TESIS DE LA UNIVERSIDAD DE ZARAGOZA

2022 158

Mario Pérez Tarragona

Multi-Phase Power Factor Correction for Domestic Induction Heating

Director/es

Héctor Sarnago Andía
Óscar Lucía Gil

ISSN 2254-7606

Prensas de la Universidad
Universidad Zaragoza

ISSN 2254-7606

Universidad Zaragoza
1542

Tesis Doctoral

MULTI-PHASE POWER FACTOR CORRECTION FOR DOMESTIC INDUCTION HEATING

Autor

Mario Pérez Tarragona

Director/es

Héctor Sarnago Andía
Óscar Lucía Gil

UNIVERSIDAD DE ZARAGOZA
Escuela de Doctorado

Programa de Doctorado en Ingeniería Electrónica

2020

Departamento de Química Inorgánica
Universidad Zaragoza
1542
iSQCH
Instituto de Síntesis Química y Catálisis Homogénea
CSIC
Consejo Superior de Investigaciones Científicas

PhD Thesis

New Insights into Trifluoromethyl Gold Chemistry

Memoria presentada por **Alberto Pérez Bitrián**, Graduado en Química y Máster Universitario en Química Molecular y Catálisis Homogénea, para optar al grado de Doctor en Ciencias Químicas con "Mención de Doctorado Internacional" por la Universidad de Zaragoza.

Zaragoza, 5 de mayo de 2020

New Insights into Trifluoromethyl Gold Chemistry

Esta Tesis Doctoral se presenta en la modalidad de Tesis por compendio de publicaciones, e incluye cinco artículos publicados en revistas científicas internacionales que se encuentran indexadas en el Journal Citations Reports. Todas ellas pertenecen al primer cuartil (Q1) dentro de su categoría.

Las publicaciones incluidas en la Tesis son las siguientes:

1. **Gold(I) Fluorohalides: Theory and Experiment**
   Miguel Baya, Alberto Pérez-Bitrián, Sonia Martínez-Salvador, José M. Casas, Babil Menjón, Jesús Orduna. *Chemistry – A European Journal* **2017**, *23*, 1512−1515.
   DOI: 10.1002/chem.201605655.

2. **Gold(II) Trihalide Complexes from Organogold(III) Precursors**
   Miguel Baya, Alberto Pérez-Bitrián, Sonia Martínez-Salvador, Antonio Martín, José M. Casas, Babil Menjón, Jesús Orduna. *Chemistry – A European Journal* **2018**, *24*, 1514−1517.
   DOI: 10.1002/chem.201705509.

3. **An Organogold(III) Difluoride with a *trans* Arrangement**
   Alberto Pérez-Bitrián, Miguel Baya, José M. Casas, Antonio Martín, Babil Menjón, Jesús Orduna. *Angewandte Chemie International Edition* **2018**, *57*, 6517–6521.
   DOI: 10.1002/anie.201802379.
   Angewandte Chemie **2018**, *130*, 6627–6631.
   DOI: 10.1002/ange.201802379.

4. **Anionic Derivatives of Perfluorinated Trimethylgold**

   Alberto Pérez-Bitrián, Sonia Martínez-Salvador, Miguel Baya, José M. Casas, Antonio Martín, Babil Menjón, Jesús Orduna. *Chemistry – A European Journal* **2017**, *23*, 6919–6929.

   DOI: 10.1002/chem.201700927.

5. **$(CF_3)_3Au$ as a Highly Acidic Organogold(III) Fragment**

   Alberto Pérez-Bitrián, Miguel Baya, José M. Casas, Larry R. Falvello, Antonio Martín, Babil Menjón. *Chemistry – A European Journal* **2017**, *23*, 14918–14930.

   DOI: 10.1002/chem.201703352.

BABIL MENJÓN RUIZ, Investigador Científico del CSIC en el Instituto de Síntesis Química y Catálisis Homogénea (Universidad de Zaragoza – CSIC)

JOSÉ MARÍA CASAS DEL POZO, Catedrático de Universidad del Departamento de Química Inorgánica de la Facultad de Ciencias de la Universidad de Zaragoza

CERTIFICAN:

Que la presente Memoria titulada "New Insights into Trifluoromethyl Gold Chemistry" ha sido realizada en el Departamento de Química Inorgánica de la Universidad de Zaragoza y en el Instituto de Síntesis Química y Catálisis Homogénea (ISQCH) bajo su dirección y AUTORIZAN su presentación para que sea calificada como Tesis Doctoral en la modalidad de compendio de publicaciones.

Zaragoza, a 5 de mayo de 2020.

Fdo. Dr. Babil Menjón Ruiz Fdo. Prof. Dr. José María Casas del Pozo

Abstract

The chemistry of gold trifluoromethyl complexes containing one to three CF_3 groups has been investigated. The gold(I) $[PPh_4][CF_3AuX]$ complexes (X = Cl, Br, I) have been prepared, which easily undergo oxidation with halogens, X_2, to afford the corresponding $[PPh_4][CF_3AuX_3]$ complexes. By means of tandem mass spectrometry, the unprecedented mixed $[F{-}Au{-}X]^-$ anions have been detected to arise from the former upon CF_2 extrusion in the gas phase, whereas the rare $[Au^{II}X_3]^-$ anions (X = Cl, Br) are formed upon Au−C bond homolysis in the latter. The first organogold(III) difluoride with a *trans* arrangement, $[PPh_4][trans\text{-}(CF_3)_2AuF_2]$, has been prepared by reaction of $[PPh_4][CF_3AuCF_3]$ and XeF_2 and it has been thoroughly characterized. The unimolecular decomposition of the $[trans\text{-}(CF_3)_2AuF_2]^-$ anion enabled the detection in the gas phase of the whole series of $[CF_3AuF_x]^-$ anions (x = 1, 2, 3), as well as $[Au^{II}F_3]^-$ and $[Au^{I}F_2]^-$ in further stages of the experiment. The fluoride ligands in $[PPh_4][trans\text{-}(CF_3)_2AuF_2]$ are readily replaced by any other heavier halide and cyanide, with retention of the stereochemistry. In fact, the comparison of the crystal structure of the isoleptic ans isomorphous complexes $[PPh_4][trans\text{-}(CF_3)_2M(CN)_2]$ (M = Ag, Au) led to the conclusion that Au(III) and Ag(III) have similar covalent radii in their square-planar geometry. An efficient entry to the $(CF_3)_3Au$ unit has been found through the complex $[PPh_4][(CF_3)_3AuI]$, which is formed upon photooxidative addition of CF_3I to $[PPh_4][CF_3AuCF_3]$. This Au(III) species opens the door to the synthesis of different anionic derivatives for which no $[(CH_3)_3AuX]^-$ counterpart is known. Additionally, the fluorinated analogue of trimethyl gold, $(CF_3)_3Au{\cdot}OEt_2$, has been prepared and is presented as a suitable synthon of the unsaturated 14-electron species $(CF_3)_3Au$, which has been assessed to be the strongest R_3Au Lewis acid to date (R = organyl group). This T-shaped $(CF_3)_3Au$ unit is characterized by a marked stereochemical stability with an associated reluctance to undergo reductive elimination of $CF_3{-}CF_3$, which is in sharp contrast with the behavior observed for the non-fluorinated analogue $(CH_3)_3Au$. A number of neutral complexes containing ligands with different donor abilities and donor atoms have been prepared and characterized, showing a significantly higher stability in contrast with their non-fluorinated analogues. Decomposition pathways of the prepared anionic complexes are different in the gas phase, where only unimolecular processes occur, and in the condensed phase, where lower-energy intermolecular paths are open.

Resumen

Se ha realizado un estudio exhaustivo de la química de trifluorometil complejos de oro que contienen entre uno y tres grupos CF_3. Con ese objetivo, se han preparado los complejos de oro(I) $[PPh_4][CF_3AuX]$ (X = Cl, Br, I), que son oxidados fácilmente por halógenos, X_2, para dar lugar a los complejos $[PPh_4][CF_3AuX_3]$ correspondientes. Mediante espectrometría de masas en tándem, los primeros conducen a los aniones mixtos $[F{-}Au{-}X]^-$ a través de la extrusión de CF_2 en fase gas, mientras que los aniones $[Au^{II}X_3]^-$ (X = Cl, Br) se generan por homólisis del enlace Au−C en los complejos de Au(III). Por reacción de $[PPh_4][CF_3AuCF_3]$ con XeF_2 se ha preparado y caracterizado totalmente el primer difluoruro organometálico de oro(III) con disposición *trans*, $[PPh_4][trans\text{-}(CF_3)_2AuF_2]$. El estudio de la descomposición unimolecular del anión $[trans\text{-}(CF_3)_2AuF_2]^-$ ha permitido detectar las especies $[CF_3AuF_x]^-$ (x = 1, 2, 3) en fase gas, así como los aniones $[Au^{II}F_3]^-$ y $[Au^{I}F_2]^-$ en etapas posteriores del experimento. Además, los ligandos fluoruro en el complejo $[PPh_4][trans\text{-}(CF_3)_2AuF_2]$ son sustituidos fácilmente por los halogenuros más pesados y por cianuro, con retención de la estereoquímica. De hecho, por comparación de las estructuras cristalinas de las especies isolépticas e isomorfas $[PPh_4][trans\text{-}(CF_3)_2M(CN)_2]$ (M = Ag, Au), se pudo concluir que Au(III) y Ag(III) tienen radios covalentes similares en su geometría plano cuadrada. La obtención del complejo $[PPh_4][(CF_3)_3AuI]$ por fotoadición oxidante de CF_3I sobre $[PPh_4][CF_3AuCF_3]$ constituye la ruta de acceso más apropiada al fragmento $(CF_3)_3Au$. Esta especie de Au(III) abre la puerta a la síntesis de diferentes derivados aniónicos, cuyos análogos $[(CH_3)_3AuX]^-$ no se conocen. Además, se ha preparado el análogo fluorado del trimetil oro, $(CF_3)_3Au{\cdot}OEt_2$, que es un sintón adecuado de la especie insaturada de 14 electrones $(CF_3)_3Au$. Este fragmento es el ácido de Lewis R_3Au (R = grupo organilo) más fuerte descrito hasta la fecha. Esta unidad $(CF_3)_3Au$, que presenta forma de T, se caracteriza por una marcada estabilidad estereoquímica y una baja tendencia a la eliminación reductora de $CF_3{-}CF_3$, contrariamente al comportamiento observado para el análogo no fluorado $(CH_3)_3Au$. También se han preparado y caracterizado diversos complejos neutros con ligandos de diferente capacidad dadora y distintos átomos dadores, que presentan una estabilidad muy superior a sus análogos no fluorados. Los complejos aniónicos de Au(III) descritos presentan vías de descomposición distintas en fase gas, donde solo ocurren procesos unimoleculares, y en fase condensada, donde son posibles caminos intermoleculares de menor energía.

List of Abbreviations

*a*HF	Anhydrous hydrogen fluoride
av.	Average
bpy	2,2′-bipyridine
Bu	Butyl
CID	Collision-Induced Dissociation
COSY	Correlation Spectroscopy
Cy	Cyclohexyl
DCTB	*trans*-2-[3-(4-*tert*-butylphenyl)-2-methyl-2-propenylidene]malononitrile (MALDI matrix)
DFT	Density Functional Theory
diglyme	Bis(2-methoxyethyl) ether
4-dmap	4-(dimethylamino)pyridine
dme	1,2-dimethoxyethane
dmf	Dimethylformamide
dmso	Dimethyl sulfoxide
DSC	Differential Scanning Calorimetry
DTA	Differential Thermal Analysis
δ	Chemical shift (in NMR)
ESI	Electrospray Ionization
Et	Ethyl
FIA	Fluoride Ion Affinity
Hbzq	Benzo[*h*]quinoline
HOMO	Highest Occupied Molecular Orbital
HRMS	High-resolution mass spectrometry
HSAB	Hard and Soft (Lewis) Acids and Bases
IDipp	1,3-bis(2,6-diisopropylphenyl)imidazol-2-ylidene
Im	*N*-methylimidazole
*i*Pr	Isopropyl
IR	Infrared spectroscopy
J	Coupling constant (in NMR)

LUMO	Lowest Unoccupied Molecular Orbital
MALDI	Matrix-Assisted Laser Desorption/Ionization
Me	Methyl
MS^n	Tandem Mass Spectrometry (*n* = stage of the experiment)
m.p.	Melting point
m/z	mass-to-charge ratio (in mass spectrometry)
$n\mathrm{Bu}^{\mathrm{F}}$	Perfluoro *n*-butyl
NHC	N-Heterocyclic Carbene
NMR	Nuclear Magnetic Resonance
Ph	Phenyl
phen	1,10-phenantroline
pmdta	N,N,N',N',N''-pentamethyldiethylenetriamine
ppm	Parts per million (chemical shift units)
py	Pyridine
Q-ToF	Quadrupole-Time-of-Flight
SIDipp	1,3-bis(2,6-diisopropylphenyl)-4,5-dihydroimidazol-2-ylidene
SIMes	1,3-bis(2,4,6-trimethylphenyl)-4,5-dihydroimidazol-2-ylidene
*t*Bu	*tert*-butyl
Tf	CF_3SO_2
TGA	Thermogravimetric Analysis
thf	Tetrahydrofuran
tht	Tetrahydrothiophene
TM	Transition Metal
tmeda	Tetramethylethylenediamine
TS	Transition State
v	Wavenumber (in IR)
χ	Electronegativity

All other abbreviations which are not so common will be explained along the text in due course.

List of Compounds

I	$[PPh_4][CF_3AuCF_3]$
II	CF_3AuCO
1	$[PPh_4][CF_3AuCl]$
2	$[PPh_4][CF_3AuBr]$
3	$[PPh_4][CF_3AuI]$
4	$[F{-}Au{-}Cl]^-$
5	$[F{-}Au{-}Br]^-$
6	$[F{-}Au{-}I]^-$
7	$[PPh_4][CF_3AuCl_3]$
8	$[PPh_4][CF_3AuBr_3]$
9	$[PPh_4][CF_3AuI_3]$
10	$[AuCl_3]^-$
11	$[AuBr_3]^-$
12	$[PPh_4][\textit{trans}\text{-}(CF_3)_2AuF_2]$
13	$[CF_3AuF_3]^-$
14	$[CF_3AuF_2]^-$
15	$[CF_3AuF]^-$
16	$[AuF_3]^-$
17	$[AuF_2]^-$
18	$[PPh_4][\textit{trans}\text{-}(CF_3)_2AuCl_2]$
19	$[PPh_4][\textit{trans}\text{-}(CF_3)_2AuBr_2]$
20	$[PPh_4][\textit{trans}\text{-}(CF_3)_2AuI_2]$
21	$[PPh_4][\textit{trans}\text{-}(CF_3)_2Au(CN)_2]$
21*	$[PPh_4][\textit{trans}\text{-}(CF_3)_2Au(^{13}CN)_2]$
22	$[PPh_4][(CF_3)_3AuI]$
23	$[PPh_4][\textit{trans}\text{-}(\textit{n}Bu^F)(CF_3)_2AuI]$
24	$[PPh_4][(CF_3)_3AuF]$
25	$[PPh_4][(CF_3)_3AuCl]$
25′	$[PPh_3CH_2Ph][(CF_3)_3AuCl]$
26	$[PPh_4][(CF_3)_3AuBr]$

27	$[PPh_4][(CF_3)_3Au(CN)]$
28	$(CF_3)_3Au{\cdot}OEt_2$
29	$(CF_3)_3Au(CN\mathit{t}Bu)$
30	$(CF_3)_3Au(NCMe)$
31	$(CF_3)_3Au(py)$
32	$(CF_3)_3Au(PMe_3)$
33	$(CF_3)_3Au(PPh_3)$
34	$(CF_3)_3Au(Opy)$
35	$(CF_3)_3Au(OPPh_3)$
36	$(CF_3)_3Au(tht)$
37	$(CF_3)_3Au(SPPh_3)$

Roman numbers are given for complexes used as starting materials, previously described in the literature.

Those species which have been only detected in the gas phase by tandem mass spectrometry are identified by a number written in *italics*.

Table of contents

Introduction

I.1. A short overview on gold chemistry

Gold is a unique element found native in Nature, which has fascinated mankind for millennia because of its beauty and unalterability. Its usage in jewelry and currency, among others, gives clear evidence of the omnipresence of gold along history.[1,2] Nevertheless, the chemistry of gold remained largely unexplored due to the remarkable inertness of the bulk metal at ambient conditions. In fact, it had a late start, but has been rapidly developing since the last decades of the 20th century. Nowadays it has evolved into an important field of research with many applications in areas such as catalysis, medicine, or nanotechnology.[3,4]

Relativistic effects play a decisive role in determining the properties of gold and its compounds.[5-8] They are important in the chemistry of other 5d elements as well, but a pronounced maximum is reached at the Au atom in Group 11 (Figure I.1). As a consequence of the high nuclear charge of the gold atom, the speed of the 6s electrons is not negligible with respect to the speed of light and leads to an increase in the mass of these electrons and a contraction and stabilization of the 6s orbital (direct relativistic effect). This stabilization results in a more effective shielding of the nuclear charge, which leads to an expansion and destabilization of the 5d orbitals (indirect relativistic effect).

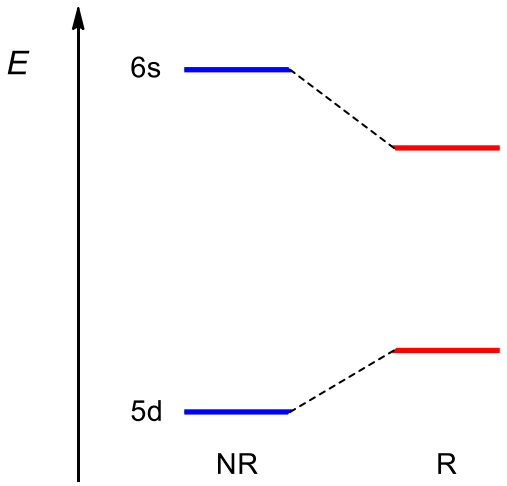

Figure I.1. Schematic view of the relativistic (R) and non-relativistic (NR) orbital energies for AuH (adapted from Ref. [7c]).

The smaller energy gap between the 6s and the 5d orbitals, which is consequence of the stabilization of the former and destabilization of the latter, accounts for the yellow color of gold. Otherwise, the excitation energy between those valence levels would be much larger and would lie in the UV, as for most metals, instead of being small enough to absorb blue light. These relativistic effects also account for the unique atomic properties of gold, such as its high electronegativity (2.54 in the Pauling scale),[9] electron affinity (–2.309 eV)[10] and the first ionization potential (9.2255 eV).[10] In fact, the high exothermic character of the electron affinity of gold justifies the unusual stability of the auride anion Au^-, which can be found in some ionic structures as in that of CsAu.[11] According to this, gold could be regarded as a pseudohalogen, since it is actually almost as electronegative as iodine (2.66 in the Pauling scale),[9] and its electron affinity is not qualitatively different from that of this element (–3.059 eV).[10]

Several oxidation states are known for gold, ranging from –I to V,[2,3,12] the most common being I and III. In the former, with closed-shell $[Xe]4f^{14}5d^{10}$ configuration, a linear coordination is favored as a consequence of the high s-character of the LUMO, which derives from the high stabilization of the 6s orbitals with respect to the 6p.[8d] In the latter, a $[Xe]4f^{14}5d^{8}$ configuration leads to low-spin complexes with square-planar stereochemistry. Aurophilicity plays a key role in Au(I) complexes, as it justifies the conformation and aggregation of these compounds and is responsible for a number of photophysical phenomena.[13] Aurophilic interactions have been assigned a dispersive nature, the dispersion actually increasing because of the relativistic effects, and being comparable in energy to hydrogen bonds. They are mainly established between seemingly closed-shell Au(I) centers (d^{10}), yet a few examples of aurophilicity involving Au(III) centers have also been investigated.[13a,14]

A quite different chemical element is fluorine. The marked chemical inertness of gold is in sharp contrast with the fierceness of fluorine. The large electronegativity and the small atomic size of fluorine make this element especially appropriate to stabilize high oxidation states, such as Au(V).[15] In fact, when fluoride ligands are coordinated to gold centers, compounds of singular properties are formed.[16-19] Similarly, fluorinated ligands, among which the CF_3 is the simplest one, also impart interesting properties to gold complexes when coordinated to this metal and have allowed for the still-ongoing development of a rich chemistry.[17,20] These kinds of compounds and their most salient characteristics will be presented in the next sections.

I.2. The fluorides of gold

The existence of gold fluorides was reported only after the isolation of fluorine by Henri Moissan[21] and the chemistry of these compounds has always remained much less explored than that of the heavier homologues chlorine, bromine and iodine.[16-19] This may be due to the difficulties in handling these highly-reactive species, which are moisture sensitive and which usually require specialized equipment for its synthesis and characterization.

The oxidation state III in gold is significantly stabilized because of the relativistic effects in comparison to oxidation state I, as commented above.[8c] This fact is clearly brought to light for binary gold fluorides, since AuF_3 is the simplest isolable one. It has been actually used as precursor for the preparation of most of the gold fluorides known.[16-19] After failed efforts by Lehnen[22] and Ruff,[23] Sharpe succeeded in preparing AuF_3 in 1949 by using BrF_3 as the fluorinating agent.[24] His method consisted in dissolving gold powder in BrF_3, which is liquid at room temperature, whereby $AuF_3 \cdot BrF_3$ was formed. Upon pyrolysis at 180 ºC of this adduct, which can also be formulated as $[BrF_2]^+[AuF_4]^-$, AuF_3 could be obtained (Scheme I.1). However, since it contained a very little amount of bromine as an impurity, other methods were developed later, such as halogen exchange reaction of F_2 and $AuCl_3$ at high temperatures,[25] or the direct synthesis from the elements (Scheme I.1).[26]

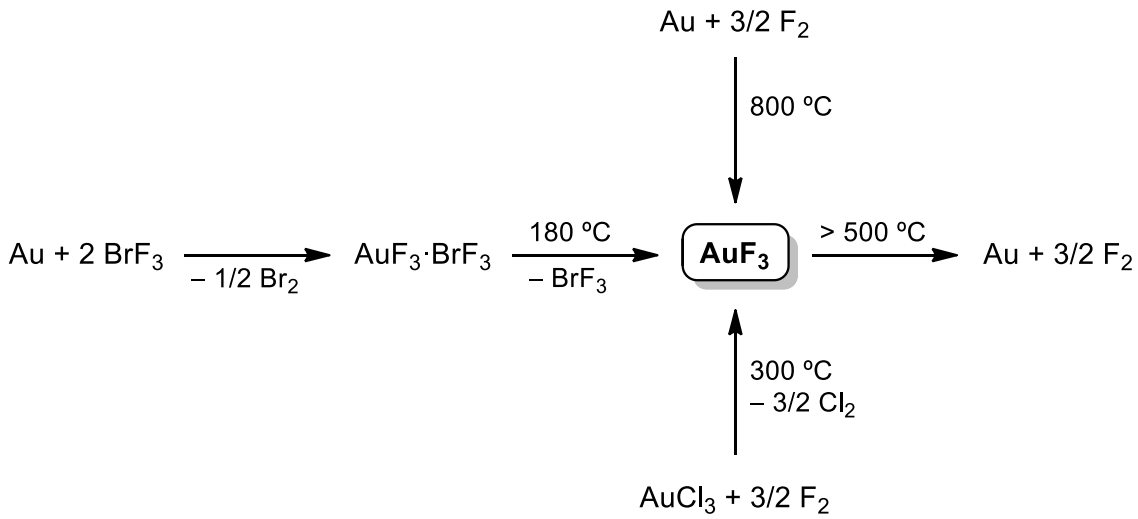

Scheme I.1. Different synthetic routes to prepare AuF_3 and thermal decomposition of the compound.[24-26]

AuF_3 is an orange solid, which decomposes thermally at around 500 ºC to render metallic gold, with fluorine release. It is also readily hydrolyzed to give $Au(OH)_3$ and HF in an exothermic way, and reacts violently with benzene and alcohol. However, it is able to yield chlorofluorocarbons upon reaction with CCl_4 at 40 ºC.[24] Only recently, it has been shown that small amounts of AuF_3 can be dissolved in MeCN below –25 ºC with formation of AuF_3(NCMe).[27] After an initial study by X-ray powder diffraction,[25c] the structure of AuF_3 in the solid state could be established by single-crystal X-ray diffraction.[26b,28] The compound was found to be a polymeric fluoride-bridged helical chain (Figure I.2). Indeed, it consists of approximately square-planar AuF_4 units linked by two *cis* bridging fluorides, with the bridging Au–F bond lengths being longer (204 pm) than the terminal distances (191 pm). Additionally, the chains are cross-linked by weak fluorine contacts (269 pm). In the gas phase, however, the monomer AuF_3 exhibits an almost T-shaped structure, as calculated by computational methods and established by gas-phase electron diffraction.[8c,29-31] Additionally, dimeric Au_2F_6 has been detected in matrix-isolation experiments[29] and its planar structure has been determined by gas-phase electron diffraction.[31]

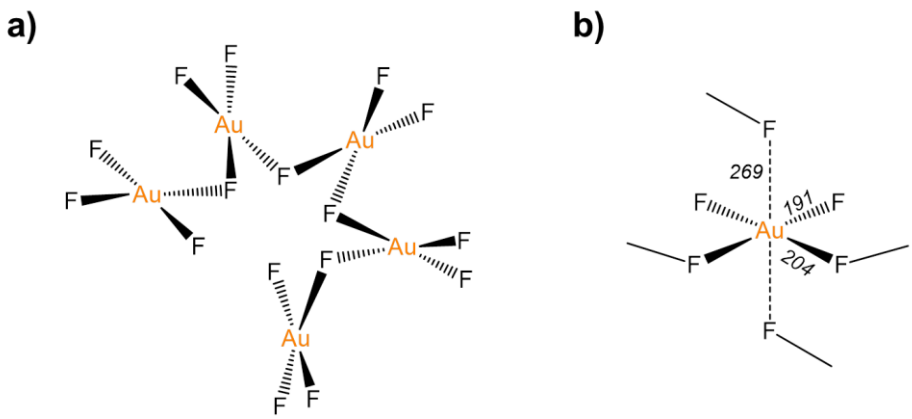

Figure I.2. a) Scheme of the crystal structure of AuF_3. b) Gold environment in the polymeric structure of AuF_3. Terminal and bridging Au–F distances, as well as weak contacts are indicated [pm], as reported by Bartlett et al. in 1967.[26b]

The related $[AuF_4]^-$ anion was first synthesized in 1959 as its potassium salt upon reaction of gold metal, KCl and BrF_3.[32] It is far more stable than AuF_3. This binary species is highly electrophilic and reacts with a number of metal fluorides to afford

different salts of the square-planar $[AuF_4]^-$ anion.[16-19,33] $M^I[AuF_4]$ salts are known for alkali cations, as well as for other metallic or more complex monocations (e.g. AgF^+ or XeF_5^+). Additionally, $M^{II}[AuF_4]_2$ salts have been prepared with a variety of dications such as earth-alkaline Mg^{2+} and Ba^{2+}, as well as other d-block metals (e.g. Ni^{2+} or Zn^{2+}), including Au^{2+}, which gives an overall Au_3F_8 stoichiometry.[34] Interestingly, the first salts of $[AuF_4]^-$ with organic cations, $[NR_4]^+$ (R = Me, Et), were recently isolated upon reaction of AuF_3 with the corresponding $[NR_4]Br$ in a Br_2/BrF_3 mixture.[27] The Au–F bond lengths in these two salts show very little variation: 189.9–191.6 pm. These salts are especially interesting, since they can be handled in many dry organic solvents, contrary to AuF_3 or even $Cs[AuF_4]$. For instance, solutions of $Q[AuF_4]$ (Q = Cs^+ or $[NMe_4]^+$) in pyridine rendered a mixture of pyridine fluoride gold(III) species, being AuF_3(py) the main product in CH_2Cl_2 solution.[27]

Contrary to these stable Au(III) fluorides, the simplest Au(I) fluoride AuF is very unstable and has not been isolated as a pure substance. Theoretical calculations on the lattice energy of AuF demonstrated that the synthesis from the elements is an endergonic process and also that it would disproportionate to Au and AuF_3, according to thermodynamic data.[35] In 1992, the first spectroscopic evidence for the existence of AuF was presented during the etching of gold films using O_2-CF_4 and O_2-SF_6 plasmas, but the authors also admitted that the observed emission could equally arise from AuO, AuF^+ or AuO^+.[36] Soon after, theoretical calculations predicted the formation of AuF in the gas phase,[37] and its spectroscopic properties were anticipated.[38] In 1994, Schwarz and coworkers finally reported clear evidence of the existence of this elusive species in the gas phase by using neutralization-reionization mass spectrometry.[39] Its existence was later confirmed by microwave spectroscopy.[40,41] Interestingly, in a noble-gas matrix, AuF coordinates a noble gas atom giving [NgAuF] species (Ng = Ne, Ar).[29] The complex anion $[AuF_2]^-$ should be more stable, as has been predicted by theoretical calculations.[8d] However, it has only been detected in the gas phase via tandem mass spectrometry.[42] Additionally, it appeared among the decomposition products of $[AuF_4]^-$ in its ESI(−) mass spectrum, together with the Au(II) anion $[AuF_3]^-$.[27]

Similarly, although computational studies on the properties of AuF_2 and related molecules have been performed,[38,43] this open-shell binary species has only been detected and characterized under cryogenic conditions in neon and argon matrices.[29] Quantum-chemical calculations demonstrated that AuF_2 is stable against homolytic

bond cleavage and disproportionation.[29] Recent theoretical investigations showed that under high pressures, AuF_2 should be stable and exhibit a bulk structure of quasi-linear molecules interacting among them.[44,45] The related binary, open-shell gold fluoride AuF_4 has never been observed. In fact, oxidation state IV in gold is elusive and only recently the AuO^{2+} dication has been detected by mass spectrometry and characterized theoretically.[46] However, in recent studies, it has been shown that AuF_4 might be stable under high pressure and should therefore be experimentally synthesized.[44,45] Interestingly, two different structures have been predicted for AuF_4: a tetragonal structure containing square-planar molecular AuF_4 units[45] and a monoclinic one consisting of a polymer containing two non-equivalent AuF_6 octahedral units connected through two bridging fluorides.[44]

The highest oxidation state currently known for gold, Au(V), is achieved only with fluorine.[15] The only two Au(V) species known are indeed gold fluorides: the binary AuF_5 and the anionic $[AuF_6]^-$. Since the first Au(V) complex $[Xe_2F_{11}][AuF_6]$ was synthesized by reaction of AuF_3 with an excess of XeF_6,[47] various other $[AuF_6]^-$ salts with different counterions have been prepared (Scheme I.2).[16-19,48] For example, upon reaction of $[Xe_2F_{11}][AuF_6]$ and CsF the cesium salt $Cs[AuF_6]$ was formed.[47] However, KrF_2 can react directly with elemental gold to render $[KrF][AuF_6]$.[49] Additionally, oxidation of $[AuF_4]^-$ salts, dissolved in anhydrous HF (*a*HF), with F_2 and UV light at room temperature also yields the corresponding $[AuF_6]^-$ salts.[48] A similar procedure using photodissociated F_2 is also useful to prepare $M^{II}[AuF_6]_2$ salts, starting from AuF_3 and the appropriate MF_2 species. The $[AuF_6]^-$ anion exhibits an octahedral geometry, as established by X-ray diffraction on single crystals of $[Xe_2F_{11}][AuF_6]$,[50] and by Mössbauer spectroscopy.[51]

The binary compound AuF_5 is prepared by thermal decomposition of $[KrF][AuF_6]$ or $[O_2][AuF_6]$ and is obtained in pure form as a dark red solid after sublimation (Scheme I.3).[49,52] It is a dimer in the solid state, Au_2F_{10}, as established by single-crystal X-ray diffraction.[53] It is an extremely powerful oxidant and fluorinating agent, which makes it difficult to handle. In *a*HF solution it releases F_2 with reduction to AuF_3 (Scheme I.3). The five-coordinate monomer AuF_5 is actually the strongest neutral Lewis acid known to date.[54]

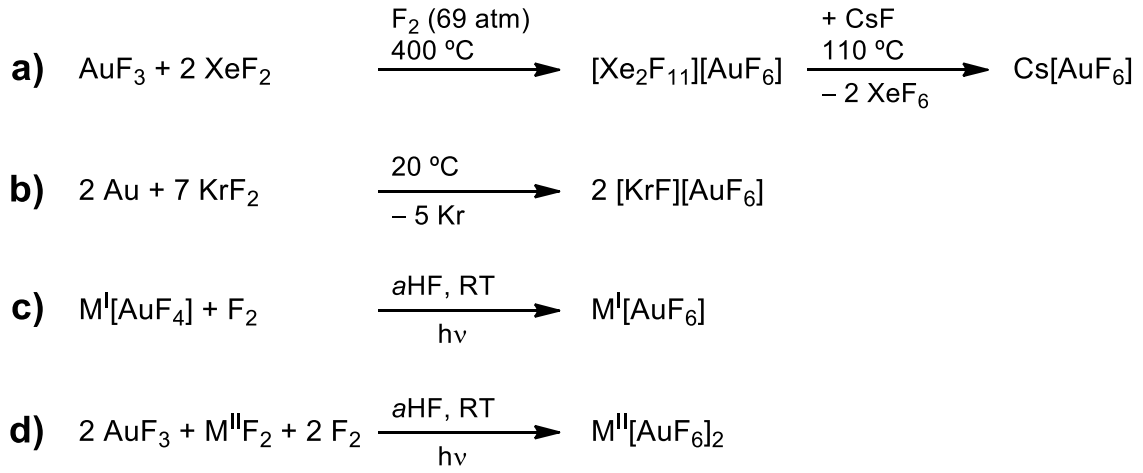

Scheme I.2. Examples of different synthetic routes to prepare $[AuF_6]^-$ salts: a) first preparation by Leary and Bartlett;[47] b) direct access from elemental gold;[49] c) fluorination of a $M^I[AuF_4]$ salt;[48] d) synthesis of $M^{II}[AuF_6]_2$ salts by direct fluorination.[48]

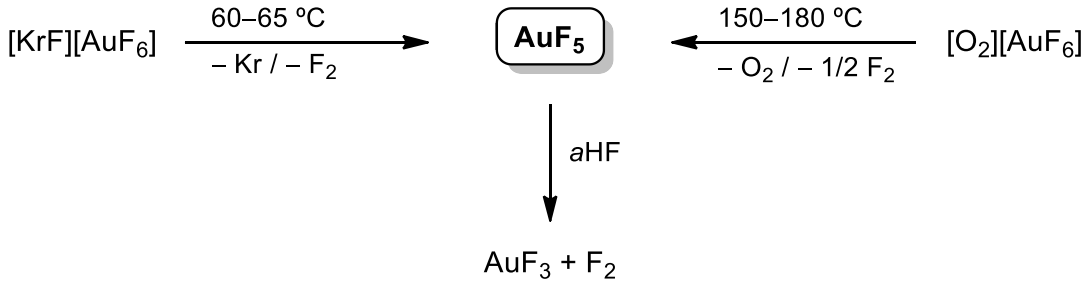

Scheme I.3. Synthetic routes to prepare AuF_5 and its decomposition in *a*HF.[49,52,53]

The neutral molecule AuF_6 has been claimed to be the strongest oxidizer according to computational calculations,[55] but it has never been prepared nor even detected. In fact, the most powerful oxidizers currently known, namely NiF_4 and AgF_3 dissolved in acidified *a*HF (whereby solvated cationic Ni(IV) and Ag(III) species are formed), are not able to oxidize the $[AuF_6]^-$ anion to AuF_6.[56] However, recent theoretical investigations have shown that AuF_6 might exist under high pressure.[44,45]

The extremely high oxidation state Au(VII) was reported for a putative AuF_7 species in 1986.[57] Its formulation, however, was later challenged[58] and computational calculations finally confirmed that AuF_7 as such is intrinsically unstable, being best formulated as an adduct of AuF_5 with an end-on coordinated F_2 molecule, $AuF_5 \cdot F_2$.[59]

This result also illustrates the strong Lewis acidity of AuF_5. Recent theoretical calculations also corroborated the instability of AuF_7 as a Au(VII) species,[60] which makes Au(V) the highest oxidation state known for Au.[15]

Gold fluorides are highly reactive and therefore, its chemistry is difficult to develop, as clearly demonstrated along this section. The introduction of appropriate ancillary ligands can lead to a substantial stabilization of the Au−F unit in mixed gold fluoride complexes.[16] This way, the properties and reactivity of Au−F bonds can be studied under milder conditions, as will be discussed in the following section.

I.3. The chemistry of organogold fluoride complexes

Organometallic fluorides can be defined as those compounds which contain metal−fluorine (M−F) and metal−carbon (M−C) bonds at the same metal center.[61] Their properties largely differ from those of their heavier-halide homologues. For late-transition metals (TM), this fact can be justified by the filled/filled orbital interactions discussed by Caulton.[62] According to this hypothesis, destabilizing interactions appear between halide lone-pair electrons and filled d orbitals of the late-TM. Thus, within a series of organometallic halide complexes, it is reasonable to expect that these destabilizing interactions would reach the maximum in the case of fluorine, which is the strongest π donor and leads to short M−F bonds.[63] Until recently, organometallic fluoride complexes have been much less studied than their heavier-halide homologues, mainly because of the lack of suitable synthetic procedures to introduce the fluoride ligand.[64] However, convenient synthetic routes have been developed in the last years.[16,61]

The distinct effects that fluoride ligands impart to metal centers are especially conspicuous in gold chemistry.[16,17] Gold is a “soft acid” (according to Pearson’s HSAB theory)[65] or a “class b” metal (based on the original classification of Ahrland, Chatt and Davies)[66] in its most common oxidation states I and III. Accordingly, coordination of large polarizable ligands is preferred.[67] Since fluoride is a hard base, the soft-hard difference in Au−F bonds becomes prominent, which together with the dπ–pπ repulsion between the fluoride and the gold center,[61,62] makes these bonds very labile and reactive.

Organogold fluorides form a relatively new class of compounds, generally difficult to isolate, and characterized by their high reactivity.[16,17] Thus, despite being largely sought, these complexes are still scarce. Although Willner and coworkers generated and studied spectroscopically a mixture of species $[(CF_3)_xAuF_{4-x}]^-$ (x = 1–3) in 2004, their isolation was not possible.[68] The first organogold(I) fluoride was isolated by the group of Sadighi in 2005, making use of an N-heterocyclic carbene (NHC) ligand to stabilize the "Au–F" fragment.[69] Complex (SIDipp)AuF (SIDipp = 1,3-bis(2,6-diisopropylphenyl)-4,5-dihydroimidazol-2-ylidene) was prepared by protonolysis of the *tert*-butoxide precursor with $Et_3N{\cdot}3HF$ (Scheme I.4a). Computational calculations located a substantial negative charge on the fluoride ligand, demonstrating the highly ionic character of the Au–F bond. This complex was later found to react with 3-hexyne to form a (*trans*-β-fluorovinyl)gold(I) species (Scheme I.4b) in a reversible way, from which the fluoroalkene could be obtained upon reaction with trifluoroacetic acid.[70] A catalytic version of this overall hydrofluorination reaction could actually be developed. The mononuclear complex (SIDipp)AuF enabled to prepare the only other organogold(I) fluoride complex currently known, namely the dinuclear derivative with a bridging fluoride ligand, $[\{(SIDipp)Au\}_2(\mu\text{-}F)]BF_4$ (Scheme I.4c).[71] Additionally, the $[CF_3AuF]^-$ anion was detected to arise in the gas phase by collision-induced-dissociation of the precursor $[Au(O_2CCF_3)_2]^-$.[42] It is worth noting that the Werner-type complex $(PPh_3)AuF$ could not be prepared by halide metathesis from the well-known chloride complex $(PPh_3)AuCl$ and AgF.[72]

The chemistry of organogold(III) fluorides is also recent, but comparatively more developed, with several reports since 2010.[16] A small set of monofluoride derivatives is currently known, which comprises 15 complexes, including $[PPh_4][(CF_3)_3AuF]$, to be described in Chapter 3. Interestingly, the number of isolated organogold(III) fluorides decreases dramatically when the number of fluorine atoms directly bound to the metal increases. In fact, only 6 difluoride derivatives have been prepared (including $[PPh_4][trans\text{-}(CF_3)_2AuF_2]$, which will appear in Chapter 2) and just a single organogold(III) trifluoride species has been isolated (see below).

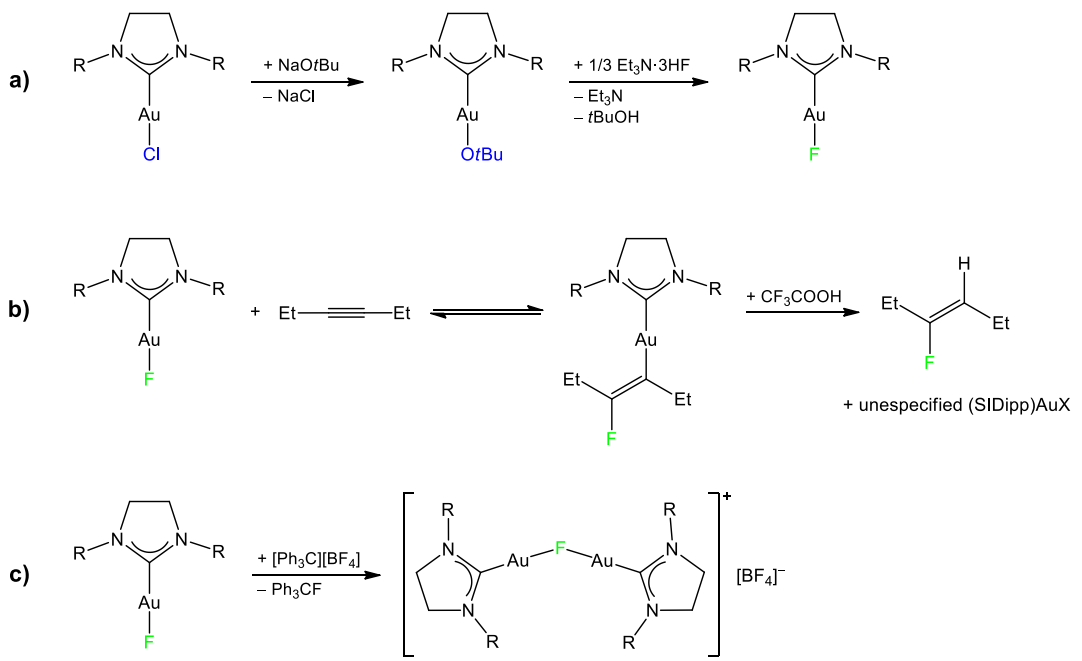

Scheme I.4. a) Synthesis of the first organogold(I) fluoride complex (R = 2,6-diisopropylphenyl), reported by Sadighi et al. in 2005,[69] b) its reactivity towards alkynes,[70] and c) its use for the synthesis of a dinuclear μ-fluoro cationic organogold(I) complex.[71]

Methods for introducing a fluoride ligand include the use of AgF and a heavier-halide precursor, as already exploited by Moissan in the late XIX century.[73] This way, the Toste group prepared the first terminal organogold(III) fluoride complexes $CF_3AuF(4\text{-}Me\text{-}C_6H_4)(PPh_3)$ and $CF_3AuF(4\text{-}F\text{-}C_6H_4)(PCy_3)$, which contain a single fluoride ligand (Scheme I.5a).[74] Soon after, the Nevado group prepared a set of organometallic gold(III) monofluoro derivatives containing a cyclometalated (N^C^C)-ligand framework using a similar procedure (Scheme I.5b).[75] Additionally, they studied the reactivity of the Au−F bond in one of the (N^C^C)AuF complexes towards different terminal alkynes and aryl boronic acids to obtain alkynyl[75] and aryl[76] derivatives, respectively (Scheme I.6). Similarly, using a 2-phenylpyridine-based C^N ligand to stabilize the Au(III) center,[77] they prepared two new monofluoride complexes (C^N)AuRF (Scheme I.5c; R = CH_3, 3,5-$(CF_3)_2$-C_6H_3).

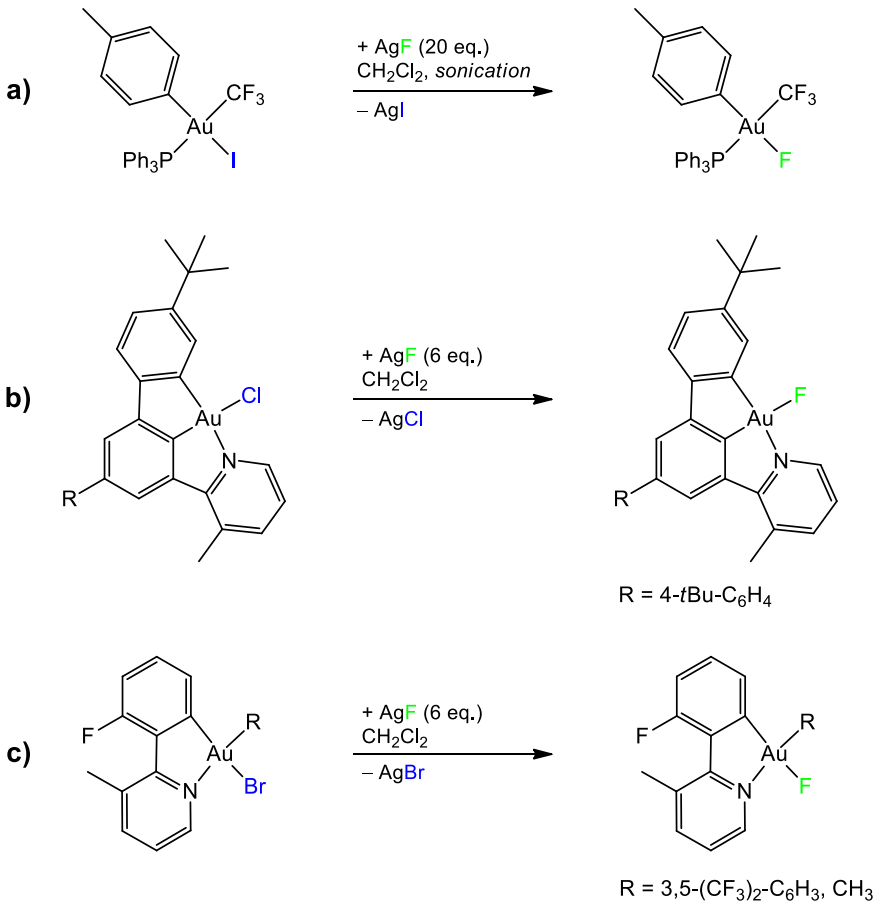

Scheme I.5. Organogold(III) fluoride complexes containing one Au–F bond, prepared by halide-exchange reactions with AgF: a) One of the examples reported by the Toste group.[74] b) One of the examples of the organogold(III) fluoride complexes containing a N^C^C ligand reported by the Nevado group.[75] c) Organogold(III) fluoride complexes containing a C^N ligand reported by the Nevado group.[76]

The C^N platform was also successfully used by Nevado and coworkers to isolate two organogold(III) difluoride complexes, which were also prepared by facile halide exchange with AgF (Scheme I.7a).[76] However, some years before, the Toste group had reported the preparation of the first organogold(III) difluoride complex using XeF_2 to reach the oxidation state III, while introducing two fluoride ligands (Scheme I.7b).[78] The monomeric compound, *cis*-(IDipp)Au(CH_3)F_2 (IDipp = 1,3-bis(2,6-diisopropylphenyl)imidazol-2-ylidene), was in equilibrium with a cationic double fluoride-bridged dimer, which was actually the species that crystallizes preferentially. In fact, no crystallographic evidence of the monomeric species has been found thus far. The binuclear species is favored at high concentrations and also by the other ligands, as

concluded from similar reactions with related systems. The difluoride complex rapidly reacts with aryl boronic acids to afford the C–C coupling product. The stability of *cis*-(IDipp)Au(CH_3)F_2 is exceptional for this kind of compounds, since the oxidation of other alkyl gold(I) analogues (IDipp)AuR with XeF_2 affords mixtures of the C(sp^3)–F coupling product and alkenes resulting from β-hydride elimination, if the R group contains at least a hydrogen atom in that position.[79] However, in several cases, *cis*-(IDipp)AuF_2R intermediates were observed by ^{19}F NMR spectroscopy but could not be isolated.

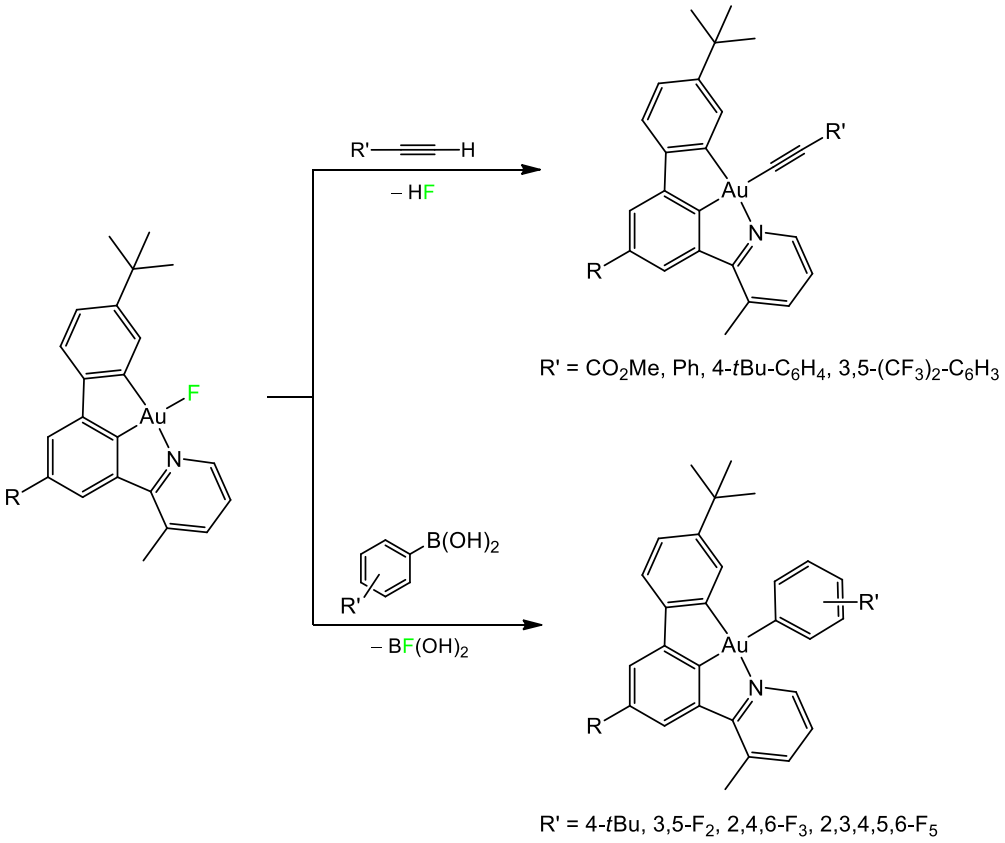

Scheme I.6. Reactivity of Nevado's organogold(III) fluoride complex containing a N^C^C ligand (R = 4-*t*Bu-C_6H_4) towards terminal alkynes and aryl boronic acids.[75,76]

Most organogold(III) difluoride species described thus far exhibit a *cis* stereochemistry[76,78,79] and, in fact, no *trans* organogold(III) difluoride complex had been reported prior our compound [PPh_4][*trans*-$(CF_3)_2AuF_2$], which will be presented in Chapter 2. Following our report, two more *trans* organogold(III) difluoride derivatives were prepared by the Riedel group (see below). Additionally, cationic Werner-type

gold(III) difluoride complexes with *trans* arrangement, containing imidazole and pyridine ligands, were reported later.[80] Interestingly, and as in our own case, the latter were also prepared by oxidation of the corresponding Au(I) species with XeF_2, again leading to a *trans* stereochemistry instead of the *cis* arrangement found by Toste in the aforementioned analogous process (Scheme I7.b).[78,79]

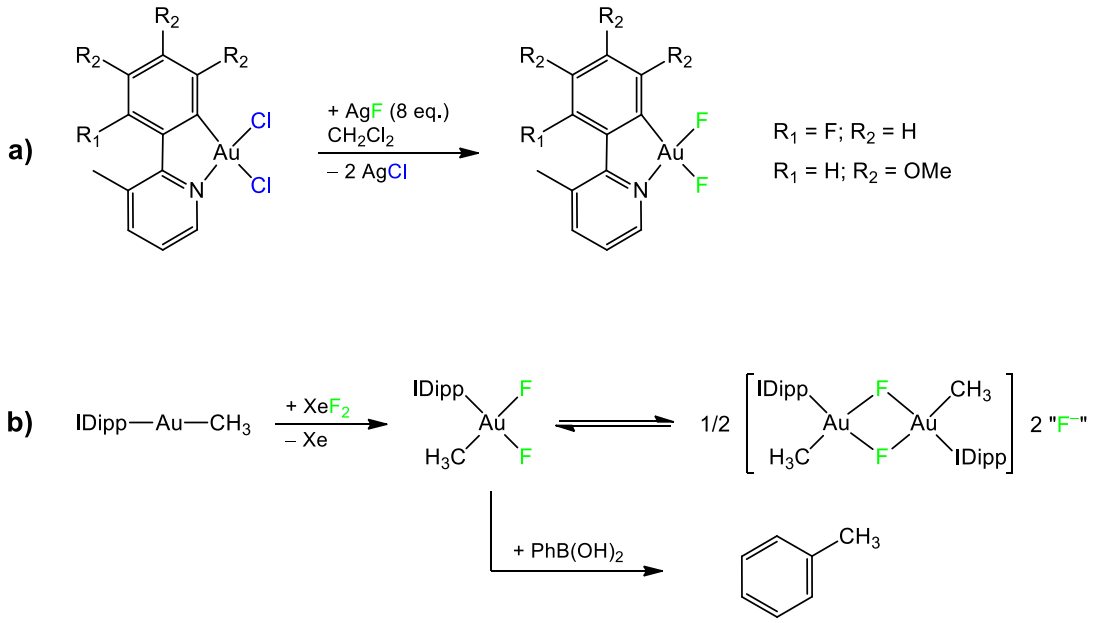

Scheme I.7. Synthesis of *cis*-difluoride organogold(III) complexes by a) halide-exchange reaction with AgF,[76] and b) oxidation of a gold(I) precursor with XeF_2. Although other Au(I) precursors containing the SIDipp ligand and the *t*Bu group were used, the example shown is the only one which allowed to isolate the mononuclear complex. The counterions of the dimer are formally F^- anions, but their nature was not unambiguously established in the structure refinement.[78]

The only organogold(III) trifluoride complex that has been isolated and characterized to date, AuF_3(SIMes) (SIMes = 1,3-bis(2,4,6-trimethylphenyl)-4,5-dihydroimidazol-2-ylidene), was reported by Riedel and coworkers in 2018.[81] It was prepared by careful reaction of AuF_3 and the SIMes ligand in dichloromethane (Scheme I.8). Coordination of the carbene ligand tames the reactivity of the strong-oxidizing AuF_3 unit. This complex is, in fact, more stable than AuF_3(NCMe), which is detected in solution at low temperature[27] The fluoride in the *trans* position of the SIMes (Au–F: 197.2(1) pm) in compound AuF_3(SIMes) seems to be more weakly bound to the Au(III) center than the mutually *trans*-standing fluoride ligands (Au–F: 191.9(1) pm av.). In fact, it was found

to be stereoselectively substituted by a chloride or a pentafluoroorthotellurate group upon treatment with Me_3SiX reagents (X = Cl, $OTeF_5$), leading to the corresponding difluoride complexes with *trans* stereochemistry (Scheme I.8).[82]

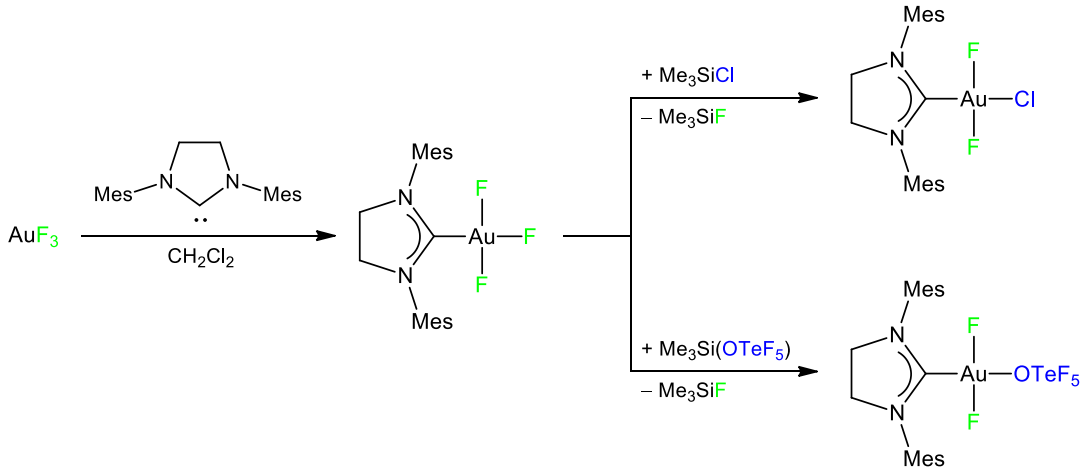

Scheme I.8. Synthesis of the only known organogold(III) trifluoride complex reported by the Riedel group (Mes = mesityl),[81] and its reactivity towards Me_3SiX reagents.[82]

Organogold fluorides play an important role in a variety of fluorination processes.[83] The current interest in preparing new fluorinated organic molecules with interesting applications via gold catalysis has stimulated the search for this kind of species.[16,17] In particular, in the area of redox gold catalysis,[4b,84] the main difficulty was to overcome the high oxidation potential of the redox couple Au^{III}/Au^{I} (1.41 V) compared to the well-studied Pd^{II}/Pd^{0} system (0.95 V).[85] In those cases, a stoichiometric external oxidant is generally required,[4b,84] as for instance XeF_2.[78-80] However, when searching for the fluorination of organic substrates, C–F reductive elimination seems to be the key turnover step in the catalytic cycle, since it is thermodynamically favorable, yet exhibits high activation barriers.[86] In fact, in some cases the reductive elimination process does not result in fluorination but in C–C bond formation.

I.4. The trifluoromethyl group in transition-metal chemistry

Organofluorine chemistry has been established over the years as a well-defined research field owing to the importance of C−F bonds in a myriad of applications.[87] C−F bonds

are the strongest bonds formed by carbon with any chemical element (485 kJ mol^{-1}).[88] Fluorination of an organic molecule causes marked changes in its physicochemical properties, which is a consequence of the highly polarized C−F bond.[87d,89] The significant $C^{\delta+}$−$F^{\delta-}$ component is indeed responsible for the unusual thermal stability and low chemical activity of the compounds, which also exhibit changes in their volatility, lipophilicity, ability to form hydrogen bonds or π-donor behavior. Although fluorine is the 13th element in the Earth's crust,[90] the vast majority of organofluorine compounds currently known are synthetic and very few natural products have been identified to contain fluorine.[91]

The most simple perfluorinated organic group CF_3, was unknown until Swarts prepared $PhCF_3$ in 1898.[92] This group gives a clear example of the effects caused by fluorination, since its properties are significantly different from those of its non-fluorinated analogue CH_3 (Figure I.3). The group electronegativity in Pauling units rises from 2.28 in the methyl to 3.49 in the trifluoromethyl group, which makes CF_3 even more electronegative than chlorine (χ_{Cl} = 3.16).[9, 93] Moreover, according to its effective van der Waals radius (220 pm), the CF_3 group is similar in size to an isopropyl group.[94] The reactivity of a CF_3 group is also significantly different from that of a CH_3 group. Therefore, all these differences justify that "the trifluoromethyl group should be considered more appropriately as a distinct functional group rather than as a substituted methyl group", as claimed by Prof. Ritter.[86b]

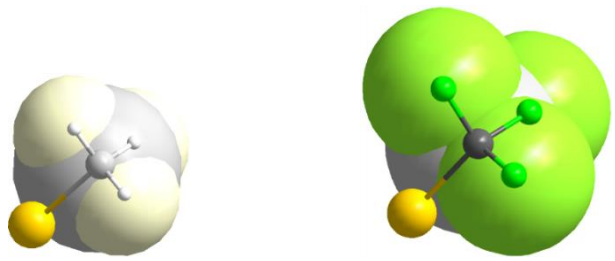

	M–CH_3	**M–CF_3**
χ [Pauling units]	2.28	3.49
r_{vdW} [pm]	180	220

Figure I.3. Comparison between CH_3 and CF_3 groups bound to a generic TM: χ = group electronegativity in Pauling units; r_{vdW} = effective van der Waals radius in pm.

The striking differences between both alkyl groups are especially remarkable in organometallic chemistry.[95] In fact, TM trifluoromethyl complexes generally show an enhanced thermal stability with respect to their methyl analogues. This higher stability has been attributed at least in part by assuming the existence of fluoride negative hyperconjugation[96] and M−C π-back-bonding between filled d orbitals of the metal center and σ* orbitals of the CF_3 group.[97] This leads to an explanation of the [M]−CF_3 bonding through three indistinguishable resonance structures (Scheme I.9).

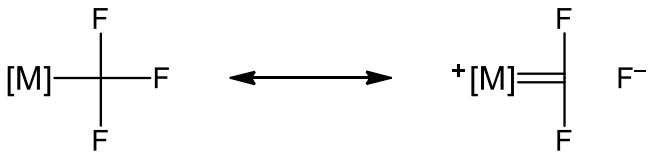

Scheme I.9. One of the three indistinguishable resonance structures involving fluoride negative hyperconjugation and M−C π-back-bonding for the [M]−CF_3 unit.

Structural and spectroscopic features of TM trifluoromethyl complexes are in agreement with this model, and include:

a) Shortening of the M−C bond.
b) Elongation of the C−F bonds with respect to the values found in non-metallic organofluorine compounds.
c) Lower frequency associated with the ν(C–F) vibration modes.
d) Signals appearing at considerably higher frequencies in ^{19}F NMR spectra when compared to non-metallic organofluorine compounds.

Although the CF_3 group has been traditionally considered as electron-withdrawing,[95] it has recently been proposed to act as a better σ-donor than a methyl group in TM chemistry.[98,99] In particular, the [M]−CF_3 σ bond has been calculated to have a significant 2s character from the C atom, enhanced by contributions from the C−F σ* orbitals.[98a] In contrast, the π-back-donation to the C−F σ* orbitals is relatively weak, and becomes insignificant in the methyl analogues. This model involves highly polarized $M^{\delta-}$−$C^{\delta+}$ bonds with high positive charge on the CF_3 carbon as the ground state. This polarized bond is opposite to the precise electronegativity concept and, moreover, it is not in agreement with the high electronegativity of the CF_3 group. What seems clear is that the CF_3 group imposes a higher *trans* influence than CH_3 in its TM

complexes. M−CF_3 bonds are generally shorter,[98a,100] especially in mid and late-TM, since for comparable titanium complexes, the Ti−CF_3 bond length has been found to be longer than the Ti−CH_3 distances calculated in their non-fluorinated analogues.[101]

The CF_3 group has also been considered as a redox non-innocent σ-ligand able to induce ligand-field inversion in late-TM complexes,[102] in which the d orbitals of the metal are substantially stabilized and the LUMO is predominantly formed by a combination of the orbitals of the ligands, contrary to the classical ligand-field splitting. The most controversial trifluoromethyl complex has been the $[(CF_3)_4Cu]^-$ anion. Its bonding scheme and the oxidation state of the metal center have been discussed[102,103] since Snyder first formulated it as a linear organocopper(I) species $[CF_3CuCF_3]^-$ with two additional CF_3^+ and CF_3^-.[104] Calculations on the electronic structures of the heavier homologues $[(CF_3)_4Ag]^-$[105] and $[(CF_3)_4Au]^-$[106] have unveiled ligand-field inversion in all three Group 11 metal complexes. This implies that the frontier orbitals of these derivatives are mainly ligand-centered, with a substantial contribution of the 6s metal orbital in the gold species due to relativistic stabilization (Figure I.1). The $[(CF_3)_4M]^-$ complexes (M = Cu, Ag, Au) show qualitatively similar behavior in the gas phase: the observed homolytic splitting of the M−C bonds denotes a marked covalent character of this bond,[106] contrary to the ionic model initially suggested for the copper derivative.[104]

The chemistry of TM complexes containing perfluoroalkyl ligands has significantly evolved in the last decades,[95,107] since the synthesis of the very first TM perfluoroorganyl complex, $CF_3Mn(CO)_5$, which was reported by the groups of Closson,[108] Stone[109] and McClellan,[110] independently. Nowadays, a good number of TM trifluoromethyl complexes are known, especially for mid and late-TM. However, the development of the chemistry of these derivatives has been historically hindered by the scarcity of appropriate synthetic methods to coordinate the CF_3 group to metal centers.[95,107d]

I.4.1. Synthesis of transition-metal trifluoromethyl complexes

The synthesis of TM trifluoromethyl derivatives faces the difficulty that organolithium CF_3Li and organomagnesium CF_3MgX reagents are not available for synthetic

purposes, contrary to their non-fluorinated analogues.[111] In fact, the easy generation of the stabilized singlet difluorocarbene :CF_2 from CF_3Li renders its synthesis difficult.[112] It is worth noting that the perfluoroethyl homologue LiC_2F_5, which is more stable, has been prepared and its structure has been determined in the solid state.[113] Despite being for a long time invoked as a transient species in a variety of trifluoromethylation processes, the CF_3^- anion was not identified in the condensed phase until 2014,[114] when Prakash et al. were able to stabilize it with the $[K(18\text{-crown-}6)]^+$ cation. This unusual salt, $[K(18\text{-crown-}6)]^+CF_3^-$, was characterized by ^{19}F and ^{13}C NMR at −78 ºC (Scheme I.10a).[115] However, Grushin and coworkers demonstrated the existence of naked CF_3^- anion by preparation (Scheme I.10b) and crystallization of the ionic salt $[K(\text{crypt-}222)]^+CF_3^-$, in which the K^+ cation encapsulated by the enclosing cryptand ligand is inaccessible to the CF_3^- anion.[116] Nevertheless, the solid-state structure of this salt has been controversial.[117] These results are very recent and therefore have been not been exploited from a synthetic point of view yet. However, a variety of different synthetic methods to introduce the CF_3 group into the coordination sphere of a TM exist nowadays, which are summarized in Scheme I.11 and will be described next.[95]

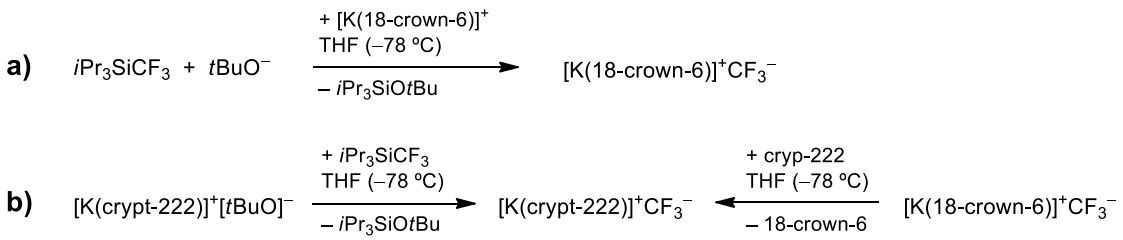

Scheme I.10. Generation and isolation of the discrete CF_3^- anion with a) the $[K(18\text{-crown-}6)]^+$ cation;[115] and b) the $[K(\text{crypt-}222)]^+$ cation.[116]

Thermal decarbonylation of an acyl complex, [M]−C(O)CF_3, afforded the first TM trifluoromethyl complex, $CF_3Mn(CO)_5$, (Scheme I.12).[108-110] The same method was successfully used later on.[107d,118] Decarboxylation of [M]−OC(O)CF_3 precursors has also been used to reach other [M]−CF_3 species, as for instance the well-known $Hg(CF_3)_2$, which can be prepared from $Hg(O_2CCF_3)_2$ in the presence of K_2CO_3.[119]

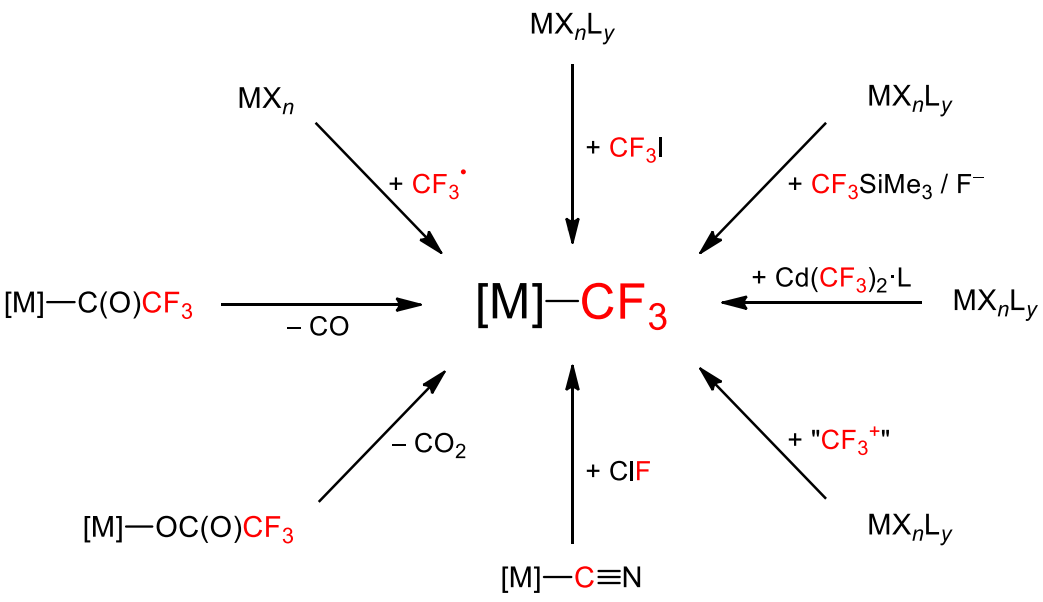

Scheme I.11. Overview of the general methods to introduce CF_3 groups into the coordination sphere of a TM.[95]

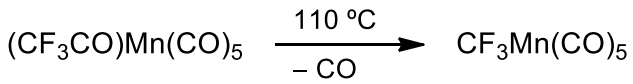

Scheme I.12. Synthesis of the first TM trifluoromethyl complex.[108-110]

More vigorous methods which also require specific equipment have been developed, but they have not found wide use.[120] Thus, direct fluorination of the corresponding methyl analogues at low temperature afforded $Hg(CF_3)_2$[121] and $W(CF_3)_6$,[122] whereby the M–C bonds are preserved (Scheme I.13). Another methodology which cannot be implemented in standard synthetic laboratories because of the expensive and complicated equipment is the use of plasma-generated $CF_3^{\bullet}$ radicals, obtained by homolytic cleavage of the CF_3–CF_3 bond caused by electric glow discharge.[120] These radicals can combine with the appropriate precursor, either element halides or element atoms, to afford the corresponding [M]–CF_3 derivative, as long as the final product is stable enough to withstand the high-energy conditions required. For example, low-temperature cocondensation of metal vapors with trifluoromethyl radicals furnished a number of unsaturated Group 10[123] and Group 11[124] trifluoromethyl derivatives, which were stabilized by PMe_3 coordination (Scheme I.14).

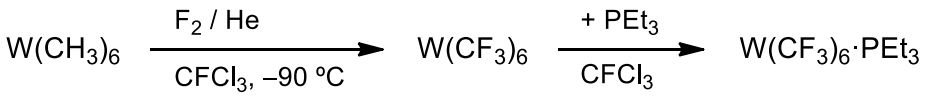

Scheme I.13. Direct fluorination of $W(CH_3)_6$ and further stabilization.[122]

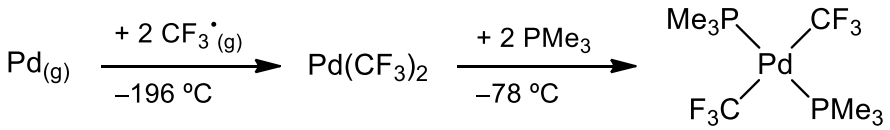

Scheme I.14. First synthesis of a TM trifluoromethyl complex by combination of metal vapors and plasma-generated $CF_3^{\bullet}$ radicals.[123]

The transformation of cyano ligands, [M]−CN, into trifluoromethyl groups, [M]−CF_3 arised as a promising method after Willner and coworkers successfully applied it for the synthesis of $[B(CF_3)_4]^-$.[125] They were able to prepare this weakly coordinating anion by fluorination of $[B(CN)_4]^-$ with ClF or ClF_3 in *a*HF. The process bears some relationship with the transformation of nitriles, RCN, into trifluoromethyl groups, RCF_3, in organic molecules, using BrF_3.[126] In TM chemistry, the synthesis of gold[68] and platinum[127] trifluoromethyl derviatives from the corresponding cyano complexes $[Au(CN)_4]^-$, $[Pt(CN)_4]^{2-}$ or $[Pt(CN)_6]^{2-}$ by reaction with ClF in *a*HF or CH_2Cl_2 was also attempted. However, unlike in the $[B(CF_3)_4]^-$ case,[125] these processes were non-selective and afforded complex reaction mixtures of trifluoromethyl derivatives from which no single species could be isolated. The lack of selectivity and the high stability requirements, together with the need for special equipment, are important drawbacks.

An interesting reagent to coordinate CF_3 groups to TM centers in low oxidation states is CF_3I.[95,107d] This reagent shows inverted $I^{\delta+}$–$C^{\delta-}$ polarity with respect to CH_3I,[128] according to the higher electronegativity of the CF_3 group with respect to iodine.[9,93] This versatile reagent, obtained by Emeléus in 1948,[129] was one of the first available trifluoromethyl precursors used to prepare TM complexes, the first examples being (η^5-C_5H_5)Co(CO)(CF_3)I[130] and $CF_3Fe(CO)_4I$ (Scheme I.15).[131] It is interesting to note that CF_3I is a source of $CF_3^{\bullet}$ radicals especially under thermal, photochemical, electrochemical or chemical activation.[132] In organotransition metal chemistry, it has been successfully applied to d^8 and d^{10} metal precursors.[95,107d]

$$Fe(CO)_5 \xrightarrow[-\,CO]{+\,CF_3I} CF_3Fe(CO)_4I$$

Scheme I.15. One of the first syntheses of a TM trifluoromethyl complex by oxidative addition of CF_3I to a low-valent derivative.[131]

Probably the most used method to prepare TM trifluoromethyl complexes has been via metathesis or transmetalation processes by using different CF_3-transfer reagents.[95,107d] To this aim, Group 12 metal compounds have been widely used. The first of these reagents to be available was $Hg(CF_3)_2$, which was initially prepared by oxidation of elemental mercury with CF_3I under thermal or photochemical activation.[133] By ligand exchange reaction of $Hg(CF_3)_2$ and $Cd(CH_3)_2$, different $Cd(CF_3)_2{\cdot}L$ adducts were isolated (L = dme, diglyme, thf or py).[134] A more convenient route was later reported using CF_3I as the trifluoromethylating agent.[135] Cadmium reagents were preferred over mercurials due to their higher reactivity. In particular, $Cd(CF_3)_2{\cdot}dme$ became the most popular reagent of this family.[95,107d] Different zinc complexes are known (e.g. $Zn(CF_3)_2$, CF_3ZnX (X = Cl, Br, I) and $Zn(CF_3)_2(py)_2$),[95] but with poorer trifluoromethylating ability than $Cd(CF_3)_2{\cdot}dme$.[107d]

Owing mainly to the toxicity of cadmium, the well-performing $Cd(CF_3)_2{\cdot}dme$ reagent has been superseded by the commercially available Ruppert–Prakash reagent, Me_3SiCF_3. This convenient and safer reactant is typically used in the presence of a hard Lewis base, usually F^-.[136] Upon coordination of the fluoride to Me_3SiCF_3 at low temperature in thf, a five-coordinate Si(IV) species is generated, $[Me_3Si(CF_3)F]^-$,[137] which can readily transfer the CF_3 group to the appropriate metal precursor (Scheme I.16). However, when a metal fluoride, hydroxide or alkoxide complex is used as precursor, no additional fluoride source is required.[95] Concomitant formation of volatile Me_3SiF occurs, which can be easily separated. This methodology, although largely known in organic synthesis,[136] was applied in organotransition metal chemistry in 1997.[138]

When Me_3SiCF_3 is used in combination with AgF as the fluoride source in a N-donor solvent, solutions of trifluoromethyl silver, "CF_3Ag", are generated, which have themselves been used as trifluoromethylating agents.[139] Some representative examples include a number of Rh,[140] Ir,[140] Ni,[141] Pd[142] or Au[143] trifluoromethyl complexes.

In these "CF_3Ag" solutions, there are equilibrium mixtures of various species, including CF_3Ag(solvent) and $[CF_3AgCF_3]^-$.[139c,144] The latter anion, $[CF_3AgCF_3]^-$, has been isolated only recently as its Cs^+, $[NBu_4]^+$ and $[PPh_4]^+$ salts by our group[105] and that of Pérez-Temprano,[142] independently.

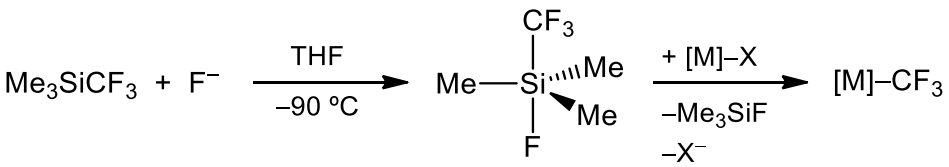

Scheme I.16. General trifluoromethylation of a TM with the Me_3SiCF_3/F^- system. The reaction proceeds via the five-coordinate intermediate shown.[137]

In addition to the nucleophilic trifluoromethylating species just described, several electrophilic trifluoromethylating reagents are also known.[145] The most popular is probably Umemoto's reagent (Figure I.4),[146] which exhibits a high stability under ambient conditions and is commercially available since year 2000.[145a] Some iodine(III) compounds have also arisen as very efficient electrophilic trifluoromethylating species, among which Togni's reagents are probably the best known (Figure I.4).[147] Both Umemoto's and Togni's reagents have been successfully used to prepare high-valent Ni(IV)[148] and Pd(IV) complexes,[149] from their corresponding M(II) precursors.

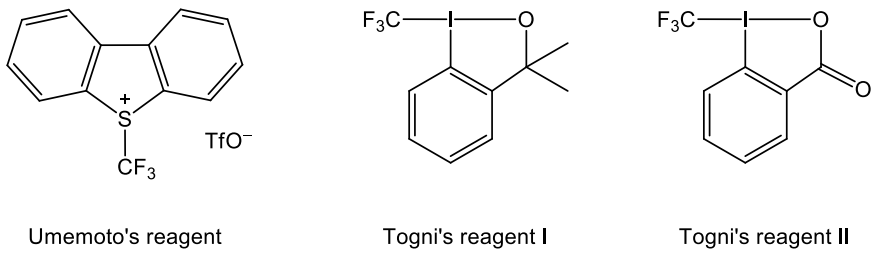

Figure I.4. Selection of electrophilic trifluoromethylating reagents.

I.4.2. Reactivity patterns of transition-metal trifluoromethyl complexes

Transition-metal trifluoromethyl complexes display an interesting reactivity which widely differs from that of their non-fluorinated analogues.[86,95,107d,e] Some of the most prominent reactivity patters include:[95]

a) Trifluoromethylation of organic molecules.
b) Formation of difluorocarbenes by C−F activation.
c) Stabilization of complexes with metals in high oxidation states and highly acidic metal fragments.

I.4.2.1. Trifluoromethylation of organic molecules

The trifluoromethyl group alters the physicochemical and/or biological properties of organic molecules, so that they frequently find interesting applications as pharmaceuticals, agrochemicals or in material science.[87h,89b,150] For this reason, many efficient and selective synthetic routes have been developed over the years to incorporate this valuable substituent to organic molecules. Among them, TM mediated or catalyzed trifluoromethylation processes have become very popular owing to the plethora of CF_3 sources and metal substrates currently available, which are actually able to promote CF_3 transfer.[86,89a,95,99,132b,136,151] Compounds containing M−CF_3 bonds are proposed to participate in these processes, but they are not always isolated or even detected. It is interesting to note that TM catalyzed and mediated C−CF_3 bond formation is challenging because of the strong M−CF_3 bonds deriving from the bonding interactions between the metal d orbitals and the C−F σ* orbitals of the CF_3 group.[97] This often results in a higher activation barrier for the C−CF_3 reductive elimination.[86,95,107d,e,152] The most suitable complexes are those containing late-TM, mainly Group 10 and Group 11 metals.

Probably the most used trifluoromethylating copper-based system has been *in-situ* generated "CF_3Cu",[86a,99,132b,136a,151b,f,h,j] which was discovered in the late 1960s,[153] yet its precise nature is still unknown.[154] However, some well-defined copper complexes have resulted useful in the transfer of CF_3 groups to organic molecules, as for instance (NHC)Cu(CF_3) species,[155] (phen)Cu(CF_3),[156] or the $[CF_3CuCF_3]^-$ anion.[157,158] In fact, the cesium salt of the $[CF_3CuCF_3]^-$ anion has been selectively prepared and isolated very recently, and its role in the trifluoromethylation of arenes has been investigated experimentally and computationally.[158]

The development of trifluoromethylation reactions by using Cu(III) complexes is very recent. Most of the studied C−CF_3 bond-formation reactions mediated of catalyzed by

copper(III) involve neutral $(CF_3)_3AuL$ complexes[159] (L = py,[160] bpy,[161] phen).[162] In some of these reactions, radical trifluoromethylation processes occur,[160,161] as it also happens with the homoleptic $[(CF_3)_4Cu]^-$, which is able to transfer $CF_3^\bullet$ radicals under photoirradiation.[106] Concerted reductive elimination processes leading to R−CF_3 from anionic $[(CF_3)_3CuR]^-$ complexes (R = alkyl, aryl) have been also reported recently (Scheme I.17).[163]

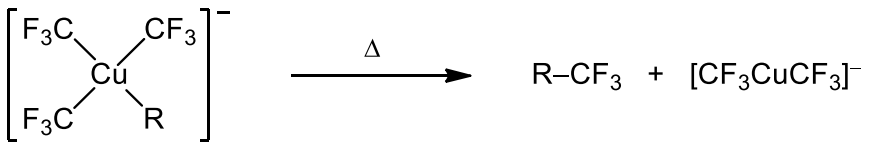

Scheme I.17. Reductive elimination R−CF_3 (R = alkyl, aryl) from Cu(III) trifluoromethyl complexes. The cation is $[NBu_4]^+$.[163]

Trifluoromethylation reactions catalyzed or mediated by palladium complexes have been thoroughly investigated.[86,95,99,151b,d,e,g-l,152] Interestingly, the reductive elimination affording the trifluoromethylated organic molecule is highly dependent on the nature of the ancillary ligands at the Pd(II) center, and particularly on their steric requirements. For example, in a series of bis(phosphino)ferrocene ligands used by Sanford and coworkers, it was found that the rate of reductive elimination increases with the size of the phosphine substituents.[164] The key role of the steric demand of the ligands has also been assessed by computational studies.[165] It has further been suggested that the changes in steric repulsions to access the transition state (TS) are actually responsible for the energy barriers of the reductive elimination of Ph−CF_3.[166]

Reductive elimination from octahedral Pd(IV) complexes also takes place under mild conditions. The Sanford group reported in 2010 the synthesis of the first Pd(IV)−CF_3 complex and described the first reductive elimination of aryl−CF_3 from a Pd(IV) center (Scheme I.18),[167] the mechanism of which was later investigated.[168] Trifluoromethylation of benzo[*h*]quinoline (Hbzq) in moderate yields was also achieved via reductive elimination from the octahedral complex $(bzq)Pd^{IV}(CF_3)(OAc)_2(OH_2)$,[149] which is generated by electrophilic trifluoromethylation of the dinuclear Pd(II) derivative $[Pd(bzq)(\mu\text{-}O_2CMe)]_2$ through an oxidation−fragmentation sequence proceeding via a Pd^{III}–Pd^{III} or Pd^{IV}←Pd^{II} intermediate.[169]

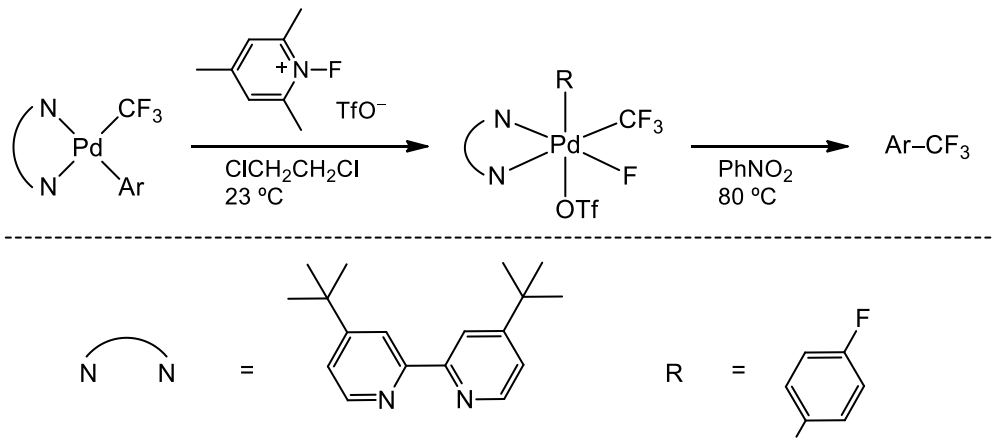

Scheme I.18. Synthesis of the first Pd(IV) trifluoromethyl complex and subsequent C(sp^2)−CF_3 bond formation.[167]

Ni-mediated trifluoromethylation of arenes has only been recently achieved. Initial studies by Vicic[170] and Grushin[171] were rather unsuccessful, and oxidatively-induced aryl−CF_3 bond formation from Ni(II) complexes was demonstrated in 2018 by Klein and van der Vlugt.[172] An in-depth study by Sanford and coworkers on the reductive elimination of Ph−CF_3 from (P^P)Ni(Ph)(CF_3) complexes when treated with ferrocinium salts showed a great dependence on the diphosphine ligand, P^P.[173] Aryl−CF_3 bond-formation processes from isolated Ni(III)[174] and Ni(IV)[148a,c] complexes containing a tris(pyrazolyl)borate scaffold have also been reported by the Sanford group. Complex $(CF_3)_2NiF_2(py)_2$, obtained by reaction of $(CF_3)_2Ni(py)_2$ with XeF_2, was the first Ni(IV) derivative to enable direct C−H trifluoromethylation of arenes.[175]

I.4.2.2. Formation of difluorocarbenes

Many TM trifluoromethyl derivatives are prone to undergo C−F bond activation. These processes are found mainly in those cases with significant fluoride negative hyperconjugation in the [M]−CF_3 unit (Scheme I.9), which leads to substantial weakening of the C−F bonds in α position.[95] Fluoride abstraction is generally promoted by Brønsted or Lewis acids whereby a metal difluorocarbene species, [M]=CF_2, is formed (Scheme I.19a).[107b,176] The stability of these [M]=CF_2 compounds significantly depends on the particular metal, its oxidation state, and on the nature of the

other coordinated ligands. Some of these [M]=CF_2 complexes are stable enough to be detected in solution and even isolated and characterized.[107b,176] However, many of them are highly reactive and readily undergo hydrolysis via nucleophilic attack by a molecule of water, whereby HF elimination affords a carbonyl complex [M]–CO (Scheme I.19b). Hence, sometimes they can only be proposed as reaction intermediates. Some of these species will be discussed next.

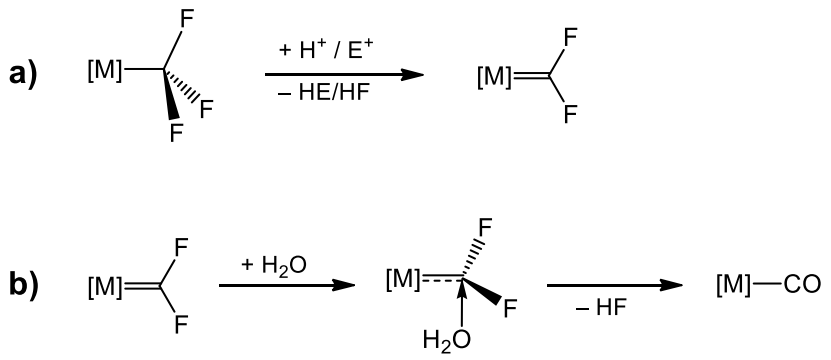

Scheme I.19. a) Formation of a metal difluorocarbene complex by attack of an electrophile (E^+) or a Brønsted acid (H^+) on a TM trifluoromethyl derivative. b) Transformation of a difluorocarbene complex to a carbonyl one via nucleophilic attack by water.[107b,176]

Most of the isolated TM difluorocarbene complexes contain early and mid-TM. In fact, the [M]=CF_2 unit seems to be particularly stable for d^6 Group 8 metals.[95] For instance, direct treatment of complex $Ru(CF_3)Cl(CO)(MeCN)(PPh_3)_2$ with dry HCl affords the difluorocarbene derivative, which is easily hydrolyzed to the carbonyl derivative (Scheme I.20).[177] Additionally, it also reacts with MeOH and Me_2NH to yield the corresponding fluorocarbene species (Scheme I.20). On the other hand, complex $RuHF(CO)L_2$ (L = P*t*Bu_2Me) reacts with Me_3SiCF_3 to directly afford a [Ru]=CF_2 species, $RuHF(CF_2)(CO)L_2$, instead of the expected [Ru]−CF_3 compound.[138,178] This is due to an α-fluorine migration from the proposed intermediate $RuH(CF_3)(CO)L_2$, the metal center of which would act as a Lewis acid. A different route to generate a difluorocarbene complex is via two-electron reduction of a metal trifluoromethyl derivative. It actually occurs by α-F elimination, as in the case of $(\eta^5\text{-}C_5Me_5)Ir^I(CF_2)(L)$ complexes (L = CO, PMe_3), which were prepared from their corresponding $(\eta^5\text{-}C_5Me_5)Ir^{III}(CF_3)I(L)$ precursors upon reaction with KC_8.[179]

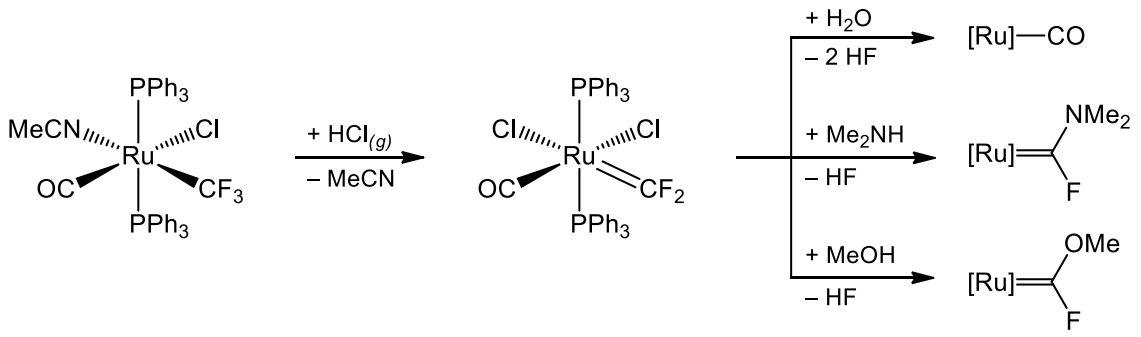

Scheme I.20. Transformation of a [Ru]−CF_3 unit into a [Ru]=CF_2 one and its subsequent reactivity towards different nucleophiles.[177]

When moving from early to late-TM, diflurocarbene complexes become more reactive and therefore more difficult to detect or even isolate. Anyway, they are usually invoked as intermediates in the fluoride-abstraction process of [M]−CF_3 derivatives.[95] For example, in the neutral complexes *cis*-$(CF_3)_2Pt(py)_2$ and *cis*-$(CF_3)_2Pt(L^\wedge L)$ (L^L = bpy, tmeda), the transformation of one CF_3 group into a CO ligand requires the action of strong acids such as aqueous HCl or $HClO_4$.[180] In the case of the homoleptic complex anion $[(CF_3)_4Pt]^{2-}$, however, the reaction occurs simply by the action of ambient moisture, whereby compound $[NBu_4][(CF_3)_3Pt(CO)]$ is formed.[181] By reaction of $[NBu_4][(CF_3)_3Pt(CO)]$ with pyridine-2-thiol in the presence of $ONMe_3$, the *gem* difluorinated $[NBu_4][(CF_3)_2Pt(CF_2NC_5H_2S\text{-}\kappa C,\kappa S)]$ derivative was isolated in good yield (Scheme I.21). This complex can be considered to contain a difluorocarbene-platinum fragment stabilized by intramolecular base coordination, which arises from C−F activation and subsequent C−N coupling (Scheme I.21). It was actually the first clear evidence of the involvement of highly reactive [Pt]=CF_2 unit along the degradation of a Pt−CF_3 bond in the presence of acids.[181]

The first Group 10 difluorocarbene complex to be isolated was the tetrahedral derivative $Ni(CF_2)(dppe)\{P(OMe)_3\}$, which was prepared by reduction of compound $Ni(CF_3)(dppe)(O_2CCF_3)$ with KC_8 in the presence of $P(OMe)_3$ (Scheme I.22).[182] Together with $Ni(CF_2)\{P(OMe)_3\}_3$, they are the only examples of formal d^{10} metal fluorocarbenes. Additionally, Ni(II) and Pd(II) difluorocarbene complexes containing the pincer ligand $\kappa P,\kappa C,\kappa P$-(2,6-($iPr_2$PO)$_2$-$C_6H_3$) were prepared in solution upon treatment of the corresponding trifluoromethyl derivative with a Lewis acid, but only the nickel species could be crystallized.[183] In the case of Group 11 metals, no

difluorocarbene complex has been isolated so far,[95] but gold difluorocarbenoid complexes have been detected for the first time recently, as will be described in the next section.

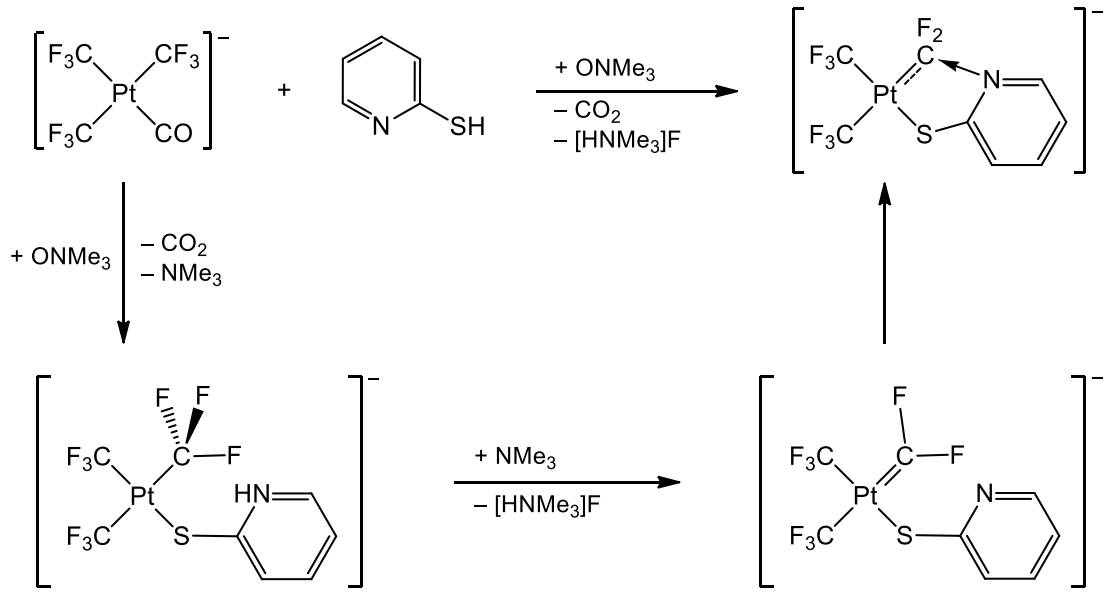

Scheme I.21. Formation of a [Pt]=CF_2 complex fragment stabilized by intramolecular base coordination (upper path) and suggested reaction mechanism (lower path). In all cases the cation is $[NBu_4]^+$.[181]

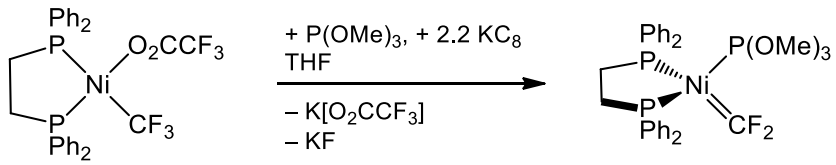

Scheme I.22. Synthesis of one of the first Group 10 metal difluorocarbene complex with d^{10} electron count. The oxidation states changes from II to 0 and the complex changes its geometry from square-planar to tetrahedral.[182]

I.4.2.3. Stabilization of high oxidation states and highly acidic metal fragments.

Trifluoromethyl ligands are especially suited to stabilize complexes of TM in high oxidation states. This is mainly due to the marked electron-withdrawing character of the CF_3 ligand, which derives from its high group electronegativity and the hardness of the

C-donor atom. This same reason makes it also appropriate to afford highly acidic organometallic "$M(CF_3)_n$" moieties.[95]

For instance, trifluoromethyl ligands are able to stabilize Cu(III) complexes,[159-163,184] among which the complex anion $[(CF_3)_4Cu]^-$ has been subject of much debate regarding its oxidation state.[102-104,106] Very few complexes are known containing silver is its highest oxidation state III.[15a,c,d] Although complexes $[PPh_4][(CF_3)_3Ag(CH_3)]$ and $[PPh_4][trans\text{-}(CF_3)_3Ag(CN)]$ have been prepared and thoroughly characterized, some other Ag(III) trifluoromehyl derivatives have only been detected by NMR spectroscopy.[185] Interesting examples of Ag(III) trifluoromethyl derivatives have been recently synthesized in our group. The homoleptic $[(CF_3)_4Ag]^-$ anion has been prepared and isolated as its $[PPh_4]^+$ salt via one-pot reaction of the organosilver(I) derivative $[CF_3AgCF_3]^-$ with $PhI(O_2CCF_3)_2$ and Me_3SiCF_3 in the presence of CsF (Scheme I.23).[105] Additionally, the first organosilver(III) fluoride complex, $[(CF_3)_3AgF]^-$, has been prepared by chlorination of $[CF_3AgCF_3]^-$, to afford $[(CF_3)_3AgCl]^-$, and subsequent treatment with AgF (Scheme I.23).[186]

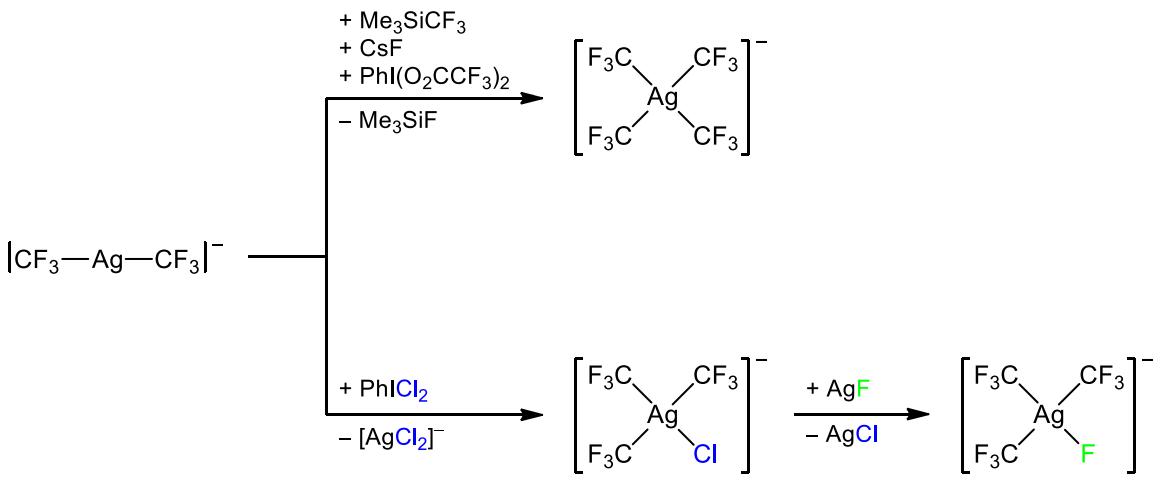

Scheme I.23. Synthesis of Ag(III) trifluoromethyl complexes reported by Joven-Sancho et al. In all cases the cation is $[PPh_4]^+$.[105,186]

A very useful strategy to access trifluoromethyl complexes in high oxidation states is by oxidative addition processes. Besides RX reagents such as CF_3I, which introduce an additional organic group, oxidative addition of halogens has also been useful in the synthesis of Group 10 metal derivatives in oxidation state IV (Figure I.5). For example,

the square-planar organoplatinum(II) compound $[NBu_4]_2[(CF_3)_4Pt]$ reacts with halogens X_2 (X = Cl, Br, I) in a stereoselective way to afford octahedral organoplatinum(IV) complexes $[NBu_4]_2[trans\text{-}(CF_3)_4PtX_2]$.[187] Additionally, reaction of the parent Pt(II) compound with $SOCl_2$ in acetone at room temperature enables to obtain the *cis* isomer of $[NBu_4]_2[(CF_3)_4PtCl_2]$.[188] This reaction proceeds through the intermediate species $[trans\text{-}(CF_3)_4PtCl(SOCl)]^{2-}$, which evolves into the complex $[NBu_4]_2[cis\text{-}(CF_3)_4PtCl_2]$, whereby the "$(CF_3)_4Pt$" unit undergoes a stereochemical rearrangement. The *cis* isomer is more reactive than the *trans* species and reacts with the equimolar amount of aqueous HCl to afford $[NBu_4]_2[fac\text{-}(CF_3)_3PtCl_3]$. However, to obtain the *mer* isomer, oxidative addition of Cl_2 to $[NBu_4]_2[(CF_3)_3PtCl]$ in CH_2Cl_2 is required.[188]

Although oxidation state IV is less common for lighter Group 10 metals, Ni(IV)[148,175,190] and Pd(IV),[148b,149,167,168,189,191] complexes can also be stabilized by coordination of CF_3 groups (Figure I.5). Many of them bear a tripodal ligand, the only exception in the case of nickel being $(CF_3)_2NiF_2(py)_2$, which is obtained by reaction of $cis\text{-}(CF_3)_2Ni(py)_2$ with XeF_2.[175]

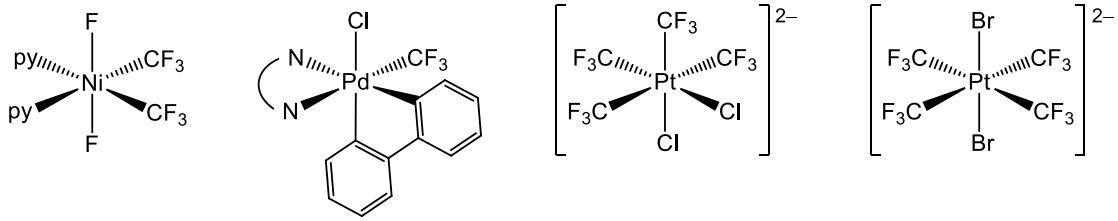

Figure I.5. Examples of Group 10 metal trifluoromethyl complexes in oxidation state IV, obtained by oxidation of suitable M(II) precursors. The cation is $[NBu_4]^+$ where appropriate.[175,187-189]

The compounds just discussed contain up to four CF_3 groups per metal atom and there are very few species containing a greater ratio. Regarding homoleptic derivatives, the Au(V) $[Au(CF_3)_6]^-$ anion has been calculated to be unstable.[60] Complexes $U(CF_3)_6$ and $W(CF_3)_6$ appear in the literature, but they are poorly characterized.[122,192] The homoleptic Pt(IV) complex $[Pt(CF_3)_6]^{2-}$ has been detected to arise in the reaction of $[Pt(CN)_6]^{2-}$ with ClF in CH_2Cl_2, but could not be isolated from the complex reaction mixture.[127] The complexes with the highest CF_3 content which have been isolated and

characterized to date are the anionic derivatives $[(CF_3)_5PtX]^{2-}$ (X = Cl, Br, I) and $[(CF_3)_5PtL]^-$ (L = CO, MeCN, py, H_2O, tht), reported by our group (Scheme I.24).[193]

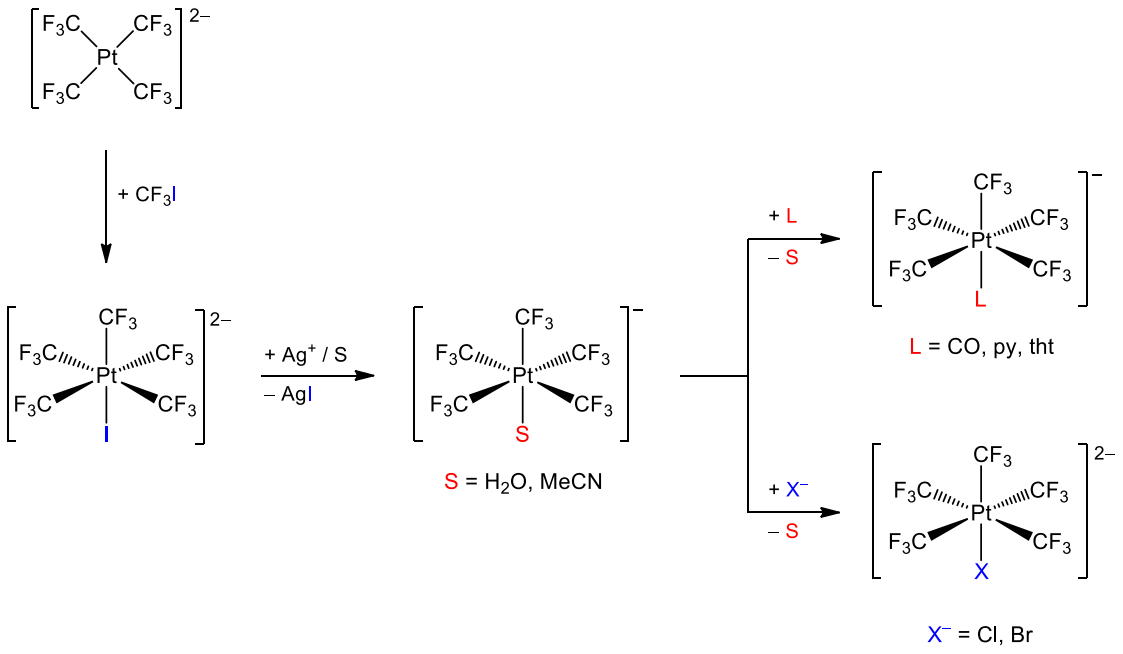

Scheme I.24. Synthetic routes to access highly trifluoromethylated Pt(IV) derivatives containing neutral and anionic ligands. In all cases the cation is $[NBu_4]^+$.[193]

An interesting evidence of the electron-withdrawing character of the CF_3 group in comparison with other related ligands is given by the homologous series of compounds $[X_3Pt(CO)]^-$ (X = CF_3, C_6F_5, C_6Cl_5, Cl, Br, I). Within this series, complex $[(CF_3)_3Pt(CO)]^-$ shows the highest ν(CO) value (Table I.1).[181a] This fact suggests that with X = CF_3, the metal center has the least electron density, and accordingly, the $(CF_3)_3Pt^-$ fragment exhibits the highest Lewis acidity. We will turn to this idea later on.

Table I.1. Vibrational frequency ν(CO) of the Pt(II) monocarbonyl $Q[X_3Pt(CO)]$ compounds (Q^+ being a cation).[a]

X	ν(CO) [cm^{-1}][b]
CF_3	2117
C_6F_5	2084
C_6Cl_5	2073
Cl	2098
Br	2089
I	2075

[a] Adapted from Table 1 in Ref. [181a]. [b] IR spectra were registered in CH_2Cl_2 solution.

I.5. Gold trifluoromethyl complexes

Whereas the first gold methyl complexes were prepared in 1939,[194] the first gold trifluoromethyl complexes were not reported until 1973 by Johnson and Puddephatt.[195] The chemistry of gold trifluoromethyl complexes has experienced a significant development ever since because of the interesting reactivity, properties and applications of these compounds.[20] This is in contrast with the few higher perfluoroalkyls currently known. In fact, only $(C_2F_5)Au(PEt_3)$ had been detected prior to the beginning of this Thesis but it was not isolated.[196] However, a set of Au(I) and Au(III) complexes containing primary and secondary perfluoroalkyl ligands has been isolated and characterized recently.[197] On the other hand, it has to be noted that the chemistry of gold with fluoroaryl ligands was largely developed in our Department over the years by R. Usón, A. Laguna, M. Laguna, and their coworkers.[198]

Gold trifluoromethyl derivatives are more stable than their non-fluorinated analogues, as it occurs with other TM trifluoromethyl complexes. An interesting example which clearly evidences this fact is the comparison between the pairs of homoleptic complex anions $[CF_3AuCF_3]^-$ / $[CH_3AuCH_3]^-$ and $[(CF_3)_4Au]^-$ / $[(CH_3)_4Au]^-$. Whereas the $[PPh_4][(CF_3)_xAu]$ salts start to decompose at 275 ºC (x = 2) and 370 ºC (x = 4), respectively,[199] their non-fluorinated analogues $[Li(pmdta)][(CH_3)_xAu]$ (x = 2, 4) readily decompose at 140 ºC.[200] This difference can be attributed to stronger $Au{-}CF_3$ bonds compared to $Au{-}CH_3$ ones, which becomes clear from the corresponding Au−C distances. Taking the same couples of compounds, it can be observed that for both of them, $Au{-}CF_3$ bonds are shorter than $Au{-}CH_3$ ones (Table I.2).[199,201] Additionally, when comparing the $Au{-}CF_3$ bond length between the species in the two oxidation states I and III, it is observed that they are longer in the Au(III) derivatives, whereas the C−F bonds are shorter (132(1) pm av.) than in the Au(I) species (137.8(3) pm av.). A rehybridization of the orbitals involved in the Au−C and C−F bonds when changing the coordination number and the oxidation state of the gold center may account for this difference, the 2s character of the C atom decreasing in the Au(III)−C orbital whereas it increases in the C−F orbitals.[20]

Table I.2. Au−C bond distances in the homoleptic Au(I) and Au(III) methyl and trifluoromethyl complexes.

	***d*(Au−C) [pm, av.]**	
	X = H[201]	**X = F[199]**
$Q[(CX_3)_2Au]$	207.5(6) (Q = $[NBu_4]^+$)	203.3(2) (Q = $[PPh_4]^+$)
$Q[(CX_3)_4Au]$	210.0(4) (Q = $[NMe_2(CH_2Ph)_2]^+$)	208.0(7) (Q = $[NBu_4]^+$)

Gold complexes containing CF_3 ligands can be prepared by using the wide variety of synthetic methods currently available for the generation of M−CF_3 bonds (see previous section). Most of the Au(I) complexes have been prepared by using Me_3SiCF_3 as the trifluoromethylating reagent in the presence of a fluoride source, whereas Au(III) derivatives have been mainly synthesized by oxidative addition reactions, either of halogens, X_2, or alkyl halides, RX.[20]

Many neutral gold(I) trifluoromethyl complexes CF_3AuL are known.[20] For example, a series of complexes where L is a phosphine or a fluorophosphine was obtained by treatment of the chloride derivative AuClL with $Cd(CF_3)_2$·dme (Scheme I.25a).[196,202] Similarly, Puddephatt and coworkers prepared complex $CF_3Au(CNMe)$ and used it for the preparation of gold films by chemical vapor deposition.[203] The less toxic reagent Me_3SiCF_3 has enabled to prepare trifluoromethyl complexes starting from AuL(OR) complexes (L = phosphine; R = $CH(CF_3)_2$, Ph; Scheme I.25b).[204] The combination of Me_3SiCF_3 with AgF in a N-donor solvent, whereby "CF_3Ag" is formed, enabled to prepare gold(I) complexes containing different phosphine, phosphite, isocyanide and NHC ligands, starting from the corresponding choro or iodo derivarives (Scheme I.25c).[143] By reaction of $[N(PPh_3)_2][AuCl(C_6F_5)]$ with "CF_3Ag", a mixture of $[(CF_3)_xAu(C_6F_5)_{2-x}]^-$ anions (x = 0, 1, 2) was obtained, together with minor amounts of $[CF_3AgCF_3]^-$.[143] From this mixture, single crystals of $[N(PPh_3)_2][CF_3Au(C_6F_5)]$ were obtained and studied by X-ray diffraction.

Although collision-induced dissociation of the $[Au(O_2CCF_3)_2]^-$ anion enabled the detection in the gas phase of complex anions $[CF_3Au(O_2CCF_3)]^-$ and $[CF_3AuF]^-$,[42] complex $[CF_3AuCF_3]^-$ was the first anionic gold(I) trifluoromethyl derivative which was prepared in practical amounts. It is synthesized by reaction of AuCl or AuCl(tht) and Me_3SiCF_3 in the presence of F^-, as reported by Tyrra[205] and our own group,[199] independently (Scheme I.26a). When $AuCl_3$ is used as the starting material, a mixture of the Au(I) and the Au(III) homoleptic species is obtained, which can be successfully

separated using $[PPh_4]^+$ as the cation (Scheme I.26b).[199] Different salts of the $[CF_3AuCF_3]^-$ anion are known, containing cations such as $[PPh_4]^+$,[199] $[NMe_4]^+$,[205] $[N(PPh_3)_2]^+$,[205] $[K(18\text{-crown-}6)]^+$,[205] $[Ag(py)_2]^+$,[206] $[Au\{(F_3CC_6H_4)_3P\}_2]^+$,[207] or simply Cs^+.[158] The salt $[NMe_4][CF_3AuCF_3]$ was found to generate monodisperse gold nanoparticles by hydrolytic decomposition.[205] This process was suggested to proceed via α-F bond activation, whereby a short-lived CF_3AuCO species was formed, which decomposed further.

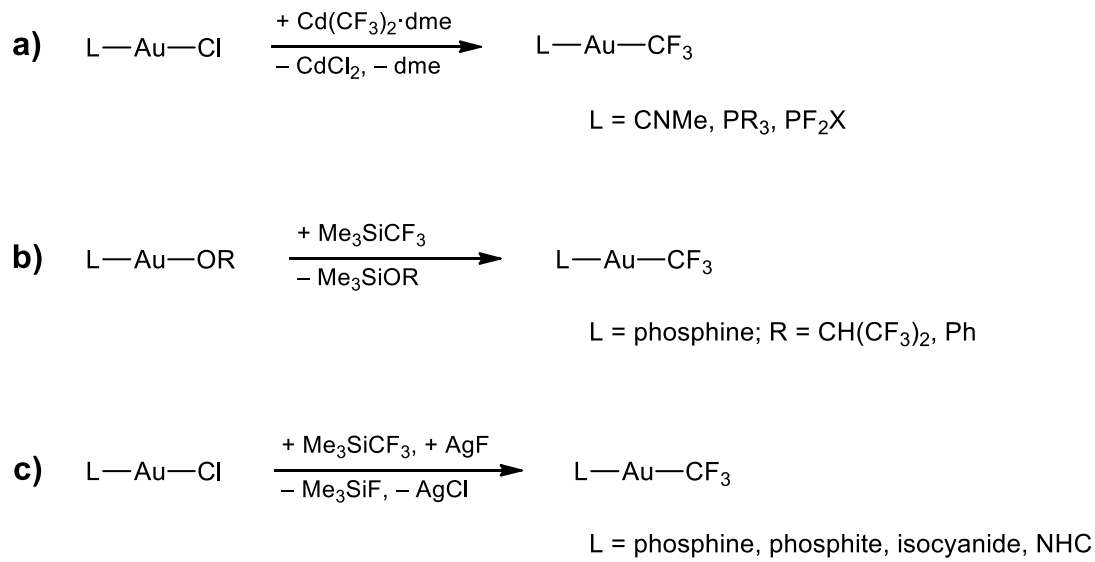

Scheme I.25. Synthesis of neutral Au(I) trifluoromethyl complexes via transmetalation.[143,196,202-204]

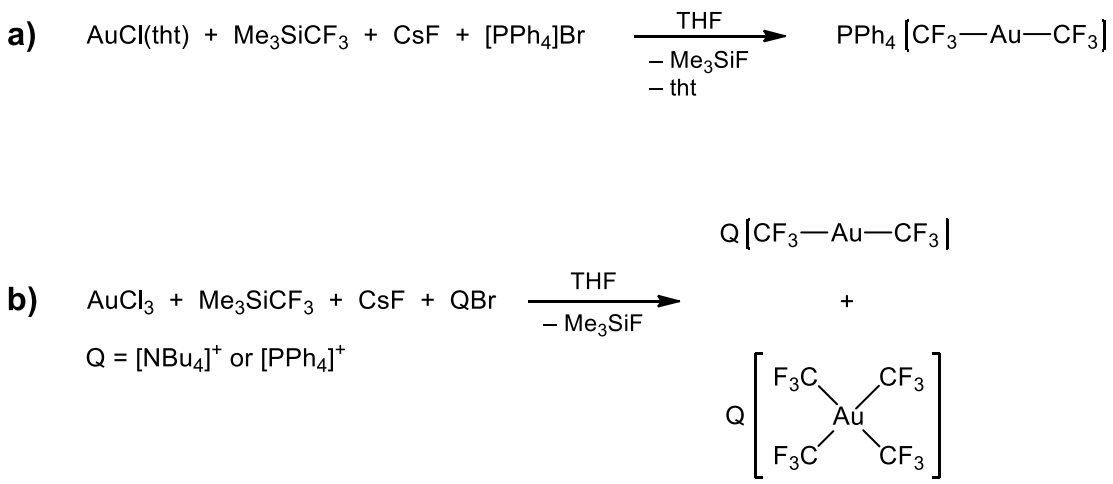

Scheme I.26. Synthesis of the homoleptic $[CF_3AuCF_3]^-$ and $[(CF_3)_4Au]^-$ anions.[199]

The gold(I) carbonyl derivative CF_3AuCO could be prepared by low-temperature reaction of $[PPh_4][CF_3AuCF_3]$ and $BF_3{\cdot}OEt_2$ in CH_2Cl_2, as later reported by our group (Scheme I.27a).[199,208] This compound is highly moisture-sensitive, rapidly decomposing to Au^0 in the presence of water. However, under rigorously anhydrous conditions it could be crystallized and studied by single-crystal X-ray diffraction. Additionally, it is worth noting the high *ν*(CO) vibration in the solid state for CF_3AuCO (2194 cm^{-1}) within the homologous series of neutral XAuCO compounds shown in Table I.3,[199,208] which denotes the significant electron-withdrawing character of the CF_3 group in comparison with other related ligands.

Table I.3. Vibrational frequency *ν*(CO) of the Au(I) neutral monocarbonyl XAuCO compounds.[a]

X	*ν*(CO) [cm^{-1}][b]
CF_3	2194 (solid)
	2180 (CH_2Cl_2)
Cl	2162 (CH_2Cl_2)
OSO_2F	2195 (solid)
$BH(pz^*)_3$[c]	2144 (solid)
	2125 (cyclohexane)

[a] Adapted from Table 1 in Ref. [199]. [b] Experimental details are given for each compound. [c] pz* = 3,5-bis(trifluoromethyl)pyrazolyl.

The CO ligand is highly labile, being readily substituted at 0 ºC by neutral ligands to afford complexes CF_3AuL (L = *t*BuNC, MeCN, py, tht),[199] and by Br^-, whereby complex $[CF_3AuBr]^-$ is formed (Scheme I.27b).[209] Complex CF_3AuCO can thus be considered as a convenient synthon of the "CF_3Au" fragment.[199] Its formation might proceed through a difluorocarbene intermediate, which could not be detected, probably due to fast hydrolysis occurring even at −80 ºC.[199,208] The transient CF_3AuCF_2 species could be possibly stabilized by Et_2O coordination before evolving to the final carbonyl product. Interestingly, related gold(I) difluorocarbenoid species R_3PAuCF_2X were detected recently, but could not be isolated.[207] In fact, these gold difluorocarbene complexes are so deprived of electron density, that they bind even weakly coordinating anions such as triflate or triflimide (X = OTf, NTf_2). These compounds were characterized at −50 ºC by NMR spectroscopy, since they rapidly decompose above that temperature (Scheme I.28).

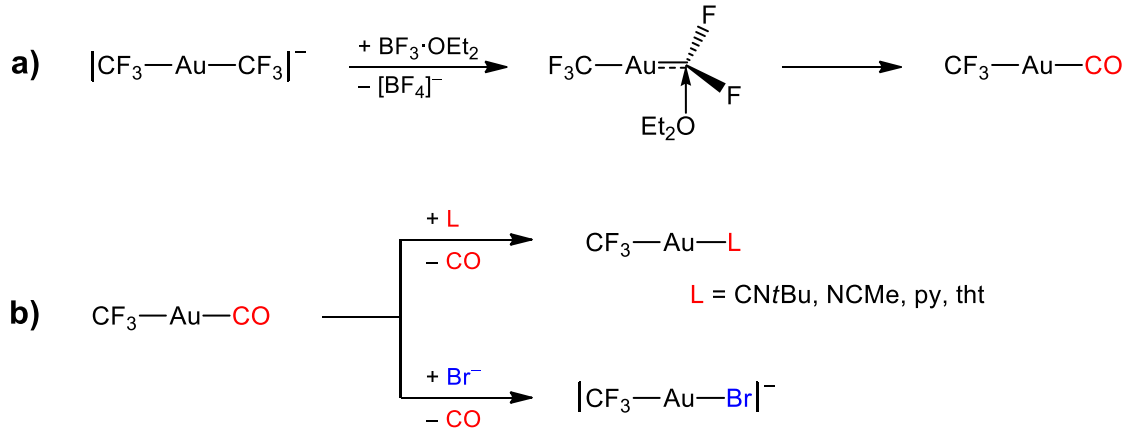

Scheme I.27. a) Suggested reaction path for the synthesis of CF_3AuCO.[199,208] b) Synthesis of neutral and anionic Au(I) trifluoromethyl complexes by substitution of the highly labile CO ligand in CF_3AuCO. In all cases the cation is $[PPh_4]^+$.[199,209]

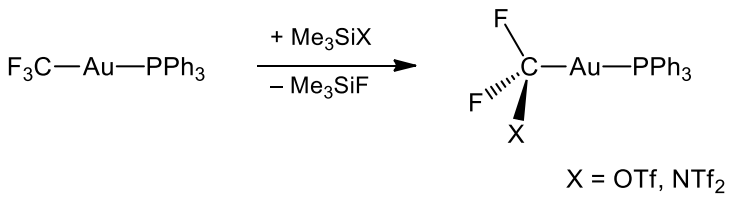

Scheme I.28. Generation of neutral gold(I) difluorocarbenoid complexes in CH_2Cl_2. They were detected at −50 ºC by NMR spectroscopy. In the case of the triflate anion, other phosphines have also been used.[207]

The salt $[Ag(py)_2][CF_3AuCF_3]$ is useful to prepare the dinuclear Au(II) species $(CF_3)_4Au_2(py)_2$, which is obtained upon UV irradiation (λ = 352 nm) of a $CDCl_3$ or CD_3CN solution of this precursor (Figure I.6).[206] It contains a very short unsupported Au(II)−Au(II) bond (250.62(9) pm) which is of covalent nature, as shown by DFT calculations.[210] The compound was characterized in the solid state, but no data could be obtained in solution, as it disproportionates into a mixture of $CF_3Au(py)$ and $(CF_3)_3Au(py)$.[210] Only another dinuclear Au(II) complex is currently known, which contains two bridging bis(ylide) ligands (Figure I.6).[211] This compound, $(CF_3)_2Au_2\{\mu\text{-}Ph_2P(CH_2)_2\}_2$, in which the CF_3 ligands are found in the Au(II)−Au(II) axis, was prepared by exchange reaction of the axial chloride ligands in $AuCl_2\{\mu\text{-}Ph_2P(CH_2)_2\}_2$ with $Cd(CF_3)_2\cdot dme$.[211]

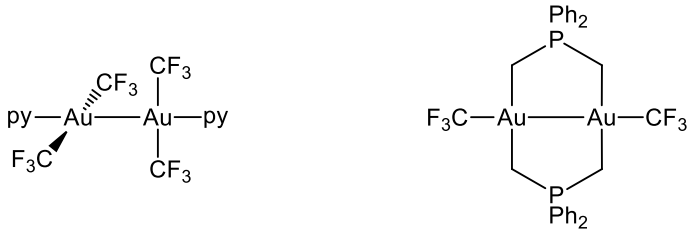

Figure I.6. The only two Au(II) trifluoromethyl complexes isolated to date.[206, 211]

Compound $[PPh_4][CF_3AuCF_3]$ is also oxidized by halogens X_2 to render the oxidative addition products, $[PPh_4][trans\text{-}(CF_3)_2AuX_2]$ (X = Cl, Br, I), as shown in Scheme I.29a.[199] Analogous halogenation reactions have been useful to access neutral trifluoromethyl gold(III) derivatives (Scheme I.29b). One interesting example is that of complex $CF_3Au(IDipp)$, which also reacts with halogens and ICl to afford the *trans* Au(III) complexes.[143] These Au(III) derivatives were isolated in high yield except in the case of *trans*-$CF_3Au(IDipp)I_2$, which is unstable and rapidly eliminates CF_3I even at low temperature. However, upon UV irradiation, CF_3X is reductively eliminated from *trans*-$CF_3Au(IDipp)X_2$ (X = Cl, Br; Scheme I.29b).[143]

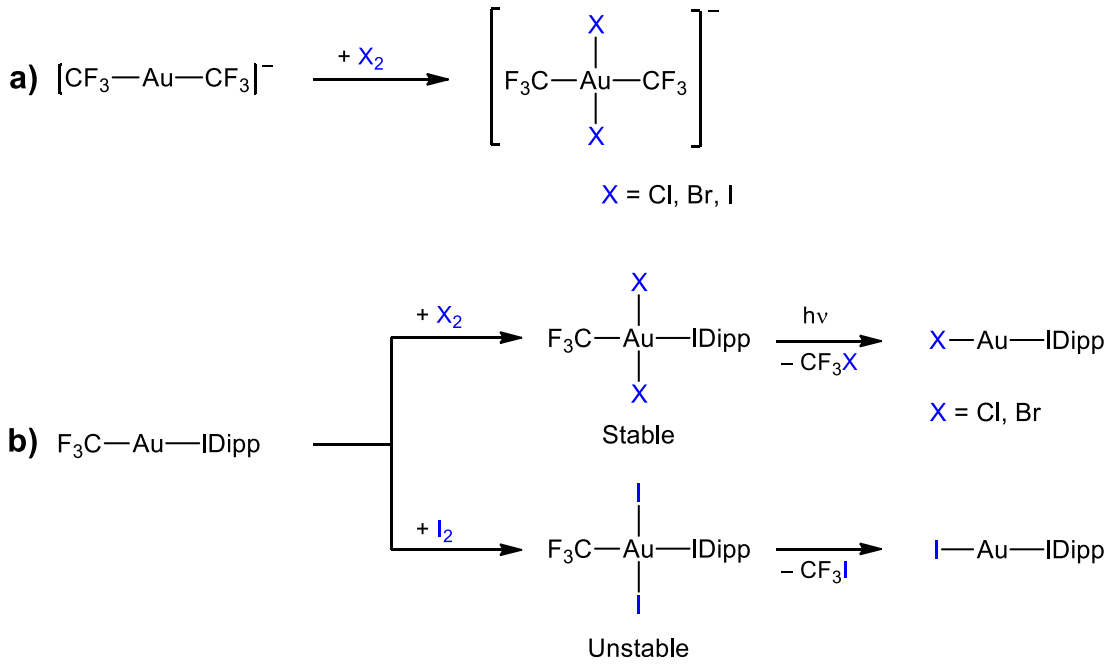

Scheme I.29. Oxidative addition of halogens X_2 to: a) Anionic Au(I) trifluoromethyl species. In all cases the cation is $[PPh_4]^+$.[199] b) Neutral Au(I) trifluoromethyl compounds and subsequent thermal or photochemical reductive eliminations. Cl_2 was used in the form of $PhICl_2$. Complex *trans*-$CF_3Au(IDipp)I_2$ is unstable and was detected but not isolated.[143]

Another method that has been widely used to access Au(III) trifluoromethyl complexes is via oxidative addition of CF_3I. In fact, it was already used to prepare the first gold trifluoromethyl derivatives.[195,212] They were isolated upon reaction of CH_3AuL (L = phosphine) with CF_3I, the product depending on the precise phosphine ligand. When L = PMe_3, PMe_2Ph, mixtures of the *cis* and *trans* isomers of the Au(III) complexes $CF_3Au(CH_3)_2L$ were obtained (Scheme I.30), which were dependent on the solvent. From these mixtures, only the *trans* isomers were isolated. The stoichiometry of the obtained products requires that the reaction proceeds via a two-step process: 1) oxidative addition of CF_3I to the Au(I) compound to give a $CF_3Au(CH_3)IL$ intermediate, and 2) subsequent CH_3 for I exchange effected by still unreacted Au(I) complex. However, for L = PPh_3, the Au(I) species $CF_3Au(PPh_3)$ was the only isolated product (Scheme I.30), probably formed by the reductive elimination of CH_3I from the putative intermediate $CF_3Au(CH_3)I(PPh_3)$, which was not detected. In the case of L = $PMePh_2$, a mixture of the Au(I) and Au(III) species was obtained (Scheme I.30). Similar results as in the case of the PPh_3 derivative were later obtained when carrying out analogous reactions starting from $\{CH(SiMe_3)_2\}Au(PPh_3)$[213] and $CH_3Au(PCy_3)$,[214] the latter leading to $CF_3Au(PCy_3)$ only upon irradiation of the mixture with ambient light.

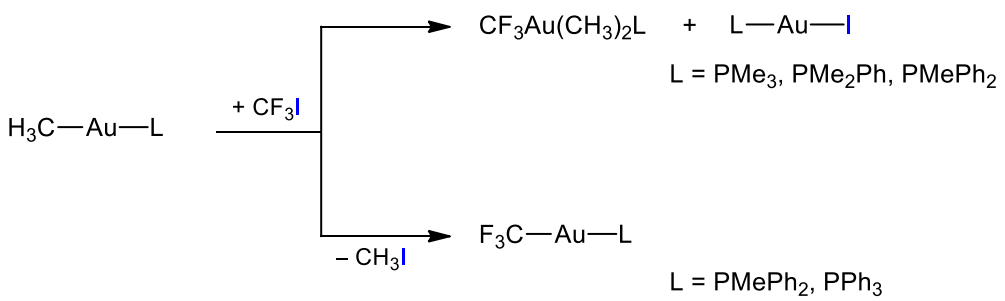

Scheme I.30. Oxidative addition of CF_3I to different Au(I) methyl complexes. The observed reaction products depend on the precise phosphine ligand.[195,212]

Oxidative addition of CF_3I to $CF_3Au(PR_3)$ complexes (R = Me, Et) gave mixtures of the *cis* and *trans* isomers of $(CF_3)_2AuI(PR_3)$, the *cis* one being the major product.[196,202b] These compounds undergo ligand-exchange processes with the starting gold(I) material to give mixtures of $(CF_3)_3Au(PR_3)$ and $AuI(PR_3)$.[196] Compound $(CF_3)_3Au(PMe_3)$ was actually prepared from $(CF_3)_2AuI(PMe_3)$ via a transmetalation reaction with

$Cd(CF_3)_2 \cdot dme$ in a CF_3I atmosphere to prevent reductive elimination of this molecule from the parent species.[202b]

A radical pathway was initially suggested to operate in the aforementioned oxidative addition processes of CF_3I, since the reactions were inhibited in the presence of a radical scavenger.[196,202b,212] This proposal was recently confirmed by Toste, who thoroughly studied the mechanism of the oxidative addition of CF_3I to phosphine aryl Au(I) complexes under near-UV light.[214] The reaction was found to proceed via a photoinitiated radical chain mechanism (Scheme I.31). First, a photoexcited molecule $[CF_3I]^*$ would oxidize the Au(I) precursor while generating the radical anion $[CF_3I]^{\bullet-}$. Homolytic cleavage of the C−I bond of $[CF_3I]^{\bullet-}$ would generate I^- and $CF_3^\bullet$ radicals, able to oxidize the Au(I) species to a three-coordinate Au(II) intermediate. The latter molecule would abstract an iodine atom from CF_3I, whereby the $CF_3^\bullet$ radicals are regenerated.

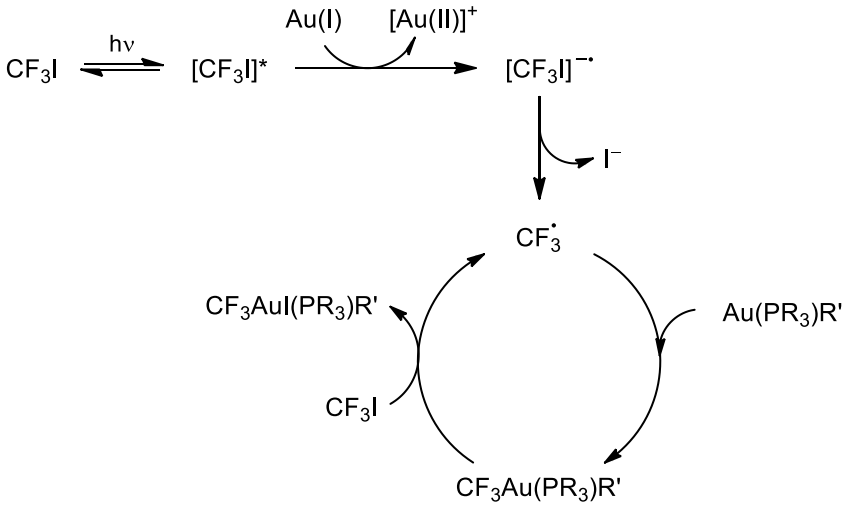

Scheme I.31. Proposed radical chain mechanism for the photoinitiated oxidative addition of CF_3I to Au(I) complexes. PR_3 = phosphine; R′ = aryl.[214]

Other varied methods have been used to prepare $[Au]-CF_3$ compounds, but have been exploited to a lesser extent because of the need of special requirements or being of little synthetic use.[20] For example, the naked compound $(CF_3)_3Au$ was apparently isolated in a matrix as an unstable species from the gas-phase reaction of Au atoms and $CF_3^\bullet$ radicals, and further stabilized upon coordination of PMe_3 to afford complex $(CF_3)_3Au(PMe_3)$.[124] Dinuclear complexes $[(CF_3)_2Au(\mu\text{-}X)]_2$ (X = Br, I) have been

similarly prepared by vapor cocondensation of gold atoms and CF_3X.[215] On the other hand, the reaction between $[NBu_4][Au(CN)_4]$ and ClF in CH_2Cl_2 afforded a mixture of species of stoichiometry $[(CF_3)_{4-x-y}AuCl_xF_y]^-$ (x = 0–2, y = 0–4), the main components being $[(CF_3)_3AuF]^-$, $[(CF_3)_4Au]^-$ and [*trans*-$(CF_3)_2AuFCl]^-$.[68] These species were perfectly characterized by NMR spectroscopy, but no compound could be isolated.

Among the anions just mentioned, the homoleptic $[(CF_3)_4Au]^-$ is of especial interest, since the delocalization of its negative charge over 12 fluorine atoms makes it an unusual weakly coordinating anion with a flat shape, according to computational calculations performed by Preiss and Krossing.[216] In fact, it has been used for the preparation of superconducting organic materials.[217] The synthesis of the first simple salt of the homoleptic $[(CF_3)_4Au]^-$ anion was described in our group by reaction of $AuCl_3$ and Me_3SiCF_3 in the presence of CsF (Scheme I.26b).[199] It could be isolated with $[PPh_4]^+$ as the counterion, after separation from the $[CF_3AuCF_3]^-$ anion, which arises from the partial reduction of the starting material during the reaction. This anion is highly stable and does not react with Lewis acids such as $BF_3{\cdot}OEt_2$ or Me_3SiOTf in CH_2Cl_2.[199] However, the neutral difluorocarbene complex $(CF_3)_3Au(CF_2)$ seems to be experimentally feasible.[216] In the gas phase, the $[(CF_3)_4Au]^-$ anion undergoes CF_2 extrusion, giving rise to $[(CF_3)_3AuF]^-$.[106] The synthesis and study of this organogold(III) fluoride complex is part of this Thesis (see Chapter 3). Additionally, $[(CF_3)_4Au]^-$ formally eliminates C_2F_6, whereby the $[CF_3AuCF_3]^-$ anion is formed. The calculated energy for the homolytic dissociation of a Au–CF_3 in the Au(III) homoleptic complex (ΔG^o = 197.5 kJ mol^{-1}) is considerably higher than that of the lighter Group 11 metals Cu (ΔG^o = 120.9 kJ mol^{-1}) and Ag (ΔG^o = 132.2 kJ mol^{-1}). These calculations were also confirmed by the experimental evaluation of the strength of the Au–CF_3 bond by energy-resolved mass spectrometry (ERMS).[106] Unlike the Cu and Ag analogues, the ability of $[(CF_3)_4Au]^-$ to transfer $CF_3^{\bullet}$ radicals to arenes upon UV photoirradiation is almost negligible, according to the higher stability of the Au−CF_3 bond.[106]

A number of studies were actually undertaken on the potential activity of some Au(III) trifluoromethyl complexes as trifluoromethylating agents, especially in the last years. As discussed in the previous section, reductive elimination of C_{aryl}–CF_3 remains a challenging step due to the strong M−CF_3 bonds. In fact, complexes $CF_3Au(aryl)I(PR_3)$ undergo C_{aryl}–I reductive elimination rather than C_{aryl}–CF_3 bond formation when heated at 110 ºC in toluene-d_8. However, upon treatment of the complexes with $AgSbF_6$, C_{aryl}–

CF_3 reductive elimination occurs in less than 1 min (Scheme I.32a).[214] A subsequent study on this system showed that the selectivity of the reductive elimination depends on the halide ligand (Scheme I.32b).[74] In the case of the fluoride derivative within the halide series $CF_3Au(4\text{-}Me\text{-}C_6H_4)(PPh_3)X$, only reductive elimination of C_{aryl}–CF_3 takes place. This process becomes less important when going down the halogen group and is actually absent in the case of the iodide derivative, for which only C_{aryl}–I is observed. The mechanism of the reductive elimination was later studied computationally and the key role of the halide ligand was confirmed,[218] again pointing out the large differences between fluoride and its heavier homologues. In addition, it was found both experimentally and theoretically that dissociation of the phosphine was the initial step prior to reductive elimination from a three-coordinate species.[214,218]

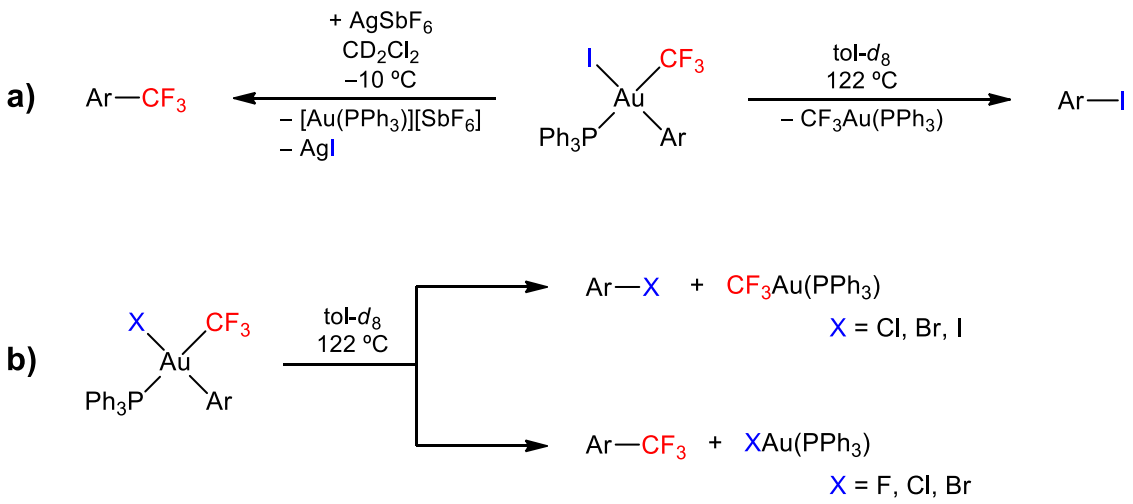

Scheme I.32. a) Divergent reductive elimination from Au(III) complexes.[214] b) Halide-dependent reductive elimination from Au(III) complexes. The selectivity for C_{aryl}–CF_3 bond formation increases in the order X = I < Br < Cl < F, being inexistent when X = I and exclusive when X = F (Ar = aryl).[74]

The particular behavior of CF_3 ligands in this kind of processes significantly differs from that of their closely related CHF_2. In a recent study, C_{aryl}–CHF_2 bond formation from $(CHF_2)AuCl(4\text{-}F\text{-}C_6H_4)$ (PCy_3) was found to be much faster than that of its trifluoromethyl analogue, $CF_3AuCl(4\text{-}F\text{-}C_6H_4)(PCy_3)$.[219] In particular, reductive elimination of C_{aryl}–CHF_2 takes place with full conversion and quantitative formation of the product at 115 ºC after 80 min in CCl_4, whereas C_{aryl}–CF_3 only occurs at 150 ºC

after 6 h with 90% of conversion and only generates the trifluoromethylated arene in 34% yield. Additionally, the mechanism is completely different: unlike the phosphine dissociation pathway proposed for the [Au]–CF_3 derivatives,[214,218] a concerted C–C reductive elimination pathway through a three-membered-ring TS seems to be preferred for the CHF_2 analogues.

C_{aryl}–CF_3 coupling has also been achieved at gold centers through a photoinitiated process via a chain radical mechanism.[220] In particular, an aryl radical, which is generated upon reaction of an aryldiazonium salt with the photoredox catalyst $[Ru(bpy)_3][PF_6]_2$, is added to the Au(I) complex to generate a Au(II) intermediate. In turn, this intermediate is oxidized to a Au(III) cation species from which reductive elimination takes place.

Finally, a very interesting mechanism was found for the formal C(sp^3)–CF_3 reductive elimination from gold(III) centers. The reaction does not consist in a real reductive elimination, but it involves the cleavage and reassembly of a CF_3 group catalyzed by $B(C_6F_5)_3$ through a series of three steps, including a fluoride abstraction, a migratory insertion and a C–F reductive elimination.[221] In fact, the authors themselves already referred to it as a “fluoride-rebound mechanism”. This methodology enabled the preparation of highly-functionalized organic derivatives and pharmaceuticals, as well as ^{18}F-labeled CF_3-containing compounds which can be promising as radiotracers for positron emission tomography.

I.6. Thematic focus and Thesis structure

This Doctoral Thesis is placed within the previously explained context of Inorganic and Organometallic Chemistry and, in particular, it deals with organogold complexes, gold fluorides and gold trifluoromethyl derivatives. It covers the synthesis and characterization of organogold complexes containing different number of CF_3 ligands. The fundamental behavior of many of these compounds in the gas phase has been studied by tandem mass spectrometry and the observed results have been rationalized with the aid of quantum-chemical calculations. Our results are divided into three different chapters.

Chapter 1. *Monotrifluoromethyl Gold Complexes as Precursors of Highly Unstable Species*

This chapter focuses on the synthesis and characterization of complexes with $[PPh_4][CF_3AuX_n]$ stoichiometry (X = Cl, Br, I; n = 1, 3). Their study by tandem mass spectrometry enabled us to detect highly unstable species which were previously unknown (see Scheme I.33). Results corresponding to this Chapter include:

a) The detection of the mixed gold(I) fluorohalides $[F{-}Au{-}X]^-$ (X = Cl, Br, I), obtained via CF_2 extrusion from the parent $[CF_3AuX]^-$ anions.
b) The detection of gold(II) trihalides $[AuX_3]^-$ (X = Cl, Br), which arise from the unexpected homolytic splitting of the only Au−C bond in the organogold(III) $[CF_3AuX_3]^-$ anions.

These results are included in the following two peer-reviewed articles:

M. Baya, A. Pérez-Bitrián, S. Martínez-Salvador, J. M. Casas, B. Menjón, J. Orduna. Gold(I) Fluorohalides: Theory and Experiment. *Chem. Eur. J.* **2017**, *23*, 1512−1515. DOI: 10.1002/chem.201605655.

M. Baya, A. Pérez-Bitrián, S. Martínez-Salvador, A. Martín, J. M. Casas, B. Menjón, J. Orduna. Gold(II) Trihalide Complexes from Organogold(III) Precursors. *Chem. Eur. J.* **2018**, *24*, 1514−1517. DOI: 10.1002/chem.201705509.

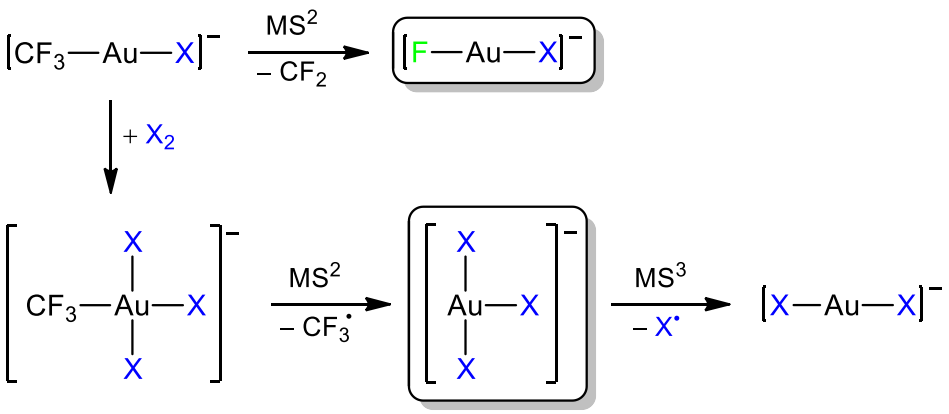

Scheme I.33. Schematic overview of Chapter 1.

Chapter 2. *An Organogold(III) Difluoride with a* trans *Arrangement*

This Chapter is dedicated to the synthesis, characterization and study of the first organogold(III) difluoride with a *trans* stereochemistry, $[PPh_4][trans\text{-}(CF_3)_2AuF_2]$ (see Scheme I.34). Additionally, its properties in the gas phase were investigated and further unstable organogold fluoride anions were detected. Initial studies on its reactivity are also presented.

These results are included in the following peer-reviewed article:

A. Pérez-Bitrián, M. Baya, J. M. Casas, A. Martín, B. Menjón, J. Orduna. An Organogold(III) Difluoride with a *trans* Arrangement. *Angew. Chem. Int. Ed.* **2018**, *57*, 6517–6521. DOI: 10.1002/anie.201802379. *Angew. Chem.* **2018**, *130*, 6627–6631. DOI: 10.1002/ange.201802379.

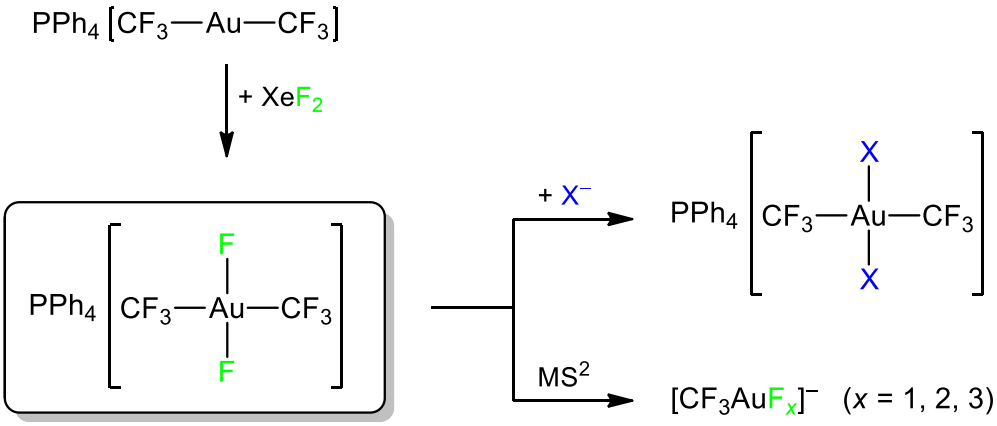

Scheme I.34. Schematic overview of Chapter 2.

Chapter 3. *Anionic and Neutral Derivatives of the Highly Acidic $(CF_3)_3Au$ Unit*

In this Chapter, an efficient synthetic access to the $(CF_3)_3Au$ fragment is described and its chemistry is investigated. With this aim, several anionic and neutral derivatives containing this unit have been synthesized, including the perfluorinated analogue of trimethyl gold, $(CF_3)_3Au{\cdot}OEt_2$, which serves as a convenient synthon of the $(CF_3)_3Au$ moiety (Scheme I.35). The properties of this unsaturated fragment are analyzed and compared to those of its non-fluorinated analogue $(CH_3)_3Au$. Finally, the decomposition

of the anionic derivatives is investigated in the gas phase (unimolecular) by tandem mass spectrometry, as well as in the condensed phase (bulk matter).

Results corresponding to this section are included in the following peer-reviewed papers:

A. Pérez-Bitrián, S. Martínez-Salvador, M. Baya, J. M. Casas, A. Martín, B. Menjón, J. Orduna. Anionic Derivatives of Perfluorinated Trimethylgold. *Chem. Eur. J.* **2017**, *23*, 6919–6929. DOI: 10.1002/chem.201700927.

A. Pérez-Bitrián, M. Baya, J. M. Casas, L. R. Falvello, A. Martín, B. Menjón. $(CF_3)_3Au$ as a Highly Acidic Organogold(III) Fragment. *Chem. Eur. J.* **2017**, *23*, 14918–14930. DOI: 10.1002/chem.201703352.

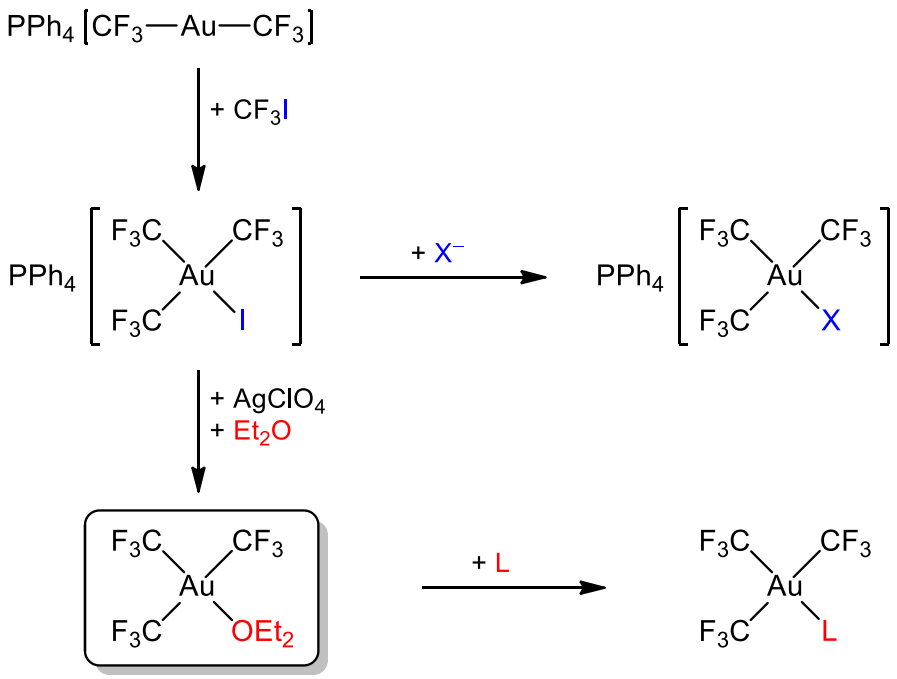

Scheme I.35. Schematic overview of Chapter 3.

I.7. References

[1] a) C. Corti, R. Holliday (Eds.), *Gold: Science and Applications*, CRC Press, Boca Raton (FL), **2010**; b) H. Schmidbaur (Ed.), *Gold: Progress in Chemistry, Biochemistry and Technology*, John Wiley & Sons, Chichester, **1999**; c) R. J. Puddephatt, *The Chemistry of Gold*, Elsevier, Amsterdam, **1978**.

[2] a) M. C. Gimeno, in *Modern Supramolecular Gold Chemistry: Gold-Metal Interactions and Applications* (Ed.: A. Laguna), Wiley-VCH, Weinheim, **2008**, pp. 1–64; b) G. J. Hutchings, M. Brust, H. Schmidbaur. Gold—an introductory perspective. *Chem. Soc. Rev.* **2008**, *37*, 1759.

[3] H. G. Raubenheimer, H. Schmidbaur. The Late Start and Amazing Upswing in Gold Chemistry. *J. Chem. Educ.* **2014**, *91*, 2024.

[4] a) M. D. Đurović, Ž. D. Bugarčić, R. van Eldik. Stability and reactivity of gold compounds – From fundamental aspects to applications. *Coord. Chem. Rev.* **2017**, *338*, 186; b) M. Joost, A. Amgoune, D. Bourissou. Reactivity of Gold Complexes towards Elementary Organometallic Reactions. *Angew. Chem. Int. Ed.* **2015**, *54*, 15022; *Angew. Chem.* **2015**, *127*, 15234.

[5] a) P. Pyykkö. Relativistic Effects in Chemistry: More Common Than You Thought. *Annu. Rev. Phys. Chem.* **2012**, *63*, 45; b) P. Schwerdtfeger, M. Lein, in *Gold Chemistry: Applications and Future Directions in the Life Sciences* (Ed.: F. Mohr), Wiley-VCH, Weinheim, **2009**, pp. 183–247; c) H. Schmidbaur, S. Cronje, B. Djordjevic, O. Schuster. Understanding gold chemistry through relativity. *Chem. Phys.* **2005**, *311*, 151; d) P. Schwerdtfeger. Relativistic Effects in Properties of Gold. *Heteroat. Chem.* **2002**, *13*, 578; e) N. Bartlett. Relativistic Effects and the Chemistry of Gold. *Gold Bull.* **1998**, *31*, 22; f) P. Pyykkö. Relativistic Effects in Structural Chemistry. *Chem. Rev.* **1988**, *88*, 563; g) P. Pyykkö, J.-P. Desclaux. Relativity and the Periodic System of Elements. *Acc. Chem. Res.* **1979**, *12*, 276.

[6] a) A. Leyva-Pérez, A. Corma. Similarities and Differences between the "Relativistic" Triad Gold, Platinum, and Mercury in Catalysis. *Angew. Chem. Int. Ed.* **2012**, *51*, 614; *Angew. Chem.* **2012**, *124*, 636; b) D. J. Gorin, F. D. Toste. Relativistic effects in homogeneous gold catalysis. *Nature* **2007**, *446*, 395.

[7] a) P. Pyykkö. Theoretical chemistry of gold. III. *Chem. Soc. Rev.* **2008**, *37*, 1967; b) P. Pyykkö. Theoretical chemistry of gold. II. *Inorg. Chim. Acta* **2005**, *358*, 4113; c) P. Pyykkö. Theoretical Chemistry of Gold. *Angew. Chem. Int. Ed.* **2004**, *43*, 4412; *Angew. Chem.* **2004**, *116*, 4512.

[8] a) R. Wesendrup, J. K. Laerdahl, P. Schwerdtfeger. Relativistic effects in gold chemistry. VI. Coupled cluster calculations for the isoelectronic series $AuPt^-$, Au_2, and $AuHg^+$. *J. Chem. Phys.* **1999**, *110*, 9457; b) P. Schwerdtfeger, G. A. Bowmaker. Relativistic effects in gold chemistry. V. Group 11 dipole polarizabilities and weak bonding in monocarbonyl compounds. *J. Chem. Phys.* **1994**, *100*, 4487; c) P. Schwerdtfeger, P. D. W. Boyd, S. Brienne, A. K. Burrell. Relativistic Effects in Gold Chemistry. 4. Gold(III) and Gold(V) Compounds. *Inorg. Chem.* **1992**, *31*, 3411; d) P. Schwerdtfeger, P. D. W. Boyd, A. K. Burrell, W. T. Robinson, M. J. Taylor. Relativistic Effects in Gold Chemistry. 3. Gold(I) Complexes. *Inorg. Chem.* **1990**, *29*, 3593; e) P. Schwerdtfeger. Relativistic Effects in Gold Chemistry. 2. The Stability of Complex Halides of Gold(III). *J. Am. Chem. Soc.* **1989**, *111*, 7261; f) P. Schwerdtfeger, M. Dolg, W. H. E. Schwarz, G. A. Bowmaker, P. D. W. Boyd. Relativistic effects in gold chemistry. I. Diatomic gold compounds. *J. Chem. Phys.* **1989**, *91*, 1762.

[9] J. E. Huheey, E. A. Keiter, R. L. Keiter, in *Inorganic Chemistry: Principles of Structure and Reactivity*, 4th ed., Harper-Collins, New York (NY), **1993**, pp. 182–199.

[10] D. R. Lide (Ed.), *CRC Handbook of Chemistry and Physics*, CRC Press, Boca Raton (FL), **2005**.

[11] M. Jansen. The chemistry of gold as an anion. *Chem. Soc. Rev.* **2008**, *37*, 1826.

[12] a) A. L. Balch, T. Y. Garcia, in *Gold: Science and Applications* (Eds.: C. Corti, R. Holliday), CRC Press, Boca Raton (FL), **2010**, pp. 31−50; b) M. C. Gimeno, A. Laguna, in *Comprehensive Coordination Chemistry II, Vol 6.* (Eds.: J. A. McCleverty, T. J. Meyer), Elsevier, Oxford, **2003**, pp. 911–1145.

[13] a) H. Schmidbaur, A. Schier. Aurophilic interactions as a subject of current research: an up-date. *Chem. Soc. Rev.* **2012**, *41*, 370; b) H. Schmidbaur, A. Schier. A briefing on aurophilicity. *Chem. Soc. Rev.* **2008**, *37*, 1931; c) H. Schmidbaur. The Aurophilicity Phenomenon: A Decade of Experimental Findings, Theoretical Concepts and Emerging Applications. *Gold Bull.* **2000**, *33*, 3.

[14] A. N. Chernyshev, M. V. Chernysheva, P. Hirva, V. Y. Kukushkin, M. Haukka. Weak aurophilic interactions in a series of Au(III) double salts. *Dalton Trans.* **2015**, *44*, 14523.

[15] a) A. Higelin, S. Riedel, in *Modern Synthesis Processes and Reactivity of Fluorinated Compounds* (Eds.: H. Groult, F. R. Leroux, A. Tressaud), Elsevier, Amsterdam, **2017**, pp. 561−586; b) T. Schlöder, S. Riedel, in *Comprehensive Inorganic Chemistry II, Vol. 9* (Eds.: J. Reedijk, K. Poeppelmeier), Elsevier, Amsterdam, **2013**, pp. 227−243; c) S. Riedel, in *Comprehensive Inorganic Chemistry II, Vol. 2* (Eds.: J. Reedijk, K. Poeppelmeier), Elsevier, Amsterdam, **2013**, pp. 187−221; d) S. Riedel, M. Kaupp. The highest oxidation states of the transition metal elements. *Coord. Chem. Rev.* **2009**, *253*, 606.

[16] W. J. Wolf, F. D. Toste, in *The Chemistry of Organogold Compounds, Vol. 1* (Eds.: Z. Rappoport, J. F. Liebman, I. Marek), belonging to Patai's Chemistry of Functional Groups, Wiley, Chichester, **2014**, pp. 391–408.

[17] M. N. Pillay, W. E. Van Zyl. Fluoro-, Fluoroalkyl-, and Heterofluorogold Complexes. *Comments Inorg. Chem.* **2012**, *33*, 122.

[18] F. Mohr. The Chemistry of Gold-fluoro compounds: A continuing challenge for Gold Chemists. *Gold Bull.* **2004**, *37*, 164.

[19] B. G. Müller. Fluorides of Copper, Silver, Gold, and Palladium. *Angew. Chem. Int. Ed. Engl.* **1987**, *26*, 1081; *Angew. Chem.* **1987**, *99*, 1120.

[20] J. Gil-Rubio, J. Vicente. Gold trifluoromethyl complexes. *Dalton Trans.* **2015**, *44*, 19432.

[21] H. Moissan. Préparation et propriétés du fluorure de platine anhydre. *C. R. Acad. Sci.* **1889**, *109*, 807.

[22] V. Lenher. Fluoride of Gold. *J. Am. Chem. Soc.* **1903**, *25*, 1136.

[23] O. Ruff. Über die Fluoride der Edelmetalle. *Ber. Dtsch. Chem. Ges.* **1913**, *46*, 920.

[24] A. G. Sharpe. Auric Fluoride and Related Compounds. *J. Chem. Soc.* **1949**, 2901.

[25] a) U. Engelmann, B. G. Müller. Tetrafluoroaurate(III) der Lanthaniden $MF[AuF_4]_2$ (M = Tm, Yb, Lu). *Z. Anorg. Allg. Chem.* **1993**, *619*, 1661; b) U. Engelmann, B. G. Müller. Tetrafluoroaurate(III) der Lanthaniden $M_2F[AuF_4]_5$ (M = Tb, Dy, Ho, Er). *Z. Anorg. Allg. Chem.* **1992**, *618*, 43; c) L. B. Asprey, F. H. Kruse, K. H. Jack, R. Maitland. Preparation and Properties of Crystalline Gold Trifluoride. *Inorg. Chem.* **1964**, *3*, 602.

[26] a) I. C. Tornieporth-Oetting, T. M. Klapötke. Laboratory Scale Direct Synthesis of Pure AuF_3. *Chem. Ber.* **1995**, *128*, 957; b) F. W. B. Einstein, P. R. Rao, J. Trotter, N. Bartlett. The Crystal Structure of Gold Trifluoride. *J. Chem. Soc. A* **1967**, 478.

[27] M. A. Ellwanger, S. Steinhauer, P. Golz, H. Beckers, A. Wiesner, B. Braun-Cula, T. Braun, S. Riedel. Taming the High Reactivity of Gold(III) Fluoride: Fluorido Gold(III) Complexes with N-Based Ligands. *Chem. Eur. J.* **2017**, *23*, 13501.

[28] B. Žemva, K. Lutar, A. Jesih, W. J. Casteel, Jr., A. P. Wilkinson, D. E. Cox, R. B. Von Dreele, H. Borrmann, N. Bartlett. Silver Trifluoride: Preparation, Crystal Structure, Some Properties, and Comparison with AuF_3. *J. Am. Chem. Soc.* **1991**, *113*, 4192.

[29] a) X. Wang, L. Andrews, F. Brosi, S. Riedel. Matrix Infrared Spectroscopy and Quantum-Chemical Calculations for the Coinage-Metal Fluorides: Comparisons of Ar–AuF, Ne–AuF, and Molecules MF_2 and MF_3. *Chem. Eur. J.* **2013**, *19*, 1397; b) X. Wang, L. Andrews, K. Willmann, F. Brosi, S. Riedel. Investigation of Gold Fluorides and Noble Gas Complexes by Matrix-Isolation Spectroscopy and Quantum-Chemical Calculations. *Angew. Chem. Int. Ed.* **2012**, *51*, 10628; *Angew. Chem.* **2012**, *124*, 10780.

[30] A. Schulz, M. Hargittai. Structural Variations and Bonding in Gold Halides: A Quantum Chemical Study of Monomeric and Dimeric Gold Monohalide and Gold Trihalide Molecules, AuX, Au_2X_2, AuX_3, and Au_2X_6 (X = F, Cl, Br, I). *Chem. Eur. J.* **2001**, *7*, 3657.

[31] B. Réffy, M. Kolonits, A. Schulz, T. M. Klapötke, M. Hargittai. Intriguing Gold Trifluoride−Molecular Structure of Monomers and Dimers: An Electron Diffraction and Quantum Chemical Study. *J. Am. Chem. Soc.* **2000**, *122*, 3127.

[32] R. D. Peacock. Potassium Tetrafluoroaurate(III). *Chem. Ind.* **1959**, 904.

[33] M. Leblanc, V. Maisonneuve, A. Tressaud. Crystal Chemistry and Selected Physical Properties of Inorganic Fluorides and Oxide-Fluorides. *Chem. Rev.* **2015**, *115*, 1191.

[34] a) O. Graudejus, A. P. Wilkinson, N. Bartlett. Structural Features of $Ag[AuF_4]$ and $Ag[AuF_6]$ and the Stuctural Relationship of $Ag[AgF_4]_2$ and $Au[AuF_4]_2$ to $Ag[AuF_4]_2$. *Inorg. Chem.* **2000**, *39*, 1545; b) R. Schmidt, B. G. Müller. Einkristalluntersuchungen an $Au[AuF_4]_2$ und CeF_4, zwei unerwarteten Nebenprodukten. *Z. Anorg. Allg. Chem.* **1999**, *625*, 605; c) S. H. Elder, G. M. Lucier, F. J. Hollander, N. Bartlett. Synthesis of Au(II) Fluoro Complexes and Their Structural and Magnetic Properties. *J. Am. Chem. Soc.* **1997**, *119*, 1020.

[35] T. C. Waddington. The lattice energies and thermodynamic properties of the hypothetical compounds AuF and CuF. *Trans. Faraday Soc.* **1959**, *55*, 1531.

[36] K. L. Saenger, C. P. Sun. Yellow emission bands produced during gold etching in O_2-CF_4 rf glow-discharge plasmas: Evidence for gas-phase AuF. *Phys. Rev. A* **1992**, *46*, 670.

[37] P. Schwerdtfeger, J. S. McFeaters, R. L. Stephens, M. J. Liddell, M. Dolg, B. A. Hess. Can AuF be synthesized? A theoretical study using relativistic configuration interaction and plasma modeling techniques. *Chem. Phys. Lett.* **1994**, *218*, 362.

[38] P. Schwerdtfeger, J. S. McFeaters, M. J. Liddell, J. Hrušák, H. Schwarz. Spectroscopic properties for the ground states of AuF, AuF^+, AuF_2, and Au_2F_2: A pseudopotential scalar relativistic Møller–Plesset and coupled-cluster study. *J. Chem. Phys.* **1995**, *103*, 245.

[39] D. Schröder, J. Hrušák, I. C. Tornieporth-Oetting, T. M. Klapötke, H. Schwarz. Neutral Gold(I) Fluoride Does Indeed Exist. *Angew. Chem. Int. Ed. Engl.* **1994**, *33*, 212; *Angew. Chem.* **1994**, *106*, 223.

[40] C. J. Evans, M. C. L. Gerry. Confirmation of the Existence of Gold(I) Fluoride, AuF: Microwave Spectrum and Structure. *J. Am. Chem. Soc.* **2000**, *122*, 1560.

[41] T. Okabayashi, Y. Nakaoka, E. Yamazaki, M. Tanimoto. Millimeter- and submillimeter-wave spectroscopy of AuF in the ground $X^1\Sigma^+$ state. *Chem. Phys. Lett.* **2002**, *366*, 406.

[42] N. J. Rijs, R. A. J. O'Hair. Forming trifluoromethylmetallates: competition between decarboxylation and C–F bond activation of group 11 trifluoroacetate complexes, $[CF_3CO_2ML]^-$. *Dalton Trans.* **2012**, *41*, 3395.

[43] X. Li, J. Cai. Electron Density Properties and Metallophilic Interactions of Gold Halides AuX_2 and Au_2X (X = F–I): *Ab Initio* Calculations. *Int. J. Quantum Chem.* **2016**, *116*, 1350.

[44] G. Liu, X. Feng, L. Wang, S. A. T. Redfern, X. Yong, G. Gao, H. Liu. Theoretical investigation of the valence states in Au *via* the Au–F compounds under high pressure. *Phys. Chem. Chem. Phys.* **2019**, *21*, 17621.

[45] J. Lin, S. Zhang, W. Guan, G. Yang, Y. Ma. Gold with +4 and +6 Oxidation States in AuF_4 and AuF_6. *J. Am. Chem. Soc.* **2018**, *140*, 9545.

[46] S. Dhaif Allah Al Harbi, M. Mogren Al Mogren, A. Elmarghany, D. Ben Abdallah, B. Mehnen, R. Linguerri, M. Hochlaf. Gold with +4 oxidation state compounds: mass spectrometric and theoretical characterization of AuO^{2+}. *Phys. Chem. Chem. Phys.* **2019**, *21*, 16120.

[47] K. Leary, N. Bartlett. A New Oxidation State of Gold: The Preparation and some Properties of $[AuF_6]^-$ Salts. *J. Chem. Soc., Chem. Commun.* **1972**, 903.

[48] Z. Mazej, in *Modern Synthesis Processes and Reactivity of Fluorinated Compounds* (Eds.: H. Groult, F. R. Leroux, A. Tressaud), Elsevier, Amsterdam, **2017**, pp. 587–607.

[49] J. H. Holloway, G. J. Schrobilgen. Krypton Fluoride Chemistry; a Route to AuF_5, $KrF^+AuF_6^-$, $Xe_2F_3^+AuF_6^-$, and $NO^+AuF_6^-$: The KrF^+–$XeOF_4$ System. *J. Chem. Soc., Chem. Commun.* **1975**, 623.

[50] a) K. Leary, A. Zalkin, N. Bartlett. Crystal Structure of $Xe_2F_{11}^+AuF_6^-$ and the Raman Spectrum of $Xe_2F_{11}^+$. *Inorg. Chem.* **1974**, *13*, 775; b) K. Leary, A. Zalkin, N. Bartlett. Crystal Structure of $[Xe_2F_{11}]^+[AuF_6]$. *J. Chem. Soc., Chem. Commun.* **1973**, 131.

[51] G. Kaindl, K. Leary, N. Bartlett. Mössbauer study of quinquevalent gold compounds. *J. Chem. Phys.* **1973**, *59*, 5050.

[52] M. J. Vasile, T. J. Richardson, F. A. Stevie, W. E. Falconer. Preparation and Characterization of Gold Pentafluoride. *J. Chem. Soc., Dalton Trans.* **1976**, 351.

[53] I.-C. Hwang, K. Seppelt. Gold Pentafluoride: Structure and Fluoride Ion Affinity. *Angew. Chem. Int. Ed.* **2001**, *40*, 3690; *Angew. Chem.* **2001**, *113*, 3803.

[54] L. Greb. Lewis Superacids: Classifications, Candidates, and Applications. *Chem. Eur. J.* **2018**, *24*, 17881.

[55] R. Craciun, D. Picone, R. T. Long, S. Li, D. A. Dixon, K. A. Peterson, K. O. Christe. Third Row Transition Metal Hexafluorides, Extraordinary Oxidizers, and Lewis Acids: Electron Affinities, Fluoride Affinities, and Heats of Formation of WF_6, ReF_6, OsF_6, IrF_6, PtF_6, and AuF_6. *Inorg. Chem.* **2010**, *49*, 1056.

[56] B. Žemva, N. Bartlett. The room temperature preparation of metastable fluorides and potent oxidizers. *J. Fluorine Chem.* **2006**, *127*, 1463.

[57] A. A. Timakov, V. N. Prusakov, Y. V. Drobyshevskii. Gold heptafluoride. *Dokl. Akad. Nauk SSSR* **1986**, *291*, 125.

[58] S. Riedel, M. Kaupp. Has AuF_7 Been Made? *Inorg. Chem.* **2006**, *45*, 1228.

[59] D. Himmel, S. Riedel. After 20 Years, Theoretical Evidence That "AuF_7" Is Actually $AuF_5 \cdot F_2$. *Inorg. Chem.* **2007**, *46*, 5338.

[60] J. Conradie, A. Ghosh. Theoretical Search for the Highest Valence States of the Coinage Metals: Roentgenium Heptafluoride May Exist. *Inorg. Chem.* **2019**, *58*, 8735.

[61] E. F. Murphy, R. Murugavel, H. W. Roesky. Organometallic Fluorides: Compounds Containing Carbon−Metal−Fluorine Fragments of d-Block Metals. *Chem. Rev.* **1997**, *97*, 3425.

[62] K. G. Caulton. The influence of π-stabilized unsaturation and filled/filled repulsions in transition metal chemistry. *New J. Chem.* **1994**, *18*, 25.

[63] K. Fagnou, M. Lautens. Halide Effects in Transition Metal Catalysis. *Angew. Chem. Int. Ed.* **2002**, *41*, 26; *Angew. Chem.* **2002**, *114*, 26.

[64] N. M. Doherty, N. W. Hoffman. Transition-Metal Fluoro Compounds Containing Carbonyl, Phosphine, Arsine, and Stibine Ligands. *Chem. Rev.* **1991**, *91*, 553.

[65] a) R. G. Pearson. Recent Advances in the Concept of Hard and Soft Acids and Bases. *J. Chem. Educ.* **1987**, *64*, 561; b) R. G. Pearson. Hard and Soft Acids and Bases. *J. Am. Chem. Soc.* **1963**, *85*, 3533.

[66] S. Ahrland, J. Chatt, N. R. Davies. The relative affinities of ligand atoms for acceptor molecules and ions. *Q. Rev. Chem. Soc.* **1958**, *12*, 265.

[67] R. J. Puddephatt, in *The Chemistry of Gold*, Elsevier, Amsterdam, **1978**, pp. 22–24.

[68] E. Bernhardt, M. Finze, H. Willner. Synthesis and NMR spectroscopic investigation of salts containing the novel $[Au(CF_3)_nX_{4-n}]^-$ (n = 4–1, X = F, CN, Cl) anions. *J. Fluorine Chem.* **2004**, *125*, 967.

[69] D. S. Laitar, P. Müller, T. G. Gray, J. P. Sadighi. A Carbene-Stabilized Gold(I) Fluoride: Synthesis and Theory. *Organometallics* **2005**, *24*, 4503.

[70] J. A. Akana, K. X. Bhattacharyya, P. Müller, J. P. Sadighi. Reversible C−F Bond Formation and the Au-Catalyzed Hydrofluorination of Alkynes. *J. Am. Chem. Soc.* **2007**, *129*, 7736.

[71] C. M. Wyss, B. K. Tate, J. Bacsa, M. Wieliczko, J. P. Sadighi. Dinuclear μ-fluoro cations of copper, silver and gold. *Polyhedron* **2014**, *84*, 87.

[72] T. Mathieson, A. Schier, H. Schmidbaur. Tris[(triphenylphosphine)gold(I)]oxonium Dihydrogentrifluoride as the Product of an Attempted Preparation of [(Triphenylphosphine)gold(I)] Fluoride. *Z. Naturforsch. B* **2000**, *55*, 1000.

[73] a) H. Moissan. Recherches sûr les propriétés et la préparation du fluorure d'éthyle. *Ann. Chim. Phys. Ser. 6* **1890**, *19*, 266; b) H. Moissan. Préparation et propriétés du fluorure d'éthyle. *C. R. Acad. Sci.* **1888**, *107*, 260.

[74] M. S. Winston, W. J. Wolf, F. D. Toste. Halide-Dependent Mechanisms of Reductive Elimination from Gold(III). *J. Am. Chem. Soc.* **2015**, *137*, 7921.

[75] R. Kumar, A. Linden, C. Nevado. Luminescent (N^C^C) Gold(III) Complexes: Stabilized Gold(III) Fluorides. *Angew. Chem. Int. Ed.* **2015**, *54*, 14287; *Angew. Chem.* **2015**, *127*, 14495.

[76] R. Kumar, A. Linden, C. Nevado. Evidence for Direct Transmetalation of Au^{III}–F with Boronic Acids. *J. Am. Chem. Soc.* **2016**, *138*, 13790.

[77] R. Kumar, C. Nevado. Cyclometalated Gold(III) Complexes: Synthesis, Reactivity, and Physicochemical Properties. *Angew. Chem. Int. Ed.* **2017**, *56*, 1994; *Angew. Chem.* **2017**, *129*, 2024.

[78] N. P. Mankad, F. D. Toste. C−C Coupling Reactivity of an Alkylgold(III) Fluoride Complex with Arylboronic Acids. *J. Am. Chem. Soc.* **2010**, *132*, 12859.

[79] N. P. Mankad, F. D. Toste. C(sp^3)–F reductive elimination from alkylgold(III) fluoride complexes. *Chem. Sci.* **2012**, *3*, 72.

[80] M. Albayer, R. Corbo, J. L. Dutton. Well defined difluorogold(III) complexes supported by N-ligands. *Chem. Commun.* **2018**, *54*, 6832.

[81] M. A. Ellwanger, S. Steinhauer, P. Golz, T. Braun, S. Riedel. Stabilization of Lewis Acidic AuF_3 as an N-Heterocyclic Carbene Complex: Preparation and Characterization of [AuF_3(SIMes)]. *Angew. Chem. Int. Ed.* **2018**, *57*, 7210; *Angew. Chem.* **2018**, *130*, 7328.

[82] M. A. Ellwanger, C. von Randow, S. Steinhauer, Y. Zhou, A. Wiesner, H. Beckers, T. Braun, S. Riedel. Tuning the Lewis acidity of difluorido gold(III) complexes: the synthesis of [$AuClF_2$(SIMes)] and [$AuF_2(OTeF_5)$(SIMes)]. *Chem. Commun.* **2018**, *54*, 9301.

[83] a) J. Miró, C. del Pozo. Fluorine and Gold: A Fruitful Partnership. *Chem. Rev.* **2016**, *116*, 11924; b) M. N. Hopkinson, A. D. Gee, V. Gouverneur. Gold Catalysis and Fluorine. *Isr. J. Chem.* **2010**, *50*, 675.

[84] a) M. N. Hopkinson, A. Tlahuext-Aca, F. Glorius. Merging Visible Light Photoredox and Gold Catalysis. *Acc. Chem. Res.* **2016**, *49*, 2261; b) M. Livendahl, A. M. Echavarren. Gold(I) Catalysis in Cross-Coupling Reactions. *Chim. Oggi* **2012**, *30*, 19; c) H. A. Wegner, M. Auzias. Gold for C–C Coupling Reactions: A Swiss-Army-Knife Catalyst? *Angew. Chem. Int. Ed.* **2011**, *50*, 8236; *Angew. Chem.* **2011**, *123*, 8386; d) M. N. Hopkinson, A. D. Gee, V. Gouverneur. Au^I/Au^{III} Catalysis: An Alternative Approach for C–C Oxidative Coupling. *Chem. Eur. J.* **2011**, *17*, 8248; e) P. Garcia, M. Malacria, C. Aubert, V. Gandon, L. Fensterbank. Gold-Catalyzed Cross-Couplings: New Opportunities for C–C Bond Formation. *ChemCatChem* **2010**, *2*, 493.

[85] S. G. Bratsch. Standard Electrode Potentials and Temperature Coefficients in Water at 298.15 K. *J. Phys. Chem. Ref. Data* **1989**, *18*, 1.

[86] a) T. Liang, C. N. Neumann, T. Ritter. Introduction of Fluorine and Fluorine-Containing Functional Groups. *Angew. Chem. Int. Ed.* **2013**, *52*, 8214; *Angew. Chem.* **2013**, *125*, 8372; b) T. Furuya, A. S. Kamlet, T. Ritter. Catalysis for fluorination and trifluoromethylation. *Nature* **2011**, *473*, 470.

[87] a) T. Braun, R. P. Hughes (Eds.), *Organometallic Fluorine Chemistry*, Springer, Cham (Switzerland), **2015**; b) P. Kirsch, *Modern Fluoroorganic Chemistry: Synthesis, Reactivity, Applications*, 2nd ed., Wiley-VCH, Weinheim, **2013**; c) T. Okazoe. Overview on the history of organofluorine chemistry from the viewpoint of material industry. *Proc. Jpn. Acad., Ser. B* **2009**, *85*, 276; d) D. O'Hagan. Understanding organofluorine chemistry. An introduction to the C–F bond. *Chem. Soc. Rev.* **2008**, *37*, 308; e) K. Uneyama, *Organofluorine Chemistry*, Blackwell Publishing, Oxford, **2006**; f) J. Percy (Ed.), *Science of Synthesis, Vol. 34: Fluorine*, Thieme, Stuttgart, **2005**; g) R. D. Chambers, *Fluorine in Organic Chemistry*, Blackwell Publishing, Oxford, **2004**; h) D. M. Lemal. Perspective on Fluorocarbon Chemistry. *J. Org. Chem.* **2004**, *69*, 1; i) G. Sandford. Perfluoroalkanes. *Tetrahedron* **2003**, *59*, 437; j) T. Hiyama, *Organofluorine Compounds: Chemistry and Applications* (Ed.: H. Yamamoto), Springer, Berlin, **2000**; k) G. Sanford. Organofluorine chemistry. *Phil. Trans. R. Soc. Lond. A* **2000**, *358*, 455; l) B. Baasner, H. Hagemann, J. C. Tatlow, *Houben-Weyl Methods of Organic Chemistry, Vol. E10: Organo-Fluorine Compounds*, 4th ed., Thieme, Stuttgart, **1999**; m) R. E. Banks, J. C. Tatlow. A guide to modern organofluorine chemistry. *J. Fluorine Chem.* **1986**, *33*, 227.

[88] J. E. Huheey, E. A. Keiter, R. L. Keiter, in *Inorganic Chemistry: Principles of Structure and Reactivity*, 4th ed., Harper-Collins, New York (NY), **1993**, pp. A21–A34.

[89] a) D. L. Orsi, R. A. Altman. Exploiting the unusual effects of fluorine in methodology. *Chem. Commun.* **2017**, *53*, 7168; b) B. E. Smart. Fluorine substituent effects (on bioactivity). *J. Fluorine Chem.* **2001**, *109*, 3; c) Y. Kobayashi, I. Kumadaki. Valence Bond Isomers of Aromatic Compounds Stabilized by Trifluoromethyl Groups. *Acc. Chem. Res.* **1981**, *14*, 76; d) J. A. Young. Fluorine Compounds as Teaching Aids in Organic Theory. *J. Chem. Educ.* **1970**, *47*, 733.

[90] P. Enghag, in *Encyclopedia of the Elements*, Wiley-VCH, Weinheim, **2004**, pp. 1073–1076.

[91] a) L. Ma, A. Bartholome, M. H. Tong, Z. Qin, Y. Yu, T. Shepherd, K. Kyeremeh, H. Deng, D. O'Hagan. Identification of a fluorometabolite from *Streptomyces* sp. MA37: (2*R*3*S*4*S*)-5-fluoro-2,3,4-trihydroxypentanoic acid. *Chem. Sci.* **2015**, *6*, 1414; b) K. K. J. Chan, D. O'Hagan. The Rare Fluorinated Natural Products and Biotechnological Prospects for Fluorine Enzymology. *Methods Enzymol.* **2012**, *516*, 219; c) D. O'Hagan, D. B. Harper. Fluorine-containing natural products. *J. Fluorine Chem.* **1999**, *100*, 127.

[92] F. Swarts. Sur quelques dérivés fluorés du toluol. *Bull. Acad. R. Belg.* **1898**, *35*, 375.

[93] S. G. Bratsch. A Group Electronegativity Method with Pauling Units. *J. Chem. Educ.* **1985**, *62*, 101.

[94] G. Bott, L. D. Field, S. Sternhell. Steric Effects. A Study of a Rationally Designed System. *J. Am. Chem. Soc.* **1980**, *102*, 5618.

[95] M. Á. García-Monforte, S. Martínez-Salvador, B. Menjón. The Trifluoromethyl Group in Transition Metal Chemistry. *Eur. J. Inorg. Chem.* **2012**, 4945.

[96] P. von Ragué Schleyer, A. J. Kos. The importance of negative (anionic) hyperconjugation. *Tetrahedron* **1983**, *39*, 1141.

[97] a) T. Leyssens, D. Peeters, A. G. Orpen, J. N. Harvey. How Important Is Metal−Ligand Back-Bonding toward YX_3 Ligands (Y = N, P, C, Si)? An NBO Analysis. *Organometallics* **2007**, *26*, 2637; b) H. C. Clark, J. H. Tsai. Bonding in fluorinated organometallic compounds. *J. Organomet. Chem.* **1967**, *7*, 515.

[98] a) A. G. Algarra, V. V. Grushin, S. A. Macgregor. Natural Bond Orbital Analysis of the Electronic Structure of $[L_nM(CH_3)]$ and $[L_nM(CF_3)]$ Complexes. *Organometallics* **2012**, *31*, 1467; b) J. Goodman, V. V. Grushin, R. B. Larichev, S. A. Macgregor, W. J. Marshall, D. C. Roe. Fluxionality of $[(Ph_3P)_3M(X)]$ (M = Rh, Ir). The Red and Orange Forms of $[(Ph_3P)_3Ir(Cl)]$. Which Phosphine Dissociates Faster from Wilkinson's Catalyst? *J. Am. Chem. Soc.* **2010**, *132*, 12013; c) J. Goodman, V. V. Grushin, R. B. Larichev, S. A. Macgregor, W. J. Marshall, D. C. Roe. Fluxionality of $[(Ph_3P)_3Rh(X)]$: The Extreme Case of X = CF_3. *J. Am. Chem. Soc.* **2009**, *131*, 4236.

[99] O. A. Tomashenko, V. V. Grushin. Aromatic Trifluoromethylation with Metal Complexes. *Chem. Rev.* **2011**, *111*, 4475.

[100] a) P. Sgarbossa, A. Scarso, G. Strukul, R. A. Michelin. Platinum(II) Complexes with Coordinated Electron-Withdrawing Fluoroalkyl and Fluoroaryl Ligands: Synthesis, Reactivity, and Catalytic Activity. *Organometallics* **2012**, *31*, 1257; b) T. G. Appleton, H. C. Clark, L. E. Manzer. The *trans*-influence: its measurement and significance. *Coord. Chem. Rev.* **1973**, *10*, 335; c) T. G. Appleton, M. H. Chisholm, H. C. Clark, L. E. Manzer. Trifluoromethylplatinum Complexes and the Nature of the Pt–CF_3 Bond. *Inorg. Chem.* **1972**, *11*, 1786.

[101] F. L. Taw, A. E. Clark, A. H. Mueller, M. T. Janicke, T. Cantat, B. L. Scott, P. J. Hay, R. P. Hughes, J. L. Kiplinger. Titanium(IV) Trifluoromethyl Complexes: New

Perspectives on Bonding from Organometallic Fluorocarbon Chemistry. *Organometallics* **2012**, *31*, 1484.

[102] R. Hoffmann, S. Alvarez, C. Mealli, A. Falceto, T. J. Cahill, III, T. Zeng, G. Manca. From Widely Accepted Concepts in Coordination Chemistry to Inverted Ligand Fields. *Chem. Rev.* **2016**, *116*, 8173.

[103] a) C. Gao, G. Macetti, J. Overgaard. Experimental X-ray Electron Density Study of Atomic Charges, Oxidation States, and Inverted Ligand Field in $Cu(CF_3)_4^-$. *Inorg. Chem.* **2019**, *58*, 2133; b) R. C. Walroth, J. T. Lukens, S. N. MacMillan, K. D. Finkelstein, K. M. Lancaster. Spectroscopic Evidence for a $3d^{10}$ Ground State Electronic Configuration and Ligand Field Inversion in $[Cu(CF_3)_4]^{1-}$. *J. Am. Chem. Soc.* **2016**, *138*, 1922; c) C. M. Lemon, M. Huynh, A. G. Maher, B. L. Anderson, E. D. Bloch, D. C. Powers, D. G. Nocera. Electronic Structure of Copper Corroles. *Angew. Chem. Int. Ed.* **2016**, *55*, 2176; *Angew. Chem.* **2016**, *128*, 2216; d) J. P. Snyder. Distinguishing Copper d^8 and d^{10} Configurations in a Highly Ionic Complex; A Nonformal Metal Oxidation State. *Angew. Chem. Int. Ed. Engl.* **1995**, *34*, 986; *Angew. Chem.* **1995**, *107*, 1076; e) M. Kaupp, H. G. von Schnering. Formal Oxidation State versus Partial Charge—A Comment. *Angew. Chem. Int. Ed. Engl.* **1995**, *34*, 986; *Angew. Chem.* **1995**, *107*, 1076;

[104] J. P. Snyder. Elusiveness of Cu^{III} Complexation; Preference for Trifluoromethyl Oxidation in the Formation of $[Cu^{I}(CF_3)_4]^-$ Salts. *Angew. Chem. Int. Ed. Engl.* **1995**, *34*, 80; *Angew. Chem.* **1995**, *107*, 112.

[105] D. Joven-Sancho, M. Baya, A. Martín, B. Menjón. Homoleptic Trifluoromethyl Derivatives of Ag^{I} and Ag^{III}. *Chem. Eur. J.* **2018**, *24*, 13098.

[106] M. Baya, D. Joven-Sancho, P. J. Alonso, J. Orduna, B. Menjón. M−C Bond Homolysis in Coinage-Metal $[M(CF_3)_4]^-$ Derivatives. *Angew. Chem. Int. Ed.* **2019**, *58*, 9954; *Angew. Chem.* **2019**, *131*, 10059.

[107] a) R. P. Hughes. Fluorine as a ligand substituent in organometallic chemistry: A second chance and a second research career. *J. Fluorine Chem.* **2010**, *131*, 1059; b) R. P. Hughes. Conversion of Carbon–Fluorine Bonds α to Transition Metal Centers to Carbon–Hydrogen, Carbon–Carbon, and Carbon–Heteroatom Bonds. *Eur. J. Inorg. Chem.* **2009**, *2009*, 4591; c) F. G. A. Stone. Fluorocarbon metal compounds—role models in organotransition metal chemistry. *J. Fluorine Chem.* **1999**, *100*, 227; d) J. A. Morrison. Trifluoromethyl-Containing Transition Metal Complexes. *Adv. Organomet. Chem.* **1993**, *35*, 211; e) R. P. Hughes. Organo-Transition Metal Compounds Containing Perfluorinated Ligands. *Adv. Organomet. Chem.* **1990**, *31*, 183; f) F. G. A. Stone. The Role of Fluorocarbons in Oxidative−Addition and −Elimination Reactions. *Pure Appl. Chem.* **1972**, *30*, 551; g) R. Nyholm. Transition-metal Complexes of Some Perfluoro-ligands. *Q. Rev. Chem. Soc.* **1970**, *24*, 1.

[108] T. H. Coffield, J. Kozikowski, R. D. Closson, in *International Conference on Coordination Chemistry*, Chemical Society (Special Publication No. 13), London, **1959**, p. 126.

[109] H. D. Kaesz, R. B. King, F. G. A. Stone. Chemistry of the Metal Carbonyls VIII. *Z. Naturforsch. B* **1960**, *15*, 763.

[110] W. R. McClellan. Perfluoroalkyl and Perfluoroacyl Metal Carbonyls. *J. Am. Chem. Soc.* **1961**, *83*, 1598.

[111] a) D. J. Burton, L. Lu. Fluorinated Organometallic Compounds. *Top. Curr. Chem.* **1997**, *193*, 45; b) D. J. Burton, Z.-Y. Yang, P. A. Morken. Fluorinated Organometallics: Vinyl, Alkynyl, Allyl, Benzyl, Propargyl and Aryl: Fluorinated Organometallic Reagents in Organic Synthesis. *Tetrahedron* **1994**, *50*, 2993.

[112] J. Kvíčala, J. Štambaský, S. Böhm, O. Paleta. Equilibrium structures of isolated (halogenated) fluorolithiomethanes. *J. Fluorine Chem.* **2002**, *113*, 147.

[113] B. Waerder, S. Steinhauer, B. Neumann, H.-G. Stammler, A. Mix, Y. V. Vishnevskiy, B. Hoge, N. W. Mitzel. Solid-State Structure of a Li/F Carbenoid: Pentafluoroethyllithium. *Angew. Chem. Int. Ed.* **2014**, *53*, 11640; *Angew. Chem.* **2014**, *126*, 11824.

[114] a) S. K. Ritter. A Fleeting Chemistry No More. *Chem. Eng. News* **2014**, *92*(36), 4; b) N. Santschi, R. Gilmour. The (Not So) Ephemeral Trifluoromethanide Anion. *Angew. Chem. Int. Ed.* **2014**, *53*, 11414; *Angew. Chem.* **2014**, *126*, 11598.

[115] G. K. S. Prakash, F. Wang, Z. Zhang, R. Haiges, M. Rahm, K. O. Christe, T. Mathew, G. A. Olah. Long-Lived Trifluoromethanide Anion: A Key Intermediate in Nucleophilic Trifluoromethylations. *Angew. Chem. Int. Ed.* **2014**, *53*, 11575; *Angew. Chem.* **2014**, *126*, 11759.

[116] A. Lishchynskyi, F. M. Miloserdov, E. Martin, J. Benet-Buchholz, E. C. Escudero-Adán, A. I. Konovalov, V. V. Grushin. The Trifluoromethyl Anion. *Angew. Chem. Int. Ed.* **2015**, *54*, 15289; *Angew. Chem.* **2015**, *127*, 15504.

[117] a) R. L. Harlow, J. Benet-Buchholz, F. M. Miloserdov, A. I. Konovalov, W. J. Marshall, E. C. Escudero-Adán, E. Martin, A. Lishchynskyi, V. V. Grushin. On the Structure of $[K(crypt\text{-}222)]^+CF_3^-$. *Helv. Chim. Acta* **2018**, *101*, e1800015; b) F. M. Miloserdov, A. I. Konovalov, E. Martin, J. Benet-Buchholz, E. C. Escudero-Adán, A. Lishchynskyi, V. V. Grushin. The Trifluoromethyl Anion: Evidence for $[K(crypt\text{-}222)]^+CF_3^-$. *Helv. Chim. Acta* **2017**, *100*, e1700032; c) S. Becker, P. Müller. A Reinterpretation of the Crystal Structure Analysis of $[K(crypt\text{-}222)]^+CF_3^-$: No Proof for the Trifluoromethanide Ion. *Chem. Eur. J.* **2017**, *23*, 7081.

[118] a) A. Maleckis, M. S. Sanford. Synthesis of Fluoroalkyl Palladium and Nickel Complexes via Decarbonylation of Acylmetal Species. *Organometallics* **2014**, *33*, 3831; b) B. D. Panthi, S. L. Gipson, A. Franken. Comparison of the Thermal and Reductive Decarbonylation of a Rhodium Trifluoroacetyl Diphosphine Complex. *Organometallics* **2010**, *29*, 5890; c) H. Huang, R. P. Hughes, A. L. Rheingold. Synthesis and Structural Characterization of New Perfluoroacyl and Perfluoroalkyl Group 6 Transition Metal Compounds. *Organometallics* **2010**, *29*, 1948.

[119] R. Eujen. Bis(Trifluoromethyl)Mercury. *Inorg. Synth.* **1986**, *24*, 52.

[120] R. J. Lagow, J. A. Morrison. New Methods for the Synthesis of Trifluoromethyl Organometallic Compounds. *Adv. Inorg. Chem. Radiochem.* **1980**, *23*, 177.

[121] E. K. S. Liu, R. J. Lagow. The Preservation of Metal–Carbon Bonds and Metalloid–Carbon Bonds during Direct Fluorination: a Surprise Even to Fluorine Chemists. *J. Am. Chem. Soc.* **1976**, *98*, 8270.

[122] R. J. Lagow, in *Fluorine Chemistry at the Millennium* (Ed.: R. E. Banks), Elsevier, Oxford, **2000**, pp. 283−296.

[123] D. W. Firsich, R. J. Lagow. Novel Synthesis of σ-Bonded Palladium and Nickel Compounds by Co-condensation of Metal Vapour with Alkyl Free Radicals. *J. Chem. Soc., Chem. Commun.* **1981**, 1283.

[124] M. A. Guerra, T. R. Bierschenk, R. J. Lagow. The generality of metal atom-free radical reactions and synthesis of new trifluoromethylalkyls of gold(III) and silver. *J. Organomet. Chem.* **1986**, *307*, C58.

[125] a) E. Bernhardt, M. Finze, H. Willner. Mechanistic Study on the Fluorination of $K[B(CN)_4]$ with ClF Enabling the High Yield and Large Scale Synthesis of $K[B(CF_3)_4]$ and $K[(CF_3)_3BCN]$. *Inorg. Chem.* **2011**, *50*, 10268; b) E. Bernhardt, G. Henkel, H. Willner, G. Pawelke, H. Bürger. Synthesis and Properties of the

Tetrakis(trifluoromethyl)borate Anion, $[B(CF_3)_4]^-$: Structure Determination of $Cs[B(CF_3)_4]$ by Single-Crystal X-ray Diffraction. *Chem. Eur. J.* **2001**, *7*, 4696.

[126] a) S. Rozen. Attaching the Fluorine Atom to Organic Molecules Using BrF_3 and Other Reagents Directly Derived from F_2. *Acc. Chem. Res.* **2005**, *38*, 803; b) S. Rozen, D. Rechavi, A. Hagooly. Novel reactions with the underutilized BrF_3: The chemistry with nitriles. *J. Fluorine Chem.* **2001**, *111*, 161; c) M. T. Baker, J. A. Ruzicka, J. H. Tinker. One step synthesis of 1,1,1,4,4,4-hexafluorobutane from succinonitrile. *J. Fluorine Chem.* **1999**, *94*, 123; d) T. E. Stevens. Fluorination of Some Nitriles and Ketones with Bromine Trifluoride. *J. Org. Chem.* **1961**, *26*, 1627.

[127] S. Balters, E. Bernhardt, H. Willner, T. Berends. Synthesen und NMR-Untersuchungen von Salzen mit den neuen Anionen $[PtX_n(CF_3)_{6-n}]^{2-}$ (n = 0 - 5, X = F, OH, Cl, CN) und die Kristallstrukturanalyse von $K_2[(CF_3)_2F_2Pt(\mu\text{-}OH)_2PtF_2(CF_3)_2]\cdot 2H_2O$. *Z. Anorg. Allg. Chem.* **2004**, *630*, 257.

[128] J. Banus, H. J. Emeléus, R. N. Haszeldine. The Heterolytic Fission of the Carbon–Iodine Bond in Trifluoroiodomethane. *J. Chem. Soc.* **1951**, 60.

[129] A. A. Banks, H. J. Emeléus, R. N. Haszeldine, V. Kerrigan. The Reaction of Bromine Trifluoride and Iodine Pentafluoride with Carbon Tetrachloride, Tetrabromide, and Tetraiodide and with Tetraiodoethylene. *J. Chem. Soc.* **1948**, 2188.

[130] R. B. King, P. M. Treichel, F. G. A. Stone. Chemistry of the Metal Carbonyls. XII. New Complexes Derived from Cyclopentadienylcobalt Dicarbonyl. *J. Am. Chem. Soc.* **1961**, *83*, 3593.

[131] R. B. King, S. L. Stafford, P. M. Treichel, F. G. A. Stone. Chemistry of the Metal Carbonyls. XV. Fluorocarbon Derivatives of Iron Carbonyl. *J. Am. Chem. Soc.* **1961**, *83*, 3604.

[132] a) N. O. Brace. Syntheses with perfluoroalkyl radicals from perfluoroalkyl iodides. A rapid survey of synthetic possibilities with emphasis on practical applications. Part one: alkenes, alkynes and allylic compounds. *J. Fluorine Chem.* **1999**, *93*, 1; b) M. A. McClinton, D. A. McClinton. Trifluoromethylations and Related Reactions in Organic Chemistry. *Tetrahedron* **1992**, *48*, 6555.

[133] a) H. J. Emeléus, R. N. Haszeldine. Organometallic Fluorine Compounds. Part II. The Synthesis of Bistrifluoromethylmercury. *J. Chem. Soc.* **1949**, 2953; b) H. J. Emeléus, R. N. Haszeldine. Organometallic Fluorine Compounds. Part I. The Synthesis of Trifluoromethyl and Pentafluoroethyl Mercurials. *J. Chem. Soc.* **1949**, 2948.

[134] L. J. Krause, J. A. Morrison. Trifluoromethyl Group 2B Compounds: Bis(trifluoromethyl)cadmium·Base. New, More Powerful Ligand-Exchange Reagents and Low-Temperature Difluorocarbene Sources. *J. Am. Chem. Soc.* **1981**, *103*, 2995.

[135] H. Lange, D. Naumann. Bis(perfluororgano)cadmium-Verbindungen: Ein einfaches darstellungsverfahren. *J. Fluorine Chem.* **1984**, *26*, 1.

[136] a) X. Liu, C. Xu, M. Wang, Q. Liu. Trifluoromethyltrimethylsilane: Nucleophilic Trifluoromethylation and Beyond. *Chem. Rev.* **2015**, *115*, 683; b) G. K. S. Prakash, M. Mandal. Nucleophilic trifluoromethylation tamed. *J. Fluorine Chem.* **2001**, *112*, 123; c) R. P. Singh, J. M. Shreeve. Nucleophilic Trifluoromethylation Reactions of Organic Compounds with (Trifluoromethyl)trimethylsilane. *Tetrahedron* **2000**, *56*, 7613; d) G. K. S. Prakash, A. K. Yudin. Perfluoroalkylation with Organosilicon Reagents. *Chem. Rev.* **1997**, *97*, 757.

[137] N. Maggiarosa, W. Tyrra, D. Naumann, N. V. Kirij, Y. L. Yagupolskii. $[Me_3Si(CF_3)F]^-$ and $[Me_3Si(CF_3)_2]^-$: Reactive Intermediates in Fluoride-Initiated Trifluoromethylation with Me_3SiCF_3 — An NMR Study. *Angew. Chem. Int. Ed.* **1999**, *38*, 2252; *Angew. Chem.* **1999**, *111*, 2392.

[138] D. Huang, K. G. Caulton. New Entries to and New Reactions of Fluorocarbon Ligands. *J. Am. Chem. Soc.* **1997**, *119*, 3185.

[139] a) W. Tyrra, D. Naumann. Perfluoroorganosilver(I) compounds. *J. Fluorine Chem.* **2004**, *125*, 823; b) W. Tyrra. Silver(I) Fluoride and Related Compounds in Chemical Synthesis. *Heteroat. Chem.* **2002**, *13*, 561; c) W. E. Tyrra. Oxidative perfluoroorganylation methods in group 12–16 chemistry: The reactions of haloperfluoroorganics and In and InBr, a convenient new route to AgR_f ($R_f = CF_3$, C_6F_5) and reactions of AgR_f with group 12–16 elements. *J. Fluorine Chem.* **2001**, *112*, 149.

[140] B. J. Truscott, F. Nahra, A. M. Z. Slawin, D. B. Cordes, S. P. Nolan. Fluoride, bifluoride and trifluoromethyl complexes of iridium(I) and rhodium(I). *Chem. Commun.* **2015**, *51*, 62.

[141] C.-P. Zhang, H. Wang, A. Klein, C. Biewer, K. Stirnat, Y. Yamaguchi, L. Xu, V. Gomez-Benitez, D. A. Vicic. A Five-Coordinate Nickel(II) Fluoroalkyl Complex as a Precursor to a Spectroscopically Detectable Ni(III) Species. *J. Am. Chem. Soc.* **2013**, *135*, 8141.

[142] S. Martínez de Salinas, Á. L. Mudarra, J. Benet-Buchholz, T. Parella, F. Maseras, M. H. Pérez-Temprano. New Vistas in Transmetalation with Discrete "$AgCF_3$" Species: Implications in Pd-Mediated Trifluoromethylation Reactions. *Chem. Eur. J.* **2018**, *24*, 11895.

[143] M. Blaya, D. Bautista, J. Gil-Rubio, J. Vicente. Synthesis of Au(I) Trifluoromethyl Complexes. Oxidation to Au(III) and Reductive Elimination of Halotrifluoromethanes. *Organometallics* **2014**, *33*, 6358.

[144] D. Naumann, W. Wessel, J. Hahn, W. Tyrra. Darstellung, NMR-spektroskopische Charakterisierung und Reaktionen von Perfluoralkylsilber(I)-Verbindungen. *J. Organomet. Chem.* **1997**, *547*, 79.

[145] a) T. Umemoto, in *Modern Synthesis Processes and Reactivity of Fluorinated Compounds* (Eds.: H. Groult, F. R. Leroux, A. Tressaud), Elsevier, Amsterdam, **2017**, pp. 265−287; b) N. Shibata, A. Matsnev, D. Cahard. Shelf-stable electrophilic trifluoromethylating reagents: A brief historical perspective. *Beilstein J. Org. Chem.* **2010**, *6*, 65; c) T. Umemoto. Electrophilic Perfluoroalkylating Agents. *Chem. Rev.* **1996**, *96*, 1757.

[146] H. Li. Umemoto's Reagent. *Synlett* **2012**, *23*, 2289.

[147] P. Eisenberger, S. Gischig, A. Togni. Novel 10-I-3 Hypervalent Iodine-Based Compounds for Electrophilic Trifluoromethylation. *Chem. Eur. J.* **2006**, *12*, 2579.

[148] a) E. A. Meucci, S. N. Nguyen, N. M. Camasso, E. Chong, A. Ariafard, A. J. Canty, M. S. Sanford. Nickel(IV)-Catalyzed C–H Trifluoromethylation of (Hetero)arenes. *J. Am. Chem. Soc.* **2019**, *141*, 12872; b) N. M. Camasso, A. J. Canty, A. Ariafard, M. S. Sanford. Experimental and Computational Studies of High-Valent Nickel and Palladium Complexes. *Organometallics* **2017**, *36*, 4382; c) J. R. Bour, N. M. Camasso, M. S. Sanford. Oxidation of Ni(II) to Ni(IV) with Aryl Electrophiles Enables Ni-Mediated Aryl–CF_3 Coupling. *J. Am. Chem. Soc.* **2015**, *137*, 8034; d) N. M. Camasso, M. S. Sanford. Design, synthesis, and carbon-heteroatom coupling reactions of organometallic nickel(IV) complexes. *Science* **2015**, *347*, 1218.

[149] Y. Ye, N. D. Ball, J. W. Kampf, M. S. Sanford. Oxidation of a Cyclometalated Pd(II) Dimer with "CF_3^+": Formation and Reactivity of a Catalytically Competent Monomeric Pd(IV) Aquo Complex. *J. Am. Chem. Soc.* **2010**, *132*, 14682.

[150] a) E. P. Gillis, K. J. Eastman, M. D. Hill, D. J. Donnelly, N. A. Meanwell. Applications of Fluorine in Medicinal Chemistry. *J. Med. Chem.* **2015**, *58*, 8315; b) T. Fujiwara, D. O'Hagan. Successful fluorine-containing herbicide agrochemicals. *J. Fluorine Chem.*

2014, *167*, 16; c) S. K. Ritter. Dabbling In Fluorine. *Chem. Eng. News* **2012**, *90*(9), 10; d) S. Purser, P. R. Moore, S. Swallow, V. Gouverneur. Fluorine in medicinal chemistry. *Chem. Soc. Rev.* **2008**, *37*, 320; e) K. Müller, C. Faeh, F. Diederich. Fluorine in Pharmaceuticals: Looking Beyond Intuition. *Science* **2007**, *317*, 1881; f) W. R. Dolbier, Jr. Fluorine chemistry at the millennium. *J. Fluorine Chem.* **2005**, *126*, 157; g) H.-J. Böhm, D. Banner, S. Bendels, M. Kansy, B. Kuhn, K. Müller, U. Obst-Sander, M. Stahl. Fluorine in Medicinal Chemistry. *ChemBioChem* **2004**, *5*, 637; h) P. Jeschke. The Unique Role of Fluorine in the Design of Active Ingredients for Modern Crop Protection. *ChemBioChem* **2004**, *5*, 570.

[151] a) P. Gao, X.-R. Song, X.-Y. Liu, Y.-M. Liang. Recent Developments in the Trifluoromethylation of Alkynes. *Chem. Eur. J.* **2015**, *21*, 7648; b) C. Alonso, E. Martínez de Marigorta, G. Rubiales, F. Palacios. Carbon Trifluoromethylation Reactions of Hydrocarbon Derivatives and Heteroarenes. *Chem. Rev.* **2015**, *115*, 1847; c) J. Xu, X. Liu, Y. Fu. Recent advance in transition-metal-mediated trifluoromethylation for the construction of C(sp^3)–CF_3 bonds. *Tetrahedron Lett.* **2014**, *55*, 585; d) G. Landelle, A. Panossian, S. Pazenok, J.-P. Vors, F. R. Leroux. Recent advances in transition metal-catalyzed Csp^2-monofluoro-, difluoro-, perfluoromethylation and trifluoromethylthiolation. *Beilstein J. Org. Chem.* **2013**, *9*, 2476; e) P. Chen, G. Liu. Recent Advances in Transition-Metal-Catalyzed Trifluoromethylation and Related Transformations. *Synthesis* **2013**, *45*, 2919; f) T. Liu, Q. Shen. Progress in Copper-Mediated Formation of Trifluoromethylated Arenes. *Eur. J. Org. Chem.* **2012**, 6679; g) Y. Ye, M. S. Sanford. Investigations into Transition-Metal-Catalyzed Arene Trifluoromethylation Reactions. *Synlett* **2012**, *23*, 2005; h) X.-F. Wu, H. Neumann, M. Beller. Recent Developments on the Trifluoromethylation of (Hetero)Arenes. *Chem. Asian J.* **2012**, *7*, 1744; i) T. Besset, C. Schneider, D. Cahard. Tamed Arene and Heteroarene Trifluoromethylation. *Angew. Chem. Int. Ed.* **2012**, *51*, 5048; *Angew. Chem.* **2012**, *124*, 5134; j) Z. Jin, G. B. Hammond, B. Xu. Transition-Metal-Mediated Fluorination, Difluoromethylation, and Trifluoromethylation. *Aldrichimica Acta* **2012**, *45*, 67; k) S. Roy, B. T. Gregg, G. W. Gribble, V.-D. Le, S. Roy. Trifluoromethylation of aryl and heteroaryl halides. *Tetrahedron* **2011**, *67*, 2161; l) R. J. Lundgren, M. Stradiotto. Transition-Metal-Catalyzed Trifluoromethylation of Aryl Halides. *Angew. Chem. Int. Ed.* **2010**, *49*, 9322; *Angew. Chem.* **2010**, *122*, 9510; m) J.-A. Ma, D. Cahard. Strategies for nucleophilic, electrophilic, and radical trifluoromethylations. *J. Fluorine Chem.* **2007**, *128*, 975; n) M. Schlosser. CF_3-Bearing Aromatic and Heterocyclic Building Blocks. *Angew. Chem. Int. Ed.* **2006**, *45*, 5432; *Angew. Chem.* **2006**, *118*, 5558.

[152] V. V. Grushin. The Organometallic Fluorine Chemistry of Palladium and Rhodium: Studies toward Aromatic Fluorination. *Acc. Chem. Res.* **2010**, *43*, 160.

[153] a) Y. Kobayashi, I. Kumadaki. Trifluoromethylation of aromatic compounds. *Tetrahedron Lett.* **1969**, *10*, 4095; b) V. C. R. McLoughlin, J. Thrower. A route to fluoroalkyl-substituted aromatic compounds involving fluoroalkylcopper intermediates. *Tetrahedron* **1969**, *25*, 5921.

[154] D. M. Wiemers, D. J. Burton. Pregeneration, Spectroscopic Detection and Chemical Reactivity of (Trifluoromethyl)copper, an Elusive and Complex Species. *J. Am. Chem. Soc.* **1986**, *108*, 832.

[155] G. G. Dubinina, H. Furutachi, D. A. Vicic. Active Trifluoromethylating Agents from Well-Defined Copper(I)−CF_3 Complexes. *J. Am. Chem. Soc.* **2008**, *130*, 8600.

[156] a) H. Morimoto, T. Tsubogo, N. D. Litvinas, J. F. Hartwig. A Broadly Applicable Copper Reagent for Trifluoromethylations and Perfluoroalkylations of Aryl Iodides and Bromides. *Angew. Chem. Int. Ed.* **2011**, *50*, 3793; *Angew. Chem.* **2011**, *123*, 3877; b) M. Oishi, H. Kondo, H. Amii. Aromatic trifluoromethylation catalytic in copper. *Chem. Commun.* **2009**, 1909.

[157] G. G. Dubinina, J. Ogikubo, D. A. Vicic. Structure of Bis(trifluoromethyl)cuprate and Its Role in Trifluoromethylation Reactions. *Organometallics* **2008**, *27*, 6233.

[158] S. Martínez de Salinas, Á. L. Mudarra, C. Odena, M. Martínez Belmonte, J. Benet-Buchholz, F. Maseras, M. H. Pérez-Temprano. Exploring the Role of Coinage Metalates in Trifluoromethylation: A Combined Experimental and Theoretical Study. *Chem. Eur. J.* **2019**, *25*, 9390.

[159] L. Liu, Z. Xi. Organocopper(III) Compounds with Well-defined Structures Undergo Reductive Elimination to Form C—C or C–Heteroatom Bonds. *Chin. J. Chem.* **2018**, *36*, 1213.

[160] S.-L. Zhang, C. Xiao, H.-X. Wan. Diverse copper(III) trifluoromethyl complexes with mono-, bi- and tridentate ligands and their versatile reactivity. *Dalton Trans.* **2018**, *47*, 4779.

[161] a) S. Guo, D. I. AbuSalim, S. P. Cook. Aqueous Benzylic C–H Trifluoromethylation for Late-Stage Functionalization. *J. Am. Chem. Soc.* **2018**, *140*, 12378; b) X. Tan, Z. Liu, H. Shen, P. Zhang, Z. Zhang, C. Li. Silver-Catalyzed Decarboxylative Trifluoromethylation of Aliphatic Carboxylic Acids. *J. Am. Chem. Soc.* **2017**, *139*, 12430; c) A. M. Romine, N. Nebra, A. I. Konovalov, E. Martin, J. Benet-Buchholz, V. V. Grushin. Easy Access to the Copper(III) Anion $[Cu(CF_3)_4]^-$. *Angew. Chem. Int. Ed.* **2015**, *54*, 2745; *Angew. Chem.* **2015**, *127*, 2783.

[162] S.-L. Zhang, W.-F. Bie. Isolation and characterization of copper(III) trifluoromethyl complexes and reactivity studies of aerobic trifluoromethylation of arylboronic acids. *RSC Adv.* **2016**, *6*, 70902.

[163] a) Z. Lu, H. Liu, S. Liu, X. Leng, Y. Lan, Q. Shen. A Key Intermediate in Copper-Mediated Arene Trifluoromethylation, $[n\mathrm{Bu}_4\mathrm{N}][\mathrm{Cu}(\mathrm{Ar})(\mathrm{CF}_3)_3]$: Synthesis, Characterization, and $C(sp^2)-CF_3$ Reductive Elimination. *Angew. Chem. Int. Ed.* **2019**, *58*, 8510; *Angew. Chem.* **2019**, *131*, 8598; b) M. Paeth, S. B. Tyndall, L.-Y. Chen, J.-C. Hong, W. P. Carson, X. Liu, X. Sun, J. Liu, K. Yang, E. M. Hale, D. L. Tierney, B. Liu, Z. Cao, M.-J. Cheng, W. A. Goddard III, W. Liu. Csp^3–Csp^3 Bond-Forming Reductive Elimination from Well-Defined Copper(III) Complexes. *J. Am. Chem. Soc.* **2019**, *141*, 3153.

[164] D. M. Ferguson, J. R. Bour, A. J. Canty, J. W. Kampf, M. S. Sanford. Aryl–CF_3 Coupling from Phosphinoferrocene-Ligated Palladium(II) Complexes. *Organometallics* **2019**, *38*, 519.

[165] V. I. Bakhmutov, F. Bozoglian, K. Gómez, G. González, V. V. Grushin, S. A. Macgregor, E. Martin, F. M. Miloserdov, M. A. Novikov, J. A. Panetier, L. V. Romashov. CF_3–Ph Reductive Elimination from $[(Xantphos)Pd(CF_3)(Ph)]$. *Organometallics* **2012**, *31*, 1315.

[166] P. Anstaett, F. Schoenebeck. Reductive Elimination of $ArCF_3$ from Bidentate Pd^{II} Complexes: A Computational Study. *Chem. Eur. J.* **2011**, *17*, 12340.

[167] N. D. Ball, J. W. Kampf, M. S. Sanford. Aryl−CF_3 Bond-Forming Reductive Elimination from Palladium(IV). *J. Am. Chem. Soc.* **2010**, *132*, 2878.

[168] N. D. Ball, J. B. Gary, Y. Ye, M. S. Sanford. Mechanistic and Computational Studies of Oxidatively-Induced Aryl−CF_3 Bond-Formation at Pd: Rational Design of Room Temperature Aryl Trifluoromethylation. *J. Am. Chem. Soc.* **2011**, *133*, 7577.

[169] D. C. Powers, E. Lee, A. Ariafard, M. S. Sanford, B. F. Yates, A. J. Canty, T. Ritter. Connecting Binuclear Pd(III) and Mononuclear Pd(IV) Chemistry by Pd–Pd Bond Cleavage. *J. Am. Chem. Soc.* **2012**, *134*, 12002.

[170] G. G. Dubinina, W. W. Brennessel, J. L. Miller, D. A. Vicic. Exploring Trifluoromethylation Reactions at Nickel: A Structural and Reactivity Study. *Organometallics* **2008**, *27*, 3933.

[171] J. Jover, F. M. Miloserdov, J. Benet-Buchholz, V. V. Grushin, F. Maseras. On the Feasibility of Nickel-Catalyzed Trifluoromethylation of Aryl Halides. *Organometallics* **2014**, *33*, 6531.

[172] L. S. Jongbloed, N. Vogt, A. Sandleben, B. de Bruin, A. Klein, J. I. van der Vlugt. Nickel–Alkyl Complexes with a Reactive PNC-Pincer Ligand. *Eur. J. Inorg. Chem.* **2018**, 2408.

[173] J. R. Bour, P. Roy, A. J. Canty, J. W. Kampf, M. S. Sanford. Oxidatively Induced Aryl–CF_3 Coupling at Diphosphine Nickel Complexes. *Organometallics* **2020**, *39*, 3.

[174] J. R. Bour, N. M. Camasso, E. A. Meucci, J. W. Kampf, A. J. Canty, M. S. Sanford. Carbon–Carbon Bond-Forming Reductive Elimination from Isolated Nickel(III) Complexes. *J. Am. Chem. Soc.* **2016**, *138*, 16105.

[175] F. D'Accriscio, P. Borja, N. Saffon-Merceron, M. Fustier-Boutignon, N. Mézailles, N. Nebra. C−H Bond Trifluoromethylation of Arenes Enabled by a Robust, High-Valent Nickel(IV) Complex. *Angew. Chem. Int. Ed.* **2017**, *56*, 12898; *Angew. Chem.* **2017**, *129*, 13078.

[176] P. J. Brothers, W. R. Roper. Transition-Metal Dihalocarbene Complexes. *Chem. Rev.* **1988**, *88*, 1293.

[177] G. R. Clark, S. V. Hoskins, W. R. Roper. Difluorocarbene complexes of ruthenium derived from trifluoromethyl compounds. $RuCl_2(CF_2)(CO)(PPh_3)_2$, $RuCl_2(CFNMe_2)(CO)(PPh_3)_2$, $RuCl_2(CFOMe)(CO)(PPh_3)_2$ and the structure of $Ru(CF_3)(HgCF_3)(CO)_2(PPh_3)_2$. *J. Organomet. Chem.* **1982**, *234*, C9.

[178] D. Huang, P. R. Koren, K. Folting, E. R. Davidson, K. G. Caulton. Facile and Reversible Cleavage of C−F Bonds. Contrasting Thermodynamic Selectivity for Ru−CF_2H vs F−Os=CFH. *J. Am. Chem. Soc.* **2000**, *122*, 8916.

[179] a) C. J. Bourgeois, R. P. Hughes, J. Yuan, A. G. DiPasquale, A. L. Rheingold. α- and β-Fluorine Elimination Reactions Induced by Reduction of Iridium−Fluoroalkyl Complexes. Selective Formation of Fluoroalkylidene and Hydrofluoroalkene Ligands. *Organometallics* **2006**, *25*, 2908; b) R. P. Hughes, R. B. Laritchev, J. Yuan, J. A. Golen, A. N. Rucker, A. L. Rheingold. A Simple Route to Difluorocarbene and Perfluoroalkylidene Complexes of Iridium. *J. Am. Chem. Soc.* **2005**, *127*, 15020.

[180] T. G. Appleton, R. D. Berry, J. R. Hall, D. W. Neale. Displacement of norbornadiene (NBD) from $Pt(CF_3)_2(NBD)$ by weak donor ligands L, and reactions of *cis*-$Pt(CF_3)_2L_2$ with water and acids. *J. Organomet. Chem.* **1989**, *364*, 249.

[181] a) S. Martínez-Salvador, J. Forniés, A. Martín, B. Menjón, I. Usón. Stepwise Degradation of Trifluoromethyl Platinum(II) Compounds. *Chem. Eur. J.* **2013**, *19*, 324; b) S. Martínez-Salvador, B. Menjón, J. Forniés, A. Martín, I. Usón. Trapping a Difluorocarbene–Platinum Fragment by Base Coordination. *Angew. Chem. Int. Ed.* **2010**, *49*, 4286; *Angew. Chem.* **2010**, *122*, 4382.

[182] D. J. Harrison, A. L. Daniels, I. Korobkov, R. T. Baker. d^{10} Nickel Difluorocarbenes and Their Cycloaddition Reactions with Tetrafluoroethylene. *Organometallics* **2015**, *34*, 5683.

[183] G. M. Lee, I. Korobkov, R. T. Baker. d^8 Nickel and palladium difluorocarbenes derived from trifluoromethyl POCOP-type pincer complexes. *J. Organomet. Chem.* **2017**, *847*, 270.

[184] M. A. Willert-Porada, D. J. Burton, N. C. Baenziger. Synthesis and X-Ray Structure of Bis(trifluoromethyl)(*N*,*N*-diethyldithiocarbamato)-copper; a Remarkably Stable Perfluoroalkylcopper(III) Complex. *J. Chem. Soc., Chem. Commun.* **1989**, 1633.

[185] R. Eujen, B. Hoge, D. J. Brauer. Preparation and NMR Spectra of the (Trifluoromethyl)argentates(III) $[Ag(CF_3)_nX_{4-n}]^-$, with X = CN (n = 1−3), CH_3, $C{\equiv}CC_6H_{11}$, Cl, Br (n = 2, 3), and I (n = 3), and of Related Silver(III) Compounds. Structures of $[PPh_4][trans\text{-}Ag(CF_3)_2(CN)_2]$ and $[PPh_4][Ag(CF_3)_3(CH_3)]$. *Inorg. Chem.* **1997**, *36*, 1464.

[186] D. Joven-Sancho, M. Baya, A. Martín, J. Orduna, B. Menjón. The First Organosilver(III) Fluoride, $[PPh_4][(CF_3)_3AgF]$. *Chem. Eur. J.* **2020**, *26*, 4471.

[187] B. Menjón, S. Martínez-Salvador, M. A. Gómez-Saso, J. Forniés, L. R. Falvello, A. Martín, A. Tsipis. Oxidative Addition of Halogens to Homoleptic Perfluoromethyl or Perfluorophenyl Derivatives of Platinum(II): A Comparative Study. *Chem. Eur. J.* **2009**, *15*, 6371.

[188] S. Martínez-Salvador, P. J. Alonso, J. Forniés, A. Martín, B. Menjón. Efficient and stereoselective syntheses of isomeric trifluoromethyl-platinum(IV) chlorides. *Dalton Trans.* **2011**, *40*, 10440.

[189] J. M. Racowski, N. D. Ball, M. S. Sanford. C–H Bond Activation at Palladium(IV) Centers. *J. Am. Chem. Soc.* **2011**, *133*, 18022.

[190] a) E. Chong, J. W. Kampf, A. Ariafard, A. J. Canty, M. S. Sanford. Oxidatively Induced C–H Activation at High Valent Nickel. *J. Am. Chem. Soc.* **2017**, *139*, 6058; b) E. A. Meucci, N. M. Camasso, M. S. Sanford. An Organometallic Ni^{IV} Complex That Participates in Competing Transmetalation and $C(sp^2)$–O Bond-Forming Reductive Elimination Reactions. *Organometallics* **2017**, *36*, 247.

[191] A. Maleckis, M. S. Sanford. Facial Tridentate Ligands for Stabilizing Palladium(IV) Complexes. *Organometallics* **2011**, *30*, 6617.

[192] a) R. J. Lagow, L. L. Gerchman, R. A. Jacob (Massachusetts Institute of Technology, Cambridge, MA), US-A 3992424, 1976, p. 7; [R. J. Lagow, L. L. Gerchman, R. A. Jacob, *Chem. Abstr.* **1977**, *86*, 72887]; b) R. J. Lagow, L. L. Gerchman, R. A. Jacob (Massachusetts Institute of Technology, Cambridge, MA), US-A 3954585, 1976, p. 8; [R. J. Lagow, L. L. Gerchman, R. A. Jacob, *Chem. Abstr.* **1976**, *85*, 160324].

[193] S. Martínez-Salvador, J. Forniés, A. Martín, B. Menjón. Highly Trifluoromethylated Platinum Compounds. *Chem. Eur. J.* **2011**, *17*, 8085.

[194] F. H. Brain, C. S. Gibson. The Organic Compounds of Gold. Part VII. Methyl and Ethyl Compounds. *J. Chem. Soc.* **1939**, 762.

[195] A. Johnson, R. J. Puddephatt. Oxidative addition reactions of methylgold(I) compounds. *Inorg. Nucl. Chem. Lett.* **1973**, *9*, 1175.

[196] H. K. Nair, J. A. Morrison. Formation of group 11 trifluoromethyl derivatives by reaction of $Cd(CF_3)_2{\cdot}$glyme with representative Au, Ag, and Cu complexes: isolation of $Au(CF_3)_3(PMe_3)$, $Au(CF_3)_3(PEt_3)$, $AuI(CF_3)_2(PMe_3)$, $AuCF_3(PMe_3)$, $AuCF_3(PEt_3)$ and $AgCF_3(PMe_3)$; observation of $CuCF_3(PMe_3)$. *J. Organomet. Chem.* **1989**, *376*, 149.

[197] A. Portugués, I. López-García, J. Jiménez-Bernad, D. Bautista, J. Gil-Rubio. Photoinitiated Reactions of Haloperfluorocarbons with Gold(I) Organometallic Complexes: Perfluoroalkyl Gold(I) and Gold(III) Complexes. *Chem. Eur. J.* **2019**, *25*, 15535.

[198] a) A. Luquin, E. Cerrada, M. Laguna, in *Gold Chemistry: Applications and Future Directions in the Life Sciences* (Ed.: F. Mohr), Wiley-VCH, Weinheim, **2009**, pp. 93−181; b) R. Usón, A. Laguna. Recent Development in arylgold chemistry. *Coord.*

Chem. Rev. **1986**, *70*, 1; c) R. Usón. Some new developments in aryl-gold and aryl-platinum chemistry. *Pure Appl. Chem.* **1986**, *58*, 647; d) R. Usón, A. Laguna, J. Vicente. Arylgold Chemistry. *Synth. React. Inorg. Met.-Org. Chem.* **1977**, *7*, 463.

[199] S. Martínez-Salvador, L. R. Falvello, A. Martín, B. Menjón. Gold(I) and Gold(III) Trifluoromethyl Derivatives. *Chem. Eur. J.* **2013**, *19*, 14540.

[200] S. Komiya, T. A. Albright, R. Hoffmann, J. K. Kochi. The Stability of Organogold Compounds. Hydrolytic, Thermal, and Oxidative Cleavages of Dimethylaurate(I) and Tetramethylaurate(III). *J. Am. Chem. Soc.* **1977**, *99*, 8440.

[201] D. Zhu, S. V. Lindeman, J. K. Kochi. X-ray Crystal Structures and the Facile Oxidative (Au−C) Cleavage of the Dimethylaurate(I) and Tetramethylaurate(III) Homologues. *Organometallics* **1999**, *18*, 2241.

[202] a) A. Gräfe, T. Kruck. Übergangsmetall-Trifluormethyl-Komplexe: Erste Trifluormethyl-Komplexe von Gold mit Fluorphosphan-Liganden. *J. Organomet. Chem.* **1996**, *506*, 31; b) R. D. Sanner, J. H. Satcher, Jr., M. W. Droege. Synthesis and Characterization of (Trifluoromethyl)gold Complexes. *Organometallics* **1989**, *8*, 1498.

[203] N. H. Dryden, J. G. Shapter, L. L. Coatsworth, P. R. Norton, R. J. Puddephatt. $[CF_3Au(C{\equiv}NMe)]$ as a Precursor for CVD of Gold. *Chem. Mater.* **1992**, *4*, 979.

[204] Y. Usui, J. Noma, M. Hirano, S. Komiya. C−Si bond cleavage of trihalomethyltrimethylsilane by alkoxo- and aryloxogold or -copper complexes. *Inorg. Chim. Acta* **2000**, *309*, 151.

[205] D. Zopes, S. Kremer, H. Scherer, L. Belkoura, I. Pantenburg, W. Tyrra, S. Mathur. Hydrolytic Decomposition of Tetramethylammonium Bis(trifluoromethyl)aurate(I), $[NMe_4][Au(CF_3)_2]$: A Route for the Synthesis of Gold Nanoparticles in Aqueous Medium. *Eur. J. Inorg. Chem.* **2011**, 273.

[206] D. Zopes, C. Hegemann, W. Tyrra, S. Mathur. $[(CF_3)_4Au_2(C_5H_5N)_2]$ – a new alkyl gold(II) derivative with a very short Au–Au bond. *Chem. Commun.* **2012**, *48*, 8805.

[207] A. G. Tskhovrebov, J. B. Lingnau, A. Fürstner. Gold Difluorocarbenoid Complexes: Spectroscopic and Chemical Profiling. *Angew. Chem. Int. Ed.* **2019**, *58*, 8834; *Angew. Chem.* **2019**, *131*, 8926.

[208] S. Martínez-Salvador, J. Forniés, A. Martín, B. Menjón. $[Au(CF_3)(CO)]$: A Gold Carbonyl Compound Stabilized by a Trifluoromethyl Group. *Angew. Chem. Int. Ed.* **2011**, *50*, 6571; *Angew. Chem.* **2011**, *123*, 6701.

[209] S. Martínez-Salvador, L. R. Falvello, A. Martín, B. Menjón. A hexanuclear gold carbonyl cluster. *Chem. Sci.* **2015**, *6*, 5506.

[210] X.-G. Xiong, P. Pyykkö. Unbridged Au(II)–Au(II) bonds are theoretically allowed. *Chem. Commun.* **2013**, *49*, 2103.

[211] H. H. Murray, J. P. Fackler, Jr., L. C. Porter, D. A. Briggs, M. A. Guerra, R. J. Lagow. Synthesis and X-ray Crystal Structures of $[Au(CH_2)_2PPh_2]_2(CF_3)_2$, $[Au(CH_2)_2PPh_2]_2(C_6F_5)_2$, and $[PPN][Au(C_6F_5)_4]$: Two Dinuclear Gold(II) Ylide Complexes Containing Alkyl and Aryl Ligands and a Tetrakis(pentafluorophenyl)aurate(III) Anion Complex. *Inorg. Chem.* **1987**, *26*, 357.

[212] A. Johnson, R. J. Puddephatt. Reactions of Trifluoromethyl Iodide with Methylgold(I) Complexes. Preparation of Trifluoromethyl-gold(I) and -gold(III) Complexes. *J. Chem. Soc., Dalton Trans.* **1976**, 1360.

[213] F. Glockling, V. B. Mahale. Bis-(trimethylsilyl)methylgold(I) and tris-(trimethylsilyl)methylgold(I) complexes. *J. Chem. Res. (S)* **1978**, 170.

[214] M. S. Winston, W. J. Wolf, F. D. Toste. Photoinitiated Oxidative Addition of CF_3I to Gold(I) and Facile Aryl-CF_3 Reductive Elimination. *J. Am. Chem. Soc.* **2014**, *136*, 7777.

[215] J. L. Margrave, K. H. Whitmire, R. H. Hauge, N. T. Norem. Synthesis and Characterization of Bis(trifluoromethyl)gold m-Halide Dimers: X-ray Structural Characterization of $[Au(CF_3)_2(\mu\text{-}I)]_2$. *Inorg. Chem.* **1990**, *29*, 3252.

[216] U. Preiss, I. Krossing. A Computational Study of $[M(CF_3)_4]^-$ (M = Cu, Ag, Au) and their Properties as Weakly Coordinating Anions. *Z. Anorg. Allg. Chem.* **2007**, *633*, 1639.

[217] a) J. A. Schlueter. Tetrathiafulvalene-Based Conductors Containing Organometallic Components. *Top. Organomet. Chem.* **2009**, *27*, 1; b) U. Geiser, J. A. Schlueter. Conducting Organic Radical Cation Salts with Organic and Organometallic Anions. *Chem. Rev.* **2004**, *104*, 5203; c) J. A. Schlueter, U. Geiser, A. M. Kini, H. H. Wang, J. M. Williams, D. Naumann, T. Roy, B. Hoge, R. Eujen. Trifluoromethylmetallate anions as components of molecular charge transfer salts and superconductors. *Coord. Chem. Rev.* **1999**, *190-192*, 781; d) J. A. Schlueter, U. Geiser, J. M. Williams, J. D. Dudek, M. E. Kelly, J. P. Flynn, R. R. Wilson, H. I. Zakowicz, P. P. Sche, D. Naumann, T. Roy, P. G. Nixon, R. W. Winter, G. L. Gard. Rational Design of Organic Superconductors Through the Use of the Large, Discrete Molecular Anions $M(CF_3)_4^-$ (M= Cu, Ag, Au) and $SO_3CF_2CH_2SF_5^-$. *Synth. Met.* **1997**, *85*, 1453; e) J. A. Schlueter, J. M. Williams, U. Geiser, H. H. Wang, A. M. Kini, M. E. Kelly, J. D. Dudek, D. Naumann, T. Roy. New Organic Superconductors in the System $(ET)_2M(CF_3)_4$(Solvent) (*M* = Cu, Ag, Au): Dramatic Effects of Organometallic Anion and Solvent Replacement. *Mol. Cryst. Liq. Cryst.* **1996**, *285*, 43; f) J. A. Schlueter, U. Geiser, H. H. Wang, M. E. Kelly, J. D. Dudek, J. M. Williams, D. Naumann, T. Roy. Synthesis and Physical Properties of a Novel, Highly Tunable Family of Organic Superconductors: $(ET)_2M(CF_3)_4$(1,1,2-trihaloethane) (M = Cu, Ag, Au). *Mol. Cryst. Liq. Cryst.* **1996**, *284*, 195; g) J. A. Schlueter, J. M. Williams, U. Geiser, J. D. Dudek, S. A. Sirchio, M. E. Kelly, J. S. Gregar, W. H. Kwok, J. A. Fendrich, J. E. Schirber, W. R. Bayless, D. Naumann, T. Roy. Synthesis and Characterization of Two New Organic Superconductors, k_L- and k_H-[Bis(ethylenedisulfanyl)tetrathiafulvalene]$_2Au(CF_3)_4$·(1,1,2-Trichloroethane) *via* Microelectrocrystallization. *J. Chem. Soc., Chem. Commun.* **1995**, 1311.

[218] R. Bhattacharjee, A. Nijamudheen, A. Datta. Direct and Autocatalytic Reductive Elimination from Gold Complexes ([$(Ph_3P)Au(Ar)(CF_3)(X)$], X = F, Cl, Br, I): The Key Role of Halide Ligands. *Chem. Eur. J.* **2017**, *23*, 4169.

[219] S. Liu, K. Kang, S. Liu, D. Wang, P. Wei, Y. Lan, Q. Shen. The Difluoromethylated Organogold(III) Complex *cis*-$[Au(PCy_3)(4\text{-}F\text{-}C_6H_4)(CF_2H)(Cl)]$: Preparation, Characterization, and Its $C(sp^2)$–CF_2H Reductive Elimination. *Organometallics* **2018**, *37*, 3901.

[220] S. Kim, F. D. Toste. Mechanism of Photoredox-Initiated C−C and C−N Bond Formation by Arylation of IPrAu(I)−CF_3 and IPrAu(I)−Succinimide. *J. Am. Chem. Soc.* **2019**, *141*, 4308.

[221] M. D. Levin, T. Q. Chen, M. E. Neubig, C. M. Hong, C. A. Theulier, I. J. Kobylianskii, M. Janabi, J. P. O'Neil, F. D. Toste. A catalytic fluoride-rebound mechanism for $C(sp^3)$-CF_3 bond formation. *Science* **2017**, *356*, 1272.

Objectives

Fluorine and fluorinated groups confer distinct properties to transition metal centers to which they get bound. In particular, the simplest perfluorinated ligand, CF_3, has special properties that substantially differ from those of the methyl group and, for instance, leads to more stable transition-metal complexes. In comparison with the huge progress made in the last decades in organogold chemistry and gold catalysis, the chemistry of gold perfluoroalkyl compounds has remained much less developed. Gold trifluoromethyl complexes exhibit singular structural and chemical properties, which make them potentially interesting for a number of applications. On the other hand, organogold fluoride complexes were unknown before 2005 and are therefore a relatively new class of compounds, with still few representatives. Nowadays, they are of exceptional interest because of their important role in a wide variety of gold-mediated and gold-catalyzed fluorination processes.

The main purpose of this Thesis is to study the fundamental chemistry of organogold complexes containing up to three CF_3 groups, with special focus on molecules also containing fluoride ligands. Following their syntheses and characterization, we will investigate their properties, including stability, reactivity, and behavior in the gas phase, where only intramolecular processes operate. Under these unimolecular conditions we have been able to detect rare and highly unstable species, which are usually elusive in the condensed phase.

The known complex $[PPh_4][CF_3AuCF_3]$ has been our starting material from which most of our new compounds are derived. Typical reagents enabling to obtain organogold(III) complexes from this Au(I) precursor include halogens, XeF_2 and CF_3I. In this regard, we were particularly interested in the study of the properties of the rather unexplored $(CF_3)_3Au$ unit and its derivatives, since trimethyl gold has been a key species in organogold chemistry but little knowledge existed on its perfluorinated analogue previous to this work.

Methodology

M.1. General synthetic procedures and materials

Unless otherwise stated, reactions and manipulations were carried out under purified argon using Schlenk techniques in oven-dried or flame-dried glassware. Previously degassed solvents were dried with an MBraun SPS-800 System in case of CH_2Cl_2, Et_2O, *n*-hexane and thf. All other solvents, namely acetone, acetonitrile and isopropanol, were dried over activated 3 Å molecular sieves prior to degasification. Deuterated solvents for NMR spectroscopy were also dried over activated 4Å (CD_2Cl_2) or 3Å (CD_3CN) molecular sieves and next degassed.

In all the work presented in this Thesis, compound $[PPh_4][CF_3AuCF_3]$ (**I**) is used as the starting material. Its preparation was carried out as described a few years ago in our group,[1] and needs AuCl(tht) as precursor, which was prepared according to a literature procedure.[2] The synthesis of complex **I** consists on the coordination of two CF_3 groups to a gold center by means of Me_3SiCF_3 in the presence of CsF. In Chapter 2 and Chapter 3, compound **I** is directly used to access compounds of different stoichiometries; i.e. $[\textit{trans}\text{-}(CF_3)_2AuX_2]^-$ complexes (Chapter 2) and derivatives containing the fragment $(CF_3)_3Au$ (Chapter 3). However, the starting material for the synthesis of compounds described in Chapter 1 is CF_3AuCO (**II**), which is obtained upon low-temperature treatment of **I** with $BF_3{\cdot}OEt_2$ in CH_2Cl_2. This synthetic procedure to obtain **II** was recently developed in our group[1,3] and the suitability of this compound as a useful synthon of the CF_3Au fragment was also explored.[1,4] The synthesis of $[PPh_4][(CF_3)_3AuI]$ (**22**), which is described in Chapter 3 and was used as a starting material for further reactions, was scaled up to obtain 2.5 g.

All other chemicals were purchased from standard commercial suppliers and used as received. Solutions (0.25 M) of Cl_2 and Br_2 were prepared by passing a slow stream of dry Cl_2*(g)* through CCl_4 or by diluting a measured volume of Br_2 in CCl_4, respectively. Both of them were titrated before use. The solution (1.857 M) of CF_3I in *n*-hexane was prepared by condensing a measured volume of dry CF_3I*(g)* and subsequent addition of a measured amount of dry *n*-hexane. Samples of AgCl and AgBr were prepared by precipitation from aqueous solutions of $AgNO_3$ with the corresponding halide. Finally, we had to be especially cautious when using $AgClO_4$ for the synthesis of $(CF_3)_3Au{\cdot}OEt_2$ (**28**), since perchlorate salts are potentially explosive when in contact with organic solvents and ligands.[5] For this reason, only small amounts of **28** were prepared and we

did not actually encounter any problem working under the conditions described in this Thesis. In spite of its potential explosive character, $AgClO_4$ was used because the resulting $[PPh_4]ClO_4$ salt formed in the synthesis of **28** can be cleanly removed (see Chapter 3).

M.2. Characterization techniques

Different spectroscopic and analytical techniques have been used for the characterization of the compounds prepared in this Thesis. The equipment used and the procedures associated to each technique are described in the following sections.

M.2.1. Nuclear Magnetic Resonance

Nuclear magnetic resonance (NMR) spectroscopy is the most powerful and probably the most widespread technique for the characterization of diamagnetic compounds in solution in the field of inorganic chemistry.[6] In fact, it often allows to fully establish the molecular configuration of a precise species. ^{1}H and ^{13}C are by far the most useful nuclei to be routinely measured not only in organic chemistry and biochemistry laboratories, but also in research in organometallic and coordination chemistry.

In the field of fluorine and organofluorine chemistry, ^{19}F arises as the most helpful nucleus to be measured, since it possesses a nuclear spin I = ½, and ^{19}F NMR spectroscopy becomes the most powerful technique to structurally characterize fluorinated compounds in solution.[7] In addition, its natural abundance of 100% and its high gyromagnetic ratio (about 0.94 times that of ^{1}H) make ^{19}F a “routine” spin that can be easily measured. The range of chemical shifts, δ_F, covers a region of around 600 ppm. Hence, δ_F changes substantially with a small variation in the structure of the studied molecule. The most accepted internal reference for the measurement of ^{19}F NMR spectra is trichlorofluoromethane ($CFCl_3$).[8] However, other secondary references such as trifluoroacetic acid, hexafluorobenzene, trifluoromethylbenzene or ethyl trifluoroacetate have been used, especially in the past. Furthermore, coupling constants between chemically inequivalent ^{19}F nuclei or between ^{19}F and neighboring ^{1}H, ^{13}C or ^{31}P nuclei are very variable and characteristic of the environment. It is also interesting to

note that, despite $^{1}H–^{1}H$ coupling, $^{19}F–^{19}F$ coupling can be transmitted both through bonds and through space.[7]

In the case of metal trifluoromethyl complexes, [M]–CF_3 chemical shifts are usually found between +40 and –40 ppm (relative to the $CFCl_3$ reference).[7] In the particular case of gold trifluoromethyl compounds, it has been observed that ^{19}F chemical shifts appear in a much narrower range in Au(I) complexes (less than 10 ppm) than in Au(III) derivatives (more than 35 ppm).[9] However, the range in which fluoride ligands [M]–F appear is extremely large, from positive numbers up to +164.5 ppm in WF_6,[7] to negative δ_F lower than –300 ppm, as in some recently-reported organogold(III) fluoride complexes *trans*-AuF_2(SIMes)X.[10]

^{19}F NMR spectroscopy has been the most widely used technique in the development of this Thesis, not only to characterize the final isolated products, but also to follow the progress of the reactions and check if a process was finished, or to characterize the products arising from the thermolysis of a specific complex. Additionally, ^{1}H, ^{13}C and ^{31}P NMR spectra have been recorded when the characterization of a species required it. In relation to this, $^{19}F–^{19}F$ decoupling experiments or two-dimensional $^{19}F–^{19}F$ and $^{1}H–^{1}H$ COSY experiments have aided in characterizing the prepared complexes when needed.

NMR spectra were recorded on Bruker ARX 300 or AV 400 spectrometers. Most of the measurements were carried out at room temperature. However, in the case of thermally unstable products or dynamic processes which required to be slowed down, measurements were performed at lower temperatures. Chemical shifts (δ in ppm) are given with respect to the standard references: $SiMe_4$ (^{1}H and ^{13}C), $CFCl_3$ (^{19}F), and 85% aqueous H_3PO_4 (^{31}P). NMR parameters associated with the $[PPh_4]^+$ and $[PPh_3CH_2Ph]^+$ are unexceptional and are not described at any point. Simulations of NMR spectra which required to be satisfactorily analyzed were carried out using gNMR.[11]

Trace solvents appearing in ^{1}H and ^{13}C spectra have been assigned according to literature values.[12] Different literature sources have been also used to assign the ^{19}F NMR signals and to identify the organic fluorinated products arising from the thermolyses of the different complexes.[8,13] Gold trifluoromethyl species were identified according to a previous report[14] or with the aid of previous results obtained during the development of this Thesis.

M.2.2. Infrared spectroscopy

Infrared (IR) spectroscopy allows to know which functional groups exist in a molecule, according to their characteristic vibrational frequencies. Within the framework of this Thesis, IR has been especially useful in the characterization of metal–halide (M–X) bonds. In coordination complexes, these vibrations depend on the oxidation number of the metal center, its mass and its coordination number, as well as on the stereochemistry of the precise species.[15] The M–X stretching bands appear in a specific region depending on the halide ligand.[16] The stretching frequencies of terminal M–X bonds in organometallic complexes decrease on going down the halogen group: 800–400 cm^{-1} for ν(M–F), 550–200 cm^{-1} for ν(M–Cl), 450–140 cm^{-1} for ν(M–Br) and 260–100 cm^{-1} for ν(M–I). Similarly, the C≡N bond exhibits also a characteristic stretching frequency, usually in the 2000–2300 cm^{-1} range,[17] which is very useful for identifying complexes containing ligands such as cyano,[18] nitriles[19] or isonitriles.[20] Complexes containing these ligands are also described in this work.

The IR spectra of the complexes presented in this Thesis were recorded on neat solid samples using a PerkinElmer Spectrum FT–IR spectrometer (4000–250 cm^{-1}) equipped with an ATR (attenuated total reflectance) device, therefore avoiding any sample preparation. Due to the range of measurement, no M–Br or M–I could be observed.

M.2.3. Mass spectrometry

Mass spectrometry is a very sensitive technique which is useful for determining the composition (empirical formula) of a compound under study as long as gaseous ions can be produced from it.[21] It has the additional advantage that very little amount of sample is required to perform the analysis. In mass spectrometers, gas-phase ions are generated, separated according to their mass-to-charge ratio (*m/z*) using electric or magnetic fields in a high-vacuum and counted in a detector. Several methods are available for the ionization of the sample, as well as for the separation of the ions by their *m/z* ratio.

With the aim of characterizing the anionic compounds presented in this Thesis, matrix-assisted laser desorption/ionization (MALDI) or electrospray ionization (ESI) have been used to generate the gaseous ion species.[21,22] MALDI uses a solid matrix which is co-crystallized along with the sample. A short UV-laser pulse vaporizes the sample and the

matrix at the same time, forming a dense gas cloud that expands supersonically into the vacuum and ions are generated during this expansion. In the case of ESI, which is a soft ionization method that does not barely fragment the parent species, ions are directly transferred from solution into the gas phase. In particular, a fine aerosol is created in a strong electric field from a solution containing the ionic species under study. Evaporation of the solvent contained in the drops results in the generation of individually charged ions.

Standard mass spectra (MS) of the anionic species presented in this Thesis were registered by MALDI-TOF techniques on Bruker MicroFlex or AutoFlex spectrometers, using DCTB (*trans*-2-[3-(4-*tert*-butylphenyl)-2-methyl-2-propenylidene]malononitrile) as the matrix in all cases due to its good performance. High-resolution mass spectra (HRMS) were registered using electrospray ionization (ESI) techniques on a MicroToF-Q (Bruker Daltonics) spectrometer, using sodium formate clusters as external reference. No clear peaks were detected for any of the neutral species described in this Thesis by using either positive or negative MALDI or ESI techniques.

M.2.4. Single crystal X-ray diffraction

X-ray diffraction analysis on single crystals provides structural information of the complex under study. Fluoride complexes as those reported in this Thesis have the problem of being moisture sensitive and therefore, M–F bonds can be easily hydrolyzed. This leads to two challenges when using this technique to characterize gold fluoride complexes:[23] (a) handling of moisture-sensitive crystals, and (b) distinguishing between Au–OH and Au–F bonds. The second problem arises from the fact that both ligands have similar electron density, but it can be overcome if the data quality is enough to identify the Au–OH proton in a difference electron density map. The structures of two fluoride complexes are presented in this Thesis, $[PPh_4][$*trans*-$(CF_3)_2AuF_2]$ (**12**) (Chapter 2) and $[PPh_4][(CF_3)_3AuF]$ (**24**) (Chapter 3). In both cases, no hydrogen atom corresponding to an OH group was found in the difference electron density map. Furthermore, the ^1H and ^{19}F NMR of the single crystals were recorded after the data collection and the mass spectra (ESI–) were registered, checking that the Au–F bonds were not hydrolyzed.

Regarding the CF_3 groups, they usually appear highly disordered over two or more positions.[24] Two reasons account for this rotational disorder: (a) they exhibit a high symmetry, and (b) the rotation around a threefold symmetry axis has a very low energy barrier. Hence, they have to be modeled by using soft restraints as two sets of positions with the same or different partial occupancies summing to unity.

During the development of this Thesis, single crystals suitable of X-ray diffraction analysis were obtained by slow evaporation of the solvent of a saturated solution of the corresponding compound or by slow diffusion of a layer of a solvent in which the complex is insoluble into a solution of the corresponding compound, both solvents being miscible.

X-ray intensity data were collected on an Oxford Diffraction Xcalibur diffractometer. The radiation used in all cases was graphite-monochromated Mo-Kα (λ = 71.073 pm). The diffraction frames were integrated and corrected from absorption by using the program CrysAlisPro.[25] The structures were solved by Patterson and Fourier methods and refined by full-matrix least squares on F^2 with ShelxL.[26] All non-H atoms were assigned anisotropic displacement parameters and refined without positional constraints. All H atoms were constrained to idealized geometries and assigned isotropic displacement parameters equal to 1.2 times the U_{iso} values of their attached parent atoms.

M.2.5. Elemental analyses

Elemental analysis allows to determine the weight percentage of carbon, hydrogen, nitrogen and sulfur in the compound under analysis. Additionally, if the composition of the complex is known in advance, for example by means of HRMS, elemental analyses serve as an indication of the sample purity by comparison of the obtained values against those expected for the pure compound.[21]

In this Thesis, elemental analyses were performed to check the purity of the samples. The analyses of all the compounds were carried out with a PerkinElmer 2400 CHNS/O Series II microanalyzer.

M.3. Tandem mass spectrometry (MS^n)

The gas phase chemistry of gold has been thoroughly investigated in the last decades, since the study of gold complexes in the gas phase under high-vacuum conditions is one of the best methods to investigate and understand their fundamental properties.[27] The main advantage is that they allow a high level of control over the experimental conditions, therefore circumventing some of the problems arising when studying condensed-phase reactivity. Some of these complications include the presence of solvent molecules or counter ions that can interact with the species under study, or the formation of new species (oligomers, etc.) present in complex equilibria. Moreover, gas-phase experiments open up a great opportunity to investigate highly unstable and reactive species, sometimes containing elements in unusual oxidation states, owing to the lack of interactions between the mass-selected ions with the environment and also among themselves. The results obtained in gas-phase experiments are better understood with the aid of computational calculations and, at the same time, these experiments serve to validate calculated properties of gold complexes. In fact, the improved performance of theoretical methods to accurately describe metal complexes and the progress done in the equipment for gas-phase experiments have led to a better understanding not only of the fundamental chemistry of coinage-metal complexes, but have also indirectly helped gain knowledge on condensed-phase processes.[28]

The technique of tandem mass spectrometry (MS/MS or MS^n, where *n* is the number of stages of mass spectrometry) has been widely used to study the gas phase chemistry of organogold complexes.[29] In particular, it has served to investigate the fragmentation reactions of organogold ions aiming at identifying their structures or their unimolecular decomposition pathways. Charged species, as the anionic complexes presented in this Thesis, can be easily brought into the gas phase via electrospray ionization (ESI; see Section M.2.3). At this point, two possibilities exist: either more than one mass analyzer needs to be used to separate ions according to their *m/z* ratio, or the ions are trapped in a small volume of space where repeated experiments can be performed. Both of them will be further described below. The ions must be then fragmented, which is usually achieved by means of collision-induced dissociation (CID).[30] This activation method consists in the thermal excitation of the ions upon collision with an inert gas such as helium. Some of the translational energy of the accelerated ions is transformed into

internal energy and the increase of the latter induces the unimolecular decomposition or fragmentation of these excited ions.

One the most used analyzers in tandem mass spectrometry is the quadrupole ion trap (or simply ion trap) due to its versatility and good capabilities to performing several MS/MS operations (MS^n).[31] Once the gaseous ions are injected into the ion trap, they are captured inside and their trajectories controlled through oscillating electric fields. The ions of a specific *m/z* ratio are retained in the trap by selectively ejecting all others, and are afterwards excited by CID (MS^2). The fragment ions are then detected to generate a daughter ion mass spectrum and can also be subsequently studied. The next stage of the experiment, MS^3, is achieved by ejecting all other fragment ions except the new one under study from the trap, and repeating the same operations as in the MS^2 experiment just described. Therefore, reiterated MS/MS operations are separated in time, yet take place in the same ion trap. The combination of the capabilities of the quadrupole ion trap and ESI as the ionization technique, provides a powerful "complete gas-phase chemical laboratory", as stated by Prof. O'Hair.[32]

On the other hand, tandem mass spectrometry can also be carried out in a quadrupole/orthogonal-ToF (Time-of-Flight) spectrometer (Q-ToF), where ions are thermally excited by CID in a collision cell placed between two analyzers.[31] In these instruments, a single ion is selected as passing through a quadrupole (MS^1) and then arrives to a collision cell within which it is fragmented. Finally, the ionic fragments formed by CID are introduced in an orthogonal-ToF analyzer (MS^2), which is used to separate the fragments according to their *m/z* ratio and collect the daughter ion spectrum. In the ToF analyzer, ions are accelerated by an electric field for a specific time and then are allowed to travel freely along a tube. Since the lightest ions will acquire higher speeds, they will reach the detector first.

Despite the Q-ToF analyzer is more sensitive and exhibits a higher resolution (lower *m/z* fragment ions can be detected and even the exact mass of the fragments can be determined), it also suffers from some disadvantages in comparison to the ion trap.[31] The first one is that only MS^2 experiments can be carried out due to the settings of the equipment. Additionally, the fragmentation is milder in the ion trap, where the fragment ions do not collide with the inert gas, contrary to the situation in a Q-ToF spectrometer. Therefore, more unstable species are more easily detected in an ion trap.

According to this, both tandem mass spectrometry techniques have been used in this Thesis, depending on our target in a specific study. The experiments were performed according to the following indications:

a) ESI-ion trap mass spectra were recorded on a Bruker Esquire 3000+ spectrometer (Bruker Daltonics). Analyses were carried out in negative ion mode, with Smart Parameter Settings optimized for each *m/z* ratio. The nebulizer (N_2) gas pressure, drying gas (N_2) flow rate and drying gas temperature were kept at 0.7 bar, 4.0 dm^3 min^{-1} and 350 ºC, respectively. Spectra were acquired in the *m/z* 50–1000 range, and the mass axis was externally calibrated with a tuning mix (from Agilent Technologies). 5 ppm solutions of the samples were transferred into the ESI source by means of a syringe pump at a flow rate of 4.0 mm^3 min^{-1}. ESI-CID-MS^n analyses were carried out using He as the collision gas and an isolation width for the precursor ion of 5 m/z units. Fragmentation amplitudes in the range 0.5–2.0 V were optimized to obtain the maximum ion current.
b) ESI-MS^2 Q-ToF spectra were recorded on a MicroToF-Q spectrometer (Bruker Daltonics) operated at a nebulizer (N_2) gas pressure of 0.8 bar, drying gas (N_2) flow rate 4.0 dm^3 min^{-1} and drying gas temperature 200 ºC. The mass axis was externally calibrated using 10 mM sodium formate. 2 ppm solutions of the samples in MeOH were transferred into the ESI source by means of a syringe pump at a flow rate of 4 mm^3 min^{-1}. ESI-CID-MS^2 analyses were carried out selecting precursor ions by means of the quadrupole filter using an isolation width of 5 *m/z* units and using N_2 as the collision gas. Collision energies in the range 30–60 eV were optimized to obtain the maximum fragment ion current for every sample.

M.4. Computational calculations

Theoretical DFT calculations are essential to understand some of the properties of the complexes described in this Thesis. In particular, computational calculations used in combination with tandem mass spectrometry allow to have an alternative laboratory of gas-phase chemistry in high vacuum and understand all the processes happening there.[28] Therefore, the most favorable process among several possible ones can be

elucidated and/or justified via theoretical calculations. Furthermore, the mechanisms of those processes and the involved transition states can be determined. More interestingly, DFT methods also allow to know the structure of the ions detected by tandem mass spectrometry. On the other hand, DFT calculations have also been very useful in the assessment of the Lewis acidity of the $(CF_3)_3Au$ fragment (Chapter 3), since several methods rely on quantum theoretical numbers or calculated thermodynamic parameters.[33]

Quantum mechanical calculations were performed with the Gaussian09 package[34] at the DFT/M06 level of theory.[35] C, F, Cl, Br, I and Au atoms have been described using Ahlrichs' Def2-QZVPD, a Quadruple-Zeta-Valence basis set including Polarization and Diffuse basis functions,[36] as obtained from the EMSL Basis Set Library.[37] Alternatively, when lighter atoms (including H) were involved, SDD basis set and its corresponding effective core potentials[38] with additional sets of f-type functions[39] were used to describe the Au centers, and light atoms (H, C, N, O, F, Si, P, and S) were described with a 6-31G** basis set.[40] The potential energy surfaces of the studied complexes have been examined in the gas phase and frequency calculations have been subsequently performed to check if stationary points were local minima or transition states. The methodology described here is general and applies to the whole Thesis, although particular methods for specific calculations were also used when required.

M.5. Thermal analyses

Thermal analysis experiments are useful for determining changes occurring in a sample upon heating.[21] Thermogravimetric analysis (TGA) shows how the mass of the sample changes on heating according to a programmed ramp rate and thus, volatiles or decomposition products can be identified. In thermal differential analysis (DTA), which can be simultaneously recorded, the temperature of the sample is compared to that of an internal reference (usually Al_2O_3 or SiC). Both undergo the same heating procedure and therefore, endothermic or exothermic changes in the sample can be identified relative to the reference, providing data on phase changes. The information that can be obtained from differential scanning calorimetry (DSC) is similar to that obtained from the DTA curve. In DSC, the sample and the reference are maintained at the same temperature

throughout the heating program by means of independent power suppliers. Differences in the amount of heat required are registered against the furnace temperature.

The thermogravimetric and differential thermal analyses (TGA/DTA) of the complexes prepared in this thesis were performed using a SDT 2960 instrument on powder samples (2–5 mg) in open platinum holders at heating rate of 10 ºC min^{-1} under N_2 atmosphere. When required, differential scanning calorimetry (DSC) experiments were performed using a DSC Q-2000 from TA instruments at a heating rate of 10 ºC min^{-1}. In this case, powder samples (2–5 mg) were placed in sealed aluminum holders. Melting points were taken at the maximum of the DTA peak and verified by visual inspection of the samples placed on glass plates using an Olympus BH-2 microscope fitted with a Linkam TMS-91 temperature controller with hot stage.

M.6. Thermolyses in the condensed phase

Powder samples of the complexes were placed in glass NMR tubes under inert atmosphere (Ar) and were thermolyzed during 5–10 min, depending on each particular case. The heating temperature was chosen in each case to be slightly above the corresponding onset point of decomposition, as determined in the TGA/DTA experiments. Once thermolyzed, the sample was chilled in N_2*(l)* and the residue was dissolved in CD_2Cl_2. Some insoluble metallic gold was obtained in most cases. The ^{19}F NMR spectrum of this solution was recorded immediately and the mass spectrometry experiment (MALDI or ESI) was next performed. Mass spectrometry was essential to detect NMR-invisible species such as $[AuX_2]^-$ anions (X = Cl, Br, I), as well as to determine the number of positions in which the $[PPh_4]^+$ cation was trifluoromethylated.

M.7. References

[1] S. Martínez-Salvador, L. R. Falvello, A. Martín, B. Menjón. Gold(I) and Gold(III) Trifluoromethyl Derivatives. *Chem. Eur. J.* **2013**, *19*, 14540.

[2] a) R. Usón, A. Laguna, M. Laguna. (Tetrahydrothiophene)Gold(I) or Gold(III) Complexes. *Inorg. Synth.* **1989**, *26*, 85; b) R. Usón, A. Laguna, in *Organometallic Syntheses, Vol.3* (Eds.: R. B. King, J. J. Eisch), Elsevier, Amsterdam, **1986**, pp. 322–342.

[3] S. Martínez-Salvador, J. Forniés, A. Martín, B. Menjón. [Au(CF_3)(CO)]: A Gold Carbonyl Compound Stabilized by a Trifluoromethyl Group. *Angew. Chem. Int. Ed.* **2011**, *50*, 6571; *Angew. Chem.* **2011**, *123*, 6701.

[4] S. Martínez-Salvador, L. R. Falvello, A. Martín, B. Menjón. A hexanuclear gold carbonyl cluster. *Chem. Sci.* **2015**, *6*, 5506.

[5] W. C. Wolsey. Perchlorate Salts, Their Uses and Alternatives. *J. Chem. Educ.* **1973**, *50*, A335.

[6] M. T. Weller, N. A. Young, in *Characterization Methods in Inorganic Chemistry*, Oxford, New York (NY), **2017**, pp. 66–111.

[7] P. S. Pregosin, in *NMR in Organometallic Chemistry*, Wiley-VCH, Weinheim, **2012**, pp. 146–155.

[8] S. Berger, S. Braun, H.-O. Kalinowski, *NMR-Spektroskopie der Nichtmetallen, Band 4, ^{19}F-NMR-Spektroskopie*, Thieme, Stuttgart, **1994**.

[9] J. Gil-Rubio, J. Vicente. Gold trifluoromethyl complexes. *Dalton Trans.* **2015**, *44*, 19432.

[10] M. A. Ellwanger, C. von Randow, S. Steinhauer, Y. Zhou, A. Wiesner, H. Beckers, T. Braun, S. Riedel. Tuning the Lewis acidity of difluorido gold(III) complexes: the synthesis of [AuClF_2(SIMes)] and [AuF_2(OTeF_5)(SIMes)]. *Chem. Commun.* **2018**, *54*, 9301.

[11] Adept Scientific, *gNMR V 5.1*, **2005**.

[12] G. R. Fulmer, A. J. M. Miller, N. H. Sherden, H. E. Gottlieb, A. Nudelman, B. M. Stoltz, J. E. Bercaw, K. I. Goldberg. NMR Chemical Shifts of Trace Impurities: Common Laboratory Solvents, Organics, and Gases in Deuterated Solvents Relevant to the Organometallic Chemist. *Organometallics* **2010**, *29*, 2176.

[13] a) W. R. Dolbier, Jr., *Guide to Fluorine NMR for Organic Chemists*, 2nd ed., John Wiley & Sons, Hoboken (NJ), **2016**; b) A. Foris. ^{19}F and ^{1}H NMR spectra of halocarbons. *Magn. Reson. Chem.* **2004**, *42*, 534; c) J. W. Emsley, L. Phillips, V. Wray. Flourine coupling constants. *Prog. Nucl. Magn. Reson. Spectrosc.* **1976**, *10*, 83; d) J. W. Emsley, L. Phillips. Fluorine chemical shifts. *Prog. Nucl. Magn. Reson. Spectrosc.* **1971**, *7*, 1.

[14] E. Bernhardt, M. Finze, H. Willner. Synthesis and NMR spectroscopic investigation of salts containing the novel [Au$(CF_3)_nX_{4-n}]^-$ (n = 4–1, X = F, CN, Cl) anions. *J. Fluorine Chem.* **2004**, *125*, 967.

[15] R. J. H. Clark. Metal-halogen stretching frequencies in inorganic complexes. *Spectrochim. Acta* **1965**, *21*, 955.

[16] K. Nakamoto, in *Infrared and Raman Spectra of Inorganic and Coordination Compounds, Part B*, 6th ed., John Wiley & Sons, Hoboken (NJ), **2009**, pp. 283–290.

[17] K. Nakamoto, in *Infrared and Raman Spectra of Inorganic and Coordination Compounds, Part B*, 6th ed., John Wiley & Sons, Hoboken (NJ), **2009**, pp. 110–120.

[18] P. Rigo, A. Turco. Cyanide phosphine complexes of transition metals. *Coord. Chem. Rev.* **1974**, *13*, 133.

[19] B. v. Ahsen, B. Bley, S. Proemmel, R. Wartchow, H. Willner, F. Aubke. Synthesen und Schwingungsspektren der homoleptischen Acetonitrilkomplex-Kationen [Au$(NCCH_3)_2]^+$, [Pd$(NCCH_3)_4]^{2+}$, [Pt$(NCCH_3)_4]^{2+}$ und des Adduktes $CH_3CN{\cdot}SbF_5$. Kristallstrukturen der Salze [M$(NCCH_3)_4$][$SbF_6]_2{\cdot}CH_3CN$, M = Pd, Pt. *Z. Anorg. Allg. Chem.* **1998**, *624*, 1225.

[20] F. A. Cotton, F. Zingales. The Donor-Acceptor Properties of Isonitriles as Estimated by Infrared Study. *J. Am. Chem. Soc.* **1961**, *83*, 351.

[21] M. T. Weller, N. A. Young, in *Characterization Methods in Inorganic Chemistry*, Oxford, New York (NY), **2017**, pp. 222–236.

[22] W. Henderson, J. S. McIndoe, in *Mass Spectrometry of Inorganic, Coordination and Organometallic Compounds*, John Wiley & Sons, Chichester, **2005**, pp. 47–105.

[23] S. L. Benjamin, W. Levason, G. Reid. Medium and high oxidation state metal/non-metal fluoride and oxide–fluoride complexes with neutral donor ligands. *Chem. Soc. Rev.* **2013**, *42*, 1460.

[24] P. Müller. Practical suggestions for better crystal structures. *Crystallogr. Rev.* **2009**, *15*, 57.

[25] Rigaku Oxford Diffraction, *Program CrysAlisPro 1.171.38.41r*, **2015**.

[26] *ShelxL Version 2014/8*. G. Sheldrick. Crystal structure refinement with SHELXL. *Acta Crystallogr. Sect. C* **2015**, *71*, 3.

[27] J. M. Weber, in *The Chemistry of Organogold Compounds, Vol. 1* (Eds.: Z. Rappoport, J. F. Liebman, I. Marek), belonging to Patai's Chemistry of Functional Groups, Wiley, Chichester, **2014**, pp. 41–56.

[28] J. Roithová, D. Schröder. Theory meets experiment: Gas-phase chemistry of coinage metals. *Coord. Chem. Rev.* **2009**, *253*, 666.

[29] R. A. J. O'Hair, in *The Chemistry of Organogold Compounds, Vol. 1* (Eds.: Z. Rappoport, J. F. Liebman, I. Marek), belonging to Patai's Chemistry of Functional Groups, Wiley, Chichester, **2014**, pp. 57–106.

[30] W. Henderson, J. S. McIndoe, in *Mass Spectrometry of Inorganic, Coordination and Organometallic Compounds*, John Wiley & Sons, Chichester, **2005**, pp. 1–21.

[31] W. Henderson, J. S. McIndoe, in *Mass Spectrometry of Inorganic, Coordination and Organometallic Compounds*, John Wiley & Sons, Chichester, **2005**, pp. 22–46.

[32] R. A. J. O'Hair. The 3D quadrupole ion trap mass spectrometer as a complete chemical laboratory for fundamental gas-phase studies of metal mediated chemistry. *Chem. Commun.* **2006**, 1469.

[33] L. Greb. Lewis Superacids: Classifications, Candidates, and Applications. *Chem. Eur. J.* **2018**, *24*, 17881.

[34] M. J. Frisch, G. W. Trucks, H. B. Schlegel, G. E. Scuseria, M. A. Robb, J. R. Cheeseman, G. Scalmani, V. Barone, B. Mennucci, G. A. Petersson, H. Nakatsuji, M. Caricato, X. Li, H. P. Hratchian, A. F. Izmaylov, J. Bloino, G. Zheng, J. L. Sonnenberg, M. Hada, M. Ehara, K. Toyota, R. Fukuda, J. Hasegawa, M. Ishida, T. Nakajima, Y. Honda, O. Kitao, H. Nakai, T. Vreven, J. A. Montgomery Jr., J. E. Peralta, F. Ogliaro, M. Bearpark, J. J. Heyd, E. Brothers, K. N. Kudin, V. N. Staroverov, T. Keith, R. Kobayashi, J. Normand, K. Raghavachari, A. Rendell, J. C. Burant, S. S. Iyengar, J. Tomasi, M. Cossi, N. Rega, J. M. Millam, M. Klene, J. E. Knox, J. B. Cross, V. Bakken, C. Adamo, J. Jaramillo, R. Gomperts, R. E. Stratmann, O. Yazyev, A. J. Austin, R. Cammi, C. Pomelli, J. W. Ochterski, R. L. Martin, K. Morokuma, V. G. Zakrzewski, G. A. Voth, P. Salvador, J. J. Dannenberg, S. Dapprich, A. D. Daniels, Ö. Farkas, J. B. Foresman, J. V. Ortiz, J. Cioslowski, D. J. Fox; *Gaussian 09, Revision D.01*, Gaussian, Inc., Wallingford (CT), **2013**.

[35] Y. Zhao, D. G. Truhlar. The M06 suite of density functionals for main group thermochemistry, thermochemical kinetics, noncovalent interactions, excited states, and transition elements: two new functionals and systematic testing of four M06-class functionals and 12 other functionals. *Theor. Chem. Acc.* **2008**, *120*, 215.

[36] D. Rappoport, F. Furche. Property-optimized Gaussian basis sets for molecular response calculations. *J. Chem. Phys.* **2010**, *133*, 134105.

[37] a) EMSL Basis Set Library obtained from: https://bse.pnl.gov/bse/portal; b) K. L. Schuchardt, B. T. Didier, T. Elsethagen, L. Sun, V. Gurumoorthi, J. Chase, J. Li, T. L. Windus. Basis Set Exchange: A Community Database for Computational Sciences. *J. Chem. Inf. Model.* **2007**, *47*, 1045; c) D. Feller. The Role of Databases in Support of Computational Chemistry Calculations. *J. Comput. Chem.* **1996**, *17*, 1571.

[38] D. Andrae, U. Häußermann, M. Dolg, H. Stoll, H. Preuß. Energy-adjusted *ab initio* pseudopotentials for the second and third row transition elements. *Theor. Chim. Acta* **1990**, *77*, 123.

[39] a) A. Höllwarth, M. Böhme, S. Dapprich, A. W. Ehlers, A. Gobbi, V. Jonas, K. F. Köhler, R. Stegmann, A. Veldkamp, G. Frenking. A set of d-polarization functions for pseudo-potential basis sets of the main group elements Al–Bi and f-type polarization functions for Zn, Cd, Hg. *Chem. Phys. Lett.* **1993**, *208*, 237; b) A. W. Ehlers, M. Böhme, S. Dapprich, A. Gobbi, A. Höllwarth, V. Jonas, K. F. Köhler, R. Stegmann, A. Veldkamp, G. Frenking. A set of f-polarization functions for pseudo-potential basis sets of the transition metals Sc–Cu, Y–Ag and La–Au. *Chem. Phys. Lett.* **1993**, *208*, 111.

[40] a) M. M. Francl, W. J. Pietro, W. J. Hehre, J. S. Binkley, M. S. Gordon, D. J. DeFrees, J. A. Pople. Self-consistent molecular orbital methods. XXIII. A polarization-type basis set for second-row elements. *J. Chem. Phys.* **1982**, *77*, 3654; b) W. J. Hehre, R. Ditchfield, J. A. Pople. Self–Consistent Molecular Orbital Methods. XII. Further Extensions of Gaussian–Type Basis Sets for Use in Molecular Orbital Studies of Organic Molecules. *J. Chem. Phys.* **1972**, *56*, 2257.

Contributions

The contribution of the candidate to each of the publications that constitute this Doctoral Thesis, together with the results and conclusions derived from each of them, is explained in the three following chapters. As described in the last section of the Introduction, the chapter division is established according to the number of CF_3 groups coordinated to the gold center. Therefore, Chapter 1 focuses on the study of monotrifluoromethyl gold complexes, Chapter 2 deals with complexes containing two CF_3 groups in *trans* arrangement, and Chapter 3 addresses the study of the $(CF_3)_3Au$ unit.

Chapter 1

Monotrifluoromethyl Gold Complexes as Precursors of Highly Unstable Species

This chapter is based on the following two peer-reviewed papers:

M. Baya, A. Pérez-Bitrián, S. Martínez-Salvador, J. M. Casas, B. Menjón, J. Orduna. Gold(I) Fluorohalides: Theory and Experiment. *Chem. Eur. J.* **2017**, *23*, 1512−1515. DOI: 10.1002/chem.201605655.

M. Baya, A. Pérez-Bitrián, S. Martínez-Salvador, A. Martín, J. M. Casas, B. Menjón, J. Orduna. Gold(II) Trihalide Complexes from Organogold(III) Precursors. *Chem. Eur. J.* **2018**, *24*, 1514−1517. DOI: 10.1002/chem.201705509.

1.1. Introduction and objectives

Gold halides are the most thoroughly studied group of gold compounds. These chemical species are of a remarkable simplicity, yet very interesting from both a theoretical and a practical point of view, exhibiting peculiar bonding and structural characteristics.[1] This group of compounds encompasses a wide variety of species including gold in oxidation states ranging from I to V, the preferred oxidation state depending on the particular halide. Thus, low oxidation states are more stable in the case of iodine, as in AuI or $[AuI_2]^-$, while fluorine rather stabilizes high oxidation states, as in AuF_5 or $[AuF_6]^-$. Additionally, the binary halides AuX, AuX_2, AuX_3 and AuF_5 show different properties when they appear as single molecules (that is, in the gas phase or trapped in inert matrices) or associated in the condensed phase.[2]

The binary gold(I) halides, AuX, have been isolated for the heavier analogues X = Cl, Br, I. They exhibit polymeric structures in the solid state, yet are dimeric Au_2X_2 molecules (X = Cl, Br) in the gas phase.[1] In contrast, AuF has only been detected in the gas phase.[3] The anionic $[AuF_2]^-$ has not been isolated either, but it has been detected in the gas phase as one of the ions deriving from the trifluoroacetate complex $[Au(O_2CCF_3)_2]^-$ (Scheme 1.1).[4] Countless salts of the $[AuX_2]^-$ anions are known for X = Cl, Br, I.[1] They all are two-coordinate with a linear geometry, being this tendency stressed by relativistic effects.[5] The covalency of the Au−X bond in these species has been calculated to increase on going down the halogen group. In fact, the Au−F bond in the $[AuF_2]^-$ anion exhibits a strong ionic character.[6] It is also interesting to note that the bond strength in the whole series of $[AuX_2]^-$ anions (X = F, Cl, Br, I) decreases from X = F to X = I,[7] being this trend opposite to that found for the stability of their

neutral AuX congeners.[2b] Unlike the symmetric gold dihalides, non-symmetric derivatives have been far less investigated. In particular, the geometries of the $[XAuY]^-$ anions (X = Cl, Br, I) were optimized and their photodetachment spectra theoretically predicted.[8] Additionally, mixed cyanide halide anions $[XAuCN]^-$ (X = F, Cl, Br, I) have also been studied, although the $[FAuCN]^-$ anion could not be experimentally detected.[9] The mixed $[CF_3AuBr]^-$ anion was recently prepared in our group and isolated as its $[PPh_4]^+$ salt,[10] whereas the $[CF_3AuF]^-$ species has only been detected in the gas phase (Scheme 1.1).[4]

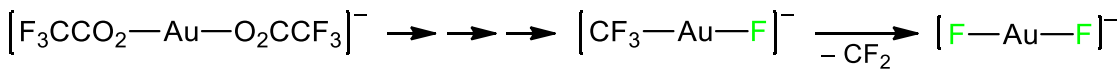

Scheme 1.1. Detection of the mixed $[CF_3AuF]^-$ and the symmetric $[AuF_2]^-$ anions in the gas phase *via* tandem mass spectrometry.[4]

In the case of gold(III) trihalides, the lighter binary compounds AuF_3, $AuCl_3$ and $AuBr_3$ have been isolated and characterized, whereas the heaviest homologue AuI_3 seems to be thermodynamically unstable, decomposing into AuI and I_2.[1] The trigonal planar AuI_3 molecule was once claimed to be stabilized in a cuprate lattice,[11] but later suggested to be a gold(I) species instead.[12] In fact, the stability of these species decreases from AuF_3 to AuI_3.[2b] Unlike the air- and moisture-sensitive AuF_3, which crystallizes as a polymeric helical chain (see Introduction),[13] $AuCl_3$[14] and $AuBr_3$[15] exhibit dimeric structures. Monomeric AuX_3 molecules (d^8) have also been the focus of several experimental and theoretical studies.[2,16-18] In all cases they are T-shaped minima,[2b] except in the case of AuI_3, which is better described as an adduct of I_2 and AuI.[2b,18]

Gold(III) AuX_3 monomers tend to form square-planar complexes by coordination of a fourth ligand or by oligomerization.[19] In the case of the gold(III) tetrahalides $[AuX_4]^-$, they are known for all halogens X = F, Cl, Br, I.[1] Several salts of these complex anions have been prepared, but the first salts of $[AuF_4]^-$ with organic cations $[NR_4]^+$ (R = Me, Et) have been reported only recently.[20] As just described for the monovalent $[AuX_2]^-$ anions, the covalency of the Au–X bonds in $[AuX_4]^-$ anions also increases on going down the halogen group.[21] The stability of these species follows the same trend as in AuX_3 and $[AuX_2]^-$, being $[AuF_4]^-$ the most stable within the series.[17d,21]

Gold(II) dihalides AuX_2 have been for a long time unknown. Although a black solid with stoichiometry $AuCl_2$ was initially isolated, it is in fact a mixed-valence species best formulated as $Au^I[Au^{III}Cl_4]$.[22] It was not only until more than 20 years later when the actual mononuclear $AuCl_2$ and $AuBr_2$ derivatives were indirectly detected in the gas phase.[23] This contribution opened the door to the study of mononuclear gold(II) halides and pseudohalides.[24] In fact, some years later, the monomeric AuF_2 was also characterized by means of matrix-isolation spectroscopy.[16] Concerning the three-coordinate $[AuX_3]^-$ ions, they have been suggested to be involved in the reduction of square-planar $[AuX_4]^-$ anions.[25] However, only the anionic gold(II) trihalide $[AuCl_3]^-$ has been recently detected upon fragmentation of $[AuCl_4]^-$ in a photochemically excited state.[26]

The species described in the previous paragraph are of special relevance since gold(II) is one of the unusual oxidation states of this element.[27] In fact, the chemistry of gold(II) complexes in the condensed phase is dominated by dinuclear species containing Au−Au bonds.[28-30] These dinuclear gold(II) derivatives are mainly obtained by oxidation of dinuclear gold(I) complexes containing bridging ligands. However, some interesting examples of unsupported Au(II)−Au(II) bonds have been reported in the last years.[30,31] On the contrary, mononuclear gold(II) species are elusive in the condensed phase[28] and little is known about their chemical behavior.[32]

Three-coordinate gold(II) species have been repeatedly suggested as intermediates in radical addition reactions to gold(I) compounds[33] and in gold-catalyzed reactions,[34] but little evidence has been found thus far. Unimolecular techniques have made possible the detection of some of some open-shell d^9 species either in matrices or in the gas phase.[16,35] Nevertheless, a scarce number of mononuclear gold(II) species have been isolated. Although a gold(II) phthalocyanine complex was reported in 1965,[36] the results could not be later reproduced and no gold(II) species could be obtained.[37] A macrocyclic thioether ligand allowed the isolation of the first mononuclear gold(II) complex, $[Au([9]aneS_3)_2]^{2+}$ ($[9]aneS_3$ = 1,4,7-trithiacyclononane).[38] Some years later, the analogous $[Au([9]aneS_2O)_2]^{2+}$ complex ($[9]aneS_2O$ = 1-oxa-4,7-dithiacyclononane),[39] where the non-bonding sulfur atom was replaced by an oxygen atom, was described. However, EPR spectroscopy and computational calculations suggested that the thioether ligands in these complexes might be non-innocent.[40] Neutral porphyrinato gold complexes have been identified as gold(II) species based on

EPR data,[41] but the isolation and thorough characterization of a stable porphyrinato gold(II) complex was reported only recently.[42]

Probably the most famous mononuclear gold(II) complexes isolated to date are $[AuXe_4]^{2+}$ and some others containing Au−Xe bonds, which were prepared by Seppelt and coworkers.[43] Two additional species which clearly contain gold in oxidation state II are $[Au(HF)_2][SbF_6]_2 \cdot 2HF$[44] and $Au[SbF_6]_2$,[45] and which were also isolated from superacidic HF/SbF_5 mixtures. Compound $Au[SbF_6]_2$ was obtained by fluorination of gold in *a*HF solution containing SbF_5, but further reaction with F_2 afforded $Au^{II}[SbF_6]_2Au^{II}[Au^{III}F_4]_2$. This compound could be easily transformed into the mixed-valence species $Au^{II}[Au^{III}F_4]_2$ upon reaction with $KAuF_4$.[45] In an attempt to prepare AuF_2 by addition of KF to $Au[SbF_6]_2$ in *a*HF solution, the same species $Au[AuF_4]_2$ was obtained.[45] The crystal structure of this species has been thoroughly studied,[45,46] although Au^{2+} cations in solid lattices stabilized by weakly basic SO_3F^- ligands or solvated in strongly acidic HSO_3F had been already identified some years before.[47]

In this chapter, the synthesis and characterization of monoalkyl gold(I) and gold(III) complexes of stoichiometry $[PPh_4][CF_3AuX_n]$ (X = Cl, Br, I; n = 1, 3) is described, together with our attempts to prepare the corresponding fluoride complexes. Within the aforementioned context, previously unknown gold halide anions were experimentally detected in the gas phase by tandem mass spectrometry and were further studied. Our results include:

a) The whole series of mixed gold(I) fluorohalides $[F{-}Au{-}X]^-$ (X = Cl, Br, I) obtained via CF_2 extrusion from the parent $[CF_3AuX]^-$ anions.
b) Gold(II) trihalides $[AuX_3]^-$ (X = Cl, Br), which arise from the unexpected homolytic splitting of the only Au−C bond in the organogold(III) $[CF_3AuX_3]^-$ anions.

1.2. Synthesis and characterization of the $[PPh_4][CF_3AuX]$ complexes (X = Cl, Br, I)

Previously in our group, the carbonyl compound CF_3AuCO (**II**) was demonstrated to be a useful synthon of the "CF_3Au" unit.[48] In particular, the equimolar reaction of **II** and $[PPh_4]Br$ rendered the anionic derivative $[PPh_4][CF_3AuBr]$ (**2**) by replacement of the highly labile carbonyl ligand.[10] Following a similar procedure, we managed to synthesize the analogous chloride $[PPh_4][CF_3AuCl]$ (**1**) and iodide $[PPh_4][CF_3AuI]$ (**3**) derivatives (Scheme 1.2), which were isolated as withe solids in high yield. Our attempts to prepare the fluoride complex $[PPh_4][CF_3AuF]$ starting from **3** and AgF were unsuccessful, as were also for Schmidbaur and coworkers when trying to prepare $(Ph_3P)AuF$ complexes from the corresponding chloride derivative.[49] However, the $[CF_3AuF]^-$ anion had already been detected in the gas phase (see Scheme 1.1).[4] In fact, no anionic gold(I) fluoride derivative has been isolated to date and only two neutral organogold(I) fluoride complexes have been prepared: (SIDipp)AuF and $[\{(SIDipp)Au\}_2(\mu\text{-}F)]BF_4$.[50]

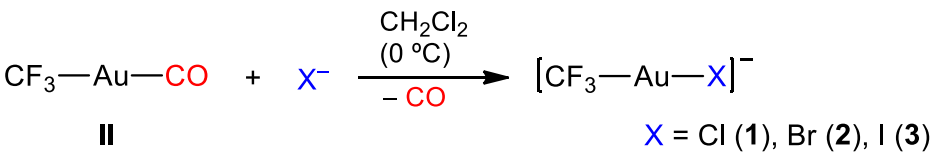

Scheme 1.2. Synthesis of the organogold(I) complexes **1**–**3**. In all cases the cation is $[PPh_4]^+$.

The ^{19}F NMR spectra of the three compounds **1**–**3** show a single signal corresponding to the CF_3 group, which moves downfield when increasing the electronegativity of the halogen atom.[a] No ligand scrambling was observed to occur in solution at room temperature, since the signal corresponding to the $[CF_3AuCF_3]^-$ anion was not observed. Additionally, neither the signal of $[CF_3AuCF_3]^-$ nor those corresponding to the $[AuX_2]^-$ anions were found in the mass spectra (ESI−) of the $[CF_3AuX]^-$ derivatives.

[a] This trend is contrary to that observed for the organogold(III) derivatives $[PPh_4][CF_3AuX_3]$ (X = Cl (**7**), Br (**8**), I (**9**)), which will be described in Section 1.4. See Figure 1.5 for a comparison of the correlation in both sets of compounds.

Compounds **1**−**3** are thermally stable species, which is in sharp contrast with the behavior of their non-fluorinated analogues, none of which are known to exist in the condensed phase. Only the heavier $[CH_3AuI]^-$ analogue, and its related copper and silver analogues, have been recently detected to arise in the gas-phase reaction of M^- and CH_3I.[51]

Single crystals of **1** suitable for X-ray diffraction were obtained by slow diffusion of a *n*-hexane layer into a CH_2Cl_2 solution of the compound at 4 ºC. The gold atom is in a linear coordination environment (Figure 1.1). The Au−CF_3 bond length, 200.1(7) pm is substantially shorter than that found for the bromo analogue (211.9(5) pm),[10] and also shorter than the distance observed in the carbonyl CF_3AuCO derivative (204.7(14) pm)[48,52] and in the homoleptic $[CF_3AuCF_3]^-$ anion in its $[N(PPh_3)_2]^+$ (206.6(6) pm)[53] and $[PPh_4]^+$ (203.3(2) pm)[48] salts.

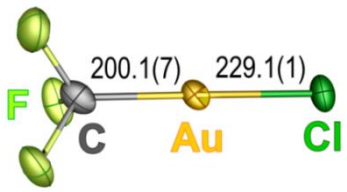

Figure 1.1. Displacement-ellipsoid diagram (50% probability) of the $[CF_3AuCl]^-$ anion as found in single crystals of **1**. Selected bond lengths [pm] with estimated standard deviations are indicated. C−Au−Cl angle: 178.1(2)º.

The optimized geometries of the anions of both **1** and **2** at the DFT/M06 level of calculation (Figure 1.2a) show slight differences with the experimentally established structures in the solid state (Table 1.1). These differences in the Au−CF_3 and Au−X bond lengths (X = Cl, Br) within each pair of anions can be attributed to the existence of crystal packing effects,[54] since no residual intense electron-density peaks appears in the model to make distances unreliable. Two aspects are interesting to note when comparing the optimized structures of the anions of compounds **1**−**3** in the gas phase:

1) The Au−CF_3 distance shows a smooth variation when going from chlorine to iodine (Table 1.1, Figure 1.2a).

2) The Au−X distances are consistently longer than those calculated for the symmetric $[AuX_2]^-$ anions (Table 1.2).

Table 1.1. Comparison of the interatomic distances [pm] in the structurally characterized $[CF_3AuX]^-$ anions and in their related equilibrium structures optimized at the DFT/M06 level of calculation.

	Au−C		**Au−X**	
X	Experimental	Calculated	Experimental	Calculated
Cl	200.1(7)	206.1	229.1(1)	234.4
Br	211.9(5)[a]	207.1	240.5(1)[a]	247.2
I	-	208.8	-	263.6

[a] Values taken from Ref. [10].

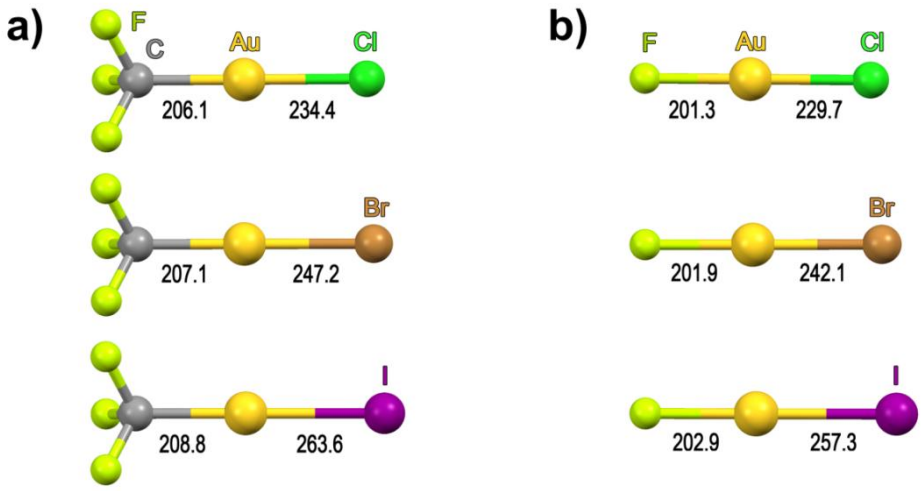

Figure 1.2. Optimized geometries at the DFT/M06 level for the a) $[CF_3AuX]^-$ and b) $[FAuX]^-$ anions. Relevant bond lengths [pm] are indicated.

1.3. Gas phase behavior of the $[CF_3AuX]^-$ anions (X = Cl, Br, I)

Compounds **1**−**3** form an ideal set for mass-spectrometry studies due to their anionic nature, their simple stoichiometry and the analogous character of the X ligand. Thus, these experiments provide information of their unimolecular decomposition processes as a function of the halide, X.

The compounds were easily transferred to the gas phase by electrospray ionization (ESI). Once the $[CF_3AuX]^-$ anions were confined into an ion trap and thermally excited by intense collision with an inert gas (He), the mixed $[F{-}Au{-}X]^-$ anions (X = Cl (***4***), Br (***5***), I (***6***)) were formed and clearly detected in all three cases (Figure 1.3, Scheme 1.3a). The used experimental conditions (see Methodology) avoid side-reactions, such as ligand scrambling and/or disproportionation, which might complicate their isolation in

the condensed phase. In fact, although Schwerdtfeger and coworkers suggested that these species could be prepared by addition of a fluoride salt to AuX (X = Cl, Br, I) species,[5] it seems that they have not been prepared in the condensed phase thus far.

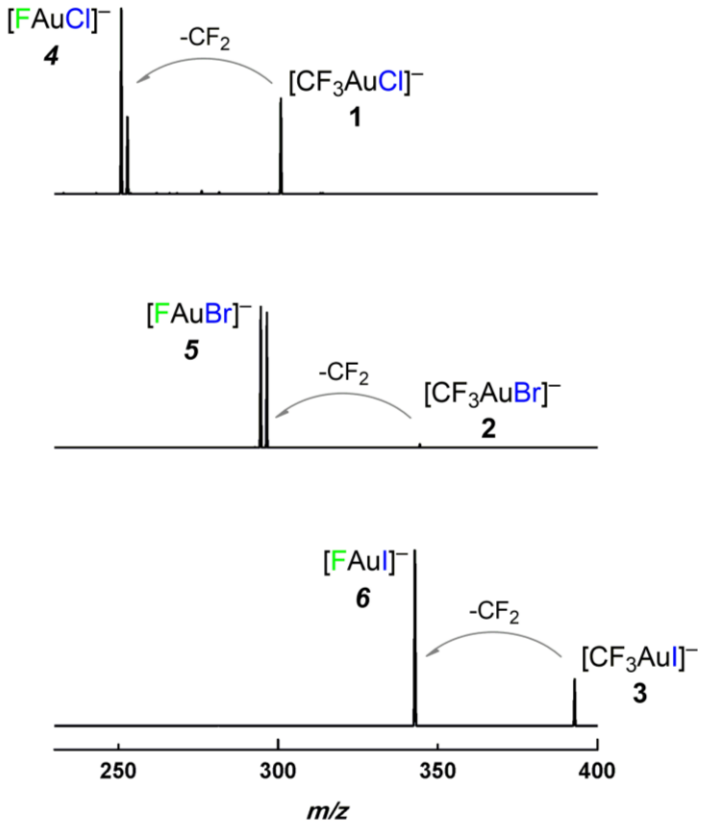

Figure 1.3. Detection of the mixed $[F{-}Au{-}X]^-$ anions (X = Cl (***4***), Br (***5***), I (***6***)) formed by collision-induced dissociation of the corresponding $[CF_3AuX]^-$ species in quadrupole ion-trap MS^2 experiments.

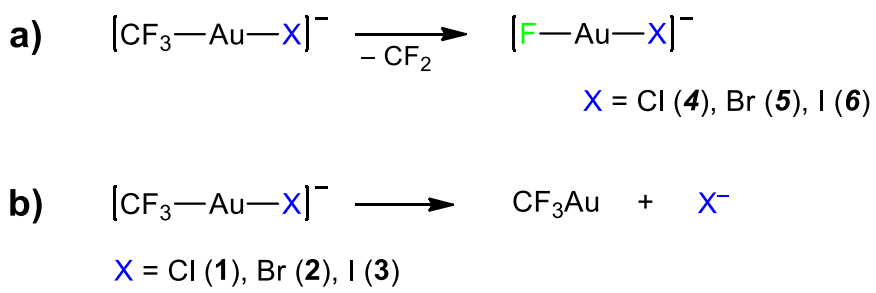

Scheme 1.3. Competing dissociation processes undergone by the $[CF_3AuX]^-$ anions (X = Cl, Br, I) in the gas phase.

Although difluorocarbene extrusion was the main decomposition pathway, halide dissociation could also be observed in all three cases (Scheme 1.3b) by performing ESI-Q-ToF MS^2 experiments allowing the detection of lower *m/z* relationships (see Methodology). The Au−X bond dissociation energy calculated for the $[CF_3AuX]^-$ species decreases on going from X = Cl (288.1 kJ mol^{-1}) to X = Br (275.0 kJ mol^{-1}) and to X = I (266.4 kJ mol^{-1}). A similar trend was observed in the analogous decomposition analyses for $[AuX_2]^-$ anions.[7] In all cases, the gold(I) species CF_3Au must be formed, yet it cannot be detected due to its neutral character. Its nature is also intriguing, since two tautomers can be in equilibrium, as shown in Scheme 1.4. We have optimized the geometries of both tautomers and found that the two of them are energy minima, the difluorocarbene species being destabilized by ΔE = 40.2 kJ mol^{-1} with respect to the trifluoromethyl one.

Scheme 1.4. Tautomeric equilibrium applying to the CF_3Au species.

The geometries of species ***4***−***6*** were optimized at the DFT/M06 level of calculation. Linear structures with $C_{\infty v}$ symmetry were found in all three cases (Figure 1.2b). Au−F distances are ca. 10 pm longer than in the diatomic AuF molecule (191.84 pm),[3a,b] and comparable to that of the neutral (SIDipp)AuF complex (Au−F 202.8(8) pm).[50b] The Au−X bond in species ***4***−***6*** is also similarly elongated with respect to the corresponding diatomic AuX molecules (Table 1.2),[55] yet shorter than in the $[CF_3AuX]^-$ anions **1**−**3**, as can be observed in Figure 1.2. This difference might be assigned to the strong *trans* influence of the CF_3 group.[56] By contrast, no significant variation appears in the Au−F distance when a noble gas (Ng) is coordinated to the AuF unit in NgAuF compounds.[16,57]

Table 1.2. Interatomic distances [pm] in the equilibrium structures obtained for the linear $[FAuX]^-$ and $[AuX_2]^-$ anions at the DFT/M06 level of calculation. Data corresponding to AuX molecules are included for comparison.

	$[FAuX]^-$		**$[AuX_2]^-$**	**AuX[a]**
X	Au−F[b]	Au−X	Au−X	Au−X
Cl	201.3	229.7	231.8	222.6
Br	201.9	242.1	244.7	233.9
I	202.9	257.3	261.7	250.6

[a] Values taken from Ref. [55]. [b] In the free diatomic AuF molecule, Au−F = 191.84 pm.[3a,b]

To gain a deeper insight into the CF_2 extrusion from compounds **1**–**3**, we performed computational calculations on the mechanism of the process. In the presence of an external acid, metal trifluoromethyl complexes undergo α-fluoride abstraction yielding metal difluorocarbene species.[58] The generally accepted mechanism in the absence of an external acid also involves a difluorocarbene metal intermediate $[M]CF_2$, according to the tautomeric equilibrium shown in Scheme 1.4 for the species CF_3Au. This mechanism was identified in the case of organoruthenium systems[59] and it was actually the same mechanism calculated to apply in the decomposition of the linear $[CF_3MR]^-$ (M = Cu, Ag, Au, R = F, CF_3, O_2CCF_3) in the gas phase.[4] In our case, however, this was not the most favorable mechanism, as a lower-energy path was found. Both mechanisms are compared in Scheme 1.5 and the energy profile for our new alternative mechanism is shown in Figure 1.4 for the transformation of $[CF_3MI]^-$ (**3**) into $[F–Au–I]^-$ (***6***).

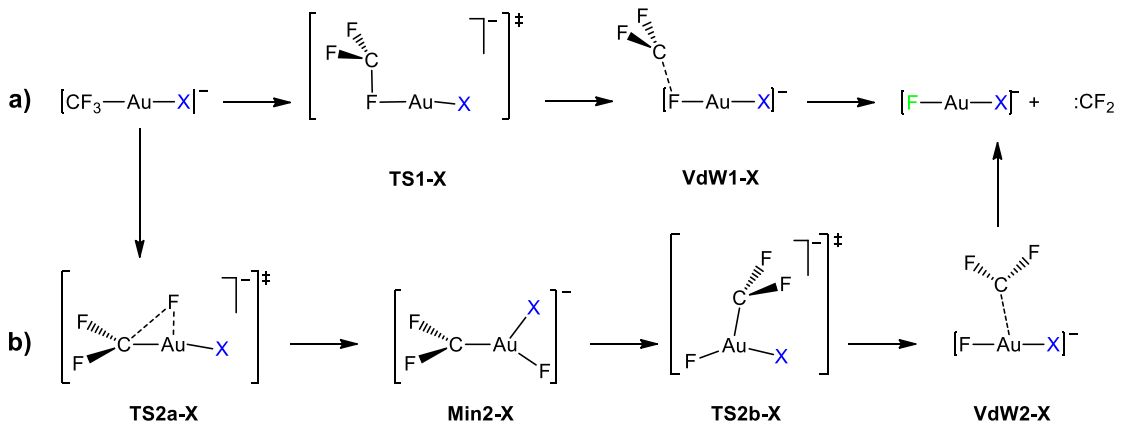

Scheme 1.5. Mechanisms of the formation of the mixed gold(I) $[F–Au–X]^-$ anions through a) the CF_2 extrusion path, and b) the classical path involving a $[M]CF_2$ intermediate.

Our new alternative mechanism (Scheme 1.5a) can be described in the following steps:

1) Weakening of the Au–C bond and formation of a Au–F bond through a transient $Au(\eta^2\text{-}F–CF_2)$ species (Scheme 1.6).

2) Loss of the Au–C interaction giving rise to a transition state (TS1-X) involving an uncommon fluoride-bridging $F_2C–F–[Au]$ unit, which in turns evolves to a van der Waals complex (VdW1-X).

3) Release of the unsaturated :CF_2 from the van der Waals complex, giving rise to the triatomic [F−Au−X]$^-$ species. This step requires a small dissociation energy < 12 kJ mol^{-1} in all three cases.

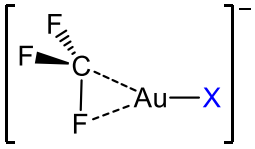

Scheme 1.6. Structural pattern showing the interactions in the transient species formed upon thermal excitation of [CF_3AuX]$^-$ anions.

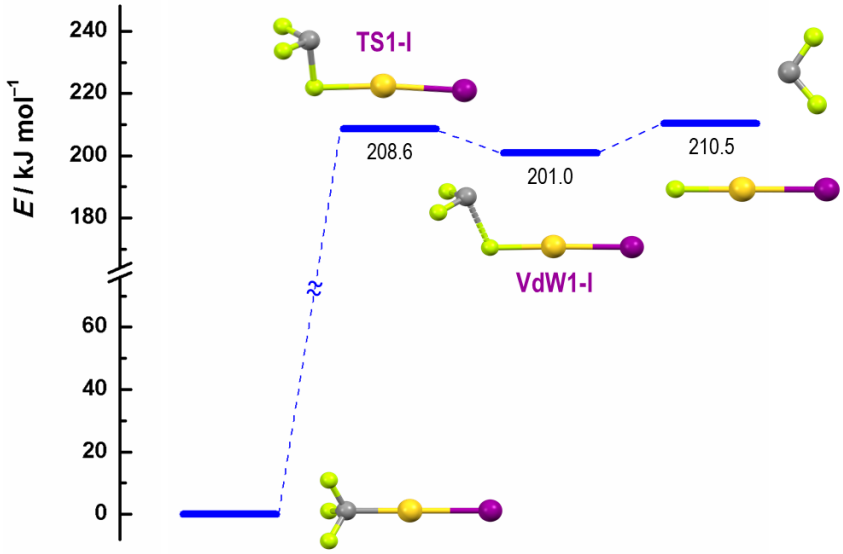

Figure 1.4. Energy profile of the lower-energy CF_2 extrusion path from the [CF_3AuI]$^-$ derivative (Scheme 1.5a). The energy barrier in the mechanism involving a [M]CF_2 intermediate (Scheme 1.5b) increases up to 244.4 kJ mol^{-1}.

This CF_2 extrusion mechanism can also apply to the CF_2 insertion into the Au−F bond due to the microreversibility principle. Thus, there is almost no energy barrier in the insertion process, which leads to a large stabilization, and in which the carbon atom gradually increases the number of substituents from two (:CF_2) to four in the final product [CF_3AuX]$^-$. This process might thus be experimentally feasible and, in fact, the insertion of the CH_2 moiety into Au−Cl bonds is already known.[60]

Similar structures to those of the transient species and the transition state involved in our mechanism are also found in the chemistry of lithium carbenoids.[61] For example, a Li(η^2-F−CF_2) interaction was found to be a global minimum for CF_3Li in the gas phase,[62] as well as for KCF_3 in a modeled thf solvation environment.[63] Both CF_3Li and the Li(CF_2CF_3)·2Et_2O dimer[64] release the corresponding fluorinated carbene giving rise to LiF, in a process that sometimes occurs violently.[65] Actually, complexes **1**−**3** can be accurately referred to as gold carbenoids, since they are able to release CF_2 without requiring a proper metal carbene intermediate.

1.4. Synthesis and characterization of the [PPh_4][CF_3AuX_3] complexes (X = Cl, Br, I)

The monoalkyl gold(I) complexes **1**−**3** undergo oxidative addition of the corresponding halogen X_2 affording complexes [PPh_4][CF_3AuX_3] (X = Cl (**7**), Br (**8**), I (**9**); Scheme 1.7). These compounds were isolated as air-stable solids in high yield. We thoroughly tried to prepare complex [PPh_4][CF_3AuF_3] too, but all our attempts were unsuccessful. Our different strategies included the reaction of **3** and XeF_2 or the treatment of **9** with both AgF and XeF_2. It is interesting to note that the [CF_3AuF_3]$^-$ anion was previously detected in solution, but not isolated.[66] It is actually expected to be an extremely reactive species, decomposing even in contact with the glass of the schlenk. This is one of the reasons why so few gold trifluoride complexes have been detected thus far.[20] In fact, only one has been recently isolated, AuF_3(SIMes), thanks to the stability that an NHC ligand confers to the AuF_3 unit.[67]

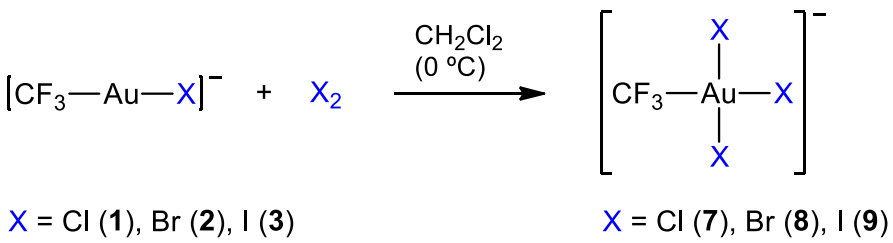

Scheme 1.7. Synthesis of the monoalkyl gold(III) anionic complexes **7**−**9**. In all cases the cation is [PPh_4]$^+$.

It is worth noting that, whereas several arylgold(III) compounds with a single Au–C bond, $[RAuX_3]^-$ (X = Cl, Br) are known,[68] monoalkyl gold(III) derivatives are still scarce.[69] In fact, although trifluoromethyl neutral derivatives of $CF_3Au(PR_3)X_2$ stoichiometry (X = Br, I; R = Me, Et, Ph) have been prepared,[70] complexes **7**–**9** are, to the best of our knowledge, the first alkyl $[RAuX_3]^-$ species to have been isolated.

In the ^{19}F NMR spectra of compounds **7**–**9** there is just one singlet corresponding to the only trifluoromethyl group coordinated to the gold center. When we compare the chemical shifts of these signals, it can be observed that they nicely correlate with the electronegativity of the halogen in the Sanderson scale (Figure 1.5, left).[71] In particular, the signal shifts upfield when increasing the electronegativity of the halogen. The chemical shift reported for the trifluoride analogue[66] also follows this trend, which is contrary to that observed for the gold(I) precursors **1**–**3** (Figure 1.5, left). If we take all the ^{13}C NMR spectra of complexes **1**–**3** and **7**–**9** together, we observe that the signals in the organogold(III) derivatives are more shielded than in the organogold(I) precursors. The $^1J(^{19}F,^{13}C)$ are slightly larger in the gold(III) species, but they increase from X = Cl to X = I in both sets of Au(I) and Au(III) compounds. Additionally, the experimental chemical shifts δ_C correlate very well with the electronegativity of the halogen in both sets of compounds, being the signal deshielded when decreasing the electronegativity of the halogen (Figure 1.5, right).

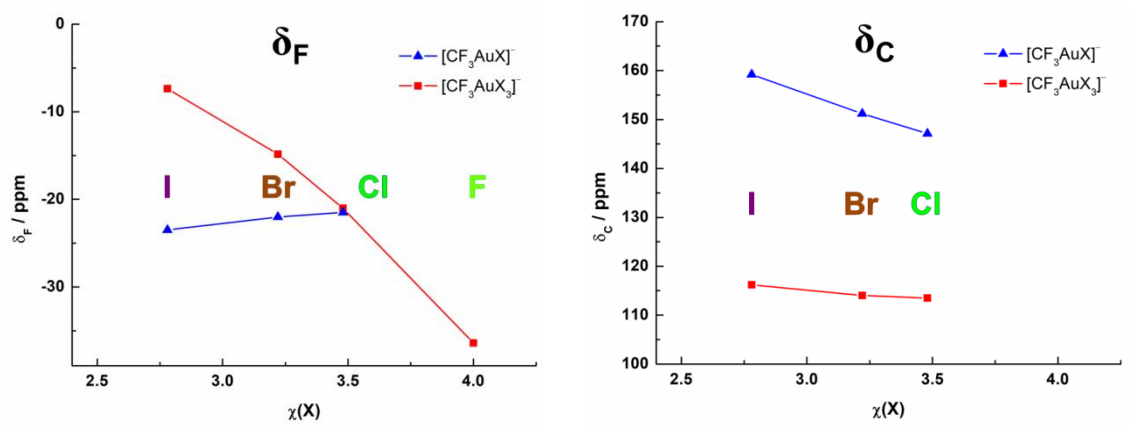

Figure 1.5. Correlation between the experimental chemical shift values of compounds $[PPh_4][CF_3AuX]$ (**1**–**3**) and $[PPh_4][CF_3AuX_3]$ (**7**–**9**) and the electronegativity of the involved halogen χ(X) in the Sanderson scale:[71] δ_F (left) and δ_C (right). All ^{19}F NMR spectra were registered in CD_2Cl_2 at room temperature. For the $[CF_3AuF_3]^-$ derivative, δ_F values are taken from Ref. [66].

Single crystals of **7** suitable for X-ray diffraction were obtained by slow diffusion of a *n*-hexane layer into a CH_2Cl_2 solution of the compound at 4 ºC. As expected, the coordination of the gold atom changes from linear in **1** to a square-planar geometry in **7** (Figure 1.6). Interestingly, both distances in the CF_3–Au–Cl axis are longer in the organogold(III) species **7** than in **1**. The lengthening of the Au–Cl distance in the chloride *trans* to the trifluoromethyl ligand with respect to the mutually *trans*-standing choride ligands appears as a consequence of the high *trans* influence of the CF_3 group.[56]

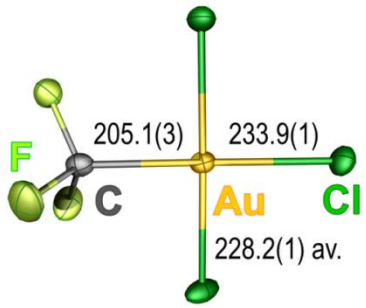

Figure 1.6. Displacement-ellipsoid diagram (50% probability) of the $[CF_3AuCl_3]^-$ anion as found in single crystals of **7**. Selected bond lengths [pm] with estimated standard deviations are indicated.

Single crystals of **9**, obtained by a similar procedure used in the case of complex **7**, could also be analyzed by X-ray diffraction. The gold center is also in a square-planar environment (Figure 1.7) but, due to crystal symmetry, all four coordination sites are identical. This means that the CF_3 group and the three iodide ligands appear overlapped, showing 0.25 and 0.75 occupancy, respectively. Thus, no reliable Au–C and Au–I distances could be obtained. Additionally, since no residual intense electron-density peaks appear in the model, the presence of any triodide anion, $[I_3]^-$, can be excluded and compound **9** is therefore accurately formulated as a square-planar gold(III) species of formula $[PPh_4][CF_3AuX_3]$. Additionally, its existence can also be confirmed because of the good agreement of the NMR data in solution of **9** within the whole series of $[CF_3AuX_3]^-$ anions (X = F, Cl, Br, I; see Figure 1.5). This is of special interest because Au(III) is not always formed in the presence of I_2, being the oxidative addition strongly dependent on the ligands of the gold(I) precursor.[72]

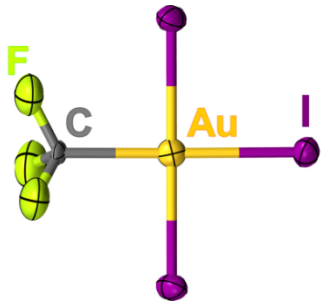

Figure 1.7. Thermal ellipsoid diagram (50% probability) of the $[CF_3AuI_3]^-$ anion as found in single crystals of **9**. The CF_3 group and the I^- ligands appear disordered and mutually overlapped over the four coordination sites due to crystal symmetry.

1.5. Decomposition studies on $[PPh_4][CF_3AuX_3]$ complexes (X = Cl, Br, I)

With the aim of gaining a deeper insight into the properties of compounds **7**–**9**, we studied their decomposition processes under two related but quite different conditions: in the gas phase and in the condensed phase. These conditions ensure the independence of any kind of solvent and enable to distinguish between inter- and intramolecular decomposition processes.

1.5.1. Thermolyses in the condensed phase

The thermal stability of compounds **7**–**9** was determined by TGA/DTA experiments. In all cases, clean elimination of CF_3X was observed as the first decomposition step (Scheme 1.8), as shown in Figure 1.8 for compound **8**. After the onset of decomposition was determined, the thermolyses were performed in NMR tubes under inert atmosphere (see Methodology). In all three cases, the solid sample changed color when was heated above the corresponding onset of decomposition, but no melting process was observed. This was the expected behavior, since no endothermic peak corresponding to a melting process was observed in the DTA curve (blue line in Figure 1.8 for the case of **8**). The decomposition rendered, as expected, the halomethanes CF_3X as the main fluorinated species, which were identified by ^{19}F NMR, with the concomitant formation of $[AuX_2]^-$ anions, which were detected by mass spectrometry (ESI–). No $[CF_3AuX]^-$ was detected in any case. Photochemical elimination processes of CF_3X[73] and longer

perfluorocarbon halides[33a] from other organogold(III) derivatives have been recently reported.

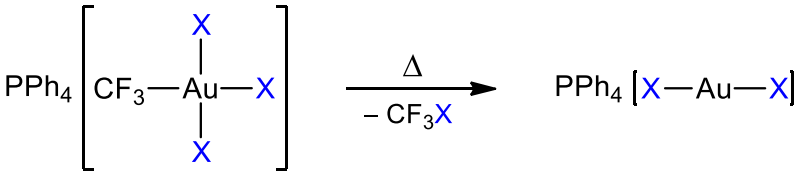

Scheme 1.8. First decomposition process observed for complexes **7**–**9** in the condensed phase.

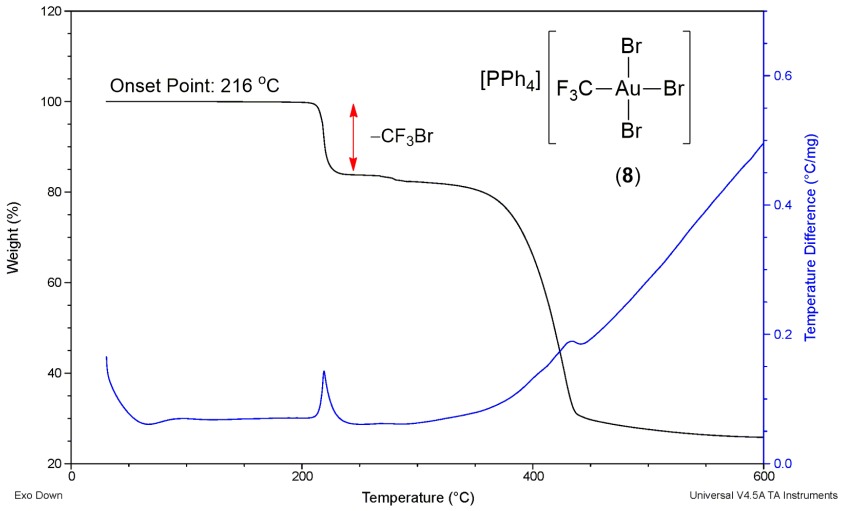

Figure 8. TGA (black trace, vertical scale on the left) and DTA (blue trace, vertical scale on the right) of compound **8** recorded on heating at 10 ºC min^{-1}. Loss of one equivalent of CF_3Br (17.6% theor.) is indicated.

1.5.2. Thermolyses in the gas phase

The unimolecular decomposition of $[CF_3AuX_3]^-$ anions in the gas phase was studied by tandem mass spectrometry (MS^n). The general fragmentation paths observed upon collision-induced dissociation (CID) for the anions of complexes **7**–**9** in MS^2 experiments are shown in Scheme 1.9. Elimination of CF_3X is observed in all cases (Scheme 1.9b), but this is not the only decomposition pathway. Thus, it is reasonable to assume that intermolecular processes may take place in the condensed phase, where this is the only decomposition pathway observed (Scheme 1.8). The iodo derivative $[CF_3AuI_3]^-$ (**9**) undergoes I_2 elimination, regenerating the organogold(I) species

$[CF_3AuI]^-$ (**3**). This fragmentation path (Scheme 1.9c) is also present in the decomposition of the bromo derivative $[CF_3AuBr_3]^-$ (**8**), but not in the chloro complex **7**.

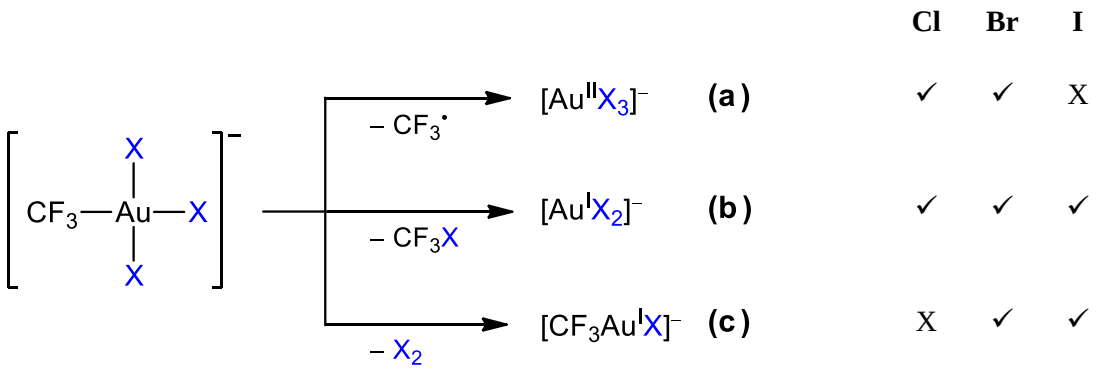

Scheme 1.9. General fragmentation paths observed for the $[CF_3AuX_3]^-$ anions in the gas phase.

In addition to these two-electron reduction processes, a one-electron reduction was also detected in the case of $[CF_3AuCl_3]^-$ (**7**) and $[CF_3AuBr_3]^-$ (**8**) anions (Scheme 1.9a). This process involves the homolytic cleavage of the Au–CF_3 bond and formation of the gold(II) anions $[AuCl_3]^-$ (***10***) and $[AuBr_3]^-$ (***11***), respectively (Figure 1.9). Therefore, when going down the group, the homolytic cleavage of the Au–CF_3 bond (Scheme 1.9a) is less favored, as opposed to X_2 elimination (Scheme 1.9c).

The $CF_3^{\bullet}$ radical dissociation pathway is important because unlike in main-group organoelement chemistry,[74] homolytic cleavage of M–C bonds is not very common in organotransition-metal chemistry.[75] In addition to the importance of radical processes in gold chemistry,[76] further and definite evidence of the generation of trifluoromethyl radicals from homoleptic Group 11 $[(CF_3)_4M]^-$ complexes has been recently obtained.[77]

In a further step of tandem mass spectrometry, MS^3, we performed experiments on anions ***10*** and ***11***, observing the homolytic splitting of a Au–X bond, leading to the formation of the gold(I) dihalides $[AuX_2]^-$ (X = Cl, Br) (Scheme 1.10). Interestingly, no halide X^- dissociation was observed at any stage of the described processes.

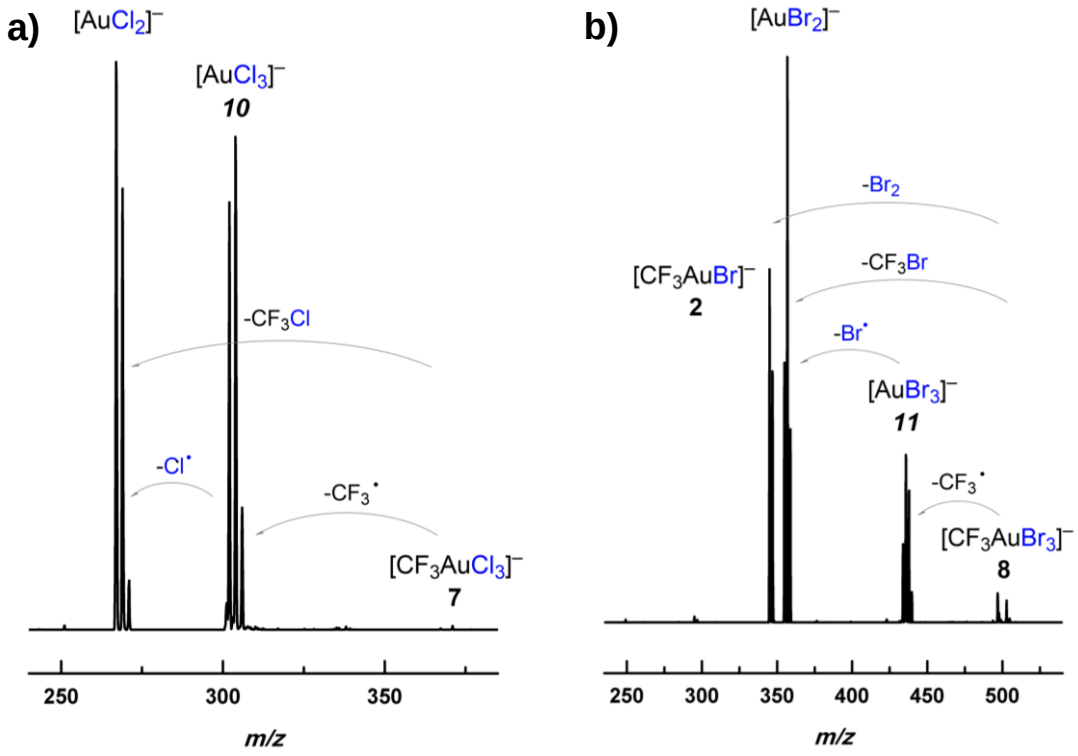

Figure 1.9. Quadrupole ion-trap MS^2 results of the collision-induced dissociation (CID) of the anions of a) **7**, $[CF_3AuCl_3]^-$; and b) **8**, $[CF_3AuBr_3]^-$.

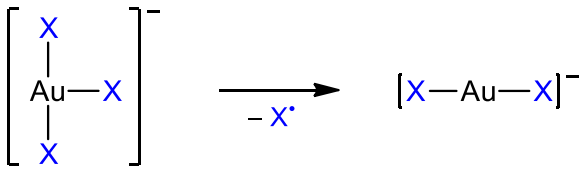

Scheme 1.10. Formation of the linear $[AuX_2]^-$ (X = Cl, Br) anions upon homolytic cleavage of a Au−X bond in the corresponding $[AuX_3]^-$ anions in the gas phase.

1.6. Computational calculations on the $[AuX_3]^-$ anions

Calculated Au−C bond enthalpies for the complex anions **7**−**9**, as well as for the related $[CF_3AuF_3]^-$, show that they decrease with the electronegativity of the halogen (Table 1.3). T-shaped geometries have been calculated as energy minima in all cases (Figure 1.10a), whereas Y-shaped structures were identified as transition states. The equilibrium geometries of $[AuF_3]^-$ and $[AuCl_3]^-$ anions were also calculated recently.[78] The T-shaped geometries of our anionic open-shell d^9 $[AuX_3]^-$ species show two main

differences with those of the well-studied monomeric, neutral and diamagnetic d^8 AuX_3 molecules:[2ab,16-18]

- $[AuX_3]^-$ anions are energy minima in all cases, whereas monomeric AuI_3 is better described as a side-on iodine adduct of AuI: $IAu(I_2)$.[2b,18] In fact, T-shaped AuI_3 was found to be a transition state.

- Whereas the Au−X bond lengths in the neutral species are virtually identical,[2b] the distance to the X stem-ligand in the $[AuX_3]^-$ anions is about 15 pm longer that those found in the crosspiece (Figure 1.10).

Table 1.3. Parameters calculated for the T-shaped minima of the mononuclear $[AuX_3]^-$ species in the gas phase.

X =	**F**	**Cl**	**Br**	**I**
$[F_3C{-}AuX_3]^-$ bond enthalpy [kJ mol^{-1}]	278	208	183	155
X^- dissociation enthalpy [kJ mol^{-1}][a]	290	219	201	179
$X^\bullet$ dissociation enthalpy [kJ mol^{-1}][b]	166	120	90	81
Vertical detachment energy [eV][c]	5.19	4.90	4.71	4.26
Adiabatic detachment energy [eV] [d]	4.64	4.56	4.41	3.82
Spin density on Au [%][e]	62	42	31	21
Spin density on stem X [%][e]	26	37	46	52

[a] Heterolytic Au−X bond dissociation enthalpy as indicated in Scheme 1.11 (left). [b] Homolytic Au−X bond dissociation enthalpy as indicated in Scheme 1.11 (right). [c] The oxidized species is in an excited state. [d] The oxidized species is in the ground state. [e] Based on Mulliken charges and populations; the unassigned spin density is located symmetrically on the X ligands at the crosspiece (see Figure 1.11).

In the $[AuX_3]^-$ anions, the spin density is mainly located in the stem axis, which can justify the difference in the Au−X distances in the neutral and the anionic species (Figure 1.10). However, this spin density gradually migrates along the stem axis from the metal to the X ligand, when going from fluorine to iodine (Table 1.3, Figure 1.11). Additionally, the T-shaped $[AuX_3]^-$ species are connected to their neutral counterparts (Scheme 1.11) by large vertical electron-detachment energies (Table 1.3) or, inversely, AuX_3 are related to the corresponding anionic species by large electron affinity values. Since all these electron affinity values exceed that of Cl (−3.63 eV), all AuX_3 species can be considered as superhalogens.[24b,78,79]

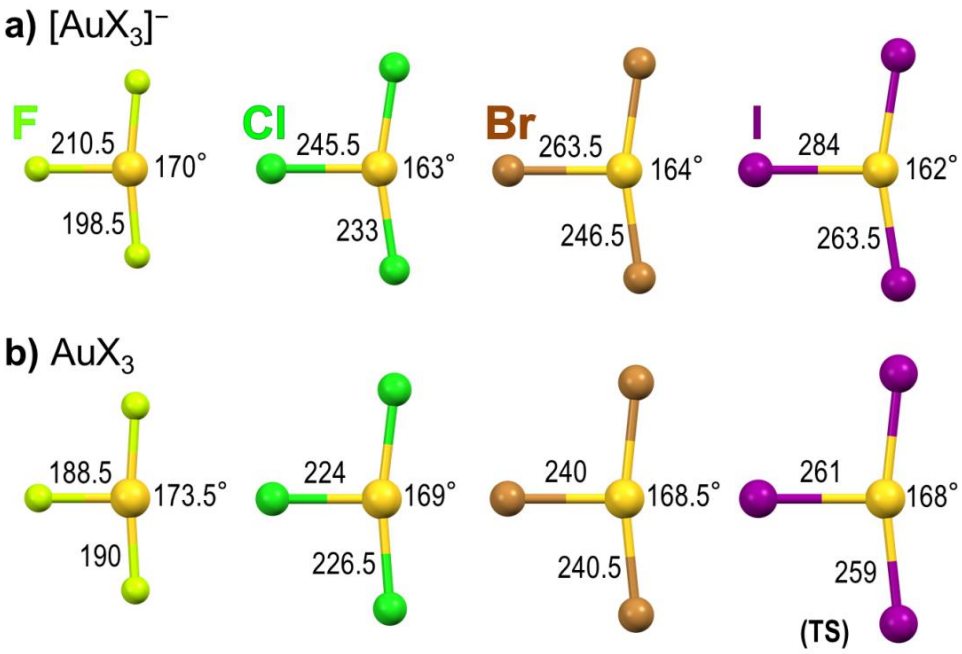

Figure 1.10. T-shaped polytopes optimized at the DFT/M06 level of the a) mononuclear anionic $[AuX_3]^-$ and b) mononuclear neutral AuX_3 species. All of them are identified as minima, except for the neutral AuI_3 species, which is a transition state. Our results on the neutral AuX_3 species are in good agreement with previous calculations.[2b] Structural parameters (bond lengths in pm; angles in degrees) are indicated.

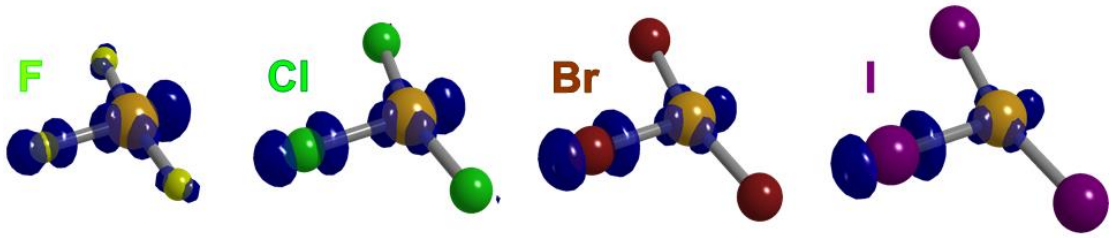

Figure 1.11. Spin density contour of all the T-shaped $[AuX_3]^-$ anions according to the Mulliken charges and populations given in Table 1.3.

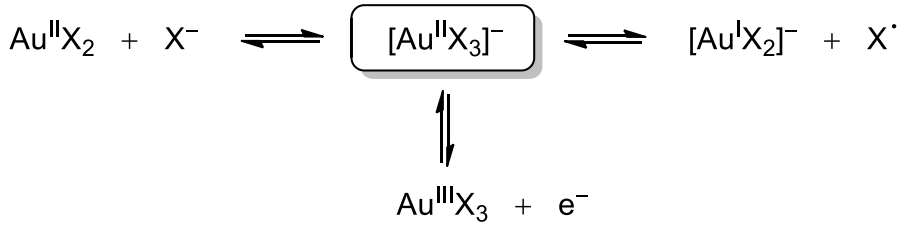

Scheme 1.11. Processes connecting the gold(II) $[AuX_3]^-$ anions with relevant neighbor species.

The most favored fragmentation process of the $[AuX_3]^-$ anions is the homolytic cleavage of Au−X bonds, giving rise to the linear $[AuX_2]^-$ anions and releasing an halogen atom $X^\bullet$, instead of the dissociation of a X^- ligand (Table 1.3, Scheme 1.11). This is actually the experimental observation in MS^3 experiments described in the previous section for X = Cl, Br (Scheme 1.10). Additionally, our calculations show that neutral AuX_2 molecules behave as unsaturated species, the coordination of a X^- ligand being very exergonic in all cases (Table 1.3). Finally, gold(II) $[AuX_3]^-$ anions are very prone to undergoing disproportionation, since the $X^\bullet$ atoms generated upon the easy Au−X bond homolysis recombine with fresh $[AuX_3]^-$ to give $[AuX_4]^-$ in a highly exergonic process (Scheme 1.12).

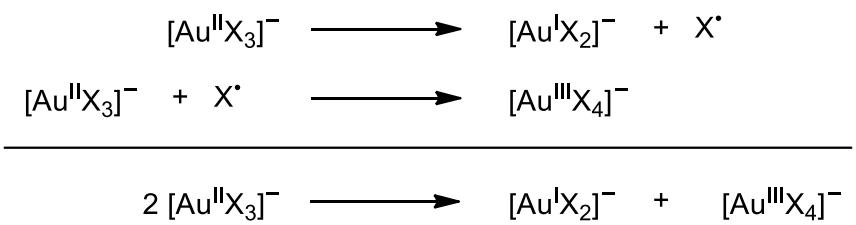

Scheme 1.12. Disproportionation process undergone by the $[AuX_3]^-$ anions. Disproportionation enthalpy values (ΔH_{dis}) are as follows: X = F, −186 kJ mol^{-1}; X = Cl, −132 kJ mol^{-1}; X = Br, −103 kJ mol^{-1}; X = I, −74 kJ mol^{-1}.

1.7. Summary

- Compounds $[PPh_4][CF_3AuCl]$ (**1**) and $[PPh_4][CF_3AuI]$ (**3**) are prepared from CF_3AuCO (**II**), following a similar procedure to that used for $[PPh_4][CF_3AuBr]$ (**2**).[10] Compounds **1**−**3** are thermally stable species that do not undergo ligand scrambling in solution.

- Compounds **1**−**3** behave as gold carbenoids, undergoing CF_2 extrusion in the gas phase to afford the mixed gold(I) fluorohalides $[F{-}Au{-}X]^-$ (***4***−***6***). The detection of these species demonstrate that AuF can be stabilized by coordination of the heavier halides, as suggested by Schwerdtfeger.[5]

- An unconventional CF_2 insertion/extrusion mechanism has been found, which involves an uncommon fluoride-bridging $F_2C{-}F{-}[Au]$ unit as the transition state, instead of a $[Au]CF_2$ intermediate.

- Compounds **1**−**3** undergo oxidative addition of the corresponding halogen X_2 to afford $[PPh_4][CF_3AuX_3]$ complexes (**7**−**9**), which are the first monoalkyl gold(III) trihalide derivatives prepared to date. However, neither $[PPh_4][CF_3AuF]$ nor $[PPh_4][CF_3AuF_3]$ could be prepared, probably because of their extremely high reactivity.

- Complexes **7**−**9** cleanly eliminate CF_3X upon heating above their onset of decomposition and without melting, with concomitant formation of the corresponding $[AuX_2]^-$ anions (Scheme 1.8).

- The gold(II) trihalide complexes $[AuX_3]^-$ (X = Cl (***10***), Br(***11***)) are formed in the gas phase upon homolytic cleavage of the only Au−C bond existing in the parent anions of **7** and **8**. T-shaped structures have been found as energy minima for all gold(II) trihalides $[AuX_3]^-$ (X = F, Cl, Br, I; Figure 1.10a).

- Compounds ***10*** and ***11*** undergo dissociation of $X^\bullet$ in the gas phase with one-electron reduction in the metal center (Scheme 1.10). This path is more favored than the non-reducing halide X^- dissociation (Scheme 1.11), as it has also been checked by computational calculations in the case of all gold trihalide anions (Table 1.3). These species actually show a marked tendency to undergo dismutation (Scheme 1.12).

1.8. References

[1] H. G. Raubenheimer, S. Cronje, in *Gold: Progress in Chemistry, Biochemistry and Technology* (Ed.: H. Schmidbaur), John Wiley & Sons, Chichester, **1999**, pp. 557−632.

[2] a) M. Hargittai. Structural Effects in Molecular Metal Halides. *Acc. Chem. Res.* **2009**, *42*, 453; b) A. Schulz, M. Hargittai. Structural Variations and Bonding in Gold Halides: A Quantum Chemical Study of Monomeric and Dimeric Gold Monohalide and Gold Trihalide Molecules, AuX, Au_2X_2, AuX_3, and Au_2X_6 (X = F, Cl, Br, I). *Chem. Eur. J.*

2001, *7*, 3657; c) M. Hargittai. Molecular Structure of Metal Halides. *Chem. Rev.* **2000**, *100*, 2233.

[3] a) T. Okabayashi, Y. Nakaoka, E. Yamazaki, M. Tanimoto. Millimeter- and submillimeter-wave spectroscopy of AuF in the ground $X^1\Sigma^+$ state. *Chem. Phys. Lett.* **2002**, *366*, 406; b) C. J. Evans, M. C. L. Gerry. Confirmation of the Existence of Gold(I) Fluoride, AuF: Microwave Spectrum and Structure. *J. Am. Chem. Soc.* **2000**, *122*, 1560; c) D. Schröder, J. Hrušák, I. C. Tornieporth-Oetting, T. M. Klapötke, H. Schwarz. Neutral Gold(I) Fluoride Does Indeed Exist. *Angew. Chem. Int. Ed. Engl.* **1994**, *33*, 212; *Angew. Chem.* **1994**, *106*, 223.

[4] N. J. Rijs, R. A. J. O'Hair. Forming trifluoromethylmetallates: competition between decarboxylation and C–F bond activation of group 11 trifluoroacetate complexes, $[CF_3CO_2ML]^-$. *Dalton Trans.* **2012**, *41*, 3395.

[5] P. Schwerdtfeger, P. D. W. Boyd, A. K. Burrell, W. T. Robinson, M. J. Taylor. Relativistic Effects in Gold Chemistry. 3. Gold(I) Complexes. *Inorg. Chem.* **1990**, *29*, 3593.

[6] X.-G. Xiong, Y.-L. Wang, C.-Q. Xu, Y.-H. Qiu, L.-S. Wang, J. Li. On the gold–ligand covalency in linear $[AuX_2]^-$ complexes. *Dalton Trans.* **2015**, *44*, 5535.

[7] S. J. Grabowski, J. M. Ugalde, D. M. Andrada, G. Frenking. Comparison of Hydrogen and Gold Bonding in $[XHX]^-$, $[XAuX]^-$, and Isoelectronic $[NgHNg]^+$, $[NgAuNg]^+$ (X = Halogen, Ng = Noble Gas). *Chem. Eur. J.* **2016**, *22*, 11317.

[8] S. Mishra. Theoretical Calculation of the Photodetachment Spectra of $XAuY^-$ (X, Y = Cl, Br, and I). *J. Phys. Chem. A* **2007**, *111*, 9164.

[9] H.-T. Liu, X.-G. Xiong, P. D. Dau, Y.-L. Wang, J. Li, L.-S. Wang. The mixed cyanide halide Au(I) complexes, $[XAuCN]^-$ (X = F, Cl, Br, and I): evolution from ionic to covalent bonding. *Chem. Sci.* **2011**, *2*, 2101.

[10] S. Martínez-Salvador, L. R. Falvello, A. Martín, B. Menjón. A hexanuclear gold carbonyl cluster. *Chem. Sci.* **2015**, *6*, 5506.

[11] J.-H. Choy, Y.-I. Kim, S.-J. Hwang, P. V. Huong. Trigonal Planar (D_{3h}) AuI_3 Complex Stabilized in a Solid Lattice. *J. Phys. Chem. B* **2000**, *104*, 7273.

[12] a) J.-H. Choy, Y.-I. Kim. Gold Valence in $(AuI_3)_{0.25}Bi_2Sr_2CaCu_2O_y$ by XPS and XANES Spectroscopy. *J. Phys. Chem. B* **2003**, *107*, 3348; b) M. L. Munzarová, R. Hoffmann. Strong Electronic Consequences of Intercalation in Cuprate Superconductors: The Case of a Trigonal Planar AuI_3 Complex Stabilized in the $Bi_2Sr_2CaCu_2O_y$ Lattice. *J. Am. Chem. Soc.* **2002**, *124*, 5542.

[13] a) B. Zemva, K. Lutar, A. Jesih, W. J. Casteel, Jr., A. P. Wilkinson, D. E. Cox, R. B. Von Dreele, H. Borrmann, N. Bartlett. Silver Trifluoride: Preparation, Crystal Structure, Some Properties, and Comparison with AuF_3. *J. Am. Chem. Soc.* **1991**, *113*, 4192; b) F. W. B. Einstein, P. R. Rao, J. Trotter, N. Bartlett. The Crystal Structure of Gold Trifluoride. *J. Chem. Soc. A* **1967**, 478.

[14] E. S. Clark, D. H. Templeton, C. H. MacGillavry. The Crystal Structure of Gold(III) Chloride. *Acta Crystallogr.* **1958**, *11*, 284.

[15] K.-P. Lörcher, J. Strähle. Die Kristallstruktur des Gold(III)bromids / The Crystal Structure of Gold(III) Bromide. *Z. Naturforsch. B* **1975**, *30*, 662.

[16] a) X. Wang, L. Andrews, F. Brosi, S. Riedel. Matrix Infrared Spectroscopy and Quantum-Chemical Calculations for the Coinage-Metal Fluorides: Comparisons of Ar–AuF, Ne–AuF, and Molecules MF_2 and MF_3. *Chem. Eur. J.* **2013**, *19*, 1397; b) X. Wang, L. Andrews, K. Willmann, F. Brosi, S. Riedel. Investigation of Gold Fluorides

and Noble Gas Complexes by Matrix-Isolation Spectroscopy and Quantum-Chemical Calculations. *Angew. Chem. Int. Ed.* **2012**, *51*, 10628; *Angew. Chem.* **2012**, *124*, 10780.

[17] a) I. J. Blackmore, A. J. Bridgeman, N. Harris, M. A. Holdaway, J. F. Rooms, E. L. Thompson, N. A. Young. Experimental Evidence for a Jahn–Teller Distortion in $AuCl_3$. *Angew. Chem. Int. Ed.* **2005**, *44*, 6746; *Angew. Chem.* **2005**, *117*, 6904; b) M. Hargittai, A. Schulz, B. Réffy, M. Kolonits. Molecular Structure, Bonding, and Jahn−Teller Effect in Gold Chlorides: Quantum Chemical Study of $AuCl_3$, Au_2Cl_6, $AuCl_4^-$, AuCl, and Au_2Cl_2 and Electron Diffraction Study of Au_2Cl_6. *J. Am. Chem. Soc.* **2001**, *123*, 1449; c) B. Réffy, M. Kolonits, A. Schulz, T. M. Klapötke, M. Hargittai. Intriguing Gold Trifluoride−Molecular Structure of Monomers and Dimers: An Electron Diffraction and Quantum Chemical Study. *J. Am. Chem. Soc.* **2000**, *122*, 3127; d) P. Schwerdtfeger, P. D. W. Boyd, S. Brienne, A. K. Burrell. Relativistic Effects in Gold Chemistry. 4. Gold(III) and Gold(V) Compounds. *Inorg. Chem.* **1992**, *31*, 3411.

[18] a) M.-J. Crawford, T. M. Klapötke. Hydrides and Iodides of Gold. *Angew. Chem. Int. Ed.* **2002**, *41*, 2269; *Angew. Chem.* **2002**, *114*, 2373; b) T. Söhnel, R. Brown, L. Kloo, P. Schwerdtfeger. The Stability of Gold Iodides in the Gas Phase and the Solid State. *Chem. Eur. J.* **2001**, *7*, 3167.

[19] P. Schwerdtfeger. Relativistic Effects in Gold Chemistry. 2. The Stability of Complex Halides of Gold(III). *J. Am. Chem. Soc.* **1989**, *111*, 7261.

[20] M. A. Ellwanger, S. Steinhauer, P. Golz, H. Beckers, A. Wiesner, B. Braun-Cula, T. Braun, S. Riedel. Taming the High Reactivity of Gold(III) Fluoride: Fluorido Gold(III) Complexes with N-Based Ligands. *Chem. Eur. J.* **2017**, *23*, 13501.

[21] W.-L. Li, Y. Li, C.-Q. Xu, X.-B. Wang, E. Vorpagel, J. Li. Periodicity, Electronic Structures, and Bonding of Gold Tetrahalides $[AuX_4]^-$ (X = F, Cl, Br, I, At, Uus). *Inorg. Chem.* **2015**, *54*, 11157.

[22] D. B. Dell'Amico, F. Calderazzo, F. Marchetti, S. Merlino. Synthesis and Molecular Structure of $[Au_4Cl_8]$, and the Isolation of $[Pt(CO)Cl_5]^-$ in Thionyl Chloride. *J. Chem. Soc., Dalton Trans.* **1982**, 2257.

[23] D. Schröder, R. Brown, P. Schwerdtfeger, X.-B. Wang, X. Yang, L.-S. Wang, H. Schwarz. Gold Dichloride and Gold Dibromide with Gold Atoms in Three Different Oxidation States. *Angew. Chem. Int. Ed.* **2003**, *42*, 311; *Angew. Chem.* **2003**, *115*, 323.

[24] a) Z. Huang, Y. Yuan, L. Sun, X. Wang, Y. Li. Computational insights into CH_3MX (M = Cu, Ag and Au; X = H, F, Cl, Br and I). *RSC Adv.* **2016**, *6*, 84016; b) X. Li, J. Cai. Electron Density Properties and Metallophilic Interactions of Gold Halides AuX_2 and Au_2X (X = F–I): *Ab Initio* Calculations. *Int. J. Quantum Chem.* **2016**, *116*, 1350; c) H.-G. Cho, L. Andrews. Infrared Spectra of CX_3–AuCl and CX_2–$AuCl_2$ Generated in Reactions of Laser-Ablated Gold Atoms with Chlorofluoromethanes and Carbon Tetrachloride. *Organometallics* **2014**, *33*, 4315; d) H.-G. Cho, L. Andrews. Infrared Spectra of CH_3–MX and CH_2X–MH Prepared in Reactions of Laser-Ablated Gold, Platinum, Palladium, and Nickel Atoms with CH_3Cl and CH_3Br. *Organometallics* **2013**, *32*, 2753; e) H.-T. Liu, Y.-L. Wang, X.-G. Xiong, P. D. Dau, Z. A. Piazza, D.-L. Huang, C.-Q. Xu, J. Li, L.-S. Wang. The electronic structure and chemical bonding in gold dihydride: AuH_2^- and AuH_2. *Chem. Sci.* **2012**, *3*, 3286; f) Y. Gong, L. Andrews. Matrix Infrared Spectroscopic and Theoretical of the Difluoroamino Metal Fluoride Molecules: F_2NMF (M = Cu, Ag, Au). *Inorg. Chem.* **2012**, *51*, 667; g) H.-G. Cho, L. Andrews. Infrared Spectra of CH_3–MF and Several Fragments Prepared by Methyl Fluoride Reactions with Laser-Ablated Cu, Ag, and Au Atoms. *Inorg. Chem.* **2011**, *50*, 10319; h) S. Mishra, V. Vallet, W. Domcke. Importance of Spin–Orbit Coupling for the Assignment of the Photodetachment Spectra of AuX_2^- (X = Cl, Br, and I). *ChemPhysChem* **2006**, *7*, 723; i) L. Andrews, X. Wang, L. Manceron, K. Balasubramanian. The Gold Dihydride Molecule, AuH_2: Calculations of Structure,

Stability, and Frequencies, and the Infrared Spectrum in Solid Hydrogen. *J. Phys. Chem. A* **2004**, *108*, 2936; j) L. Andrews, X. Wang. Infrared Spectra and Structures of the Stable CuH_2^-, AgH_2^-, AuH_2^-, and AuH_4^- Anions and the AuH_2 Molecule. *J. Am. Chem. Soc.* **2003**, *125*, 11751; k) B. Dai, J. Yang. Assignment of photoelectron spectra of AuX_2 (X = Cl, Br, and I) clusters. *Chem. Phys. Lett.* **2003**, *379*, 512.

[25] a) S. Eustis, M. A. El-Sayed. Molecular Mechanism of the Photochemical Generation of Gold Nanoparticles in Ethylene Glycol: Support for the Disproportionation Mechanism. *J. Phys. Chem. B* **2006**, *110*, 14014; b) S. Eustis, H.-Y. Hsu, M. A. El-Sayed. Gold Nanoparticle Formation from Photochemical Reduction of Au^{3+} by Continuous Excitation in Colloidal Solutions. A Proposed Molecular Mechanism. *J. Phys. Chem. B* **2005**, *109*, 4811; c) K. Kurihara, J. Kizling, P. Stenius, J. H. Fendler. Laser and Pulse Radiolytically Induced Colloidal Gold Formation in Water and in Water-in-Oil Microemulsions. *J. Am. Chem. Soc.* **1983**, *105*, 2574; d) M. Asai, S. Tazuke, S. Okamura, T. Ohno, S. Kato. Flash Photolysis of a Gold(III) Complex. *Chem. Lett.* **1973**, *2*, 993; e) J. H. Baxendale, A.-M. Koulkès-Pujo. Une étude par radiolyse pulsée sur l'espèce transitoire au II. *J. Chim. Phys.* **1970**, *67*, 1602.

[26] J. C. Marcum, S. H. Kaufman, J. M. Weber. Gas-Phase Experiments on Au(III) Photochemistry. *J. Phys. Chem. A* **2011**, *115*, 3006.

[27] a) H. G. Raubenheimer, H. Schmidbaur. The Late Start and Amazing Upswing in Gold Chemistry. *J. Chem. Educ.* **2014**, *91*, 2024; b) A. L. Balch, T. Y. Garcia, in *Gold: Science and Applications* (Eds.: C. Corti, R. Holliday), CRC Press, Boca Ratón (FL), **2010**, pp. 31−50; c) M. C. Gimeno, in *Modern Supramolecular Gold Chemistry: Gold-Metal Interactions and Applications* (Ed.: A. Laguna), Wiley-VCH, Weinheim, **2008**, pp. 1−64; d) M. C. Gimeno, A. Laguna, in *Comprehensive Coordination Chemistry II* (Eds.: J. A. McCleverty, T. J. Meyer), Pergamon, Oxford, **2003**, pp. 911−1145; e) H. Schmidbaur, K. C. Dash. Compounds of Gold in Unusual Oxidation States. *Adv. Inorg. Chem. Radiochem.* **1982**, *25*, 239.

[28] a) K. Heinze. The Quest for Mononuclear Gold(II) and Its Potential Role in Photocatalysis and Drug Action. *Angew. Chem. Int. Ed.* **2017**, *56*, 16126; *Angew. Chem.* **2017**, *129*, 16342; b) A. Laguna, M. Laguna. Coordination chemistry of gold(II) complexes. *Coord. Chem. Rev.* **1999**, *193–195*, 837.

[29] a) C. Sun, N. Mirzadeh, S.-X. Guo, J. Li, Z. Li, A. M. Bond, J. Zhang, S. K. Bhargava. Unprecedented Formation of a Binuclear Au(II)–Au(II) Complex through Redox State Cycling: Electrochemical Interconversion of Au(I)–Au(I), Au(II)–Au(II), and Au(I)–Au(III) in Binuclear Complexes Containing the Carbanionic Ligand $C_6F_4PPh_2$. *Inorg. Chem.* **2019**, *58*, 13999; b) P. Jerabek, B. von der Esch, H. Schmidbaur, P. Schwerdtfeger. Influence of Relativistic Effects on Bonding Modes in M(II) Dinuclear Complexes (M = Au, Ag, and Cu). *Inorg. Chem.* **2017**, *56*, 14624; c) L. Nilakantan, K. R. Pichaandi, M. M. Abu-Omar, D. R. McMillin, P. R. Sharp. Synthesis, characterization and DFT study of digold(II) naphth-di-yl complex. *J. Organomet. Chem.* **2017**, *844*, 30; d) B. R. Reiner, M. W. Bezpalko, B. M. Foxman, C. R. Wade. Lewis Acid Catalysis with Cationic Dinuclear Gold(II,II) and Gold(III,III) Phosphorus Ylide Complexes. *Organometallics* **2016**, *35*, 2830; e) N. Mirzadeh, M. A. Bennett, S. K. Bhargava. Cycloaurated complexes of aryl carbanions: Digold(I), Digold(II) and beyond. *Coord. Chem. Rev.* **2013**, *257*, 2250; f) A. A. Mohamed, H. E. Abdou, J. P. Fackler, Jr. Coordination chemistry of gold(II) with amidinate, thiolate and ylide ligands. *Coord. Chem. Rev.* **2010**, *254*, 1253.

[30] a) T. Dann, D.-A. Roşca, J. A. Wright, G. G. Wildgoose, M. Bochmann. Electrochemistry of Au^{II} and Au^{III} pincer complexes: determination of the Au^{II}–Au^{II} bond energy. *Chem. Commun.* **2013**, *49*, 10169; b) D.-A. Roşca, D. A. Smith, D. L. Hughes, M. Bochmann. A Thermally Stable Gold(III) Hydride: Synthesis, Reactivity, and Reductive Condensation as a Route to Gold(II) Complexes. *Angew. Chem. Int. Ed.*

2012, *51*, 10643; *Angew. Chem.* **2012**, *124*, 10795; c) D. Zopes, C. Hegemann, W. Tyrra, S. Mathur. $[(CF_3)_4Au_2(C_5H_5N)_2]$ – a new alkyl gold(II) derivative with a very short Au–Au bond. *Chem. Commun.* **2012**, *48*, 8805; d) J. Coetzee, W. F. Gabrielli, K. Coetzee, O. Schuster, S. D. Nogai, S. Cronje, H. G. Raubenheimer. Structural Studies of Gold(I, II, and III) Compounds with Pentafluorophenyl and Tetrahydrothiophene Ligands. *Angew. Chem. Int. Ed.* **2007**, *46*, 2497; *Angew. Chem.* **2007**, *119*, 2549; e) S. A. Yurin, D. A. Lemenovskii, K. I. Grandberg, I. G. Il'ina, L. G. Kuz'mina. Synthesis and structure of the first dinuclear gold complex with the Au—Au bond containing no bridging ligands. *Russ. Chem. Bull.* **2003**, *52*, 2752; f) V. W.-W. Yam, C.-K. Li, C.-L. Chan, K.-K. Cheung. Synthesis, Structural Characterization, and Photophysics of Dinuclear Gold(II) Complexes $[\{Au(dppn)Br\}_2](PF_6)_2$ and $[\{Au(dppn)I\}_2](PF_6)_2$ with an Unsupported Au^{II}–Au^{II} Bond. *Inorg. Chem.* **2001**, *40*, 7054; g) V. W.-W. Yam, S. W.-K. Choi, K.-K. Cheung. Synthesis, photophysics and thermal redox reactions of a $[\{Au(dppn)Cl\}_2]^{2+}$ dimer with an unsupported Au^{II}–Au^{II} bond. *Chem. Commun.* **1996**, 1173.

[31] X.-G. Xiong, P. Pyykkö. Unbridged Au(II)–Au(II) bonds are theoretically allowed. *Chem. Commun.* **2013**, *49*, 2103.

[32] M. D. Đurović, Ž. D. Bugarčić, R. van Eldik. Stability and reactivity of gold compounds – From fundamental aspects to applications. *Coord. Chem. Rev.* **2017**, *338*, 186.

[33] a) A. Portugués, I. López-García, J. Jiménez-Bernad, D. Bautista, J. Gil-Rubio. Photoinitiated Reactions of Haloperfluorocarbons with Gold(I) Organometallic Complexes: Perfluoroalkyl Gold(I) and Gold(III) Complexes. *Chem. Eur. J.* **2019**, *25*, 15535; b) S. Kim, F. D. Toste. Mechanism of Photoredox-Initiated C−C and C−N Bond Formation by Arylation of IPrAu(I)−CF_3 and IPrAu(I)−Succinimide. *J. Am. Chem. Soc.* **2019**, *141*, 4308; c) M. S. Winston, W. J. Wolf, F. D. Toste. Photoinitiated Oxidative Addition of CF_3I to Gold(I) and Facile Aryl-CF_3 Reductive Elimination. *J. Am. Chem. Soc.* **2014**, *136*, 7777; d) A. Johnson, R. J. Puddephatt. Reactions of Trifluoromethyl Iodide with Methylgold(I) Complexes. Preparation of Trifluoromethyl-gold(I) and -gold(III) Complexes. *J. Chem. Soc., Dalton Trans.* **1976**, 1360; e) A. Johnson, R. J. Puddephatt. Mechanistic Studies of Reactions of Benzenethiol with Methyl Derivatives of Platinum(II) and Gold-(I) and -(III). *J. Chem. Soc., Dalton Trans.* **1975**, 115.

[34] a) P. Veit, C. Volkert, C. Förster, V. Ksenofontov, S. Schlicher, M. Bauer, K. Heinze. Gold(II) in redox-switchable gold(I) catalysis. *Chem. Commun.* **2019**, *55*, 4615; b) M. N. Hopkinson, A. Tlahuext-Aca, F. Glorius. Merging Visible Light Photoredox and Gold Catalysis. *Acc. Chem. Res.* **2016**, *49*, 2261; c) L. Huang, M. Rudolph, F. Rominger, A. S. K. Hashmi. Photosensitizer-Free Visible-Light-Mediated Gold-Catalyzed 1,2-Difunctionalization of Alkynes. *Angew. Chem. Int. Ed.* **2016**, *55*, 4808; *Angew. Chem.* **2016**, *128*, 4888; d) A. Tlahuext-Aca, M. N. Hopkinson, B. Sahoo, F. Glorius. Dual gold/photoredox-catalyzed C(sp)–H arylation of terminal alkynes with diazonium salts. *Chem. Sci.* **2016**, *7*, 89; e) S. Kim, J. Rojas-Martin, F. D. Toste. Visible light-mediated gold-catalysed carbon(sp^2)–carbon(sp) cross-coupling. *Chem. Sci.* **2016**, *7*, 85; f) X.-z. Shu, M. Zhang, Y. He, H. Frei, F. D. Toste. Dual Visible Light Photoredox and Gold-Catalyzed Arylative Ring Expansion. *J. Am. Chem. Soc.* **2014**, *136*, 5844; g) B. Sahoo, M. N. Hopkinson, F. Glorius. Combining Gold and Photoredox Catalysis: Visible Light-Mediated Oxy- and Aminoarylation of Alkenes. *J. Am. Chem. Soc.* **2013**, *135*, 5505.

[35] H. Schwarz. Relativistic Effects in Gas-Phase Ion Chemistry: An Experimentalist's View. *Angew. Chem. Int. Ed.* **2003**, *42*, 4442; *Angew. Chem.* **2003**, *115*, 4580.

[36] A. MacCragh, W. S. Koski. The Phthalocyanine of Gold. *J. Am. Chem. Soc.* **1965**, *87*, 2496.

[37] E. W. Y. Wong, A. Miura, M. D. Wright, Q. He, C. J. Walsby, S. Shimizu, N. Kobayashi, D. B. Leznoff. Gold(II) Phthalocyanine Revisited: Synthesis and Spectroscopic Properties of Gold(III) Phthalocyanine and an Unprecedented Ring-Contracted Phthalocyanine Analogue. *Chem. Eur. J.* **2012**, *18*, 12404.

[38] A. J. Blake, J. A. Greig, A. J. Holder, T. I. Hyde, A. Taylor, M. Schröder. Bis(1,4,7-trithiacyclononane)gold Dication: A Paramagnetic, Mononuclear Au^{II} Complex. *Angew. Chem. Int. Ed. Engl.* **1990**, *29*, 197; *Angew. Chem.* **1990**, *102*, 203.

[39] D. Huang, X. Zhang, E. J. L. McInnes, J. McMaster, A. J. Blake, E. S. Davies, J. Wolowska, C. Wilson, M. Schröder. Crystallographic, Electrochemical, and Electronic Structure Studies of the Mononuclear Complexes of Au(I)/(II)/(III) with [9]aneS_2O ([9]aneS_2O = 1-oxa-4,7-dithiacyclononane). *Inorg. Chem.* **2008**, *47*, 9919.

[40] a) J. L. Shaw, J. Wolowska, D. Collison, J. A. K. Howard, E. J. L. McInnes, J. McMaster, A. J. Blake, C. Wilson, M. Schröder. Redox Non-innocence of Thioether Macrocycles: Elucidation of the Electronic Structures of Mononuclear Complexes of Gold(II) and Silver(II). *J. Am. Chem. Soc.* **2006**, *128*, 13827; b) M. Kampf, J. Griebel, R. Kirmse. EPR-spektroskopische Charakterisierung (X-, Q-Band) monomerer Ag^{II}- und Au^{II}-Komplexe der Thiakronenether [12]anS_4, [16]anS_4, [18]anS_6 und [27]anS_9. *Z. Anorg. Allg. Chem.* **2004**, *630*, 2669.

[41] a) S. Preiß, J. Melomedov, A. Wünsche von Leupoldt, K. Heinze. Gold(III) tetraarylporphyrin amino acid derivatives: ligand or metal centred redox chemistry? *Chem. Sci.* **2016**, *7*, 596; b) Z. Ou, K. M. Kadish, W. E, J. Shao, P. J. Sintic, K. Ohkubo, S. Fukuzumi, M. J. Crossley. Substituent Effects on the Site of Electron Transfer during the First Reduction for Gold(III) Porphyrins. *Inorg. Chem.* **2004**, *43*, 2078; c) K. M. Kadish, W. E, Z. Ou, J. Shao, P. J. Sintic, K. Ohkubo, S. Fukuzumi, M. J. Crossley. Evidence that gold(III) porphyrins are not electrochemically inert: facile generation of gold(II) 5,10,15,20-tetrakis(3,5-di-*tert*-butylphenyl)porphyrin. *Chem. Commun.* **2002**, 356.

[42] S. Preiß, C. Förster, S. Otto, M. Bauer, P. Müller, D. Hinderberger, H. Hashemi Haeri, L. Carella, K. Heinze. Structure and reactivity of a mononuclear gold(II) complex. *Nat. Chem.* **2017**, *9*, 1249.

[43] a) T. Drews, S. Seidel, K. Seppelt. Gold–Xenon Complexes. *Angew. Chem. Int. Ed.* **2002**, *41*, 454; *Angew. Chem.* **2002**, *114*, 470; b) S. Seidel, K. Seppelt. Xenon as a Complex Ligand: The Tetra Xenono Gold(II) Cation in $AuXe_4^{2+}(Sb_2F_{11}^-)_2$. *Science* **2000**, *290*, 117.

[44] I.-C. Hwang, K. Seppelt. The Reduction of AuF_3 in Super Acidic Solution. *Z. Anorg. Allg. Chem.* **2002**, *628*, 765.

[45] S. H. Elder, G. M. Lucier, F. J. Hollander, N. Bartlett. Synthesis of Au(II) Fluoro Complexes and Their Structural and Magnetic Properties. *J. Am. Chem. Soc.* **1997**, *119*, 1020.

[46] a) O. Graudejus, A. P. Wilkinson, N. Bartlett. Structural Features of $Ag[AuF_4]$ and $Ag[AuF_6]$ and the Stuctural Relationship of $Ag[AgF_4]_2$ and $Au[AuF_4]_2$ to $Ag[AuF_4]_2$. *Inorg. Chem.* **2000**, *39*, 1545; b) R. Schmidt, B. G. Müller. Einkristalluntersuchungen an $Au[AuF_4]_2$ und CeF_4, zwei unerwarteten Nebenprodukten. *Z. Anorg. Allg. Chem.* **1999**, *625*, 605.

[47] F. G. Herring, G. Hwang, K. C. Lee, F. Mistry, P. S. Phillips, H. Willner, F. Aubke. Generation of Au^{2+} Ions in the Solid State or in Fluorosulfuric Acid Solution and Their Identification by ESR. *J. Am. Chem. Soc.* **1992**, *114*, 1271.

[48] S. Martínez-Salvador, L. R. Falvello, A. Martín, B. Menjón. Gold(I) and Gold(III) Trifluoromethyl Derivatives. *Chem. Eur. J.* **2013**, *19*, 14540.

[49] T. Mathieson, A. Schier, H. Schmidbaur. Tris[(triphenylphosphine)gold(I)]oxonium Dihydrogentrifluoride as the Product of an Attempted Preparation of [(Triphenylphosphine)gold(I)] Fluoride. *Z. Naturforsch. B* **2000**, *55*, 1000.

[50] a) C. M. Wyss, B. K. Tate, J. Bacsa, M. Wieliczko, J. P. Sadighi. Dinuclear μ-fluoro cations of copper, silver and gold. *Polyhedron* **2014**, *84*, 87; b) D. S. Laitar, P. Müller, T. G. Gray, J. P. Sadighi. A Carbene-Stabilized Gold(I) Fluoride: Synthesis and Theory. *Organometallics* **2005**, *24*, 4503.

[51] a) S. Muramatsu, K. Koyasu, T. Tsukuda. Formation of Grignard Reagent-like Complex $[CH_3–M–I]^-$ via Oxidative Addition of CH_3I on Coinage Metal Anions M^- (M = Cu, Ag, Au) in the Gas Phase. *Chem. Lett.* **2017**, *46*, 676; b) S. Muramatsu, K. Koyasu, T. Tsukuda. Oxidative Addition of CH_3I to Au^- in the Gas Phase. *J. Phys. Chem. A* **2016**, *120*, 957.

[52] S. Martínez-Salvador, J. Forniés, A. Martín, B. Menjón. $[Au(CF_3)(CO)]$: A Gold Carbonyl Compound Stabilized by a Trifluoromethyl Group. *Angew. Chem. Int. Ed.* **2011**, *50*, 6571; *Angew. Chem.* **2011**, *123*, 6701.

[53] D. Zopes, S. Kremer, H. Scherer, L. Belkoura, I. Pantenburg, W. Tyrra, S. Mathur. Hydrolytic Decomposition of Tetramethylammonium Bis(trifluoromethyl)aurate(I), $[NMe_4][Au(CF_3)_2]$: A Route for the Synthesis of Gold Nanoparticles in Aqueous Medium. *Eur. J. Inorg. Chem.* **2011**, 273.

[54] A. Martín, A. G. Orpen. Structural Systematics. 6. Apparent Flexibility of Metal Complexes in Crystals. *J. Am. Chem. Soc.* **1996**, *118*, 1464.

[55] J. R. Brown, P. Schwerdtfeger, D. Schröder, H. Schwarz. Experimental and Theoretical Studies of Diatomic Gold Halides. *J. Am. Soc. Mass Spectrom.* **2002**, *13*, 485.

[56] a) A. G. Algarra, V. V. Grushin, S. A. Macgregor. Natural Bond Orbital Analysis of the Electronic Structure of $[L_nM(CH_3)]$ and $[L_nM(CF_3)]$ Complexes. *Organometallics* **2012**, *31*, 1467; b) P. Sgarbossa, A. Scarso, G. Strukul, R. A. Michelin. Platinum(II) Complexes with Coordinated Electron-Withdrawing Fluoroalkyl and Fluoroaryl Ligands: Synthesis, Reactivity, and Catalytic Activity. *Organometallics* **2012**, *31*, 1257; c) T. G. Appleton, H. C. Clark, L. E. Manzer. The *trans*-influence: its measurement and significance. *Coord. Chem. Rev.* **1973**, *10*, 335; d) T. G. Appleton, M. H. Chisholm, H. C. Clark, L. E. Manzer. Trifluoromethylplatinum Complexes and the Nature of the Pt–CF_3 Bond. *Inorg. Chem.* **1972**, *11*, 1786.

[57] a) S. A. Cooke, M. C. L. Gerry. XeAuF. *J. Am. Chem. Soc.* **2004**, *126*, 17000; b) J. M. Thomas, N. R. Walker, S. A. Cooke, M. C. L. Gerry. Microwave Spectra and Structures of KrAuF, KrAgF, and KrAgBr; ^{83}Kr Nuclear Quadrupole Coupling and the Nature of Noble Gas−Noble Metal Halide Bonding. *J. Am. Chem. Soc.* **2004**, *126*, 1235; c) C. J. Evans, D. S. Rubinoff, M. C. L. Gerry. Noble gas–metal chemical bonding: the microwave spectra, structures and hyperfine constants of Ar–AuF and Ar–AuBr. *Phys. Chem. Chem. Phys.* **2000**, *2*, 3943.

[58] a) M. Á. García-Monforte, S. Martínez-Salvador, B. Menjón. The Trifluoromethyl Group in Transition Metal Chemistry. *Eur. J. Inorg. Chem.* **2012**, 4945; b) R. P. Hughes. Conversion of Carbon–Fluorine Bonds α to Transition Metal Centers to Carbon–Hydrogen, Carbon–Carbon, and Carbon–Heteroatom Bonds. *Eur. J. Inorg. Chem.* **2009**, *2009*, 4591; c) P. J. Brothers, W. R. Roper. Transition-Metal Dihalocarbene Complexes. *Chem. Rev.* **1988**, *88*, 1293.

[59] a) D. Huang, P. R. Koren, K. Folting, E. R. Davidson, K. G. Caulton. Facile and Reversible Cleavage of C−F Bonds. Contrasting Thermodynamic Selectivity for Ru−CF_2H vs F−Os=CFH. *J. Am. Chem. Soc.* **2000**, *122*, 8916; b) D. Huang, K. G. Caulton. New Entries to and New Reactions of Fluorocarbon Ligands. *J. Am. Chem. Soc.* **1997**, *119*, 3185.

[60] A. N. Nesmeyanov, É. G. Perevalova, E. I. Smyslova, V. P. Dyadchenko, K. I. Grandberg. Reaction of gold compounds and diazomethane. *Bull. Acad. Sci. USSR Div. Chem. Sci. (Engl. Transl.)* **1977**, *26*, 2417.

[61] a) V. H. Gessner. Stability and reactivity control of carbenoids: recent advances and perspectives. *Chem. Commun.* **2016**, *52*, 12011; b) V. Capriati, in *Contemporary Carbene Chemistry* (Eds.: R. A. Moss, M. P. Doyle), John Wiley & Sons: Hoboken (NJ), **2014**, pp. 325–362; c) V. Capriati, S. Florio. Anatomy of Long-Lasting Love Affairs with Lithium Carbenoids: Past and Present Status and Future Prospects. *Chem. Eur. J.* **2010**, *16*, 4152.

[62] J. Kvíčala, J. Štambaský, S. Böhm, O. Paleta. Equilibrium structures of isolated (halogenated) fluorolithiomethanes. *J. Fluorine Chem.* **2002**, *113*, 147.

[63] G. K. S. Prakash, F. Wang, Z. Zhang, R. Haiges, M. Rahm, K. O. Christe, T. Mathew, G. A. Olah. Long-Lived Trifluoromethanide Anion: A Key Intermediate in Nucleophilic Trifluoromethylations. *Angew. Chem. Int. Ed.* **2014**, *53*, 11575; *Angew. Chem.* **2014**, *126*, 11759.

[64] B. Waerder, S. Steinhauer, B. Neumann, H.-G. Stammler, A. Mix, Y. V. Vishnevskiy, B. Hoge, N. W. Mitzel. Solid-State Structure of a Li/F Carbenoid: Pentafluoroethyllithium. *Angew. Chem. Int. Ed.* **2014**, *53*, 11640; *Angew. Chem.* **2014**, *126*, 11824.

[65] a) R. D. Chambers, in *Fluorine in Organic Chemistry*, 2nd ed., Blackwell Publishing Ltd, Oxford, **2004**, pp. 137−161; b) D. M. Roddick. Safe generation of (perfluoroethyl)lithium. *Chem. Eng. News* **1997**, *75*(40), 6.

[66] E. Bernhardt, M. Finze, H. Willner. Synthesis and NMR spectroscopic investigation of salts containing the novel $[Au(CF_3)_nX_{4-n}]^-$ (n = 4–1, X = F, CN, Cl) anions. *J. Fluorine Chem.* **2004**, *125*, 967.

[67] M. A. Ellwanger, S. Steinhauer, P. Golz, T. Braun, S. Riedel. Stabilization of Lewis Acidic AuF_3 as an N-Heterocyclic Carbene Complex: Preparation and Characterization of $[AuF_3(SIMes)]$. *Angew. Chem. Int. Ed.* **2018**, *57*, 7210; *Angew. Chem.* **2018**, *130*, 7328.

[68] a) R. Usón, A. Laguna, B. Bergareche. Dihalo pentafluorophenyl tetrahydrothiophen gold(III) complexes, their preparation and reactions. *J. Organomet. Chem.* **1980**, *184*, 411; b) P. Braunstein, R. J. H. Clark. Synthesis and Properties of Arylgold(III) Compounds. *Inorg. Chem.* **1974**, *13*, 2224.

[69] H. Schmidbaur, A. Grohmann, M. E. Olmos, in *Gold: Progress in Chemistry, Biochemistry and Technology* (Ed.: H. Schmidbaur), John Wiley & Sons, Chichester, **1999**, pp. 647–746.

[70] R. D. Sanner, J. H. Satcher, Jr., M. W. Droege. Synthesis and Characterization of (Trifluoromethyl)gold Complexes. *Organometallics* **1989**, *8*, 1498.

[71] a) J. E. Huheey, E. A. Keiter, R. L. Keiter, in *Inorganic Chemistry: Principles of Structure and Reactivity*, 4th ed., Harper-Collins, New York (NY), **1993**, pp. 182–199; b) R. T. Sanderson, in *Simple Inorganic Substances*, Krieger, Malabar (FL), **1989**, p. 23; c) R. T. Sanderson. Principles of Electronegativity Part I. General Nature. *J. Chem. Educ.* **1988**, *65*, 112.

[72] a) D. Schneider, O. Schuster, H. Schmidbaur. Attempted Oxidative Addition of Halogens to (Isocyanide)gold(I) Complexes. *Organometallics* **2005**, *24*, 3547; b) D. Schneider, A. Schier, H. Schmidbaur. Governing the oxidative addition of iodine to gold(I) complexes by ligand tuning. *Dalton Trans.* **2004**, 1995.

[73] M. Blaya, D. Bautista, J. Gil-Rubio, J. Vicente. Synthesis of Au(I) Trifluoromethyl Complexes. Oxidation to Au(III) and Reductive Elimination of Halotrifluoromethanes. *Organometallics* **2014**, *33*, 6358.

[74] P. J. Barker, J. N. Winter, in *The Chemistry of the Metal−Carbon Bond, Vol. 2* (Eds.: F. R. Hartley, S. Patai), John Wiley & Sons, Chichester, **1985**, pp. 151–218.

[75] a) K. A. Smoll, W. Kaminsky, K. I. Goldberg. Photolysis of Pincer-Ligated Pd^{II}–Me Complexes in the Presence of Molecular Oxygen. *Organometallics* **2017**, *36*, 1213; b) P. M. Kozlowski, B. D. Garabato, P. Lodowski, M. Jaworska. Photolytic properties of cobalamins: a theoretical perspective. *Dalton Trans.* **2016**, *45*, 4457.

[76] a) D. Zhu, S. V. Lindeman, J. K. Kochi. X-ray Crystal Structures and the Facile Oxidative (Au−C) Cleavage of the Dimethylaurate(I) and Tetramethylaurate(III) Homologues. *Organometallics* **1999**, *18*, 2241; b) R. J. Puddephatt. Reactivity and Mechanism in Organogold Chemistry. *Gold Bull.* **1977**, *10*, 108.

[77] M. Baya, D. Joven-Sancho, P. J. Alonso, J. Orduna, B. Menjón. M−C Bond Homolysis in Coinage-Metal $[M(CF_3)_4]^-$ Derivatives. *Angew. Chem. Int. Ed.* **2019**, *58*, 9954; *Angew. Chem.* **2019**, *131*, 10059.

[78] a) A. K. Srivastava, N. Misra. The Highest Oxidation State of Au Revealed by Interactions with Successive Cl Ligands and Superhalogen Properties of $AuCl_n$ ($n = 1$–6) Species. *Int. J. Quantum Chem.* **2014**, *114*, 1513; b) P. Koirala, M. Willis, B. Kiran, A. K. Kandalam, P. Jena. Superhalogen Properties of Fluorinated Coinage Metal Clusters. *J. Phys. Chem. C* **2010**, *114*, 16018; c) K. A. Barakat, T. R. Cundari, H. Rabaâ, M. A. Omary. Disproportionation of Gold(II) Complexes. A Density Functional Study of Ligand and Solvent Effects. *J. Phys. Chem. B* **2006**, *110*, 14645.

[79] a) G. L. Gutsev, A. I. Boldyrev. The Theoretical Investigation of the Electron Affinity of Chemical Compounds. *Adv. Chem. Phys.* **1985**, *61*, 169; b) G. L. Gutsev, A. I. Boldyrev. DVM-Xα Calculations on the Ionization Potentials of MX_{k+1}^- Complex Anions and the Electron Affinities of MX_{k+1} "Superhalogens". *Chem. Phys.* **1981**, *56*, 277.

Chapter 2

An Organogold(III) Difluoride with a *trans* Arrangement

This chapter is based on the following peer-reviewed paper:

A. Pérez-Bitrián, M. Baya, J. M. Casas, A. Martín, B. Menjón, J. Orduna. An Organogold(III) Difluoride with a *trans* Arrangement. *Angew. Chem. Int. Ed.* **2018**, *57*, 6517–6521. DOI: 10.1002/anie.201802379. *Angew. Chem.* **2018**, *130*, 6627–6631. DOI: 10.1002/ange.201802379.

2.1. Introduction and objectives

Fluoride[1] and trifluoromethyl[2] ligands are of prominent importance in the coordination chemistry of gold, as described in the Introduction. However, complexes containing both ligands attached to the same gold center are very scarce. For example, the simplest gold(I) $[CF_3AuF]^-$ anion has only been detected in the gas phase,[3] and our efforts to isolate it, described in the preceding Chapter 1, were unsuccessful thus far. Moreover, before the beginning of this Thesis, the only isolated gold derivatives incorporating both ligands had been reported by Toste and coworkers as part of two series of organogold(III) halide complexes of stoichiometries $CF_3Au(4\text{-Me-}C_6H_4)(PPh_3)X$ and $CF_3Au(4\text{-F-}C_6H_4)(PCy_3)X$ (X = F, Cl, Br, I).[4]

When considering gold(III) complexes, both the purely inorganic $[AuF_4]^-$ and the homoleptic organometallic $[(CF_3)_4Au]^-$ derivatives are well known. The first one is very reactive and it has been isolated with different cations,[1,5] including tetraalkyl ammonium ones.[6] Its alkali salts have also been recently studied by matrix-isolation spectroscopy.[7] The homoleptic $[(CF_3)_4Au]^-$ anion, which shows ligand-field inversion[8] was recently characterized in the solid state[9] and also studied in the gas phase.[8] Additionally, both theoretic calculations and experimental observation enable to consider this homoleptic complex as a weakly coordinating anion,[10] which is in agreement with its lack of reactivity.[9]

On the other hand, complexes containing only both fluoride and trifluoromethyl ligands had not been previously isolated. However, even one year before the first organogold fluoride complex was prepared,[11] the four possible complex anions in between $[AuF_4]^-$ and $[(CF_3)_4Au]^-$, namely $[(CF_3)_xAuF_{4-x}]^-$ (x = 1–3), were spectroscopically detected and characterized by ^{13}C and ^{19}F NMR, but could not be separated from the complex reaction mixtures containing different trifluoromethyl gold anions.[12]

In Chapter 1 we have described our attempts to obtain salts of the $[CF_3AuF_3]^-$ anion starting from species containing a single CF_3 ligand already attached to the metal center. In Chapter 3, the synthesis and properties of the $[(CF_3)_3AuF]^-$ anion as its $[PPh_4]^+$ salt will be discussed as part of the whole organogold(III) $[(CF_3)_3AuX]^-$ anionic series (X = F, Cl, Br, I). The complex anion $[CF_3AuCF_3]^-$ was found to be oxidized by halogens, X_2, affording the *trans* dihalide derivatives [*trans*-$(CF_3)_2AuX_2]^-$.[9] Thus, a synthesis of an organogold(III) difluoride containing trifluoromethyl ligands seemed to be feasible starting from the homoleptic organogold(I) species $[PPh_4][CF_3AuCF_3]$ (**I**).

In the synthesis of gold(III) difluoride complexes, xenon difluoride has proved to be a suitable fluorinating and oxidizing agent. This colorless crystalline solid can be considered as a tamed version of elemental F_2: it is relatively easy to handle, but still very reactive.[13] The first organogold(III) difluoride complexes were obtained precisely by reaction of gold(I) (NHC)AuR precursors (NHC = N-heterocyclic carbene; R = alkyl) with XeF_2.[14] Additionally, shortly after our results on this topic were published, Dutton and coworkers reported on the synthesis of the first cationic gold(III) difluoride complexes containing pyridine and imidazole ligands using XeF_2.[15] In particular, complexes [*trans*-$AuF_2(py)_2][BF_4]$, [*trans*-$Au(4\text{-dmap})_2F_2$][OTf] (4-dmap = 4-(dimethylamino)pyridine) and [*trans*-$AuF_2(Im)_2$][OTf] (Im = *N*-methylimidazole) were prepared by reaction of the corresponding gold(I) complex with XeF_2 (Scheme 2.1), but only the imidazole derivative could be studied by X-ray diffraction. Alternatively, they were also prepared by displacement of 4-pyridinecarnonitrile ligands with KF in the presence of 18-crown-6 in acetonitrile.

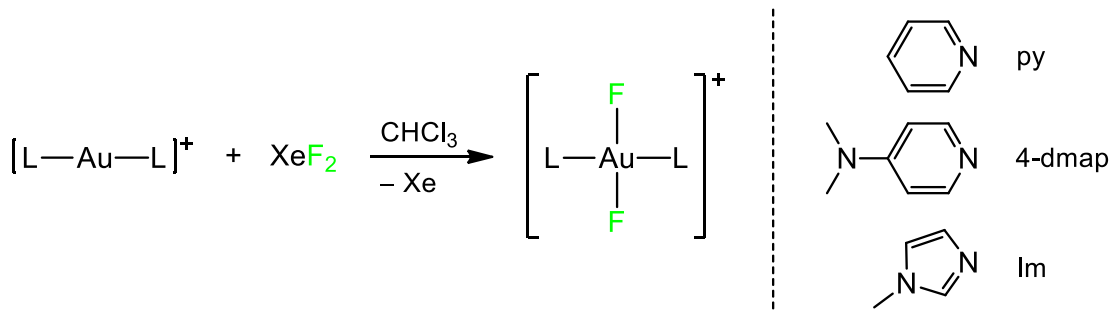

Scheme 2.1. Synthesis of cationic gold(III) difluoride complexes reported by the group of Dutton, with N-ligands L indicated on the right.[15] The anion is $[BF_4]^-$ for the pyridine complex and $[OTf]^-$ for the 4-dmap and Im derivatives.

After the publication of our results, two more *trans* difluoride organogold(III) complexes have been reported by the Riedel group, *trans*-$AuClF_2$(SIMes) and *trans*-$AuF_2(OTeF_5)$(SIMes).[16] It is interesting to note that they were prepared by substitution of a fluoride ligand in the gold(III) precursor AuF_3(SIMes), instead of by oxidation of a gold(I) species.

In this chapter, the stereoselective and efficient synthesis of the first organogold(III) difluoride with a *trans* stereochemistry is described. Additionally, its properties in the gas phase are analyzed, with a special emphasis on the detection and study of further organogold fluoride species. Finally, initial investigations on its reactivity are discussed.

2.2. Synthesis and characterization of $[PPh_4][trans\text{-}(CF_3)_2AuF_2]$

The homoleptic organogold(I) derivative $[PPh_4][CF_3AuCF_3]$ (**I**) cleanly reacts with XeF_2 in CH_2Cl_2 at 0 °C (Scheme 2.2) to render the organogold(III) difluoride complex $[PPh_4][trans\text{-}(CF_3)_2AuF_2]$ (**12**). The reaction is quantitative and stereoselective. Eventually, the complex is isolated as a white solid in excellent yield (94%). Although the reaction can be carried out using a previously flame-dried schlenk, the compound is moisture-sensitive and turns yellowish when in contact with glassware for some minutes at room temperature, even under argon atmosphere. Hence, it is better stored at low temperature. However, under completely dry conditions, it is thermally stable and decomposes above 250 °C.

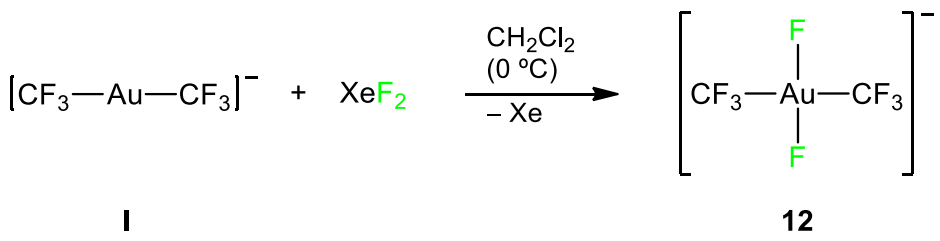

Scheme 2.2. Synthesis of the organogold(III) difluoride complex **12**. The cation is $[PPh_4]^+$.

The stereochemistry of compound **12** could be easily assigned by means of ^{19}F NMR spectroscopy, since it shows a characteristic pattern (Figure 2.1). The signal corresponding to the CF_3 groups appears as a triplet at δ_F = –46.16 ppm with $^3J(^{19}F,^{19}F)$

= 16.5 Hz. For its part, the signal belonging to the fluoride ligands appears at high field (δ_F = –324.96 ppm) as a septet with the same coupling constant, at a similar chemical shift to other related species (Table 2.1). It is interesting to note that in the case of related processes previously reported by the group of Toste, the stereochemistry of the addition was *cis* instead.[14] However, a *trans* stereochemistry was also obtained later by Dutton and coworkers when oxidizing pyridine- and imidazole-based cationic gold(I) precursors with XeF_2.[15]

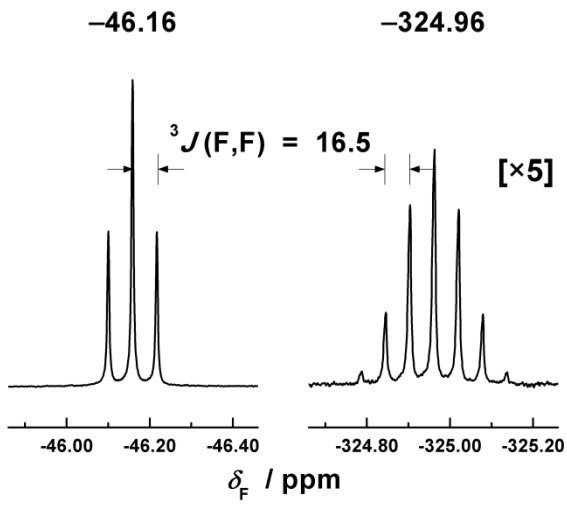

Figure 2.1. ^{19}F NMR spectrum of compound **12** in CD_3CN solution at room temperature. δ_F [ppm] and *J* [Hz] are indicated.

Table 2.1. Relevant spectroscopic and crystallographic data of isolated *trans* difluoride gold(III) complexes.

	δ_F(Au–F) [ppm]	ν(Au–F) [cm^{-1}]	Au–F bond lengths [pm, av.]
[PPh_4][*trans*-$(CF_3)_2AuF_2$] (**12**)	–324.96[a]	598	199.0(3)
[*trans*-$AuF_2(py)_2$][BF_4][b]	–237.28[a]	[c]	[c]
[*trans*-Au(4-dmap)$_2F_2$][OTf][b]	–249.40[a]	[c]	[c]
[*trans*-$AuF_2(Im)_2$][OTf][b]	–284.03[a]	[c]	191.6(3)
trans-$AuClF_2$(SIMes)[d]	–325.9[e]	594	192.6(2)
trans-$AuF_2(OTeF_5)$(SIMes)[d]	–310.5[e]	613	191.8(2)

[a] ^{19}F NMR spectra registered in CD_3CN at room temperature. [b] Values taken from Ref. [15]. [c] Not reported. [d] Values taken from Ref. [16]. [e] ^{19}F NMR spectra registered in CD_2Cl_2 at room temperature.

We were also able to grow single crystal of complex **12** and check, by single-crystal X-ray diffraction methods, that it exhibits the same stereochemistry in the solid state as in

solution (Figure 2.2). The Au–C bond lengths (205.4(5) pm av.) are between those observed in the homoleptic organogold(I) $[PPh_4][CF_3AuCF_3]$ (203.3(2) pm av.) and organogold(III) $[PPh_4][(CF_3)_4Au]$ (208.0(7) pm av.) derivatives.[9] In turn, the Au–F distances (199.0(3) pm av.) are significantly longer than those found in the $[NMe_4][AuF_4]$ salt (191.1(5) pm av.).[6] Virtually identical Au–F bond lengths were found in the *cis*-difluorides (N^C)AuF_2 reported by Nevado (198.2(4) pm av.).[17] Au–F bond lengths are also slightly shorter in the *trans*-standing fluoride ligands in the neutral $[AuF_3(SIMes)]$ complex (191.9(1) pm av.)[18] and in other *trans* gold(III) difluorides, as shown in Table 2.1. However, it is similar to the Au–F distance *trans* to the SIMes ligand in $AuF_3(SIMes)$ (197.2(1) pm). The IR-active ν(Au–F) mode (B_{1u}) of **12** (598 cm^{-1}) is indistinguishable from those reported for the $[NMe_4]^+$ (597 cm^{-1}) and $[NEt_4]^+$ (598 cm^{-1}) salts of the $[AuF_4]^-$ anion,[6] as well as for the neutral complex $AuF_3(SIMes)$ (604 cm^{-1})[16] and related *trans* difluorides (Table 2.1).

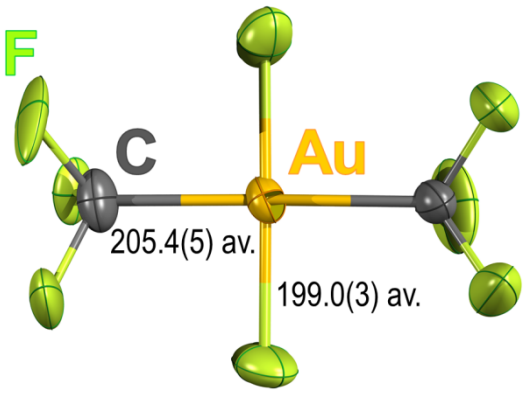

Figure 2.2. Displacement-ellipsoid diagram (50% probability) of the $[trans\text{-}(CF_3)_2AuF_2]^-$ anion as found in single crystals of **12**. Only one set of the rotationally disordered F atoms found in one of the CF_3 groups is shown. Selected bond lengths [pm] with estimated standard deviations are indicated.

2.3. Gas-phase behavior of $[trans\text{-}(CF_3)_2AuF_2]^-$

The anion of **12**, $[trans\text{-}(CF_3)_2AuF_2]^-$ was studied by tandem mass spectrometry to get an insight into its behavior in the gas phase. Several unimolecular decomposition pathways were observed in MS^2 (Scheme 2.3, Figure 2.3). The most favored process is the extrusion of CF_2, which involves the formation of the trifluoride $[CF_3AuF_3]^-$ anion

(***13***), with no change in the oxidation state of the metal (Scheme 2.3a). Interestingly, a CF_2 extrusion has also been observed in the unimolecular decomposition of the homoleptic anions $[CF_3AuCF_3]^-$[3] and $[(CF_3)_4Au]^-$.[8] In MS^3, complex ***13*** dissociates homolytically a $CF_3^{\bullet}$ radical (Scheme 2.3a) giving rise to the gold(II) trifluoride anion $[AuF_3]^-$ (***16***) through an analogous process to that described in Chapter 1, and which enabled the detection of gold(II) trihalides $[AuCl_3]^-$ (***10***) and $[AuBr_3]^-$ (***11***). A T-shape structure was found to be the most stable geometry for all these d^9 species (see Chapter 1). Anion ***16*** also shows a similar behavior to its heavier homologues ***10*** and ***11***, dissociating a fluorine atom and giving rise to gold difluoride anion $[AuF_2]^-$ (***17***).

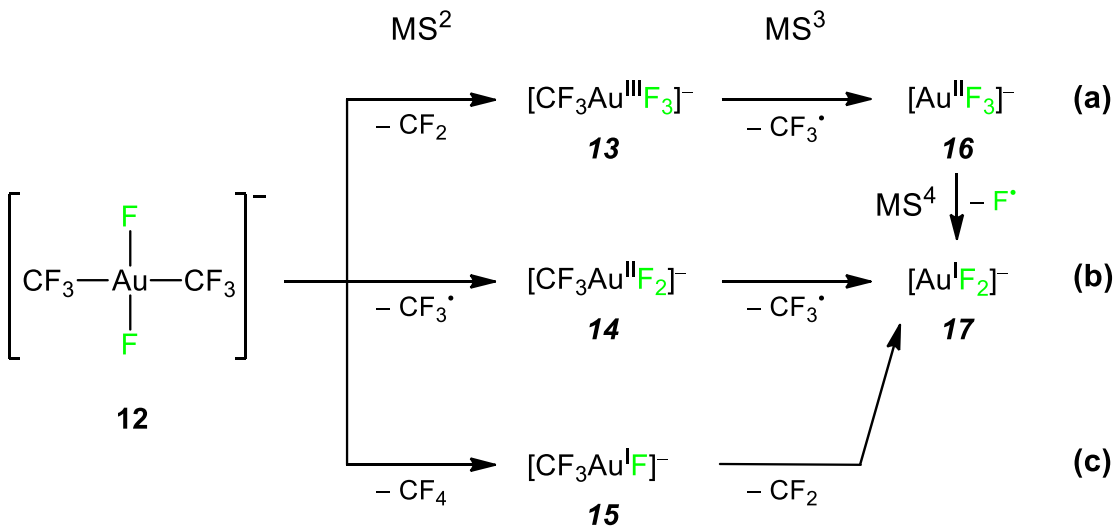

Scheme 2.3. Unimolecular fragmentation paths experimentally observed by tandem mass spectrometry for the $[trans\text{-}(CF_3)_2AuF_2]^-$ anion and for the $[CF_3AuF_x]^-$ anions (x = 1, 2, 3) derived therefrom.

The $[trans\text{-}(CF_3)_2AuF_2]^-$ anion also undergoes homolytic cleavage of a Au–CF_3 bond giving rise to the organogold(II) difluoride $[CF_3AuF_2]^-$ species (***14***), in which the oxidation state of gold is reduced by one unit (Scheme 2.3b). Anion ***14*** suffers a second bond homolysis in MS^3 to yield $[AuF_2]^-$ (***17***). Additionally, a formal reductive elimination of CF_4 or double radical dissociation, with the corresponding reduction of the metal center by two units, leads to small amounts of the mixed organogold(I) $[CF_3AuF]^-$ (***15***) species (Scheme 2.3c). Whereas $[CF_3AuF]^-$ (***15***),[3] $[AuF_3]^-$ (***16***)[6] and $[AuF_2]^-$ (***17***)[3] have been recently detected in the gas phase, $[CF_3AuF_3]^-$ (***13***) had only been previously detected in solution.[12]

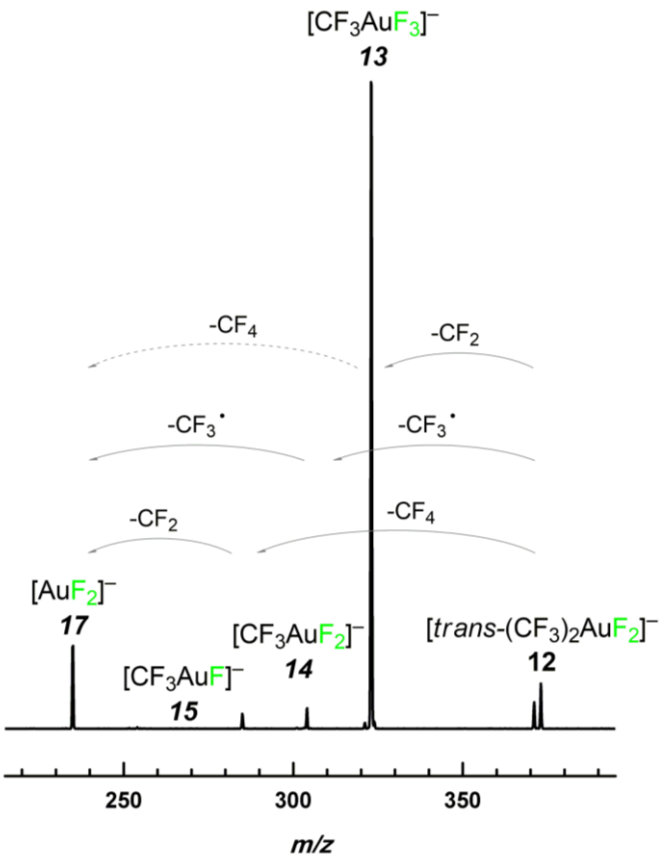

Figure 2.3. Quadrupole ion-trap MS^2 results of the collision-induced dissociation (CID) of the anion of **12**, [*trans*-$(CF_3)_2AuF_2]^-$. All the $[CF_3AuF_x]^-$ anions (x = 1 (***15***), 2 (***14***), 3(***13***)), as well as $[AuF_2]^-$ (***17***) can be observed.

The geometries of the detected organogold fluorides $[CF_3AuF_x]^-$ (x = 1 (***15-DFT***), 2 (***14-DFT***), 3(***13-DFT***)) were optimized at the DFT/M06 level (Figure 2.4 and Figure 2.5). Interestingly, the CF_3–Au–F axis in the gold(III) compound ***13-DFT*** is very similar to the linear gold(I) species ***15-DFT***, regardless of the coordination number and the oxidation state of gold. However, the unsaturated organogold(II) species ***14-DFT*** has been found to be fluxional and two T-shaped isomers have been located as a local minimum (*trans* isomer) and a global minimun (*cis* isomer), respectively (Figure 2.5). The latter is stabilized by ΔH = –16.2 kJ mol^{-1} and both are connected through an interconversion path with a transition state at only +0.7 kJ mol^{-1} above our arbitrary reference. The Au–C bond length in the *cis* isomer of ***14-DFT*** (Figure 2.5c) is quite similar to the Au–C distance in ***13-DFT*** and ***15-DFT*** (Figure 2.4). However, it is significantly elongated in the transition state and even longer in the *trans* isomer. This

elongation is related to the increasing spin density of the unpaired electron delocalized onto the CF_3 group, which is insignificant in the *cis* isomer but becomes 54% in the *trans* isomer. Therefore, the CF_3 group delocalizes the spin density similarly to iodine in the related $[AuI_3]^-$ anion (see Chapter 1), which indicates a significant degree of covalency for the Au–CF_3 bond.[19]

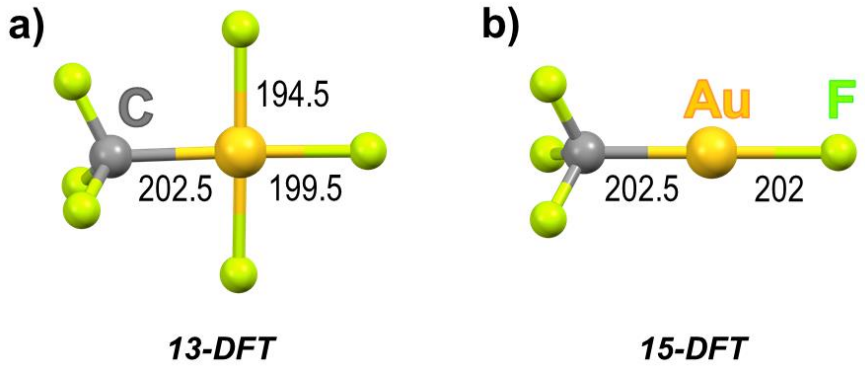

Figure 2.4. Geometries of a) the $[CF_3Au^{III}F_3]^-$ anion (***13-DFT***) and b) the $[CF_3Au^{I}F]^-$ (***15-DFT***) anion, optimized at the DFT/M06 level. Relevant bond lengths [pm] are indicated.

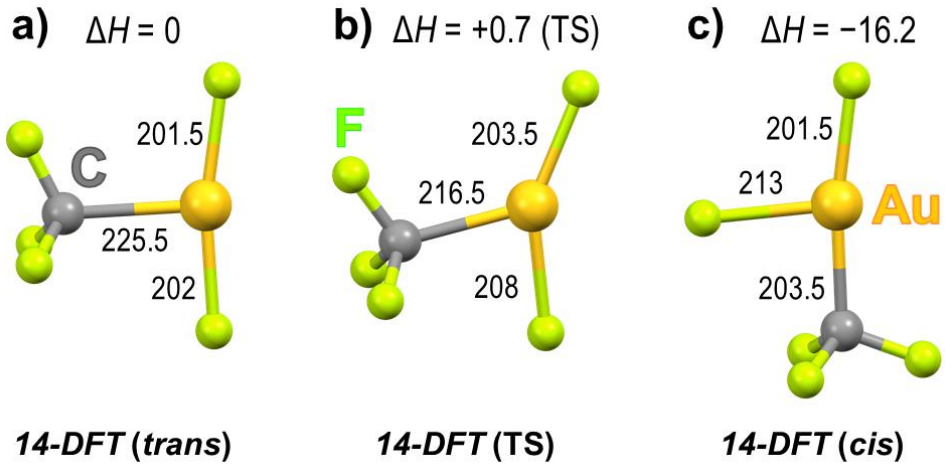

Figure 2.5. Geometries of the stationary points located on the potential energy surface of the unsaturated $[CF_3Au^{II}F_2]^-$ anion (***14-DFT***) optimized at the DFT/M06 level: a) *trans* isomer, b) transition state, and c) *cis* isomer. Relative stabilities (ΔH in kJ mol^{-1}) and relevant bond lengths [pm] are indicated.

2.4. Reactivity of [PPh$_4$][*trans*-(CF$_3$)$_2$AuF$_2$]

To gain a deeper understanding of our difluoride complex [PPh$_4$][*trans*-(CF$_3$)$_2$AuF$_2$] (**12**), its reactivity was tested. In particular, the metathesis reaction with heavier halides was examined, being the results in agreement with the typical behavior of a hard ligand like fluoride bound to a "class *b*" metal like Au(III), according to the HSAB theory.[20]

The fluoride ligands in **12** are easily replaced by any other heavier halide in acetone solution (Scheme 2.4), quantitatively yielding the corresponding [PPh$_4$][*trans*-(CF$_3$)$_2$AuX$_2$] derivatives (X = Cl (**18**), Br (**19**), I (**20**)). These complexes were also recently prepared by oxidative addition of the corresponding halogen, X$_2$, to the homoleptic [PPh$_4$][CF$_3$AuCF$_3$] compound.[9] Interestingly, the ^{19}F chemical shifts of the CF$_3$ groups in all derivatives of the [PPh$_4$][*trans*-(CF$_3$)$_2$AuX$_2$] series (X = F (**12**), Cl (**18**), Br (**19**), I (**20**)) correlate very accurately with the electronegativity of the corresponding halogen in the Sanderson scale (Figure 2.6).[21] We also tried to obtain mixed [PPh$_4$][*trans*-(CF$_3$)$_2$AuFX] complexes by reacting compound **12** and one equivalent of KX or Me$_3$SiX. However, all our attempts were unsuccessful and resulted in mixtures of the corresponding [PPh$_4$][*trans*-(CF$_3$)$_2$AuX$_2$] derivatives and unreacted **12**.

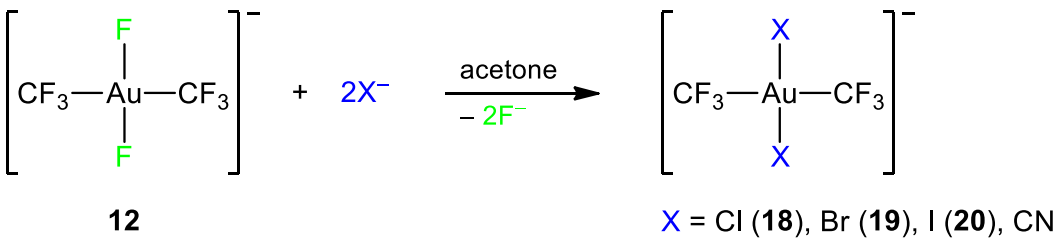

Scheme 2.4. Halide exchange reactions of **12** with KX, yielding compounds **18**–**21**. In all cases the cation is [PPh$_4$]$^+$.

Additionally, the fluoride ligands are also replaced by cyanide to render complex [PPh$_4$][*trans*-(CF$_3$)$_2$Au(CN)$_2$] (**21**), which was isolated as a highly-stable white solid, decomposing only above 350 °C. Complex [PPh$_4$][*trans*-(CF$_3$)$_2$Au(^{13}CN)$_2$] (**21***) was similarly obtained for spectroscopic purposes. Our results validate the assignment of the anion of **21**, [*trans*-(CF$_3$)$_2$Au(CN)$_2$]$^-$, which had been previously detected in solution.[12] The structure of the anion of **21** could be determined by single-crystal X-ray diffraction

methods (Figure 2.7), confirming the *trans* stereochemistry also in the solid state. The shorter Au–CN distance with respect to the Au–CF_3 bond is in line with the bond lengths found in the homoleptic $[Au(CN)_4]^-$ (200.6(7) pm av.)[22] and $[(CF_3)_4Au]^-$ (208.0(7) pm av.)[9] anions.

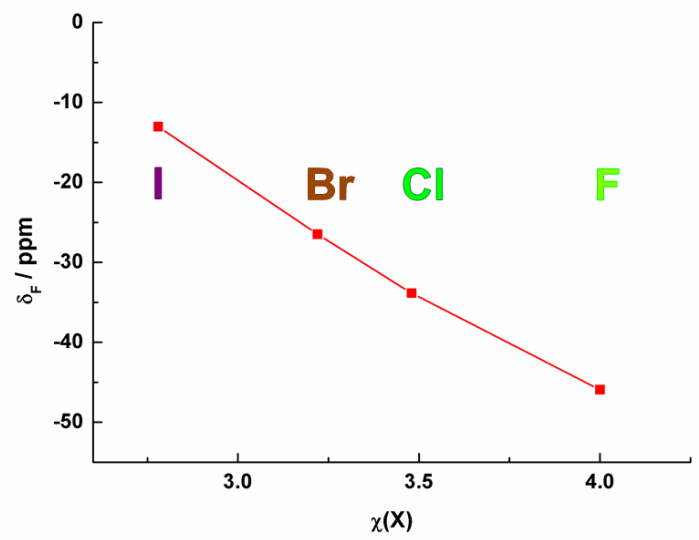

Figure 2.6. Correlation between the experimental δ_F values of the $[PPh_4][trans\text{-}(CF_3)_2AuX_2]$ complexes (X = F (**12**), Cl (**18**), Br (**19**), I (**20**)) and the electronegativity of the involved halogen $\chi(X)$ in the Sanderson scale.[21] All ^{19}F NMR spectra were registered in CD_2Cl_2 at room temperature. For the heavier-halide derivatives **18**–**20**, δ_F values are taken from Ref. [9].

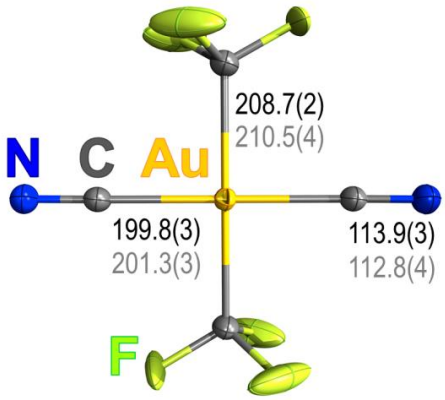

Figure 2.7. Displacement-ellipsoid diagram (50% probability) of the $[trans\text{-}(CF_3)_2Au(CN)_2]^-$ anion as found in single crystals of **21**. Only one set of the rotationally disordered F atoms found in the symmetry-related CF_3 groups is shown. Selected bond lengths [pm] with estimated standard deviations are indicated. The same bond lengths in the homologous silver derivative $[trans\text{-}(CF_3)_2Ag(CN)_2]^-$ are indicated in gray.[23]

It is interesting to note that the Au–C bond lengths in the anion of **21** do not significantly differ from those in the isoleptic and isostructural silver(III) analogue [*trans*-$(CF_3)_2Ag(CN)_2]^-$ (see Figure 2.7 for comparison).[23] Both species seem to be isomorphous, with no sign of significant cation/anion interaction, and similar standard deviations in the structural parameters determined. Thus, it can be concluded that Ag^{III} and Au^{III} have comparable covalent radii. Previous studies determined that Au^{I} has a smaller size than Ag^{I} due to relativistic effects in gold,[24] being this unusual difference less significant in the case of oxidation state II in these metals.[25] We now conclude that there is no difference in their covalent radii when shifting to oxidation state III, which is in agreement with their virtually identical crystal radii in square-planar environments (81 (Ag^{3+}) vs. 82 (Au^{3+}) pm).[26] It is also in keeping with the decrease in the relativistic Au–L bond contraction on going from Au^{I} to Au^{III} complexes.[27]

2.5. Summary

- A stereoselective and efficient synthetic route has been described for the synthesis of the first organogold(III) difluoride with *trans* stereochemistry, [PPh_4][*trans*-$(CF_3)_2AuF_2$] (**12**), by reaction of the homoleptic organogold(I) species [PPh_4][CF_3AuCF_3] (**I**) with XeF_2. The product has been fully characterized in solution and in the solid state.

- The study of complex [PPh_4][*trans*-$(CF_3)_2AuF_2$] (**12**) by tandem mass spectrometry has enabled the detection in the gas phase of the whole series of organogold fluorides $[CF_3AuF_x]^-$ (x = 1 (***15***), 2 (***14***), 3(***13***)), containing gold in oxidation states I, II and III, respectively. Their geometries have been optimized at the DFT/M06 level. In further stages of the experiment, other gold fluorides such as $[AuF_3]^-$ (***16***) and $[AuF_2]^-$ (***17***) have been detected.

- The computational study of the isomers of the organogold(II) anion $[CF_3AuF_2]^-$ (***14***) has shown that the spin density distribution depends on the precise stereochemistry of the species, even under a same characteristic molecular shape (polytope).

- The fluoride ligands in [PPh_4][*trans*-$(CF_3)_2AuF_2$] (**12**) can be easily replaced by any heavier halide and by cyanide, the latter yielding the new [PPh_4][*trans*-$(CF_3)_2Au(CN)_2$] derivative (**21**) with retention of the stereochemistry.

- The determination of the crystal structure of complex $[PPh_4][trans\text{-}(CF_3)_2Au(CN)_2]$ (**21**) in comparison with the isoleptic silver(III) derivative,[23] has allowed to conclude that Au^{III} and Ag^{III} have similar covalent radii, at least in their most common square-planar geometry.

2.6. References

[1] W. J. Wolf, F. D. Toste, in *The Chemistry of Organogold Compounds, Vol. 1* (Eds.: Z. Rappoport, J. F. Liebman, I. Marek), belonging to Patai's Chemistry of Functional Groups, Wiley, Chichester, **2014**, pp. 391–408.

[2] J. Gil-Rubio, J. Vicente. Gold trifluoromethyl complexes. *Dalton Trans.* **2015**, *44*, 19432.

[3] N. J. Rijs, R. A. J. O'Hair. Forming trifluoromethylmetallates: competition between decarboxylation and C–F bond activation of group 11 trifluoroacetate complexes, $[CF_3CO_2ML]^-$. *Dalton Trans.* **2012**, *41*, 3395.

[4] M. S. Winston, W. J. Wolf, F. D. Toste. Halide-Dependent Mechanisms of Reductive Elimination from Gold(III). *J. Am. Chem. Soc.* **2015**, *137*, 7921.

[5] a) M. Leblanc, V. Maisonneuve, A. Tressaud. Crystal Chemistry and Selected Physical Properties of Inorganic Fluorides and Oxide-Fluorides. *Chem. Rev.* **2015**, *115*, 1191; b) F. Mohr. The Chemistry of Gold-fluoro compounds: A continuing challenge for Gold Chemists. *Gold Bull.* **2004**, *37*, 164; c) B. G. Müller. Fluorides of Copper, Silver, Gold, and Palladium. *Angew. Chem. Int. Ed. Engl.* **1987**, *26*, 1081; *Angew. Chem.* **1987**, *99*, 1120.

[6] M. A. Ellwanger, S. Steinhauer, P. Golz, H. Beckers, A. Wiesner, B. Braun-Cula, T. Braun, S. Riedel. Taming the High Reactivity of Gold(III) Fluoride: Fluorido Gold(III) Complexes with N-Based Ligands. *Chem. Eur. J.* **2017**, *23*, 13501.

[7] F. A. Redeker, M. A. Ellwanger, H. Beckers, S. Riedel. Investigation of Molecular Alkali Tetrafluorido Aurates by Matrix-Isolation Spectroscopy. *Chem. Eur. J.* **2019**, *25*, 15059.

[8] M. Baya, D. Joven-Sancho, P. J. Alonso, J. Orduna, B. Menjón. M−C Bond Homolysis in Coinage-Metal $[M(CF_3)_4]^-$ Derivatives. *Angew. Chem. Int. Ed.* **2019**, *58*, 9954; *Angew. Chem.* **2019**, *131*, 10059.

[9] S. Martínez-Salvador, L. R. Falvello, A. Martín, B. Menjón. Gold(I) and Gold(III) Trifluoromethyl Derivatives. *Chem. Eur. J.* **2013**, *19*, 14540.

[10] U. Preiss, I. Krossing. A Computational Study of $[M(CF_3)_4]^-$ (M = Cu, Ag, Au) and their Properties as Weakly Coordinating Anions. *Z. Anorg. Allg. Chem.* **2007**, *633*, 1639.

[11] D. S. Laitar, P. Müller, T. G. Gray, J. P. Sadighi. A Carbene-Stabilized Gold(I) Fluoride: Synthesis and Theory. *Organometallics* **2005**, *24*, 4503.

[12] E. Bernhardt, M. Finze, H. Willner. Synthesis and NMR spectroscopic investigation of salts containing the novel $[Au(CF_3)_nX_{4-n}]^-$ (n = 4–1, X = F, CN, Cl) anions. *J. Fluorine Chem.* **2004**, *125*, 967.

[13] a) M. Tramšek, B. Žemva. Synthesis, Properties and Chemistry of Xenon(II) Fluoride. *Acta Chim. Slov.* **2006**, *53*, 105; b) M. A. Tius. Xenon Difluoride in Synthesis. *Tetrahedron* **1995**, *51*, 6605.

[14] a) N. P. Mankad, F. D. Toste. C(sp^3)–F reductive elimination from alkylgold(III) fluoride complexes. *Chem. Sci.* **2012**, *3*, 72; b) N. P. Mankad, F. D. Toste. C−C Coupling Reactivity of an Alkylgold(III) Fluoride Complex with Arylboronic Acids. *J. Am. Chem. Soc.* **2010**, *132*, 12859.

[15] M. Albayer, R. Corbo, J. L. Dutton. Well defined difluorogold(III) complexes supported by N-ligands. *Chem. Commun.* **2018**, *54*, 6832.

[16] M. A. Ellwanger, C. von Randow, S. Steinhauer, Y. Zhou, A. Wiesner, H. Beckers, T. Braun, S. Riedel. Tuning the Lewis acidity of difluorido gold(III) complexes: the synthesis of [$AuClF_2$(SIMes)] and [$AuF_2(OTeF_5)$(SIMes)]. *Chem. Commun.* **2018**, *54*, 9301.

[17] R. Kumar, A. Linden, C. Nevado. Evidence for Direct Transmetalation of Au^{III}–F with Boronic Acids. *J. Am. Chem. Soc.* **2016**, *138*, 13790.

[18] M. A. Ellwanger, S. Steinhauer, P. Golz, T. Braun, S. Riedel. Stabilization of Lewis Acidic AuF_3 as an N-Heterocyclic Carbene Complex: Preparation and Characterization of [AuF_3(SIMes)]. *Angew. Chem. Int. Ed.* **2018**, *57*, 7210; *Angew. Chem.* **2018**, *130*, 7328.

[19] a) E. Ruiz, J. Cirera, S. Alvarez. Spin density distribution in transition metal complexes. *Coord. Chem. Rev.* **2005**, *249*, 2649; b) J. Cano, E. Ruiz, S. Alvarez, M. Verdaguer. Spin Density Distribution in Transition Metal Complexes: Some Thoughts and Hints. *Comments Inorg. Chem.* **1998**, *20*, 27.

[20] a) R. G. Pearson. Recent Advances in the Concept of Hard and Soft Acids and Bases. *J. Chem. Educ.* **1987**, *64*, 561; b) R. J. Puddephatt, in *The Chemistry of Gold*, Elsevier, Amsterdam, **1978**, pp. 22–24; c) S. Ahrland. Factors Contributing to (b)-behaviour in Acceptors. *Struct. Bonding (Berlin)* **1966**, *1*, 207; d) R. G. Pearson. Hard and Soft Acids and Bases. *J. Am. Chem. Soc.* **1963**, *85*, 3533; e) S. Ahrland, J. Chatt, N. R. Davies. The relative affinities of ligand atoms for acceptor molecules and ions. *Q. Rev. Chem. Soc.* **1958**, *12*, 265.

[21] a) J. E. Huheey, E. A. Keiter, R. L. Keiter, in *Inorganic Chemistry: Principles of Structure and Reactivity*, 4th ed., Harper-Collins: New York (NY), **1993**, pp. 182–199; b) R. T. Sanderson, in *Simple Inorganic Substances*, Krieger: Malabar (FL), **1989**, p. 23; c) R. T. Sanderson. Principles of Electronegativity Part I. General Nature. *J. Chem. Educ.* **1988**, *65*, 112.

[22] P. G. Jones, C. Thöne. Tetraphenylarsonium Tetracyanoaurate(III) Dichloromethane Solvate. *Acta Crystallogr. Sect. C* **1989**, *45*, 11.

[23] R. Eujen, B. Hoge, D. J. Brauer. Preparation and NMR Spectra of the (Trifluoromethyl)argentates(III) $[Ag(CF_3)_nX_{4-n}]^-$, with X = CN (n = 1−3), CH_3, $C{\equiv}CC_6H_{11}$, Cl, Br (n = 2, 3), and I (n = 3), and of Related Silver(III) Compounds. Structures of [PPh_4][*trans*-$Ag(CF_3)_2(CN)_2$] and [PPh_4][$Ag(CF_3)_3(CH_3)$]. *Inorg. Chem.* **1997**, *36*, 1464.

[24] a) U. M. Tripathi, A. Bauer, H. Schmidbaur. Covalent radii of four-co-ordinate copper(I), silver(I) and gold(I): crystal structures of [$Ag(AsPh_3)_4$]BF_4 and [$Au(AsPh_3)_4$]BF_4. *J. Chem. Soc., Dalton Trans.* **1997**, 2865; b) A. Bayler, A. Schier, G. A. Bowmaker, H. Schmidbaur. Gold Is Smaller than Silver. Crystal Structures of [Bis(trimesitylphosphine)gold(I)] and [Bis(trimesitylphosphine)silver(I)] Tetrafluoroborate. *J. Am. Chem. Soc.* **1996**, *118*, 7006; c) M. S. Liao, W. H. E. Schwarz. Effective radii of the monovalent coin metals. *Acta Crystallogr. Sect. B* **1994**, *50*, 9.

[25] S. Preiß, C. Förster, S. Otto, M. Bauer, P. Müller, D. Hinderberger, H. Hashemi Haeri, L. Carella, K. Heinze. Structure and reactivity of a mononuclear gold(II) complex. *Nat. Chem.* **2017**, *9*, 1249.

[26] R. D. Shannon, in *Encyclopedia of Inorganic Chemistry, Vol. 2* (Ed.: R. B. King), Wiley, Chichester, **1994**, pp. 929–942.

[27] a) P. Schwerdtfeger, M. Lein, in *Gold Chemistry: Applications and Future Directions in the Life Sciences* (Ed.: F. Mohr), Wiley-VCH, Weinheim, **2009**, pp. 183–247; b) P. Schwerdtfeger, P. D. W. Boyd, S. Brienne, A. K. Burrell. Relativistic Effects in Gold Chemistry. 4. Gold(III) and Gold(V) Compounds. *Inorg. Chem.* **1992**, *31*, 3411.

Chapter 3

Anionic and Neutral Derivatives of the Highly Acidic $(CF_3)_3Au$ Unit

This chapter is based on the following two peer-reviewed papers:

A. Pérez-Bitrián, S. Martínez-Salvador, M. Baya, J. M. Casas, A. Martín, B. Menjón, J. Orduna. Anionic Derivatives of Perfluorinated Trimethylgold. *Chem. Eur. J.* **2017**, *23*, 6919–6929. DOI: 10.1002/chem.201700927.

A. Pérez-Bitrián, M. Baya, J. M. Casas, L. R. Falvello, A. Martín, B. Menjón. $(CF_3)_3Au$ as a Highly Acidic Organogold(III) Fragment. *Chem. Eur. J.* **2017**, *23*, 14918–14930. DOI: 10.1002/chem.201703352.

3.1. Introduction and objectives

The first organogold compounds were prepared by Pope and Gibson in 1907,[1] but it was not until 1939 when the first gold methyl complexes were reported by Brain and Gibson.[2] In 1942, the synthesis of the first organogold(III) species containing the R_3Au moiety was described.[3] This compound was formed by reaction of CH_3Li either with Au_2Br_6 or $[(CH_3)_2Au(\mu\text{-}Br)]_2$ in Et_2O solution at –65 ºC and was formulated by Gilman and Woods as "trimethyl gold" (Scheme 3.1). However, they already stated that the compound most probably contained an additional Et_2O molecule coordinated to the gold center at the fourth coordination site. Trimethyl gold was described as an unstable species because of the lability of the Et_2O ligand and the readiness of the $(CH_3)_3Au$ fragment to undergo reductive elimination of ethane above –40 ºC in Et_2O solution (Scheme 3.2). This made its characterization difficult and in fact, it has not been isolated to date. Trimethyl gold could however be stabilized to a greater extent with ylides or ligands containing Group 15 donor atoms, the resulting compounds being stable at or above room temperature.[4]

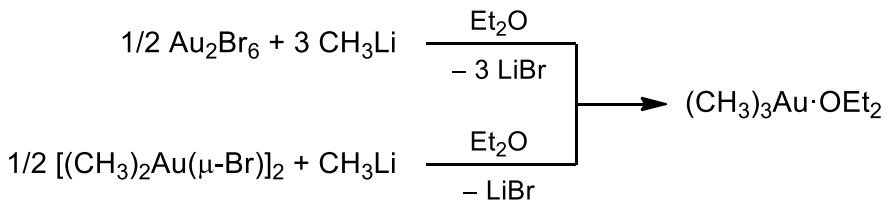

Scheme 3.1. Synthesis of trimethyl gold at –65 ºC, as reported by Gilman and Woods.[3]

$$(CH_3)_3Au{\cdot}OEt_2 \longrightarrow (CH_3)_3Au + Et_2O \qquad \text{(i)}$$

$$(CH_3)_3Au \longrightarrow CH_3Au + CH_3CH_3 \qquad \text{(ii)}$$

$$2\ CH_3Au \longrightarrow 2\ Au + CH_3CH_3 \qquad \text{(iii)}$$

Scheme 3.2. Decomposition of trimethyl gold above –40 ºC in Et_2O solution.[3a]

In their initial report, Gilman and Woods stabilized the $(CH_3)_3Au$ unit by replacing the Et_2O ligand at low temperature with amines such as ethylenediamine, 2-aminopyridine and benzylamine.[3a] Ligand displacement reactions also served to obtain different phosphine complexes of stoichiometry $(CH_3)_3Au(PR_3)$ (R = Me, Ph), starting either from $(CH_3)_3Au{\cdot}OEt_2$ or from $(CH_3)_3Au(NH_2CH_2CH_2NH_2)Au(CH_3)_3$.[5] Triethylphosphine was found to replace trimethylphosphine in $(CH_3)_3Au(PMe_3)$ at 50 ºC giving rise to $(CH_3)_3Au(PEt_3)$,[6] yet this reaction was not useful to obtain the triphenylphosphine derivative.[6a] Phosphine ligands were also found to be replaced by ylides, which allowed to prepare a handful of ylide complexes of trimethyl gold.[7] Methylation of $(CH_3)_2AuI(PR_3)$, formed by treatment of $[(CH_3)_2Au(\mu\text{-}I)]_2$ with PR_3, was later used by Tobias and coworkers to prepare $(CH_3)_3Au(PR_3)$ (R = Me, Et, Ph), as shown in Scheme 3.3.[8] This method resulted also useful in the synthesis of the only known arsine derivative of trimethyl gold, $(CH_3)_3Au(AsMe_3)$,[8a] as well as for the ylide complex $(CH_3)_3Au(CH_2PMe_3)$.[9]

$$1/2\ [(CH_3)_2Au(\mu\text{-}I)]_2 \xrightarrow{+\ PR_3} (CH_3)_2AuI(PR_3) \xrightarrow[-\ LiI]{+\ CH_3Li} (CH_3)_3Au(PR_3)$$

Scheme 3.3. Synthesis of $(CH_3)_3Au(PR_3)$ (R = Me, Et, Ph) by alkylation of $(CH_3)_2AuI(PR_3)$.[8]

Trimethyl gold phosphine derivatives were found to appear also as products of the oxidative addition of CH_3I to CH_3AuL compounds (L = phosphine).[10-12] The overall reaction is a two-step process which includes oxidative addition (Scheme 3.4i) and alkyl transfer (Scheme 3.4ii). Since the second step is very quick, the dialkylgold(III) intermediate could not be even detected, but the $(CH_3)_3AuL$ product was directly obtained. In the case of L = PPh_3, $(CH_3)_3Au(PPh_3)$ undergoes subsequent reductive elimination (Scheme 3.4iii) and finally $IAu(PPh_3)$ and C_2H_6 are produced. However,

$(CH_3)_3Au(PMe_3)$ is more stable and does not undergo reductive elimination. Instead, it participates in a further slow reaction with $IAu(PMe_3)$ and CH_3I to afford complex *cis*-$(CH_3)_2AuI(PMe_3)$, while in contrast no $IAu(PMe_3)$ was obtained. Therefore, the less bulky phosphine PMe_3 did allow to isolate this intermediate complex which is the formal product of the oxidative addition shown in Scheme 3.4i. The analogous *cis*-$(CH_3)_2AuIL$ compound was also isolated for L = PMe_2Ph, whereas a mixture of *cis*-$(CH_3)_2AuIL$, IAuL and C_2H_6 was found for L = $PMePh_2$. It could be thus concluded that the reaction products were dependent on the bulkiness and basicity of the phosphine, the rate of the reductive elimination step increasing as it does the size of the ligand.[12a]

$$CH_3AuL + CH_3I \longrightarrow (CH_3)_2AuIL \qquad \text{(i)}$$

$$(CH_3)_2AuIL + CH_3AuL \rightleftharpoons (CH_3)_3AuL + IAuL \qquad \text{(ii)}$$

$$(CH_3)_3AuL \longrightarrow C_2H_6 + CH_3AuL \qquad \text{(iii)}$$

Scheme 3.4. Formation of $(CH_3)_3AuL$ derivatives (L = phosphine) via oxidative addition of CH_3I to a CH_3AuL complex. Step (iii) applies only when L = PPh_3 and $PMePh_2$.[11,12]

This method had the main disadvantage of the limited stability of the $(CH_3)_3AuL$ under the reaction conditions, but also the rather slow oxidative addition. A more convenient procedure to prepare trialkyl gold derivatives was reported soon after, which also allowed for the preparation of complexes with dissimilar organic groups. The process involved the oxidative addition of alkyl halides to *in-situ*-prepared dialkylaurate(I) complexes (Scheme 3.5).[13]

$$CH_3AuL \xrightarrow{+\,CH_3Li} (CH_3)_2AuL^-Li^+ \xrightarrow[-\,LiI]{+\,CH_3I} (CH_3)_3AuL$$

Scheme 3.5. Formation of $(CH_3)_3AuL$ derivatives (L = phosphine) via oxidative addition of CH_3I to in-situ-generated dimethylaurate(I) salts.[13]

The number of currently known trimethyl gold derivatives is still scarce and anionic $[(CH_3)_3AuX]^-$ species are completely unknown.[4] In this regard, the $[(CH_3)_3AuI]^-$ anion has been postulated to be formed in the reaction between $[CH_3AuCH_3]^-$ and CH_3I either in the condensed or in the gas phase, yet has never been detected nor isolated, and only

the products of reductive elimination are obtained.[14] Additionally, various salts of the homoleptic $[(CH_3)_4Au]^-$ anion are known, which can be considered as a $[(CH_3)_3AuR]^-$ species with R = CH_3.[14b,15] Nevertheless, theoreticians and experimentalists have become interested in trimethyl gold and its derivatives because of the intrinsic simplicity and prototypical nature of these species.[4]

Initial studies on the reactivity of $(CH_3)_3Au{\cdot}OEt_2$ revealed that it reacts with HCl or thiols leading to cleavage of a Au–C bond and release of methane, yet it seems to be unreactive towards phenol and trichloroacetic acid.[3a] Moreover, in the presence of Au_2Br_6, dimethylgold bromide is formed. The reactivity of trimethyl gold phosphine complexes was also investigated and the mechanisms of different processes were elucidated.[16] Mercuric salts were found to stereoespecifically cleave one of the mutually *trans*-standing methyl groups in $(CH_3)_3Au(PPh_3)$ in a variety of solvents via a S_E2 mechanism.[17] The same phosphine derivative also reacts with CH_3Li to afford the tetramethylaurate(III) salt $Li[(CH_3)_4Au]$.[15d] Additionally, complex $(CH_3)_3Au(PMe_2Ph)$ undergoes methyl for bromide exchange with $Br_3Au(PMe_2Ph)$ to render *cis*-$(CH_3)_2AuBr(PMe_2Ph)$.[18] On the other hand, several NMR studies were carried out on the phosphine substitution reaction and an associative mechanism via a five-coordinate intermediate was proposed.[6b,19] However, ligand exchange and *cis-trans* isomerization in related $(CH_3)_2RAu(PPh_3)$ (R = alkyl) were found to be independent processes, since the latter occurs through a dissociative and unimolecular mechanism.[20]

The decomposition pathways of trimethyl gold derivatives have been also thoroughly investigated. Following the initial studies by Gilman and Woods,[3a] Coates and Parkin detected C_2H_6 as the only volatile in the thermal decomposition of $(CH_3)_3Au(PMe_3)$, which proceeds through the organogold(I) species $CH_3Au(PMe_3)$ and finally renders PMe_3 and gold.[5] Detailed mechanistic studies concluded that the decomposition of these derivatives proceeds via a dissociative and unimolecular mechanism,[20,21] as indicated in Scheme 3.2. In fact, the dissociation of the phosphine was experimentally found to be the limiting step (Scheme 3.2i), as was later demonstrated by advanced calculations.[22] Eventually, fast reductive elimination of C_2H_6 from a putative three-coordinate intermediate takes place (Scheme 3.2ii).

In contrast to the thorough knowledge acquired on trimethyl gold and its derivatives, the chemistry of the homologous fluorinated fragment $(CF_3)_3Au$ has remained far less

developed thus far, despite the increasing interest in gold trifluoromethyl complexes.[23] This might be due to the lack of appropriate synthetic methods currently available. The $(CF_3)_3Au$ unit seems to have been prepared as an unstable species by the cocondensation of gold vapors with trifluoromethyl radicals, followed by matrix isolation (Scheme 3.6a).[24] As in the case of its non-fluorinated analogue, the $(CF_3)_3Au$ fragment could be stabilized upon coordination of an additional ligand to render complex $(CF_3)_3Au(PMe_3)$. This same adduct was later prepared in high yield by treatment of $(CF_3)_2AuI(PMe_3)$ with $(CF_3)_2Cd{\cdot}dme$ in the presence of excess of CF_3I (Scheme 3.6b).[25] Complexes $(CF_3)_3Au(PR_3)$ (R = Me, Et) have also been observed to appear in the ligand exchange reaction between $CF_3Au(PR_3)$ and $(CF_3)_2AuI(PR_3)$, the latter being formed upon oxidative addition of CF_3I onto the former, as shown in Scheme 3.6c.[26] No reductive elimination of C_2F_6 from any of these complexes has been described.

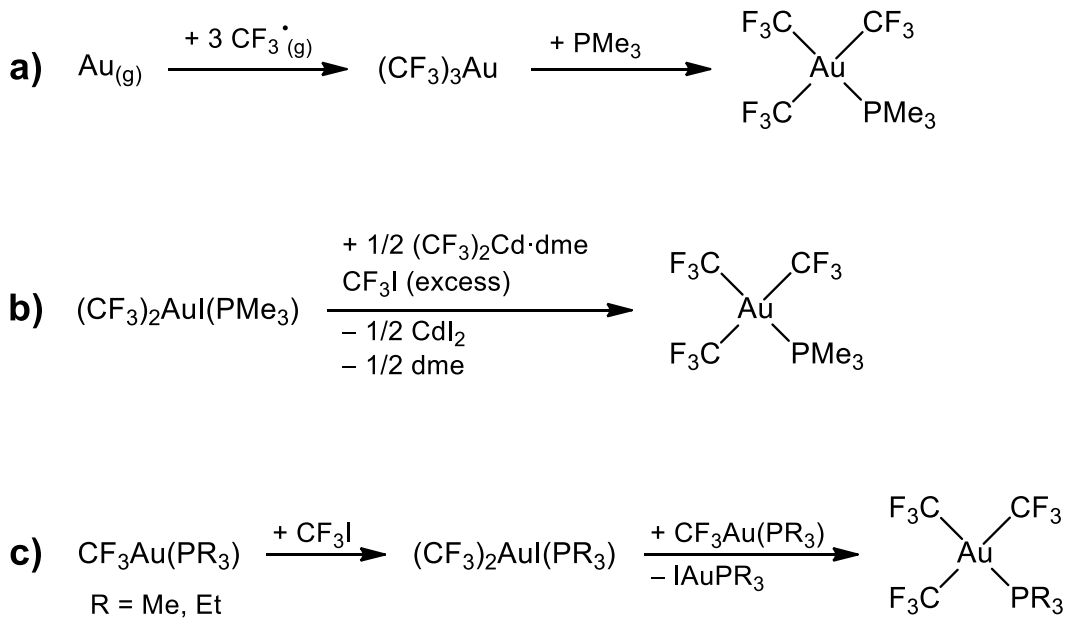

Scheme 3.6. Previous reported syntheses of $(CF_3)_3Au$ and its derivatives by a) gas phase reaction of gold vapors and trifluoromethyl radicals;[24] b) transmetallation;[25] and c) oxidative addition of CF_3I and subsequent ligand exchange.[26] The $(CF_3)_2AuI(PR_3)$ species consists of a mixture of *cis* and *trans* isomers, where the *cis* isomer is the major product.[25]

Treatment of $[NBu_4][Au(CN)_4]$ with ClF in CH_2Cl_2 was non-selective and afforded a complex mixture of trifluoromethyl derivatives among which some $[(CF_3)_3AuX]^-$

anions (X = F, Cl, CN) were detected by ^{19}F NMR spectroscopy, but could not be isolated.[27] Finally, previous attempts carried out in our group to obtain derivatives containing the $(CF_3)_3Au$ moiety via the cleavage of one of the Au–C bonds in the homoleptic $[(CF_3)_4Au]^-$ anion failed due to the high stability and inertness of this species,[28] which can be actually considered a weakly coordinating anion.[29]

In this chapter, a new and more convenient synthetic approach to the homologous fluorinated fragment of trimethyl gold, $(CF_3)_3Au$, is described and its chemistry is explored. In particular, we focus on the synthesis of anionic and neutral derivatives, including the etherate complex $(CF_3)_3Au{\cdot}OEt_2$, which serves as a convenient synthon of the 14-electron species $(CF_3)_3Au$. The properties of this unsaturated fragment are analyzed and compared to those of its non-fluorinated analogue. These properties include its stereochemistry, its Lewis acidity, its stability and its affinity towards different ligands. Finally, the decomposition of the anionic derivatives is investigated under two related but quite different conditions: in the gas phase by tandem mass spectrometry, where only intramolecular decomposition pathways operate, and in the condensed phase, where intermolecular decomposition paths are also possible.

3.2. Synthesis of $[PPh_4][(CF_3)_3AuI]$: a new synthetic entry to the $(CF_3)_3Au$ unit

The homoleptic organogold(I) compound $[PPh_4][CF_3AuCF_3]$ (**I**) cleanly undergoes oxidative addition of CF_3I in MeCN solution at room temperature (Scheme 3.7) yielding the square-planar triorganogold(III) derivative $[PPh_4][(CF_3)_3AuI]$ (**22**), which can be isolated as a white solid in very good yield (90%). This compound shows a characteristic ^{19}F NMR spectrum consisting of a quartet and a septet in 2:1 integrated ratio, due to the two chemically inequivalent CF_3 groups, which are mutually coupled (Figure 3.1). The great difference in the reaction rate observed upon photoirradiation (10 min vs. 4 days in the dark) is clear evidence of a radical mechanism. Similar photoinitiated oxidative addition reactions have also been found in related systems.[25,26,30] Given the stoichiometry of product **22**, it is impossible to distinguish between a *cis* or a *trans* addition. However, the reaction of **I** with nBu^{F}I stereoselectively affords $[PPh_4][trans\text{-}(n\text{Bu}^F)(CF_3)_2AuI]$ (**23**; Scheme 3.7). Hence, since

both perfluoroalkyl iodides contain similar α-C atoms with $I^{\delta+}$–$C^{\delta-}$ bond polarity, a *trans* stereochemistry can be assigned to the oxidative addition reaction in both cases. Compound **23** was the first reported case of a perfluorobutyl group coordinated to a gold center, but a handful of them have been isolated and fully characterized recently.[30a]

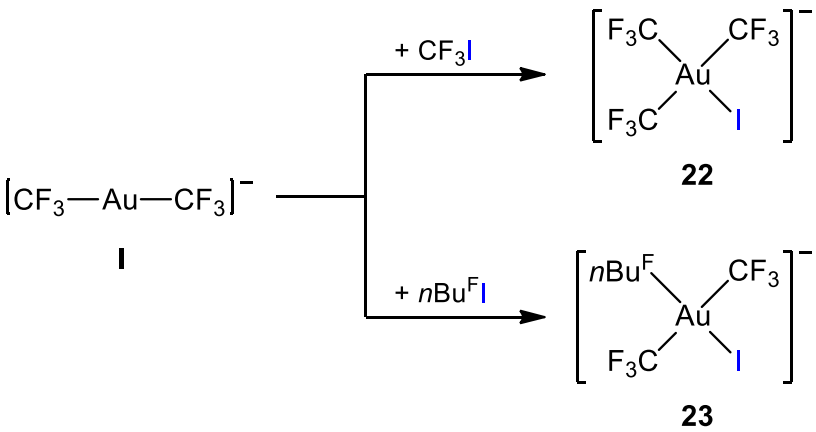

Scheme 3.7. Oxidative addition of R^FI reagents (R^F = CF_3, nBu^F) to the homoleptic anionic species **I** to afford complexes **22** and **23**. In all cases the cation is $[PPh_4]^+$.

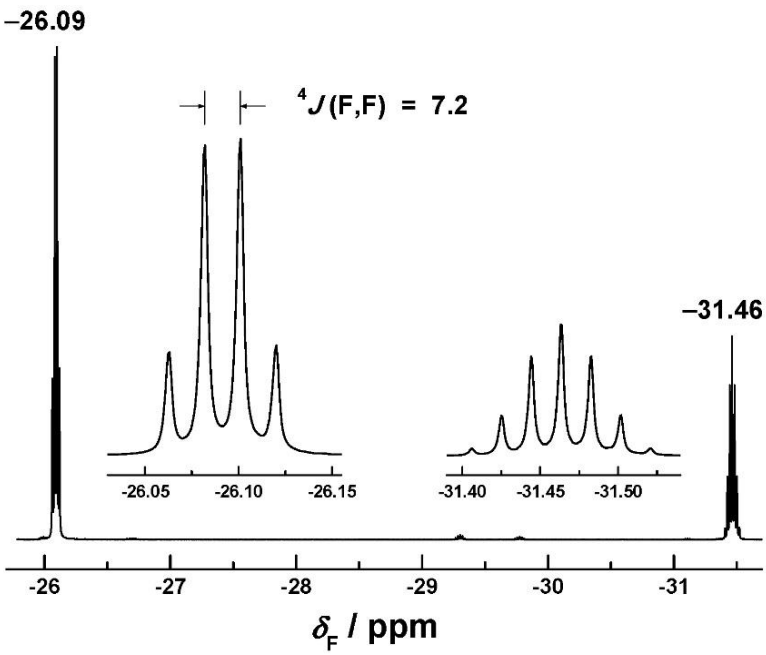

Figure 3.1. ^{19}F NMR spectrum (376.308 MHz) of compound **22** in CD_2Cl_2 solution at room temperature: δ_F [ppm] and J [Hz] values are indicated.

It is also worth noting that no anionic derivative of the non-fluorinated trimethyl gold, $[(CH_3)_3AuX]^-$, seems to be known.[4] In fact, although the $[(CH_3)_3AuI]^-$ anion might be involved in the reaction of $[CH_3AuCH_3]^-$ and MeI, the compound undergoes metal reduction and affords a mixture of ethane and methane in the absence of stabilizing ligands.[14b] Not even in the gas phase, using a high concentration of MeI or the longest possible times, does the reaction occur.[14a] In contrast, the fluorinated $(CF_3)_3Au$ moiety can be stabilized by any other halide in addition to iodide, as will be described in the next section.

3.3. Synthesis and characterization of various anionic derivatives of $(CF_3)_3Au$

The relative stability of gold halides towards substitution in solution increases when going down the halogen group, which is in agreement with the preference of gold(III), a "class b" metal ion or "soft acid", to bind larger and more polarizable ligands.[31] Thus, to prepare the lighter halide complexes of the $(CF_3)_3Au$ fragment starting from the iodo-derivative **22**, AgX salts are suitable reagents, since the precipitation of the extremely insoluble AgI at room temperature acts as a driving force for the reaction. Using this procedure, all the organogold(III) halide complexes in the $[PPh_4][(CF_3)_3AuX]$ series (X = F (**24**), Cl (**25**), Br (**26**)) could be easily obtained in good yield (Scheme 3.8). The fluoride complex **24**, which is one of the few organogold(III) monofluoride complexes reported to date,[32] can also be prepared by treatment of **22** with XeF_2 (Scheme 3.8). This compound is moisture-sensitive, yet very stable in the solid state (up to 267 ºC). Additionally, the cyano-complex $[PPh_4][(CF_3)_3Au(CN)]$ (**27**) was prepared by reaction of **22** with KCN (Scheme 3.8).

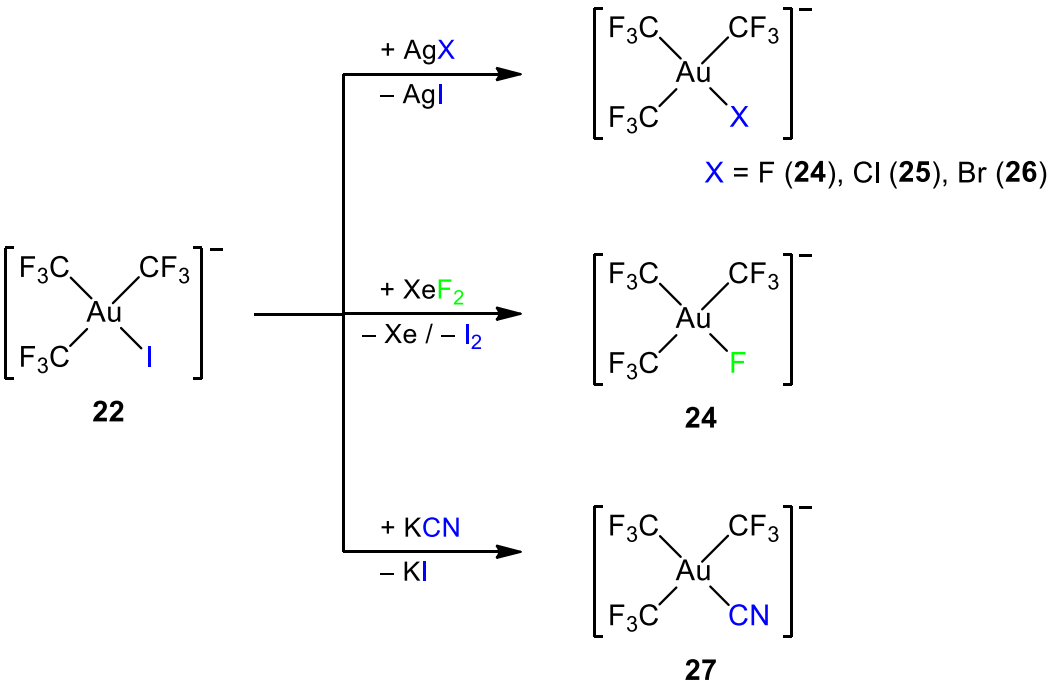

Scheme 3.8. Synthetic procedures affording the whole family of anionic complexes **24–27**, starting from the iodo-derivative **22**. In all cases the cation is $[PPh_4]^+$.

The characterization of these complexes by ^{19}F NMR spectroscopy is in agreement with the previous assignments to the $[(CF_3)_3AuX]^-$ anions (X = F, Cl, CN) detected in solution.[27] All complexes **24–27** show the typical pattern of a septet and a quartet in 1:2 integrated ratio in their ^{19}F NMR spectra. In the case of the fluoro-derivative **24**, these signals show an additional splitting due to the coupling to the fluoride ligand (Figure 3.2). In turn, the signal corresponding to the fluoride appears as a quartet of septets at very high field (δ_F = –254.41 ppm). In this case, both CF_3 signals show the widest separation, which denotes the most different environment for each of the chemically inequivalent CF_3 groups. Interestingly, when going down the halogen group, the signals get closer and their relative positions become even inverted in the iodo-derivative **22**. This trend is similar to that observed in the isoleptic Pt(II) derivatives $[(CF_3)_3PtX]^{2-}$.[33] Moreover, the "inverted" arrangement in compound **22** has been associated to ligands exhibiting some π-acceptor character,[33] as in the case of the cyano-complex **27**. Similar to the trends observed in the series of compounds described in Chapter 1 and Chapter 2, the ^{19}F NMR chemical shifts of both CF_3 signals within the series of halide complexes nicely correlate with the halogen's electronegativity in the

Sanderson scale (Figure 3.3).[34] In particular, the dependence is more marked for the *trans*-standing CF_3 groups and contrary for each kind of CF_3.

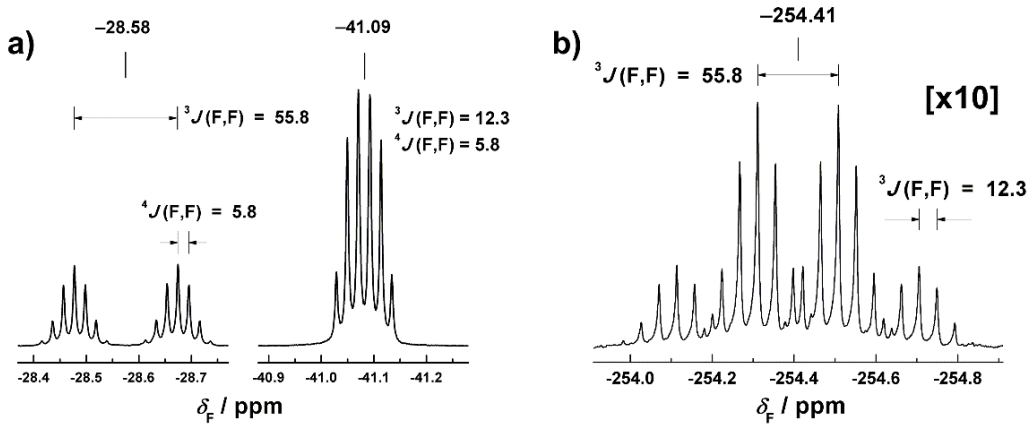

Figure 3.2. ^{19}F NMR spectrum (282.231 MHz) of compound **24** in CD_2Cl_2 solution at room temperature: a) CF_3 region; b) Au–F signal, with δ_F [ppm] and *J* [Hz] values indicated.

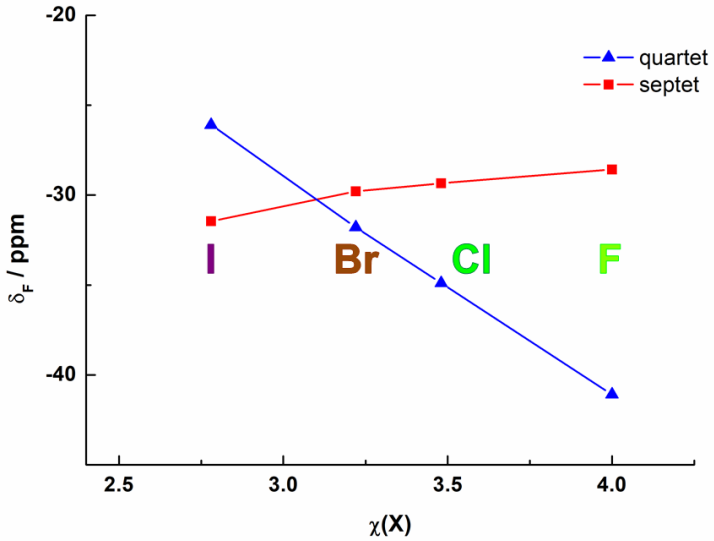

Figure 3.3. Correlation between the experimental δ_F values of the $[PPh_4][(CF_3)_3AuX]$ complexes (X = F (**24**), Cl (**25**), Br (**26**), I (**22**)) and the electronegativity of the involved halogen χ(X) in the Sanderson scale.[34] All ^{19}F NMR spectra were registered in CD_2Cl_2 at room temperature to enable proper comparison.

We also succeeded in obtaining single-crystals of compounds **24** and **27** suitable for X-ray diffraction analysis. In both square-planar complexes (Figure 3.4), the Au–C bond

length of the mutually *trans* CF_3 groups is longer than that *trans* to the X ligand, as a consequence of the higher *trans* influence of the CF_3 group.[35] This can also be the reason why the Au–F bond in **24** (198.99(14) pm) is elongated with respect to the $[AuF_4]^-$ anion (191.1(5) pm av. when crystallized as its $[NMe_4]^+$ salt).[36] In the case of the cyano-complex **27**, a longer Au–CN bond (205.9(3) pm) than in the homoleptic $[AsPh_4][Au(CN)_4]$ derivative (200.6(7) pm av.)[37] is also observed. In fact, focusing on the CF_3–Au–CN axis, the elongation of the Au–CN bond and shortening of the Au–CF_3 bond render two similar Au–C distances (205.9(3) pm vs. 206.8(3) pm), despite the different nature of the ligands and the hybridization of the C-donor atom in each case.

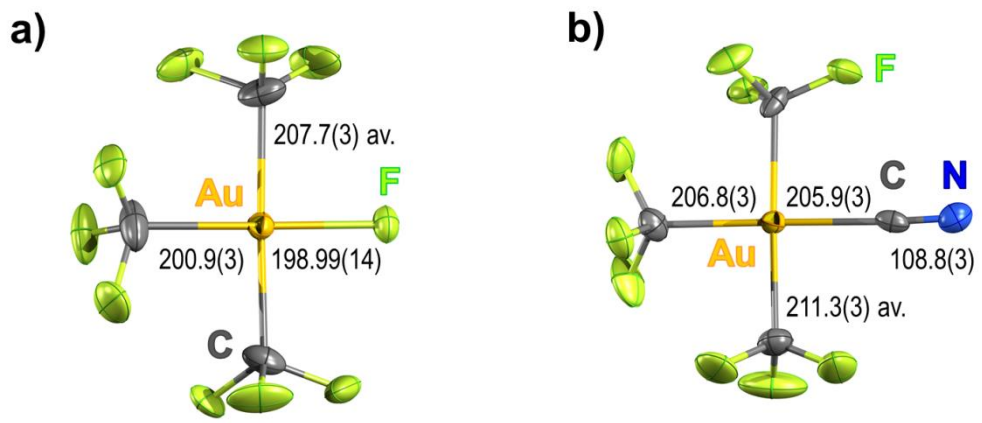

Figure 3.4. Displacement-ellipsoid diagram (50% probability) of: a) the $[(CF_3)_3AuF]^-$ anion as found in single crystals of **24** (with only one set of the rotationally disordered F atoms found in the CF_3 groups shown); and b) the $[(CF_3)_3AuCN]^-$ anion as found in single crystals of **27** (with only one set of the F atoms belonging to one of the CF_3 *cis* to CN at half occupancy given). Selected bond lengths [pm] with estimated standard deviations are indicated.

Complex **24** belongs to the small group of structurally-characterized organgold(III) mono fluorides.[32] The Au–F bond length in the $[(CF_3)_3AuF]^-$ anion (198.99(14) pm) is slightly shorter that that found in the neutral derivatives (N^C)Au(3,5-$(CF_3)_2$-C_6H_3)F (201.1(4) pm),[32a] (N^C)Au(CH_3)F (202.3(7) pm)[32a] and CF_3AuF(4-Me-C_6H_4)(PPh_3) (203.08(18) pm),[32c] and much shorter than that found in the pincer complex (N^C^C)AuF (226.4(3) pm).[32b] In general, the structural parameters of the $[(CF_3)_3AuF]^-$ anion in the crystal show satisfactory agreement with those calculated by Preiss and Krossing in the gas phase.[29] Finally, it has to be noted that complex **24** is isostructural with the isoleptic silver(III) derivative $[PPh_4][(CF_3)_3AgF]$.[38]

3.4. Synthesis of $(CF_3)_3Au{\cdot}OEt_2$

The room temperature treatment of $[PPh_4][(CF_3)_3AuI]$ (**22**) with the equimolar amount of $AgClO_4$ in a CH_2Cl_2/Et_2O mixture affords the solvento complex $(CF_3)_3Au{\cdot}OEt_2$ (**28**) in solution, with concomitant precipitation of AgI (Scheme 3.9). By replacing the initial solvent mixture with Et_2O/*n*-hexane (1:3 v/v) and cooling the new mixture at –80 ºC overnight, solutions of **28** can be freed from the accompanying $[PPh_4]ClO_4$ and AgI by filtration. These colorless solutions of the etherate **28** are reasonably stable at room temperature and suitable for most synthetic purposes. It is worth noting that the adduct **28** shows greatly enhanced thermal stability with respect to the non-fluorinated trimethyl gold etherate $(CH_3)_3Au{\cdot}OEt_2$, which decomposes at about –40 to –35 ºC rendering gold, methane and ethane.[3]

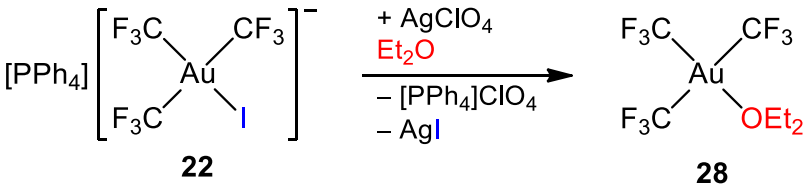

Scheme 3.9. Synthetic procedure to prepare the etherate $(CF_3)_3Au{\cdot}OEt_2$ (**28**).

The room temperature ^{19}F NMR spectrum of compound **28** shows two broad bands in 1:2 integrated ratio, which are resolved into the typical pattern of a septet and a quartet of $(CF_3)_3Au$ derivatives at low temperature. This behavior justifies the lability of Et_2O ligand, which undergoes rapid exchange in solution at room temperature. In fact, even small amounts of free Et_2O in the sample cause the broadening of the signal without significant shift in the corresponding δ_F values. We thoroughly tried to isolate compound **28** as a pure substance but all our attempts were unsuccessful due to its hygroscopic character and high solubility in Et_2O and *n*-hexane even at low temperatures. After evaporation of the solvent mixture at 0 ºC, extraction with *n*-hexane and crystallization at –80 ºC, a deliquescent white solid was obtained, which melted just above 0 ºC. The ^{19}F NMR spectrum in CD_2Cl_2 (Figure 3.5a) is consistent with that of the reaction media. However, a slight amount of free Et_2O still remained in the material, as observed in the low-temperature ^{1}H NMR spectrum (Figure 3.5b), and could not be completely removed without altering the integrity of **28**. The signals corresponding to

coordinated Et_2O appear downfield shifted with respect to those of the free molecule.[39] The spectroscopic evidence for the existence of etherate **28** is further supported by the presence of similarly deshielded signals in salts of the oxonium cation $[H(OEt_2)_2]^+$ with weakly coordinating anions[40] and in the related complex $(C_6F_5)Au{\cdot}OEt_2$.[41]

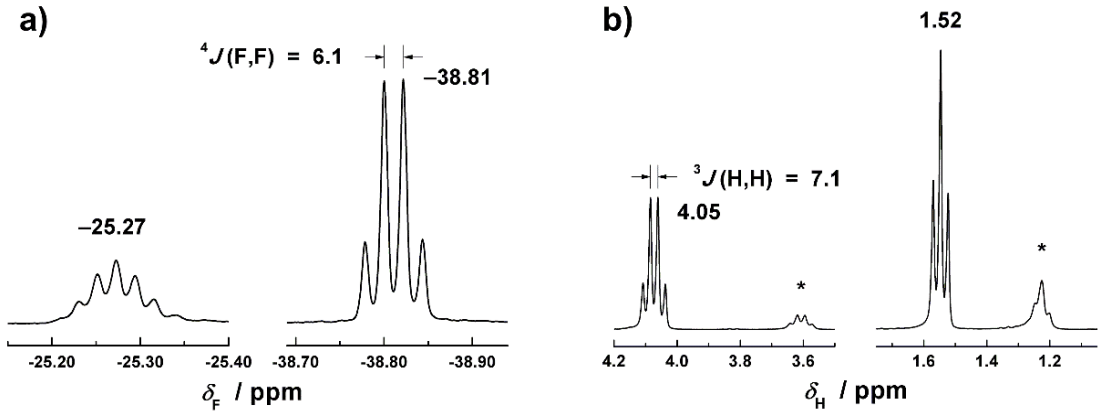

Figure 3.5. ^{19}F (a) and ^1H (b) NMR spectra of etherate **28** in CD_2Cl_2 solution at –60 ºC. δ_F [ppm] and *J* [Hz] values are indicated. Asterisks denote signals corresponding to free Et_2O.[39]

3.5. Synthesis and characterization of neutral derivatives of $(CF_3)_3Au$

The lability of the Et_2O ligand in complex **28** and its reasonable thermal stability make this species very useful for synthetic purposes. In fact, the weakly coordinated ether molecule in **28** can be readily replaced by many other neutral ligands (Scheme 3.10). We chose a variety of representative C, N, P, O and S ligands covering a wide range of donor abilities so as to explore the stability of the corresponding complexes. Eventually, we isolated and fully characterized a handful of different $(CF_3)_3AuL$ derivatives with L being CN*t*Bu (**29**), NCMe (**30**), py (**31**), PMe_3 (**32**), PPh_3 (**33**), Opy (**34**), $OPPh_3$ (**35**), tht (**36**) and $SPPh_3$ (**37**). It has to be noted that complex $(CF_3)_3Au(PMe_3)$ (**32**) had been previously prepared by different procedures.[24-26] On the other hand, similar attempts to prepare related silver complexes with PR_3 ligands (R = Me, Ph, OMe) starting from $(CF_3)_3Ag{\cdot}solv$ (solv = dmso, NCMe, dmf, or other N-bases) were unsuccessful.[42]

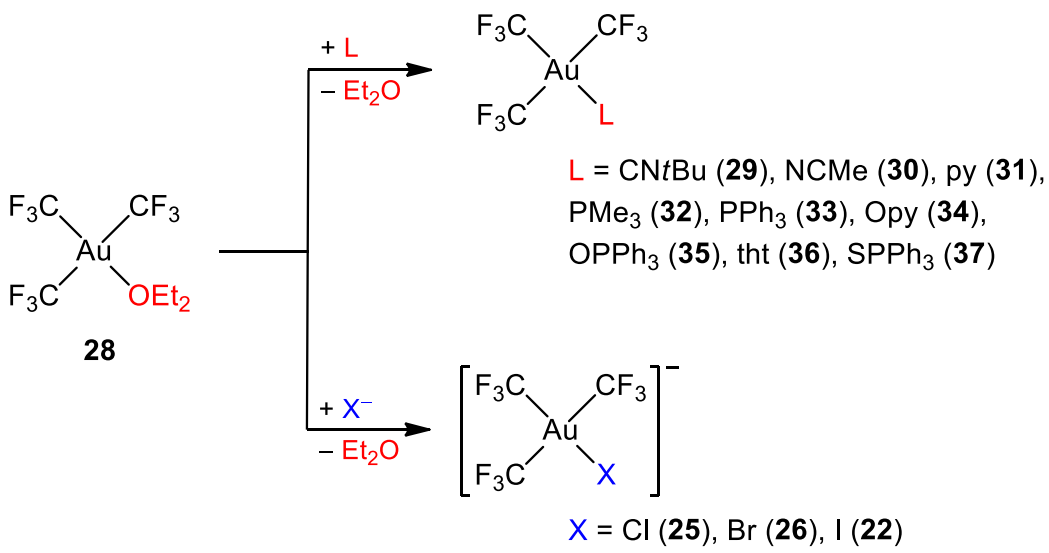

Scheme 3.10. Replacement of the labile Et_2O ligand in **28** by a variety of monodentate neutral and anionic ligands to afford neutral derivatives **29–37** and anionic complexes **22, 25** and **26**, for which the cation is $[PPh_4]^+$. By using cation $[PPh_3CH_2Ph]^+$, complex **25′** was also isolated.

All complexes show in their ^{19}F NMR spectra the typical pattern previously described for four-coordinated complexes containing the $(CF_3)_3Au$ fragment. It consists of two signals in 1:2 integrated ratio, typically a septet and a quartet, with an additional coupling in the case of the phosphine complexes **32** and **33**, due to coupling to the corresponding ^{31}P nucleus. The signals appear "inverted" in complexes containing π-acceptor ligands, namely CN*t*Bu (**29**), PMe_3 (**32**) and PPh_3 (**33**), as also observed in the cyano-complex **27** and in the related Pt(II) systems.[33]

The crystal and molecular structure of all neutral derivatives **29–37** prepared from etherate **28** were established by X-ray diffraction methods (Figure 3.6). A direct comparison with the related non-fluorinated derivative could be made only in the case of $(CF_3)_3Au(PPh_3)$ (**33**). The Au–P bond in **33** (239.27(6) pm) is longer than in compound $(CH_3)_3Au(PPh_3)$ (234.8(6) pm).[7a] The structural features of compound $(CF_3)_3Au(tht)$ (**36**) also compare well with those of the related complex $(C_6F_5)_3Au(tht)$.[43] Furthermore, in the classical coordination complexes Cl_3AuL (L = py,[44] PPh_3,[45] tht[46]), the Au–L bonds are shorter than in the related $(CF_3)_3AuL$ derivatives, a characteristic which is also observed when comparing compound **29** and its bromide analogue $Br_3Au(CN\mathit{t}Bu)$ (Table 3.1).[47] These differences derive from the higher *trans* influence of the CF_3 group.[35] On the other hand, in compounds **32**, **33** and

36 containing soft P- and S-donor ligands, the Au–CF_3 bond lengths in each molecule are identical within the experimental error (Table 3.2), despite the weaker *trans* influence of these soft ligands compared to that of the CF_3 group. Moreover, these distances are virtually identical to the Au–CF_3 bond lengths in the homoleptic anionic derivative $[NBu_4][(CF_3)_4Au]$ (208.0(7) pm av.).[28] Nevertheless, in complexes **29**, **30**, **31**, **34**, **35** and **37** the Au–C bond *trans* to L is shorter than those located *trans* to each other (Table 3.2).

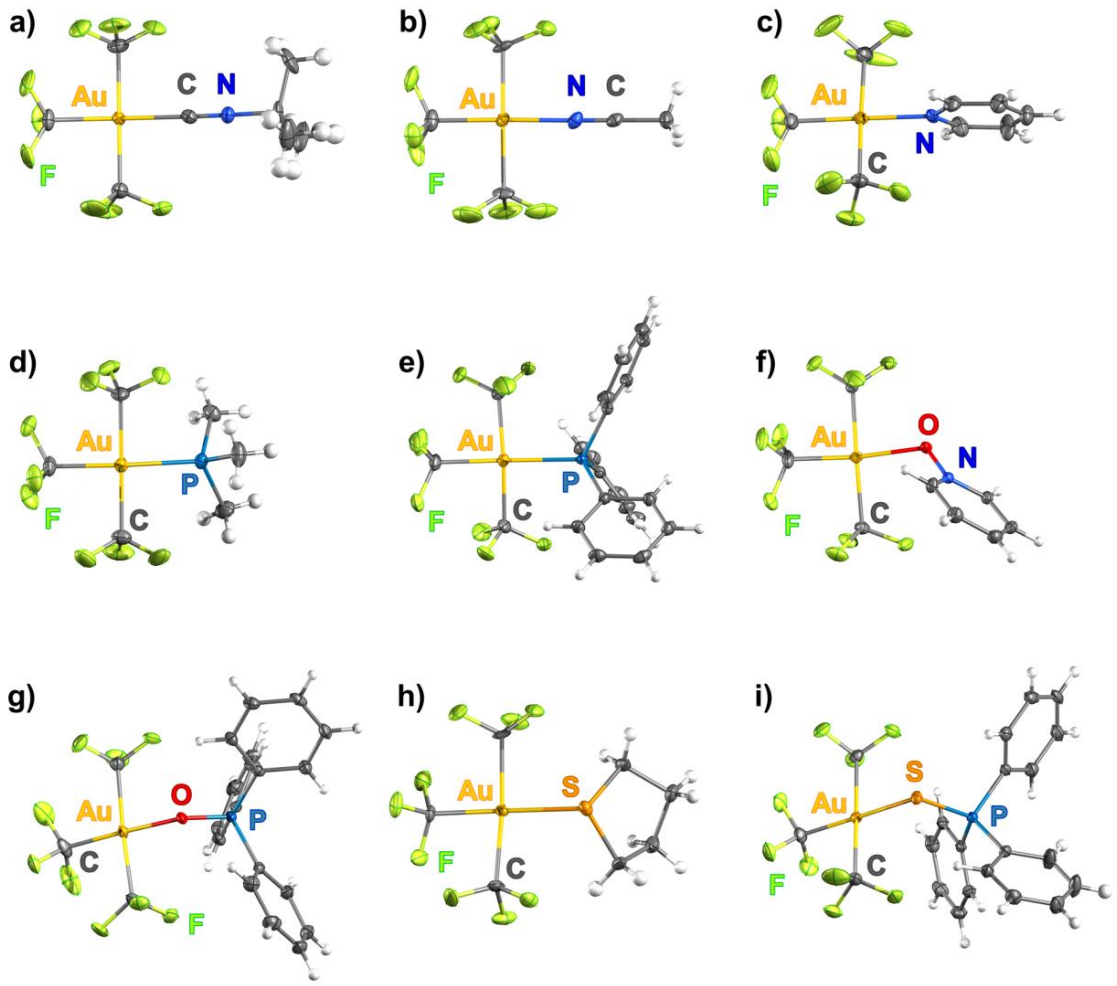

Figure 3.6. Displacement-ellipsoid diagrams (50% probability) of the neutral derivatives $(CF_3)_3AuL$: a) L = CN*t*Bu (**29**); b) L = NCMe (**30**); c) L = py (**31**); d) L = PMe_3 (**32**); e) L = PPh_3 (**33**); f) L = Opy (**34**); g) L = $OPPh_3$ (**35**); h) L = tht (**36**); i) L = $SPPh_3$ (**37**). In **29** and **31** only one set of the rotationally disordered F atoms found in two of the CF_3 groups is shown.

Table 3.1. Comparison of the Au–L bond lengths [pm] in $(CF_3)_3AuL$ complexes and related X_3AuL species.

L	$(CF_3)_3AuL$	X_3AuL
py	207.5(6)	199.3(7) (X = Cl)[44]
PPh_3	239.27(6)	232.9(2) (X = Cl)[45]
tht	238.9(2)[a]	232.6(2) (X = Cl)[46]
CN*t*Bu	204.3(5)	199(1) (X = Br)[47]

[a] Average values for the two crystallographically independent molecules in the unit cell.

Table 3.2. Au–CF_3 bond lengths [pm] in $(CF_3)_3AuL$ complexes.[a]

L	CF_3–Au–CF_3 axis[b]	CF_3–Au–E axis
CN*t*Bu (**29**)	208.5(6)	205.8(5)
NCMe (**30**)[c]	208.6(6)	201.7(6)
py (**31**)	207.4(9)	202.9(7)
PMe_3 (**32**)[c]	208.6(10)	208.3(10)
PPh_3 (**33**)	209.8(2)	209.0(3)
Opy (**34**)	207.8(3)	202.5(3)
$OPPh_3$ (**35**)	208.2(3)	200.1(3)
tht (**36**)[c]	208.8(8)	206.2(7)
$SPPh_3$ (**37**)	208.7(2)	205.3(2)

[a] A *trans* arrangement is meant in the indicated CF_3–Au–CF_3 and CF_3–Au–E units, E denoting a main-group donor atom. [b] Average of two independent values. [c] Average values for the two crystallographically independent molecules in the unit cell.

The Et_2O ligand in **28** can be also replaced by halide ligands X^-, giving rise to the corresponding anionic derivatives $[(CF_3)_3AuX]^-$ (X = Cl (**25**), Br (**26**), I (**22**)), which can be isolated as their $[PPh_4]^+$ salts (Scheme 3.10). This route allows for the easy introduction of different cations to crystallize the corresponding $[(CF_3)_3AuX]^-$ anion. For example, when etherate **28** reacts with $[PPh_3CH_2Ph]Cl$ in Et_2O/*n*-hexane (1:3 v/v), the $[PPh_3CH_2Ph][(CF_3)_3AuCl]$ salt (**25′**) can be easily isolated in very good yield.

Single crystals of **25′** were obtained by slow diffusion of a layer of *n*-hexane into a solution of the compound in CH_2Cl_2 and were analyzed by X-ray diffraction methods. The anion of **25′** exhibits a square-planar geometry (Figure 3.7) with structural parameters similar to those obtained for other anionic derivatives (Figure 3.4). The higher *trans* influence of the trifluoromethyl group[35] accounts for the longer Au–C distance of the mutually *trans*-standing CF_3 groups with respect to that of the Au–C bond *trans* to chloride. The bond lengths in the CF_3–Au–Cl axis are very similar to those found in $[PPh_4][CF_3AuCl_3]$ (**4**) (Au–C: 204.3(3) vs. 205.1(3) pm; Au–Cl: 232.56(6) vs. 233.9(1) pm; see Chapter 1). Although single crystals of **25**, which

contains the $[PPh_4]^+$ cation, could similarly be obtained, some disorder was found between the chloride ligand and one of the mutually *trans*-standing CF_3 groups, which precluded from obtaining reliable geometrical parameters. This is likely due to the S_4 symmetry of the $[PPh_4]^+$ cation, which gives rise to a high symmetry pattern in the crystal lattice. The less symmetric cation $[PPh_3CH_2Ph]^+$ breaks this symmetry pattern and allowed to obtain accurate structural data of the $[(CF_3)_3AuCl]^-$ anion.

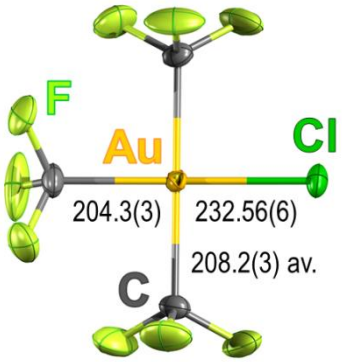

Figure 3.7. Displacement-ellipsoid diagram (50% probability) of the $[(CF_3)_3AuCl]^-$ anion as found in single crystals of **25′**. Selected bond lengths [pm] with estimated standard deviations are indicated.

3.6. Properties of the $(CF_3)_3Au$ fragment. Comparison of $(CF_3)_3Au$ versus $(CH_3)_3Au$

The $(CF_3)_3Au$ and $(CH_3)_3Au$ fragments are prototypical examples of unsaturated 14-valence-electron species. This is the reason why they have attracted the attention of several research groups, becoming the focus of a number of theoretical studies by Hoffmann,[20a] Nakamura[22] and Krossing.[29] A comparative theoretical study of both $(CX_3)_3Au$ moieties was undertaken using the same level of theory to gain a deeper understanding of their similarities and their differences. The different properties under study are described in the following sections.

3.6.1. Stereochemistry

Both $(CF_3)_3Au$ and $(CH_3)_3Au$ fragments have been calculated to exhibit a T-shape structure as the most energetically favored geometry, which is in agreement with

previous results.[20a,22,29] The Au–C bond *trans* to the void is the shortest one in both cases because of the lack of any *trans* influence. For their part, the mutually *trans*-standing CX_3 groups (X = H, F) display a fairly linear arrangement (Figure 3.8a and Figure 3.8b). However, a Y-shape structure appears as an additional local minimum at nearly the same energy only in the case of $(CH_3)_3Au$ (Figure 3.8c), the Y and T polytopes being connected by a very low energy profile. Thus, the $(CH_3)_3Au$ fragment is stereochemically labile, opposite to the more pronounced stereochemical stability of the $(CF_3)_3Au$ moiety, for which the T polytope is greatly favored (Figure 3.9).

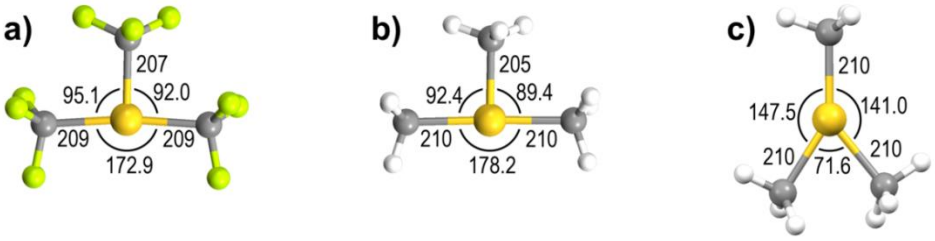

Figure 3.8. Lower-energy structures for the unsaturated $(CX_3)_3Au$ in the gas phase as calculated by DFT methods: a) T-shape polytope for X = F (global minimum); b) T-shape polytope for X = H (global minimum); c) Y-shape polytope for X = H (local minimum). Interatomic distances [pm] and angles [º] are indicated.

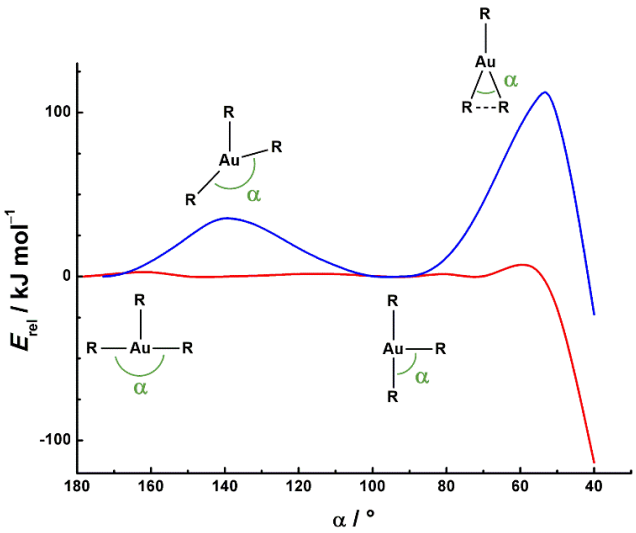

Figure 3.9. Comparative energy profiles of the $(CX_3)_3Au$ fragments (X = H, red trace; X = F, blue trace), as a function of the indicated α angle. Low α values lead to reductive elimination of CX_3–CX_3. Schematic structures above the profile lines refer to transition states, and those depicted below refer to energy minima.

The frontier orbitals of the T-shaped $(CF_3)_3Au$ polytope were analyzed (Figure 3.10) and the HOMO was identified as a mainly Au–C bonding orbital involving the mutually *trans*-standing CF_3 groups. The LUMO has a perpendicular arrangement, and exhibits a highly directional empty orbital responsible for the acidic properties of the fragment, which will be discussed in the following section. Contrary to what might be expected, an antibonding interaction arises between the empty metal-centered lobe of the LUMO and filled F(p) orbitals, suggesting very little affinity for the adjacent F substituents, as will be discussed later.

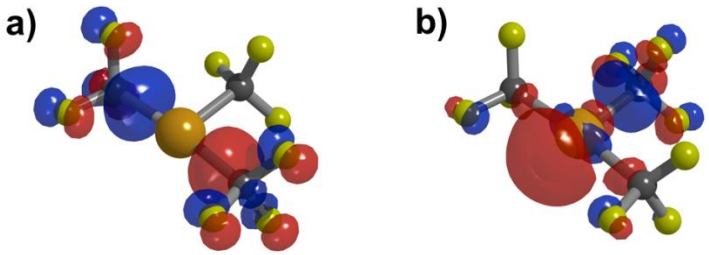

Figure 3.10. Frontier orbitals of the $(CF_3)_3Au$ unit: a) HOMO, and b) LUMO.

3.6.2. Lewis acidity

Unlike the strength of Brønsted acids, which is experimentally measured and quantified according to the well-known pH and pK_a scales,[48] no unified scale exists for the measurement of Lewis acidity. Different methods are used nowadays, which Greb classified into three different classes: intrinsic, global and effective.[49] The intrinsic methods do not rely on the formation of an acid–base pair, but rather on the analysis of the electronic structure of the free Lewis acid, by means of spectroscopy (for example via ^{29}Si NMR chemical shifts of silicocations $[R_3Si]^+$)[50] or quantum theoretical calculations like the LUMO energy[51] or the global electrophilicity index.[52] Global methods consider the thermochemistry of the process of formation of a Lewis acid–base adduct. The most representative method of this class is the fluoride ion affinity (FIA), which is defined as the binding enthalpy of a fluoride ion with a Lewis acid in the gas phase and was introduced by Haartz and McDaniel in 1973.[53] Because the initial experimental determinations were complicated and not very accurate, computational methods are now preferred. Due to the problems appearing in the calculation of the naked fluoride ion, the FIA values are obtained by nearly isodesmic reactions using the

known experimental FIA of COF_2 (209 kJ mol^{-1}) as an anchor point (Scheme 3.11).[51,54] Following this approach, Christe and coworkers developed a quantitative pF$^-$ scale of Lewis acidity, by dividing the FIA values (in kcal mol^{-1}) by 10.[54] Effective methods use the variation of a spectroscopic parameter of a probe molecule (Lewis base) upon interaction with an electron acceptor to determine Lewis acidity. Probably the most widely used is the Gutmann–Beckett method, which makes use of the chemical shift variation of the ^{31}P NMR signal of Et_3PO ($\Delta\delta_P$) upon coordination to a Lewis acid (Scheme 3.12).[55] Consistent trends are also obtained by using Ph_3PO as the probe molecule.[56] Additionally, Riedel and coworkers have recently reported the use of ^{13}C NMR chemical shifts of the C-donor atom of the SIMes ligand as a measure of the Lewis acidity of gold species.[57]

$$COF_3^- + A \xrightarrow{\Delta H\ \text{(calculated)}} AF^- + COF_2$$

$$COF_2 + F^- \xrightarrow{\Delta H = -209\ \text{kJ mol}^{-1}} CF_3O^-$$

$$A + F^- \xrightarrow{-\Delta H = \text{FIA}} AF^-$$

Scheme 3.11. Calculation of the FIA for a Lewis acid A by using COF_2 as the reference fluoride carrier (experimental FIA = 209 kJ mol^{-1}).[49,51,54]

$$A + Et_3PO \xrightarrow{\Delta\delta_P\ (Et_3PO)} A{\cdot}OPEt_3$$

Scheme 3.12. Assessment of the Lewis acidity of a Lewis acid A by the Gutmann-Beckett method.[55] An extension of this scale has been developed by using Ph_3PO instead of Et_3PO.[56]

We have chosen one method of each class to assess the Lewis acidity of the $(CF_3)_3Au$ fragment. First, the LUMO of the T-shaped $(CF_3)_3Au$ polytope is located at –4.34 eV, much lower than in its non-fluorinated analogue $(CH_3)_3Au$ (–2.71 eV), which proves the higher acidity of the fluorinated moiety. In addition, the $(CF_3)_3Au$ moiety is more acidic than $(C_6F_5)_3B$ (–3.93 eV), but not as much as $(CF_3)_3B$ (–4.77 eV).[51]

The FIA value of our fluorinated T-shaped $(CF_3)_3Au$ fragment, calculated by using COF_2 as the reference fluoride carrier is 433 kJ mol^{-1}, again indicating its substantially

higher Lewis acidity in comparison with the non-fluorinated $(CH_3)_3Au$ unit (FIA = 298 kJ mol^{-1}). However, it is still a weaker acid than the superacidic $(CF_3)_3B$ (FIA = 556 kJ mol^{-1}).[51,58] On the quantitative pF$^-$ scale, the Lewis acidity of $(CF_3)_3Au$ (pF$^-$ = 10.3) is similar to that of AsF_5 (pF$^-$ = 10.6) and $(C_6F_5)_3B$ (pF$^-$ = 10.8), whereas the non-fluorinated $(CH_3)_3Au$ is as acidic as SeF_4 (pF$^-$ = 7.1).[54] A comparison of the pF$^-$ values of $(CF_3)_3Au$ with related neutral species is shown in Figure 3.11. Interestingly, $(C_6F_5)_3B$ (FIA = 452 kJ mol^{-1})[51] seems to be slightly more acidic than $(CF_3)_3Au$ according to their FIA values, which can be attributed to the much stronger B–F bond (732 kJ mol^{-1}) with respect to the Au–F bond (294.1 kJ mol^{-1}) for the respective diatomic neutral fluorides.[59] This makes the FIA method especially unfavorable for gold, since it is a soft acid ("class b" metal) and the fluoride ion is a hard base.[31]

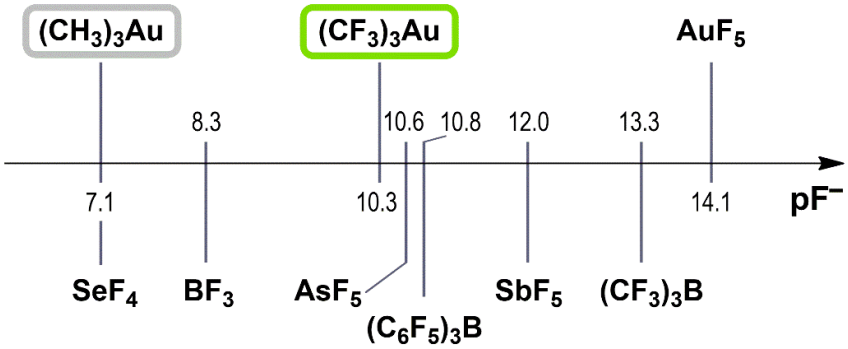

Figure 3.11. Lewis acidity scale (highest range) in pF$^-$ values[54] for selected neutral AX_n species.

According to the Gutmann–Beckett method, the δ_P of Et_3PO suffers a downfield shift of $\Delta\delta_P$ = 33.4 ppm upon coordination to the $(CF_3)_3Au$ unit, which again ranks it as a stronger Lewis acid than $(C_6F_5)_3B$ ($\Delta\delta_P$ = 30.6 ppm).[56,60] Similarly, the δ_P of Ph_3PO is also much deshielded in $(CF_3)_3Au(OPPh_3)$ ($\Delta\delta_P'$ = 24.8 ppm) than in $(C_6F_5)_3B(OPPh_3)$ ($\Delta\delta_P'$ = 20.3 ppm).[56,61] On this scale, it could be demonstrated that the $(CF_3)_3Au$ unit is also a stronger Lewis acid than $(C_6F_5)_3Au$ ($\Delta\delta_P'$ = 17.1 ppm).[41a]

3.6.3. Stability and decomposition pathways

For reductive elimination to occur at the unsaturated $(CX_3)_3Au$ units, two alkyl groups must become close enough as to enable C–C coupling. Hence, we have modeled both

systems by gradually reducing the C–Au–C angle between two *cis*-standing groups from 90º to 40º. In the case of $(CF_3)_3Au$, reductive elimination of hexafluoroethane requires rather high activation energy (≈ 112 kJ mol^{-1}). However, reductive elimination of ethane at the $(CH_3)_3Au$ moiety has been found to be a clearly exergonic process with a very low activation barrier (≈ 7 kJ mol^{-1}), which is in agreement with the almost fluxional behavior of this unit (see Section 3.6.1) that allows two methyl groups to approach to each other easily.

The electronegativity of the alkyl group CX_3 seems to be also a determining factor of the stability of the $(CX_3)_3Au$ units towards reductive elimination of C_2X_6, this process being more favored with the least electronegative substituents. Thus, considering the series of mainly σ-donor ligands CF_3, CH_3 and H, with electronegativity values of 3.49, 2.28 and 2.20 in Pauling units, respectively,[34a,62] we have demonstrated that reductive elimination is more favored with the less electronegative CH_3 than with CF_3. The least electronegative hydride ligand is not even able to stabilize the high-valent species AuH_3, which is better formulated as a dihydrogen adduct of AuH, $HAu(H_2)$.[63] A similar trend is actually observed in the case of gold trihalides (see Chapter 1 for an in-depth description), the heavier halide AuI_3 being better described as an end-on iodine adduct of AuI, $IAu(I_2)$,[64] contrary to the T-shaped lighter homologues.[64b,65]

Another potential decomposition path of our $(CF_3)_3Au$ unit would be through fluorotropic processes, namely a 1,2-F shift, which is actually the origin of the instability of the isoleptic $(CF_3)_3B$.[58] Other very strong Lewis acids, such as $Al(C_6F_5)_3$[66] and $Al(OC(CF_3)_3)_3$,[67] also suffer from similar drawbacks. In the case of the elusive superacidic species $(CF_3)_3B$, a 1,2-F shift affording the $(CF_3)_2B(CF_2)F$ saturated species is energetically favored because the hard F^- anion forms very strong bonds with boron and also the kinetic barrier is easily overcome.

In our $(CF_3)_3Au$ fragment (**A**), the energy of the system rises when forcing the F atom of a CF_3 group to approach the metal center (Figure 3.12), in accord with the antibonding interaction between the empty metal-centered lobe of the LUMO and filled F(p) orbitals (Figure 3.10). In the case of a *cis*-1,2-F shift, even the highest point in which the F atom occupies the empty coordination site (**B-*cis***) is metastable and reverts to the initial stage **A** spontaneously when the only restraint applied is removed. On the other hand, although the endpoint of the *trans*-1,2-F shift (**B-*trans***) is higher in energy,

it is a local minimum. Hence, both square-planar saturated stereoisomers **B-*cis*** and **B-*trans*** are less stable than the T-shaped, 14-electron unit **A**. This destabilization due to the 1,2-F shift is due to the greater energy required for the C–F bond-breaking, which is not surpassed by that liberated in the formation of the Au–F bond. This is in contrast to the favorable energy balance in the analogous fluorotropic process in the case of $(CF_3)_3B$, which also requires a geometric rearrangement[68] to form the final tetrahedral shape in $(CF_3)_2B(CF_2)F$.

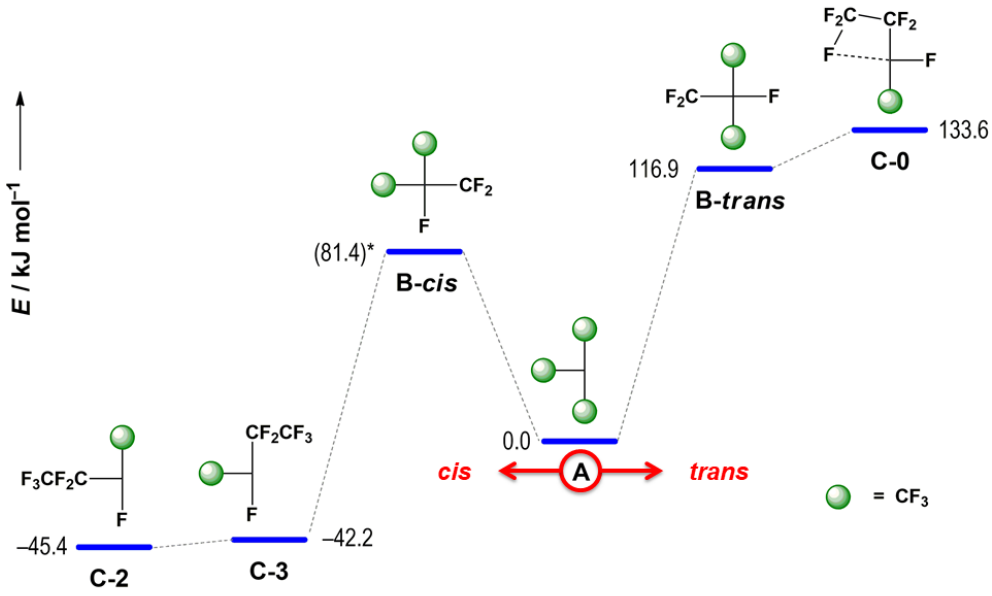

Figure 3.12. Energy scheme calculated for the [Au]–CF_3 ⇌ F–Au←CF_2 fluorine shift and subsequent CF_2 insertion into remaining Au–CF_3 bonds relative to the parent species $(CF_3)_3Au$ (**A**).

Stereoisomer **B-*cis*** is significantly stabilized upon CF_2 insertion into any of the Au–CF_3 bonds, giving rise to $CF_3CF_2Au(CF_3)F$ (**C**), in two of its isomeric forms, not very different in energy (Figure 3.12). The insertion of CF_2 into the *trans* Au–CF_3 bond affords a species (**C-2**) with a distorted Y geometry, which is slightly more stable than the insertion into the *cis* Au–CF_3 bond, which gives rise to a regular T-shaped structure (**C-3**). However, the related insertion process in the **B-*trans*** species, gives just a single stereoisomer (**C-0**) which is even more destabilized. In fact, the high electronegativity of fluorine favors a secondary Au···F bonding interaction with one of the β-F atoms of the perfluoroalkyl chain, or with an α-F atom if the first interaction is removed,

destabilizing the system even more. These interactions are not observed in stereoisomers **C-2** and **C-3**, which proves the stronger *trans* influence of perfluoroalkyl ligands with respect to fluoride.

It can be therefore concluded, that the 1,2-F shift in the $(CF_3)_3Au$ unit cannot be considered a feasible decomposition path because of its destabilizing effect. This adds to the high intrinsic stability of the T-shaped $(CF_3)_3Au$ fragment, which originates from its marked stereochemical stability and its reluctance to undergo reductive elimination of C_2F_6.

3.6.4. Ligand affinity of the $(CF_3)_3Au$ fragment

Since all evidence points to a dissociative mechanism as the initial step in reductive elimination processes undergone by trialkyl gold(III) derivatives, the ease of L dissociation is a key aspect to determine the reaction progress in R_3AuL systems. We therefore decided to calculate the affinity of the $(CF_3)_3Au$ unit for a range of neutral ligands including those of complexes **28–37** and some others selected for comparative purposes. First, the structures of all these R_3AuL derivatives were optimized by DFT calculations. The geometry of the $(CF_3)_3Au$ moiety compares well with those experimentally established by single-crystal X-ray diffraction. However, the calculated Au–E distances are slightly longer and therefore Au–E dissociation values D_e may be underestimated.

The order of our calculated ligand strength towards the $(CF_3)_3Au$ fragment as the Au–E dissociation values, D_e, is represented in Figure 3.13. It is interesting to note, that relative affinity scales are also known for some fundamental gold units such as AuCl[69] and the bare Au^+ cation.[70] In the case of our $(CF_3)_3Au$ unit, the most stable compounds are the phosphine derivatives, the more basic PMe_3 (**32**: D_e = 229 kJ mol^{-1}) providing even higher stability than PPh_3 (**33**: D_e = 204 kJ mol^{-1}). The stability of the compounds containing semipolar pnictogen oxide ligands, pyO (**34**: D_e = 151 kJ mol^{-1}) and Ph_3PO (**35**: D_e = 173 kJ mol^{-1}) is exceeded by that of the softer sulfide Ph_3PS (**37**: D_e = 183 kJ mol^{-1}). Intermediate values are obtained for py (**31**: D_e = 169 kJ mol^{-1}) and *t*BuNC (**29**: D_e = 178 kJ mol^{-1}), which are in turn more stable than the related complexes formed with the heavier-element homologues PC_5H_5 (D_e = 152 kJ mol^{-1}) and *t*BuNSi (D_e = 139

kJ mol^{-1}). The weaker σ-donor and better π-acceptor capability of the phosphabenzene ligand with respect to pyridine[71] may account for the lower stability of $(CF_3)_3Au(PC_5H_5)$ in comparison with $(CF_3)_3Au$(py). Similar stabilization is attained with soft thioether ligands such as tht (**36**: D_e = 149 kJ mol^{-1}) and its related open-chain Et_2S (D_e = 166 kJ mol^{-1}).

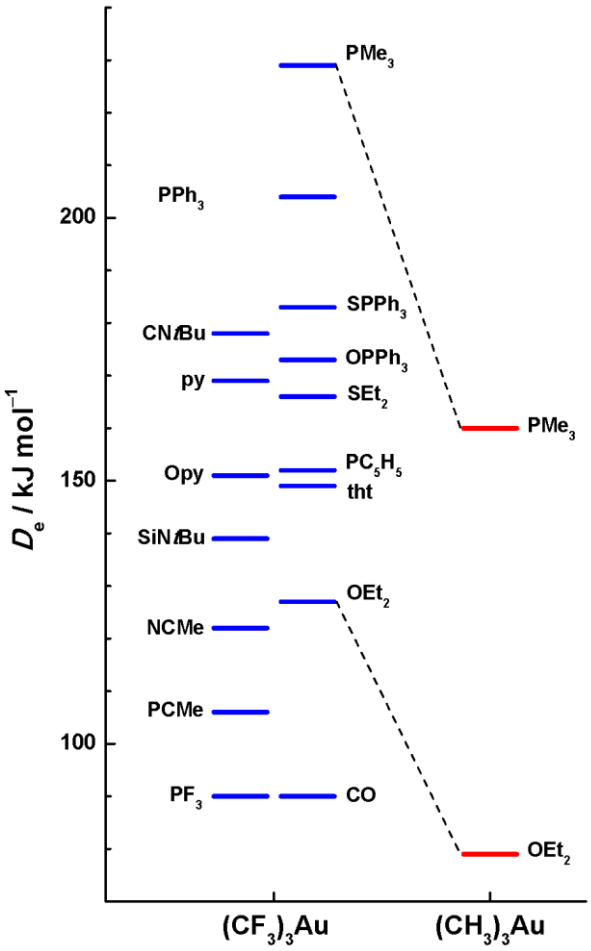

Figure 3.13. Affinity scale of the $(CF_3)_3Au$ unit for a variety of neutral L ligands based on the dissociation energy D_e calculated for the corresponding $(CF_3)_3Au$–L bond. D_e values are compared for L = Et_2O, PMe_3 with the significantly less stable $(CH_3)_3Au$–L complexes (right).

The modest D_e value required to dissociate L in the derivatives containing the hard and weakly coordinating ligands[72] Et_2O (**28**: D_e = 127 kJ mol^{-1}) and MeCN (**30**: D_e = 122 kJ mol^{-1}), makes them suitable synthons for the naked $(CF_3)_3Au$ unit. The complex formed with the heavier-element homologue of acetonitrile MeC≡P is significantly less stable (D_e = 106 kJ mol^{-1}), but unlike for MeC≡N, a side-on coordination is preferred.

The derivatives with the typical π-acceptor ligands CO and PF_3 were the least stable of the whole calculated series (D_e = 90 kJ mol^{-1} in both cases). The poor σ-donor ability of CO and PF_3 ligands results in weaker [Au]–L σ bonds. Moreover, no significant synergic reinforcement through π-backbonding from the $(CF_3)_3Au$ unit should be expected. In fact, we were unable to prepare the carbonyl compound $(CF_3)_3Au(CO)$ by replacement of the Et_2O ligand in the labile derivative **28**, at least under the experimental conditions used for complexes **29–37** (Scheme 3.10).

Coordination of Et_2O and PMe_3, chosen as representative examples for weakly and strongly coordinated ligands, to the non-fluorinated $(CH_3)_3Au$ moiety provides significant less stabilization (L = Et_2O: D_e = 79 kJ mol^{-1}; L = PMe_3: D_e = 160 kJ mol^{-1}). This is in agreement with the experimental observations, the derivative $(CF_3)_3Au{\cdot}OEt_2$ (**28**) being easily handled in solution at room temperature, in contrast to its non-fluorinated analogue $(CH_3)_3Au{\cdot}OEt_2$, which begins to decompose at –40 ºC.[3] Similarly, $(CF_3)_3Au(PPh_3)$ (**33**) is stable up to 251 ºC, whereas its non-fluorinated analogue $(CH_3)_3Au(PPh_3)$ already decomposes at 120 ºC.[5]

In agreement with our DFT calculations, complexes **29–37** show high thermal stability, as established by combined TGA/DTA analysis. Interestingly, the small size of some of the $(CF_3)_3AuL$ derivatives and the lack of significant intermolecular interactions in the solid state, result in high volatility of complexes with L = MeCN (**30**), py (**31**), PMe_3 (**32**) and tht (**36**), which boil between 205 and 223 ºC at atmospheric pressure. $(CF_3)_3Au(CN\mathit{t}Bu)$ (**29**) decomposes at 125 ºC, but all other complexes with L = PPh_3 (**33**), Opy (**34**), $OPPh_3$ (**35**) and $SPPh_3$ (**37**) exhibit high thermal stability with decomposition temperatures within a range between 220 and 302 ºC, complex **37** being the most stable. Interestingly, pyridine *N*-oxide derivative **34** undergoes oxygen extrusion upon heating at 210 ºC for 5 minutes, giving rise to the pyridine complex **31**.

3.7. Thermolytic studies on the anionic derivatives of $(CF_3)_3Au$

In addition to the analyses performed for our neutral derivatives **29–37** to rank their stability, we also carried out thermolytic studies on our isolated anionic complexes **22** and **24–27** under two related but quite different experimental conditions: in the gas phase and in the condensed phase. These conditions ensure that the results obtained are

intrinsic of each substance, since no solvent is involved. They also enable distinction between inter- and intramolecular decomposition pathways.

3.7.1. Unimolecular thermolyses in the gas phase

The anionic derivatives $[(CF_3)_3AuX]^-$ (X = F, Cl, Br, I, CN) were studied by tandem mass spectrometry, since they are charged species and form an ideal set for the study of their unimolecular decomposition pathways as function of a single variable, X. The energetic experimental conditions required to induce fragmentation in the parent ions point out their intrinsic stability. Moreover, these experimental conditions ensure that only intramolecular decomposition pathways operate.

The general decomposition pattern observed for the set of anionic derivatives $[(CF_3)_3AuX]^-$ (X = F, Cl, Br, I, CN) is shown in Scheme 3.13, but some variations exist depending on the precise halide X. The formal reductive elimination of C_2F_6 with concomitant formation of $[CF_3AuX]^-$ operates in all cases, being the main fragmentation path in all the derivatives except in the case of the fluoride complex (Figure 3.14a). In this case, the main fragmentation path involves CF_2 extrusion, whereby the difluoride species $[(CF_3)_2AuF_2]^-$ is formed. This non-reductive fragmentation is less important on going down the halogen group and is actually absent in the case of the iodo derivative (Figure 3.14b). Formal reductive elimination of C_2F_6 is largely favored over that of CF_3X in all cases. In fact, elimination of CF_3CN is not observed in the cyano derivative.

The formal reductive elimination of C_2F_6 was calculated to be a high-energy process in the naked $(CF_3)_3Au$ fragment, as described in Section 3.6.1. This is in line with the highly-energetic experimental conditions required for these unimolecular decompositions to occur. However, a two-step $CF_3^{\bullet}$ radical dissociation may probably take place, since this kind of process has been also observed in other gold(III) trifluoromethyl derivatives (see Chapter 1 and Chapter 2).

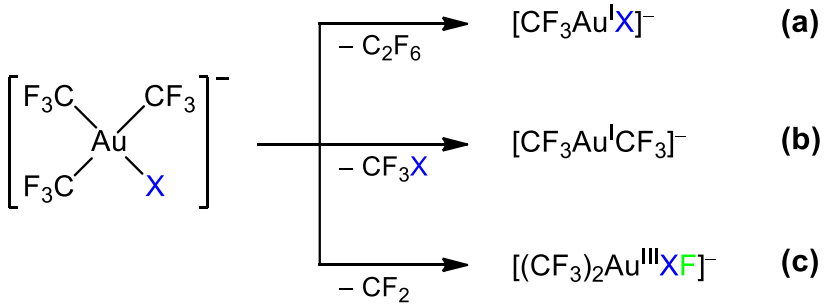

Scheme 3.13. Primary unimolecular fragmentation paths experimentally observed by tandem mass spectrometry (MS^2) for the $[(CF_3)_3AuX]^-$ anions (X = F, Cl, Br, I, CN). Significant variations apply to each particular case.

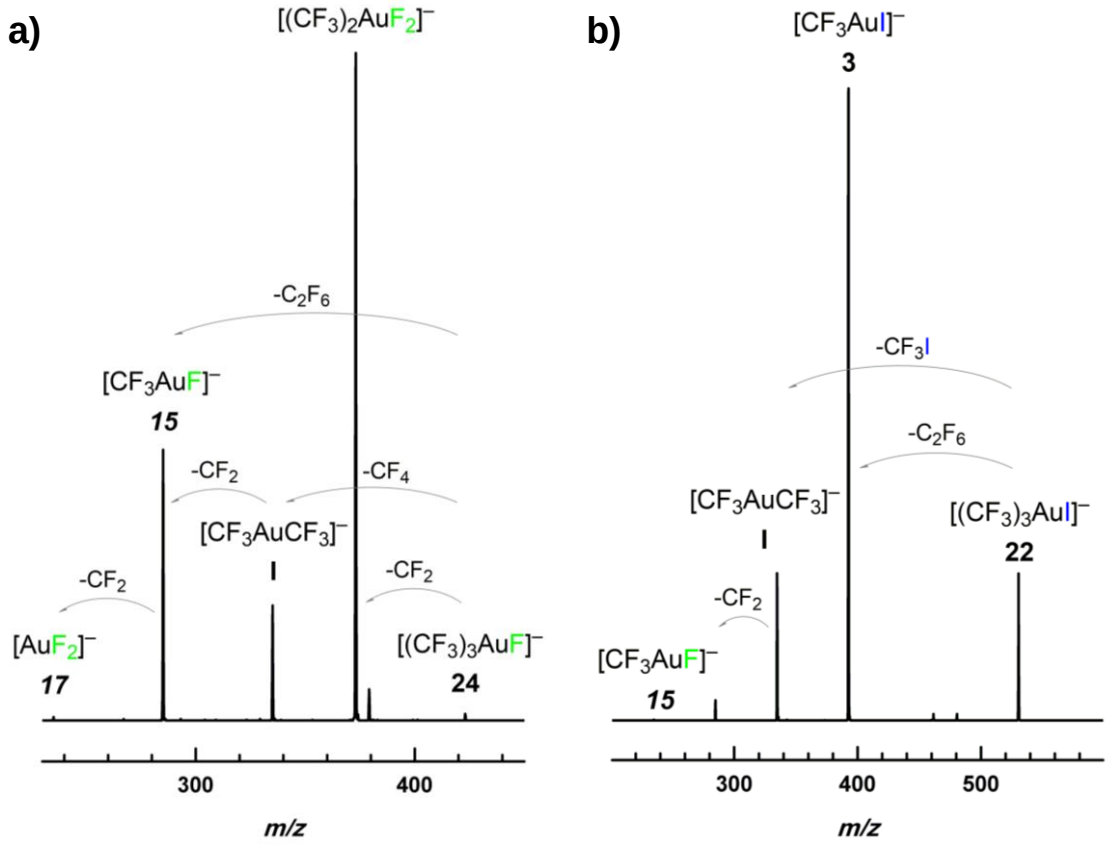

Figure 3.14. Quadrupole ion-trap MS^2 results of the collision-induced dissociation (CID) of the anion of a) **24**, $[(CF_3)_3AuF]^-$; and b) **22**, $[(CF_3)_3AuI]^-$.

3.7.2. Thermolyses in the condensed phase

The stability of the anionic derivatives containing the $(CF_3)_3Au$ unit, **22** and **24–27**, was checked by a combined TGA/DTA analysis of the corresponding solid samples. All

these compounds show unusually high stability, the decomposition temperature ranging from 245 ºC in the case of the iodo derivative **22** to 350 ºC in the case of the cyano complex **27**. Once their decomposition temperature was determined, the bulk solids were thermolyzed above that temperature in sealed tubes under an argon atmosphere and the products were analyzed by means of ^{19}F NMR spectroscopy and mass spectrometry (see Methodology).

No C_2F_6 was detected in the decomposition of any of these complexes, thus confirming that the formal reductive elimination of C_2F_6 observed in the gas phase does not actually take place as a single-step CF_3–CF_3 elimination, but rather as a two-step $CF_3^{\bullet}$ radical dissociation (see above). Additionally, variable amounts of metallic gold appeared, as well as the fluorosilicate anion $[SiF_5]^-$, denoting the formation of highly active species, able to attack the glass tube. In all cases, non-regioselective trifluoromethylation of the cation at one or two positions of the phenyl rings was observed.

As a representative example, we studied the thermolysis of the iodo derivative **22** at 250 ºC, a temperature which is only slightly above the onset of decomposition of this compound (245 ºC). Its decomposition produces CF_3I and $[CF_3AuCF_3]^-$ (**I**) as required for the reductive elimination shown in Scheme 3.14a. This process occurs only to a minor extent in the gas phase (Figure 3.14b), therefore indicating that intermolecular paths operate in the condensed phase. The existence of intermolecular processes is further evidenced by the presence of $[(CF_3)_4Au]^-$ and $[CF_3AuI]^-$ (**3**) among the decomposition products. The lack of C_2F_6 justifies that the latter compound cannot arise from reductive elimination of C_2F_6 from the starting compound **22**. The exchange process given in Scheme 3.14b may rather account for its formation. The homoleptic anion $[CF_3AuCF_3]^-$ (**I**) acts therefore as a trifluoromethylating agent towards complex anion $[(CF_3)_3AuI]^-$ (**22**).

This intermolecular exchange process takes place at a temperature which is above the melting points of $[PPh_4][(CF_3)_3AuI]$ (**22**, m.p. 171 ºC) and $[PPh_4][CF_3AuCF_3]$ (**I**, m.p. 193 ºC),[28] therefore enabling a fluid contact between both organogold derivatives. The independent equimolar reaction between preformed **22** and **I** (Scheme 3.14b) carried out at 200 ºC, a temperature at which **22** has not decomposed yet, allowed us to confirm this exchange process. Similar exchange reactions are known to occur in solution among gold(III) halide complexes and more active trifluoromethylating agents such as

$(CF_3)_2Cd{\cdot}dme$.[25,26] Related processes in solution among $[Au^{III}]$–X and $[Au^{I}]$–CH_3 derivatives are also known,[11,12,20b,73] but the singularity of the one described here is due to the fact that it takes place in the melt and gives rise to the anionic homoleptic $[(CF_3)_4Au]^-$ species.

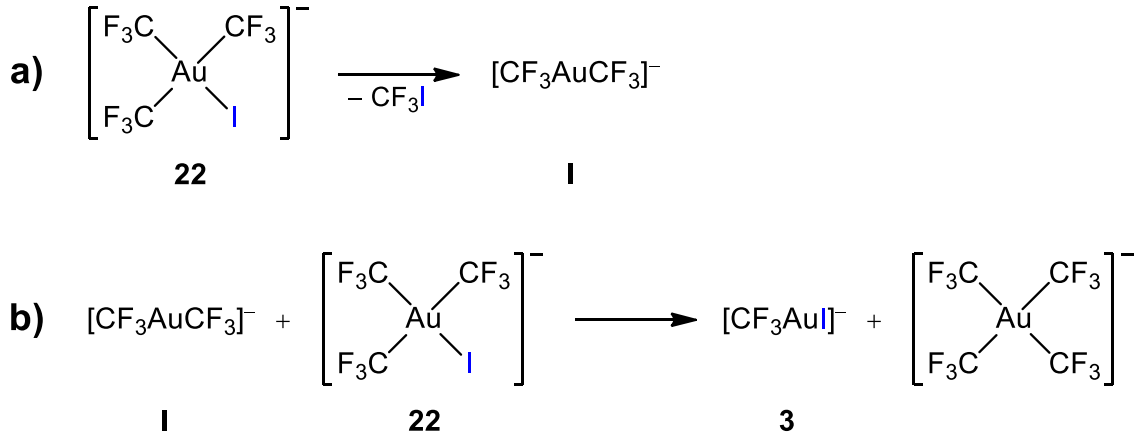

Scheme 3.14. Intermolecular decomposition paths observed upon thermolysis of **22** at 250 ºC in condensed phase: a) Reductive elimination, and b) ligand exchange. Process b) was independently investigated using equimolar amounts of preformed **I** and **22**. In both initial **22** and **I** the cation is $[PPh_4]^+$, but the phenyl rings are once or twice trifluoromethylated during the thermolytic process.

3.8. Summary

- The organogold(III) compound $[PPh_4][(CF_3)_3AuI]$ (**22**) was cleanly obtained by photoinduced oxidative addition of CF_3I to the homoleptic organogold(I) precursor $[PPh_4][CF_3AuCF_3]$ (**I**) in high yield and under mild conditions (Scheme 3.7). Compound **22** constitutes a convenient and efficient entry to the $(CF_3)_3Au$ moiety, which was virtually unexplored until now.

- The anionic derivatives $[PPh_4][(CF_3)_3AuX]$ (X = F (**24**), Cl (**25**), Br (**26**), CN (**27**)) have been prepared from complex **22** in high yield by halide exchange with the appropriate reagents (Scheme 3.8). These compounds are very stable, as demonstrated by TGA/DTA experiments. This is of special importance since no analogous $[(CH_3)_3AuX]^-$ complex is known.[4]

- The fluorinated analogue of trimethyl gold, $(CF_3)_3Au{\cdot}OEt_2$ (**28**) has been prepared and characterized (Scheme 3.9). It is significantly more stable than its non-fluorinated analogue, which already decomposes above –40 ºC in Et_2O solution.[3]

- The high lability and modest dissociation energy of the Et_2O ligand in $(CF_3)_3Au{\cdot}OEt_2$ (**28**) make this compound a convenient synthon of the unsaturated 14-electron species $(CF_3)_3Au$. In fact, the Et_2O ligand can be readily replaced by a variety of neutral L ligands including a wide range of donors, and this way, complexes **29–37** were prepared therefrom (Scheme 3.10). Thus, we have considerably expanded the chemistry of the $(CF_3)_3Au$ fragment.

- The most fundamental intrinsic properties of the $(CF_3)_3Au$ moiety have been investigated with the aid of DFT methods, and compared to those of its non-fluorinated analogue, $(CH_3)_3Au$. The naked $(CF_3)_3Au$ fragment has been calculated to exhibit a T-shape structure as the most energetically favored. Its high stereochemical stability and the high energy barrier required for the reductive elimination of CF_3–CF_3 account for the high stability of the $(CF_3)_3Au$ fragment. In contrast, the $(CH_3)_3Au$ unit is stereochemically labile and undergoes almost barrierless reductive elimination of CH_3–CH_3.

- In the few cases where the comparison can be experimentally established, the stability of the $(CF_3)_3AuL$ compounds largely exceed that of the non-fluorinated $(CH_3)_3AuL$ derivatives. This has been rationalized in terms of stronger $(CX_3)_3Au$–L interactions when X = F. In the set of ligands L chosen for the ligand affinity scale of the $(CF_3)_3Au$ fragment (Figure 3.13), P-donor ligands proved to be particularly versatile, since they cover the whole range of stability from the highly basic PMe_3 (upper limit) to the poor donor PF_3 (lower limit).

- The $(CF_3)_3Au$ fragment has been found to be probably the strongest neutral organogold R_3Au Lewis acid, as assessed by different theoretical and experimental methods. Fluorination of $(CH_3)_3Au$ makes the $(CF_3)_3Au$ unit much more acidic, which is in agreement with the stronger electron-withdrawing properties of the CF_3 group.[74] In fact, it exhibits higher acidity that $(C_6F_5)_3Au$ or $(C_6F_5)_3B$.

- The decomposition pathways of anionic derivatives $[PPh_4][(CF_3)_3AuX]$ have been investigated and compared in two different but related conditions; i.e. in the gas phase

and in the condensed phase. Different decomposition mechanisms were found depending on the aggregation state. Whereas high-energy processes operate at the unimolecular level (gas phase), lower-energy intermolecular pathways are open in the condensed phase (solvent-free reaction media), where ligand exchange processes occur.

3.9. References

[1] a) W. J. Pope, C. S. Gibson. The alkyl compounds of gold. *J. Chem. Soc., Trans.* **1907**, *91*, 2061; b) W. J. Pope, C. S. Gibson. The alkyl compounds of gold. Diethylauric bromide. *Proc. Chem. Soc., London* **1907**, *23*, 245.

[2] F. H. Brain, C. S. Gibson. The Organic Compounds of Gold. Part VII. Methyl and Ethyl Compounds. *J. Chem. Soc.* **1939**, 762.

[3] a) H. Gilman, L. A. Woods. Trimethylgold. *J. Am. Chem. Soc.* **1948**, *70*, 550; b) L. A. Woods, H. Gilman. Trialkylgold Compounds. *Proc. Iowa Acad. Sci.* **1942**, *49*, 286.

[4] a) H. Schmidbaur, A. Grohmann, M. E. Olmos, in *Gold: Progress in Chemistry, Biochemistry and Technology* (Ed.: H. Schmidbaur), John Wiley & Sons, Chichester, **1999**, pp. 647–746; b) H. Schmidbaur, A. Grohmann, M. E. Olmos, A. Schier, in *The Chemistry of Organic Derivatives of Gold and Silver* (Eds.: S. Patai, Z. Rappoport), belonging to Patai's Chemistry of Functional Groups, Wiley, Chichester, **1999**, pp. 227–311; c) G. K. Anderson. The Organic Chemistry of Gold. *Adv. Organomet. Chem.* **1982**, *20*, 39; d) H. Schmidbaur, *Au: Organogold Compounds*, in Gmelin-Handbuch der Anorganischen Chemie, Springer, Berlin, 8th ed., Springer-Verlag, Berlin, **1980**; e) R. J. Puddephatt, in *The Chemistry of Gold*, Elsevier, Amsterdam, **1978**, pp. 98–156; f) B. Armer, H. Schmidbaur. Organogold Chemistry. *Angew. Chem. Int. Ed. Engl.* **1970**, *9*, 101; *Angew. Chem.* **1970**, *82*, 120.

[5] G. E. Coates, C. Parkin. Tertiary Phosphine Complexes of Trimethylgold: Infrared Spectra of Complexes of Gold and Some Other Metals. *J. Chem. Soc.* **1963**, 421.

[6] a) H. Schmidbaur, A. Shiotani. Organogold-Chemie, VI. Darstellung komplexer Organogold-Verbindungen durch Liganden-Substitutionsreaktionen. *Chem. Ber.* **1971**, *104*, 2821; b) A. Shiotani, H.-F. Klein, H. Schmidbaur. Nuclear Magnetic Resonance Spectra and Ligand Substitution Reactions of Methylgold and Trimethylgold Complexes. *J. Am. Chem. Soc.* **1971**, *93*, 1555.

[7] a) J. Stein, J. P. Fackler, Jr., C. Paparizos, H.-W. Chen. Structure and Properties of Transition-Metal Ylide Complexes. 2. Organometallic Complexes of Gold(III). *J. Am. Chem. Soc.* **1981**, *103*, 2192; b) J. P. Fackler, Jr., C. Paparizos. Trimethylgold(III) Complexes of Reactive Sulfoxonium and Sulfonium Ylides. *J. Am. Chem. Soc.* **1977**, *99*, 2363; c) H. Schmidbaur, R. Franke. Organogold chemistry. XVI. Trimethylgold Trimethylphosphonium-methylid and Related Compounds. *Inorg. Chim. Acta* **1975**, *13*, 79.

[8] a) C. F. Shaw, R. S. Tobias. Bonding in Methygold(I) and Trimethygold(III) Compounds. Nuclear Magnetic Resonance, Raman, and Infrared Spectra and Normal Coordinates. *Inorg. Chem.* **1973**, *12*, 965; b) S. W. Krauhs, G. C. Stocco, R. S. Tobias. Trends in $(CH_3)_2YAuP(C_6H_5)_3$ Compounds ($Y^- = Cl^-, CH_3^-, \square\text{-}C_5H_5^-$). Proton Magnetic Resonance and Vibrational Spectra. *Inorg. Chem.* **1971**, *10*, 1365.

[9] H. Schmidbaur. Inorganic Chemistry with Ylides. *Acc. Chem. Res.* **1975**, *8*, 62.

[10] A. Shiotani, H. Schmidbaur. Organogold-chemie IX. Versuche zur Oxydativen Addition an Organogold-Komplexen. *J. Organomet. Chem.* **1972**, *37*, C24.

[11] a) A. Tamaki, J. K. Kochi. Oxidative addition in the coupling of alkylgold(I) with alkyl halides. *J. Organomet. Chem.* **1974**, *64*, 411; b) A. Tamaki, J. K. Kochi. Catalytic mechanism involving oxidative addition in the coupling of alkylgold(I) with alkyl halides. *J. Organomet. Chem.* **1972**, *40*, C81.

[12] a) A. Johnson, R. J. Puddephatt. Oxidative addition reactions of methyl iodide with some methylgold(I) compounds. *J. Organomet. Chem.* **1975**, *85*, 115; b) A. Johnson, R. J. Puddephatt. Oxidative addition reactions of methylgold(I) compounds. *Inorg. Nucl. Chem. Lett.* **1973**, *9*, 1175.

[13] a) A. Tamaki, J. K. Kochi. Reactions of Dialkylaurate(I) with Electrophiles: Synthesis of Trialkylgold(III) Compounds. *J. Chem. Soc., Dalton Trans.* **1973**, 2620; b) A. Tamaki, J. K. Kochi. Dialkylaurate(I) complexes and the synthesis of trialkylgold(III) compounds. *J. Organomet. Chem.* **1973**, *51*, C39.

[14] a) N. J. Rijs, G. B. Sanvido, G. N. Khairallah, R. A. J. O'Hair. Gas phase synthesis and reactivity of dimethylaurate. *Dalton Trans.* **2010**, *39*, 8655; b) S. Komiya, T. A. Albright, R. Hoffmann, J. K. Kochi. The Stability of Organogold Compounds. Hydrolytic, Thermal, and Oxidative Cleavages of Dimethylaurate(I) and Tetramethylaurate(III). *J. Am. Chem. Soc.* **1977**, *99*, 8440.

[15] a) D. Zhu, S. V. Lindeman, J. K. Kochi. X-ray Crystal Structures and the Facile Oxidative (Au−C) Cleavage of the Dimethylaurate(I) and Tetramethylaurate(III) Homologues. *Organometallics* **1999**, *18*, 2241; b) S. Komiya, S. Ochiai, Y. Ishizaki. Isolation of Stable Tetraalkylammonium Tetraalkylaurate(III) Complexes. *Inorg. Chem.* **1992**, *31*, 3168; c) G. W. Rice, R. S. Tobias. Isolation of Thermally Stable Compounds Containing the Dimethylaurate(I) and Tetramethylaurate(III) Anions. *Inorg. Chem.* **1976**, *15*, 489; d) G. W. Rice, R. S. Tobias. Synthesis of Tetramethylaurate(III). Studies on the Structures of $Li[(CH_3)_2Au]$ and $Li[(CH_3)_4Au]$ in Solution. *Inorg. Chem.* **1975**, *14*, 2402.

[16] J. K. Kochi, in *Organometallic Mechanisms and Catalysis*, Academic Press, New York (NY), **1978**, pp. 262–283.

[17] B. J. Gregory, C. K. Ingold. Mechanism of Electrophilic Substitution at a Saturated Carbon Atom. Part XI. Bimolecular and Unimolecular Substitution of Mercury for Gold in Alkylgold Complexes. *J. Chem. Soc. B* **1969**, 276.

[18] R. J. Puddephatt, P. J. Thompson. Methyl for Halogen Exchange Reactions Between Palladium(II), Platinum(II), Gold(I), and Gold(III) Complexes. *J. Chem. Soc., Dalton Trans.* **1975**, 1810.

[19] H. Schmidbaur, A. Shiotani, H.-F. Klein. Organogold-Chemie, VII. NMR-Spektroskopische Studien von Liganden-Austauschreaktionen an zweifach und vierfach koordinierten Goldatomen. *Chem. Ber.* **1971**, *104*, 2831.

[20] a) S. Komiya, T. A. Albright, R. Hoffmann, J. K. Kochi. Reductive Elimination and Isomerization of Organogold Complexes. Theoretical Studies of Trialkylgold Species as Reactive Intermediates. *J. Am. Chem. Soc.* **1976**, *98*, 7255; b) A. Tamaki, S. A. Magennis, J. K. Kochi. Catalysis by Gold. Alkyl Isomerization, Cis–Trans Rearrangement, and Reductive Elimination of Alkylgold(III) Complexes. *J. Am. Chem. Soc.* **1974**, *96*, 6140.

[21] A. Tamaki, S. A. Magennis, J. K. Kochi. Rearrangement and Decomposition of Trialkylgold(III) Complexes. *J. Am. Chem. Soc.* **1973**, *95*, 6487.

[22] W. Nakanishi, M. Yamanaka, E. Nakamura. Reactivity and Stability of Organocopper(I), Silver(I), and Gold(I) Ate Compounds and Their Trivalent Derivatives. *J. Am. Chem. Soc.* **2005**, *127*, 1446.

[23] J. Gil-Rubio, J. Vicente. Gold trifluoromethyl complexes. *Dalton Trans.* **2015**, *44*, 19432.

[24] M. A. Guerra, T. R. Bierschenk, R. J. Lagow. The generality of metal atom-free radical reactions and synthesis of new trifluoromethylalkyls of gold(III) and silver. *J. Organomet. Chem.* **1986**, *307*, C58.

[25] R. D. Sanner, J. H. Satcher, Jr., M. W. Droege. Synthesis and Characterization of (Trifluoromethyl)gold Complexes. *Organometallics* **1989**, *8*, 1498.

[26] H. K. Nair, J. A. Morrison. Formation of group 11 trifluoromethyl derivatives by reaction of $Cd(CF_3)_2$·glyme with representative Au, Ag, and Cu complexes: isolation of $Au(CF_3)_3(PMe_3)$, $Au(CF_3)_3(PEt_3)$, $AuI(CF_3)_2(PMe_3)$, $AuCF_3(PMe_3)$, $AuCF_3(PEt_3)$ and $AgCF_3(PMe_3)$; observation of $CuCF_3(PMe_3)$. *J. Organomet. Chem.* **1989**, *376*, 149.

[27] E. Bernhardt, M. Finze, H. Willner. Synthesis and NMR spectroscopic investigation of salts containing the novel $[Au(CF_3)_nX_{4-n}]^-$ (n = 4–1, X = F, CN, Cl) anions. *J. Fluorine Chem.* **2004**, *125*, 967.

[28] S. Martínez-Salvador, L. R. Falvello, A. Martín, B. Menjón. Gold(I) and Gold(III) Trifluoromethyl Derivatives. *Chem. Eur. J.* **2013**, *19*, 14540.

[29] U. Preiss, I. Krossing. A Computational Study of $[M(CF_3)_4]^-$ (M = Cu, Ag, Au) and their Properties as Weakly Coordinating Anions. *Z. Anorg. Allg. Chem.* **2007**, *633*, 1639.

[30] a) A. Portugués, I. López-García, J. Jiménez-Bernad, D. Bautista, J. Gil-Rubio. Photoinitiated Reactions of Haloperfluorocarbons with Gold(I) Organometallic Complexes: Perfluoroalkyl Gold(I) and Gold(III) Complexes. *Chem. Eur. J.* **2019**, *25*, 15535; b) M. Joost, A. Amgoune, D. Bourissou. Reactivity of Gold Complexes towards Elementary Organometallic Reactions. *Angew. Chem. Int. Ed.* **2015**, *54*, 15022; *Angew. Chem.* **2015**, *127*, 15234; c) M. S. Winston, W. J. Wolf, F. D. Toste. Photoinitiated Oxidative Addition of CF_3I to Gold(I) and Facile Aryl-CF_3 Reductive Elimination. *J. Am. Chem. Soc.* **2014**, *136*, 7777; d) R. J. Puddephatt. Reactivity and Mechanism in Organogold Chemistry. *Gold Bull.* **1977**, *10*, 108; e) A. Johnson, R. J. Puddephatt. Reactions of Trifluoromethyl Iodide with Methylgold(I) Complexes. Preparation of Trifluoromethyl-gold(I) and -gold(III) Complexes. *J. Chem. Soc., Dalton Trans.* **1976**, 1360.

[31] a) R. G. Pearson. Recent Advances in the Concept of Hard and Soft Acids and Bases. *J. Chem. Educ.* **1987**, *64*, 561; b) R. J. Puddephatt, in *The Chemistry of Gold*, Elsevier, Amsterdam, **1978**, pp. 22–24; c) S. Ahrland. Factors Contributing to (b)-behaviour in Acceptors. *Struct. Bonding (Berlin)* **1966**, *1*, 207; d) R. G. Pearson. Hard and Soft Acids and Bases. *J. Am. Chem. Soc.* **1963**, *85*, 3533; e) S. Ahrland, J. Chatt, N. R. Davies. The relative affinities of ligand atoms for acceptor molecules and ions. *Q. Rev. Chem. Soc.* **1958**, *12*, 265.

[32] a) R. Kumar, A. Linden, C. Nevado. Evidence for Direct Transmetalation of Au^{III}–F with Boronic Acids. *J. Am. Chem. Soc.* **2016**, *138*, 13790; b) R. Kumar, A. Linden, C. Nevado. Luminescent (N^C^C) Gold(III) Complexes: Stabilized Gold(III) Fluorides. *Angew. Chem. Int. Ed.* **2015**, *54*, 14287; *Angew. Chem.* **2015**, *127*, 14495; c) M. S. Winston, W. J. Wolf, F. D. Toste. Halide-Dependent Mechanisms of Reductive Elimination from Gold(III). *J. Am. Chem. Soc.* **2015**, *137*, 7921.

[33] S. Martínez-Salvador, J. Forniés, A. Martín, B. Menjón, I. Usón. Stepwise Degradation of Trifluoromethyl Platinum(II) Compounds. *Chem. Eur. J.* **2013**, *19*, 324.

[34] a) J. E. Huheey, E. A. Keiter, R. L. Keiter, in *Inorganic Chemistry: Principles of Structure and Reactivity*, 4th ed., Harper-Collins, New York (NY), **1993**, pp. 182–199; b) R. T. Sanderson, in *Simple Inorganic Substances*, Krieger, Malabar (FL), **1989**, p. 23; c) R. T. Sanderson. Principles of Electronegativity Part I. General Nature. *J. Chem. Educ.* **1988**, *65*, 112.

[35] a) A. G. Algarra, V. V. Grushin, S. A. Macgregor. Natural Bond Orbital Analysis of the Electronic Structure of $[L_nM(CH_3)]$ and $[L_nM(CF_3)]$ Complexes. *Organometallics* **2012**, *31*, 1467; b) P. Sgarbossa, A. Scarso, G. Strukul, R. A. Michelin. Platinum(II) Complexes with Coordinated Electron-Withdrawing Fluoroalkyl and Fluoroaryl Ligands: Synthesis, Reactivity, and Catalytic Activity. *Organometallics* **2012**, *31*, 1257; c) T. G. Appleton, H. C. Clark, L. E. Manzer. The *trans*-influence: its measurement and significance. *Coord. Chem. Rev.* **1973**, *10*, 335; d) T. G. Appleton, M. H. Chisholm, H. C. Clark, L. E. Manzer. Trifluoromethylplatinum Complexes and the Nature of the Pt–CF_3 Bond. *Inorg. Chem.* **1972**, *11*, 1786.

[36] M. A. Ellwanger, S. Steinhauer, P. Golz, H. Beckers, A. Wiesner, B. Braun-Cula, T. Braun, S. Riedel. Taming the High Reactivity of Gold(III) Fluoride: Fluorido Gold(III) Complexes with N-Based Ligands. *Chem. Eur. J.* **2017**, *23*, 13501.

[37] P. G. Jones, C. Thöne. Tetraphenylarsonium Tetracyanoaurate(III) Dichloromethane Solvate. *Acta Crystallogr. Sect. C* **1989**, *45*, 11.

[38] D. Joven-Sancho, M. Baya, A. Martín, J. Orduna, B. Menjón. The First Organosilver(III) Fluoride, $[PPh_4][(CF_3)_3AgF]$. *Chem. Eur. J.* **2020**, *26*, 4471.

[39] G. R. Fulmer, A. J. M. Miller, N. H. Sherden, H. E. Gottlieb, A. Nudelman, B. M. Stoltz, J. E. Bercaw, K. I. Goldberg. NMR Chemical Shifts of Trace Impurities: Common Laboratory Solvents, Organics, and Gases in Deuterated Solvents Relevant to the Organometallic Chemist. *Organometallics* **2010**, *29*, 2176.

[40] a) P. W. Siu, K. Hazin, D. P. Gates. $H(OEt_2)_2[P(1,2\text{-}O_2C_6Cl_4)_3]$: Synthesis, Characterization, and Application as a Single-Component Initiator for the Carbocationic Polymerization of Olefins. *Chem. Eur. J.* **2013**, *19*, 9005; b) I. Krossing, A. Reisinger. Perfluorinated Alkoxyaluminate Salts of Cationic Brønsted Acids: Synthesis, Structure, and Characterization of $[H(OEt_2)_2][Al\{OC(CF_3)_3\}_4]$ and $[H(THF)_2][Al\{OC(CF_3)_3\}_4]$. *Eur. J. Inorg. Chem.* **2005**, 1979; c) U. Wietelmann, W. Bonrath, T. Netscher, H. Nöth, J.-C. Panitz, M. Wohlfahrt-Mehrens. Tris(oxalato)phosphorus Acid and Its Lithium Salt. *Chem. Eur. J.* **2004**, *10*, 2451; d) S. Rannabauer, T. Habereder, H. Nöth, W. Schnick. Synthesis, Spectroscopic Properties, and Crystal Structure of the Oxonium Acid $[H(OEt_2)_2]^+[Ti_2Cl_9]^-$. *Z. Naturforsch. B* **2003**, *58*, 745; e) D. Stasko, S. P. Hoffmann, K.-C. Kim, N. L. P. Fackler, A. S. Larsen, T. Drovetskaya, F. S. Tham, C. A. Reed, C. E. F. Rickard, P. D. W. Boyd, E. S. Stoyanov. Molecular Structure of the Solvated Proton in Isolated Salts. Short, Strong, Low Barrier (SSLB) H-bonds. *J. Am. Chem. Soc.* **2002**, *124*, 13869; f) D. Vagedes, G. Erker, R. Fröhlich. Synthesis and structural characterization of $[H(OEt_2)_2]^+[(C_3H_3N_2)\{B(C_6F_5)_3\}_2]^-$ — a Brønsted acid with an imidazole-derived 'non-coordinating' anion. *J. Organomet. Chem.* **2002**, *641*, 148; g) S. J. Lancaster, A. Rodriguez, A. Lara-Sanchez, M. D. Hannant, D. A. Walker, D. H. Hughes, M. Bochmann. $[H_2N\{B(C_6F_5)_3\}_2]^-$: A New, Remarkably Stable Diborate Anion for Metallocene Polymerization Catalysts. *Organometallics* **2002**, *21*, 451; h) L. D. Henderson, W. E. Piers, G. J. Irvine, R. McDonald. Anion Stability in Stannylium, Oxonium, and Silylium Salts of the Weakly Coordinating Anion $[C_6F_4\text{-}1,2\text{-}\{B(C_6F_5)_2\}_2(\mu\text{-}OCH_3)]^-$. *Organometallics* **2002**, *21*, 340; i) P. Jutzi, C. Müller, A. Stammler, H.-G. Stammler. Synthesis, Crystal Structure, and Application of the Oxonium Acid $[H(OEt_2)_2]^+[B(C_6F_5)_4]^-$. *Organometallics* **2000**, *19*, 1442; j) M. Brookhart, B. Grant, A. F. Volpe, Jr. $[(3,5\text{-}(CF_3)_2C_6H_3)_4B]^-[H(OEt_2)_2]^+$: A Convenient Reagent for Generation and Stabilization of Cationic, Highly Electrophilic Organometallic Complexes. *Organometallics* **1992**, *11*, 3920; k) S. P. Kolesnikov, I. V.

Lyudkovskaya, M. Y. Antipin, Y. T. Struchkov, O. M. Nefedov. Etherates of Friedel-Crafts acids with a short hydrogen bond: Symmetrical $[Et_2O...H...OEt_2]^+$ cation in the crystal structure of the etherate $(Et_2O)_2 \cdot HZnCl_3$. *Bull. Acad. Sci. USSR Div. Chem. Sci. (Engl. Transl.)* **1985**, *34*, 74.

[41] a) R. Usón, A. Laguna, M. Laguna, J. Jiménez, M. E. Durana. Tris(pentafluorophenyl)gold(III) Complexes with O-, N- or S-donor Ligands. *Inorg. Chim. Acta* **1990**, *168*, 89; b) L. G. Vaughan, W. A. Sheppard. Organogold Chemistry II. Tris(pentafluorophenyl)gold(III). *J. Organomet. Chem.* **1970**, *22*, 739.

[42] R. Eujen, B. Hoge, D. J. Brauer. Preparation and NMR Spectra of the (Trifluoromethyl)argentates(III) $[Ag(CF_3)_nX_{4-n}]^-$, with X = CN (n = 1−3), CH_3, $C{\equiv}CC_6H_{11}$, Cl, Br (n = 2, 3), and I (n = 3), and of Related Silver(III) Compounds. Structures of $[PPh_4]$[*trans*-$Ag(CF_3)_2(CN)_2$] and $[PPh_4][Ag(CF_3)_3(CH_3)]$. *Inorg. Chem.* **1997**, *36*, 1464.

[43] J. Coetzee, W. F. Gabrielli, K. Coetzee, O. Schuster, S. D. Nogai, S. Cronje, H. G. Raubenheimer. Structural Studies of Gold(I, II, and III) Compounds with Pentafluorophenyl and Tetrahydrothiophene Ligands. *Angew. Chem. Int. Ed.* **2007**, *46*, 2497; *Angew. Chem.* **2007**, *119*, 2549.

[44] H.-N. Adams, J. Strähle. Die Pyridinaddukte der Goldhalogenide. 1. Darstellung und Struktur von $[Hpy][AuCl_4]$, $AuCl_3 \cdot py$, $[AuCl_2(py)_2]Cl \cdot H_2O$ und $[AuCl_2(py)_2][AuCl_2]$. *Z. Anorg. Allg. Chem.* **1982**, *485*, 65.

[45] R. J. Staples, T. Grant, J. P. Fackler, Jr., A. Elduque. Structure of trichloro(triphenylphosphine)gold(III), $[AuCl_3\{P(C_6H_5)_3\}]$. *Acta Crystallogr. Sect. C* **1994**, *50*, 39.

[46] P. G. Jones, E. Bembenek. Crystal structure of (tetrahydrothiophene)-trichlorogold(III), $C_4H_8AuCl_3S$. *Z. Kristallogr.* **1993**, *208*, 126.

[47] D. Schneider, O. Schuster, H. Schmidbaur. Attempted Oxidative Addition of Halogens to (Isocyanide)gold(I) Complexes. *Organometallics* **2005**, *24*, 3547.

[48] D. Himmel, V. Radtke, B. Butschke, I. Krossing. Basic Remarks on Acidity. *Angew. Chem. Int. Ed.* **2018**, *57*, 4386; *Angew. Chem.* **2018**, *130*, 4471.

[49] L. Greb. Lewis Superacids: Classifications, Candidates, and Applications. *Chem. Eur. J.* **2018**, *24*, 17881.

[50] K. Müther, P. Hrobárik, V. Hrobáriková, M. Kaupp, M. Oestreich. The Family of Ferrocene-Stabilized Silylium Ions: Synthesis, ^{29}Si NMR Characterization, Lewis Acidity, Substituent Scrambling, and Quantum-Chemical Analyses. *Chem. Eur. J.* **2013**, *19*, 16579.

[51] H. Böhrer, N. Trapp, D. Himmel, M. Schleep, I. Krossing. From unsuccessful H_2-activation with FLPs containing $B(Ohfip)_3$ to a systematic evaluation of the Lewis acidity of 33 Lewis acids based on fluoride, chloride, hydride and methyl ion affinities. *Dalton Trans.* **2015**, *44*, 7489.

[52] a) A. R. Jupp, T. C. Johnstone, D. W. Stephan. Improving the Global Electrophilicity Index (GEI) as a Measure of Lewis Acidity. *Inorg. Chem.* **2018**, *57*, 14764; b) A. R. Jupp, T. C. Johnstone, D. W. Stephan. The global electrophilicity index as a metric for Lewis acidity. *Dalton Trans.* **2018**, *47*, 7029; c) M. Méndez, A. Cedillo. Gas phase Lewis acidity and basicity scales for boranes, phosphines and amines based on the formation of donor–acceptor complexes. *Comput. Theor. Chem.* **2013**, *1011*, 44; d) R. G. Parr, L. v. Szentpály, S. Liu. Electrophilicity Index. *J. Am. Chem. Soc.* **1999**, *121*, 1922.

[53] J. C. Haartz, D. H. McDaniel. Fluoride Ion Affinity of Some Lewis Acids. *J. Am. Chem. Soc.* **1973**, *95*, 8562.

[54] K. O. Christe, D. A. Dixon, D. McLemore, W. W. Wilson, J. A. Sheehy, J. A. Boatz. On a quantitative scale for Lewis acidity and recent progress in polynitrogen chemistry. *J. Fluorine Chem.* **2000**, *101*, 151.

[55] a) M. A. Beckett, G. C. Strickland, J. R. Holland, K. S. Varma. A convenient n.m.r. method for the measurement of Lewis acidity at boron centres: correlation of reaction rates of Lewis acid initiated epoxide polymerizations with Lewis acidity. *Polymer* **1996**, *37*, 4629; b) U. Mayer, V. Gutmann, W. Gerger. The Acceptor Number — A Quantitative Empirical Parameter for the Electrophilic Properties of Solvents. *Monatsh. Chem.* **1975**, *106*, 1235.

[56] H. Großekappenberg, M. Reißmann, M. Schmidtmann, T. Müller. Quantitative Assessment of the Lewis Acidity of Silylium Ions. *Organometallics* **2015**, *34*, 4952.

[57] M. A. Ellwanger, C. von Randow, S. Steinhauer, Y. Zhou, A. Wiesner, H. Beckers, T. Braun, S. Riedel. Tuning the Lewis acidity of difluorido gold(III) complexes: the synthesis of $[AuClF_2(SIMes)]$ and $[AuF_2(OTeF_5)(SIMes)]$. *Chem. Commun.* **2018**, *54*, 9301.

[58] M. Finze, E. Bernhardt, M. Zähres, H. Willner. Rearrangement Reactions of the Transient Lewis Acids $(CF_3)_3B$ and $(CF_3)_3BCF_2$: An Experimental and Theoretical Study. *Inorg. Chem.* **2004**, *43*, 490.

[59] Y. R. Luo, *Comprehensive Handbook of Chemical Bond Energies*, CRC Press, Boca Ratón (FL), **2007**.

[60] M. A. Beckett, D. S. Brassington, S. J. Coles, M. B. Hursthouse. Lewis acidity of tris(pentafluorophenyl)borane: crystal and molecular structure of $B(C_6F_5)_3{\cdot}OPEt_3$. *Inorg. Chem. Commun.* **2000**, *3*, 530.

[61] a) G. J. P. Britovsek, J. Ugolotti, A. J. P. White. From $B(C_6F_5)_3$ to $B(OC_6F_5)_3$: Synthesis of $(C_6F_5)_2BOC_6F_5$ and $C_6F_5B(OC_6F_5)_2$ and Their Relative Lewis Acidity. *Organometallics* **2005**, *24*, 1685; b) M. A. Beckett, D. S. Brassington, M. E. Light, M. B. Hursthouse. Organophosphoryl adducts of tris(pentafluorophenyl)borane; crystal and molecular structure of $B(C_6F_5)_3{\cdot}Ph_3PO$. *J. Chem. Soc., Dalton Trans.* **2001**, 1768.

[62] S. G. Bratsch. A Group Electronegativity Method with Pauling Units. *J. Chem. Educ.* **1985**, *62*, 101.

[63] a) X. Wang, L. Andrews. Infrared Spectra and DFT Calculations for the Gold Hydrides AuH, $(H_2)AuH$, and the AuH_3 Transition State Stabilized in $(H_2)AuH_3$. *J. Phys. Chem. A* **2002**, *106*, 3744; b) X. Wang, L. Andrews. Gold Hydrides AuH and $(H_2)AuH$ and the AuH_3 Transition State Stabilized in $(H_2)AuH_3$: Infrared Spectra and DFT Calculations. *J. Am. Chem. Soc.* **2001**, *123*, 12899; c) N. B. Balabanov, J. E. Boggs. Lowest Singlet and Triplet States of Copper, Silver, and Gold Trihydrides: an ab Initio Study. *J. Phys. Chem. A* **2001**, *105*, 5906; d) C. A. Bayse. Interaction of Dihydrogen with Gold (I) Hydride: Prospects for Matrix-Isolation Studies. *J. Phys. Chem. A* **2001**, *105*, 5902; e) C. A. Bayse, M. B. Hall. Prediction of the Geometries of Simple Transition Metal Polyhydride Complexes by Symmetry Analysis. *J. Am. Chem. Soc.* **1999**, *121*, 1348.

[64] a) M.-J. Crawford, T. M. Klapötke. Hydrides and Iodides of Gold. *Angew. Chem. Int. Ed.* **2002**, *41*, 2269; *Angew. Chem.* **2002**, *114*, 2373; b) A. Schulz, M. Hargittai. Structural Variations and Bonding in Gold Halides: A Quantum Chemical Study of Monomeric and Dimeric Gold Monohalide and Gold Trihalide Molecules, AuX, Au_2X_2, AuX_3, and Au_2X_6 (X = F, Cl, Br, I). *Chem. Eur. J.* **2001**, *7*, 3657; c) T. Söhnel, R. Brown, L. Kloo, P. Schwerdtfeger. The Stability of Gold Iodides in the Gas Phase and the Solid State. *Chem. Eur. J.* **2001**, *7*, 3167.

[65] a) I. J. Blackmore, A. J. Bridgeman, N. Harris, M. A. Holdaway, J. F. Rooms, E. L. Thompson, N. A. Young. Experimental Evidence for a Jahn–Teller Distortion in $AuCl_3$. *Angew. Chem. Int. Ed.* **2005**, *44*, 6746; *Angew. Chem.* **2005**, *117*, 6904; b) B. Réffy, M.

Kolonits, A. Schulz, T. M. Klapötke, M. Hargittai. Intriguing Gold Trifluoride−Molecular Structure of Monomers and Dimers: An Electron Diffraction and Quantum Chemical Study. *J. Am. Chem. Soc.* **2000**, *122*, 3127; c) X. Wang, L. Andrews, F. Brosi, S. Riedel. Matrix Infrared Spectroscopy and Quantum-Chemical Calculations for the Coinage-Metal Fluorides: Comparisons of Ar–AuF, Ne–AuF, and Molecules MF_2 and MF_3. *Chem. Eur. J.* **2013**, *19*, 1397; d) X. Wang, L. Andrews, K. Willmann, F. Brosi, S. Riedel. Investigation of Gold Fluorides and Noble Gas Complexes by Matrix-Isolation Spectroscopy and Quantum-Chemical Calculations. *Angew. Chem. Int. Ed.* **2012**, *51*, 10628; *Angew. Chem.* **2012**, *124*, 10780.

[66] a) J. Chen, E. Y.-X. Chen. Unsolvated $Al(C_6F_5)_3$: structural features and electronic interaction with ferrocene. *Dalton Trans.* **2016**, *45*, 6105; b) T. Belgardt, J. Storre, H. W. Roesky, M. Noltemeyer, H.-G. Schmidt. Tris(pentafluorophenyl)alane: A Novel Aluminum Organyl. *Inorg. Chem.* **1995**, *34*, 3821; c) J. L. W. Pohlmann, F. E. Brinckmann. Preparation and Characterization of Group III A Derivatives. *Z. Naturforsch. B* **1965**, *20*, 5.

[67] a) A. Kraft, N. Trapp, D. Himmel, H. Böhrer, P. Schlüter, H. Scherer, I. Krossing. Synthesis, Characterization, and Application of Two $Al(OR^F)_3$ Lewis Superacids. *Chem. Eur. J.* **2012**, *18*, 9371; b) L. O. Müller, D. Himmel, J. Stauffer, G. Steinfeld, J. Slattery, G. Santiso-Quiñones, V. Brecht, I. Krossing. Simple Access to the Non-Oxidizing Lewis Superacid $PhF\rightarrow Al(OR^F)_3$ ($R^F=C(CF_3)_3$). *Angew. Chem. Int. Ed.* **2008**, *47*, 7659; *Angew. Chem.* **2008**, *120*, 7772.

[68] a) E. I. Davydova, T. N. Sevastianova, A. Y. Timoshkin. Molecular complexes of group 13 element trihalides, pentafluorophenyl derivatives and Lewis superacids. *Coord. Chem. Rev.* **2015**, *297-298*, 91; b) L. A. Mück, A. Y. Timoshkin, G. Frenking. Design of Neutral Lewis Superacids of Group 13 Elements. *Inorg. Chem.* **2012**, *51*, 640.

[69] P. Pyykkö, N. Runeberg. Comparative Theoretical Study of N-Heterocyclic Carbenes and Other Ligands Bound to Au^I. *Chem. Asian J.* **2006**, *1*, 623.

[70] D. Schröder, H. Schwarz, J. Hrušák, P. Pyykkö. Cationic Gold(I) Complexes of Xenon and of Ligands Containing the Donor Atoms Oxygen, Nitrogen, Phosphorus, and Sulfur. *Inorg. Chem.* **1998**, *37*, 624.

[71] a) C. Müller, D. Vogt. Phosphinines as ligands in homogeneous catalysis: recent developments, concepts and perspectives. *Dalton Trans.* **2007**, 5505; b) P. Le Floch, F. Mathey. Transition metals in phosphinine chemistry. *Coord. Chem. Rev.* **1998**, *178-180*, 771.

[72] J. A. Davies, F. R. Hartley. Complexes of the Platinum Metals Containing Weak Donor Ligands. *Chem. Rev.* **1981**, *81*, 79.

[73] G. W. Rice, R. S. Tobias. Mechanism of the alkylation of dialkylgold(III) compounds with alkylgold(I) complexes. *J. Organomet. Chem.* **1975**, *86*, C37.

[74] M. Á. García-Monforte, S. Martínez-Salvador, B. Menjón. The Trifluoromethyl Group in Transition Metal Chemistry. *Eur. J. Inorg. Chem.* **2012**, 4945.

Conclusions

Conclusiones

Conclusions

In this Thesis, the chemistry of gold trifluoromethyl compounds has been explored and substantially expanded. The conclusions obtained along the dissertation are summarized at the end of each chapter. In the following lines, some general remarks and the most important conclusions are given.

a) Mixed gold(I) fluorohalide complexes $[F{-}Au{-}X]^-$ have been detected in the gas phase for the first time. They arise by CF_2 extrusion from the corresponding $[CF_3AuX]^-$ anions (X = Cl, Br, I) through an unconventional mechanism involving an uncommon fluoride-bridging $F_2C{-}F{-}[Au]$ unit as the transition state. These $[CF_3AuX]^-$ species can therefore be referred to as gold carbenoids.
b) Complexes $[PPh_4][CF_3AuX_3]$ can be prepared by oxidative addition of halogens, X_2, to the corresponding $[PPh_4][CF_3AuX]$ precursors (X = Cl, Br, I) and they are the first monoalkyl gold(III) trihalide derivatives prepared. In the gas phase, homolytic cleavage of the only Au−C bond in $[CF_3AuX_3]^-$ gives rise to gold(II) trihalide complexes $[AuX_3]^-$ (X = Cl, Br), which undergo subsequent dissociation of $X^\bullet$ involving one-electron reduction in the metal center.
c) The first example of an organogold(III) difluoride with *trans* stereochemistry, $[PPh_4][trans\text{-}(CF_3)_2AuF_2]$ has been prepared by reaction of $[PPh_4][CF_3AuCF_3]$ and XeF_2. Neither $[PPh_4][CF_3AuF]$ nor $[PPh_4][CF_3AuF_3]$ could be obtained, probably because of their extremely high reactivity. However, these complex anions were detected to arise in the unimolecular decomposition of $[trans\text{-}(CF_3)_2AuF_2]^-$ in the gas phase, together with the Au(II) species $[CF_3AuF_2]^-$. Similarly to the chloride and bromide homologues, anion $[CF_3AuF_3]^-$ gives rise to $[AuF_3]^-$ and $[AuF_2]^-$ in consecutive stages of the tandem mass experiment.
d) Au(III) and Ag(III) have similar covalent radii, at least in their most common square-planar geometry, as concluded from the comparison of the crystal structures of the isoleptic and isomorphous complexes $[PPh_4][trans\text{-}(CF_3)_2M(CN)_2]$ (M = Ag, Au).
e) Compound $[PPh_4][(CF_3)_3AuI]$ is obtained by photooxidative addition of CF_3I to $[PPh_4][CF_3AuCF_3]$ and offers a convenient entry to the $(CF_3)_3Au$ unit, the chemistry of which had remained virtually unexplored. Anionic derivatives, for which the non-fluorinated analogues are unknown, have been prepared therefrom, including the fluoride complex $[PPh_4][(CF_3)_3AuF]$. Perfluorinated

trimethyl gold, $(CF_3)_3Au{\cdot}OEt_2$, is substantially more stable than its non-fluorinated analogue. It arises as a suitable synthon of the unsaturated 14-electron species $(CF_3)_3Au$, as demonstrated by the preparation of a number of neutral complexes, $(CF_3)_3AuL$, with L covering a wide range of donor atoms and donor abilities.

f) The $(CF_3)_3Au$ fragment is probably the strongest R_3Au Lewis acid, being actually more acidic than $(C_6F_5)_3Au$ or $(C_6F_5)_3B$. In contrast to the $(CH_3)_3Au$ unit, the fluorinated T-shaped fragment is stereochemically stable and reluctant to undergo reductive elimination of CF_3–CF_3. Additionally, the stability of its derivatives is significantly higher than that of their non-fluorinated counterparts owing to the stronger $(CF_3)_3Au$–L interactions.

g) Decomposition pathways of the aforementioned anionic complexes are different in the gas phase, where only unimolecular processes take place, and in the condensed phase, where lower-energy intermolecular paths may easily occur.

At this point, some future research possibilities arise. First of all, the preparation of the organogold fluoride complexes $[CF_3AuF]^-$ and $[CF_3AuF_3]^-$ should be possible, but may require the use of specific material and more inert solvents, as well as inorganic cations with low acidity (e.g. Cs^+). Moreover, the reactivity of the prepared organogold fluorides should be more thoroughly investigated, as they might find applications in fluorination processes. Furthermore, new stereochemical patterns and bonding systems of gold trifluoromethyl complexes, including the use of more sophisticated ligands, could be the target so as to better understand the nature of these species and the Au–CF_3 bonds, both in the bulk and in the gas phase. This would also entail the study of reductive elimination processes involving the CF_3 group. Finally, due to the current interest in the participation of organogold(III) complexes in synthetic and catalytic processes, the $(CF_3)_3Au$ system may find interesting applications as a Lewis acid catalyst, merging the reactivity potential of organogold complexes with the acidity of $(C_6F_5)_3B$.

Conclusiones

Los resultados obtenidos en esta Tesis Doctoral han contribuido de forma significativa a la ampliación de la química de los trifluorometil complejos de oro. Al final de cada capítulo se incluyen las conclusiones propias del mismo. A continuación se recogen las conclusiones más importantes que se han obtenido a lo largo del trabajo.

a) Los fluorohalogenuros mixtos de oro(I) $[F{-}Au{-}X]^-$ se han detectado en fase gas por primera vez. Estos se generan por extrusión de CF_2 de los correspondientes aniones $[CF_3AuX]^-$ (X = Cl, Br, I) mediante un mecanismo poco convencional que transcurre a través de un estado de transición con una unidad que contiene un fluoruro puente, $F_2C{-}F{-}[Au]$. Por tanto, las especies $[CF_3AuX]^-$ pueden ser consideradas como carbenoides de oro.
b) Los complejos $[PPh_4][CF_3AuX_3]$ se obtienen por adición oxidante del halógeno, X_2, sobre el precursor correspondiente $[PPh_4][CF_3AuX]$ (X = Cl, Br, I), y son los primeros derivados triahalogenuro de oro(III) descritos con un solo grupo alquilo. En fase gas, la ruptura homolítica del único enlace Au−C en los complejos $[CF_3AuX_3]^-$ da lugar a los trihalogenuros de oro(II) $[AuX_3]^-$ (X = Cl, Br), que a su vez disocian $X^\bullet$, con la reducción del metal en un electrón.
c) Se ha preparado el primer difluoruro organometálico de oro(III) con estereoquímica *trans*, $[PPh_4][trans\text{-}(CF_3)_2AuF_2]$, por reacción entre $[PPh_4][CF_3AuCF_3]$ y XeF_2. Los complejos $[PPh_4][CF_3AuF]$ y $[PPh_4][CF_3AuF_3]$ no se han podido obtener, probablemente debido a su elevada reactividad. Sin embargo, estos aniones complejos se detectan en la descomposición unimolecular del anión $[trans\text{-}(CF_3)_2AuF_2]^-$ en fase gas, junto con la especie de Au(II) $[CF_3AuF_2]^-$. De manera similar a los homólogos de cloro y bromo, el anión $[CF_3AuF_3]^-$ da lugar a $[AuF_3]^-$ y $[AuF_2]^-$ en etapas posteriores de la espectrometría de masas en tándem.
d) Los centros de Au(III) y Ag(III) tienen radios covalentes similares, al menos en su geometría plano cuadrada, que es la más común. A esta conclusión se llega por comparación de las estructuras cristalinas de los complejos isolépticos e isomorfos $[PPh_4][trans\text{-}(CF_3)_2M(CN)_2]$ (M = Ag, Au).
e) El complejo $[PPh_4][(CF_3)_3AuI]$ se obtiene por fotoadición oxidante de CF_3I sobre el compuesto $[PPh_4][CF_3AuCF_3]$ y supone una vía de acceso apropiada a la unidad $(CF_3)_3Au$, cuya química era prácticamente desconocida. A partir de él,

se han preparado derivados aniónicos, cuyos análogos no fluorados se desconocen, y entre los que se incluye el fluoro complejo $[PPh_4][(CF_3)_3AuF]$. El trimetil oro perfluorado, $(CF_3)_3Au{\cdot}OEt_2$, es significativamente más estable que su análogo no fluorado. Este compuesto se presenta como un sintón de la especie insaturada de 14 electrones $(CF_3)_3Au$, como se ha demostrado mediante la preparación de diversos complejos neutros $(CF_3)_3AuL$, en que los ligandos L tienen distinta capacidad dadora y cubren un amplio rango de átomos dadores.

f) El fragmento $(CF_3)_3Au$ es probablemente el ácido de Lewis R_3Au conocido más fuerte, superando en acidez a especies como $(C_6F_5)_3Au$ o $(C_6F_5)_3B$. Dicha unidad presenta forma de T y, al contrario que el fragmento $(CH_3)_3Au$, es estereoquímicamente estable y muestra una baja tendencia a la eliminación reductora de CF_3–CF_3. Además, la estabilidad de sus derivados es significativamente superior a la de sus análogos no fluorados debido a que las interacciones $(CF_3)_3Au$–L son más fuertes.

g) Los complejos aniónicos preparados presentan vías de descomposición distintas en fase gas, donde únicamente tienen lugar procesos unimoleculares, y en fase condensada, donde pueden existir caminos intermoleculares de menor energía.

En este punto, surgen diversas posibilidades de investigación futuras. En primer lugar, la preparación de $[CF_3AuF]^-$ y $[CF_3AuF_3]^-$ debería ser posible, pero probablemente requieran el uso de material específico o de disolventes más inertes, así como de cationes inorgánicos poco ácidos (por ejemplo, Cs^+). Además, la reactividad de los fluoruros organometálicos de oro preparados se debería investigar en mayor profundidad, pues pueden resultar útiles en procesos de fluoración. Por otro lado, podrían estudiarse nuevos patrones estereoquímicos y sistemas de enlace de trifluorometil complejos de oro, que incluyan el uso de ligandos más sofisticados. De esta manera, se entendería mejor la naturaleza de estas especies y de los enlaces Au–CF_3, tanto en fase condensada como en fase gas. Esto implicaría el estudio de procesos de eliminación reductora en los que participara el grupo CF_3. Finalmente, dentro del interés actual en los complejos organometálicos de oro(III) por su implicación en procesos sintéticos y catalíticos, se podría estudiar el sistema $(CF_3)_3Au$, pues podría actuar como un catalizador ácido de Lewis con importantes aplicaciones, combinando la reactividad de los complejos organometálicos de oro con la acidez de la especie $(C_6F_5)_3B$.

Publications

ChemPubSoc Europe
DOI: 10.1002/chem.201605655
CHEMISTRY A European Journal
Communication

Gold Fluorides

Gold(I) Fluorohalides: Theory and Experiment

Miguel Baya,[a] Alberto Pérez-Bitrián,[a] Sonia Martínez-Salvador,[a] José M. Casas,[a] Babil Menjón,*[a] and Jesús Orduna[b]

Dedicated to Prof. Dr. Elena Lalinde on the occasion of her 60th birthday

Abstract: The anionic trifluoromethylgold(I) derivatives $[CF_3AuX]^-$, which have been prepared and isolated as their $[PPh_4]^+$ salts in good yield, undergo thermally induced difluorocarbene extrusion in the gas phase, giving rise to the mixed gold(I) fluorohalide complexes [F–Au–X]$^-$ (X = Cl, Br, I). These triatomic species have been detected by tandem mass spectrometry (MS2) experiments and their properties have been analyzed by DFT methods. The CF_2 extrusion mechanism from the Au–CF_3 moiety serves as a model for the CF_2 insertion into the Au–F bond, since both reactivity channels are connected by the microreversibility principle.

Gold halides are simple chemical species of great theoretical and practical importance.[1] The binary halides AuX, AuX_2, AuX_3, and AuF_5 exhibit quite different properties when associated in the condensed phase or as single molecules,[2] either in the gas phase or trapped in inert matrices.[3,4] Thus, genuine gold(II) chloride, $AuCl_2$, has only been detected in the gas phase,[5] whereas a solid with identical stoichiometry is, in fact, a mixed-valence species best formulated as $Au^{I}[Au^{III}Cl_4]$.[6] Moreover, the instability of gold(I) fluoride, AuF, in the condensed phase seems to derive from intermolecular processes leading to disproportionation into Au^0 and AuF_3 rather than from intrinsic thermodynamic reasons.[7,8]

On the whole and despite intensive research on the subject, gold fluorides still today remain challenging and rare species; especially those with the metal in low oxidation state.[9] A few ligand-supported gold(I) fluorides stabilized by neutral donors are currently known. Thus, the AuF moiety is known to form loose complexes with noble gases, FAuNg (Ng = Ne, Ar, Kr, Xe),[3,10] and much more robust complexes with NHC ligands that enable their isolation in the condensed phase: $[\{(NHC)Au\}_n(\mu\text{-}F)]^{(n-1)+}$ (n = 1 or 2; NHC = 1,3-bis(2,6-diisopropylphenyl)-4,5-dihydroimidazol-2-ylidene).[11] To the best of our knowledge, however, no anionic gold(I) fluoride derivative is currently known apart from the symmetric $[AuF_2]^-$ complex recently detected by Rijs and O'Hair in the sequential decomposition of $[Au(OAc^F)_2]^-$ in the gas phase ($OAc^F = CF_3CO_2$).[12]

Herein we report the experimental detection of the whole series of mixed gold(I) fluorohalides [F–Au–X]$^-$ (X = Cl, Br, I) in the gas phase, together with their optimized equilibrium structures and their calculated stabilities. The mechanism of CF_2 insertion into the Au–F bond to give a CF_3 group offers new insight into the relation and mutual transformation of these fundamental C_1 fluorocarbon units.

The trifluoromethylgold(I) derivatives $[PPh_4][CF_3AuX]$ (**1**–**3**) are obtained and isolated as pure substances by the procedure used to prepare the bromo derivative,[13] which involves replacing the highly labile CO ligand in the gold carbonyl derivative CF_3AuCO[14] with the corresponding halide (Scheme 1).[15]

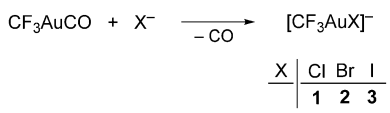

Scheme 1. Method to synthesize the organogold(I) derivatives **1**–**3** (see the Supporting Information for details). In all cases the cation is $[PPh_4]^+$.

Geometry optimizations of the mixed $[CF_3AuX]^-$ derivatives at the DFT/M06 level of calculation yield linear structures (Figure 1) with the geometric parameters given in Table 1. The optimized geometry of the $[CF_3AuBr]^-$ anion in the gas phase shows reasonable agreement with that experimentally established for compound **2** in the solid state (X-ray diffraction).[13] The Au–CF_3 distance shows little variation with the halide going from chlorine (206.1 pm) to iodine (208.8 pm), and the Au–X distances are just marginally longer than those calculated for the symmetric halides $[AuX_2]^-$ (Table 1; Supporting Information, Table S1). In the ^{19}F NMR spectra of compounds **1**–**3**, the signal corresponding to the CF_3 group suffers a steady downfield shift with increasing electronegativity of the halide ligand: I < Br < Cl (Supporting Information, Figure S1). This means that the F atoms are deshielded in the same order.

The mononuclear organogold(I) halides **1**–**3** are thermally stable compounds. To the best of our knowledge, no related

[a] Dr. M. Baya, A. Pérez-Bitrián, Dr. S. Martínez-Salvador, Dr. J. M. Casas, Dr. B. Menjón
Instituto de Síntesis Química y Catálisis Homogénea (iSQCH)
CSIC-Universidad de Zaragoza
C/ Pedro Cerbuna 12, 50009 Zaragoza (Spain)
E-mail: menjon@unizar.es

[b] Dr. J. Orduna
Instituto de Ciencia de Materiales de Aragón (ICMA)
CSIC-Universidad de Zaragoza
C/ Pedro Cerbuna 12, 50009 Zaragoza (Spain)

Supporting information and the ORCID identification number(s) for the author(s) of this article can be found under: http://dx.doi.org/10.1002/chem.201605655.

$[CH_3AuX]^-$ species have been obtained yet in the condensed phase, and only recently has the heavier $[CH_3AuI]^-$ derivative been detected to arise by oxidative addition of I–CH_3 to the bare Au^- anion in the gas phase.[16] A related organocopper(I) derivative, $[CF_3CuI]^-$, was proposed as a key intermediate in Cu-assisted arene trifluoromethylation processes, but it was not detected.[17] Compounds **1**–**3** show reasonable stability towards ligand scrambling that might otherwise lead to the symmetric species $[CF_3AuCF_3]^-$ and $[AuX_2]^-$. In fact, no such rearrangement was experimentally observed to occur in solution at room temperature.[18] Moreover, given their anionic nature, compounds **1**–**3** are ideal species for mass-spectrometry studies, which should provide valuable information on fundamental processes taking place at the unimolecular level.[19]

Negatively charged $[CF_3AuX]^-$ complexes are efficiently transferred to the gas-phase by electrospray ionization (ESI) techniques starting from room-temperature CH_2Cl_2/MeOH solutions of the pure compounds **1**–**3**. Their standard MS show no sign of ligand scrambling. Upon collision-induced activation of mass-selected $[CF_3AuX]^-$ ions, the mixed $[F–Au–X]^-$ ions are formed and clearly detected in all three cases (Figure 2, Scheme 2). These experimental conditions preclude side-reactions, such as ligand scrambling and/or disproportionation that might hinder the preparation of the $[F–Au–X]^-$ species in the condensed phase. Halide dissociation (Scheme 2 b) is a competing process that is also observed to occur in all cases (Supporting Information, Figures S2–S4). Calculated Au–X bond dissociated energies [kcal mol^{-1}] in the $[CF_3AuX]^-$ complexes are as follows: 68.9 (Cl) > 65.7 (Br) > 63.7 (I).

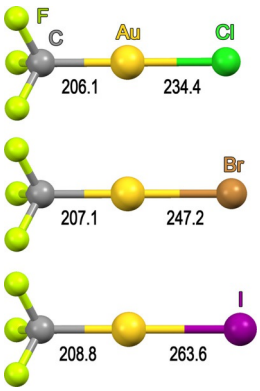

Figure 1. Geometries of the anionic $[CF_3AuX]^-$ derivatives optimized at the DFT/M06 level with relevant structural parameters indicated (see Table 1).

Table 1. Interatomic distances [pm] in the equilibrium structures obtained for the linear $[CF_3AuX]^-$ and $[FAuX]^-$ anions at the DFT/M06 level of calculation.[a]

	$[CF_3AuX]^-$		$[FAuX]^-$		$[AuX_2]^-$	AuX[b]
X	Au–C[c]	Au–X	Au–F[d]	Au–X	Au–X	Au–X
Cl	206.1	234.4	201.3	229.7	231.8	222.6
Br	207.1[e]	247.2[e]	201.9	242.1	244.7	233.9
I	208.8	263.6	202.9	257.3	261.7	250.6

[a] Data corresponding to symmetric $[AuX_2]^-$ anions and diatomic AuX molecules are also included for comparison. All the triatomic species are exactly linear, as are the $[CF_3AuX]^-$ anions. [b] Values taken from Ref. [21]. [c] Similar Au–C distances were found in the crystal structures of the homoleptic salts $[N(PPh_3)_2][Au(CF_3)_2]$ (206.5(6) pm)[36] and $[PPh_4][Au(CF_3)_2]$ (203.3(2) pm).[14a] [d] In the free diatomic AuF molecule, Au–F = 191.84 pm.[8] [e] Experimental interatomic distances in the crystal of $[PPh_4][CF_3AuBr]$ are as follows: Au–C 211.9(5) pm and Au–Br 240.5(1) pm.[13]

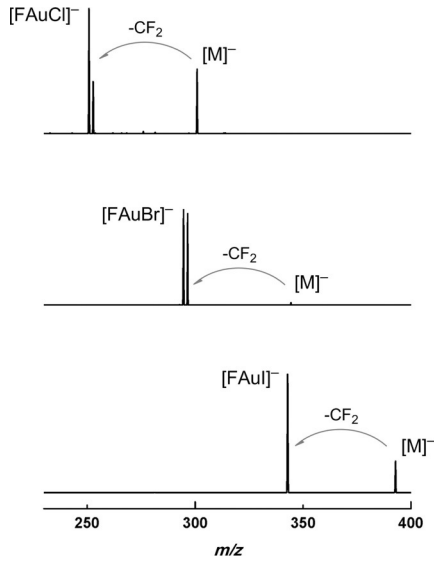

Figure 2. Detection of the mixed $[FAuX]^-$ anions (X = Cl, Br, I) formed by collision-induced dissociation of the corresponding $[CF_3AuX]^-$ species (labeled $[M]^-$) in quadrupole ion-trap MS^2 experiments.

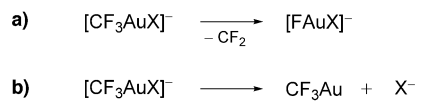

Scheme 2. Competing dissociation processes undergone by the $[CF_3AuX]^-$ anions in the gas phase.

Geometry optimizations of the triatomic $[F–Au–X]^-$ anions were performed to find out their structural arrangement and the results were characterized vibrationally (see the Supporting Information for details). All three anions show a linear structure with $C_{\infty v}$ symmetry (Figure 3) and the interatomic distances given in Table 1. Taking the neutral diatomic AuF molecule as a reference (Au–F 191.84 pm),[8] the coordination of an additional X^- ligand results in elongation of the Au–F bond by ca. 10 pm,[20] thus becoming comparable to the bond length observed in the neutral FAu(NHC) complex (Au–F 202.8(8) pm).[11b] In the same way, the Au–X bond is elongated by a similar amount with respect to the diatomic AuX molecules[21] upon F^- coordination. Addition of F^- to the heavier gold halides, AuX, was precisely the method originally suggested by Schwerdtfeger to prepare the mixed $[F–Au–X]^-$ derivatives.[22] However, we are not aware that this method has yielded any positive results so far.

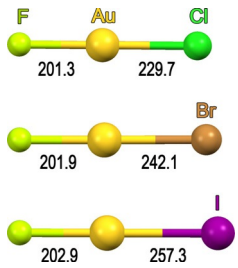

Figure 3. Geometries of the mixed $[FAuX]^-$ anions optimized at the DFT/M06 level with relevant structural parameters indicated (see Table 1).

In the absence of external acids,[23] decomposition of trifluoromethyl metal derivatives is commonly assumed to follow the tautomeric equilibrium shown in Scheme 3 a as identified by

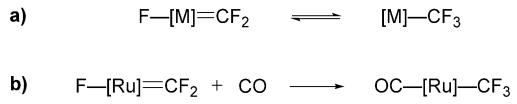

Scheme 3. Tautomeric equilibrium applying to trifluoromethyl metal derivatives: a) in general, and b) evidenced in ruthenium(II) systems; [Ru] = $(R_3P)RuH(CO)$ and PR_3 = P*i*Pr_3, PMe*t*Bu_2.[24]

Caulton in organoruthenium systems (Scheme 3 b).[24] This mechanism was also suggested to apply to the decomposition of $[CF_3MR]^-$ ions in the gas phase (M = Cu, Ag, Au; R = F, CF_3, OAc^F).[12] With regard to our own system, this mechanism is commented on in detail in the Supporting Information.

We have now found a lower-energy path for the $[CF_3AuX]^-$ decomposition that differs from the standard mechanism as no difluorocarbene metal intermediate $[M]CF_2$ is involved. This alternative mechanism (Figure 4) comprises the following

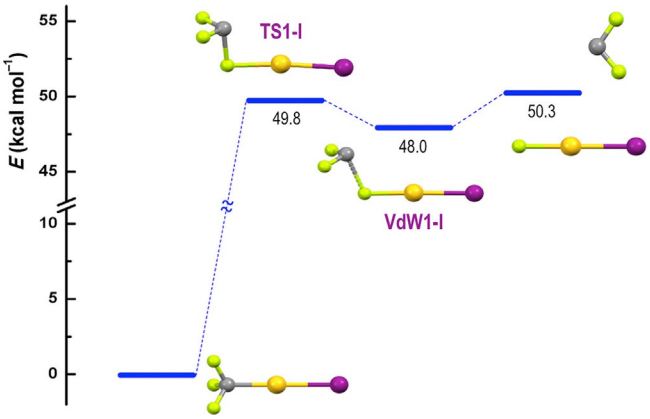

Figure 4. Energy profile of the lower-energy CF_2 extrusion path from the organogold $[CF_3Aul]^-$ derivative (see the Supporting Information, Figures S7 and S8 for structural details of the intermediates involved). The same but reverse profile applies to the CF_2 insertion into the Au–F bond. For color code, see Figure 1.

steps: 1) weakening of the Au–C bond in favor of a Au–F bond through a transient η^2-coordinated F_2C–F unit (Scheme 4 a); 2) complete loss of the Au–C interaction in the transition state (**TS1**), which features an uncommon fluoride-bridging F_2C–F–[Au] unit (Scheme 4 b); and 3) release of the unsaturated :CF_2 unit from the ensuing van der Waals complex (**VdW1**) that leaves the triatomic $[F–Au–X]^-$ species. The last step involves just a small dissociation threshold of < 3 kcal mol^{-1}.

Owing to the microreversibility principle, the mechanism just discussed also applies to the :CF_2 insertion into the Au–F bond. Thus, the interaction of free :CF_2 with the electron density of the F ligand results in slight stabilization and entails little structural modification in any of the moieties involved. This interaction confirms the inherently ambiphilic character of the singlet fluorinated divalent carbon atom that bears both a lone pair and an empty p orbital, the latter being involved in partial F(p)→C(p) π-donation.[25–29] The strengthening of this

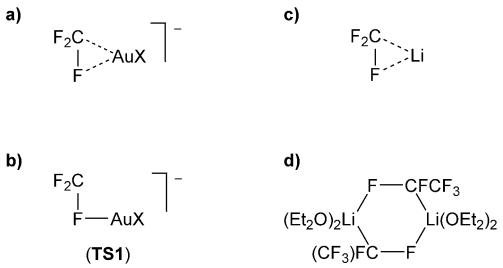

Scheme 4. Structural patterns involving C–F···M interactions: a) transient species formed upon thermal excitation of $[CF_3AuX]^-$; b) transition state in the CF_2 extrusion/insertion path given in Figure 4 (see the Supporting Information, Figure S7 for structural details); c) global minimum calculated for $LiCF_3$ in the gas phase;[33a] d) central core of the $Li(CF_2CF_3)\cdot 2\,Et_2O$ dimer in the crystal.[32].

F_2C···F–[Au] interaction in the initial van der Waals complex leads to significant elongation of the Au–F bond, which, in the transition state (Au–F ca. 215 pm; Scheme 4 b), is substantially longer than in the fluoride-bridged dinuclear complex $[\{(NHC)Au\}_2(\mu\text{-}F)][BF_4]$ (Au–F 206.0(1) pm).[11a] The metallotropic shift from F to C through a transient Au(η^2-F–CF_2) species (Scheme 4 a) leads to the final insertion product $[CF_3AuX]^-$. Along the reaction path, the carbon atom gradually increases the number of substituents from two in the initial carbene to three in the transition state and four in the final product. The global insertion process takes place in an almost barrierless way and results in large stabilization, so it might be experimentally feasible.[30]

It is worth noting that the structures of both the transition state and the transient species referred to in the mechanism just discussed find support in the chemistry of lithium carbenoids.[31] Thus, the bridging role of the F–C unit was substantiated in the crystal structure of the $Li(CF_2CF_3)\cdot 2\,Et_2O$ dimer (Scheme 4 d),[32] while a Li(η^2-F–CF_2) interaction was found to be the global minimum for $LiCF_3$ in the gas phase (Scheme 4 c).[33] Both perfluoroalkyl lithium systems are known to release the corresponding fluorinated carbene upon LiF elimination in a sometimes violent process.[34] Considering that our gold systems also release CF_2 without the need of any actual metal carbene intermediate, they can properly be termed gold carbenoids.[35]

In summary, the anionic organogold(I) $[CF_3AuX]^-$ complexes (X = Cl, Br, I) are found to perform as gold carbenoids, since they undergo CF_2 extrusion in the gas phase affording the mixed gold(I) fluorohalide $[F–Au–X]^-$ complexes. The experimental detection of these simple, triatomic species demonstrates that AuF can indeed be stabilized by heavier-halide coordination, as formerly suggested by Schwerdtfeger.[22] These species might, however, be difficult to isolate in the condensed phase unless facile ligand scrambling is precluded. An unconventional CF_2 insertion/extrusion mechanism not involving any metal carbene intermediate has been identified, which might be relevant to difluoromethylation processes mediated by late transition metals.

Acknowledgements

This work was supported by the Spanish MINECO/FEDER (Project CTQ2015-67461-P), and the Gobierno de Aragón and Fondo Social Europeo (Grupo Consolidado E21: Química Inorgánica y de los Compuestos Organometálicos). The Instituto de Biocomputación y Física de Sistemas Complejos (BIFI) and the Centro de Supercomputación de Galicia (CESGA) are greatfully acknowledged for generous allocation of computational resources. A.P.B. thanks the Spanish Ministerio de Educación, Cultura y Deporte for a grant (FPU15/03940).

Keywords: difluorocarbene · gold carbenoids · gold fluorides · organogold compounds · trifluoromethyl compounds

[1] H. Raubenheimer, S. Cronje, in *Gold: Progress in Chemistry, Biochemistry and Technology* (Ed.: H. Schmidbaur), John Wiley & Sons, Chichester (UK), **1999**, Ch. 16, pp. 557–632.
[2] M. Hargittai, *Acc. Chem. Res.* **2009**, *42*, 453; A. Schulz, M. Hargittai, *Chem. Eur. J.* **2001**, *7*, 3657; M. Hargittai, *Chem. Rev.* **2000**, *100*, 2233.
[3] a) X. Wang, L. Andrews, F. Brosi, S. Riedel, *Chem. Eur. J.* **2013**, *19*, 1397; b) X. Wang, L. Andrews, K. Willmann, F. Brosi, S. Riedel, *Angew. Chem. Int. Ed.* **2012**, *51*, 10628; *Angew. Chem.* **2012**, *124*, 10780.
[4] a) I. J. Blackmore, A. J. Bridgeman, N. Harris, M. A. Holdaway, J. F. Rooms, E. L. Thompson, N. A. Young, *Angew. Chem. Int. Ed.* **2005**, *44*, 6746; *Angew. Chem.* **2005**, *117*, 6904; b) B. Réffy, M. Kolonits, A. Schulz, T. M. Klapötke, M. Hargittai, *J. Am. Chem. Soc.* **2000**, *122*, 3127.
[5] D. Schröder, R. Brown, P. Schwerdtfeger, X.-B. Wang, X. Yang, L.-S. Wang, H. Schwarz, *Angew. Chem. Int. Ed.* **2003**, *42*, 311; *Angew. Chem.* **2003**, *115*, 323.
[6] D. B. dell'Amico, F. Calderazzo, F. Marchetti, S. Merlino, *J. Chem. Soc. Dalton Trans.* **1982**, 2257.
[7] a) P. Schwerdtfeger, J. S. McFeaters, M. J. Liddell, J. Hrušák, H. Schwarz, *J. Chem. Phys.* **1995**, *103*, 245; b) D. Schröder, J. Hrušák, I. C. Tornieporth-Oetting, T. M. Klapötke, H. Schwarz, *Angew. Chem. Int. Ed. Engl.* **1994**, *33*, 212; *Angew. Chem.* **1994**, *106*, 223.
[8] a) T. Okabayashi, Y. Nakaoka, E. Yamazaki, M. Tanimoto, *Chem. Phys. Lett.* **2002**, *366*, 406; b) C. J. Evans, M. C. L. Gerry, *J. Am. Chem. Soc.* **2000**, *122*, 1560.
[9] a) F. Mohr, *Gold Bull.* **2004**, *37*, 164; b) N. Bartlett, *Gold Bull.* **1998**, *31*, 22; c) B. G. Müller, *Angew. Chem. Int. Ed. Engl.* **1987**, *26*, 1081; *Angew. Chem.* **1987**, *99*, 1120.
[10] a) S. A. Cooke, M. C. L. Gerry, *J. Am. Chem. Soc.* **2004**, *126*, 17000; b) J. M. Thomas, N. R. Walker, S. A. Cooke, M. C. L. Gerry, *J. Am. Chem. Soc.* **2004**, *126*, 1235; c) C. J. Evans, D. S. Rubinoff, M. C. L. Gerry, *Phys. Chem. Chem. Phys.* **2000**, *2*, 3943.
[11] a) C. M. Wyss, B. K. Tate, J. Bacsa, M. Wieliczko, J. P. Sadighi, *Polyhedron* **2014**, *84*, 87; b) D. S. Laitar, P. Müller, T. G. Gray, J. P. Sadighi, *Organometallics* **2005**, *24*, 4503.
[12] N. J. Rijs, R. A. J. O'Hair, *Dalton Trans.* **2012**, *41*, 3395.
[13] S. Martínez-Salvador, L. R. Falvello, A. Martín, B. Menjón, *Chem. Sci.* **2015**, *6*, 5506.
[14] a) S. Martínez-Salvador, L. R. Falvello, A. Martín, B. Menjón, *Chem. Eur. J.* **2013**, *19*, 14540; b) S. Martínez-Salvador, J. Forniés, A. Martín, B. Menjón, *Angew. Chem. Int. Ed.* **2011**, *50*, 6571; *Angew. Chem.* **2011**, *123*, 6701.
[15] Our attempts to prepare the fluoro derivative $[CF_3AuF]^-$ in the condensed phase failed thus far. This organogold fluoride complex, however, was formed in the gas phase by collision-induced fragmentation of the homoleptic $[CF_3AuCF_3]^-$ anion (see Ref. [12]).
[16] S. Muramatsu, K. Koyasu, T. Tsukuda, *J. Phys. Chem. A* **2016**, *120*, 957.
[17] G. E. Carr, R. D. Chambers, T. F. Holmes, D. G. Parker, *J. Chem. Soc. Perkin Trans. 1* **1988**, 921.
[18] The peaks corresponding to the symmetric species $[CF_3AuCF_3]^-$ and $[AuX_2]^-$ were absent in the mass spectra (ESI) of the mixed $[CF_3AuX]^-$ derivatives.
[19] a) R. A. J. O'Hair, in *The Chemistry of Organogold Compounds, Vol. 1* (Eds.: Z. Rappoport, I. Marek, J. F. Liebman), *Patai's Chemistry of Functional Groups*, John Wiley & Sons, Chichester, UK, **2014**, Ch. 9, pp. 391–408; b) J. Roithová, D. Schröder, *Coord. Chem. Rev.* **2009**, *253*, 666.
[20] Coordination of a noble gas to the AuF molecule causes, in turn, no significant variation in the Au–F distance (see Refs. [3, 10]).
[21] J. R. Brown, P. Schwerdtfeger, D. Schröder, H. Schwarz, *J. Am. Soc. Mass Spectrom.* **2002**, *13*, 485.
[22] P. Schwerdtfeger, P. D. W. Boyd, A. K. Burrell, W. T. Robinson, M. J. Taylor, *Inorg. Chem.* **1990**, *29*, 3593.
[23] The action of external acids on trifluoromethyl metal derivatives, $[M]CF_3$, is known to promote α-fluoride abstraction yielding difluorocarbene metal species, $[M]CF_2$, with various degrees of stability: a) M. A. García-Monforte, S. Martínez-Salvador, B. Menjón, *Eur. J. Inorg. Chem.* **2012**, 4945; b) R. P. Hughes, *Eur. J. Inorg. Chem.* **2009**, 4591; c) P. J. Brothers, W. R. Roper, *Chem. Rev.* **1988**, *88*, 1293.
[24] a) D. Huang, P. R. Koren, K. Folting, E. R. Davidson, K. G. Caulton, *J. Am. Chem. Soc.* **2000**, *122*, 8916; b) D. Huang, K. G. Caulton, *J. Am. Chem. Soc.* **1997**, *119*, 3185.
[25] The relatively strong Lewis acidity of singlet CF_2 is clearly evidenced by its computed fluoride ion affinity (FIA) in the gas phase: −46.0 kcal mol^{-1} (see Ref. [26]). This value is in excellent agreement with the recently evaluated adiabatic gas-phase bond dissociation enthalpy of the $(CF_3)^-$ anion into singlet CF_2 and F^- at 298 K: 46.7 kcal mol^{-1} (see Ref. [27]). Further evidence of the acidic character of CF_2 is shown by its electrophilic behavior towards alkenes in cycloaddition processes (see Ref. [28]) as well as by its ability to form ylides $^-CF_2–B^+$ with neutral monodentate Lewis bases (B; see Ref. [29]).
[26] D. A. Dixon, D. Feller, G. Sandrone, *J. Phys. Chem. A* **1999**, *103*, 4744.
[27] G. K. S. Prakash, F. Wang, Z. Zhang, R. Haiges, M. Rahm, K. O. Christe, T. Mathew, G. A. Olah, *Angew. Chem. Int. Ed.* **2014**, *53*, 11575; *Angew. Chem.* **2014**, *126*, 11759.
[28] a) P. Pérez, *J. Phys. Chem. A* **2003**, *107*, 522; b) R. A. Moss, in *Carbene Chemistry: From Fleeting Intermediates to Powerful Reagents* (Ed.: G. Bertrand), Marcel Dekker, New York, **2002**, Ch. 3, pp. 57–101.
[29] a) J. Zheng, J.-H. Lin, J. Cai, J.-C. Xiao, *Chem. Eur. J.* **2013**, *19*, 15261; b) R. A. Moss, L. Wang, K. Krogh-Jespersen, *J. Am. Chem. Soc.* **2009**, *131*, 2128; c) D. J. Burton, Z.-Y. Yang, W. Qiu, *Chem. Rev.* **1996**, *96*, 1641.
[30] Precedents for CH_2 insertion into Au–Cl bonds are already known: A. N. Nesmeyanov, É. G. Perevalova, E. I. Smyslova, V. P. Dyadchenko, K. I. Grandberg, *Izv. Akad. Nauk SSSR Ser. Khim.* **1977**, *2610*; *Bull. Acad. Sci. USSR Div. Chem. Sci. (Engl. Transl.)* **1977**, *26*, 2417.
[31] a) V. H. Gessner, *Chem. Commun.* **2016**, *52*, 12011; b) V. Capriati, in *Contemporary Carbene Chemistry* (Eds.: R. A. Moss, M. P. Doyle), John Wiley & Sons, Hoboken, **2014**, Ch. 11, pp. 325–362; c) V. Capriati, S. Florio, *Chem. Eur. J.* **2010**, *16*, 4152.
[32] B. Waerder, S. Steinhauer, B. Neumann, H.-G. Stammler, A. Mix, Y. V. Vishnevskiy, B. Hoge, N. W. Mitzel, *Angew. Chem. Int. Ed.* **2014**, *53*, 11640; *Angew. Chem.* **2014**, *126*, 11824.
[33] a) J. Kvíčala, J. Štambaský, S. Böhm, O. Paleta, *J. Fluorine Chem.* **2002**, *113*, 147; b) a similar structural pattern was found for the potassium salt KCF_3 in a modeled THF solvation environment (see Ref. [27]).
[34] a) R. D. Chambers, *Fluorine in Organic Chemistry*, 2nd ed., Blackwell Publishing Ltd, Oxford (UK), **2004**, Ch. 6, pp. 137–161; b) D. M. Roddick, *Chem. Eng. News* **1997**, *75*(40), 6.
[35] Y. Wang, M. E. Muratore, A. M. Echavarren, *Chem. Eur. J.* **2015**, *21*, 7332.
[36] D. Zopes, S. Kremer, H. Scherer, L. Belkoura, I. Pantenburg, W. Tyrra, S. Mathur, *Eur. J. Inorg. Chem.* **2011**, 273.

Manuscript received: December 3, 2016
Accepted Article published: December 9, 2016
Final Article published: January 12, 2017

ChemPubSoc Europe
DOI: 10.1002/chem.201705509
CHEMISTRY A European Journal
Communication

Gold Complexes |Hot Paper|

Gold(II) Trihalide Complexes from Organogold(III) Precursors

Miguel Baya,[a] Alberto Pérez-Bitrián,[a] Sonia Martínez-Salvador,[a] Antonio Martín,[a] José M. Casas,[a] Babil Menjón,*[a] and Jesús Orduna[b]

Dedicated to Dr. Cristina Bohanna on the occasion of her 50th birthday

Abstract: The mononuclear gold(II) halide complexes $[AuCl_3]^-$ and $[AuBr_3]^-$ are formed in the gas phase by collision-induced homolytic splitting of the only Au–C bond in the monoalkylgold(III) precursors $[CF_3AuX_3]^-$. The geometries of the whole series of $[AuX_3]^-$ complexes (X = F, Cl, Br, I) have been calculated by DFT methods. It has also been found that the neutral AuX_2 molecules behave as unsaturated species, showing significant affinity for an additional X^- ligand. Moreover, in the open-shell $[AuX_3]^-$ anions, homolytic splitting of one of the Au–X bonds and formation of the lower-valent $[AuX_2]^-$ anions is favored over non-reducing halide dissociation. They should therefore be prone to disproportionation.

Since the indirect detection of triatomic AuX_2 halides in the gas phase (X = Cl, Br),[1] there has been increasing interest in the study of mononuclear gold(II) halides and pseudohalides.[2,3] These open-shell d^9 derivatives, however, are elusive in the condensed phase,[4–7] and their detection has been possible thanks to unimolecular techniques either in matrices or in the gas phase.[3,8] Little is known, however, about their chemical behavior.[9] Herein we report on the unexpected formation of the mononuclear $[AuCl_3]^-$ and $[AuBr_3]^-$ anions by homolytic splitting of the only Au–C bond in the monoalkyl gold(III) precursors $[CF_3AuX_3]^-$ (X = Cl, Br) in the gas phase. This experimental detection prompted us to evaluate the affinity of the neutral AuX_2 halides for an additional X^- ligand to afford the $[AuX_3]^-$ anions (ligand association) as well as the relationship of the latter singly charged species with their oxidized neutral AuX_3 counterparts (redox processes).

The monoalkyl gold(III) derivatives $[PPh_4][CF_3AuX_3]$ (X = Cl, Br, I) have been prepared by X_2 addition to the corresponding organogold(I) precursor $[PPh_4][CF_3AuX]$ (Scheme 1). They have been isolated as stable solids in good yields. The coordination environment of the gold center changes from linear to square-planar upon oxidation (Figure 1).[10] In the ^{19}F NMR spectra of the oxidized species **2**, the CF_3 signals show steady upfield shifts with the increasing electronegativity of the halogen (Figure S1 in the Supporting Information). This trend is opposite to that observed in the corresponding gold(I) precursors **1**.[11] It is worth noting that the anion of **2a** as well as the fluoro-complex $[CF_3AuF_3]^-$ had been previously detected in solution,[12] but not isolated.[13]

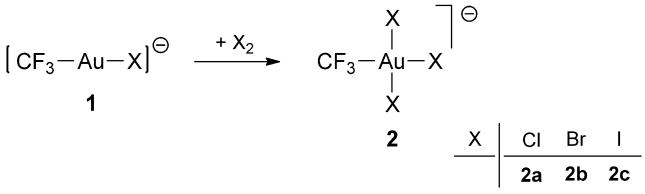

Scheme 1. Synthesis of the anionic monoalkylgold(III) derivatives **2**. In all cases the cation is $[PPh_4]^+$.

In contrast to the well-established chemistry of arylgold(II) derivatives with a single Au–C bond,[14] monoalkylgold(III) complexes are still rare.[15] In fact, no alkyl $[RAuX_3]^-$ species appear to have been isolated.

Aiming to gain insight into the fundamental properties of our monoalkylgold(III) complexes **2**, the unimolecular decomposition of the $[CF_3AuX_3]^-$ anions was studied in the gas phase by tandem mass spectrometry (MS^2; Figures S4–S8).[16] The iodo-derivative $[CF_3AuI_3]^-$ cleanly undergoes iodine elimination regenerating the parent species $[CF_3AuI]^-$ in the reverse process of that given in Scheme 1.[17] All the decomposition paths undergone by the lighter species $[CF_3AuCl_3]^-$ and $[CF_3AuBr_3]^-$ also involve reduction (Scheme 2). Thus, elimination of CF_3X or X_2 results in two-electron reduction (reductive elimination). Quite unex-

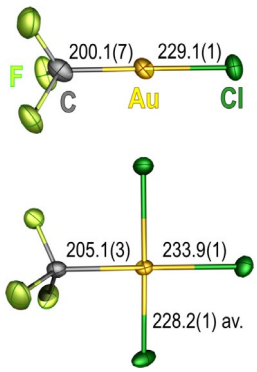

Figure 1. Displacement-ellipsoid diagrams (50% probability) of the $[CF_3AuCl]^-$ and $[CF_3AuCl_3]^-$ anions as found in single crystals of **1a** (top) and **2a** (bottom). Selected bond lengths [pm] and atom labeling as indicated.

[a] Dr. M. Baya, A. Pérez-Bitrián, Dr. S. Martínez-Salvador, Dr. A. Martín, Prof. Dr. J. M. Casas, Dr. B. Menjón
Instituto de Síntesis Química y Catálisis Homogénea (iSQCH)
CSIC-Universidad de Zaragoza
C/ Pedro Cerbuna 12, 50009 Zaragoza (Spain)
E-mail: menjon@unizar.es

[b] Dr. J. Orduna
Instituto de Ciencia de Materiales de Aragón (ICMA)
CSIC-Universidad de Zaragoza
C/ Pedro Cerbuna 12, 50009 Zaragoza (Spain)

Supporting information and the ORCID identification number(s) for the author(s) of this article can be found under https://doi.org/10.1002/chem.201705509.

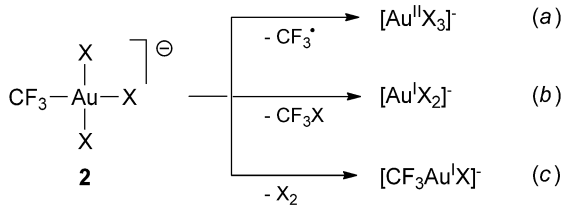

Scheme 2. General fragmentation paths observed for the monoalkylgold(III) derivatives **2** in the gas phase (Figures S4–S8). They involve metal reduction by one (path *a*) or two units (paths *b* and *c*). Path *b* is common to all three halogens (X = Cl, Br, I), whereas halogen dissociation (path *c*) is not observed for **2a** (X = Cl) and the radical path (*a*) is not observed for **2c** (X = I).

pectedly, however, a one-electron reduction is also detected, which involves the homolytic cleavage of the Au–CF_3 bond and formation of the $[AuX_3]^-$ anion. Such three-coordinate gold(II) species had been suggested to be involved in the chemical, photochemical or radiolytic reduction of the square-planar $[AuX_4]^-$ complexes.[18] Recently, the $[AuCl_3]^-$ anion was observed to arise by fragmentation of $[AuCl_4]^-$ in a photochemically excited state.[19] By performing MS^3 experiments (a further step of tandem mass spectrometry), we have additionally found that collision-induced dissociation of the $[AuX_3]^-$ species (X = Cl, Br) proceeds under homolytic splitting of a Au–X bond and formation of the gold(I) linear derivatives $[AuX_2]^-$ (Figures S9 and S10). No halide dissociation was observed in any of the fragmentation processes discussed.

Homolytic cleavage of M–C bonds is a fundamental process widely found in main-group organoelement chemistry,[20] but much less common in organotransition-metal compounds.[21] The Au–C homolysis observed in our trifluoromethyl compounds **2** seems to be a distinct feature of these monoalkylgold(III) complexes.[22] The calculated Au–C bond enthalpies are shown in Table 1.

Table 1. Parameters calculated for the mononuclear $[AuX_3]^-$ species.[a]

Parameter	X = F	X = Cl	X = Br	X = I
$[X_3Au–CF_3]^-$ bond enthalpy [kJ mol^{-1}]	278	208	183	155
X^- dissociation enthalpy [kJ mol^{-1}][b]	290	219	201	179
$X^•$ dissociation enthalpy [kJ mol^{-1}][c]	166	120	90	81
vertical detachment energy [eV][d]	5.19	4.90	4.71	4.26
adiabatic detachment energy [eV][e]	4.64	4.56	4.41	3.82
spin density on Au [%][f]	62	42	31	21
spin density on stem X [%][f]	26	37	46	52

[a] All the indicated properties and processes involve T-shaped minima (Figure 2) and have been calculated in the gas phase. [b] Heterolytic Au–X bond dissociation enthalpy as indicated in Scheme 3 (left). [c] Homolytic Au–X bond dissociation enthalpy as indicated in Scheme 3 (right). [d] The oxidized species is in an excited state. [e] The oxidized species is in the ground state. [f] Based on Mulliken charges and populations; the unassigned spin density is located symmetrically on the X ligands at the crosspiece (see Figure S15).

We have optimized the geometries of the whole series of $[AuX_3]^-$ anions[23] and have found that the T-shaped correspond with energy minima in all cases (Figure 2). On the other hand, Y-shaped structures are identified as transition states

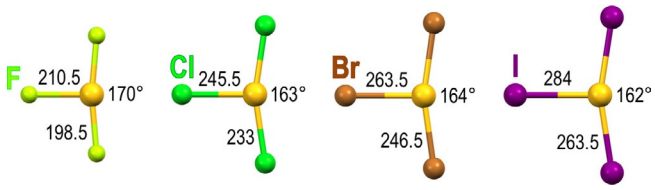

Figure 2. T-shaped polytopes for the $[AuX_3]^-$ anions optimized at the DFT/M06 level and identified as minima in the potential energy surface. Selected bond lengths [pm] and angles [°] are indicated together with atom labeling.

(Figure S16). Trigonal planar or pyramidal polytopes are not stationary points in any of these systems. The T-shaped structures of these open-shell, anionic $[AuX_3]^-$ species (d^9) show noticeable differences with those of the monomeric, diamagnetic AuX_3 molecules (d^8), which had been thoroughly studied by theoretical and experimental methods.[3,24,25] First, they are energy minima for all halide ligands, including iodide (Figure 2), whereas in the neutral case, monomeric AuI_3 is better described as a side-on iodine adduct of gold(I) iodide: $IAu(I_2)$.[25,26] The Au–X distances within each T-shaped neutral AuX_3 molecule are all virtually identical (Figure S14).[25a] In the $[AuX_3]^-$ anions, however, the Au–X distance in the stem of the T is consistently longer by about 15 pm than those found in the crosspiece (Figure 2). This difference can be ascribed to the fact that the spin density in the open-shell complexes is located mainly in the stem axis (Figure 3). It is worth noting that

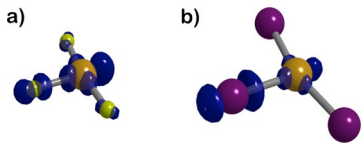

Figure 3. Spin density contour of a) the lightest $[AuF_3]^-$ and b) the heaviest $[AuI_3]^-$ anions according to the values given in Table 1. The full set is provided in Figure S15.

the spin density gradually shifts along this axis from the metal to the X ligand upon going down the halogen group (Table 1). The relationship between the mononuclear, T-shaped $[AuX_3]^-$ and AuX_3 species is given by the vertical electron-detachment energy of the former or the electron affinity of the later (Scheme 3). The large values calculated (Table 1) qualify even the heaviest T-shaped AuX_3 species as superhalogens.[27]

We have found that the neutral AuX_2 molecules behave as typical unsaturated species. Thus, the coordination of an additional X^- ligand (Scheme 3, left) is clearly exergonic in all cases

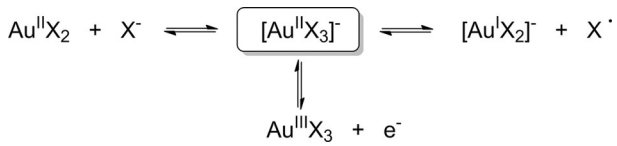

Scheme 3. Processes connecting the anionic gold(II) $[AuX_3]^-$ complexes with relevant neighbor species.

(Table 1) with enthalpy values between −179 (X = I) and −290 (X = F) kJ mol^{-1} in the gas phase, which denotes significant ligand affinity. The least endergonic fragmentation process of these $[AuX_3]^-$ anions, however, does not involve dissociation of a X^- ligand (reverse process), but rather homolytic cleavage of a Au–X bond with release of a halogen atom $X^\bullet$ and formation of the linear $[AuX_2]^-$ anions (Scheme 3, right). This lower-energy decomposition channel (Table 1) has been actually established to operate on the $[AuCl_3]^-$ and $[AuBr_3]^-$ anions by MS^3 experiments (Figures S9 and S10) as indicated above. The ability of Au^{III} to oxidize X^- ligands into $X^\bullet$ atoms indicates a marked tendency of the species under study to undergo disproportionation.[28]

In brief, the gold(II) halide complexes $[AuX_3]^-$ (X = Cl, Br) arise from the organogold(III) precursors $[CF_3AuX_3]^-$ by Au–C homolytic cleavage in the gas phase. The neutral AuX_2 molecules attain substantial stabilization by halide coordination. The $[AuX_3]^-$ anions thereby formed show T-shaped structures as energy minima for all halides. Dissociation of $X^\bullet$ atoms from these anions with one-electron metal reduction is energetically favored over halide dissociation even at the unimolecular level. This radical process underlies the tendency of simple gold(II) species to undergo dismutation. The $[AuX_3]^-$ anions (d^9) build the open-shell bridge between the diamagnetic neighbors, $[PtX_3]^-$ (d^8)[29] and $[HgX_3]^-$ (d^{10}),[30] of the relativistic triad.

Acknowledgements

This work was supported by the Spanish MINECO/FEDER (Project CTQ2015-67461-P) and the Gobierno de Aragón and Fondo Social Europeo (Grupo Consolidado E21: *Química Inorgánica y de los Compuestos Organometálicos*). The Instituto de Biocomputación y Física de Sistemas Complejos (BIFI) and the Centro de Supercomputación de Galicia (CESGA) are greatfully aknowledged for generous allocation of computational resources. A.P.-B. thanks the Spanish Ministerio de Educación, Cultura y Deporte for a grant (FPU15/03940).

Conflict of interest

The authors declare no conflict of interest.

Keywords: DFT · gold(II) · homolysis · metal halides · organogold

[1] D. Schröder, R. Brown, P. Schwerdtfeger, X.-B. Wang, X. Yang, L.-S. Wang, H. Schwarz, *Angew. Chem. Int. Ed.* **2003**, *42*, 311; *Angew. Chem.* **2003**, *115*, 323.

[2] a) X. Li, J. Cai, *Int. J. Quantum Chem.* **2016**, *116*, 1350; b) Z. Huang, Y. Yuan, L. Sun, X. Wang, Y. Li, *RSC Adv.* **2016**, *6*, 84016; c) H.-G. Cho, L. Andrews, *Organometallics* **2014**, *33*, 4315; d) H.-G. Cho, L. Andrews, *Organometallics* **2013**, *32*, 2753; e) H.-T. Liu, Y.-L. Wang, X.-G. Xiong, P. D. Dau, Z. A. Piazza, D.-L. Huang, C.-Q. Xu, J. Li, L.-S. Wang, *Chem. Sci.* **2012**, *3*, 3286; f) H.-G. Cho, L. Andrews, *Inorg. Chem.* **2011**, *50*, 10319; g) Y. Gong, L. Andrews, *Inorg. Chem.* **2012**, *51*, 667–673; h) S. Mishra, V. Vallet, W. Domcke, *ChemPhysChem* **2006**, *7*, 723; i) L. Andrews, X. Wang, L. Manceron, K. Balasubramanian, *J. Phys. Chem. A* **2004**, *108*, 2936; j) L. Andrews, X. Wang, *J. Am. Chem. Soc.* **2003**, *125*, 11751; k) B. Dai, J. Yang, *Chem. Phys. Lett.* **2003**, *379*, 512.

[3] a) X. Wang, L. Andrews, F. Brosi, S. Riedel, *Chem. Eur. J.* **2013**, *19*, 1397; b) X. Wang, L. Andrews, K. Willmann, F. Brosi, S. Riedel, *Angew. Chem. Int. Ed.* **2012**, *51*, 10628; *Angew. Chem.* **2012**, *124*, 10780.

[4] The chemistry of gold(II) in the condensed phase[5] is largely dominated by diamagnetic dinuclear compounds with Au–Au bonds.[6] Mononuclear open-shell species are still rare.[7]

[5] a) K. Heinze, *Angew. Chem. Int. Ed.* **2017**, *56*, 16126; *Angew. Chem.* **2017**, *129*, 16342; b) H. G. Raubenheimer, H. Schmidbaur, *J. Chem. Educ.* **2014**, *91*, 2024; c) A. Laguna, M. Laguna, *Coord. Chem. Rev.* **1999**, *193–195*, 837; d) H. Schmidbaur, K. C. Dash, *Adv. Inorg. Chem.* **1982**, *25*, 239.

[6] a) P. Jerabek, B. von der Esch, H. Schmidbaur, P. Schwerdtfeger, *Inorg. Chem.* **2017**, *56*, 14624; b) L. Nilakantan, K. R. Pichaandi, M. M. Abu-Omar, D. R. McMillin, P. R. Sharp, *J. Organomet. Chem.* **2017**, *844*, 30; c) N. Mirzadeh, M. A. Bennett, S. K. Bhargava, *Coord. Chem. Rev.* **2013**, *257*, 2250; d) D.-A. Roşca, D. A. Smith, D. L. Hughes, M. Bochmann, *Angew. Chem. Int. Ed.* **2012**, *51*, 10643; *Angew. Chem.* **2012**, *124*, 10795; e) S. Mathur, W. Tyrra, C. Hegemann, D. Zopes, *Chem. Commun.* **2012**, *48*, 8805; f) A. A. Mohamed, H. E. Abdou, J. P. Fackler, Jr., *Coord. Chem. Rev.* **2010**, *254*, 1253; g) J. Coetzee, W. F. Gabrielli, K. Coetzee, O. Schuster, S. D. Nogai, S. Cronje, H. G. Raubenheimer, *Angew. Chem. Int. Ed.* **2007**, *46*, 2497; *Angew. Chem.* **2007**, *119*, 2549.

[7] a) S. Preiß, C. Förster, S. Otto, M. Bauer, P. Müller, D. Hinderberger, H. H. Haeri, L. Carella, K. Heinze, *Nat. Chem.* **2017**, *9*, 1249; b) T. Drews, S. Seidel, K. Seppelt, *Angew. Chem. Int. Ed.* **2002**, *41*, 454; *Angew. Chem.* **2002**, *114*, 470; c) S. Seidel, K. Seppelt, *Science* **2000**, *290*, 117.

[8] H. Schwarz, *Angew. Chem. Int. Ed.* **2003**, *42*, 4442; *Angew. Chem.* **2003**, *115*, 4580.

[9] M. D. Đurović, Z. D. Bugarčić, R. van Eldik, *Coord. Chem. Rev.* **2017**, *338*, 186.

[10] The square-planar geometry of the $[CF_3AuI_3]^-$ anion in **2c** was established by single-crystal X-ray diffraction methods (Figure S3). Reliable Au–C and Au–I distances could not be obtained, however, owing to heavy disorder within the anion (see Supporting Information for details).

[11] a) M. Baya, A. Pérez-Bitrián, S. Martínez-Salvador, J. M. Casas, B. Menjón, J. Orduna, *Chem. Eur. J.* **2017**, *23*, 1512; b) S. Martínez-Salvador, L. R. Falvello, A. Martín, B. Menjón, *Chem. Sci.* **2015**, *6*, 5506.

[12] E. Bernhardt, M. Finze, H. Willner, *J. Fluorine Chem.* **2004**, *125*, 967.

[13] Our attempts to prepare the fluoro-derivative $[PPh_4][CF_3AuF_3]$ by reaction of **1c** with XeF_2 or by treatment of **2c** with AgF were unsuccessful thus far.

[14] For instance, aryl complexes with $[RAuX_3]^-$ stoichiometry are known with X = Cl or Br: a) R. Usón, A. Laguna, B. Bergareche, *J. Organomet. Chem.* **1980**, *184*, 411 (R = C_6F_5); b) P. Braunstein, R. J. H. Clark, *Inorg. Chem.* **1974**, *13*, 2224 (R = C_6H_4R'-*p*, where R′ = H, Cl, Br, NO_2).

[15] H. Schmidbaur, A. Grohmann, E. Olmos, in *Gold: Progress in Chemistry, Biochemistry and Technology* (Ed.: H. Schmidbaur), John Wiley & Sons, Chichester (UK), **1999**, Ch. 18, pp. 647–746.

[16] Compounds **2** undergo thermal decomposition in the condensed phase with CF_3X elimination in all cases (Figures S11–S13), whereby it is reasonable to assume that intermolecular processes operate. Photochemical elimination of CF_3X from other organogold(III) derivatives has been reported recently, see: M. Blaya, D. Bautista, J. Gil-Rubio, J. Vicente, *Organometallics* **2014**, *33*, 6358.

[17] For a thorough discussion on the delicate range of stability of Au(III) in the presence of iodide, see: D. Schneider, A. Schier, H. Schmidbaur, *Dalton Trans.* **2004**, 1995.

[18] a) S. Eustis, M. A. El-Sayed, *J. Phys. Chem. B* **2006**, *110*, 14014; b) S. Eustis, H.-Y. Hsu, M. A. El-Sayed, *J. Phys. Chem. B* **2005**, *109*, 4811; c) K. Kurihara, J. Kizling, P. Stenius, J. H. Fendler, *J. Am. Chem. Soc.* **1983**, *105*, 2574; d) M. Asai, S. Tazuke, S. Okamura, T. Ohno, S. Kato, *Chem. Lett.* **1973**, *2*, 993; e) J. H. Baxendale, A.-M. Koulkès-Pujo, *J. Chim. Phys. Phys.-Chim. Biol.* **1970**, *67*, 1602.

[19] J. C. Marcum, S. H. Kaufman, J. M. Weber, *J. Phys. Chem. A* **2011**, *115*, 3006.

[20] P. J. Barker, J. N. Winter, in *The Chemistry of the Metal–Carbon Bond, Vol. 2* (Eds.: F. R. Hartley, S. Patai), belonging to *The Chemistry of Functional Groups* (Ed.: S. Patai), John Wiley & Sons: Chichester (UK), **1985**, Ch. 3, pp. 151–218.

[21] Leading Refs.: a) K. A. Smoll, W. Kaminsky, K. I. Goldberg, *Organometallics* **2017**, *36*, 1213; b) P. M. Kozlowski, B. D. Garabato, P. Lodowski, M. Jaworska, *Dalton Trans.* **2016**, *45*, 4457.
[22] For the importance of radical processes in gold chemistry, see: a) D. Zhu, S. V. Lindeman, J. K. Kochi, *Organometallics* **1999**, *18*, 2241; b) R. J. Puddephatt, *Gold Bull.* **1977**, *10*, 108.
[23] The equilibrium geometries of the lighter anionic species $[AuF_3]^-$ and $[AuCl_3]^-$ were also calculated recently: a) A. K. Srivastava, N. Misra, *Int. J. Quantum Chem.* **2014**, *114*, 1513; b) P. Koirala, M. Willis, B. Kiran, A. K. Kandalam, P. Jena, *J. Phys. Chem. C* **2010**, *114*, 16018; c) K. A. Barakat, T. R. Cundari, H. Rabaâ, M. A. Omary, *J. Phys. Chem. B* **2006**, *110*, 14645.
[24] a) M. Hargittai, *Acc. Chem. Res.* **2009**, *42*, 453; b) I. J. Blackmore, A. J. Bridgeman, N. Harris, M. A. Holdaway, J. F. Rooms, E. L. Thompson, N. A. Young, *Angew. Chem. Int. Ed.* **2005**, *44*, 6746; *Angew. Chem.* **2005**, *117*, 6904; c) M. Hargittai, A. Schulz, B. Réffy, M. Kolonits, *J. Am. Chem. Soc.* **2001**, *123*, 1449; d) B. Réffy, M. Kolonits, A. Schulz, T. M. Klapötke, M. Hargittai, *J. Am. Chem. Soc.* **2000**, *122*, 3127; e) P. Schwerdtfeger, P. D. W. Boyd, S. Brienne, A. K. Burrell, *Inorg. Chem.* **1992**, *31*, 3411.
[25] a) A. Schulz, M. Hargittai, *Chem. Eur. J.* **2001**, *7*, 3657; b) T. Söhnel, R. Brown, L. Kloo, P. Schwerdtfeger, *Chem. Eur. J.* **2001**, *7*, 3167.
[26] M.-J. Crawford, T. M. Klapötke, *Angew. Chem. Int. Ed.* **2002**, *41*, 2269; *Angew. Chem.* **2002**, *114*, 2373.
[27] G. L. Gutsev, A. I. Boldyrev, *Adv. Chem. Phys.* **1985**, *61*, 169. See also Refs. [2a] and [23].
[28] The moderate energy cost of Au–X homolysis is largely compensated by the highly exergonic combination of the generated $X^{\bullet}$ atoms with fresh $[AuX_3]^-$ to give the well-known $[AuX_4]^-$ anions in the global bimolecular process: $2[Au^{II}X_3]^- \rightarrow [Au^{I}X_2]^- + [Au^{III}X_4]^-$ (Table S2).
[29] a) J. Joseph, K. Pradhan, P. Jena, H. Wang, X. Zhang, Y. J. Ko, K. H. Bowen, Jr., *J. Chem. Phys.* **2012**, *136*, 194305; b) S. A. Siddiqui, T. Rasheed, A. K. Pandey, *Comput. Theor. Chem.* **2012**, *979*, 119.
[30] a) V. Arcisauskaite, S. Knecht, S. P. A. Sauer, L. Hemmingsen, *Phys. Chem. Chem. Phys.* **2012**, *14*, 2651; b) L. A. Bengtsson, B. Norén, H. Stegemann, *Acta Chem. Scand.* **1995**, *49*, 391.

Manuscript received: November 20, 2017
Accepted manuscript online: December 22, 2017
Version of record online: January 16, 2018

Gold Fluorides

International Edition: DOI: 10.1002/anie.201802379
German Edition: DOI: 10.1002/ange.201802379

An Organogold(III) Difluoride with a *trans* Arrangement

Alberto Pérez-Bitrián, Miguel Baya, José M. Casas, Antonio Martín, Babil Menjón, and Jesús Orduna*

Abstract: *The trans isomer of the organogold(III) difluoride complex $[PPh_4][(CF_3)_2AuF_2]$ has been obtained in a stereoselective way and in excellent yield by reaction of $[PPh_4][CF_3AuCF_3]$ with XeF_2 under mild conditions. The compound is both thermally stable and reactive. Thus, the fluoride ligands are stereospecifically replaced by any heavier halide or by cyanide, the cyanide affording $[PPh_4][trans\text{-}(CF_3)_2Au(CN)_2]$. The organogold fluoride complexes $[CF_3AuF_x]^-$ (x = 1, 2, 3) have been experimentally detected to arise upon collision-induced dissociation of the $[trans\text{-}(CF_3)_2AuF_2]^-$ anion in the gas phase. Their structures have been calculated by DFT methods. In the isomeric forms identified for the open-shell species $[CF_3AuF_2]^-$, the spin density residing on the metal center is found to strongly depend on the precise stereochemistry. Based on crystallographic evidence, it is concluded that Au^{III} and Ag^{III} have similar covalent radii, at least in their most common square-planar geometry.*

Organometallic fluorides form a special class of compounds whose properties largely differ from those of their heavier-halide homologues.[1] The differences rely on the distinct effects induced by the most electronegative of the elements, fluorine, and are particularly conspicuous in gold chemistry.[2] Owing to their high reactivity, organogold fluorides are eagerly sought species, but even so, they are still rare today. Yet they are frequently proposed as key reaction intermediates,[3] just a few are sufficiently stable to enable isolation.[4] Focusing on gold(III), there is a small set of monofluoride derivatives currently known,[5] but the number of available compounds decreases dramatically with increasing fluoride content. Thus, whereas a handful of difluorides with formula *cis*-(NHC)RAuF_2 (R = alkyl) were detected in solution,[6] only the compounds *cis*-(N^C)AuF_2 were actually isolated.[7,8] As far as we know, the single example of organogold(III) difluoride with *trans* geometry is given by the anion $[trans\text{-}(CF_3)_2AuF_2]^-$, which was detected in solution along with the trifluoride $[CF_3AuF_3]^-$ and various other species, but could not be separated.[9] This difluoride is of especial interest not only because of its singular geometry among organogold fluorides but also because it is exactly midway between the all organometallic[10] $[(CF_3)_4Au]^-$ and the purely inorganic[11] $[AuF_4]^-$ derivatives, probably combining the stability of the former with the reactivity of the latter.[12]

Now we report on an efficient and stereoselective synthesis of the elusive species $[trans\text{-}(CF_3)_2AuF_2]^-$, isolated as its $[PPh_4]^+$ salt. Its fundamental properties in the solid state, in solution, and in the gas phase are also presented. Replacement of the F ligands takes place stereospecifically, with the *trans* stereochemistry being preserved.

The trifluoromethylgold(I) derivative $[PPh_4][(CF_3)_2Au]$ cleanly reacts with XeF_2 (Scheme 1) affording the organogold(III) difluoride $[PPh_4][trans\text{-}(CF_3)_2AuF_2]$ (**1**). The

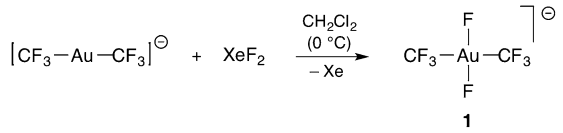

Scheme 1. Synthesis of the organogold(III) difluoride **1**. The cation is $[PPh_4]^+$.

reaction takes place in a quantitative and stereoselective way on a spectroscopic basis (^{19}F NMR). The stereochemistry of this oxidative addition is intriguing, since every known precedent proceed otherwise under formation of the *cis* isomers.[6] Compound **1** is eventually isolated as a thermally stable (Figure S13 in the Supporting Information), white solid in excellent yield (> 90 %). The compound is, however, highly moisture-sensitive and turns yellowish within hours when in contact with glassware at room temperature. Owing to its sensitivity, it is best kept at low temperature.

The stereochemistry of compound **1** in solution is readily assigned attending to the characteristic pattern of its ^{19}F NMR spectrum (Figure 1).[13] The signal corresponding to the CF_3 groups appears as a triplet with $^3J(F,F) = 16.5$ Hz; its chemical shift, $\delta_F = -46.16$ ppm, nicely follows the trend set up by the heavier-halide homologues $[PPh_4][trans\text{-}(CF_3)_2AuX_2]$ (X = Cl, Br, I)[10a] with respect to the electronegativity of the corresponding halogen (Figure S1). The well-upfield signal ($\delta_F = -324.96$ ppm) corresponds to the F ligand and appears split into a septet with the same coupling constant.

Compound **1** exhibits the same stereochemistry in the solid state as in solution, as established by single-crystal, X-ray diffraction methods (Figure 2). The Au–C bond lengths (205.4(5) pm av.) are similar to those observed in the homoleptic compound $[NBu_4][(CF_3)_4Au]$ (208.0(7) pm av.).[10a] However, the Au–F bond lengths (199.0(3) pm av.) are significantly longer than those found in the $[NMe_4][AuF_4]$

[*] A. Pérez-Bitrián, Dr. M. Baya, Prof. Dr. J. M. Casas, Dr. A. Martín, Dr. B. Menjón
Instituto de Síntesis Química y Catálisis Homogénea (iSQCH)
CSIC-Universidad de Zaragoza
C/ Pedro Cerbuna 12, 50009 Zaragoza (Spain)
E-mail: menjon@unizar.es
Dr. J. Orduna
Instituto de Ciencia de Materiales de Aragón (ICMA), CSIC-Universidad de Zaragoza
C/Pedro Cerbuna 12, 50009 Zaragoza (Spain)
Supporting information and the ORCID identification number(s) for the author(s) of this article can be found under: https://doi.org/10.1002/anie.201802379.

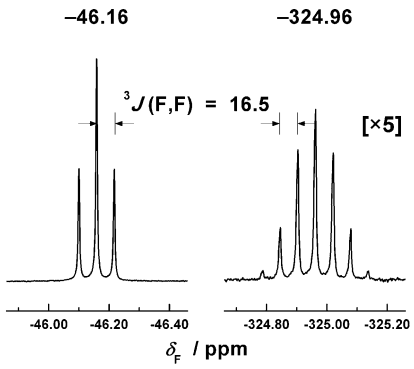

Figure 1. ^{19}F NMR spectrum of compound **1** in CD_3CN solution at room temperature with relevant parameters indicated (δ_F in ppm; J in Hz). The analysis of the [*trans*-($^{13}CF_3$)($^{12}CF_3$)AuF_2]$^-$ isotopomer is detailed in Figure S3.

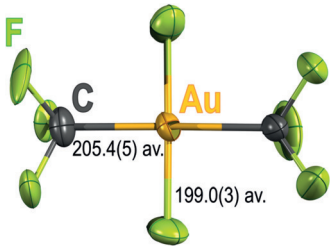

Figure 2. Displacement-ellipsoid diagram (50% probability) of the [*trans*-$(CF_3)_2AuF_2$]$^-$ anion as found in crystals of **1**. Only one set of the rotationally disordered F atoms found in one of the CF_3 groups is shown. Average Au–F and Au–C distances [pm] are indicated. For crystallographic details and CCDC number see Supporting Information.

salt (191.1(5) pm av.).[11a] Despite this lengthening, the observed frequency for the only IR-active ν(Au–F) mode (B_{1u}) in compound **1** (598 cm^{-1}; Figure S2) is indistinguishable from those reported for the [NR_4][AuF_4] salts: 597 (R = Me) and 598 cm^{-1} (R = Et).[11a] Virtually identical average Au–F interatomic distances were found in the neutral metallacyclic difluorides (N^C)AuF_2 (198.2(4) pm av.).[7]

The [*trans*-$(CF_3)_2AuF_2$]$^-$ anion shows interesting behavior in the gas phase, as examined by tandem mass spectrometry (MS^2). It undergoes various collision-induced dissociation processes (Figures S8–S12), which are summarized in Scheme 2. By far the most favored process involves CF_2 extrusion[14] and formation of the trifluoride complex [CF_3AuF_3]$^-$ with no change in the metal oxidation state

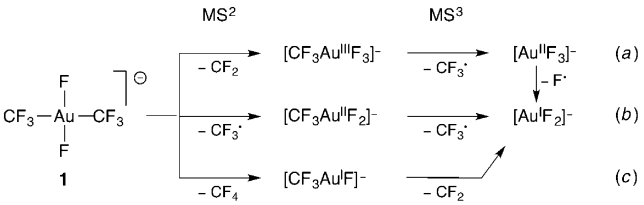

Scheme 2. Unimolecular decomposition paths experimentally detected by tandem mass spectrometry on the [*trans*-$(CF_3)_2AuF_2$]$^-$ anion, as well as on the [CF_3AuF_x]$^-$ species derived therefrom (x = 1, 2, 3). See text for details.

(Scheme 2a). All other fragmentations involve metal reduction by one (radical dissociation) or two units (reductive elimination or double radical dissociation). Thus, apparent elimination of CF_4 gives rise to small amounts of the mixed organogold(I) species [CF_3AuF]$^-$ (Scheme 2c). Homolytic splitting of a Au–CF_3 bond gives rise to the organogold(II) difluoride [CF_3AuF_2]$^-$, which again suffers Au–C homolysis to yield [AuF_2]$^-$ (Scheme 2b). The aforementioned [CF_3AuF_3]$^-$ derivative also undergoes Au-C homolytic cleavage rendering the gold(II) fluoride complex [AuF_3]$^-$ (Scheme 2a). This open-shell derivative was recently assigned a T-shaped structure.[15] It was also observed to arise by F• dissociation from the inorganic [AuF_4]$^-$ anion.[11a] With the aid of MS^4 experiments (Figure S12), we have now detected that the [AuF_3]$^-$ anion itself undergoes radical dissociation of F• atoms giving rise to [AuF_2]$^-$. This fact is in line with the behavior of the heavier homologues [$AuCl_3$]$^-$ and [$AuBr_3$]$^-$, and confirms our previous calculations.[15]

The geometries of the experimentally detected organogold fluoride complexes [CF_3AuF_x]$^-$ (x = 1, 2, 3) have been optimized by DFT methods. The saturated species of gold(III) and gold(I) show the structures depicted in Figure 3. In

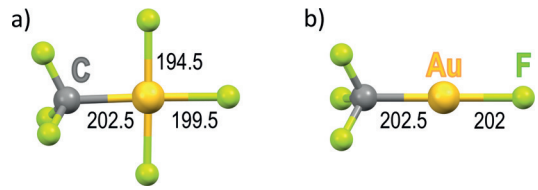

Figure 3. Geometries of a) the square-planar and b) the linear trifluoromethyl gold(III) and trifluoromethyl gold(I) fluoride complexes [CF_3AuF_3]$^-$ and [CF_3AuF]$^-$ optimized at the DFT/M06 level with relevant bond lengths [pm] indicated (see note added in proof).[28]

contrast, two isomeric forms have been located for the unsaturated gold(II) complex [CF_3AuF_2]$^-$ (Figure 4). In this case, the *trans* isomer is a local minimum and the *cis* isomer is stabilized by $\Delta H = -16.2$ kJ mol^{-1}, being identified as the global minimum. Both T-shaped isomers are connected through an interconversion path with a transition state (TS) located just +0.7 kJ mol^{-1} above our arbitrary reference (Figure S15). The low-energy profile of this interconversion

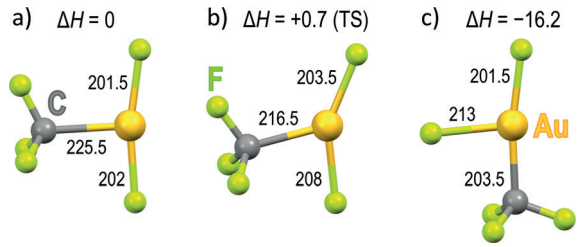

Figure 4. Geometries of the stationary points located on the potential energy surface of the unsaturated organogold(II) fluoride complex [CF_3AuF_2]$^-$, as optimized at the DFT/M06 level: a) *trans* isomer, b) transition state, and c) *cis* isomer. Relative stabilities (ΔH in kJ mol^{-1}) as well as relevant bond lengths [pm] are indicated. The energy profile of the path interconnecting all three species is shown in Figure S15.

path should result in easy fluxional behavior of the unsaturated $[CF_3AuF_2]^-$ complex. The Au–C distance (202.5 pm) calculated in the square-planar $[CF_3AuF_3]^-$ complex (Figure 3a) is slightly shorter than that experimentally found in the parent compound **1** (205.4(5) pm), denoting a comparatively smaller *trans* influence of the F ligand.[16] The entire CF_3-Au-F axis in this gold(III) compound shows little structural difference with the linear gold(I) complex $[CF_3AuF]^-$ (Figure 3b), regardless of the different oxidation state and coordination number of the metal in each case. A similar Au–C distance (203.5 pm) is calculated for the *cis* isomer of the unsaturated, open-shell $[CF_3AuF_2]^-$ complex (Figure 4); it is, however, substantially elongated in the TS (216.5 pm) and even more so in the *trans* isomer (225.5 pm). This gradual elongation follows the increasing spin density of the unpaired electron delocalized onto the CF_3 group depending on its stereochemical location (Table 1; Figure S16). Thus, the spin density on the CF_3 group is negligible in the *cis* isomer, whereas it amounts >50% in the *trans* isomer. It is worth noting that the unpaired electron is much less delocalized when the stem ligand is fluorine. In this case, the spin density resides mainly on the Au atom (72%), with just 24% delocalized onto the stem F atom. Comparing these data with those obtained for the purely inorganic $[AuX_3]^-$ anions (X = F, Cl, Br, I), it follows that the ability of the CF_3 group to delocalize spin density of the unpaired electron closely approaches that of iodine.[15] This also evidences a high degree of covalency for the Au–CF_3 bond.[17] Since the SOMO of the $[CF_3AuF_2]^-$ complex is antibonding with respect to the stem ligand (Figure S17), the corresponding Au–X bond will weaken as the spin density on that ligand increases. This explains why the stem Au–X bond (Figure 4) is comparatively much more elongated for X = CF_3 (225.5 pm in the *trans* isomer) than for X = F (213 pm in the *cis* isomer).[18] It is further concluded that the spin density at a given metal atom can be determined by the precise stereochemistry of the chemical entity, even under a same characteristic molecular shape (polytope).

Table 1: Spin density distribution [%] on the different atoms and groups along the stationary points found for the three-coordinate, open-shell organogold(II) complex $[CF_3AuF_2]^-$.[a]

Atom or group	*trans* isomer	TS	*cis* isomer
Au	34	38	72
CF_3	54	46	0
[Au]–F[b]	6/6	5/11	4/24

[a] Graphical representations are shown in Figure S16. [b] The spin densities on the metal-bound F atoms, [Au]–F, are similar in the *trans* isomer, where they are almost equivalent, but becomes progressively dissimilar in the TS and the *cis* isomer, where two distinct coordination sites are identified (Figure 4). The smaller values correspond to the (near) cross F atoms.

Once the intrinsic properties of compound **1** have been examined, we sought to test its chemical reactivity. In acetone solution, the fluoride ligands of compound **1** are readily replaced by any of the heavier halides, X^- (X = Cl, Br, I), giving rise (Scheme 3) to the corresponding [*trans*-$(CF_3)_2AuX_2]^-$ derivatives (**2–4**)[10a] in quantitative yield (^{19}F NMR). This behavior is typical of a hard ligand like fluoride, when bound to a "class *b*" metal like gold(III).[19] The fluoride ligands are also quantitatively replaced by cyanide (Scheme 3) affording $[PPh_4]$[*trans*-$(CF_3)_2Au(CN)_2$] (**5**), which is isolated as a white solid in good yield.[20] In the solid state, compound **5** exhibits unusually high stability for an organometallic species, as it melts at 209 °C and decomposes only over 350 °C (Figure S14). The labelled derivative $[PPh_4]$-[*trans*-$(CF_3)_2Au(^{13}CN)_2$] (**5***) has also been prepared and isolated for spectroscopic purposes (see Supporting Information). The stereochemistry of **5** has been established by single-crystal X-ray diffraction analysis. The structure of the anion is depicted in Figure 5. The Au atom is located at an inversion center. The Au–CN bond (199.8(3) pm) involving an sp-hybridized C-donor atom is appreciably shorter than the Au–CF_3 bond (208.7(2) pm) within the same unit. These Au–C bond lengths do not significantly differ from those, respectively observed in the homoleptic anions $[Au(CN)_4]^-$ (200.6(7) pm)[21] and $[(CF_3)_4Au]^-$ (208.0(7) pm av.).[10a]

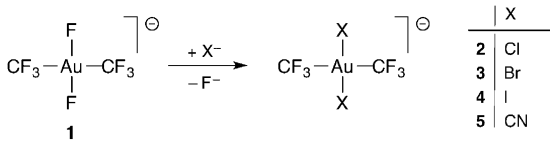

Scheme 3. Syntheses of compounds **2–5**. In all cases the cation is $[PPh_4]^+$.

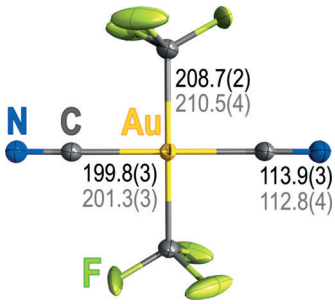

Figure 5. Displacement-ellipsoid diagram (50% probability) of the [*trans*-$(CF_3)_2Au(CN)_2]^-$ anion as found in crystals of **5** with selected interatomic distances [pm] indicated. Only one set of the rotationally disordered F atoms found in the symmetry-related CF_3 groups is shown. Values in gray correspond to the same interatomic distances in the homologous silver derivative [*trans*-$(CF_3)_2Ag(CN)_2]^-$.[22] For crystallographic details and CCDC number see Supporting Information.

It is worth noting that the Au–C bond distances in **5** show no significant difference with those found in the lighter, isoleptic and isostructural silver(III) anion [*trans*-$(CF_3)_2Ag(CN)_2]^-$, namely Ag–CN 201.3(3) pm and Ag–CF_3 210.5(4) pm (Figure 5).[22] Since crystals of both $[PPh_4]$-[*trans*-$(CF_3)_2M(CN)_2$] salts (M = Ag, Au) are isomorphous (monoclinic, space group *C*2/*c*, *Z* = 4),[23] with no sign of significant covalent cation/anion interaction, and showing similar standard deviations in the structural parameters determined, it can be concluded that Ag^{III} and Au^{III} have approximately the same covalent radii. Direct and meaningful

comparisons between isomorphous and isostructural M^{III} covalent species were not previously possible due to the lack of suitable Ag^{III} partners. Some time ago, it was concluded that Au^{I} has smaller size than Ag^{I} due to relativistic effects operating preferentially on gold.[24] This unusual size inversion substantially diminishes in Ag^{II}/Au^{II} pairs[25] and, according to our current results, fades away on shifting to oxidation state III. This trend is consistent with the decrease in the relativistic Au−L bond contraction on going from Au^{I} to Au^{III} complexes pointed out by Schwerdtfeger and coworkers.[26] The fact that the Ag^{III} and Au^{III} centers have approximately the same covalent radii is also in keeping with the virtually identical values assigned to their crystal radii in four-coordinate square-planar environments, namely 81 (Ag^{3+}) and 82 (Au^{3+}) pm.[27]

In summary, the efficient and stereoselective synthesis of $[PPh_4][trans\text{-}(CF_3)_2AuF_2]$ provides an entry to the whole family of organogold fluoride complexes with formula $[CF_3AuF_x]^-$ ($x = 1$, 2, 3). These species, containing gold in oxidation states I, II, and III, respectively, have been experimentally detected (gas phase) and their structures calculated (DFT). A detailed study of the isomeric forms of the open-shell species $[CF_3AuF_2]^-$ reveals that the spin density distribution over the complex is a function of its precise stereochemistry even under a given polytope. Finally, experimental evidence is provided to conclude that Au^{III} and Ag^{III} have comparable covalent radii, at least in a square-planar environment, which is by far the most common geometry for these d^8 centers.

Acknowledgements

This work was supported by the Spanish MINECO/FEDER (Project CTQ2015-67461-P) and the Gobierno de Aragón and Fondo Social Europeo (Grupo Consolidado E21: *Química Inorgánica y de los Compuestos Organometálicos*). The Instituto de Biocomputación y Física de Sistemas Complejos (BIFI) and the Centro de Supercomputación de Galicia (CESGA) are gratefully acknowledged for generous allocation of computational resources. A.P.-B. thanks the Spanish Ministerio de Educación, Cultura y Deporte for a grant (FPU15/03940).

Conflict of interest

The authors declare no conflict of interest.

Keywords: fluorides · geometric isomerism · gold · stereoselectivity · trifluoromethyl ligand

How to cite: *Angew. Chem. Int. Ed.* **2018**, *57*, 6517–6521
Angew. Chem. **2018**, *130*, 6627–6631

[1] E. F. Murphy, R. Murugavel, H. W. Roesky, *Chem. Rev.* **1997**, *97*, 3425.
[2] W. J. Wolf, F. D. Toste in *The Chemistry of Organogold Compounds*, *Vol. 1* (Eds.: Z. Rappoport, I. Marek, J. F. Liebman), belonging to Patai's Chemistry of Functional Groups, Wiley, Chichester, **2014**, chap. 9, pp. 391–408.
[3] J. Miró, C. del Pozo, *Chem. Rev.* **2016**, *116*, 11924.
[4] The mononuclear (SIDipp)AuF and dinuclear $[\{(SIDipp)Au\}_2(\mu\text{-}F)]BF_4$ compounds (SIDipp = 1,3-bis(2,6-diisopropylphenyl)-4,5-dihydroimidazol-2-ylidene) are the only stable organogold(I) fluoride complexes described to date: a) C. M. Wyss, B. K. Tate, J. Bacsa, M. Wieliczko, J. P. Sadighi, *Polyhedron* **2014**, *84*, 87; b) D. S. Laitar, P. Müller, T. G. Gray, J. P. Sadighi, *Organometallics* **2005**, *24*, 4503.
[5] a) A. Pérez-Bitrián, S. Martínez-Salvador, M. Baya, J. M. Casas, A. Martín, B. Menjón, J. Orduna, *Chem. Eur. J.* **2017**, *23*, 6919; b) R. Kumar, A. Linden, C. Nevado, *J. Am. Chem. Soc.* **2016**, *138*, 13790; c) R. Kumar, A. Linden, C. Nevado, *Angew. Chem. Int. Ed.* **2015**, *54*, 14287; *Angew. Chem.* **2015**, *127*, 14495; d) M. S. Winston, W. J. Wolf, F. D. Toste, *J. Am. Chem. Soc.* **2015**, *137*, 7921.
[6] a) N. P. Mankad, F. D. Toste, *Chem. Sci.* **2012**, *3*, 72; b) N. P. Mankad, F. D. Toste, *J. Am. Chem. Soc.* **2010**, *132*, 12859.
[7] See Ref. [5b], where N^C = 3-fluoro-2-(3-methylpyridin-2-yl)phenyl or 2,3,4-trimethoxy-6-(3-methylpyridin-2-yl)phenyl.
[8] Dinuclear organogold(III) compounds with formula $[\{(NHC)AuMe\}_2(\mu\text{-}F)_2]F_2$ have been reported (NHC = 1,3-bis(2,6-diisopropylphenyl)imidazol-2-ylidene (IDipp) or SIDipp), which contain a double-bridging fluoride system with inherent *cis* arrangement.[6b]
[9] E. Bernhardt, M. Finze, H. Willner, *J. Fluorine Chem.* **2004**, *125*, 967.
[10] a) S. Martínez-Salvador, L. R. Falvello, A. Martín, B. Menjón, *Chem. Eur. J.* **2013**, *19*, 14540; b) U. Preiss, I. Krossing, *Z. Anorg. Allg. Chem.* **2007**, *633*, 1639.
[11] a) M. A. Ellwanger, S. Steinhauer, P. Golz, H. Beckers, A. Wiesner, B. Braun-Cula, T. Braun, S. Riedel, *Chem. Eur. J.* **2017**, *23*, 13501; b) M. Leblanc, V. Maisonneuve, A. Tressaud, *Chem. Rev.* **2015**, *115*, 1191; c) B. G. Müller, *Angew. Chem. Int. Ed. Engl.* **1987**, *26*, 1081; *Angew. Chem.* **1987**, *99*, 1120.
[12] Trifluoromethyl gold chemistry has been thoroughly reviewed in: J. Gil-Rubio, J. Vicente, *Dalton Trans.* **2015**, *44*, 19432.
[13] The slight differences with previously reported values are probably due to the different cation used in each case, namely $[PPh_4]^+$ vs. $[NBu_4]^+$.[9]
[14] CF_2 extrusion processes in gold chemistry had been previously detected to occur at the unimolecular level in the homoleptic organogold(I) derivative $[CF_3AuCF_3]^-$ as well as in the mixed halide complexes $[CF_3AuX]^-$ (X = F, Cl, Br, I): a) M. Baya, A. Pérez-Bitrián, S. Martínez-Salvador, J. M. Casas, B. Menjón, J. Orduna, *Chem. Eur. J.* **2017**, *23*, 1512; b) N. J. Rijs, R. A. J. O'Hair, *Dalton Trans.* **2012**, *41*, 3395.
[15] M. Baya, A. Pérez-Bitrián, S. Martínez-Salvador, A. Martín, J. M. Casas, B. Menjón, J. Orduna, *Chem. Eur. J.* **2018**, *24*, 1514.
[16] A low *trans* influence for the fluoride ligand was also inferred in: E. Peris, J. C. Lee, Jr., J. R. Rambo, O. Eisenstein, R. H. Crabtree, *J. Am. Chem. Soc.* **1995**, *117*, 3485.
[17] a) E. Ruiz, J. Cirera, S. Alvarez, *Coord. Chem. Rev.* **2005**, *249*, 2649; b) J. Cano, E. Ruiz, S. Alvarez, M. Verdaguer, *Comments Inorg. Chem.* **1998**, *20*, 27.
[18] A substantially shorter Au–F bond length (190.7 pm) was estimated for the neutral, linear AuF_2 molecule: a) X. Wang, L. Andrews, F. Brosi, S. Riedel, *Chem. Eur. J.* **2013**, *19*, 1397; b) X. Wang, L. Andrews, K. Willmann, F. Brosi, S. Riedel, *Angew. Chem. Int. Ed.* **2012**, *51*, 10628; *Angew. Chem.* **2012**, *124*, 10780.
[19] a) R. G. Pearson, *J. Chem. Educ.* **1987**, *64*, 561; b) R. J. Puddephatt, *The Chemistry of Gold*, Elsevier, Amsterdam, **1978**, chap. 1, pp. 22–24; c) S. Ahrland, *Struct. Bonding (Berlin)* **1966**, *1*, 207; d) S. Ahrland, J. Chatt, N. R. Davies, *Q. Revs. Chem. Soc.* **1958**, *12*, 265.

[20] The [*trans*-$(CF_3)_2Au(CN)_2]^-$ anion had been previously detected in solution but not isolated.[9]

[21] P. G. Jones, C. Thöne, *Acta Crystallogr. Sect. C* **1989**, *45*, 11.

[22] R. Eujen, B. Hoge, D. J. Brauer, *Inorg. Chem.* **1997**, *36*, 1464.

[23] The slight difference in the cell volumes of [PPh_4]-[*trans*-$(CF_3)_2M(CN)_2$] crystals, $V = 2.7029(5)$ nm^3 (M = Ag) vs. 2.60369(8) nm^3 (M = Au), can be reasonably attributed to the thermal expansion associated to the different data-collection temperature used in each case: $T = 295(2)$ vs. 100(2) K for M = Ag and Au, respectively.

[24] a) U. M. Tripathi, A. Bauer, H. Schmidbaur, *J. Chem. Soc. Dalton Trans.* **1997**, 2865; b) A. Bayler, A. Schier, G. A. Bowmaker, H. Schmidbaur, *J. Am. Chem. Soc.* **1996**, *118*, 7006; c) M. S. Liao, W. H. E. Schwarz, *Acta Crystallogr. Sect. B* **1994**, *50*, 9.

[25] S. Preiß, C. Förster, S. Otto, M. Bauer, P. Müller, D. Hinderberger, H. H. Haeri, L. Carella, K. Heinze, *Nat. Chem.* **2017**, *9*, 1249.

[26] a) P. Schwerdtfeger, M. Lein in *Gold Chemistry: Applications and Future Directions in the Life Sciences* (Ed.: F. Mohr), Wiley-VCH, Weinheim, **2009**, chap. 4, pp. 183–247; b) P. Schwerdtfeger, P. D. W. Boyd, S. Brienne, A. K. Burrell, *Inorg. Chem.* **1992**, *31*, 3411.

[27] R. D. Shannon in *Encyclopedia of Inorganic Chemistry*, *Vol. 2* (Ed.: R. B. King), Wiley, Chichester, **1994**, pp. 929–942.

[28] **Note Added in Proof** (April 23, 2018) : After acceptance of this work, an organogold(III) compound with high fluoride content and formula (NHC)AuF_3 was reported, where NHC = 1,3-dimesityl-4,5-dihydroimidazol-2-ylidene (SIMes). We note the satisfactory agreement between the Au–F interatomic distances established experimentally for this neutral compound (X-ray) with those calculated herein for the related anionic species $[CF_3AuF_3]^-$ (Figure 3a). The just marginal elongation found in the latter case might well be due to the anionic nature of the complex: M. Ellwanger, S. Steinhauer, P. Golz, T. Braun, S. Riedel, *Angew. Chem. Int. Ed.* **2018**, *57*, DOI: 10.1002/anie.201802952; Angew. Chem. **2018**, *130*, DOI: 10.1002/ange.201802952.

Manuscript received: February 23, 2018
Accepted manuscript online: March 23, 2018
Version of record online: April 26, 2018

Organometallic Chemistry

Anionic Derivatives of Perfluorinated Trimethylgold

Alberto Pérez-Bitrián,[a] Sonia Martínez-Salvador,[a] Miguel Baya,[a] José M. Casas,[a] Antonio Martín,[a] Babil Menjón,*[a] and Jesús Orduna[b]

Dedicated to the Memory of Prof. Dr. Rafael Usón

Abstract: The homoleptic compound $[PPh_4][CF_3AuCF_3]$ cleanly undergoes photoinduced oxidative addition of CF_3I to afford the organogold(III) derivative $[PPh_4][(CF_3)_3AuI]$ in good yield and under mild conditions. This compound provides a convenient entry to the chemistry of the perfluorinated $(CF_3)_3Au$ fragment, the properties of which were analyzed with the aid of DFT methods and compared with those of the homologous non-fluorinated $(CH_3)_3Au$ moiety. It was found that reductive elimination of CX_3–CX_3 in the former (X = F) requires a much higher energy barrier than in the latter (X = H) and is therefore considerably less favored. This can be considered as one of the main features underlying the significantly higher stability associated to the $(CF_3)_3Au$ fragment and its derivatives. This unsaturated, 14-electron species can be stabilized by coordination of any of the halide ligands, including fluoride. In fact, the whole series of anionic $[PPh_4][(CF_3)_3AuX]$ complexes (X = F, Cl, Br, I, CN) has now been isolated and conveniently characterized. Evidence for intermolecular decomposition pathways upon thermolysis in the condensed phase is presented.

Introduction

More than thirty years after Pope and Gibson prepared the first organogold compounds,[1] Gilman and Woods reported the synthesis of "trimethyl gold" as a thermally unstable species decomposing above −40 °C in Et_2O solution.[2] This compound—most probably corresponding to the solvate $(CH_3)_3Au{\cdot}OEt_2$, as already pointed out by its authors—has not yet been isolated. Nevertheless, it has captured the attention over the years of both theoreticians and experimentalists due to its intrinsic simplicity and prototypical nature.[3] The lability of the Et_2O ligand and the readiness of the $(CH_3)_3Au$ fragment to undergo reductive elimination of ethane are the main reasons for its thermal instability [Eq. (1)].[3] In fact, the unsaturated $(CH_3)_3Au$ fragment can be stabilized to a greater extent by better ligands than Et_2O, namely, ylides[4] and various ligands with Group 15 donor atoms: amines,[2] phosphines,[4a,5–7] and $AsMe_3$.[6a] Even so, the number of currently known trimethylgold derivatives remains small.[8,9]

$$(CH_3)_3Au \cdot OEt_2 \rightarrow (CH_3)_3Au \rightarrow (CH_3)Au + C_2H_6 \quad (1)$$

There is now a burning interest in the progress of trifluoromethyl derivatives of both metals[10] and non-metals[11] because of their unique and advantageous properties. It is therefore surprising that the chemistry of the homologous fluorinated fragment $(CF_3)_3Au$ remains far less developed to date, probably due to the lack of appropriate synthetic methods currently available. Thus, naked $(CF_3)_3Au$ seems to have been prepared as an unstable species by gas-phase reaction of Au vapors with $CF_3^{\bullet}$ radicals followed by matrix isolation [Eq. (2)].[12] As in the preceding non-fluorinated methyl derivative, significant stabilization is accomplished by coordination of an additional ligand, namely $(CF_3)_3Au(PMe_3)$. The latter phosphine adduct was subsequently prepared by treatment of $(CF_3)_2AuI(PMe_3)$ with $(CF_3)_2Cd{\cdot}dme$ in the presence of excess of CF_3I.[13]

$$Au_{(g)} + 3\,CF_3{}^{\bullet}{}_{(g)} \rightarrow (CF_3)_3Au \quad (2)$$

Our own attempts to bring into reaction just one of the Au–CF_3 bonds in the anionic species $[(CF_3)_4Au]^-$ failed.[14] The lack of selectivity in the attempted processes can be attributed to the high stability and remarkable inertness of the symmetric $[(CF_3)_4Au]^-$ anion, which make this homoleptic species a convenient weakly coordinating anion,[15] yet one of little synthetic use. In this context, it is interesting to note that protonation of the lighter homologous species $[(CF_3)_4Cu]^-$ in the presence of 2,2′-bipyridine (bpy) afforded the neutral $(CF_3)_3Cu(bpy)$ derivative.[10b] By treating the isoleptic silver anion $[(CF_3)_4Ag]^-$ with ICl in MeCN, the neutral $(CF_3)_3Ag(NCMe)$ compound was obtained as a colorless oil, but in poor yield.[16] Treatment of $[NBu_4][Au(CN)_4]$ with ClF in CH_2Cl_2 proved to be non-selective.

[a] A. Pérez-Bitrián, Dr. S. Martínez-Salvador, Dr. M. Baya, Dr. J. M. Casas, Dr. A. Martín, Dr. B. Menjón
Instituto de Síntesis Química y Catálisis Homogénea (iSQCH)
CSIC-Universidad de Zaragoza, C/ Pedro Cerbuna 12
50009 Zaragoza (Spain)
E-mail: menjon@unizar.es

[b] Dr. J. Orduna
Instituto de Ciencia de Materiales de Aragón (ICMA)
CSIC-Universidad de Zaragoza, C/ Pedro Cerbuna 12
50009 Zaragoza (Spain)

Supporting information and the ORCID identification numbers for the authors of this article can be found under: https://doi.org/10.1002/chem.201700927.

In the complex mixtures of gold derivatives thereby obtained, some anionic $[(CF_3)_3AuX]^-$ compounds (X = F, Cl, CN) were detected by ^{19}F NMR spectroscopy, but were not isolated.[17]

We now report on a simple and efficient method enabling a convenient entry to the chemistry of the $(CF_3)_3Au$ fragment. The fundamental properties of this unsaturated, 14-electron species were analyzed with the aid of DFT methods and conveniently contrasted with those corresponding to the non-fluorinated homologous $(CH_3)_3Au$ moiety. We have succeeded in stabilizing the naked $(CF_3)_3Au$ moiety by coordination of the whole family of halide ligands, X^-, including fluoride. Synthetic methods are thus described to prepare the series of anionic compounds with the formula $[PPh_4][(CF_3)_3AuX]$ (X = F, Cl, Br, I, CN) for which no counterpart in the well-established chemistry of the non-fluorinated $(CH_3)_3Au$ fragment is currently known.[8] These fluorinated compounds exhibit unusually high thermal stability. Their decomposition pathways under various conditions were also studied in detail and are thoroughly discussed.

Results and Discussion

Synthesis of $[PPh_4][(CF_3)_3AuI]$ (1)

The homoleptic organogold(I) derivative $[PPh_4][CF_3AuCF_3]$[14] cleanly undergoes oxidative addition of CF_3I in MeCN solution at room temperature (Scheme 1) affording the triorganogold(III) species $[PPh_4][(CF_3)_3AuI]$ (**1**), which can be isolated as a white solid in good yield. Compound **1** shows a characteristic ^{19}F NMR spectrum (Figure 1) consisting of a quartet at $\delta_F = -26.09$ ppm and a septet at $\delta_F = -31.46$ ppm in 2:1 integrated ratio, corresponding to each kind of chemically inequivalent CF_3 groups, which are mutually coupled with a common $^4J(F,F) = 7.2$ Hz value.

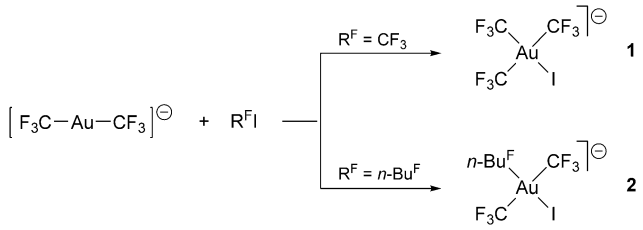

Scheme 1. Oxidative addition of R^FI reagents to the homoleptic, anionic trifluoromethylgold(I) species. In all cases the cation is $[PPh_4]^+$.

Concerning the reaction mechanism, it is interesting to note that the process requires 4 days for completion in the dark, while it proceeds quantitatively in just 10 min when exposed to daylight, as determined by ^{19}F NMR spectroscopy. The sharp rate difference observed upon photoirradiation is clear evidence that the reaction proceeds by a radical mechanism, as also found in related systems.[18] The AX_3Y stoichiometry of the obtained anion precludes any decision concerning the stereochemistry of the process. However, when the reaction is carried out under similar conditions using nBu^{F}I as the reagent, the *trans* isomer of $[PPh_4][n\text{Bu}^F(CF_3)_2AuI]$ (**2**) is stereoselectively obtained (Scheme 1; Figure S1). Given the similarity at the α-C atom in both perfluoroalkyl iodides with $I^{\delta+}$–$C^{\delta-}$ bond polarity, R^FI ($R^F = CF_3$, nPr^{F}CF$_2$), it is reasonable to conclude that their oxidative addition to compound $[PPh_4][CF_3AuCF_3]$ takes place in both cases with *trans* stereochemistry. We had previously found that the same homoleptic organogold(I) derivative also undergoes stereoselective oxidative addition of halogens, X_2, affording $[PPh_4][trans\text{-}(CF_3)_2AuX_2]$ (X = Cl, Br, I).[14]

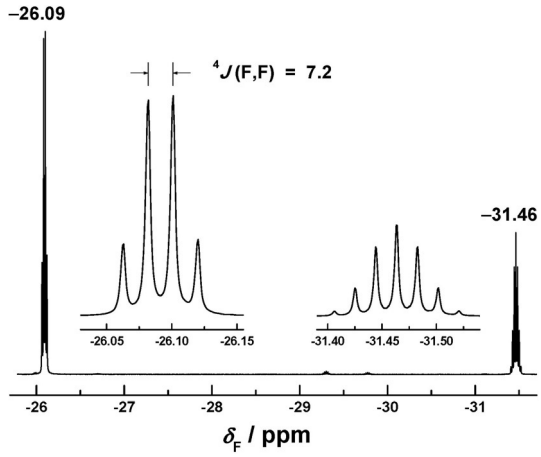

Figure 1. ^{19}F NMR spectrum of compound **1** in CD_2Cl_2 solution at room temperature with relevant parameters indicated (δ_F in ppm; J in Hz).

The clean behavior now observed for the fluorinated $[CF_3AuCF_3]^-$ species towards RI reagents (Scheme 1) is in sharp contrast with that previously reported for the non-fluorinated $[CH_3AuCH_3]^-$ homologue. In the absence of additional stabilizing ligands, the latter is known to react with MeI undergoing metal reduction and affording an 8:1 mixture of ethane and methane.[9c] Although the $[(CH_3)_3AuI]^-$ anion might, in principle, be involved in the referred process, this nonfluorinated anion has not been isolated or identified to date. It was not detected upon reaction of $[CH_3AuCH_3]^-$ and MeI in the gas phase either, not even when using favorable conditions, namely high concentrations of MeI and the longest possible reaction times.[19] Actually, we are not aware of the existence of any simple anionic $[(CH_3)_3AuX]^-$ species. In contrast, the fluorinated $(CF_3)_3Au$ fragment can be stabilized not only by iodide, but also by any other halogen ligand, as we will see next.

Synthesis and characterization of further anionic derivatives of $(CF_3)_3Au$

It is well known that gold, even in its oxidation state III, is a typical "soft acid" (Pearson HSAB)[20] or "class b" metal in the original classification of Ahrland, Chatt and Davies.[21] Thus, the relative stability of gold halides towards substitution in solution usually follows the order: F ≪ Cl < Br < I ≪ CN.[22] In order to prepare the lighter halide complexes of the $(CF_3)_3Au$ moiety starting from the iodo-derivative **1**, the use of AgX salts seemed appropriate since the extremely low solubility of AgI might help to overcome this unfavorable trend.[23] In fact, room-temperature treatment of **1** with a slight excess of AgX

(X = F, Cl, Br)[24] readily affords the whole family of halo-derivatives $[PPh_4][(CF_3)_3AuX]$ (**3**–**5**) in good yield (Scheme 2).

Additionally, the cyano-complex $[PPh_4][(CF_3)_3AuCN]$ (**6**) was prepared by simple reaction of compound **1** with KCN

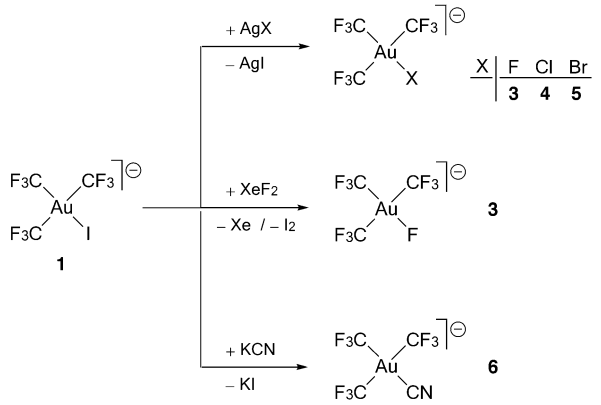

Scheme 2. Synthetic procedures affording the whole family of anionic $[(CF_3)_3AuX]^-$ derivatives. In all cases the cation is $[PPh_4]^+$.

(Scheme 2). The fluoro-derivative $[PPh_4][(CF_3)_3AuF]$ (**3**) is particularly appealing given the current interest in the synthesis of organogold fluorides.[25] It is worth noting that the $[(CF_3)_3AuF]^-$ anion had been previously identified in solution, but not isolated thus far.[17] Compound **3** can also be prepared in reasonable yield by treatment of **1** with XeF_2 (Scheme 2). Compound **3** is an extremely moisture-sensitive species. Under rigorously dry conditions and once isolated, however, compound **3** is very stable in the solid state (see below).

Compounds **3**–**6** were conveniently characterized by analytical and spectroscopic methods (see the Experimental Section). Valuable structural information in solution is provided by ^{19}F NMR spectroscopy. Our results validate previous assignments to the $[(CF_3)_3AuX]^-$ anions detected in solution (X = F, Cl, CN).[17] The room-temperature spectral pattern of all these compounds consists of two signals in 1:2 integrated ratio (typically a septet and a quartet), corresponding to the two types of chemically inequivalent CF_3 groups with no hint of fluxional exchange between them. Both sets of nuclei are mutually coupled with $^4J(F,F)$ values in the narrow 5.8–7.2 Hz range. Additional splitting of the signals is observed in the fluoro-derivative **3** (Figure 2). In the latter, the CF_3 signals show the widest separation within the series of halides (quartet: $\delta_F = -41.09$ ppm vs. septet: $\delta_F = -28.58$ ppm), revealing the most dissimilar environment for each kind of chemically inequivalent CF_3 group. Moreover, the fluorine atom directly bound to gold is much shielded, with the corresponding signal appearing at very high field: $\delta_F = -254.41$ ppm (Figure 2b). If we compare the CF_3 chemical shifts within the series of halides, $[(CF_3)_3AuX]^-$ (X = F, Cl, Br, I), it is found that they nicely correlate with the halogen's electronegativity (Figure S2). The dependence is surprisingly less marked for the CF_3 group *trans* to X and is contrary for each kind of CF_3, in such a way that the relative quartet versus septet position becomes inverted in the iodo-derivative **1** (Figure 1). Such an "inverted" arrangement was also

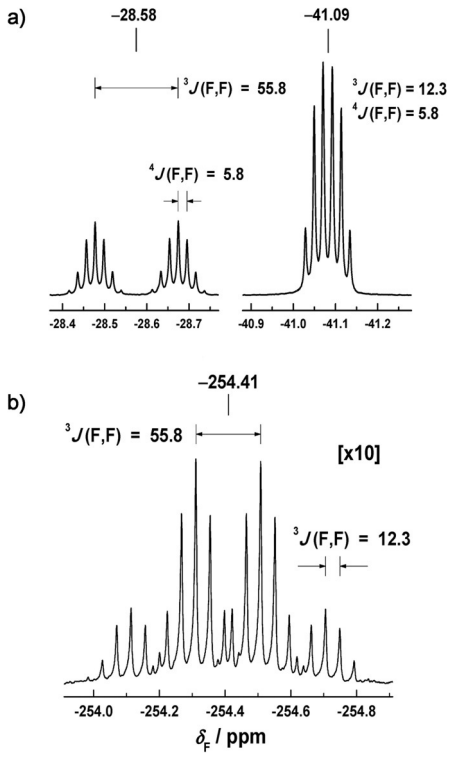

Figure 2. ^{19}F NMR spectrum of compound **3** in CD_2Cl_2 solution at room temperature with relevant parameters indicated (δ_F in ppm; *J* in Hz): a) CF_3 range; b) fluoride signal.

found in the related isoelectronic Pt^{II} derivatives,[26] and seems to be associated with ligands exhibiting certain π-acceptor character. An additional example of this apparently general trend is provided by the cyano-derivative **6**. In this compound bearing a typical π-acceptor ligand, the quartet ($\delta_F = -30.07$ ppm) and septet ($\delta_F = -34.15$ ppm) signals also show "inverted" positions.

We also sought to obtain structural information in the solid state by X-ray diffraction methods. Single crystals of the gold compounds with the lightest (**3**) and the heaviest (**1**) halogens were indeed obtained and their X-ray diffraction data were carefully analyzed. In both cases, however, and regardless of their disparate size, the monoatomic X ligands (X = F or I) in the corresponding $[(CF_3)_3AuX]^-$ anions were heavily disordered over three adjacent positions and thus, no reliable structural parameters could be finally obtained. Better results were attained for the cyano-derivative **6**, in which the diatomic CN ligand shows no apparent sign of disorder. In the $[(CF_3)_3AuCN]^-$ anion (Figure 3), the gold atom is surrounded by four C-donor ligands in a square-planar arrangement. The Au–CN bond length (205.9(3) pm) is appreciably longer than that found in the homoleptic $[AsPh_4][Au(CN)_4]$ derivative (200.6(7) pm average).[27] This elongation can be attributed to the high *trans* influence of the CF_3 group.[28] Accordingly, the Au–C bond lengths of the mutually *trans*-standing CF_3 groups (211.2(3) pm average) are also longer than the Au–CF_3 distance *trans* to CN (a ligand with low *trans* influence): Au–C(2) 206.8(3) pm. Focusing on the CF_3-Au-CN axis, it is worth noting that the elongation of the Au–CN bond and shortening of the

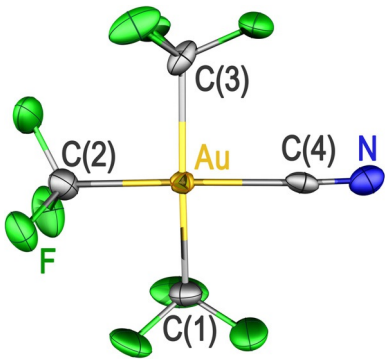

Figure 3. Displacement-ellipsoid diagram (50% probability) of the $[(CF_3)_3AuCN]^-$ anion as found in single crystals of **6** with only one set of C(1)-bound F atoms at half occupancy given. Selected bond lengths [pm] and angles [°] with estimated standard deviations: Au-C(1) 210.0(3), Au-C(2) 206.8(3), Au-C(3) 212.5(3), Au-C(4) 205.9(3), C(4)-N 108.8(3), C(1)-Au-C(2) 90.55(11), C(1)-Au-C(3) 177.03(10), C(1)-Au-C(4) 88.43(10), C(2)-Au-C(3) 90.93(10), C(2)-Au-C(4) 178.50(9), C(3)-Au-C(4) 90.13(9), Au-C(4)-N 177.0(2).

Au–CF_3 bond just discussed render both Au–C bonds similar in length (205.9(3) vs. 206.8(3) pm) despite the contrasting nature of the involved ligands and the different hybridization of the C-donor atom in each case.

All the isolated compounds containing the $(CF_3)_3Au$ moiety (**1** and **3**–**6**) show high thermal stability. They melt without decomposition in the 144–180 °C range (see the Experimental Section). Except for compound **3**,[29] well-defined processes coinciding with the melting point are observed in the corresponding DSC measurements (Figures S6–S9). These are the only significant features appearing before decomposition. A detailed study of the decomposition processes will be presented below, but we consider it appropriate to first explore the reasons underlying the unusual stability experimentally observed, especially considering that the non-fluorinated $[(CH_3)_3AuX]^-$ species are still unknown.

$(CF_3)_3Au$ versus $(CH_3)_3Au$

The $(CH_3)_3Au$ and $(CF_3)_3Au$ fragments are of fundamental importance as prototypical examples of unsaturated species with 14 valence electrons, and for this reason, they have been previously studied at different levels of theory by the research groups of Hoffmann,[3a] Nakamura,[30] and Krossing.[15] In view of the current experimental results, we considered it appropriate to undertake a comparative theoretical study of both $(CX_3)_3Au$ unsaturated species (X = H, F) using the same level of treatment. Aiming to gain a deeper understanding of their analogies and especially of their differences, we undertook calculations of their ground-state stereochemistry as well as of their most basic decomposition pathways.

Stereochemistry

Concerning the ground-state geometry, T-shape structures have been found as the most energetically favored for both $(CX_3)_3Au$ units in line with previous results.[3a, 15, 30] The obtained geometric parameters (Figure 4) are in keeping with the structural data experimentally found for the $[(CF_3)_3AuCN]^-$ anion discussed above. Accordingly, the Au–C bond *trans* to the void (no *trans* influence) is the shortest one in both cases. Besides, the mutually *trans*-standing CX_3 groups do not substantially deviate from linearity (C-Au-C > 170°). A Y-shape structure is also located as an additional local minimum at nearly the same energy for $(CH_3)_3Au$ (Figure 4c), whereas no similar structure was found to be stable in the case of $(CF_3)_3Au$. The extremely low energy profile connecting the Y and T polytopes of $(CH_3)_3Au$ (Figure 5, red trace) indicates that this non-fluorinated fragment is stereochemically labile. In contrast, the T polytope is greatly favored in the fluorinated fragment $(CF_3)_3Au$, which therefore shows a much more pronounced stereochemical stability (Figure 5, blue trace).

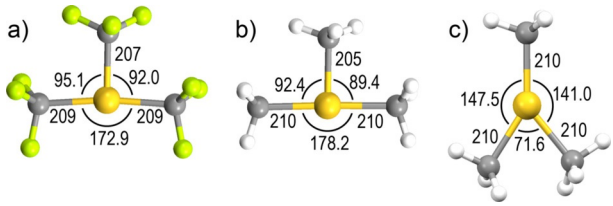

Figure 4. Lower-energy structures for the unsaturated $(CX_3)_3Au$ species in the gas phase as calculated by DFT methods: a) T-shape polytope for X = F (global minimum); b) T-shape polytope for X = H (global minimum); c) Y-shape polytope for X = H (local minimum). Indicated are the most relevant structural parameters: interatomic distances [pm] and angles [°].

It is interesting to note that a symmetric trigonal-planar arrangement would entail degenerate electron configuration for a singlet spin-state (diamagnetic). This system would be unstable and would either evolve into a triplet spin-state or undergo Jahn–Teller distortion to lower-symmetry structures as the aforementioned T or Y polytopes.[31] We have carried out geometry optimizations for both spinomers[32] of the highly symmet-

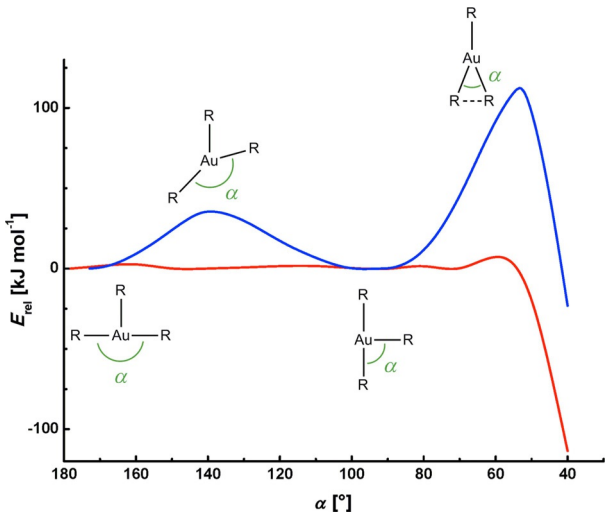

Figure 5. Comparative energy profiles of the R_3Au fragments, R = CH_3 (red trace) and CF_3 (blue trace), as a function of the indicated α angle. Low α values lead to reductive elimination of R–R. Schematic structures depicted above the profile lines refer to transition states (Figure S18) and those depicted below refer to energy minima (Figure 4).

ric trigonal-planar $(CX_3)_3Au$ species, that is, those with triplet and singlet spin-states. For the triplet-spin $(CX_3)_3Au$ spinomers ($S=1$), almost perfect trigonal-planar geometries (Figure 6)

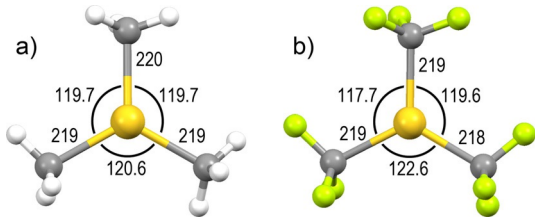

Figure 6. Optimized structures in the gas phase for the triplet-spin $(CX_3)_3Au$ spinomers as calculated by DFT methods: a) X = H; b) X = F. Indicated are the most relevant structural parameters: interatomic distances [pm] and angles [°].

with significantly longer Au–C bond lengths (≈219 pm) were found as well-defined minima at > 110 kJ mol^{-1} over the corresponding ground state. In contrast, no minimum was found for the diamagnetic spinomers ($S=0$). Following our calculations, both trigonal-planar spinomers of $(CX_3)_3Au$ are unfavorable, high-energy species, and hence they should be avoided in any feasible reaction mechanism and/or rearrangement pathway. Although this limitation might be counterintuitive in some instances, it is clear that highly symmetric trigonal-planar arrangements are energetically unaffordable.

Decomposition pathways

Early studies on the decomposition of non-fluorinated neutral $(CH_3)_3AuL$ compounds were carried out by Gilman and Woods ($L=Et_2O$)[2a] and then by Coates and Parkin ($L=PR_3$).[7] Detailed mechanistic studies were later carried out by Kochi,[33] who established that such decompositions follow a dissociative path as indicated in Equation (1). Nakamura also found, by advanced calculations,[30] that dissociation of the neutral ligand was indeed the limiting step in the unimolecular decomposition of $(CH_3)_3Au(PMe_3)$ (gas phase).[34]

For reductive elimination to occur at the unsaturated $(CX_3)_3Au$ units, two CX_3 groups must become sufficiently close as to enable C–C coupling. Following this reaction scheme, we have modeled both $(CX_3)_3Au$ systems by gradually varying the C-Au-C angle formed by two *cis*-standing groups: $90° \geq \alpha \geq 40°$. Aside from this α angle, which represents the reaction coordinate, all other structural parameters have been refined freely (no additional constraints applied). By so doing, we have found that reductive elimination of CH_3–CH_3 at the unsaturated $(CH_3)_3Au$ fragment is a clearly exergonic process with virtually no activation barrier (Figure 5, red trace). In contrast, reductive elimination of CF_3–CF_3 at the fluorinated $(CF_3)_3Au$ species was to require rather high activation energy (Figure 5, blue trace). This contrasting behavior is in line with the stereochemical properties of each fragment discussed above. The low-energy path found for reductive elimination at $(CH_3)_3Au$ is in agreement with its almost fluxional behavior that should enable the mutual approaching of two CH_3 groups with little energy cost. The marked preference of the fluorinated $(CF_3)_3Au$ fragment for a T-shape geometry should, in turn, result in substantial energy expenditure to bring two CF_3 groups together.

Another important factor governing the stability of the R_3Au systems towards R–R elimination seems to be the electronegativity of the R substituent as clearly illustrated within the series of monomeric gold(III) halides AuX_3. The lightest species, AuF_3, was found to exhibit a T-shape structure in the gas phase by electron diffraction[35] and by computational methods.[35,36] Evidence of similar geometries in matrix-trapped AuF_3 and $AuCl_3$ molecules has been recently obtained.[37] In contrast, the global minimum found for the heavier halide, AuI_3, is best formulated as an adduct of the reduced iodide AuI with an end-on iodine molecule, $IAu(I_2)$.[36] This trend found with typical $(\sigma+\pi)$-donor ligands is also paralleled in the following series of mainly σ-donor ligands (electronegativity values in parentheses): CF_3 (3.49), CH_3 (2.28) and H (2.20).[38] We have seen that $(CF_3)_3Au$ is less prone to undergo reductive elimination than $(CH_3)_3Au$, and much less so than AuH_3. The latter is, in fact, best formulated as a dihydrogen adduct of gold(I) hydride, $HAu(H_2)$.[39] It becomes apparent that reductive elimination is so much favored with the least electronegative substituents in both series that neither hydride nor iodide are able to stabilize the corresponding high-valent species AuH_3 or AuI_3.[40]

Thermolytic studies on the anionic derivatives of $(CF_3)_3Au$

We carried out detailed thermolytic studies on the isolated compounds under two related but quite different experimental conditions: in the gas phase and in the condensed phase. These conditions ensure that the results obtained are intrinsic of each substance and therefore independent of any kind of solvent. They also enable the distinction between inter- and intramolecular decomposition pathways.

Unimolecular thermolyses in the gas phase[41]

The anionic $[(CF_3)_3AuX]^-$ derivatives (X = F, Cl, Br, I, CN) were studied by tandem mass spectrometry (ESI-CID-MS^2; see the Experimental Section). Given their simple stoichiometry and the homologous character of the X ligand, these $[R_3AuX]^-$ anions form an ideal set for the study of the mechanism of their unimolecular thermal decomposition as a function of just a single variable, X. Moreover, they are charged species and therefore easily brought into the gas-phase by electrospray ionization (ESI). The $[(CF_3)_3AuX]^-$ anions were selectively confined in an ion trap and thermally excited by intensive collision with an inert gas (He). The energetic experimental conditions required to induce fragmentation in the parent ions give an indication of their intrinsic stability. The ionic fragments formed by collision-induced dissociation (CID) were detected in the second stage of the experiment (MS^2). These experimental conditions ensure that only intramolecular decomposition pathways operate. The results obtained (given in the Supporting Information) are consistent with the general decomposition pattern shown in Scheme 3, although significant variations apply to each particular case.

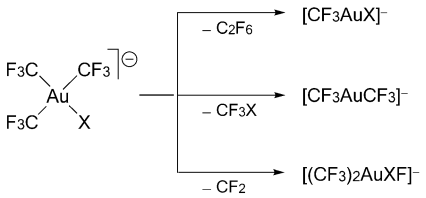

Scheme 3. Primary intramolecular decomposition paths experimentally observed by tandem mass spectrometry on the anionic species $[(CF_3)_3AuX]^-$ (X = F, Cl, Br, I, CN) with significant variations applying to each particular case.

Two primary fragmentation paths involve reductive elimination of C_2F_6 or CF_3X giving rise to the organogold(I) species $[CF_3AuX]^-$ and $[CF_3AuCF_3]^-$, respectively. These are the main mechanisms operating in the decomposition of the iodo-derivative **1** (Figure 7). It is worth noting that elimination of C_2F_6 is largely favored over that of CF_3X in all cases. In fact, in all other halo-complexes, little CF_3X is eliminated, and in the cyano complex **6**, elimination of CF_3CN was not observed at all (Figures S3–S5).

The unimolecular decomposition of the fluoro-derivative **3** sharply differs from its heavier homologues. In this case, the main fragmentation path involves CF_2 extrusion, whereby the organogold(III) difluoride $[(CF_3)_2AuF_2]^-$ is formed (Figure 8). This non-reductive fragmentation path (Scheme 3) is less important in the cyano complex **6** (Figure S5), operates just marginally in the chloro- and bromo-derivatives **4** and **5** (Figures S3 and S4) and is virtually absent in the iodo-derivative **1** (Figure 7).

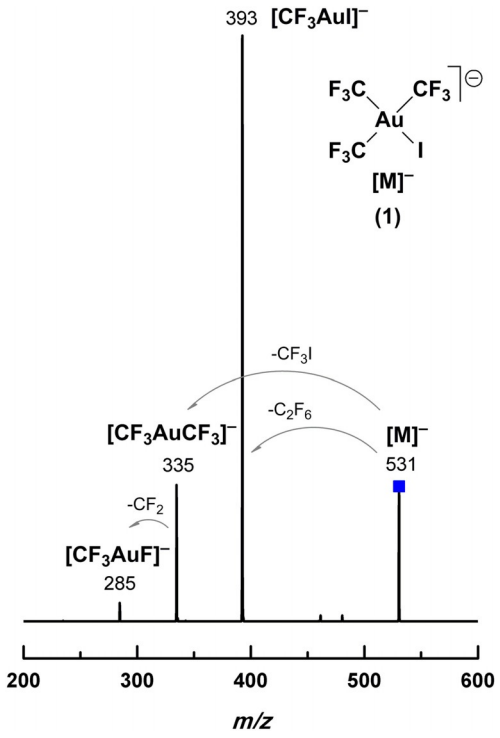

Figure 7. Quadrupole ion-trap MS^2 results of the collision-induced dissociation of the anion of **1** (labeled $[M]^-$).

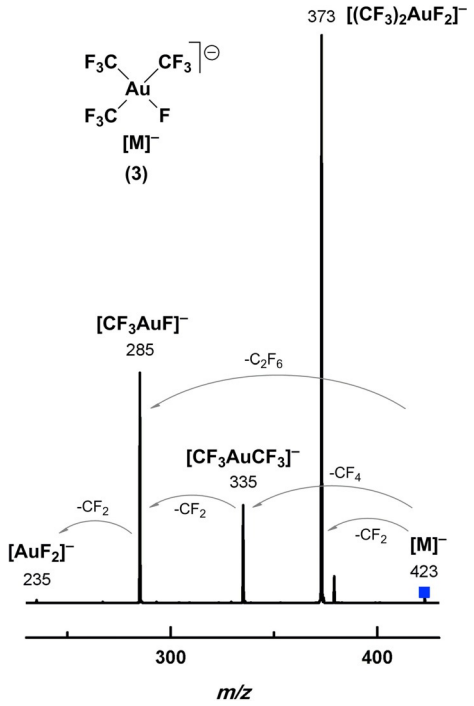

Figure 8. Quadrupole ion-trap MS^2 results of the collision-induced dissociation of the anion of **3** (labeled $[M]^-$).

Extrusion of CF_2 also takes place at secondary stages of decomposition. Thus, the organogold(I) species $[CF_3AuX]^-$ formed by C_2F_6 elimination, undergo CF_2 extrusion giving rise to tiny amounts of the $[FAuX]^-$ fluorides. This fragmentation path has been recently reported to occur on pure samples of $[PPh_4]$-$[CF_3AuX]$.[42] Also, the symmetric $[FAuF]^-$ difluoride has been recently detected to arise as a minor product in the decarboxylation of $[Au(OAc^F)_2]^-$ in the gas phase.[43]

It becomes clear that, except for the fluoro-complex **3**, the main decomposition path in the series of anionic $[(CF_3)_3AuX]^-$ derivatives involves C_2F_6 elimination. This kind of elimination has been assessed as a high-energy process in the naked $(CF_3)_3Au$ fragment, following our calculations presented above. It is worth noting, however, that the experimental conditions for these unimolecular decompositions to occur are highly energetic.

Thermolyses in the condensed phase

The stability of all the anionic compounds containing the $(CF_3)_3Au$ moiety (**1** and **3**–**6**) was checked by thermogravimetric and differential thermal analysis (TGA/DTA) of the corresponding solid samples. The results are given in the Supporting Information (Figures S10–S14). All these compounds show unusual stability. The most stable species is the cyano-derivative **6**, which decomposes at 350 °C. Even the fluoro-derivative **3** shows remarkable stability for an organogold fluoride, as it decomposes at 267 °C. The least stable of the ionic $[PPh_4]$-$[(CF_3)_3AuX]$ compounds is the iodo-complex **1**, decomposing at 245 °C.

Once the decomposition temperature was determined by TGA/DTA, the halide compounds were thermolyzed in sealed tubes under an inert atmosphere (Ar), and their decomposition products were analyzed by ^{19}F NMR spectroscopy with the aid of MS. It is worth noting that no C_2F_6 was detected in any of these bulk thermolyses, in contrast with the results observed in the gas phase. Decomposition of the iodo-derivative **1** at 250 °C (Figure S15) produces CF_3I together with $[CF_3AuCF_3]^-$ as required for the reductive elimination indicated in Scheme 4a.

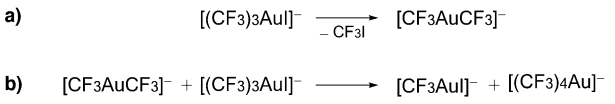

Scheme 4. Intermolecular decomposition paths observed upon thermolysis of **1** in condensed phase (Figure S15): a) reductive elimination, and b) ligand exchange. The result of the separate process (b) is given in Figure S16.

Since this process occurs to just a minor extent in the gas phase (Figure 7), it is reasonable to conclude that intermolecular paths operate in the condensed phase. Evidence for the involvement of intermolecular processes is further supplied by the presence of additional trifluoromethyl-gold derivatives among the decomposition products, namely $[(CF_3)_4Au]^-$ and $[CF_3AuI]^-$ (Figure S15). The latter compound cannot arise by reductive elimination of C_2F_6 from the starting product **1** since C_2F_6 is totally absent; its occurrence might rather be explained as the result of the exchange process given in Scheme 4b, whereby the homoleptic organogold(I) derivative $[CF_3AuCF_3]^-$ acts as a trifluoromethylating agent towards the iodo-derivative **1**. This intermolecular exchange process is made possible by the fact that it takes place at a temperature above the melting points of both compound **1** (m.p. 171 °C) and $[PPh_4]$-$[CF_3AuCF_3]$ (m.p. 193 °C),[14] thus enabling fluid contact between the relevant organogold units. Exchange was further confirmed by heating an equimolar mixture of the reagents involved at 200 °C (Figure S16), that is, well below the onset of decomposition of compound **1**.

Related exchange processes are known to occur in solution by reaction of various gold(III) halide complexes with more active trifluoromethylating agents such as $(CF_3)_2Cd{\cdot}dme$.[13,18c] Also, in non-fluorinated methylgold systems, exchange between $[Au^{III}]$-X and $[Au^{I}]$-CH_3 units in solution are well documented.[44] Nevertheless, the process given in Scheme 4b is quite singular because it takes place in the melt and leads to the full-substituted $[(CF_3)_4Au]^-$ species (Figure S16).

A feature common to all the thermolyses under study is the appearance of variable amounts of metallic gold. Although the fate of the corresponding CF_3 groups cannot be easily ascertained, the presence of the fluorosilicate anion $[SiF_5]^-$ ($\delta_F = -139$ ppm; $^1J(^{19}F,^{21}Si) = 146$ Hz)[45] denotes formation of highly active species, able to attack the vessel glass. Some CF_3H is usually observed. Moreover, trifluoromethylation of the cation at one or two positions of the phenyl rings was observed, as clearly evidenced by the appropriate mass increase in the MS (Figure S17). These trifluoromethylation processes, however, are non-regioselective giving rise to various singlets in the suitable region of the ^{19}F NMR spectrum (ca. −63 ppm).[46]

Conclusions

The organogold(III) compound $[PPh_4][(CF_3)_3AuI]$ (**1**) was cleanly obtained by photoinduced oxidative addition of CF_3I to the organogold(I) precursor $[PPh_4][CF_3AuCF_3]$. This high-yield synthesis, carried out under mild conditions, makes compound **1** a convenient entry to the chemistry of the perfluorinated $(CF_3)_3Au$ fragment. Thus, the anionic $[PPh_4][(CF_3)_3AuX]$ halide complexes [X = F (**3**), Cl (**4**), Br (**5**)] have been obtained therefrom by simple, high-yield methods. The family of anionic halides was completed with the pseudo-halide complex $[PPh_4]$-$[(CF_3)_3AuCN]$ (**6**). Some of these chemical species had been previously detected in solution by Willner and his co-workers, who correctly and competently assigned their NMR spectroscopic properties.[17] Once isolated, this series of compounds provides a complete and homogeneous set most suited for comparative studies. All of them are robust species with unusually high stability: their decomposition temperatures range from 245 °C for the iodo-derivative **1** to 350 °C for the cyano-complex **6**. This unusual stability is a remarkable feature, especially considering that no analogous $[(CH_3)_3AuX]^-$ complex with the non-fluorinated methyl group is currently known.

In order to ascertain the reasons underlying this contrasting difference, the most fundamental properties of the isoleptic $(CH_3)_3Au$ and $(CF_3)_3Au$ fragments were studied by theoretical methods, namely their stereochemistry and their tendency to undergo reductive elimination. The naked $(CF_3)_3Au$ fragment was found to exhibit a T-shape structure as the most energetically favored (Figure 4a). This fragment was found to be configurationally stable and shows a sizable energy barrier (≈ 110 kJ mol^{-1}) for reductive elimination (Figure 5, blue trace). In contrast, the non-fluorinated $(CH_3)_3Au$ moiety was found to be stereochemically labile and to undergo almost barrierless reductive elimination (Figure 5, red trace).

The thermal decomposition of all these $[PPh_4][(CF_3)_3AuX]$ compounds was carefully examined both in the gas phase (MS^2) and in the bulk (TGA/DTA). Sharply different decomposition mechanisms were identified depending on the aggregation state. Thus, high-energy processes operate at the unimolecular level (gas phase), whereas lower-energy intermolecular pathways are open in the condensed phase (bulk). Collision-induced dissociation of the $[(CF_3)_3AuF]^-$ anion in the gas phase proceeds mainly under CF_2 extrusion giving rise to the organogold(III) difluoride $[(CF_3)_2AuF_2]^-$ (Figure 8). Finally, the homoleptic organogold(I) derivative $[CF_3AuCF_3]^-$ was identified as a thermally robust trifluoromethylating agent able to operate in the condensed phase under solvent-free conditions.

In summary, the most fundamental properties of the perfluorinated $(CF_3)_3Au$ species have been examined by theoretical methods. The anionic complexes of this unsaturated 14-electron fragment with the whole series of halides (including fluoride), $[PPh_4][(CF_3)_3AuX]$, have been isolated and their decomposition paths thoroughly studied. The involvement of in-

termolecular processes in bulk systems is demonstrated even in solvent-free reaction media.

Experimental Section

General procedures and materials

Unless otherwise stated, the reactions and manipulations were carried out under purified argon using Schlenk techniques. Solvents were dried using an MBraun SPS-800 System. Compound $[PPh_4][CF_3AuCF_3]$ was obtained as described elsewhere.[14] Samples of AgCl and AgBr were prepared by precipitation from aqueous $AgNO_3$ solutions with the corresponding halide. Other chemicals were purchased from standard commercial suppliers and were used as received. Elemental analyses were carried out by using a PerkinElmer 2400 CHNS/O Series II microanalyzer. IR spectra were recorded on neat solid samples using a PerkinElmer Spectrum FT-IR spectrometer (4000–250 cm^{-1}) equipped with an ATR device. Standard mass spectra (MS) were registered by MALDI-TOF techniques on Bruker MicroFlex or AutoFlex spectrometers. ^{19}F NMR spectra were recorded at room temperature on Bruker ARX 300 or AV 400 spectrometers. Chemical shifts (δ_F in ppm) are given with respect to $CFCl_3$. Chemically inequivalent CF_3 groups are indicated as follows: CF_3-Au-CF_3 refers to the mutually *trans*-standing CF_3 groups (q = quartet), whereas CF_3-Au-X refers to the CF_3 group *trans* to the anionic X ligand (spt = septet). Thermogravimetric and differential thermal analyses (TGA/DTA) were performed under N_2 atmosphere on powder samples (2–5 mg) in open platinum holders at heating rate of 10 °C min^{-1} using a SDT 2960 instrument. Differential scanning calorimetry (DSC) experiments were performed using a DSC Q-2000 from TA instruments with powder samples (2–5 mg) in sealed aluminum holders at a heating rate of 10 °C min^{-1}. Melting points were taken at the maximum of the DSC peak and verified by visual inspection of samples placed on glass plates using an Olympus BH-2 microscope fitted with a Linkam TMS-91 temperature controller with hot stage.

Synthesis of $[PPh_4][(CF_3)_3AuI]$ (1)

Method A: A 1.857 M solution of CF_3I in *n*-hexane (2.40 cm^3, 4.45 mmol) was added to a MeCN solution (10 cm^3) of $[PPh_4][CF_3AuCF_3]$ (0.50 g, 0.74 mmol) and the mixture was stirred at room temperature in the dark for 4 days. The reaction mixture was then evaporated to dryness. Treatment of the resulting residue with *i*PrOH (3 cm^3) at −30 °C rendered a white solid which was filtered, washed with Et_2O (3×3 cm^3), vacuum dried and identified as compound **1** (0.58 g, 0.67 mmol, 90% yield). M.p. 171 °C; latent heat of fusion: $\Delta H = 34.0$ kJ mol^{-1} (Figure S6). ^{19}F NMR (Figure 1: 376.308 MHz, CD_2Cl_2): $\delta_F = -26.09$ (q, $^4J(F,F) = 7.2$ Hz, 6F, CF_3-Au-CF_3), −31.46 ppm (spt, 3F, CF_3-Au-X). IR: $\tilde{\nu} = 3057$ (w), 1588 (w), 1485 (m), 1435 (s), 1341 (w), 1316 (w), 1191 (w), 1162 (w), 1146 (s), 1098 (vs), 1064 (vs), 1045 (vs), 996 (s), 977 (m), 928 (m), 846 (w), 749 (m), 719 (vs), 686 (vs), 616 (w), 522 (vs), 453 (m), 335 (w), 303 (m), 289 (m), 277 cm^{-1} (m). MS (MALDI−): *m/z*: 531 $[(CF_3)_3AuI]^-$, 393 $[CF_3AuI]^-$, 335 $[CF_3AuCF_3]^-$. Elemental analysis calcd (%) for $C_{27}H_{20}AuF_9IP$: C 37.26, H 2.32; found: C 36.89, H 2.36.

Method B: A 1.857 M solution of CF_3I in *n*-hexane (48 mm^3, 90 μmol) was added to a MeCN solution (0.5 cm^3) of $[PPh_4][CF_3AuCF_3]$ (10 mg, 15 μmol) in a quartz tube. After 10 min exposure to sunlight, quantitative transformation to the final product was confirmed by ^{19}F NMR spectroscopy.

Oxidative addition of nBu^{F}I to $[PPh_4][CF_3AuCF_3]$

nC_4F_9I (15 mm^3, 90 μmol) was added to a MeCN solution (0.5 cm^3) of $[PPh_4][CF_3AuCF_3]$ (10 mg, 15 μmol) in a quartz tube and exposed to sunlight for 10 min. The resulting mixture was evaporated to dryness and the residue redissolved in CD_2Cl_2, being identified as $[PPh_4][trans\text{-}(n\text{Bu}^F)(CF_3)_2AuI]$ (**2**). ^{19}F NMR (Figure S1: 376.308 MHz, CD_2Cl_2): $\delta_F = -24.51$ (tt, $^4J(F,F) = 11.5$ Hz, $^5J(F,F) = 7.9$ Hz, 6F; Au-CF_3), −81.27 (tt, $^3J(F,F) \approx 0$ Hz, $^4J(F,F) = 10.1$ Hz, $^5J(F,F) = 2.9$ Hz, 3F; CF_2CF_3), −84.60 (br, 2F; α-CF_2), −114.76 (br, 2F; β-CF_2), −126.65 ppm (m_c, 2F; γ-CF_2).

Synthesis of $[PPh_4][(CF_3)_3AuF]$ (3)

Method A: A mixture of compound **1** (0.10 g, 0.11 mmol) and AgF (44 mg, 0.34 mmol) in CH_2Cl_2 (10 cm^3) was stirred in the dark for 1 h. The resulting suspension was filtered through high-quality diatomite so as to separate the silver halides. The colorless filtrate was evaporated to dryness. Treatment of the residue with Et_2O (3 cm^3) rendered a white solid, which was filtered, vacuum dried and identified as compound **3** (70 mg, 92 μmol, 80%). M.p. 180 °C. ^{19}F NMR (Figure 2: 282.231 MHz, CD_2Cl_2): $\delta_F = -28.58$ (dspt, $^3J(F,F) = 55.8$, $^4J(F,F) = 5.8$ Hz, 3F, CF_3-Au-X), −41.09 (dq, $^3J(F,F) = 12.3$, 6F, CF_3-Au-CF_3), −254.41 ppm (qspt, 1F, Au-F). IR: $\tilde{\nu} = 3062$ (w), 3024 (w), 1588 (w), 1486 (m), 1435 (s), 1392 (w), 1342 (w), 1319 (w), 1189 (w), 1174 (s), 1153 (w), 1118 (s), 1107 (vs), 1084 (vs), 1070 (vs), 1049 (vs), 996 (s), 932 (w), 884 (m), 849 (w), 797 (w), 776 (w), 752 (s), 720 (vs), 688 (vs), 616 (w), 524 (vs), 511 (vs), 479 (m), 449 (m), 399 (w), 338 (w), 312 (s), 303 (m), 277 (w), 269 cm^{-1} (w). MS: no clear peaks were detected by using either positive or negative MALDI techniques. Elemental analysis calcd (%) for $C_{27}H_{20}AuF_{10}P$: C 42.54, H 2.64; found: C 42.55, H 2.49.

Method B: To a CH_2Cl_2 solution (5 cm^3) of compound **1** (50 mg, 57 μmol) at 0 °C was added XeF_2 (4.9 mg, 29 μmol) and the mixture was stirred at that temperature for 1 h. The resulting red solution was then evaporated to dryness. After washing the brown residue with *n*-hexane (4×5 cm^3), it was redissolved in CH_2Cl_2 (5 cm^3) still at 0 °C. A second treatment with an additional portion of XeF_2 (4.9 mg, 29 μmol) and identical workup, afforded a white solid, which was identified as compound **3** (33 mg, 43 μmol, 75% yield).

Synthesis of $[PPh_4][(CF_3)_3AuCl]$ (4)

A mixture of compound **1** (0.10 g, 0.11 mmol) and AgCl (49 mg, 0.34 mmol) in Me_2CO (10 cm^3) was stirred in the dark for 1 h. The suspension was then filtered through high-quality diatomite so as to separate the silver halides. The resulting colorless solution was evaporated to dryness. Treatment of the residue with Et_2O (3 cm^3) rendered a white solid, which was filtered, vacuum dried and identified as compound **4** (67 mg, 86 μmol, 75%). M.p. 162 °C; latent heat of fusion: $\Delta H = 35.0$ kJ mol^{-1} (Figure S7). ^{19}F NMR (376.308 MHz, CD_2Cl_2): $\delta_F = -29.34$ (spt, $^4J(F,F) = 6.9$ Hz, 3F, CF_3-Au-X), −34.89 ppm (q, 6F, CF_3-Au-CF_3). IR: $\tilde{\nu} = 3062$ (w), 3029 (w), 1588 (w), 1486 (m), 1442 (m), 1436 (s), 1391 (w), 1342 (w), 1319 (w), 1189 (w), 1158 (s), 1102 (vs), 1074 (vs), 1048 (vs), 1026 (s), 997 (s), 982 (m), 932 (w), 855 (w), 848 (w), 751 (s), 719 (vs), 687 (vs), 616 (w), 523 (vs), 455 (m), 438 (w), 394 (w), 341 (vs, Au–Cl), 298 (m), 262 cm^{-1} (m). MS (MALDI−): *m/z*: 439 $[(CF_3)_3AuCl]^-$. Elemental analysis calcd (%) for $C_{27}H_{20}AuClF_9P$: C 41.64, H 2.59; found: C 41.25, H, 2.49.

Synthesis of $[PPh_4][(CF_3)_3AuBr]$ (5)

By using the procedure just described for synthesizing compound **4**, compound **5** was prepared starting from compound **1** (0.10 g, 0.11 mmol) and AgBr (65 mg, 0.34 mmol). Complex **5** was obtained as a white solid (68 mg, 83 μmol, 72% yield). M.p. 159 °C; latent heat of fusion: $\Delta H = 35.7$ kJ mol^{-1} (Figure S8). ^{19}F NMR (376.308 MHz, CD_2Cl_2): $\delta_F = -29.80$ (spt, ^4J(F,F) = 7.1 Hz, 3F, CF_3-Au-X), −31.79 ppm (q, 6F, CF_3-Au-CF_3). IR: $\tilde{\nu} = 3059$ (w), 1589 (w), 1485 (m), 1436 (s), 1390 (w), 1342 (w), 1318 (w), 1191 (w), 1154 (s), 1103 (vs), 1075 (vs), 1049 (vs), 996 (s), 978 (m), 929 (w), 852 (w), 848 (w), 750 (m), 720 (vs), 687 (vs), 616 (w), 524 (vs), 454 (w), 310 (m), 296 (m), 269 cm^{-1} (w). MS (MALDI−): *m/z*: 484 $[(CF_3)_3AuBr]^-$. Elemental analysis calcd (%) for $C_{27}H_{20}AuBrF_9P$: C 39.39, H 2.45; found: C 39.26, H 2.38.

Synthesis of $[PPh_4][(CF_3)_3AuCN]$ (6)

To a Me_2CO solution (10 cm^3) of compound **1** (0.20 g, 0.23 mmol) was added KCN (15 mg, 0.23 mmol) and the resulting mixture was stirred at room temperature for 18 h. The white suspension was then evaporated to dryness and the resulting residue was treated with CH_2Cl_2 (5 cm^3). The new suspension was filtered through high-quality diatomite and the colorless filtrate was evaporated to dryness. Treatment of the resulting residue with cold Et_2O (5 cm^3) rendered a white solid which was filtered, washed with *n*-hexane, vacuum dried, and identified as compound **6** (92 mg, 0.12 mmol, 52% yield). M.p. 144 °C; latent heat of fusion: $\Delta H = 29.2$ kJ mol^{-1} (Figure S9). ^{19}F NMR (376.308 MHz, CD_2Cl_2): $\delta_F = -30.07$ (q, ^4J(F,F) = 6.1 Hz, 6F, CF_3-Au-CF_3), −34.15 ppm (spt, 3F, CF_3-Au-X). IR: $\tilde{\nu} = 3063$ (w), 1588 (w), 1486 (m), 1444 (m), 1436 (s), 1394 (w), 1343 (w), 1318 (w), 1190 (w), 1162 (s), 1104 (vs), 1087 (s), 1059 (vs), 997 (s), 984 (m), 956 (m), 935 (w), 851 (w), 752 (s), 719 (vs), 688 (vs), 616 (w), 523 (vs), 456 (w), 425 (s), 291 (s), 271 cm^{-1} (w); C≡N vibration is not observed probably due to poor intensity. MS (MALDI−): *m/z*: 430 $[(CF_3)_3AuCN]^-$, 292 $[CF_3AuCN]^-$. Elemental analysis calcd (%) for $C_{28}H_{20}AuF_9NP$: C 43.71, H 2.62, N 1.82; found: C 43.53, H 2.57, N 1.79. Crystals suitable for X-ray diffraction analysis were obtained by slow diffusion of a layer of *n*-hexane (10 cm^3) into a solution of compound **6** (10 mg) in CH_2Cl_2 (3 cm^3) at 4 °C.

Crystallographic details

Crystal data and other details of the structure analysis are presented in Table S1. Crystals of **6** were obtained as indicated in the appropriate experimental entry. A parallelepiped-like single crystal was mounted in a quartz fiber in a random orientation and held in place with fluorinated oil. Data collection was performed at 100 K on an Oxford diffraction Xcalibur CCD diffractometer using graphite monochromated Mo-Kα radiation ($\lambda = 71.073$ nm) with a nominal crystal to detector distance of 5.0 cm. Unit cell dimensions were determined from the positions of 22 502 reflections from the main dataset. The diffraction frames were integrated and corrected for absorption by using the Crysalis RED package.[47] Lorentz and polarization corrections were applied.

The structure was solved by direct methods. All non-H atoms were assigned anisotropic displacement parameters. The positions of the H atoms were constrained to idealized geometries and assigned isotropic displacement parameters equal to 1.2 times the U_{iso} values of their respective parent atoms. In one of the CF_3 groups the F atoms are disordered over two positions which were refined with 0.5 partial occupancy. The structure was refined using the SHELXL-97 program.[48]

CCDC 1477038 contains the supplementary crystallographic data for this paper. These data are provided free of charge by The Cambridge Crystallographic Data Centre.

Tandem mass spectrometry (MS^2)

ESI-ion trap mass spectra were recorded on a Bruker Esquire 3000+ spectrometer (Bruker Daltonics). Analyses were carried out in negative ion mode, with Smart Parameter Settings optimized for each *m/z* value. The nebulizer (N_2) gas pressure, drying gas (N_2) flow rate and drying gas temperature were kept at 0.7 bar, 4.0 dm^3 min^{-1} and 350 °C, respectively. Spectra were acquired in the *m/z* 50–1000 range, and the mass axis was externally calibrated with a tuning mix (from Agilent Technologies). The 5 ppm solutions of the samples were transferred into the ESI source by means of a syringe pump at a flow rate of 4 mm^3 min^{-1}. ESI-CID-MS^2 analysis was carried out by using He as the collision gas, an optimal amplitude voltage of 1.9 V and an isolation width for the precursor ion of 5 *m/z* units.

Thermolyses in the condensed phase

Each sample (5 mg) was sealed in a glass tube under an inert atmosphere (Ar) and heated for a few minutes at a temperature slightly above that corresponding to the onset of decomposition (TGA/DTA). The soluble fluorinated species were identified by ^{19}F NMR spectroscopy with the aid of MS. Details are given in the Supporting Information.

Computational details

Quantum mechanical calculations were performed with the Gaussian 09[49] package at the DFT/M06 level of theory. SDD basis set and its ECP's were used to describe Au atoms together with additional f-type polarization functions. Light atoms (H, C and F) were described with a 6-31G** basis set. See Supporting Information for full details.

Acknowledgements

This work was supported by the Spanish MINECO/FEDER (Project CTQ2015-67461-P), and the Gobierno de Aragón and Fondo Social Europeo (Grupo Consolidado E21: Química Inorgánica y de los Compuestos Organometálicos). The Instituto de Biocomputación y Física de Sistemas Complejos (BIFI) and the Centro de Supercomputación de Galicia (CESGA) are gratefully acknowledged for generous allocation of computational resources. A.P.-B. thanks the Spanish Ministerio de Educación, Cultura y Deporte for a grant (FPU15/03940).

Conflict of interest

The authors declare no conflict of interest.

Keywords: gold · mass spectrometry · organogold chemistry · photoinitiated oxidative addition · trifluoromethyl compounds

[1] a) W. J. Pope, C. S. Gibson, *J. Chem. Soc. Trans.* **1907**, *91*, 2061; b) W. J. Pope, C. S. Gibson, *Proc. Chem. Soc. London* **1907**, *23*, 245.
[2] a) H. Gilman, L. A. Woods, *J. Am. Chem. Soc.* **1948**, *70*, 550; b) L. A. Woods, H. Gilman, *Proc. Iowa Acad. Sci.* **1943**, *49*, 286.

[3] a) S. Komiya, T. A. Albright, R. Hoffmann, J. K. Kochi, *J. Am. Chem. Soc.* **1976**, *98*, 7255; b) A. Tamaki, S. A. Magennis, J. K. Kochi, *J. Am. Chem. Soc.* **1974**, *96*, 6140; c) A. Tamaki, S. A. Magennis, J. K. Kochi, *J. Am. Chem. Soc.* **1973**, *95*, 6487.
[4] a) J. Stein, J. P. Fackler, Jr., C. Paparizos, H. W. Chen, *J. Am. Chem. Soc.* **1981**, *103*, 2192; b) J. P. Fackler, Jr., C. Paparizos, *J. Am. Chem. Soc.* **1977**, *99*, 2363; c) H. Schmidbaur, R. Franke, *Inorg. Chim. Acta* **1975**, *13*, 79.
[5] a) R. J. Puddephatt, P. J. Thompson, *J. Chem. Soc. Dalton Trans.* **1975**, 1810; b) A. Johnson, R. J. Puddephatt, *J. Organomet. Chem.* **1975**, *85*, 115.
[6] a) C. F. Shaw, R. S. Tobias, *Inorg. Chem.* **1973**, *12*, 965; b) H. Schmidbaur, A. Shiotani, *Chem. Ber.* **1971**, *104*, 2821; c) B. J. Gregory, C. K. Ingold, *J. Chem. Soc. B* **1969**, 276.
[7] G. E. Coates, C. Parkin, *J. Chem. Soc.* **1963**, 421.
[8] a) H. Schmidbaur, A. Grohmann, E. Olmos, in *Gold: Progress in Chemistry, Biochemistry and Technology* (Ed.: H. Schmidbaur), Wiley, Chichester, **1999**, pp. 647–746; b) H. Schmidbaur, A. Grohmann, M. E. Olmos, A. Schier, in *The Chemistry of Organic Derivatives of Gold and Silver* (Eds.: S. Patai, Z. Rappoport), belonging to the series *Patai's Chemistry of Functional Groups*, Wiley, Chichester, **1999**, pp. 227–311; c) G. K. Anderson, *Adv. Organomet. Chem.* **1982**, *20*, 39; d) H. Schmidbaur, *Au: Organogold Compounds, in Gmelin-Handbuch der Anorganischen Chemie*, 8th ed., Springer, Berlin, **1980**; e) B. Armer, H. Schmidbaur, *Angew. Chem. Int. Ed. Engl.* **1970**, *9*, 101; *Angew. Chem.* **1970**, *82*, 120.
[9] Various salts of the homoleptic $[(CH_3)_4Au]^-$ anion are also known, which can be considered as a $[(CH_3)_3AuR]^-$ derivative with $R=CH_3$: a) D. Zhu, S. V. Lindeman, J. K. Kochi, *Organometallics* **1999**, *18*, 2241; b) S. Komiya, S. Ochiai, Y. Ishizaki, *Inorg. Chem.* **1992**, *31*, 3168; c) S. Komiya, T. A. Albright, R. Hoffmann, J. K. Kochi, *J. Am. Chem. Soc.* **1977**, *99*, 8440; d) G. W. Rice, R. S. Tobias, *Inorg. Chem.* **1976**, *15*, 489; e) G. W. Rice, R. S. Tobias, *Inorg. Chem.* **1975**, *14*, 2402.
[10] a) R. C. Walroth, J. T. Lukens, S. N. MacMillan, K. D. Finkelstein, K. M. Lancaster, *J. Am. Chem. Soc.* **2016**, *138*, 1922; b) A. M. Romine, N. Nebra, A. I. Konovalov, E. Martin, J. Benet-Buchholz, V. V. Grushin, *Angew. Chem. Int. Ed.* **2015**, *54*, 2745; *Angew. Chem.* **2015**, *127*, 2783; c) J. Gil-Rubio, J. Vicente, *Dalton Trans.* **2015**, *44*, 19432; d) M. A. García-Monforte, S. Martínez-Salvador, B. Menjón, *Eur. J. Inorg. Chem.* **2012**, 4945.
[11] Selected Reviews: a) Y. Zhou, J. Wang, Z. Gu, S. Wang, W. Zhu, J. L. Aceña, V. A. Soloshonok, K. Izawa, H. Liu, *Chem. Rev.* **2016**, *116*, 422; b) F. Meyer, *Chem. Commun.* **2016**, *52*, 3077; c) A. Prieto, O. Baudoin, D. Bouyssi, N. Monteiro, *Chem. Commun.* **2016**, *52*, 869; d) S.-M. Wang, J.-B. Han, C.-P. Zhang, H.-L. Qin, J.-C. Xiao, *Tetrahedron* **2015**, *71*, 7949; e) C. Alonso, E. Martínez de Marigorta, G. Rubiales, F. Palacios, *Chem. Rev.* **2015**, *115*, 1847; f) X. Liu, C. Xu, M. Wang, Q. Liu, *Chem. Rev.* **2015**, *115*, 683; g) J. Charpentier, N. Früh, A. Togni, *Chem. Rev.* **2015**, *115*, 650; h) H. Egami, M. Sodeoka, *Angew. Chem. Int. Ed.* **2014**, *53*, 8294; *Angew. Chem.* **2014**, *126*, 8434; i) J. Wang, M. Sánchez-Roselló, J. L. Aceña, C. del Pozo, A. E. Sorochinsky, S. Fustero, V. A. Soloshonok, H. Liu, *Chem. Rev.* **2014**, *114*, 2432; j) E. Merino, C. Nevado, *Chem. Soc. Rev.* **2014**, *43*, 6598; k) S. Barata-Vallejo, B. Lantaño, A. Postigo, *Chem. Eur. J.* **2014**, *20*, 16806; l) P. Gao, X.-R. Song, X.-Y. Liu, Y.-M. Liang, *Chem. Eur. J.* **2015**, *21*, 7648; m) W. Zhu, J. Wang, S. Wang, Z. Gu, J. L. Aceña, K. Izawa, H. Liu, V. A. Soloshonok, *J. Fluorine Chem.* **2014**, *167*, 37; n) G. Landelle, A. Panossian, S. Pazenok, J.-P. Vors, F. R. Leroux, *Beilstein J. Org. Chem.* **2013**, *9*, 2476; o) T. Liang, C. N. Neumann, T. Ritter, *Angew. Chem. Int. Ed.* **2013**, *52*, 8214; *Angew. Chem.* **2013**, *125*, 8372; p) H. Liu, Z. Gu, X. Jiang, *Adv. Synth. Catal.* **2013**, *355*, 617; q) P. Chen, G. Liu, *Synthesis* **2013**, 2919; r) T. Besset, C. Schneider, D. Cahard, *Angew. Chem. Int. Ed.* **2012**, *51*, 5048; *Angew. Chem.* **2012**, *124*, 5134; s) X.-F. Wu, H. Neumann, M. Beller, *Chem. Asian J.* **2012**, *7*, 1744; t) Y. Ye, M. S. Sanford, *Synlett* **2012**, 2005; u) Z. Jin, G. B. Hammond, B. Xu, *Aldrichimica Acta* **2012**, *45* (3), 67; v) D. A. Nagib, D. W. C. MacMillan, *Nature* **2011**, *480*, 224; w) A. T. Parsons, S. L. Buchwald, *Nature* **2011**, *480*, 184; x) T. Furuya, A. S. Kamlet, T. Ritter, *Nature* **2011**, *473*, 470; y) O. A. Tomashenko, V. V. Grushin, *Chem. Rev.* **2011**, *111*, 4475; z) J. Nie, H.-C. Guo, D. Cahard, J.-A. Ma, *Chem. Rev.* **2011**, *111*, 455; aa) R. J. Lundgren, M. Stradiotto, *Angew. Chem. Int. Ed.* **2010**, *49*, 9322; *Angew. Chem.* **2010**, *122*, 9510; bb) N. Shibata, A. Matsnev, D. Cahard, *Beilstein J. Org. Chem.* **2010**, *6*, No. 65 DOI: 10.3762/bjoc.6.65; cc) S. Purser, P. R. Moore, S. Swallow, V. Gouverneur, *Chem. Soc. Rev.* **2008**, *37*, 320; dd) J.-A. Ma, D. Cahard, *J. Fluorine Chem.* **2007**, *128*, 975; ee) M. Schlosser, *Angew. Chem. Int. Ed.* **2006**, *45*, 5432; *Angew. Chem.* **2006**, *118*, 5558; ff) G. K. S. Prakash, M. Mandal, *J. Fluorine Chem.* **2001**, *112*, 123; gg) H. L. Yale, *J. Med. Chem.* **1959**, *1*, 121.
[12] M. A. Guerra, T. R. Bierschenk, R. J. Lagow, *J. Organomet. Chem.* **1986**, *307*, C58.
[13] R. D. Sanner, J. H. Satcher, M. W. Droege, *Organometallics* **1989**, *8*, 1498.
[14] S. Martínez-Salvador, L. R. Falvello, A. Martín, B. Menjón, *Chem. Eur. J.* **2013**, *19*, 14540.
[15] U. Preiss, I. Krossing, *Z. anorg. allg. Chem.* **2007**, *633*, 1639.
[16] D. Naumann, W. Tyrra, F. Trinius, W. Wessel, T. Roy, *J. Fluorine Chem.* **2000**, *101*, 131.
[17] E. Bernhardt, M. Finze, H. Willner, *J. Fluorine Chem.* **2004**, *125*, 967.
[18] a) M. Joost, A. Amgoune, D. Bourissou, *Angew. Chem. Int. Ed.* **2015**, *54*, 15022; *Angew. Chem.* **2015**, *127*, 15234; b) M. S. Winston, W. J. Wolf, F. D. Toste, *J. Am. Chem. Soc.* **2014**, *136*, 7777; c) H. K. Nair, J. A. Morrison, *J. Organomet. Chem.* **1989**, *376*, 149; d) R. J. Puddephatt, *Gold Bull.* **1977**, *10*, 108; e) A. Johnson, R. J. Puddephatt, *J. Chem. Soc. Dalton Trans.* **1976**, 1360.
[19] N. J. Rijs, G. B. Sanvido, G. N. Khairallah, R. A. J. O'Hair, *Dalton Trans.* **2010**, *39*, 8655.
[20] R. G. Pearson, *J. Chem. Educ.* **1987**, *64*, 561.
[21] S. Ahrland, J. Chatt, N. R. Davies, *Q. Revs. Chem. Soc.* **1958**, *12*, 265.
[22] R. J. Puddephatt, *The Chemistry of Gold*, Elsevier, Amsterdam, **1978**, pp. 22–24.
[23] The "special affinity" among silver and iodine was already noted in the mid XIX century by one of the most prominent figures in the history of chemistry: H. Sainte-Claire Deville, *C. R. Acad. Sci.* **1856**, *43*, 970; *Chem. Gaz.* **1857**, *15*, 81 (English translation).
[24] The use of AgF for replacing iodide by fluoride was already exploited by Moissan in the late XIX century: H. Moissan, *Ann. Chim. Phys. Ser. 6* **1890**, *19*, 266; H. Moissan, *C. R. Acad. Sci.* **1888**, *107*, 260.
[25] a) W. J. Wolf, F. D. Toste, in *The Chemistry of Organogold Compounds, Vol. 1* (Eds.: Z. Rappoport, I. Marek, J. F. Liebman), belonging to the series *Patai's Chemistry of Functional Groups*, Wiley, Chichester, **2014**, pp. 391–408; b) F. Mohr, *Gold Bull.* **2004**, *37*, 164.
[26] S. Martínez-Salvador, J. Forniés, A. Martín, B. Menjón, I. Usón, *Chem. Eur. J.* **2013**, *19*, 324.
[27] P. G. Jones, C. Thöne, *Acta Crystallogr. Sect. C* **1989**, *45*, 11.
[28] a) A. G. Algarra, V. V. Grushin, S. A. Macgregor, *Organometallics* **2012**, *31*, 1467; b) P. Sgarbossa, A. Scarso, G. Strukul, R. A. Michelin, *Organometallics* **2012**, *31*, 1257; c) see also Ref. [22], pp. 26–27; d) T. G. Appleton, H. C. Clark, L. E. Manzer, *Coord. Chem. Rev.* **1973**, *10*, 335; e) T. G. Appleton, M. H. Chisholm, H. C. Clark, L. E. Manzer, *Inorg. Chem.* **1972**, *11*, 1786.
[29] Highly exothermic interaction of the fluoro-derivative **3** with the aluminum holder was observed to occur at $T>160\,^{\circ}C$, probably due to fluorine transfer from gold to aluminum. This abrupt interaction hindered reliable DSC data to be obtained for this compound. The melting point was nevertheless determined by visual inspection (see the Experimental Section) and confirmed by DTA carried out on platinum holders, with which no anomalous interation was observed (Figure S11).
[30] W. Nakanishi, M. Yamanaka, E. Nakamura, *J. Am. Chem. Soc.* **2005**, *127*, 1446.
[31] a) J. Cirera, in *Comprehensive Inorganic Chemistry II: from Elements to Applications, Vol. 9* (Ed.: S. Alvarez), Elsevier, Amsterdam, **2013**, pp. 441–468; b) T. A. Albright, J. K. Burdett, M.-H. Whangbo, *Orbital Interactions in Chemistry*, 2nd ed., Wiley, Hoboken, **2013**, pp. 503–511.
[32] Spinomers are chemical species with similar stereochemistry, but different spin state: J. Cirera, E. Ruiz, S. Alvarez, *Inorg. Chem.* **2008**, *47*, 2871; see also reference [31a].
[33] J. K. Kochi, *Organometallic Mechanisms and Catalysis*, Academic Press, New York, **1978**, pp. 262–283, and references therein.
[34] In the less symmetric [AuXYZL] compounds, with all four ligands being different in nature ($X=F$, Cl, Br, I; $Y=C_6H_4Me$-4; $Z=CF_3$; $L=PPh_3$), dissociation of the neutral phosphine ligand (L) also appears to be the most kinetically favorable decomposition path, whereby the unsaturated AuXYZ species is formed: R. Bhattacharjee, A. Nijamudheen, A. Datta, *Chem. Eur. J.* **2017**, *23*, 4169.
[35] B. Réffy, M. Kolonits, A. Schulz, T. M. Klapötke, M. Hargittai, *J. Am. Chem. Soc.* **2000**, *122*, 3127.
[36] A. Schulz, M. Hargittai, *Chem. Eur. J.* **2001**, *7*, 3657.

[37] a) X. Wang, L. Andrews, F. Brosi, S. Riedel, *Chem. Eur. J.* **2013**, *19*, 1397; b) X. Wang, L. Andrews, K. Willmann, F. Brosi, S. Riedel, *Angew. Chem. Int. Ed.* **2012**, *51*, 10628; *Angew. Chem.* **2012**, *124*, 10780; c) I. J. Blackmore, A. J. Bridgeman, N. Harris, M. A. Holdaway, J. F. Rooms, E. L. Thompson, N. A. Young, *Angew. Chem. Int. Ed.* **2005**, *44*, 6746; *Angew. Chem.* **2005**, *117*, 6904.
[38] a) J. E. Huheey, E. A. Kreiter, R. L. Kreiter, *Inorganic Chemistry*, 4th ed., Harper–Collins, New York, **1993**, pp. 182–199; b) S. G. Bratsch, *J. Chem. Educ.* **1985**, *62*, 101; c) roughly similar group-electronegativity values were also obtained for CF_3 (3.22) versus CH_3 (2.45) by quantum-chemical calculations: A. R. Campanelli, A. Domenicano, F. Ramondo, I. Hargittai, *J. Phys. Chem. A* **2004**, *108*, 4940.
[39] a) X. Wang, L. Andrews, *J. Phys. Chem. A* **2002**, *106*, 3744; b) X. Wang, L. Andrews, *J. Am. Chem. Soc.* **2001**, *123*, 12899; c) N. B. Balabanov, J. E. Boggs, *J. Phys. Chem. A* **2001**, *105*, 5906; d) C. A. Bayse, *J. Phys. Chem. A* **2001**, *105*, 5902; e) C. A. Bayse, M. B. Hall, *J. Am. Chem. Soc.* **1999**, *121*, 1348.
[40] M.-J. Crawford, T. M. Klapötke, *Angew. Chem. Int. Ed.* **2002**, *41*, 2269; *Angew. Chem.* **2002**, *114*, 2373.
[41] R. A. J. O'Hair, in *The Chemistry of Organogold Compounds, Vol. 1* (Eds.: Z. Rappoport, I. Marek, J. F. Liebman), belonging to the series *Patai's Chemistry of Functional Groups*, Wiley, Chichester, **2014**, pp. 391–408.
[42] M. Baya, A. Pérez-Bitrián, S. Martínez-Salvador, J. M. Casas, B. Menjón, J. Orduna, *Chem. Eur. J.* **2017**, *23*, 1512.
[43] N. J. Rijs, R. A. J. O'Hair, *Dalton Trans.* **2012**, *41*, 3395.
[44] a) G. W. Rice, R. S. Tobias, *J. Organomet. Chem.* **1975**, *86*, C37; b) A. Tamaki, J. K. Kochi, *J. Organomet. Chem.* **1974**, *64*, 411; c) A. Johnson, R. J. Puddephatt, *Inorg. Nucl. Chem. Lett.* **1973**, *9*, 1175; d) A. Tamaki, J. K. Kochi, *J. Organomet. Chem.* **1972**, *40*, C81; see also Refs. [3b] and [5b].
[45] F. Klanberg, E. L. Muetterties, *Inorg. Chem.* **1968**, *7*, 155.
[46] W. R. Dolbier, Jr., *Guide to Fluorine NMR for Organic Chemists*, 2nd ed., Wiley, Hoboken, **2016**, p. 223–227.
[47] CrysAlis RED, CCD camera data reduction program, Oxford Diffraction: Oxford, UK, **2004**.
[48] G. M. Sheldrick, *Acta Crystallogr. Sect. A* **2008**, *64*, 112.
[49] Gaussian 09, Revision A.01, M. J. Frisch, G. W. Trucks, H. B. Schlegel, G. E. Scuseria, M. A. Robb, J. R. Cheeseman, G. Scalmani, V. Barone, B. Mennucci, G. A. Petersson, H. Nakatsuji, M. Caricato, X. Li, H. P. Hratchian, A. F. Izmaylov, J. Bloino, G. Zheng, J. L. Sonnenberg, M. Hada, M. Ehara, K. Toyota, R. Fukuda, J. Hasegawa, M. Ishida, T. Nakajima, Y. Honda, O. Kitao, H. Nakai, T. Vreven, J. A. Montgomery, Jr., J. E. Peralta, F. Ogliaro, M. Bearpark, J. J. Heyd, E. Brothers, K. N. Kudin, V. N. Staroverov, R. Kobayashi, J. Normand, K. Raghavachari, A. Rendell, J. C. Burant, S. S. Iyengar, J. Tomasi, M. Cossi, N. Rega, J. M. Millam, M. Klene, J. E. Knox, J. B. Cross, V. Bakken, C. Adamo, J. Jaramillo, R. Gomperts, R. E. Stratmann, O. Yazyev, A. J. Austin, R. Cammi, C. Pomelli, J. W. Ochterski, R. L. Martin, K. Morokuma, V. G. Zakrzewski, G. A. Voth, P. Salvador, J. J. Dannenberg, S. Dapprich, A. D. Daniels, O. Farkas, J. B. Foresman, J. V. Ortiz, J. J. Cioslowski, D. J. Fox, Gaussian, Inc., Wallingford, CT, **2009**.

Manuscript received: February 28, 2017
Accepted Article published: March 20, 2017
Final Article published: April 24, 2017

ChemPubSoc Europe
DOI: 10.1002/chem.201703352
CHEMISTRY A European Journal
Full Paper

Organogold Compounds |*Hot Paper*|

$(CF_3)_3Au$ as a Highly Acidic Organogold(III) Fragment

Alberto Pérez-Bitrián,[a] Miguel Baya,[a] José M. Casas,[a] Larry R. Falvello,[b] Antonio Martín,[a] and Babil Menjón*[a]

Dedicated to Professor Juan Forniés on the occasion of his 70th birthday

Abstract: The Lewis acidity of perfluorinated trimethylgold $(CF_3)_3Au$ was assessed by theoretical and experimental methods. It was found that the $(CF_3)_3Au$ unit is much more acidic than its nonfluorinated analogue $(CH_3)_3Au$, and probably sets the upper limit of the acidity scale for neutral organogold(III) species R_3Au. The significant acidity increase on fluorination is in line with the CF_3 group being more electron-withdrawing than CH_3. The solvate $(CF_3)_3Au{\cdot}OEt_2$ (**1**) is presented as a convenient synthon of the unsaturated, 14-electron species $(CF_3)_3Au$. Thus, the weakly coordinated ether molecule in **1** is readily replaced by a variety of neutral ligands (L) to afford a wide range of $(CF_3)_3Au{\cdot}L$ compounds, which were isolated and characterized. Most of these mononuclear compounds exhibit marked thermal stability. This enhanced stabilization can be rationalized in terms of substantially stronger [Au]–L interactions with the $(CF_3)_3Au$ unit. An affinity scale of this single-site, highly acidic organogold(III) fragment was calculated by DFT methods and experimentally mapped for various neutral monodentate ligands. The high-energy profile calculated for the fluorotropic [Au]–CF_3⇌F–[Au]←CF_2 process makes this potential decomposition path unfavorable and adds to the general stabilization of the fragment.

Introduction

Strong Lewis acids are fascinating chemical species and are eagerly sought because of their interesting and high reactivity.[1–5] Prototypical examples of strong Lewis acids in organic chemistry are carbocations R_3C^+. These highly reactive, unsaturated species were first formulated as ephemeral intermediates, but were unambiguously identified by the late Nobel laureate Olah and co-workers.[6] Isoelectronic with charged carbocations R_3C^+ are neutral boranes, R_3B, the Lewis acidic properties of which have also been thoroughly studied and widely exploited.[7] Their use as promotors in alkene polymerization processes catalyzed by alkyl metallocenes has fostered the rapid and fruitful development of an astonishing variety of boranes.[8]

In the search for ever stronger Lewis acidic boranes R_3B, it was soon realized that fluorination of the organic group R resulted in enhancement of the Lewis acidity in the corresponding $R^F{}_3B$ compounds.[9–11] In fact, the most widely used borane is by far $(C_6F_5)_3B$, which exhibits considerable Lewis acidity.[12] The perfluoromethyl derivative $(CF_3)_3B$ would be expected to exhibit even higher Lewis acidity. Although this compound has not yet been isolated as such, its derivatives $(CF_3)_3B{\cdot}L$[13] and, especially the singular carbonyl compound $(CF_3)_3B(CO)$,[14] evidence greatly enhanced acidity of the $(CF_3)_3B$ moiety.[15,16]

The CF_3 group exhibits properties that depart so markedly from those of nonfluorinated CH_3 that T. Ritter has suggested that it be considered "more appropriately as a distinct functional group" rather than just as a substituted methyl group.[17] It has traditionally been considered[18] as a compact, electron-withdrawing group with electronegativity ($\chi_{CF_3}=3.49$)[19] virtually identical to that of chlorine ($\chi_{Cl}=3.48$),[19] and it additionally exhibits a strong *trans* influence in its transition metal compounds.[20] Recently, it has also been considered as a noninnocent σ ligand able to induce inversion in the ligand-field splitting of metal d orbitals, especially in late transition metals, as in the homoleptic $[(CF_3)_4Cu]^-$ anion.[21] With regard to gold chemistry, the CF_3 group was first introduced by Puddephatt et al. in the 1970s.[22] Since that early work, the study of trifluoromethyl gold derivatives has aroused continued interest, but only recently has it developed into a hot research topic.[23]

We have recently found a convenient entry to the chemistry of the $(CF_3)_3Au$ fragment, which has emerged as a stereochemically robust moiety with a marked reluctance to undergo reductive elimination of CF_3–CF_3.[24] The anionic derivatives $[PPh_4][(CF_3)_3AuX]$ (X = F, Cl, Br, I, CN) have also been isolated and characterized. We wanted now to assess the Lewis acidity of the $(CF_3)_3Au$ unit in comparison with that of its nonfluorinated analogue $(CH_3)_3Au$ in order to establish the effect of fluori-

[a] A. Pérez-Bitrián, Dr. M. Baya, Prof. Dr. J. M. Casas, Dr. A. Martín, Dr. B. Menjón
Instituto de Síntesis Química y Catálisis Homogénea (iSQCH)
CSIC-Universidad de Zaragoza, C/ Pedro Cerbuna 12
50009 Zaragoza (Spain)
E-mail: menjon@unizar.es

[b] Prof. Dr. L. R. Falvello
Instituto de Ciencia de Materiales de Aragón (ICMA)
CSIC-Universidad de Zaragoza, C/ Pedro Cerbuna 12
50009 Zaragoza (Spain)

Supporting information and the ORCID identification numbers for the authors of this article can be found under: https://doi.org/10.1002/chem.201703352.

nation. To this end, a combination of theoretical and experimental approaches was used. Further comparison with the isoleptic $(CF_3)_3B$ species as well as with the ubiquitous $(C_6F_5)_3B$ provides parallels between transition metal and main group chemistry, and bridges what might otherwise appear to be a conceptual divide.[21,25]

Results and Discussion

The naked $(CF_3)_3Au$ species seems to have been prepared by Lagow and his co-workers[26] as the result of gas-phase reaction of Au vapors with $CF_3^{\bullet}$ radicals and subsequent matrix isolation [Eq. (1)]:

$$Au_{(g)} + 3\,CF_3{}^{\bullet}{}_{(g)} \rightarrow (CF_3)_3Au \qquad (1)$$

This procedure requires highly specialized and rather expensive equipment that cannot be afforded by most chemistry laboratories. Moreover, naked $(CF_3)_3Au$ is thermally unstable and is produced only in modest yield (≈20%), as estimated by derivatization. We sought to circumvent all these drawbacks by preparing a $(CF_3)_3Au{\cdot}L$ adduct with a weakly coordinating ligand L. The ligand of choice was Et_2O, as already used by Gilmann and Woods to stabilize the nonfluorinated $(CH_3)_3Au$.[27]

Synthesis of $(CF_3)_3Au{\cdot}OEt_2$ (1)

On room-temperature treatment of the iodo derivative $[PPh_4][(CF_3)_3AuI]$[24] with an equimolar amount of $AgClO_4$ in CH_2Cl_2/Et_2O, precipitation of AgI was observed with concomitant formation of the solvento complex $(CF_3)_3Au{\cdot}OEt_2$ (**1**) in solution (Scheme 1). Solutions of etherate **1** can be freed from the accompanying $[PPh_4]ClO_4$ salt by replacing the initial solvent mixture with Et_2O/*n*-hexane (1:3 v/v) and allowing them to stand at −80 °C, overnight. Once filtered, colorless solutions of **1** are reasonably stable at room temperature if protected from the action of light. These solutions are free of byproducts and as such are appropriate for most synthetic purposes. Interestingly, compound **1** shows greatly enhanced thermal stability relative to the nonfluorinated etherate $(CH_3)_3Au{\cdot}OEt_2$, which already decomposes at about −40 °C in Et_2O solution giving a gold mirror and a mixture of ethane and methane.[27]

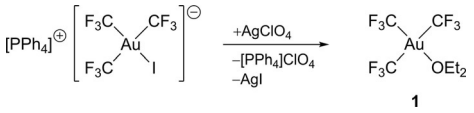

Scheme 1. Synthetic method to prepare the etherate $(CF_3)_3Au{\cdot}OEt_2$ (**1**).

The room-temperature ^{19}F NMR spectrum of **1** shows two broad bands at about −25 and −39 ppm in 1:2 integrated ratio, which are resolved at low temperature into a septet and a quartet, respectively. This behavior indicates that the Et_2O ligand is labile and undergoes rapid exchange at room temperature. In fact, even small amounts of free Et_2O in the sample result in broadening of the signal without noticeable shift in the corresponding δ_F values. Although we tried to isolate compound **1** as a pure substance, its marked hygroscopic character together with its high solubility in Et_2O and *n*-hexane even at low temperatures made our task difficult. After evaporation of ethereal solutions of **1** to dryness at 0 °C, extraction of the residue with *n*-hexane, and crystallization at −80 °C, a deliquescent white solid was eventually obtained that melted just above 0 °C.[28] The ^{19}F NMR spectrum of this solid in CD_2Cl_2 solution at −60 °C (Figure 1 a) is consistent with that observed in the initial reaction medium (Scheme 1) with just a slight shift in δ_F values, attributable to the different dielectric constants of the solvent used in each case (Et_2O/*n*-hexane versus CD_2Cl_2). In the ^1H NMR spectrum (Figure 1 b), the signals due to coordinated Et_2O [δ_H = 4.05 (CH_2) and 1.52 ppm (CH_3)] are shifted downfield with respect to those of the free molecule (δ_H = 3.43 (CH_2) and 1.15 ppm (CH_3) in CD_2Cl_2 solution);[29] that is, the corresponding protons are deshielded on coordination to the acidic $(CF_3)_3Au$ fragment (Table 1). Similarly deshielded signals were also found in salts of the oxonium cation $[H(OEt_2)_2]^+$ with weakly coordinating anions[30] as well as in the related perfluorophenyl derivative $(C_6F_5)_3Au{\cdot}OEt_2$.[31] There is therefore strong spectroscopic evidence suggesting that the solid samples obtained consist mainly of compound **1**. However, such samples always contained variable amounts of free Et_2O (see marked signals in Figure 1 b) that could not be completely removed

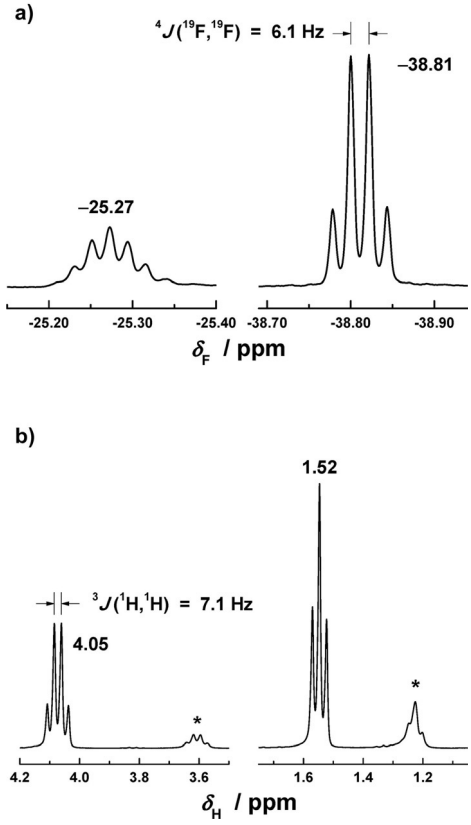

Figure 1. ^{19}F (a) and ^1H (b) NMR spectra of etherate **1** in CD_2Cl_2 solution at −60 °C . The signals marked with an asterisk correspond to free Et_2O.[29]

Table 1. Relevant NMR parameters corresponding to the neutral $(CF_3)_3Au{\cdot}L$ derivatives.[a]

Compound	$\delta_F(q)$[b]	$\delta_F(spt)$[c]	$^4J(F,F)$[d]	Other NMR signals
$(CF_3)_3Au(OEt_2)$ (**1**)[e]	−38.81	−25.27	6.1	$\delta_H = 4.05$ (q, $^3J(H,H) = 7.1$; CH_2), 1.52 (t; CH_3)
$(CF_3)_3Au(CNtBu)$ (**2**)	−29.39	−32.07	6.3	$\delta_H = 1.63$ (s)
$(CF_3)_3Au(NCMe)$ (**3**)[e]	−35.76	−27.48	6.3	$\delta_H = 2.52$ (s)
$(CF_3)_3Au(py)$ (**4**)[f]	−37.85	−28.89	6.5	$\delta_H = 8.55$ (m_c, 2H; H^o), 8.14 (tt, 1H; H^p), 7.74 (m_c, 2H; H^m)
$(CF_3)_3Au(PMe_3)$ (**5**)[g]	−30.67	−32.41	6.5	$\delta_P = 3.09$ [qspt, $^3J(F,P) = 78.8$ (*trans*), $^3J(F,P) = 10.6$ (*cis*)]; $\delta_H = 1.78$ [d, $^2J(H,P) = 12.5$]
$(CF_3)_3Au(PPh_3)$ (**6**)	−30.63	−31.19	7.4	$\delta_P = 27.90$ [qspt, $^3J(F,P) = 78.7$ (*trans*), $^3J(F,P) = 9.1$ (*cis*)]; $\delta_H = 7.70$–7.50 (aromatic)
$(CF_3)_3Au(Opy)$ (**7**)[h]	−40.22	−26.19	6.8	$\delta_H = 8.60$ (m_c, 2H; H^o), 8.03 (tt, 1H; H^p), 7.75 (m_c, 2H; H^m)
$(CF_3)_3Au(OPPh_3)$ (**8**)	−37.57	−25.83	6.9	$\delta_P = 49.90$; $\delta_H = 7.75$–7.53 (aromatic)
$(CF_3)_3Au(tht)$ (**9**)	−33.26	−28.18	6.7	$\delta_H = 3.49$ (m_c; α-CH_2), 2.18 (m_c; β-CH_2)
$(CF_3)_3Au(SPPh_3)$ (**10**)	−31.75	−29.17	7.2	$\delta_P = 47.13$; $\delta_H = 7.84$–7.57 (aromatic)

[a] Unless otherwise stated, all spectra were recorded in CD_2Cl_2 solution at room temperature; chemical shifts δ are given in ppm relative to standard references (see Experimental Section) and coupling constants J in hertz; abbreviations: s = singlet, d = doublet, t = triplet, q = quartet, spt = septet, tt = triplet of triplets, qspt = quartet of septets, m_c = multiplet centered at. [b] Signal corresponding to the mutually *trans* CF_3 groups. [c] Signal corresponding to the CF_3 group *trans* to the L ligand. [d] Coupling constant between chemically inequivalent CF_3 groups (*cis*). [e] Spectra registered in the slow-ligand-exchange region (213 K). [f] The ^1H NMR spectrum of **4** was satisfactorily analyzed as an AA′MM′X system with the following homonuclear coupling constants: $^3J(H^o,H^m) = 5.6$, $^3J(H^m,H^p) = 7.8$, $^4J(H^o,H^p) = 1.5$, $^4J(H^o,H^{o'}) = 0.5$, $^4J(H^m,H^{m'}) = 1.5$, $^5J(H^o,H^{m'}) = 0.8$. [g] The spectroscopic parameters of **5** are in keeping with previously reported data.[26,33] [h] The ^1H NMR spectrum of **7** was satisfactorily analyzed as an AA′MM′X system with the following homonuclear coupling constants: $^3J(H^o,H^m) = 6.6$, $^3J(H^m,H^p) = 7.8$, $^4J(H^o,H^p) = 1.1$, $^4J(H^o,H^{o'}) = 2.1$, $^4J(H^m,H^{m'}) = 2.1$, $^5J(H^o,H^{m'}) = 0.7$.

without altering the integrity of the main component. This failure eventually defeated our repeated efforts to isolate compound **1** in analytically pure form. The fact that two separate sets of signals are observed for coordinated and free Et_2O in the ^1H NMR spectrum at −60 °C (Figure 1 b) indicates that exchange between them has been sufficiently slowed down at that temperature.

Synthesis and characterization of neutral $(CF_3)_3Au{\cdot}L$ derivatives

The labile character of the Et_2O ligand in etherate **1** together with its reasonable thermal stability can be exploited for synthetic purposes. Thus, a number of neutral organogold(III) $(CF_3)_3Au{\cdot}L$ derivatives **2**–**10** could be prepared by replacement of the Et_2O molecule in precursor species **1** by a series of representative L ligands (Scheme 2). Similar attempts to prepare

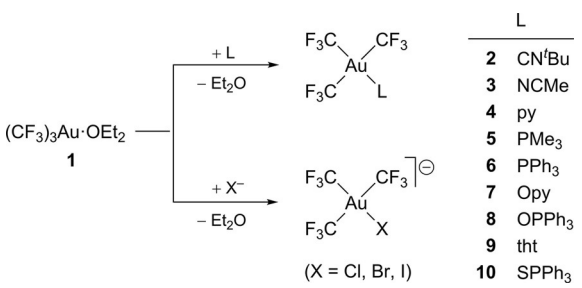

Scheme 2. Replacement of the weakly coordinated Et_2O donor molecule in compound **1** by a range of monodentate neutral L and anionic X^- ligands. The cation is $[PPh_4]^+$ where appropriate.

related silver complexes by replacement of the solvent donor ligands in $(CF_3)_3Ag{\cdot}solv$ (solv = dmso, MeCN, dmf, or other nitrogen bases) with soft donors such as PR_3 (R = Me, Ph, OMe) or AsF_3 failed.[32] The phosphine derivative $(CF_3)_3Au(PMe_3)$ (**5**) was already known; it was first prepared[26] by complexation of naked $(CF_3)_3Au$ with PMe_3 and later by treatment of $(CF_3)_2AuI(PMe_3)$ with $(CF_3)_2Cd{\cdot}dme$ in the presence of an excess of CF_3I.[33] Halide ligands X^- are also able to replace the labile Et_2O molecule in **1** to furnish the corresponding anionic $[(CF_3)_3AuX]^-$ derivatives (Scheme 2), which we isolated recently (X = Cl, Br, I).[24]

Monodentate ligands L were selected to cover a wide range of donor abilities with donor atoms including first- and second-row elements of the p block, with the aim of exploring the stability of their corresponding complexes. All these compounds were isolated and characterized by analytical and spectroscopic methods (see Experimental Section). The ^1H, ^{19}F, and ^{31}P NMR spectroscopic data obtained in solution at room temperature are listed in Table 1. Particularly valuable structural information in solution is derived from the ^{19}F NMR spectra. The general spectral pattern consists of two signals in 1:2 integrated ratio (typically a septet and a quartet), corresponding to the two types of chemically inequivalent CF_3 groups with no hint of fluxional exchange between them. Both sets of nuclei are mutually coupled with $^4J(F,F)$ values in the narrow range of 6.1–7.4 Hz. Additional splitting of the signals is observed in the phosphine complexes **5** and **6**. In the compounds bearing typical π-acceptor ligands, namely, *t*BuNC (**2**), PMe_3 (**5**), and PPh_3 (**6**), the relative positions of the quartet with respect to the septet appears to be inverted, a feature also observed in related isoelectronic Pt(II) derivatives.[34]

The crystal and molecular structures of several representative examples were experimentally established by single-crystal X-ray diffraction (Table 2). In the phosphine complexes $(CF_3)_3Au(PMe_3)$ (**5**; Figure 2 a) and $(CF_3)_3Au(PPh_3)$ (**6**; Figure 2 b), similar Au–P distances and virtually identical Au–C bond lengths are observed. The Au–P bond in compound **6** (239.27(6) pm) is longer than those in the analogous nonfluorinated compound $(CH_3)_3Au(PPh_3)$ (234.8(6) pm)[35] and the classical coordination compound $Cl_3Au(PPh_3)$ (232.9(2) pm).[36] In the

Table 2. Relevant geometric parameters of the structurally characterized $(CF_3)_3Au{\cdot}L$ derivatives.[a]

Compound	Au–C [pm] in CF_3-Au-CF_3[b]	Au–C [pm] in E-Au-C	Au–E [pm]	CF_3-Au-CF_3 [°]	$\Sigma\measuredangle$[c] [°]
$(CF_3)_3Au(CNtBu)$ (**2**)	208.5(6)	205.8(5)	204.3(5)	179.7(2)	359.9
$(CF_3)_3Au(py)$ (**4**)	207.4(9)	202.9(7)	207.5(6)	177.7(3)	360.1
$(CF_3)_3Au(PMe_3)$ (**5**)[d]	208.6(10)	208.3(10)	237.0(2)	174.5(4)	360.6
$(CF_3)_3Au(PPh_3)$ (**6**)	209.8(2)	209.0(3)	239.27(6)	175.2(1)	360.0
$(CF_3)_3Au(Opy)$ (**7**)[e]	207.8(3)	202.5(3)	207.0(2)	178.2(1)	360.0
$(CF_3)_3Au(OPPh_3)$ (**8**)[f]	208.2(3)	200.1(3)	206.2(2)	176.9(1)	360.1
$(CF_3)_3Au(tht)$ (**9**)[d]	208.8(8)	206.2(7)	238.9(2)	177.4(2)	360.1
$(CF_3)_3Au(SPPh_3)$ (**10**)[g]	208.7(2)	205.3(2)	240.55(5)	179.4(1)	360.0

[a] A *trans* arrangement is meant in the indicated CF_3-Au-CF_3 and E-Au-C units with E denoting a chemical element. [b] Average of two independent values. [c] Sum of all adjacent E-Au-E′ angles as a measure of planarity. [d] Average values for the two crystallographically independent molecules in the unit cell. [e] Au-O-N 119.26(15)°. [f] Au-O-P 131.10(11)°. [g] Au-S-P 105.90(3)°.

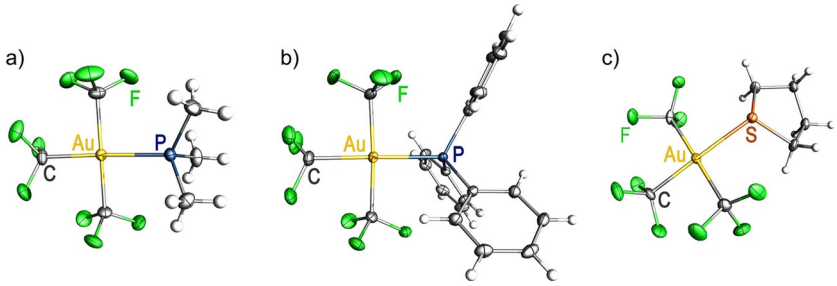

Figure 2. Displacement-ellipsoid diagram (50% probability) of: a) $(CF_3)_3Au(PMe_3)$ (**5**), b) $(CF_3)_3Au(PPh_3)$ (**6**), and c) $(CF_3)_3Au(tht)$ (**9**).

thioether complex $(CF_3)_3Au(tht)$ (**9**), the structural features of the metal coordination environment (Figure 2c) compare well with those of the perfluorophenyl derivative $(C_6F_5)_3Au(tht)$.[37] Again, the Au–S bond length in compound **9** (238.9(2) pm) is longer than that in the classical coordination complex $Cl_3Au(tht)$ (232.6(2) pm).[38] In the pyridine complex $(CF_3)_3Au(py)$ (**4**: Figure 3), the Au–N bond length (207.5(6) pm) is also substantially longer than that in the Werner-type complex $Cl_3Au(py)$ (199.3(7) pm).[39] The elongated Au–L bonds found in these $(CF_3)_3Au{\cdot}L$ compounds (L = py, PPh_3, tht) in comparison with the corresponding chlorides $Cl_3Au{\cdot}L$, are clear evidence of the strong *trans* influence of the CF_3 group.[20]

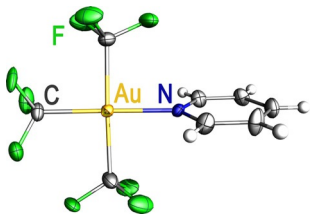

Figure 3. Displacement-ellipsoid diagram (50% probability) of $(CF_3)_3Au(py)$ (**4**). Only one set of the rotationally disordered F atoms found in two of the CF_3 groups is shown.

In compounds **5**, **6**, and **9** bearing soft PR_3 and SR_2 ligands (Figure 2), the Au–C bond lengths in each molecule are indistinguishable within the experimental error in spite of the weaker *trans* influence associated with the PR_3 or SR_2 ligands compared to that of the CF_3 group. Moreover, they do not significantly deviate from the Au–C bond length found in the homoleptic anionic derivative $[NBu_4][Au(CF_3)_4]$ (av 208.0(7) pm).[40] In complex **4**, however, the Au–C bond *trans* to the hard ligand pyridine is significantly shorter than those located *trans* to each other: 202.9(7) versus 207.4(9) pm. A distinction between the Au–C distances involving chemically inequivalent

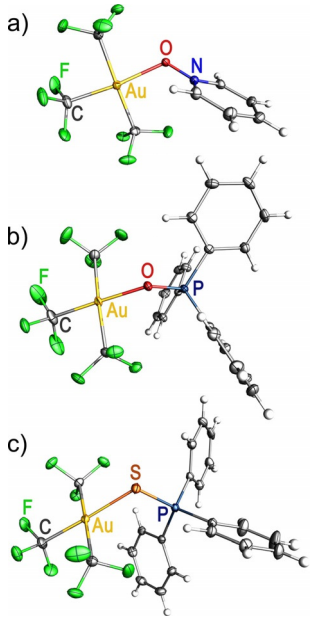

Figure 4. Displacement-ellipsoid diagram (50% probability) of: a) $(CF_3)_3Au(Opy)$ (**7**), b) $(CF_3)_3Au(OPPh_3)$ (**8**), and c) $(CF_3)_3Au(SPPh_3)$ (**10**).

CF_3 groups also becomes increasingly apparent in phosphine sulfide complex **10** (205.3(2) vs. 208.7(2) pm), pyridine *N*-oxide derivative **7** (202.5(3) vs. 207.8(3) pm), and phosphine oxide species **8** (200.1(3) vs. 208.2(3) pm), which respectively bear ligands with semipolar Ph_3P^+–S^-, py^+–O^-, and Ph_3P^+–O^- bonds.[41] In this set of compounds (Figure 4), the Au-E-N/P angles at the chalcogen atom gradually widen in the same sequence [Au-S-P 105.90(3), Au-O-N 119.26(15), Au-O-P 131.10(11)°], a trend that can probably be related to the σ-donor ability of the ligand involved.[42] The Au–S bond length in compound $(CF_3)_3Au(SPPh_3)$ (240.55(5) pm) is similar to that in thioether derivative **9** (238.9(2) pm).

In $(CF_3)_3Au(CNtBu)$ (**2**), the gold atom is surrounded by four C-donor ligands (Figure 5). The presence of a typical π-acceptor ligand, namely, CN*t*Bu, does not appear to have any significant effect on the Au–CF_3 bond length in *trans* position (Table 2). However, the Au–CN*t*Bu bond length (204.3(5) pm) is longer than that in the analogous halogenido derivative $Br_3Au(CNtBu)$ (199(1) pm).[43]

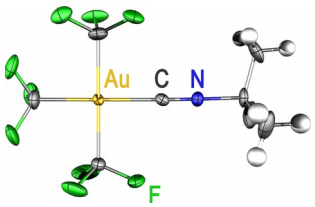

Figure 5. Displacement-ellipsoid diagram (50% probability) of $(CF_3)_3Au(CNtBu)$ (**2**) with only one set of F atoms at half-occupancy shown.

All the isolated $(CF_3)_3Au{\cdot}L$ compounds **2**–**10** show high thermal stability, as established by thermogravimetric and differential thermal analysis (TGA/DTA) of the solid materials (see Experimental Section and Figures S14–S22 in the Supporting Information). The experimentally observed stability in the neutral $(CF_3)_3Au{\cdot}L$ series as a function of the ancillary ligand L is in reasonable agreement with that predicted by theoretical calculations (see below).

The small size of some of the $(CF_3)_3Au{\cdot}L$ molecules, together with the absence of significant intermolecular interactions in the solid state, results in high volatility. Thus, the complexes with MeCN (**3**), py (**4**), PMe_3 (**5**), and tht (**9**) boil between 205 and 223 °C at atmospheric pressure. Aside from *t*BuNC complex **2**, which decomposes at 125 °C, all other compounds show high thermal stability with decomposition temperatures ranging from 220 to 302 °C. The upper value is set by $SPPh_3$ derivative **10**, which is therefore the most stable species. Pyridine *N*-oxide complex **7** undergoes oxygen extrusion on thermolysis to give pyridine complex **4**, as established by ^{19}F NMR spectroscopy (Figure S23 in the Supporting Information).

Lewis acidity of the $(CF_3)_3Au$ fragment

Previously, we found that the unsaturated $(CF_3)_3Au$ moiety is characterized by marked stereochemical stability with clear preference for a T-shaped structure.[24] This perfluorinated organogold(III) fragment is furthermore highly reluctant to undergo reductive elimination of CF_3–CF_3. Both of these characteristic features can be considered as the main reasons underlying the intrinsic stability of the $(CF_3)_3Au$ moiety. An analysis of the frontier orbitals of this d^8 R_3M fragment reveals that the HOMO (Figure 6a) can be identified as a mainly Au–C bonding orbital involving the mutually *trans* CF_3 groups. This M–C bonding interaction is slightly antibonding for the C–F bonds, a feature connected with the negative fluorine hyperconjugation traditionally considered to operate in fluoroalkyl groups.[44] The LUMO (Figure 6b) has a perpendicular arrangement and shows a highly directional empty orbital, which is responsible for the acidic properties of the unsaturated metal fragment. In this MO, antibonding interaction with filled F(p) orbitals is also observed to arise, even with the empty metal-centered lobe, for which an opposite stabilizing interaction might in turn be expected. This feature suggests that the empty coordination site has little affinity for the adjacent F substituents, as is discussed below. We now focus on the Lewis acidity of the $(CF_3)_3Au$ moiety, both in the absolute sense and in comparison with related species, such as the nonfluorinated analogue $(CH_3)_3Au$ and the isoleptic perfluoromethylborane $(CF_3)_3B$.

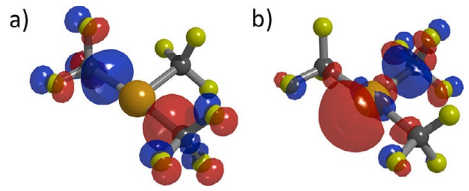

Figure 6. Frontier orbitals of the $(CF_3)_3Au$ moiety: a) HOMO, and b) LUMO.

In the absence of a universal scale, the Lewis acidity of the $(CF_3)_3Au$ fragment has been evaluated by three different criteria. The first consists of a simple estimate of the LUMO energy.[45] The LUMO of the $(CF_3)_3Au$ unit in its ground-state conformation is located at considerably lower energy (−4.34 eV) than that of the nonfluorinated $(CH_3)_3Au$ fragment (−2.71 eV), which is clear evidence of higher acidity in the former. By this intrinsic criterion, the $(CF_3)_3Au$ unit is also more acidic than $(C_6F_5)_3B$, for which a LUMO energy of −3.93 eV has been calculated, but not as much as $(CF_3)_3B$ (−4.77 eV).[45]

Another widely used criterion for evaluating the Lewis acidity of a chemical entity is the fluoride ion affinity (FIA). The absolute FIA values calculated for the T-shaped polytopes of the respective $(CX_3)_3Au$ species by using COF_2 as the reference fluoride carrier in the nearly isodesmic process indicated in Equation (2) are as follows: 433 (X = F) versus 298 kJ mol^{-1} (X = H).

$$[(CX_3)_3AuF]^- + COF_2 \rightarrow CF_3O^- + (CX_3)_3Au \qquad (2)$$

Using this criterion, Christe and co-workers have derived a quantitative scale of Lewis acidity conveniently based on pF^- values, which result from dividing the absolute fluoride affinities (kcal mol^{-1}) by 10.[46] Relevant pF^- values corresponding to

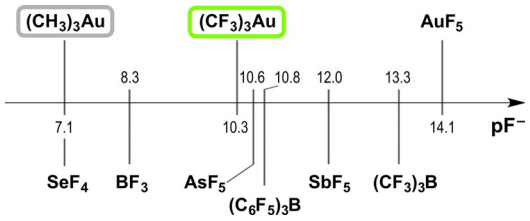

Figure 7. Lewis acidity scale in pF$^-$ values[46] for selected neutral AX_n species. Only the highest acidity range is represented here.

the $(CX_3)_3Au$ units (X = H, F) are shown in Figure 7 in graphical comparison with those of other neutral Lewis acids. On this quantitative scale, the Lewis acidity of the $(CH_3)_3Au$ fragment (pF$^-$ = 7.1) coincides with that of SeF_4. The Lewis acidity of this organogold(III) fragment is substantially enhanced on fluorination. Thus, the Lewis acidity of the perfluorinated $(CF_3)_3Au$ moiety (pF$^-$ = 10.3) is higher than that of BF_3 (pF$^-$ = 8.3) and comparable to those of $(C_6F_5)_3B$ (pF$^-$ = 10.8) and AsF_5 (pF$^-$ = 10.6). Significantly stronger Lewis acids seem to be the neutral binary pentafluorides SbF_5 (pF$^-$ = 12.0) and especially AuF_5 in its monomeric (pF$^-$ = 14.1) or dimeric (pF$^-$ = 12.9) forms.[47] The monomeric, square-pyramidal AuF_5 unit containing a highly oxidized gold(V) center (d^6 electron configuration) has, in fact, been claimed to set the current upper limit of Lewis acidity for any neutral chemical species. However, even stronger Lewis acids can be found in cationic species, among which the F^+ cation exhibits a pF$^-$ value as high as 36.1. The $(CF_3)_3Au$ unit is a much weaker Lewis acid than the superacidic isoleptic borane $(CF_3)_3B$, for which a substantially higher FIA value of 556 kJ mol^{-1} (pF$^-$ = 13.3) has been calculated.[15,45]

The close constitutional similarity of both $(CX_3)_3Au$ species (X = H, F) makes the comparison of their acidity by means of theoretical criteria particularly relevant. Nevertheless, an experimental estimate of the Lewis acidity of the $(CF_3)_3Au$ fragment has also been carried out by the Gutmann–Beckett method.[48] This method relies on the chemical shift variation, $\Delta\delta_P$, suffered by the Et_3PO base on interaction with the acidic moiety (Lewis neutralization) and has been applied to acidic species of both metals and nonmetals.[49] The δ_P value of Et_3PO changes from 46.2 ppm in the free ligand to 79.6 ppm on interaction with the $(CF_3)_3Au$ fragment (i.e., $\Delta\delta_P$ = 33.4 ppm). According to his value, the $(CF_3)_3Au$ unit can be ranked as a stronger Lewis acid than $(C_6F_5)_3B$, for which $\Delta\delta_P$ = 30.6 ppm.[49a,d] The same order is obtained by considering the intrinsic LUMO energy of $(CF_3)_3Au$ versus $(C_6F_5)_3B$, as commented on above. However, this order is inverted when considering the FIA values. This inconsistency can be attributed to the B–F bond being much stronger than the Au–F bond (732 vs. 294.1 kJ mol^{-1}) for the respective diatomic neutral fluorides.[50] The large difference between B–F and Au–F bond strengths makes the FIA criterion particularly unfavorable for gold, which is a typical soft acid (class *b* metal) that prefers to bind larger and more polarizable ligands than fluoride.[51]

Although the standard Gutmann–Beckett scale of Lewis acidity is set according to the δ_P shift of Et_3PO, consistent trends are generally obtained with Ph_3PO (δ_P = 25.1 ppm).[49a] In fact, if we compare the relative shift observed for the $(CF_3)_3Au(OPPh_3)$ complex (**8**: $\Delta\delta_P'$ = 24.8 ppm; Table 1) with that reported for $(C_6F_5)_3B(OPPh_3)$ ($\Delta\delta_P'$ = 20.3 ppm),[49a-c] we again obtain an indication of higher acidity for the organogold(III) fragment. On this secondary scale, the $(CF_3)_3Au$ unit is a stronger Lewis acid than the $(C_6F_5)_3Au$ moiety ($\Delta\delta_P'$ = 17.1 ppm).[31b]

On the [Au]–CF_3⇌F–[Au]←CF_2 process

The main source of instability for perfluoromethylborane $(CF_3)_3B$ lies in the fact that the F substituents are in close proximity to the superacidic boron center. The F$^-$ ion is a hard base that forms particularly strong bonds with boron, as mentioned above. A 1,2-F shift is therefore energetically favored (−49.7 kJ mol^{-1}), whereby the saturated species $(CF_3)_2B(CF_2)F$ is formed (Scheme 3 a). This fluorotropic process has been thoroughly studied by Willner and co-workers.[15] We wanted now to explore the role that a similar process (Scheme 3 b) might play in the chemistry of the isoleptic $(CF_3)_3Au$ fragment (hereafter denoted **A**).[52,53]

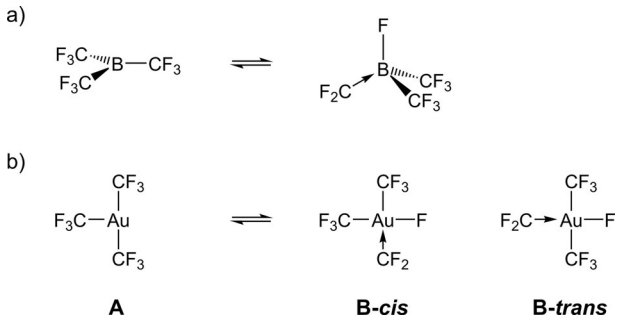

Scheme 3. Fluorotropic processes in the unsaturated, isoleptic species $(CF_3)_3B$ (a)[15] and $(CF_3)_3Au$ (b).

When a fluorine atom of one of the mutually *trans* CF_3 groups in **A** is forced to approach the metal center by varying the C-Au-F angle α, the system energy rises steadily (Figure S1a in the Supporting Information) up to the point at which the shifted F atom occupies the empty coordination site at α = 90° (**B-*cis***). Every stage in this endergonic *cis*-1,2-F shift is metastable, including the highest point **B-*cis*** (E = 81.4 kJ mol^{-1}; Figure 8)[54] and all of them revert to the initial stage **A** in a spontaneous and barrierless way when the only restraint applied is removed (α set free). We recall here that the LUMO of **A** (Figure 6 b) shows antibonding interaction of the empty metal-centered lobe with filled p orbitals of the adjacent F atoms.

A *trans*-1,2-F shift in **A** gives an even higher and qualitatively different energy profile (Figure S1b in the Supporting Information). Here, the endpoint **B-*trans*** at α = 180° is a high-energy local minimum (116.9 kJ mol^{-1}; Figure 8), and a transition state is found at α = 72.3° (333.6 kJ mol^{-1}; Figure S1b). In the optimized geometry of **B-*trans*** (Figure S3), the planar CF_2 unit is placed exactly perpendicular to the metal coordination plane (dihedral angle: 90.0°). This arrangement is unsuited for any

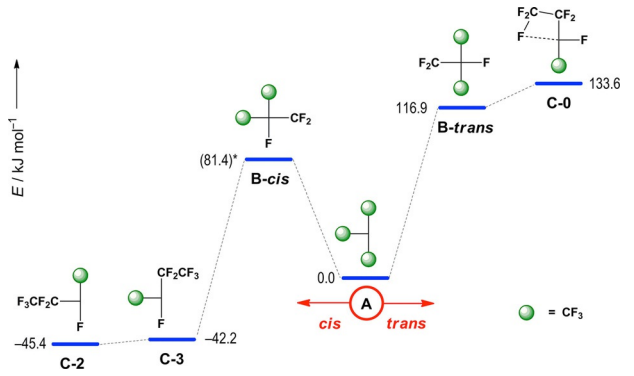

Figure 8. Energy scheme calculated for the [Au]–CF_3⇌F–[Au]←CF_2 fluorine shift (Scheme 3 b) and subsequent CF_2 insertion into remaining Au–CF_3 bonds relative to the parent $(CF_3)_3Au$ species (**A**). Optimized stationary structures are depicted in Figure S3 in the Supporting Information. An extended version of this energy scheme including higher-energy rotamers of the [Au]–C_2F_5 derivatives as well as other excited states is given in Figure S2 in the Supporting Information.

M–C π interaction to be established, and accordingly the [Au]←CF_2 interaction is depicted as a dative bond.

Although both stereoisomers (*cis* and *trans*) of **B** are standard square-planar, 16-electron species, they are less stable than the unsaturated, T-shaped, 14-electron moiety **A**. This destabilization on 1,2-F shift can be attributed to the unfavorable balance that results from the Au–F bond forming at the expense of a C–F bond breaking. This is in sharp contrast with the above-mentioned boron case, in which the fluorotropic process $(CF_3)_3B$⇌$(CF_3)_2B(CF_2)F$ indeed gives a favorable balance to the saturated species on the right. In that case, the B–F bond energy overcomes the energy expense for both the C–F bond breaking and the geometric rearrangement[9] required to go from the initially trigonal-planar $(CF_3)_3B$ unit to the final tetrahedral shape in $(CF_3)_2B(CF_2)F$ (Scheme 3 a). No such geometric rearrangement is needed in the gold **A**⇌**B** system, which is based on a basically square-planar frame (Scheme 3 b).

Stereoisomer **B-*cis*** achieves substantial stabilization on CF_2 insertion into any of the Au–CF_3 bonds giving rise to the unsaturated species $CF_3CF_2Au(CF_3)F$ (**C**) in two of its isomeric forms (Figure 8). The relative orientation of the CF_3CF_2 group gives rise to different rotamers for each stereoisomer. As they do not differ much in energy from each other (Figure S2 in the Supporting Information), only the most stable rotamer is considered here. The stereoisomer that results from CF_2 insertion into the *trans* Au–CF_3 bond is only marginally more stable (**C-2**: −45.4 kJ mol^{-1}; Figure 8) than that resulting from the *cis* insertion (**C-3**: −42.2 kJ mol^{-1}; Figure 8). A quite regular T-shaped structure is found as the optimized geometry of **C-3**, whereas a pronounced Y distortion is observed in stereoisomer **C-2** (Figure S3 in the Supporting Information).

A similar insertion process in the **B-*trans*** species gives just a single stereoisomer, namely, **C-0**, identified as a high-energy minimum in which the F ligand is located *trans* to the void (Figure S3 in the Supporting Information). This particular arrangement is energetically unfavorable, and results in additional destabilization (**C-0**: 133.6 kJ mol^{-1}; Figure 8). The high electronegativity of F favors a secondary Au···F bonding interaction with one of the β-F atoms (Figure S3 in the Supporting Information). Moreover, if this interaction is forcibly removed, a new secondary interaction is spontaneously established, this time with an α-F atom of the CF_3CF_2 group. This new arrangement is even more destabilized (**C-0′**: 142.3 kJ mol^{-1}; Figure S2 in the Supporting Information). Similar secondary interactions were not observed in stereoisomers **C-2** and **C-3**, in which the empty coordination site is *trans* to a perfluoroalkyl group (CF_3CF_2 and CF_3, respectively). If such interactions are forcibly introduced, the system suffers destabilization (Figure S2 in the Supporting Information) and reverts to the initial state when the restraints are removed. The difference in behavior between **C-0** and its stereoisomers **C-2** and **C-3** is clear evidence that fluoroalkyl ligands exert a much stronger *trans* influence than fluoride. It would also be expected that the **C-0** species would transform into any of its more stable stereoisomers **C-2** and **C-3**.

From our current study, it becomes clear that the 1,2-F shift is hindered as a potential decomposition path, and thus the stability of $(CF_3)_3Au$ (**A**) is increased. In fact, during our experimental work with this organogold(III) unit, we found no evidence of formation of metal species [Au]–CF_2CF_3 containing the perfluoroethyl group.

Ligand affinity of the $(CF_3)_3Au$ fragment

There is overwhelming evidence that trialkyl gold(III) derivatives undergo reductive elimination by a dissociative mechanism as the initial step.[55] A key point that determines the reaction progress in such R_3Au·L systems should therefore be the ease of L dissociation. Hence, we decided to calculate the affinity of the $(CF_3)_3Au$ fragment for a range of neutral ligands in order to evaluate their stability. These ligands include all those experimentally used in the synthesis of compounds $(CF_3)_3Au$·L (**1**–**10**) and are supplemented by a number of other donors selected for comparative purposes.

The gas-phase molecular structures of all these compounds were optimized by DFT calculations. The resulting minima are depicted in Figures S5–S13 of the Supporting Information, and relevant geometric parameters are given in Table 3. In many instances, the obtained geometries can be directly compared with the corresponding solid-state structures experimentally established by single-crystal X-ray diffraction (Table 2). Excellent agreement is observed in the geometry of the $(CF_3)_3Au$ unit. However, the calculated Au–E distances are, in general, slightly longer than those experimentally observed. This means that the corresponding Au–E dissociation values D_e may be underestimated in our calculations. The order of calculated D_e values is graphically represented in Figure 9 and gives a ligand affinity scale of the $(CF_3)_3Au$ fragment.[56]

The most stable compounds are clearly those formed with phosphines; the more basic PMe_3 provides even higher stability (**5**: D_e = 229 kJ mol^{-1}) than PPh_3 (**6**: D_e = 204 kJ mol^{-1}).

The stability of the compounds formed with the semipolar pnictogen oxides pyO (**7**: D_e = 151 kJ mol^{-1}) and Ph_3PO (**8**: D_e =

Table 3. Relevant geometric parameters of the indicated $(CF_3)_3Au{\cdot}L$ compounds in the gas phase as optimized by DFT methods with indication of the Au–L dissociation energy D_e).[a-c]

Compound	D_e(Au–L) [kJ mol^{-1}]	Au–E [pm]	Au–C [pm] in CX_3-Au-CX_3[d]	Au–C [pm] in E-Au-C	CX_3-Au-CX_3 [°]
$(CF_3)_3Au$[e]	–	–	209	207	172.9
$(CF_3)_3Au(OEt_2)$ (**1**)	127	224	211	204.5	176.8
$(CH_3)_3Au(OEt_2)$ (**1 H**)	*79*	*234*	*212*	*204*	*179.5*
$(CF_3)_3Au(CO)$	90	213	212	206.5	178.5
$(CF_3)_3Au(CN$*t*$Bu)$ (**2**)	178	209	211.5	206.5	178.2
$(CF_3)_3Au(SiN$*t*$Bu)$[f]	139	228[g]	212	207	179.8
$(CF_3)_3Au(NCMe)$ (**3**)	122	215	211	204	177.6
$(CF_3)_3Au(py)$ (**4**)	169	216	211	205	176.9
$(CF_3)_3Au(PCMe)$[h]	106	249[i]	212	208	179.3
$(CF_3)_3Au(PC_5H_5)$	152	248	212	208	179.7
$(CF_3)_3Au(PMe_3)$ (**5**)	229	245.5	211	209.5	174.4
$(CH_3)_3Au(PMe_3)$ (**5 H**)	*160*	*241*	*213.5*	*208*	*175.1*
$(CF_3)_3Au(PPh_3)$ (**6**)	204	248	212	210	173.1
$(CF_3)_3Au(PF_3)$	90	245.5	211.5	207.5	176.0
$(CF_3)_3Au(Opy)$ (**7**)[j]	151	217	211	204.5	176.7
$(CF_3)_3Au(OPPh_3)$ (**8**)[k]	173	215	211	204	176.4
$(CF_3)_3Au(SEt_2)$	166	251.5	211.5	208	178.6
$(CF_3)_3Au(tht)$ (**9**)	149	252	211.5	207.5	178.7
$(CF_3)_3Au(SPPh_3)$ (**10**)[l]	183	251.5	211.5	208	178.2

[a] The naked $(CF_3)_3Au$ fragment (L = nil) as well as ether and phosphine complexes of the nonfluorinated $(CH_3)_3Au$ fragment (**1 H** and **5 H**; values in italics) are also included for comparison. [b] A *trans* arrangement is meant in the indicated CX_3-Au-CX_3 (X = H, F) and E-Au-C units with E denoting a chemical element. [c] Atomic coordinates of the optimized structures are given in the Supporting Information. [d] Average value. [e] Ref. [24]. [f] The SiN*t*Bu unit shows an asymmetric side-on coordination favoring the Au–N interaction. [g] The Au–N distance is indicated; the Au–Si distance is 282 pm. [h] The PCMe unit is π-coordinated to the metal center. [i] Distance from the metal to the centroid of the π-coordinated ligand. [j] Au-O-N 118.6°. [k] Au-O-P 125.9°. [l] Au-S-P 100.7°.

173 kJ mol^{-1}) is surpassed by that of the softer sulfide Ph_3PS (**10**: D_e = 183 kJ mol^{-1}).

Intermediate stabilization is attained with py (**4**: D_e = 169 kJ mol^{-1}) and *t*BuNC (**2**: D_e = 178 kJ mol^{-1}). However, the complexes formed with the heavier-element homologues PC_5H_5 (D_e = 152 kJ mol^{-1}) and *t*BuNSi (D_e = 139 kJ mol^{-1}) are less stable. In the $(CF_3)_3Au(SiN$*t*$Bu)$ complex (Figure S6 in the Supporting Information), the silylated ligand is coordinated in a highly asymmetric way, clearly slipped towards the N atom. In the optimized geometry of the phosphabenzene complex $(CF_3)_3Au(PC_5H_5)$ (Figure S8 in the Supporting Information), little modification is observed in the heteroaromatic ring with respect to the free ligand,[57] in keeping with other structurally characterized metal complexes.[58] Thus, a planar geometry is found at the P atom with a small C-P-C angle (105°) and indistinguishable C–C distances within the ring (av 139 pm) consistent with a delocalized aromatic state. The Au–P distance (248 pm) is, however, appreciably longer than those found in linear gold(I) complexes of various substituted monodentate λ^3-phosphinine ligands: $ClAu(PC_5H_2$*t*Bu_3-2,4,6) (221.9(2) pm),[59] $ClAu(PC_5H_2Ph_2$-2,6-Me–4) (av 220.62(7) pm),[60] $ClAu(PC_5H_2R_2$-2,6-Ph-4) (223.4(3) pm for R = Me; ca. 222 pm for R = Ph),[61] $ClAu(PC_5H_2R$-2-Ph_2-4,6) (av 220.8(1) pm; R = $C_6H_3(OMe)_2$-3,4),[62] $ClAu\{PC_5HR$-2-Me-3-Ph_2-4,6} (220.40(7) pm; R = $C_6H_3Me_2$-2,3),[63] $ClAu\{PC_5H_3(SiMe_3)_2$-2,6} (221.1(2) pm), and $[Au\{PC_5H_3(SiMe_2R)_2$-2,6$\}_2][GaCl_4]$ (av 228.2(4) pm for R = Me; av 226.3(2) pm for R = CCPh).[64] The most salient difference to the homologous py complex **4** is the relative disposition of the heteroaromatic EC_5H_5 ring with respect to the metal coordination plane; the dihedral angle is much smaller for E = P (20.3°) than for E = N

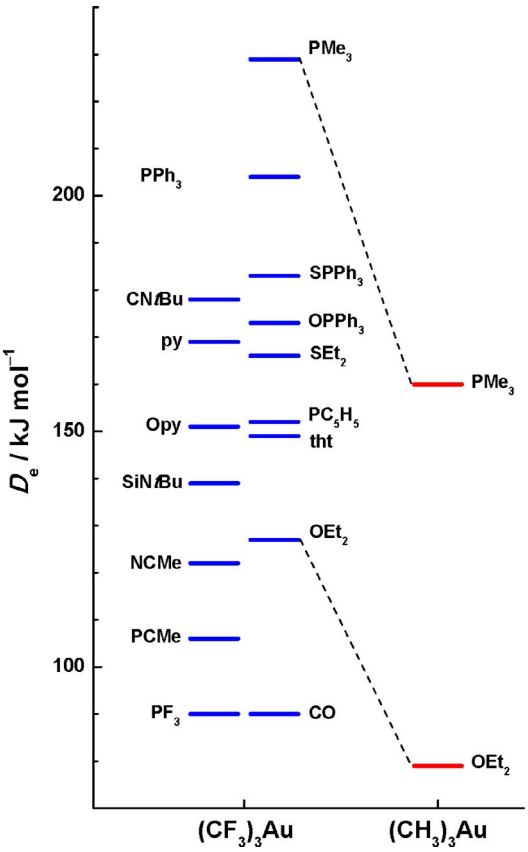

Figure 9. Affinity scale of the $(CF_3)_3Au$ fragment for various L ligands based on the dissociation energy D_e calculated for the corresponding $(CF_3)_3Au$–L bond (Table 3). Considerably lesser stabilization is achieved by coordination to the nonfluorinated $(CH_3)_3Au$ fragment (right).

(81.2°). The latter is in excellent agreement with that experimentally determined for complex **4** (78.2°). The lower stability of $(CF_3)_3Au(PC_5H_5)$ in comparison with $(CF_3)_3Au(NC_5H_5)$ can be attributed to the phosphabenzene ligand being a weaker σ donor and better π acceptor than py.[65]

Moderately stable compounds are formed with the hard ligands Et_2O (**1**) and MeCN (**3**), for which $D_e \approx 125$ kJ mol^{-1}. These Lewis bases are well known as typical weakly coordinating ligands.[66] Considering the modest D_e value required to set free the unsaturated metal fragment, these solvates are indeed suitable synthons for the naked $(CF_3)_3Au$ unit. Substantially more stabilized are complexes with soft thioether ligands, such as open-chain Et_2S ($D_e = 166$ kJ mol^{-1}) and alicyclic tht (**9**: $D_e = 149$ kJ mol^{-1}). In contrast, the complex formed with the heavier-element homologue of acetonitrile MeC≡P is significantly less stable ($D_e = 106$ kJ mol^{-1}). However, the two $(CF_3)_3Au(ECMe)$ complexes show quite different structural patterns. Thus, side-on coordination is more stable for the heavier MeC≡P ligand (Figure S7 in the Supporting Information), whereas standard end-on coordination is found for MeC≡N. Although sought by different approaches, no minimum was found for side-on coordination in the latter case. Side-on coordination of the phosphaalkyne ligand was experimentally found in the cationic gold(I) complex $[(RtBu_2P)Au(\eta^2\text{-}P{\equiv}CtBu)][SbF_6]$ ($R = C_6H_4Ph$-2).[67]

Identical stabilization is attained with the prototypical π-acceptor ligands CO and PF_3: $D_e = 90$ kJ mol^{-1}. Their complexes are the least stable in the whole set under study. As in the case of phosphabenzene, the poor σ-donor ability of the CO and PF_3 ligands results in weaker [Au]–L σ bonds. Moreover, there is little chance for the $(CF_3)_3Au$ unit to supply any significant π-backbonding contribution that might strengthen the [Au]–L bond by synergy. In fact, we were unable to prepare the carbonyl derivative $(CF_3)_3Au{\cdot}(CO)$ by replacement of the labile Et_2O molecule in compound **1**, at least under the experimental conditions that proved successful in every other case (Scheme 2).

In the set of bases L chosen for the current study, the P-donor ligands proved to be particularly versatile, as they encompass the whole stability range (Figure 9). Thus, the upper limit is set by the highly basic phosphine PMe_3, whereas the lower limit is set by the poor donor PF_3. In between are found unsaturated P-donor ligands, such as phosphabenzene and the phosphaalkyne MeC≡P.

Finally, we compared the stabilization achieved by coordination of a given ligand L to the $(CF_3)_3Au$ species with that attained with the nonfluorinated $(CH_3)_3Au$ fragment. For this purpose, we selected compounds $(CH_3)_3Au(OEt_2)$ (**1H**) and $(CH_3)_3Au(PMe_3)$ (**5H**) as representative examples of complexes with weakly and strongly coordinated ligands. In both cases, coordination to the $(CH_3)_3Au$ fragment provides substantially less stabilization (Table 3; Figure 9). Comparing the optimized geometries of the $(CX_3)_3Au(OEt_2)$ molecules (X = H, F; Figure S5 in the Supporting Information) reveals that the oxygen atom in the fluorinated derivative **1** undergoes little pyramidalization, and the sum of subtended bond angles (352°) is appreciably greater than that in the nonfluorinated counterpart **1H** (341°). This is probably an additional effect of the higher acidity of the $(CF_3)_3Au$ moiety, which should induce greater polarization of the electron density at the donor atom. Experimentally, compound **1** can be handled in solution at room temperature without noticeable decomposition, whereas **1H** already begins to decompose at −40 °C.[27] In a similar way, $(CF_3)_3Au(PPh_3)$ (**6**) is stable up to 251 °C, whereas its nonfluorinated analogue $(CH_3)_3Au(PPh_3)$ decomposes at 120 °C.[68] Thus, fluorination of the trimethylgold moiety $(CH_3)_3Au$ results in substantial stability enhancement in the corresponding $(CF_3)_3Au{\cdot}L$ derivatives, as shown experimentally and confirmed by theoretical calculations.

Conclusions

The perfluorinated $(CF_3)_3Au$ moiety is a highly acidic organogold(III) fragment. As established by theoretical and experimental methods, its Lewis acidity greatly exceeds that of the nonfluorinated analogous species $(CH_3)_3Au$, and closely approaches that of $(C_6F_5)_3B$. This result reinforces the idea of the CF_3 group acting as an efficient electron-withdrawing ligand with high electronegativity.[18] Since CF_3 is the organic group with the highest fluorine content per carbon atom, the $(CF_3)_3Au$ moiety possibly excels as the strongest Lewis acid among conceivable R_3Au organogold species.

The neutral etherate $(CF_3)_3Au{\cdot}OEt_2$ (**1**) provides a convenient experimental entry to the chemistry of the perfluorinated $(CF_3)_3Au$ moiety, which is currently underdeveloped. The modest bond dissociation energy of the coordinated Et_2O ligand together with its high lability makes compound **1** a useful synthon of the unsaturated $(CF_3)_3Au$ fragment. In fact, a range of neutral $(CF_3)_3Au{\cdot}L$ compounds (**2**–**10**) was synthesized therefrom (Scheme 2). The L ligands, which include a variety of C, N, P, O, and S donors, were selected to cover a wide range of donor abilities. Compounds **3**–**10** exhibit marked thermal stability (decomposition temperatures >200 °C). The stability of the saturated $(CF_3)_3Au{\cdot}L$ compounds largely exceeds that of the nonfluorinated $(CH_3)_3Au{\cdot}L$ analogues in the few cases in which such comparison can be experimentally established. The stabilization enhancement by fluorination was estimated to amount to 50–70 kJ mol^{-1} (Table 3; Figure 9). This remarkable stability makes the $(CF_3)_3Au$ moiety especially appealing for synthetic and applied purposes. Hence, a ligand-affinity scale that may provide a guide for reactivity studies was elaborated by DFT methods (Figure 9). Given the stereochemical stability of the T-shaped $(CF_3)_3Au$ moiety, little deformation energy is required for the metal coordination sphere to accommodate the incoming L ligand.[16,69] For this reason, our estimates of ligand dissociation energies in the series of $(CF_3)_3Au{\cdot}L$ complexes provide a reliable measure of the actual Au–L interaction energy.

The high energy profile calculated for the $[Au]{-}CF_3 \rightleftharpoons F{-}[Au] \leftarrow CF_2$ fluorine shift (Scheme 3b) makes this process less important as a potential decomposition channel, and thus represents a further source of additional stability.

In summary, fluorination of $(CH_3)_3Au$ raises the Lewis acidity of the Au center in $(CF_3)_3Au$ close to that of $(C_6F_5)_3B$ and results also in substantial stability enhancement in the corresponding

$(CF_3)_3Au{\cdot}L$ complexes. These advantageous features together with its marked stereochemical stability and its reluctance to undergo side reactions such as fluorotropism or reductive elimination[24] make the single-site $(CF_3)_3Au$ fragment appealing for reactivity and mechanistic studies. Considering also the current interest in the involvement of organogold(III) complexes in synthetic and catalytic processes,[70] the $(CF_3)_3Au$ system may find interesting applications, as it unites the reactivity potential of organogold complexes with the performance of the highly acidic $(C_6F_5)_3B$ species.

Experimental Section

General procedures and materials

Unless otherwise stated, reactions and manipulations were carried out under purified argon by using Schlenk techniques. Solvents were dried with an MBraun SPS-800 System. The parent species $[PPh_4][(CF_3)_3AuI]$ was obtained as described elsewhere.[24] Other chemicals were purchased from standard commercial suppliers and used as received. Elemental analyses were carried out with a Perkin–Elmer 2400 CHNS/O Series II microanalyzer. IR spectra were recorded on neat solid samples with a PerkinElmer Spectrum FTIR spectrometer (4000–250 cm^{-1}) equipped with an ATR device. Mass spectra were recorded with a Bruker MicroFlex or AutoFlex spectrometer. However, no clear peaks were detected for any of the neutral species $(CF_3)_3Au{\cdot}L$ (**2**–**10**) by using either positive or negative MALDI-TOF techniques. NMR spectra were recorded with Bruker ARX 300 or AV 400 spectrometers. Unless otherwise stated, the spectroscopic measurements were carried out at room temperature. Chemical shifts are given with respect to the standard references: $SiMe_4$ (^1H and ^{13}C), $CFCl_3$ (^{19}F), and 85% aqueous H_3PO_4 (^{31}P). Experimentally obtained NMR spectroscopic data are given in Table 1 and are therefore omitted in the corresponding synthetic entry. TGA/DTA was performed with an SDT 2960 instrument at heating rate of 10 °C min^{-1} under N_2 atmosphere. Melting points were taken at the maximum of the DTA peak and verified by visual inspection of samples placed on glass plates by using an Olympus BH-2 microscope fitted with a Linkam TMS-91 temperature controller with hot stage.

Caution! Although we have not encountered any problems working under the conditions detailed below (synthesis of **1**), perchlorate salts are potentially explosive when in contact with organic solvents and ligands. For this reason, only small amounts of these materials should be prepared and they should always be handled with great caution.[71]

Synthesis of $(CF_3)_3Au{\cdot}OEt_2$ (1)

Addition of an equimolar amount of $AgClO_4$ (24 mg, 0.11 mmol) to a solution of $[PPh_4][(CF_3)_3AuI]$ (0.10 g, 0.11 mmol) in CH_2Cl_2/Et_2O (2/10 mL) in the dark caused immediate precipitation of AgI. After 30 min of stirring, the solvent mixture was replaced by Et_2O/*n*-hexane (5/15 mL), and the resulting suspension was allowed to stand at −80 °C overnight. Filtering the solid off gave a solution of etherate **1**, which is suitable for most synthetic purposes (80% yield estimated on further reactions). By evaporation of this solution to dryness at 0 °C, a white residue appeared, which was redissolved in *n*-hexane. By keeping this extract at −80 °C for 2 d, a deliquescent white solid was obtained that still contained some free Et_2O (Figure 1).

Synthesis of $(CF_3)_3Au(CNtBu)$ (2)

*t*BuNC (11 μL, 92 μmol) was added to a solution of **1** (92 μmol) in Et_2O/*n*-hexane (5/15 mL), and the resulting mixture was stirred for 30 min. Removal of the solvent by vacuum evaporation afforded a white solid, which was suspended in *n*-hexane (3 mL), collected by filtration, dried, and identified as **2** (28 mg, 58 μmol, 63% yield). $^{13}C\{^1H\}$ NMR (100.577 MHz, CD_2Cl_2): $\delta_C = 29.4$ ppm (s; CH_3); IR: 2997 (w), 2283 (m; C≡N), 1617 (w), 1477 (w), 1456 (w), 1437 (w), 1379 (m), 1259 (w), 1236 (w), 1160 (m), 1131 (s), 1100 (s), 1073 (vs), 1038 (vs), 954 (m), 934 (m), 831 (m), 802 (m), 751 (w), 728 (s), 714 (s), 689 (m), 639 (w), 527 (s), 451 (w), 399 (w), 339 (w), 329 (w), 307 (w), 294 (s), 278 (m), 263 cm^{-1} (m); elemental analysis (%) calcd for $C_8H_9AuF_9N$: C 19.73, H 1.86, N 2.88; found: C 20.22, H 1.68, N 2.84. Single crystals suitable for X-ray diffraction were obtained by slow evaporation of a solution of **2** (7 mg) in Et_2O/*n*-hexane (1/2 mL) at room temperature.

Synthesis of $(CF_3)_3Au(NCMe)$ (3)

By the procedure described for the synthesis of **2**, compound **3** was prepared starting from an Et_2O/*n*-hexane solution of compound **1** (92 μmol) and MeCN (4.8 μL, 92 μmol). Complex **3** was obtained as a white solid (28 mg, 62 μmol, 68% yield); m.p. 96 °C; b.p. 209 °C. $^{13}C\{^1H\}$ NMR (100.577 MHz, CD_2Cl_2): $\delta_C = 120.5$ (s; C≡N), 3.6 ppm (s; CH_3); IR: 2959 (m), 2901 (w), 2346 (m; ν_2: C≡N), 2316 (m; $\nu_3+\nu_4$),[72] 1408 (w), 1370 (w), 1260 (m), 1170 (s), 1139 (s), 1095 (s), 1040 (vs), 1025 (vs), 955 (s), 866 (m), 799 (s), 736 (s), 716 (m), 534 (w), 460 (w), 402 (m), 321 (s), 307 (s), 266 cm^{-1} (s); elemental analysis (%) calcd for $C_5H_3AuF_9N$: C 13.49, H 0.68, N 3.15; found: C, 13.31, H 0.72, N 3.33.

Synthesis of $(CF_3)_3Au(py)$ (4)

By using the procedure described for the synthesis of **2**, compound **4** was prepared starting from an Et_2O/*n*-hexane solution of **1** (92 μmol) and py (7.4 μL, 92 μmol). Complex **4** was obtained as a white solid (29 mg, 60 μmol, 65% yield); m.p. 177 °C; b.p. 223 °C. $^{13}C\{^1H\}$ NMR (100.577 MHz, CD_2Cl_2): $\delta_C = 149.6$ (s; C^o), 142.4 (s; C^p), 127.8 ppm (s; C^m); IR: 3128 (w), 1617 (m), 1493 (w), 1460 (s), 1436 (w), 1260 (m), 1166 (s), 1126 (s), 1112 (s), 1080 (vs), 1044 (vs), 1034 (vs), 1020 (vs), 1009 (vs), 980 (s), 948 (s), 871 (w), 799 (m), 759 (s), 731 (m), 715 (m), 688 (vs), 656 (m), 526 (m), 446 (w), 432 (w), 395 (w), 341 (w), 313 (m), 303 (s), 280 (w), 262 cm^{-1} (m); elemental analysis (%) calcd for $C_8H_5AuF_9N$: C 19.89, H 1.04, N 2.90; found: C 19.91, H 1.02, N 3.08. Single crystals suitable for X-ray diffraction were obtained by slow evaporation of a solution of **4** (7 mg) in Et_2O/*n*-hexane (1/2 mL) at room temperature.

Synthesis of $(CF_3)_3Au(PMe_3)$ (5)

By using the procedure described for the synthesis of **2**, compound **5** was prepared starting from an Et_2O/*n*-hexane solution of compound **1** (92 μmol) and a 1 M solution of PMe_3 in toluene (92 μL, 92 μmol). Complex **5**, which had already been prepared by other methods,[26,33] was obtained as a white solid (24 mg, 50 μmol, 54% yield); m.p. 151 °C; b.p. 214 °C. $^{13}C\{^1H\}$ NMR (100.577 MHz, CD_2Cl_2): $\delta_C = 14.7$ ppm (d, $^1J(^{13}C,^{31}P) = 36.0$ Hz; CH_3); IR: 2936 (w), 1436 (w), 1426 (w), 1322 (w), 1302 (m), 1158 (s), 1104 (s), 1058 (vs), 1038 (vs), 1016 (vs), 958 (vs), 867 (s), 764 (m), 750 (m), 719 (m), 713 (m), 681 (w), 525 (w), 366 (w), 298 (m), 278 cm^{-1} (m); elemental analysis (%) calcd for $C_6H_9AuF_9P$: C 15.01, H 1.89; found: C 15.09, H 1.69. Single crystals suitable for X-ray diffraction were obtained by

slow evaporation of a solution of **5** (7 mg) in Et_2O/*n*-hexane (1/2 mL) at room temperature.

Synthesis of $(CF_3)_3Au(PPh_3)$ (6)

By using the procedure described for the synthesis of **2**, compound **6** was prepared starting from an Et_2O/*n*-hexane solution of compound **1** (92 μmol) and PPh_3 (24 mg, 92 μmol). Complex **6** was obtained as a white solid (34 mg, 51 μmol, 56% yield); m.p. 153 °C. $^{13}C\{^1H\}$ NMR (100.577 MHz, CD_2Cl_2): $\delta_C = 134.4$ (d, $^2J(^{13}C,^{31}P) = 11.1$ Hz; C^o), 133.0 (d, $^4J(^{13}C,^{31}P) = 3.0$ Hz; C^p), 129.7 (d, $^3J(^{13}C,^{31}P) = 11.9$ Hz; C^m), 126.6 ppm (d, $^1J(^{13}C,^{31}P) = 58.8$ Hz; C^{ipso}); IR: 3060 (w), 1587 (w), 1484 (m), 1439 (m), 1334 (w), 1316 (w), 1190 (w), 1150 (s), 1124 (s), 1099 (vs), 1049 (vs), 1033 (vs), 997 (s), 975 (m), 933 (w), 924 (w), 844 (w), 757 (m), 745 (s), 721 (m), 707 (s), 691 (vs), 617 (w), 527 (vs), 511 (s), 495 (s), 458 (m), 446 (w), 423 (m), 406 (w), 396 (w), 374 (w), 334 (w), 290 (s), 276 (w), 269 cm^{-1} (w); elemental analysis (%) calcd for $C_{21}H_{15}AuF_9P$: C 37.86, H 2.27; found: C 37.65, H 2.09. Single crystals suitable for X-ray diffraction were obtained by slow evaporation of a solution of **6** (7 mg) in Et_2O/*n*-hexane (1/2 mL) at room temperature.

Synthesis of $(CF_3)_3Au(Opy)$ (7)

By using the procedure described for the synthesis of **2**, compound **7** was prepared starting from an Et_2O/*n*-hexane solution of compound **1** (92 μmol) and Opy (8.7 mg, 92 μmol). Complex **7** was obtained as a white solid (20 mg, 40 μmol, 44% yield); m.p. 108 °C. $^{13}C\{^1H\}$ NMR (100.577 MHz, CD_2Cl_2): $\delta_C = 141.2$ (s; C^o), 137.9 (s; C^p), 128.0 ppm (s; C^m); IR: 3127 (w), 3103 (w), 1620 (w), 1479 (s), 1436 (w), 1253 (w), 1210 (m), 1163 (m), 1147 (s), 1098 (s), 1065 (vs), 1055 (vs), 1034 (vs), 1021 (vs), 932 (m), 832 (s), 810 (m), 772 (s), 734 (m), 713 (m), 689 (w), 669 (s), 643 (w), 585 (s), 556 (w), 528 (m), 473 (s), 353 (s), 306 (s), 280 (w), 264 cm^{-1} (s); elemental analysis (%) calcd for $C_8H_5AuF_9NO$: C 19.25, H 1.01, N 2.81; found: C 19.42, H 0.90, N 3.02. Crystals suitable for X-ray diffraction were obtained by slow diffusion of a layer of *n*-hexane (10 mL) into a solution of **7** (7 mg) in Et_2O (3 mL) at 4 °C.

Synthesis of $(CF_3)_3Au(OPPh_3)$ (8)

By using the procedure described for the synthesis of **2**, compound **8** was prepared starting from an Et_2O/*n*-hexane solution of compound **1** (92 μmol) and $OPPh_3$ (26 mg, 92 μmol). Complex **8** was obtained as a white solid (38 mg, 56 μmol, 61%); m.p. 145 °C. $^{13}C\{^1H\}$ NMR (100.577 MHz, CD_2Cl_2): $\delta_C = 134.2$ (d, $^4J(^{13}C,^{31}P) = 2.8$ Hz; C^p), 133.0 (d, $^2J(^{13}C,^{31}P) = 11.1$ Hz; C^o), 129.5 (d, $^3J(^{13}C,^{31}P) = 13.1$ Hz; C^m), 127.8 ppm (d, $^1J(^{13}C,^{31}P) = 108.9$ Hz; C^{ipso}); IR: 3070 (w), 1590 (w), 1485 (w), 1440 (m), 1315 (w), 1180 (m), 1163 (w), 1147 (m), 1115 (vs.; O=P), 1101 (s), 1084 (vs), 1050 (vs), 1038 (vs), 1022 (vs), 996 (vs), 985 (s), 937 (m), 851 (w), 754 (m), 746 (m), 727 (vs), 692 (s), 617 (w), 552 (s), 531 (vs), 481 (m), 442 (m), 431 (m), 400 (w), 389 (w), 352 (m), 318 (m), 309 (m), 294 (w), 281 (w), 265 cm^{-1} (m); elemental analysis (%) calcd for $C_{21}H_{15}AuF_9OP$: C 36.97, H 2.22; found: C 36.83, H 2.11. Single crystals suitable for X-ray diffraction were obtained by slow evaporation of a solution of **8** (7 mg) in Et_2O/*n*-hexane (1/2 mL) at room temperature.

Synthesis of $(CF_3)_3Au(tht)$ (9)

By using the procedure described for the synthesis of **2**, compound **9** was prepared starting from an Et_2O/*n*-hexane solution of compound **1** (92 μmol) and tht (8.2 μL, 92 μmol). Complex **9** was obtained as a white solid (17 mg, 35 μmol, 38% yield); m.p. 89 °C; b.p. 205 °C. $^{13}C\{^1H\}$ NMR (100.577 MHz, CD_2Cl_2): $\delta_C = 40.0$ (s; α-CH_2), 30.2 ppm (s; β-CH_2); IR: 2941 (w), 2873 (w), 1447 (w), 1438 (w), 1314 (w), 1278 (w), 1263 (w), 1213 (w), 1156 (s), 1127 (w), 1104 (vs), 1038 (vs), 961 (s), 896 (m), 807 (m), 730 (m), 713 (m), 666 (w), 653 (m), 528 (w), 516 (w), 477 (w), 310 (m), 295 (m), 277 (w), 266 cm^{-1} (w); elemental analysis (%) calcd for $C_7H_8AuF_9S$: C 17.08, H 1.64, S 6.52; found: C 17.07, H 1.49, S 6.72. Single crystals suitable for X-ray diffraction were obtained by slow evaporation of a solution of **9** (7 mg) in Et_2O/*n*-hexane (1/2 mL) at room temperature.

Synthesis of $(CF_3)_3Au(SPPh_3)$ (10)

By using the procedure described for the synthesis of **2**, compound **10** was prepared starting from an Et_2O/*n*-hexane solution of compound **1** (92 μmol) and $SPPh_3$ (27 mg, 92 μmol). Complex **10** was obtained as a white solid (39 mg, 56 μmol, 61% yield); m.p. 192 °C. $^{13}C\{^1H\}$ NMR (100.577 MHz, CD_2Cl_2): $\delta_C = 134.5$ (d, $^4J(^{13}C,^{31}P) = 2.9$ Hz; C^p), 133.6 (d, $^2J(^{13}C,^{31}P) = 11.2$ Hz; C^o), 130.0 (d, $^3J(^{13}C,^{31}P) = 13.4$ Hz; C^m), 126.3 ppm (d, $^1J(^{13}C,^{31}P) = 86.6$ Hz; C^{ipso}); IR: 3083 (w), 1588 (w), 1482 (w), 1439 (m), 1335 (w), 1314 (w), 1187 (w), 1150 (s), 1118 (s), 1104 (vs), 1094 (vs), 1054 (vs), 1042 (vs), 996 (s), 982 (m), 973 (m), 935 (m), 854 (w), 842 (w), 758 (m), 747 (m), 718 (s), 699 (s), 686 (s), 638 (w), 618 (m), 585 (vs; S=P), 538 (w), 517 (vs), 504 (vs), 473 (m), 447 (m), 434 (m), 403 (w), 394 (w), 352 (m), 317 (m), 290 (m), 265 cm^{-1} (m); elemental analysis (%) calcd for $C_{21}H_{15}AuF_9PS$: C 36.12, H 2.17, S 4.59; found: C 36.56, H 2.11, S 4.75. Single crystals suitable for X-ray diffraction were obtained by slow evaporation of a solution of **10** (7 mg) in Et_2O/*n*-hexane (1/2 mL) at room temperature.

Synthesis of $[PPh_4][(CF_3)_3AuCl]$

$[PPh_4]Cl$ (34 mg, 92 μmol) was added to a solution of **1** (92 μmol) in Et_2O/*n*-hexane (5/15 mL). The resulting mixture was stirred for 30 min and then concentrated to dryness. Treatment of the resulting residue with *i*PrOH (3 mL) at −30 °C gave a white solid, which was collected by filtration, washed with Et_2O (3×3 mL), and vacuum-dried (45 mg, 58 μmol, 63% yield). The compound thus obtained was identified as $[PPh_4][(CF_3)_3AuCl]$.[24]

Synthesis of $[PPh_4][(CF_3)_3AuBr]$

$[PPh_4]Br$ (39 mg, 92 μmol) was added to a solution of **1** (92 μmol) in Et_2O/*n*-hexane (5/15 mL). The resulting mixture was stirred for 30 min and then concentrated to dryness. Treatment of the resulting residue with *i*PrOH (3 mL) at −30 °C gave a white solid, which was collected by filtration, washed with Et_2O (3×3 mL), and vacuum-dried (47 mg, 57 μmol, 62% yield). The compound thus obtained was identified as $[PPh_4][(CF_3)_3AuBr]$.[24]

Reversion to $[PPh_4][(CF_3)_3AuI]$

Addition of $[PPh_4]I$ (6.6 mg, 13.8 μmol) to a CD_2Cl_2 solution of **1** (13.8 μmol) resulted in quantitative reversion to the starting material $[PPh_4][(CF_3)_3AuI]$ (^{19}F NMR).[24]

Computational details

Quantum mechanical calculations were performed with the Gaussian 09 package at the DFT/M06 level of theory. The SDD basis set and its ECPs together with additional f-type polarization functions were used to describe Au atoms. Light atoms (H, C, N, O, F, Si, P, and S) were described with a 6-31G** basis set. See Supporting Information for full details and references.

X-ray structure determinations

Crystal data and other details of the structure analyses are listed in Tables S1 and S2 in the Supporting Information. Details of diffraction data collection and structure solution can be found in the Supporting Information.

Acknowledgements

This work was supported by the Spanish MINECO/FEDER (Projects CTQ2015-67461-P and MAT2015-68200-C2-1-P) and the Gobierno de Aragón and Fondo Social Europeo (Grupo Consolidado E21: *Química Inorgánica y de los Compuestos Organometálicos*). The Instituto de Biocomputación y Física de Sistemas Complejos (BIFI) and the Centro de Supercomputación de Galicia (CESGA) are gratefully acknowledged for generous allocation of computational resources. A.P.-B. thanks the Spanish Ministerio de Educación, Cultura y Deporte for a grant (FPU15/03940).

Keywords: fluorinated ligands · gold · Lewis acids · ligand affinity · organogold chemistry

[1] *Acid Catalysis in Modern Organic Synthesis* (Eds.: H. Yamamoto, K. Ishihara), Wiley-VCH, Weinheim, **2008**.

[2] For a recent case of interrelated Brønsted and Lewis acidity, see: A. Wiesner, T. W. Gries, S. Steinhauer, H. Beckers, S. Riedel, *Angew. Chem. Int. Ed.* **2017**, *56*, 8263; *Angew. Chem.* **2017**, *129*, 8375.

[3] Very strong Lewis acids have sometimes been termed "superacids". There is, however, some disagreement on the threshold taken as the reference to apply that label. Thus, Olah considered superacids as those stronger than $AlCl_3$, the most widely used Lewis acid in Friedel–Crafts processes (see ref. [4]), whereas Krossing preferred to take the highly acidic SbF_5 as the threshold reference (see ref. [5]). To avoid confusion, in this paper we will term superacids only those species conforming to both criteria, namely, $(CF_3)_3B$ and AuF_5.

[4] a) G. A. Olah, G. K. S. Prakash, Á. Molnár, J. Sommer, *Superacid Chemistry*, 2nd ed., Wiley, Hoboken, **2009**, pp. 42–46; b) G. A. Olah, G. K. S. Prakash, A. Goeppert, *Actual. Chim.* **2006** (301–302), 68; c) G. A. Olah, J. Sommer, *La Recherche* **1979**, *10*, 624; d) G. A. Olah, G. K. S. Prakash, J. Sommer, *Science* **1979**, *206*, 13.

[5] a) A. Kraft, N. Trapp, D. Himmel, H. Böhrer, P. Schlüter, H. Scherer, I. Krossing, *Chem. Eur. J.* **2012**, *18*, 9371; b) L. O. Müller, D. Himmel, J. Stauffer, G. Steinfeld, J. Slattery, G. Santiso-Quiñones, V. Brecht, I. Krossing, *Angew. Chem. Int. Ed.* **2008**, *47*, 7659; *Angew. Chem.* **2008**, *120*, 7772.

[6] a) G. A. Olah, *J. Org. Chem.* **2005**, *70*, 2413; b) *Carbocation Chemistry* (Eds.: G. A. Olah, G. K. S. Prakash), Wiley, Hoboken, **2004**; c) G. A. Olah, *J. Org. Chem.* **2001**, *66*, 5943; d) G. A. Olah, *Angew. Chem. Int. Ed. Engl.* **1995**, *34*, 1393; *Angew. Chem.* **1995**, *107*, 1519.

[7] a) M. Hatano, K. Ishihara, in *Boron Reagents in Synthesis: ACS Symposium Series, Vol. 1236* (Ed.: A. Coca), ACS, Washington, **2016**, pp. 27–66; b) V. Rauniyar, D. G. Hall, in *Acid Catalysis in Modern Organic Synthesis Vol. 1* (Eds.: H. Yamamoto, K. Ishihara), Wiley-VCH, Weinheim, **2008**, pp. 187–239.

[8] E. Y.-X. Chen, T. J. Marks, *Chem. Rev.* **2000**, *100*, 1391.

[9] a) E. I. Davydova, T. N. Sevastianova, A. Y. Timoshkin, *Coord. Chem. Rev.* **2015**, *297–298*, 91; b) L. A. Mück, A. Y. Timoshkin, G. Frenking, *Inorg. Chem.* **2012**, *51*, 640.

[10] a) W. E. Piers, *Adv. Organomet. Chem.* **2004**, *52*, 1; b) T. Chivers, *J. Fluorine Chem.* **2002**, *115*, 1.

[11] In contrast, BF_3 is less acidic than any of the heavier halides BX_3 (X = Cl, Br, I). This atypical trend is usually rationalized by assuming a certain degree of B←X π interaction that attenuates the acidity of the boron center. Such interaction should be more efficient in the case of the fluoride (X = F) due to better overlap of the filled F(p) orbitals of appropriate symmetry with the empty B(p) orbital, which makes BF_3 the least acidic within the BX_3 family, as experimentally found: D. J. Grant, D. A. Dixon, D. Camaioni, R. G. Potter, K. O. Christe, *Inorg. Chem.* **2009**, *48*, 8811.

[12] a) G. Erker, *Dalton Trans.* **2005**, 1883; b) M. Bochmann, S. J. Lancaster, M. D. Hannant, A. Rodríguez, M. Schormann, D. A. Walker, T. J. Woodman, *Pure Appl. Chem.* **2003**, *75*, 1183; c) W. E. Piers, T. Chivers, *Chem. Soc. Rev.* **1997**, *26*, 345.

[13] M. Finze, E. Bernhardt, H. Willner, *Angew. Chem. Int. Ed.* **2007**, *46*, 9180; *Angew. Chem.* **2007**, *119*, 9340.

[14] a) M. Finze, E. Bernhardt, A. Terheiden, M. Berkei, H. Willner, D. Christen, H. Oberhammer, F. Aubke, *J. Am. Chem. Soc.* **2002**, *124*, 15385; b) A. Terheiden, E. Bernhardt, H. Willner, F. Aubke, *Angew. Chem. Int. Ed.* **2002**, *41*, 799; *Angew. Chem.* **2002**, *114*, 823.

[15] M. Finze, E. Bernhardt, M. Zähres, H. Willner, *Inorg. Chem.* **2004**, *43*, 490.

[16] A. L. Gille, T. M. Gilbert, *J. Chem. Theory Comput.* **2008**, *4*, 1681.

[17] T. Furuya, A. S. Kamlet, T. Ritter, *Nature* **2011**, *473*, 470.

[18] M. A. García-Monforte, S. Martínez-Salvador, B. Menjón, *Eur. J. Inorg. Chem.* **2012**, 4945.

[19] Electronegativity values are given according to the Sanderson scale: a) J. E. Huheey, E. A. Kreiter, R. L. Kreiter, *Inorganic Chemistry*, 4th ed., Harper–Collins, New York, **1993**, pp. 182–199; b) R. T. Sanderson, *Simple Inorganic Substances*, Krieger, Malabar, **1989**, pp. 20–28; c) S. G. Bratsch, *J. Chem. Educ.* **1985**, *62*, 101.

[20] a) A. G. Algarra, V. V. Grushin, S. A. Macgregor, *Organometallics* **2012**, *31*, 1467; b) P. Sgarbossa, A. Scarso, G. Strukul, R. A. Michelin, *Organometallics* **2012**, *31*, 1257; c) R. J. Puddephatt, *The Chemistry of Gold*, Elsevier, Amsterdam, **1978**, pp. 26–27; d) T. G. Appleton, H. C. Clark, L. E. Manzer, *Coord. Chem. Rev.* **1973**, *10*, 335; e) T. G. Appleton, M. H. Chisholm, H. C. Clark, L. E. Manzer, *Inorg. Chem.* **1972**, *11*, 1786.

[21] R. Hoffmann, S. Alvarez, C. Mealli, A. Falceto, T. J. Cahill III, T. Zeng, G. Manca, *Chem. Rev.* **2016**, *116*, 8173.

[22] a) R. J. Puddephatt, *Gold Bull.* **1977**, *10*, 108; b) A. Johnson, R. J. Puddephatt, *J. Chem. Soc. Dalton Trans.* **1976**, 1360; c) J. D. Kennedy, W. McFarlane, R. J. Puddephatt, *J. Chem. Soc. Dalton Trans.* **1976**, 745; d) A. Johnson, R. J. Puddephatt, *Inorg. Nucl. Chem. Lett.* **1973**, *9*, 1175.

[23] The chemistry of trifluoromethyl gold compounds has been reviewed recently: J. Gil-Rubio, J. Vicente, *Dalton Trans.* **2015**, *44*, 19432.

[24] A. Pérez-Bitrián, S. Martínez-Salvador, M. Baya, J. M. Casas, A. Martín, B. Menjón, J. Orduna, *Chem. Eur. J.* **2017**, *23*, 6919.

[25] a) H. Braunschweig, I. Krummenacher, M.-A. Légaré, A. Matler, K. Radacki, Q. Ye, *J. Am. Chem. Soc.* **2017**, *139*, 1802; b) C. Lichtenberg, *Angew. Chem. Int. Ed.* **2016**, *55*, 484; *Angew. Chem.* **2016**, *128*, 494; c) M. M. Hansmann, G. Bertrand, *J. Am. Chem. Soc.* **2016**, *138*, 15885; d) Z. Yang, M. Zhong, X. Ma, S. De, C. Anusha, P. Parameswaran, H. W. Roesky, *Angew. Chem. Int. Ed.* **2015**, *54*, 10225; *Angew. Chem.* **2015**, *127*, 10363; e) H. Braunschweig, R. D. Dewhurst, F. Hupp, M. Nutz, K. Radacki, C. W. Tate, A. Vargas, Q. Ye, *Nature* **2015**, *522*, 327; f) D. Martin, M. Soleilhavoup, G. Bertrand, *Chem. Sci.* **2011**, *2*, 389; g) P. P. Power, *Nature* **2010**, *463*, 171.

[26] M. A. Guerra, T. R. Bierschenk, R. J. Lagow, *J. Organomet. Chem.* **1986**, *307*, C58.

[27] a) H. Gilman, L. A. Woods, *J. Am. Chem. Soc.* **1948**, *70*, 550; b) L. A. Woods, H. Gilman, *Proc. Iowa Acad. Sci.* **1943**, *49*, 286.

[28] The related silver solvento complex $(CF_3)_3Ag{\cdot}NCMe$ was described as an oily substance at room temperature: D. Naumann, W. Tyrra, F. Trinius, W. Wessel, T. Roy, *J. Fluorine Chem.* **2000**, *101*, 131.

[29] G. R. Fulmer, A. J. M. Miller, N. H. Sherden, H. E. Gottlieb, A. Nudelman, B. M. Stoltz, J. E. Bercaw, K. I. Goldberg, *Organometallics* **2010**, *29*, 2176.

[30] a) P. W. Siu, K. Hazin, D. P. Gates, *Chem. Eur. J.* **2013**, *19*, 9005; b) I. Krossing, A. Reisinger, *Eur. J. Inorg. Chem.* **2005**, 1979; c) U. Wietelmann, W. Bonrath, T. Netscher, H. Nöth, J.-C. Panitz, M. Wohlfahrt-Mehrens, *Chem. Eur. J.* **2004**, *10*, 2451; d) S. Rannabauer, T. Habereder, H. Nöth, W. Schnick, *Z. Naturforsch. Teil B* **2003**, *58*, 745; e) D. Stasko, S. P. Hoffmann, K.-C. Kim, N. L. P. Fackler, A. S. Larsen, T. Drovetskaya, F. S. Tham, C. A. Reed, C. E. F. Rickard, P. D. W. Boyd, E. S. Stoyanov, *J. Am. Chem. Soc.* **2002**, *124*, 13869; f) S. J. Lancaster, A. Rodríguez, A. Lara-Sánchez, M. D. Hannant, D. A. Walker, D. H. Hughes, M. Bochmann, *Organometallics* **2002**, *21*, 451; g) L. D. Henderson, W. E. Piers, G. J. Irvine, R. McDonald, *Organometallics* **2002**, *21*, 340; h) D. Vagedes, G. Erker, R. Fröhlich, *J. Or-*

ganomet. Chem. **2002**, *641*, 148; i) P. Jutzi, C. Müller, A. Stammler, H.-G. Stammler, *Organometallics* **2000**, *19*, 1442; j) M. Brookhart, B. Grant, A. F. Volpe, Jr., *Organometallics* **1992**, *11*, 3920; k) S. P. Kolesnikov, I. V. Lyudkovskaya, M. Y. Antipin, Y. T. Struchkov, O. M. Nefedov, *Bull. Acad. Sci. USSR Div. Chem. Sci. (Engl. Transl.)* **1985**, *34*, 74; *Izv. Akad. Nauk SSSR Ser. Khim.* **1985**, *34*, 79.

[31] $(C_6F_5)_3Au{\cdot}OEt_2$ was first prepared by Vaughan and Sheppard, and later isolated by Usón and co-workers: a) L. G. Vaughan, W. A. Sheppard, *J. Organomet. Chem.* **1970**, *22*, 739; b) R. Usón, A. Laguna, M. Laguna, J. Jiménez, M. E. Durana, *Inorg. Chim. Acta* **1990**, *168*, 89.

[32] R. Eujen, B. Hoge, D. J. Brauer, *Inorg. Chem.* **1997**, *36*, 1464.

[33] R. D. Sanner, J. H. Satcher, M. W. Droege, *Organometallics* **1989**, *8*, 1498; see also: H. K. Nair, J. A. Morrison, *J. Organomet. Chem.* **1989**, *376*, 149.

[34] S. Martínez-Salvador, J. Forniés, A. Martín, B. Menjón, I. Usón, *Chem. Eur. J.* **2013**, *19*, 324.

[35] J. Stein, J. P. Fackler, Jr., C. Paparizos, H. W. Chen, *J. Am. Chem. Soc.* **1981**, *103*, 2192.

[36] R. J. Staples, T. Grant, J. P. Fackler, Jr., A. Elduque, *Acta Crystallogr. Sect. C* **1994**, *50*, 39.

[37] J. Coetzee, W. F. Gabrielli, K. Coetzee, O. Schuster, S. D. Nogai, S. Cronje, H. G. Raubenheimer, *Angew. Chem. Int. Ed.* **2007**, *46*, 2497; *Angew. Chem.* **2007**, *119*, 2549.

[38] P. G. Jones, E. Bembenek, *Z. Kristallogr.* **1993**, *208*, 126.

[39] H.-N. Adams, J. Strähle, *Z. Anorg. Allg. Chem.* **1982**, *485*, 65.

[40] S. Martínez-Salvador, L. R. Falvello, A. Martín, B. Menjón, *Chem. Eur. J.* **2013**, *19*, 14540.

[41] a) N. Burford, *Coord. Chem. Rev.* **1992**, *112*, 1; b) P. L. Goggin, in *Comprehensive Coordination Chemistry, Vol. 2* (Eds.: G. Wilkinson, R. D. Gillard, J. A. McCleverty), Pergamon, Oxford, **1987**, pp. 487–503; c) S. E. Livingstone, in *Comprehensive Coordination Chemistry, Vol. 2* (Eds.: G. Wilkinson, R. D. Gillard, J. A. McCleverty), Pergamon, Oxford, **1987**, pp. 633–659; d) N. M. Karayannis, L. L. Pytlewski, C. M. Mikulski, *Coord. Chem. Rev.* **1973**, *11*, 93; e) R. G. Garvey, J. H. Nelson, R. O. Rasdale, *Coord. Chem. Rev.* **1968**, *3*, 375.

[42] J. B. Cook, B. K. Nicholson, D. W. Smith, *J. Organomet. Chem.* **2004**, *689*, 860.

[43] D. Schneider, O. Schuster, H. Schmidbaur, *Organometallics* **2005**, *24*, 3547.

[44] a) X. Zhang, K. Seppelt, *Inorg. Chem.* **1997**, *36*, 5689; b) K. B. Wiberg, P. R. Rablen, *J. Am. Chem. Soc.* **1993**, *115*, 614; c) E. Magnusson, *J. Am. Chem. Soc.* **1986**, *108*, 11; d) P. von Ragué Schleyer, A. J. Kos, *Tetrahedron* **1983**, *39*, 1141; e) L. M. Stock, M. R. Wasielewski, *Prog. Phys. Org. Chem.* **1981**, *13*, 253.

[45] H. Böhrer, N. Trapp, D. Himmel, M. Schleep, I. Krossing, *Dalton Trans.* **2015**, *44*, 7489.

[46] K. O. Christe, D. A. Dixon, D. McLemore, W. W. Wilson, J. A. Sheehy, J. A. Boatz, *J. Fluorine Chem.* **2000**, *101*, 151.

[47] I.-C. Hwang, K. Seppelt, *Angew. Chem. Int. Ed.* **2001**, *40*, 3690; *Angew. Chem.* **2001**, *113*, 3803.

[48] a) M. A. Beckett, G. C. Strickland, J. R. Holland, K. S. Varma, *Polymer* **1996**, *37*, 4629; b) U. Mayer, V. Gutmann, W. Gerger, *Monatsh. Chem.* **1975**, *106*, 1235.

[49] a) H. Großekappenberg, M. Reißmann, M. Schmidtmann, T. Müller, *Organometallics* **2015**, *34*, 4952; b) G. J. P. Britovsek, J. Ugolotti, A. J. P. White, *Organometallics* **2005**, *24*, 1685; c) M. A. Beckett, D. S. Brassington, M. E. Light, M. B. Hursthouse, *J. Chem. Soc. Dalton Trans.* **2001**, 1768; d) M. A. Beckett, D. S. Brassington, S. J. Coles, M. B. Hursthouse, *Inorg. Chem. Commun.* **2000**, *3*, 530.

[50] Bond dissociation energies for the neutral diatomic BF and AuF molecules taken from: Y. R. Luo, *Comprehensive Handbook of Chemical Bond Energies*, CRC, Boca Raton, **2007**.

[51] a) R. G. Pearson, *J. Chem. Educ.* **1987**, *64*, 561; b) R. J. Puddephatt, *The Chemistry of Gold*, Elsevier, Amsterdam, **1978**, pp. 22–24; c) S. Ahrland, *Struct. Bonding* **1966**, *1*, 207; d) S. Ahrland, J. Chatt, N. R. Davies, *Q. Revs. Chem. Soc.* **1958**, *12*, 265.

[52] Related ligand-to-metal fluorine shifts seem to underlie the low stability of very strong Lewis acids, such as the naked species $Al(C_6F_5)_3$ (see ref. [53]) and $Al\{OC(CF_3)_3\}_3$ (see ref. [5]).

[53] a) J. Chen, E. Y.-X. Chen, *Dalton Trans.* **2016**, *45*, 6105; b) T. Belgardt, J. Storre, H. W. Roesky, M. Noltemeyer, H.-G. Schmidt, *Inorg. Chem.* **1995**, *34*, 3821; c) J. L. W. Pohlmann, F. E. Brinckmann, *Z. Naturforsch. Teil B* **1965**, *20*, 5.

[54] Where constraints were applied, the optimized species are characterized by their *E* values.

[55] a) J. K. Kochi, *Organometallic Mechanisms and Catalysis*, Academic Press, New York, **1978**, pp. 262–283; b) S. Komiya, T. A. Albright, R. Hoffmann, J. K. Kochi, *J. Am. Chem. Soc.* **1976**, *98*, 7255; c) A. Tamaki, S. A. Magennis, J. K. Kochi, *J. Am. Chem. Soc.* **1974**, *96*, 6140; d) A. Tamaki, S. A. Magennis, J. K. Kochi, *J. Am. Chem. Soc.* **1973**, *95*, 6487.

[56] Relative affinity scales are known for fundamental gold units, such as AuCl and the bare Au^+ cation: a) P. Pyykkö, N. Runeberg, *Chem. Asian J.* **2006**, *1*, 623; b) D. Schröder, H. Schwarz, J. Hrušák, P. Pyykkö, *Inorg. Chem.* **1998**, *37*, 624.

[57] a) V. Jonas, G. Frenking, *Chem. Phys. Lett.* **1993**, *210*, 211; b) T. C. Wong, L. S. Bartell, *J. Chem. Phys.* **1974**, *61*, 2840; c) R. L. Kuczkowski, A. J. Ashe III, *J. Mol. Spectrosc.* **1972**, *42*, 457.

[58] a) C. Elschenbroich, J. Six, K. Harms, G. Frenking, G. Heydenrich, *Eur. J. Inorg. Chem.* **2008**, 3303; b) C. Elschenbroich, S. Voss, O. Schiemann, A. Lippek, K. Harms, *Organometallics* **1998**, *17*, 4417; c) C. Elschenbroich, M. Nowotny, A. Behrendt, K. Harms, S. Wocadlo, J. Pebler, *J. Am. Chem. Soc.* **1994**, *116*, 6217; d) C. Elschenbroich, M. Nowotny, J. Kroker, A. Behrendt, W. Massa, S. Wocadlo, *J. Organomet. Chem.* **1993**, *459*, 157; e) C. Elschenbroich, M. Nowotny, A. Behrendt, W. Massa, S. Wocadlo, *Angew. Chem. Int. Ed. Engl.* **1992**, *31*, 1343; *Angew. Chem.* **1992**, *104*, 1388; f) A. J. Ashe III, W. Butler, J. C. Colburn, S. Abu-Orabi, *J. Organomet. Chem.* **1985**, *282*, 233.

[59] S. B. Clendenning, P. B. Hitchcock, G. A. Lawless, J. F. Nixon, C. W. Tate, *J. Organomet. Chem.* **2010**, *695*, 717.

[60] J. Moussa, L. M. Chamoreau, H. Amouri, *RSC Adv.* **2014**, *4*, 11539.

[61] J. Stott, C. Bruhn, U. Siemeling, *Z. Naturforsch. Teil B* **2013**, *68*, 853.

[62] S. K. Mallissery, M. Nieger, D. Gudat, *Z. Anorg. Allg. Chem.* **2010**, *636*, 1354.

[63] M. Rigo, L. Hettmanczyk, F. J. L. Heutz, S. Hohloch, M. Lutz, B. Sarkar, C. Müller, *Dalton Trans.* **2017**, *46*, 86.

[64] N. Mézailles, L. Ricard, F. Mathey, P. Le Floch, *Eur. J. Inorg. Chem.* **1999**, 2233.

[65] a) C. Müller, D. Vogt, *Dalton Trans.* **2007**, 5505; b) P. le Floch, F. Mathey, *Coord. Chem. Rev.* **1998**, *178–180*, 771.

[66] J. A. Davies, F. R. Hartley, *Chem. Rev.* **1981**, *81*, 79.

[67] R. A. Sanguramath, N. S. Townsend, J. M. Lynam, C. A. Russell, *Eur. J. Inorg. Chem.* **2014**, 1783.

[68] G. E. Coates, C. Parkin, *J. Chem. Soc.* **1963**, 421.

[69] M. A. Carvajal, J. J. Novoa, S. Alvarez, *J. Am. Chem. Soc.* **2004**, *126*, 1465.

[70] H. Schmidbaur, A. Schier, *Arabian J. Sci. Eng.* **2012**, *37*, 1187.

[71] W. C. Wolsey, *J. Chem. Educ.* **1973**, *50*, A335. In spite of its potential explosive character, $AgClO_4$ was used in the synthesis of **1** because the resulting $[PPh_4]ClO_4$ salt formed on reaction with $[PPh_4][(CF_3)_3AuI]$ (Scheme 1) can be cleanly separated from the desired compound.

[72] B. von Ahsen, B. Bley, S. Proemmel, R. Wartchow, H. Willner, F. Aubke, *Z. Anorg. Allg. Chem.* **1998**, *624*, 1225.

Manuscript received: July 19, 2017
Accepted manuscript online: August 11, 2017
Version of record online: September 26, 2017

Appendix

A.1. JCR Impact factors of the journals and candidate's contribution to the publications

This PhD Thesis is presented as a compendium of publications and it is constituted by five articles, published in 2017 and 2018. All of them are published in peer-reviewed journals indexed in the Journal Citation Reports (JCR). A list of these publications is provided below, together with the JCR Impact Factor of the journals, the JCR category and the journal position within the category. The author contribution to each of the five publications is also explained.

1. Gold(I) Fluorohalides: Theory and Experiment

Miguel Baya, Alberto Pérez-Bitrián, Sonia Martínez-Salvador, José M. Casas, Babil Menjón, Jesús Orduna. *Chem. Eur. J.* **2017**, *23*, 1512−1515.
DOI: 10.1002/chem.201605655.

Journal: Chemistry – A European Journal
Publication year: 2017
Impact factor: 5.160
JCR Category: Chemistry, Multidisciplinary
Ranking (JCR, 2017): 37/170

Contribution: The candidate carried out the synthesis and characterization of the complexes, participated actively in the analysis of the tandem mass spectrometry studies and the related computational calculations, as well as in the preparation of the manuscript.

2. Gold(II) Trihalide Complexes from Organogold(III) Precursors

Miguel Baya, Alberto Pérez-Bitrián, Sonia Martínez-Salvador, Antonio Martín, José M. Casas, Babil Menjón, Jesús Orduna. *Chem. Eur. J.* **2018**, *24*, 1514−1517.
DOI: 10.1002/chem.201705509.

Journal: Chemistry – A European Journal
Publication year: 2018

Impact factor: 5.160
JCR Category: Chemistry, Multidisciplinary
Ranking (JCR, 2018): 37/172

Contribution: The candidate carried out the synthesis and characterization of the complexes, studied their thermolyses, and participated actively in the analysis of the tandem mass spectrometry studies and the related computational calculations, as well as in the preparation of the manuscript.

3. An Organogold(III) Difluoride with a *trans* Arrangement

Alberto Pérez-Bitrián, Miguel Baya, José M. Casas, Antonio Martín, Babil Menjón, Jesús Orduna. *Angew. Chem. Int. Ed.* **2018**, *57*, 6517–6521.
DOI: 10.1002/anie.201802379.
Angew. Chem. **2018**, *130*, 6627–6631. DOI: 10.1002/ange.201802379.

Journal: Angewandte Chemie International Edition
Publication year: 2018
Impact factor: 12.257
JCR Category: Chemistry, Multidisciplinary
Ranking (JCR, 2018): 17/172

Contribution: The candidate designed the synthetic route to access the difluoride complex and carried out all the experimental part of the article, including synthesis, characterization and preparation of single-crystals for X-ray diffraction. He also analyzed all the tandem mass spectra and the related computational calculations and participated in the preparation of the manuscript.

4. Anionic Derivatives of Perfluorinated Trimethylgold

Alberto Pérez-Bitrián, Sonia Martínez-Salvador, Miguel Baya, José M. Casas, Antonio Martín, Babil Menjón, Jesús Orduna. *Chem. Eur. J.* **2017**, *23*, 6919–6929.
DOI: 10.1002/chem.201700927.

Journal: Chemistry – A European Journal
Publication year: 2017

Impact factor: 5.160
JCR Category: Chemistry, Multidisciplinary
Ranking (JCR, 2017): 37/170

Contribution: The candidate performed all the experimental part of the article, including synthesis, characterization and preparation of single-crystals for X-ray diffraction. He also performed the thermolytic studies in the condensed phase and analyzed the tandem mass spectrometry experiments to compare the results of both types of decompositions. He also participated actively in analyzing the theoretical calculations and in the preparation of the manuscript.

5. $(CF_3)_3Au$ as a Highly Acidic Organogold(III) Fragment

Alberto Pérez-Bitrián, Miguel Baya, José M. Casas, Larry R. Falvello, Antonio Martín, Babil Menjón. *Chem. Eur. J.* **2017**, *23*, 14918–14930.
DOI: 10.1002/chem.201703352.

Journal: Chemistry – A European Journal
Publication year: 2017
Impact factor: 5.160
JCR Category: Chemistry, Multidisciplinary
Ranking (JCR, 2017): 37/170

Contribution: The candidate performed all the experimental part of the article, including synthesis, characterization and preparation of single-crystals for X-ray diffraction, as well as the experimental assessment of the Lewis acidity and the stability of the compounds. He also participated actively in analyzing the computational calculations, especially to compare them to the experimental results, and in the preparation of the manuscript.

A.2. Complete list of publications of Alberto Pérez Bitrián

8. Pascal S. Engl, Andreas P. Häring, Florian Berger, Georg Berger, **Alberto Perez-Bitrián**, Tobias Ritter. C−N Cross-Couplings for Site-Selective Late-Stage Diversification via Aryl Sulfonium Salts. *J. Am. Chem. Soc.* **2019**, *141*, 13346−13351.

7. Diego Ardura, **Alberto Pérez-Bitrián**. Motivational pathways towards academic achievement in physics & chemistry: a comparison between students who opt out and those who persist. *Chem. Educ. Res. Pract.* **2019**, *20*, 618–632.

6. Diego Ardura, **Alberto Pérez-Bitrián**. The effect of motivation on the choice of chemistry in secondary schools: adaptation and validation of the Science Motivation Questionnaire II to Spanish students. *Chem. Educ. Res. Pract.* **2018**, *19*, 905–918.

5. **Alberto Pérez-Bitrián**, Miguel Baya, José M. Casas, Antonio Martín, Babil Menjón, Jesús Orduna. An Organogold(III) Difluoride with trans Arrangement. *Angew. Chem. Int. Ed.* **2018**, *57*, 6517–6521; Angew. Chem. 2018, 130, 6627–6631.

4. Miguel Baya, **Alberto Pérez-Bitrián**, Sonia Martínez-Salvador, Antonio Martín, José M. Casas, Babil Menjón, Jesús Orduna. Gold(II) Trihalide Complexes from Organogold(III) Precursors. *Chem. Eur. J.* **2018**, *24*, 1514–1517.

3. **Alberto Pérez-Bitrián**, Miguel Baya, José M. Casas, Larry R. Falvello, Antonio Martín, Babil Menjón. $(CF_3)_3Au$ as a Highly Acidic Organogold(III) Fragment. *Chem. Eur. J.* **2017**, *23*, 14918–14930.

2. **Alberto Pérez-Bitrián**, Sonia Martínez-Salvador, Miguel Baya, José M. Casas, Antonio Martín, Babil Menjón, Jesús Orduna. Anionic Derivatives of Perfluorinated Trimethylgold. *Chem. Eur. J.* **2017**, *23*, 6919–6929.

1. Miguel Baya, **Alberto Pérez-Bitrián**, Sonia Martínez-Salvador, José M. Casas, Babil Menjón, Jesús Orduna. Gold(I) Fluorohalides: Theory and Experiment. *Chem. Eur. J.* **2017**, *23*, 1512–1515.

A.3. Conference presentations of Alberto Pérez Bitrián

7. 8th Conference of Young Researches (Chemistry and Physics) of Aragón

Poster presentation: "The use of tandem mass spectrometry to study highly unstable species: the case of gold(II) trihalides".

Zaragoza (Spain), 22th November 2018.

6. XXXVI GEQO Congress Organometallic Chemistry Group

Oral presentation: "Synthesis and Properties of Organogold(III) Fluoride Complexes".

Zaragoza (Spain), 5th to 7th September 2018.

5. 22nd International Symposium on Fluorine Chemistry

Oral presentation: "Trifluoromethylgold fluoride complexes: Organometallics with distinct inorganic flavor".

Oxford (United Kingdom), 22nd to 27th July 2018.

4. 7th Conference of Young Researches (Chemistry and Physics) of Aragón

Oral flash presentation: "The $Au(CF_3)_3$ Fragment: A Strong Lewis Acid".

Zaragoza (Spain), 24th November 2016.

3. 6th EuCheMS Chemistry Congress

Oral presentation: "Anionic Derivatives of Perfluorinated Trimethylgold: Synthesis and Decomposition".

Sevilla (Spain), 11th to 15th September 2016.

2. IX School on Organometallic Chemistry "Marcial Moreno Mañas"

Oral presentation: "On the Highly Acidic, Single-Site $Au(CF_3)_3$ Fragment".

Donostia-San Sebastián (Spain), 6th to 8th July 2016.

1. XII RSEQ – Sigma Aldrich Young Researchers Symposium.

Poster presentation: "Pt(III) vs. Pt(IV) in the Oxidation of Pt(II) Complexes".

Barcelona (Spain), 3rd to 6th November 2015.

Coauthor of the following presentations:

2. XXXVI GEQO Congress Organometallic Chemistry Group

Poster presentation: "Organogold(III) Carboxylate Complexes: Synthesis and Degradation" (presented by M.Sc. Sergio González-Díaz).

Zaragoza (Spain), 5th to 7th September 2018.

1. 22nd International Symposium on Fluorine Chemistry

Poster presentation: "Gold & Trifluoromethyl, hand in hand" (presented by Dr. Miguel Baya).

Oxford (United Kingdom), 22nd to 27th July 2018.